WILEY-VCH

Klaus Schwochau

Technetium

Chemistry and Radiopharmaceutical Applications

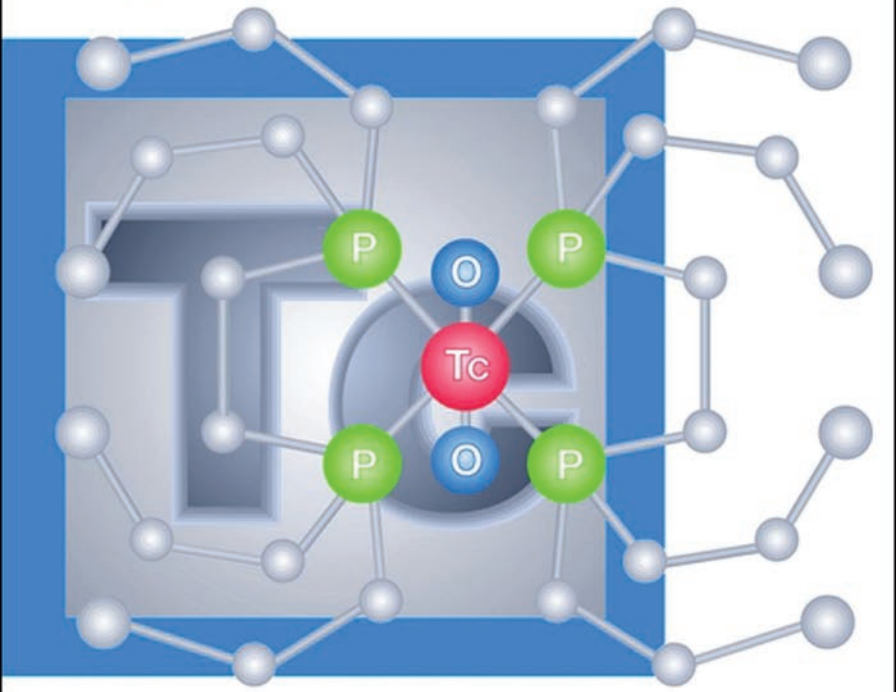

Klaus Schwochau

Technetium

WILEY-VCH

Further Reading from Wiley-VCH and John Wiley & Sons

K. H. Lieser

Nuclear and Radiochemistry. Fundamentals and Applications
1997, 4725 pages. Wiley-VCH.
ISBN 3-527-29453-8

M. E. Wolff (Ed.)

Burger's Medicinal Chemistry and Drug Discovery, 5th Edition.
1997, 3992 pages. Wiley..
ISBN 0-471-57561 (5 Volumes Set)

Klaus Schwochau

Technetium

Chemistry and Radiopharmaceutical Applications

WILEY-VCH

Weinheim · New York · Chichester · Brisbane · Singapore · Toronto

Prof. Dr. Klaus Schwochau
Institut für Chemie und Dynamik der Geospähre
Forschungszentrum Jülich GmbH
D-52425 Jülich
und
Rheinisch-Westfälische Technische Hochschule Aachen
D-52056 Aachen

Library of Congress Card No. applied for

A catalogue record for this book is available from the British Library

Die Deutsche Bibliothek Cataloguing-in-Publication Data:
A catalogue record for this book is available from Der Deutschen Bibliothek
ISBN 3-527-29496-1

Cover Illustration: W. Scheffler, D-55128 Mainz
Composition: Kühn & Weyh, D-79111 Freiburg
Printing: Strauss Offsetdruck, D-69509 Mörlenbach
Bookbinding: Großbuchbinderei J. Schäffer, D-67269 Grünstadt
Printed in the Federal Republic of Germany

Preface

The artificial radioelement of atomic number 43, technetium, is frequently considered to be a curiosity in inorganic chemistry. However, more than five decades ago, when sufficient quantities of the long-lived nuclide ^{99}Tc with a half-life of $2.13 \cdot 10^5$ a became available, investigations of its chemistry and physics soon confirmed technetium to be a true second-row transition element, filling the gap in the periodic system between manganese and rhenium. Technetium received much attention in fundamental inorganic chemistry studies at research institutions and universities. At present, the enormous number of technetium compounds, that have been isolated and characterized, documents the extensive research performed in technetium chemistry. Its rapid expansion was primarily spurred by the world-wide intention to develop technetium radiopharmaceuticals of high diagnostic efficacy labeled with the ^{99m}Tc isomer with a physical half-life of six hours. Over 80% of all radiopharmaceuticals now used in clinics are labeled with ^{99m}Tc.

This monograph represents the present status of technetium chemistry and technetium radiopharmaceuticals. It is intended for use as a handbook and a text book for inorganic and nuclear chemists, nuclear pharmacists and nuclear medicine physicians. First discussed are the discovery and occurrence of technetium, its nuclides, fundamental and analytical aspects, and its uses. Technetium chemistry is focused on in discussions of synthesis, properties, and structures of individual technetium compounds. Complex compounds are treated in the sequence of Tc oxidation states in most of part A. Part B is concerned with synthesis, composition, and structure of ^{99m}Tc radiopharmaceuticals currently used for diagnostic organ and tumor imaging, and with future prospects, including imaging of hypoxic tissue, receptor binding, and dopamine transporters. Concluding tables are provided to summarize the chapters. Each chapter terminates with the pertinent literature. Acronyms and abbreviations used in both parts of this book are listed in the appendix.

Since the mid 1960s, some excellent books on technetium have appeared: R. Colton "The Chemistry of Rhenium and Technetium", Interscience (1965), R. D. Peacock "The Chemistry of Technetium and Rhenium", Elsevier (1966), J. Steigman and W. C. Eckelman "The Chemistry of Technetium in Medicine", Nuclear Science Series (1992), and "Technetium and Rhenium. Their Chemistry and Applications", Topics in Current Chemistry (1996), edited by K. Yoshihara and T. Omori. The last book contains contributions to several aspects of technetium chemistry. However, the latest comprehensive volumes on technetium which appeared in the Gmelin Handbook of Inorganic Chemistry (8th edition, Springer) date back to 1982/83. The increasing flood of publications since then, particularly on technetium complex chemistry and radiopharmaceuticals, justifies this comprehensive monograph.

I am grateful to the late Prof. Dr. W. Herr for drawing my attention as early as the late 1950s to the artificial element technetium. I would like to express my cordial gratitude on this occasion to all my former co-workers in technetium chemistry, in particular to Dr. L. Astheimer, Mr. K. H. Linse, Dr. H. J. Schenk, Dr. H. H. Pieper, and Dr. J. Hauck. My sincere thanks are due to Prof. Dr. K. H. Lieser, Darmstadt, for his interest in this book. I would further like to thank the staff on the Central Library of the Research Center in Juelich, Germany, for actively supplying the relevant literature. Finally, my thanks are extended to the publishers for their friendly cooperation. All criticisms of this book brought to my attention will be gratefully acknowledged.

Juelich, December 1999 Klaus Schwochau

Contents

A. Chemistry

This Page Intentionally Left Blank

1 Introduction

Element 43 in the seventh subgroup of the periodic system, technetium, is the lowest atomic number radioelement. Stable, non-radioactive isotopes do not exist according to Mattauch's rule. Technetium isotopes can be produced artificially by nuclear processes. Long-lived isotopes are ^{97}Tc ($2.6 \cdot 10^6$ a), ^{98}Tc ($4.2 \cdot 10^6$ a) and ^{99}Tc ($2.1 \cdot 10^5$ a). The spectroscopic discovery of technetium in several fixed stars provided the first proof of stellar synthesis of heavy nuclides. Traces of ^{99}Tc occur in the earth's crust where they arise mainly from spontaneous fission of ^{238}U.

Among the long-lived isotopes, ^{99}Tc is the only one which is obtained in weighable amounts. It is formed in high yield by the fission of ^{235}U, and quantities of the order of kilograms can be isolated from nuclear reactor fission product waste solutions. Because of the relatively low specific activity of 17 μCi/mg (629 kBq/mg) and the weak β^--radiation (E_{max}=0.29 MeV), the laboratory handling of ^{99}Tc needs no special radiation protection.

The chemical behavior and the coordination chemistry of this second row transition element closely resemble those of the homologous element rhenium, however, detailed investigations also revealed many distinct differences. The critical temperature of superconductivity of technetium metal is remarkably high at 8.2 K. Specific catalytic properties of technetium have been demonstrated. The effectiveness of pertechnetate ions in inhibiting the corrosion of steel is noteworthy. Pertechnetate is a weakly oxidizing agent, although somewhat stronger than perrhenate. Because of the almost equal ionic radii of technetium and rhenium, their analogous compounds frequently exhibit isostructural lattices. Alkali pertechnetates are the thermally most stable compounds of technetium; $KTcO_4$ boils without decomposition at ~1000 °C.

The coordination chemistry involves the oxidation states from +7 to –1. Coordination numbers from 4 to 9 are known. Crystal field considerations and magnetic susceptibility measurements show that technetium forms low-spin compounds. Dinuclear complexes frequently display metal to metal bond character. There is some evidence that technetium complexes are thermodynamically less stable and kinetically more reactive than the corresponding complexes of rhenium. A multitude of coordination compounds of technetium has been synthesized and unambiguously characterized. Investigations of the complex chemistry have been enormously stimulated by the development of ^{99m}Tc radiopharmaceuticals.

2 Discovery

The first conclusive experimental evidence for element 43 was given by Perrier and Segrè in 1937 [1]. This discovery was a consequence of the invention of the cyclotron. A plate of natural molybdenum irradiated over a period of some months by a strong deuteron beam in the Berkeley cyclotron was presented by E. O. Lawrence of the University of California to E. Segrè at the Royal University of Palermo, Italy. The molybdenum plate showed strong radioactivity due to more than one nuclide with a half-life of months. In a cooperation of E. Segrè with C. Perrier, of the same university, a chemical investigation of the activity ruled out any radioactive isotopes of zirconium, niobium, molybdenum or ruthenium, and revealed that the activity arose from nuclides of the missing element ekamanganese of the atomic number 43 [2]. The metastable isomers ^{95m}Tc and ^{97m}Tc had been produced by the nuclear reactions:

$$^{94}_{42}\mathrm{Mo(d,n)}^{95m}_{43}\mathrm{Tc} \qquad t_{1/2} = 61\mathrm{d}$$

and

$$^{96}_{42}\mathrm{Mo(d,n)}^{97m}_{43}\mathrm{Tc} \qquad t_{1/2} = 91\mathrm{d}$$

Using concentrated fractions of these isomers, Perrier and Segrè were able to demonstrate by coprecipitations, for instance with sulphides of manganese and rhenium or with $TlReO_4$, that the element produced bore the closest resemblance to rhenium. Other experiments showed the radioactivity to volatilize with rhenium in an oxygen flow at 550 °C [2]. They could already identify several chemical properties of this artificial element [3]. In 0.4 to 5 M hydrochloric acid solution the sulphide precipitation was complete in the presence of rhenium or platinum as a carrier, but in 10 M hydrochloric acid only a very small fraction of the total activity precipitated, in contrast to the precipitation of Re_2S_7. In considering the possibility of separating element 43 and rhenium, Perrier and Segrè tried to determine partition coefficients of the radioactivity between aqueous solutions and crystals of $KReO_4$ and $CsReO_4$. They found a partition coefficient of the activity for $KReO_4$ of 2.6 and for $CsReO_4$ of 0.75 in agreement with the lower solubility of $CsTcO_4$ as compared to $KTcO_4$ [3]. In 1947 the discoverers proposed for element 43 the name "technetium" derived from the Greek word τεχνητοσ meaning artificial, in recognition of the fact that technetium was the first artificially made element, and they suggested the corresponding chemical symbol "Tc" [4]. Prior to the naming, Segrè and Wu [5] detected a 6 h activity of element 43, obviously ^{99m}Tc, by extraction of ^{99}Mo, a neutron fission product of ^{235}U.

2.1 References

[1] C. Perrier and E. Segrè, Nature (London) *140*, 193–194 (1937)
[2] C. Perrier and E. Segrè, J. Chem. Phys. *5*, 712–716 (1937)
[3] C. Perrier and E. Segrè, J. Chem. Phys. *7*, 155–156 (1939)
[4] C. Perrier and E. Segrè, Nature (London) *159*, 24 (1947)
[5] E. Segrè and C. S. Wu, Phys. Rev. *57*, 552 (1940)

3 Natural occurrence

3.1 Primordial technetium

In 1869 Mendeléev [1] predicted the existence of an element of atomic weight 100 occupying the vacant space between molybdenum and ruthenium in his Periodic System. He named this element provisionally "ekamanganese" corresponding to its position below manganese. In 1913 and 1914 Moseley [2,3] found the atomic number of elements in the Periodic System to be directly proportional to the square root of the frequency of their K or L X-ray emission and thus derived a vacant space for the atomic number 43 in addition to 61(Pm) and 75(Re). These indications of Mendeléev and Moseley stimulated numerous attempts to demonstrate the occurrence of element 43 [4,5] and the other elements lacking in nature.

In this context the systematic investigations of Noddack and Tacke [6] as well as Berg and Tacke [7] should be mentioned. It was not unexpected that when they announced in 1925 the discovery of element 75 "dvimanganese", later called rhenium, they also claimed to have detected element 43 by X-ray spectroscopy in concentrates of the minerals sperrylite ($PtAs_2$), gadolinite $\{Be_2Y_2Fe(SiO_4)_2O_2\}$, and columbite $\{(Fe,Mn)(NbO_3)_2\}$. The wavelengths of the X-ray lines interpreted as $K\alpha_1$,$K\alpha_2$, and $K\beta_1$ showed good agreement with the calculated wavelengths. Noddack, Tacke, and Berg named the alleged element 43 "masurium", commemorating the former East Prussian district of Masuria. Whereas I. Noddack (née I. Tacke) and W. Noddack [8] succeeded in isolating about 2 mg of rhenium, they could not concentrate and isolate element 43. Because no further evidence for the existence of masurium in the earth's crust was submitted, their claim to discovery was finally not accepted.

In 1934 Mattauch's rule on the stability of atomic nuclei was published [9]. Mattauch pointed out that β-stable isobar pairs do not exist when they differ only by one atomic number unit and ruled out the existence of stable isotopes of element 43. Nevertheless, the primordial occurrence of long-lived isotopes in the earth's crust could not be excluded [10], thus the search for element 43 continued. Herr [11] exposed concentrates of rhenium-rich molybdenites (MoS_2), from which Mo was separated, to an intense neutron bombardment and observed a 6 h activity of ^{99m}Tc. This activity supposedly resulted from the reaction ^{98}Tc(n,γ) ^{99m}Tc indicating the occurrence of ^{98}Tc in these ores. However, taking into account neutron reactions with possible contaminations (^{98}Mo, ^{99}Tc, ^{99}Ru, ^{235}U) of the concentrates, the occurrence of ^{98}Tc could not be demonstrated conclusively. Similar investigations were carried out by Alperovitch and Miller [12] who claimed the detection of ^{98}Tc in columbites, yttrotantalites $\{(Y,Ce)(Ta,NbTi)_2O_6\}$ and a thortveitite $\{(Y,Sc)_2(Si_2O_7)\}$. Anders (Alperovitch) et al. [13] extended the search for ^{98}Tc by neutron activation analysis mainly of the same minerals, but of different locality

and stated strong evidence for the existence of ^{98}Tc in nature. In the same year Boyd and Larson [14] published a report on the occurrence of technetium in the earth's crust after a thorough search in a variety of terrestrial substances including molybdenite and yttrotantalite. They used different analytical methods of high sensitivity such as isotopic dilution, mass spectrometry, neutron activation analysis, emission spectroscopy, spectrophotometry, and polarography, but they failed to reveal any traces of technetium in the samples analyzed. In addition, Herr et al. [15] could not detect in Precambrian columbite, gadolinite, and tantalite any enrichment of the isotopes ^{97}Mo, ^{98}Mo and ^{98}Ru as potential decay products of ^{97}Tc and^{98}Tc, respectively. Boyd et al. [16] produced the long-lived isotopes ^{97}Tc, ^{98}Tc, and ^{99}Tc by bombarding molybdenum metal with 22 MeV protons for 270 days and identified some amounts by mass spectrometry for the first time. The half-life of these isotopes was found to be considerably less than 10^8 a [14, 17], thus excluding the presence of primordial technetium in the earth's crust given the formation of the earth approximately $4.5 \cdot 10^9$ a ago.

3.2 Non-primordial technetium

Nevertheless, the earth's crust contains technetium. ^{99}Tc is predominantly formed by spontaneous fission of ^{238}U and is also produced by neutron induced fission of ^{235}U. The first isolation of naturally occuring technetium was reported by Kenna and Kuroda [18, 19], who separated about 10^{-3} µg of ^{99}Tc from 5.3 kg of Belgian Congo pitchblende. The ore contained 42.2 wt% U, 0.37 wt% Mo, 0.17 wt% Cu, 0.03 wt% Cl, less than 0.00004 wt% Ru, and 0.000002 wt% Re. Three technetium fractions were isolated from 2.0, 1.3 and 2.0 kg of pitchblende, respectively. The samples were dissolved in dilute nitric acid. Lead was precipitated as the sulphate and H_2S was passed through the filtrate. The precipitate was dissolved in ammoniacal hydrogen peroxide and excess peroxide was removed by boiling. The pH was kept at 8 or higher. To remove the bulk of the cations, the neutralized solution was passed through a cation exchange column. Copper and molybdenum were removed from the evaporated solution by precipitation with α-benzoin-oxime. Pertechnetate and perrhenate were extracted from the 5 M NaOH solution. After re-extraction into the aqueous phase, a few mg of copper were added to act as a carrier and sulphides again precipitated, filtered and dissolved. The solution was evaporated, the pH adjusted to 7, pertechnetate and perrhenate adsorbed on an anion exchange column and eluted with 0.25 M perchlorate. Finally, again copper carrier was added to the technetium fraction, the acidity adjusted to 2 N, and sulphides were precipitated [20].

The activity of the precipitate was counted with a low-background β^--counter, with a background of about 0.7 counts per min. The observed activity measured in the precipitate per kg ore was 1.8, 1.7 and 2.1 counts per min for the three pitchblende samples, respectively. The average half-thickness value of 7 ± 1 mg/cm^2 aluminum was in agreement with the accepted half-thickness value of 7.2 mg/cm^2 Al for ^{99}Tc. The atomic ratio ^{99}Tc/^{238}U in pitchblende was found to be fairly conformable with the

$^{99}Mo/^{238}U$ ratio, indicating that the ^{99}Tc in pitchblende was predominantly produced by the spontaneous fission of ^{238}U [19].

Some billion years ago natural nuclear reactors must have operated and generated ^{99}Tc as a high yield fission product by induced fission of ^{235}U with slow neutrons. The relics of a natural reactor were discovered in 1972 at the Oklo uranium mines in the Republic of Gabon, Africa. The Oklo phenomenon occurred 1.72 billion years ago and produced a greater amount of ^{99}Tc than detected in other uranium ores [20]. Ruffenach et al. [21] reported values of integrated flux of thermal neutrons for the Oklo uranium ores of up to $1.32 \cdot 10^{21}$ n · cm ^{2} and a $^{235}U/^{238}U$ atomic ratio down to 0.00410, compared to 0.00725 in normal natural uranium. If the fission yield of ^{99}Tc amounts to around 6 atom%, $0.315 \cdot 0.06 \approx 0.019$ atom% of ^{235}U should have been converted to ^{99}Tc, corresponding to about 0.2 mg of ^{99}Tc per kg of a uranium ore containing 37 wt% uranium. However, since the half-life of ^{99}Tc is $2.13 \cdot 10^{5}$ a, the isotope completely decayed to ^{99}Ru. The considerably higher abundance of ^{99}Ru in Oklo uranium ores was proved by Frejacques et al. [22].

3.3 Technetium in stars

Soon after the publication of the first and second atomic emission spectrum of technetium by Meggers and Scribner [23], Moore [24] looked for technetium lines in the spectrum of the sun. The evidence for the presence of Tc^{+}(TcII) rested chiefly on the one unblended solar line at 3195.230 Å. Later, this suggestion was shown to be erroneous [25, 26, 27]. However, in 1952 Merrill [28, 29] detected neutral technetium, (TcI) absorption lines at 4031, 4238, 4268, and 4297 Å in S-type stars. The highest intensity lines were identified in the stars R Geminorum, R-Andromeda, and AA Cygni. Stellar spectra of type S are characterized by bands of zirconium oxide and by relatively strong lines of heavy metals such as zirconium and barium. Some years later Merrill [30] also observed TcI-lines in the N-type stars TX Piscium and U Hydrae. Moreover, also M-type stars showed TcI-lines. Stars of S-, N- and M-type are relatively cold, having surface temperatures of around 3000 K. The discovery of technetium in numerous stars was of great significance to cosmological theories [31]. Considering the half-life of $2.6 \cdot 10^{6}$ a of ^{97}Tc and $2.1 \cdot 10^{5}$ a of ^{99}Tc, the isotopes which have been discussed to be produced in stars [32], the existence of technetium at the surface of stars is one of the strongest supports for the idea of nucleosynthesis of heavy elements by slow neutron capture (s-process) [33]. The time scale for neutron capture in the s-process is much longer than that for β -decay [34].

3.4 References

[1] D. Mendeléev, Liebigs Ann. Chem., Suppl-Vol. *8*, 133–229 (1872)
[2] H. G. J. Moseley, Phil. Mag. (6) *26*, 1024–1034 (1913)
[3] H. G. J. Moseley, Phil. Mag. (6) *27*, 703–714 (1914)

[4] B. T. Kenna, J. Chem. Educat. *39*, 436–442 (1962)
[5] H. W. Kirby in: Gmelin Handbook of Inorganic Chemistry, Technetium, Supplement Vol. 1, 8th ed., (H. K. Kugler and C. Keller, eds.), Springer, Berlin (1982) p. 1–11
[6] W. Noddack and I. Tacke, Naturwissenschaften *13*, 567–571 (1925)
[7] O. Berg and I. Tacke, Naturwissenschaften *13*, 571–574 (1925)
[8] I. Noddack and W. Noddack, Z. Physik. Chem. *125*, 264–274 (1927)
[9] J. Mattauch, Z. Physik *91*, 361–371 (1934)
[10] H. Jensen, Naturwissenschaften *26*, 381 (1938)
[11] W. Herr, Z. Naturforschg. *9a*, 907–908 (1954)
[12] E. A. Alperovitch and J. M. Miller, Nature *176*, 299–301 (1955)
[13] E. Anders, R. N. Sen Sarma, and P. H. Kato, J. Chem. Phys. *24*, 622–623 (1956)
[14] G. E. Boyd and Q. V. Larson, J. Physic. Chem. *60*, 707–715 (1956)
[15] W. Herr, E. Merz, P. Eberhardt, J. Geiss, C. Lang, and P. Signer, Geochim. Cosmochim. Acta *14*, 158 (1958)
[16] G. E. Boyd, J. R. Sites, Q. V. Larson, and C. R. Baldock, Phys. Rev. *99*, 1030–1031 (1955)
[17] G. E. Boyd, Phys. Rev. *95*, 113–114 (1954)
[18] B. T. Kenna and P. K. Kuroda, J. Inorg. Nucl. Chem. *23*, 142–144 (1961)
[19] B. T. Kenna and P. K. Kuroda, J. Inorg. Nucl. Chem. *26*, 493–499 (1964)
[20] P. K. Kuroda, Radiochim. Acta *63*, 9–18 (1993)
[21] J. C. Ruffenach, J. Menes, M. Lucas, R. Hagemann, and G. Nief, The Oklo Phenomenon, IAEA, Vienna, (1975) pp. 371–384
[22] C. Frejacques, C. Blain, C. Devillers, R. Hagemann, and J. C. Ruffenach, The Oklo Phenomenon, IAEA, Vienna, 509–524 (1975)
[23] W. F. Meggers and B. F. Scribner, J. Research Natl. Bur. Standards *45*, 476, RP 2161 (1950)
[24] C. E. Moore, Science *114*, 59–61 (1951)
[25] J. L. Greenstein and C. DeJager, Bull. Astron. Inst. Neth. *13*, 13–14 (1956)
[26] J. L. Greenstein, Mem. Soc. R. Sci. Liege *14*, 307 (1953)
[27] A. A. Nikitin, Astron. Zhur *35*, 18–25, (1958)
[28] P. W. Merrill, Astrophys. J. *116*, 21–26 (1952)
[29] P. W. Merrill, Science *115*, 484 (1952)
[30] P. W. Merrill, Publ. Astron. Soc. Pac. *68*, 70–71 (1956)
[31] P. Jordan, Naturwissenschaften *40*, 407–408 (1953)
[32] M. Arnould, Ann. Astrophys. *31*, 179–197 (1968)
[33] K. Takahashi, G. J. Mathews, and S. D. Bloom, Phys. Rev. *C33*, 296–301 (1986)
[34] F. Käppeler, R. Gallino, M. Busso, G. Picchio, and C. M. Raiteri, Astrophys. J. *354*, 630–643 (1990)

4 Artificial occurrence

Among the long-lived technetium isotopes only the β -emitter ^{99}Tc with a half-life of $2.13 \cdot 10^5$ a is obtained in weighable amounts, either by neutron irradiation of highly purified natural molybdenum or by induced fission of ^{235}U with thermal neutrons. Because of the high fission yield of 6.13 atom%, appreciable quantities of ^{99}Tc can be isolated from uranium fission product mixtures. Nuclear reactors with a power of 3500 MW_{th} produce about 100 g of ^{99}Tc per day or 6 TBq (~ 10 kg) ^{99}Tc/GW_{th} per year.

The total stratospheric fallout of ^{99}Tc from nuclear weapons testing was estimated at 140 TBq [1, 2]. The fission of ^{235}U and ^{239}Pu in nuclear weapons test explosions produce ^{99}Tc, which is oxidized to Tc_2O_7 in the presence of atmospheric oxygen at the high temperatures prevalent during the explosions. Tc_2O_7 reacts with water vapor to give pertechnetic acid. Radioactive fallout is very low at present as a consequence of international agreements banning nuclear weapons tests in the atmosphere [3]. The Chernobyl accident in 1986 liberated about 0.75 TBq of ^{99}Tc [2].

Releases of ^{99}Tc from nuclear power plants are low during normal operation. About 1 MBq ^{99}Tc per year is released from a 1000 MW_e reactor. With an operational experience of 6000 reactor years and a mean reactor capacity of 700 MW_e, the total calculated release of ^{99}Tc is only 4.2 GBq [2].

The short-lived ^{99m}Tc ($t_{1/2}$ = 6.0 h) is used as an organ imaging radioisotope in radiopharmaceuticals in nuclear medicine. ^{99m}Tc is produced in commercial generators and decays by γ-emission to the ^{99g}Tc ground state. Per medical investigation 20 to 1000 MBq ^{99m}Tc is applied. This radionuclide has shown the greatest increase in usage during the past two decades. However, the activity of ^{99g}Tc formed by decay of ^{99m}Tc is negligible as calculated from the ratio of the decay constants $\lambda(^{99g}\text{Tc})/\lambda(^{99m}\text{Tc})=3.2 \cdot 10^{-9}$.

The most important source of artificially occurring ^{99g}Tc is the nuclear fuel cycle. The total electricity generated by nuclear power stations over the world until the end of 1980 was 419 GW_e years [4]. Assuming that some 10 % of the fuel, from which this electricity has been produced, is reprocessed and that all the ^{99}Tc liberated by reprocessing was discharged before the end of 1980, an activity of about 825 TBq was released. After 1980 reprocessing was improved to reduce emissions. It is estimated that the ^{99g}Tc discharge is only about 10 % of that, released up until 1980, i. e. 68 TBq corresponding to 343 GW_e years up to 1983 and 234 TBq corresponding to 1187 GW_e years [5] until the end of 1993. The total global discharge of ^{99}Tc by the nuclear fuel cycle would be on the order of 1130 TBq up till the end of 1993. Summarizing the radioactivity of the relevant artificial ^{99g}Tc sources over the world would result at present in around $1.3 \cdot 10^3$ TBq, equivalent to more than 2 t of ^{99g}Tc.

4.1 Technetium in the nuclear fuel cycle

The description of technetium production in the nuclear fuel cycle and technetium release to the environment is based on a light-water reactor (LWR) designed to produce 800 MW_e years [6]. The life-time of this model reactor is considered to be 30 years. The difference in the amounts of ^{99}Tc formed in spent fuel in the pressurized water reactor (PWR) and the boiling water reactor (BWR) appears to be negligible. 35 metric tons of uranium are assumed to be the annual feed of new fuel. The ^{235}U enrichment in the fresh fuel is supposed to be 3.2 wt%, in the spent fuel 0.84 wt%. Technetium isotopes of mass numbers greater than 99 have half-lifes of less than 20 min and thus have decayed during storing of the fuel elements for 150 days after discharge from the reactor. As compared to ^{99}Tc the production of the long-lived isotopes ^{97}Tc and ^{98}Tc by thermal neutron fission can be neglected. ^{99}Tc is by far the dominant technetium isotope occurring in the nuclear fuel cycle [4]. It is also formed in high yield (atom%) from thermal neutron fission of $^{233}U(4.8)$ and $^{239}Pu(5.9)$, and fast neutron fission of $^{239}Pu(5.9)$, $^{238}U(6.3)$, and $^{232}Th(2.7)$. All of these sources may contribute to the accumulated inventory of ^{99}Tc. The specific radioactivity of ^{99}Tc normalized to fuel with a burnup of 33,000 MWd (therm) per ton of uranium is calculated to be about 14.5 Ci/t [6] corresponding to 0.85 kg of ^{99}Tc/t of uranium.

The reprocessing procedure for recovering uranium from spent fuel elements is a chemical technique known as the Purex (plutonium and uranium recovery by extraction) process [7]. The fuel elements are cut into small pieces for dissolution in 7.5 M HNO_3. The dissolution is normally incomplete. An amount of small metallic particles containing Mo, Ru, Rh, Pd, and Tc is not dissolved [8] and discharged as highly active waste [9]. Technetium, assumed to be produced during fission in its elemental state, is converted to TcO_4^-. The aqueous nitric acid liquid containing the dissolved burned-up fuel is processed through a series of solvent extractions [6].

The solvent extraction of TcO_4^- by tributyl phosphate (TBP) in *n*-dodecane was studied over a wide range of concentrations of TBP, HNO_3, NH_4NO_3, and uranium, and as a function of temperature [7, 10]. The extraction was found to proceed via the compound $HTcO_4 \cdot 3TBP$ [10]. Increasing TBP concentration from 10 to 80 vol% results in a rise of the TcO_4^- distribution coefficient D_{Tc} of almost three orders of magnitude. For any given TBP concentration D_{Tc} increases with increasing nitric acid concentration until a maximum is reached at 0.6 M HNO_3. There is almost no extraction of TcO_4^- in the absence of HNO_3. The reason for the increase of D_{Tc} up to 0.6 M HNO_3 appears to be the reduced dissociation of $HTcO_4$. Above 1.0 M HNO_3 D_{Tc} decreases rapidly due to competition of a complex formation of HNO_3 with TBP. When, by addition of $UO_2(NO_3)_2$ the aqueous phase is 0.1 M in $UO_2(NO_3)_2$, D_{Tc} is substantially increased by some orders of magnitude at HNO_3 concentrations lower than 0.1 M. Apparently, the extracted compound formed is $UO_2(NO_3)(TcO_4) \cdot 2TBP$ [7, 9, 10]. In the temperature range from 25 to 60 °C D_{Tc} was found to decrease steadily as the temperature is increased (Fig. 4.1.A).

After extraction of pertechnetate with TBP in *n*-dodecane, the uranium in the cycle may contain about 0.1 wt% of that ^{99}Tc which originally occurred in the spent fuel [6, 7, 11]. Because of restrictions on impurities of recycled uranium, it is required that the

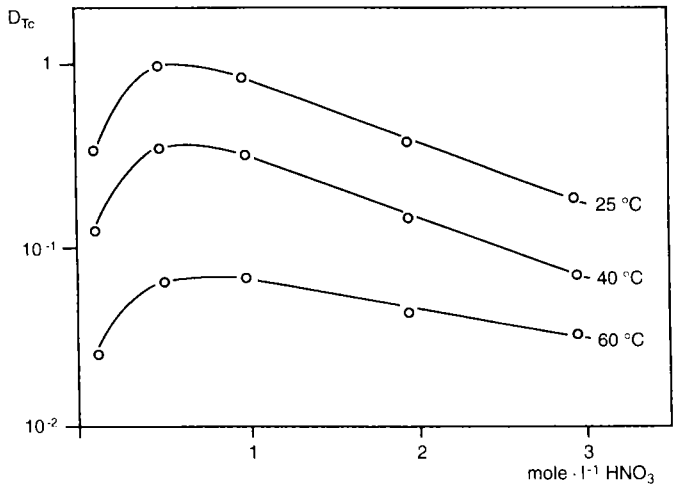

Fig. 4.1.A D_{Tc} as a function of HNO_3 concentration and temperature at a TBP concentration of 30 vol% in *n*-dodecane [7].

concentration of ^{99}Tc in uranium is only about 4 ppm. The assumption of 4 ppm ^{99}Tc in uranium implies that in 35 t of recovered uranium 0.14 kg of ^{99}Tc returns to the fuel for any year, while around 30 kg of ^{99}Tc enters the high level waste [6].

The release of ^{99}Tc from the reprocessing plant to the atmosphere may be assessed by using a so-called confinement factor. If technetium is released during the dissolution of spent fuel elements in 7.5 M HNO_3, volatile compounds formed would predominantly be Tc_2O_7 and $HTcO_4$. However, these and other volatile products would be almost quantitatively stripped by gas scrubbers containing oxidizing agents dissolved in alkaline water and would form non-volatile pertechnetate. It can be expected that the ^{99}Tc cycled through the uranium reprocessing plant remains almost completely in the process streams and does not escape. A confinement factor of 10^8 was selected due to resemblances in the chemical properties and volatility of technetium and ruthenium compounds [6]. Applying this factor to the total amount of ^{99}Tc of almost 30 kg, formed per year in the model reactor, yields a source term for reprocessing of only 0.3 mg of ^{99}Tc released to the atmosphere.

For operation of the model reactor, the input of uranium to the model plant converting UO_2 to UF_6 is assumed to be 182 t of natural uranium which is processed to about 270 t of UF_6. 13.2 wt% of 270 t of UF_6 is from uranium recycled back to the system. As mentioned above, 0.14 kg of ^{99}Tc per reactor year is returned with uranium to the fuel cycle, where it reacts with fluorine to give TcF_6. An estimate of the source term for ^{99}Tc released to the atmosphere and to water can be formed by assuming that TcF_6 is released to each pathway in the same fraction of fluoride appearing in the effluent to the total fluoride used in the process [6]. The total amount of fluoride used in the model plant for fluorination is at least 270 t of UF_6 minus 182 t of uranium, i. e. 88 t. Releases of fluoride to water account for 0.22 t and to the atmosphere for 0.11 t per model reactor year. Consequently, it may be assumed that the fraction 0.22/88 of

0.14 kg ^{99}Tc, i. e. 0.35 g is released to water and 0.11/88 of 0.14 kg ^{99}Tc, i. e. 0.175 g, to the atmosphere [6].

Significant amounts of ^{99}Tc are known to accumulate in the cascades of the gaseous diffusion enrichment plants as TcF_6. Emission of ^{99}Tc to the atmosphere result from its presence in the effluent of the cascades, but the major source are liquids used for equipment decontaminations. The relatively light TcF_6 moves toward the product end of the diffusion cascade rather than to the tails end. It can be separated from the UF_6 stream by using more or less efficient magnesium fluoride traps. ^{99}Tc may be removed from aqueous decontamination solutions by precipitation or ion exchange techniques [6]. Quantitative data are not available from which a confinement factor for ^{99}Tc can be calculated, therefore several assumptions are made. 50 wt% of the ^{99}Tc entering the model enrichment plant may follow the ^{235}U enriched UF_6, that is 70 g, while 40 wt% are assumed to remain with tails. 10 wt% of ^{99}Tc (14 g) may escape to the environment. According to some data concerning release of ^{99}Tc to water and air during gaseous diffusion enrichment of uranium in the United States [6], the mean source term ratio of water/air is around 40. Thus, per year, about 97.5 wt% of 14 g ^{99}Tc, i. e. 13.65 g, may enter the water pathway and 2.5 wt%, i. e. 0.35 g enter the atmosphere in the model enrichment plant.

The UF_6 enriched to 3.2 wt% ^{235}U constitutes the feed material to the model fuel fabrication plant. UF_6 still contains around 70 g of ^{99}Tc. 52 t UF_6 per model reactor year are converted to 40 t of UO_2 by hydrolysis of UF_6, precipitation of $(NH_4)_2U_2O_7$, calcination to UO_3, and hydrogen reduction to UO_2. During these chemical processes TcF_6 may be partially converted to Tc_2O_7 and vaporized at elevated temperature. To calculate an upper limit for ^{99}Tc release, it may be assumed that 50 wt%, i. e. 35 g of ^{99}Tc, is carried through the process and remains with the UO_2 probably in the form of TcO_2. An estimate of source terms for the environment can be made by assuming that TcF_6 is released to water and to the atmosphere in the same fraction as UF_6 [6]. Thus, per year, 99.9 % of the remaining 50 wt% of ^{99}Tc, i. e. 34.96 g, may enter the liquid waste stream and only 0.1 wt%, i. e. 35 mg, the atmosphere in the model fuel fabrication plant.

Fission products including ^{99}Tc are separated from uranium during reprocessing and retained in liquid tanks for solidification by calcination or glassification [12]. We will consider the glassification process as a model [6]. It is assumed that the model reactor creates 2 m^3 of solidified high-level waste per year, and that there are no liquid wastes associated with the solidification process. As mentioned above around 30 kg per year of ^{99}Tc is expected in the high-level radioactive waste residue which may release about 0.3 mg of ^{99}Tc to the atmosphere by solidification, assuming again a confinement factor of 10^8 as for reprocessing [6]. The solidified high-level waste containing ^{99}Tc will be transferred to a geologic repository. If it is assumed that no breach of the containment occurs, the amount of ^{99}Tc released to the atmosphere per year during the waste storage appears to be negligible.

Significant source terms assessed for ^{99}Tc releases to the environment during the different processes of the nuclear fuel cycle are summarized in Table 4.1.A [6]. The amounts expected to be released per year were calculated on the basis of the model reactor defined at the beginning of Section 4.1. The total release via effluent water

appears to be two orders of magnitude higher than the release to the atmosphere. Among the processes releasing ^{99}Tc to water, fuel fabrication and enrichment are by far the most important sources. In order to reduce the concentration of ^{99}Tc in aqueous discharges, a strong-base ion-exchange resin was suggested to bind TcO_4^- [13].

Table 4.1.A Assessment of annual ^{99}Tc releases to the environment during nuclear fuel cycle processes. The assessment is based on the model reactor defined in the text [6].

Process	Release of ^{99}Tc [g/a(MBq/a)]	
	Atmosphere	Water
Reprocessing	$3 \cdot 10^{-4}$(0.189)	0
Production of UF_6	$1.75 \cdot 10^{-1}$(110)	$3.5 \cdot 10^{-1}$(220)
Enrichment	$3.5 \cdot 10^{-1}$(220)	13.65(8586)
Fuel fabrication	$3.5 \cdot 10^{-2}$(22)	34.96(21990)
High-level waste solidification	$3 \cdot 10^{-4}$(0.189)	0
Total	$5.6 \cdot 10^{-1}$(352)	48.96(30796)

After glassification of the high-level radioactive waste, technetium appears to occur mainly in the chemical form of TcO_2 [7]. In a dry repository no chemical changes of the solidified waste are expected for a long time. However, any contact with aqueous solutions may alter the situation drastically by initiation of chemical reactions (Fig. 4.2.A) depending on the composition of the solution, the pH, redox potential and temperature [14]. The containment is assumed to resist corrosion by aqueous solutions no longer than about one hundred years [7]. Thereafter the radioactive waste is subject to water leaching, and silicates formed by glassification will be exposed to hydrolysis. In the presence of oxygen and water, TcO_2 will be oxidized to easily soluble TcO_4^-. This oxidation is expected to be enhanced radiolytically, particularly in salines [15, 16].

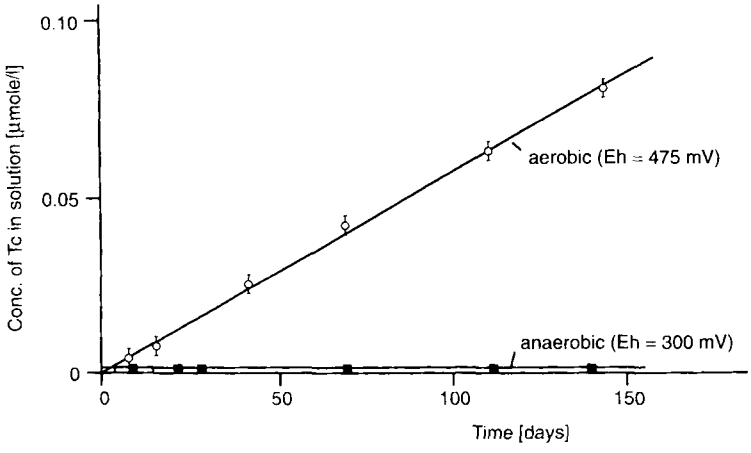

Fig. 4.2.A Dissolution of TcO_2 under anaerobic and aerobic conditions (3 mg TcO_2, 100 ml 0.1 M $NaNO_3$, 20 °C, pH 5.7 [14].

4.2 Technetium in the environment

We discussed the sources of artificial occurrence of ^{99}Tc at the beginning of this chapter and demonstrated that the nuclear fuel cycle is the predominant source of ^{99}Tc in the environment. Other, much less important, sources are the fallout from nuclear weapons testing, the Chernobyl accident, nuclear power production and the radiopharmaceutical use of the metastable ^{99m}Tc decaying to ground state ^{99}Tc. The natural occurrence of ^{99}Tc formed in the earth's crust by spontaneous fission of ^{238}U and neutron-induced fission of ^{235}U in uranium ores are negligible.

Taking into account the kind of sources and the chemistry of technetium, ^{99}Tc will be released to the environment as pertechnetate. Its behavior in the environment attracted much attention during the last two decades due to the long physical half-life of ^{99}Tc and the solubility and mobility of TcO_4^- in aquatic systems. Considerable effort has been made to understand the long-term biogeochemical behavior of ^{99}Tc, its transfer in food chains and the mechanisms controlling its mobility in diverse environments [17].

4.2.1 Retention in soils, sediments, and rocks

The pertechnetate ion will not likely be sorbed in significant amounts by soils and suspended bottom sediments of predominantly negative charge, but will be highly mobile in soils and waters and thus available for uptake in biota. The ^{99}Tc level in soil down to a depth of 25 cm was estimated in 1979 to be 10^{-14} g/g of soil [18]. This concentration was calculated from the known relative fission yield and the measured levels of ^{90}Sr and ^{137}Cs in soil, assuming that these fission products from nuclear bomb tests have nearly the same retention rates in soil.

Early sorption studies encompassed 22 soil types collected in Oregon, Washington, and Minnesota and used a batch equilibration technique. Distribution coefficients K_d for $^{95m}TcO_4^-$ were determined; this is defined as the ratio at equilibrium of the quantity of pertechnetate sorbed per gram of soil to solute per ml of solution. The K_d values for $^{95m}TcO_4^-$ ranged from 0.007 to 2.8, demonstrating the potential for accumulation in certain soils [19]. The sorption was directly correlated with increased organic carbon content and inversely correlated with increased pH. It appears that the positive charge on soil organic colloids is an important factor governing technetium retention. As pH decreases, positive charge may be expected to increase with decreased ionization of acidic groups and increased protonation of basic groups. In addition, K_d values were correlated with cation exchange capacity [19].

Recently, distribution coefficients K_d for ^{95m}Tc in Canadian Shield lake sediments were determined under oxic and anoxic conditions in a laboratory study. Untreated Winnipeg River water was used. For the oxic treatment, sediment and water were shaken for 24 h, spiked with 932 Bq of ^{95m}Tc and then shaken for another 48 h. The anoxic treatment involved purging with N_2 gas. The pH of the solution under oxic conditions was 6.7, under anoxic conditions 5.8. Under oxic conditions and the presence of 1, 10 or 50 wt% organic sediment, a mean of 98.5, 89.7 and 48.1 %, respectively, of ^{95m}Tc remained in solution, corresponding to distribution coefficients of 4.3, 6.9, and

13.0 $l \cdot kg^{-1}$ for the organic sediment. Under anoxic conditions the mean values were 96.7, 0.8, and 6.2 % of ^{95m}Tc in solutions, corresponding to K_d values of 14, 9200, and 210 $l \cdot kg^{-1}$, respectively. Consequently, considerable quantities of technetium may be sorbed to the sediment under the anoxic conditions expected for Canadian Shield lake sediments [20].

Investigations on the sorption of $^{99}TcO_4^-$ by soils revealed that about 98 % of the added pertechnetate was sorbed within a period of 2 to 5 weeks at 25 °C by 8 of 11 soils with a wide range of physical and chemical properties such as texture, pH, organic matter, free iron oxide content and cation exchange capacity. The slow kinetics observed and the insignificant reduction of ^{99}Tc sorption by addition of excess of Cl^- or $H_2PO_4^-$ tend to rule out anion exchange as the sorption mechanism. The lack of sorption exhibited by the low organic matter soils and the reduction in sorption following H_2O_2 digestion of the soils suggested a role for the living and/or non-living organic fraction of the soil. Sterilization of the previously sorbing soils by steam eliminated the sorption ability, indicating a microbial role in the sorption process [21].

Concentrations of ^{99}Tc caused by global fallout in the surface layer (< 20 cm) of paddy field soil samples in Japan collected in 1991 and 1992 near Ogata, Omagari, Morioka, Imari, and Kawazoe were measured by inductively coupled plasma mass spectrometry (ICP-MS). On a dry weight basis the ^{99}Tc concentrations ranged from 0.02–0.11 Bq per kg soil. The activity ratios of $^{99}Tc/^{137}Cs$ varied from $2.0 \cdot 10^{-3}$ to $5.2 \cdot 10^{-3}$. The theoretical activity ratio is about $3.0 \cdot 10^{-4}$. The mechanism of ^{99}Tc accumulation in paddy fields may be explained by the reduction of TcO_4^- under the reducing conditions of paddy field soil [22].

The soil chromatographic movement of ^{99}Tc through 41 selected Minnesota soils was studied to determine the short-term dynamic behavior of technetium under aerobic conditions over a wide range of physical and chemical soil properties. Under aerobic conditions ^{99}Tc occurs as TcO_4^-. Its movement was characterized by the chromatographic parameter R_f. Reduced R_f values were statistically related to elevated levels of soil organic matter. Complexation of ^{99}Tc by organic matter appeared to be weak. Pertechnetate exhibited greater retention than $^{36}Cl^-$ which may be attributed to a weak binding of TcO_4^- by organic matter [23].

The sorption of $^{95m}TcO_4^-$ on diverse soils under strictly aerobic conditions was extended to samples collected throughout the United States at locations in the states of Washington, Oregon, Colorado, Illinois, and Minnesota under arid, semi-arid and humid climates and under sagebrush, grassland, pasture land, agricultural and forest vegetation. Soils developed primarily under grassland-shrub vegetation and arid to semi-arid conditions sorbed less than 5.7 % ^{95m}Tc from solutions after 48 h equilibration. In contrast, soils developed in forests and marshlands under humid and subhumid conditions exhibited up to 31 % sorption of ^{95m}Tc over the same period. The forest-marshland soils were characterized by higher organic carbon content and contents of amorphous iron and aluminum compounds as well as lower pH values than the grassland-shrub soils. In all soils at the 48 h equilibration time, sorption was strongly correlated to organic carbon, total nitrogen, extractable iron and aluminum, several clay and silt fractions and low pH. After 1050 h of equilibration the carbon and nitrogen components significantly increased the technetium sorption [24].

The sorption of ^{99}Tc under aerobic and anaerobic conditions was determined for 34 soils that were selected from across central Canada to represent a broad range of chemical and textural characteristics. The aerobic K_d values were 0.0 and 0.5 l/kg for mineral and organic soils, respectively, the anaerobic K_d values were 18 and 68 l/kg, respectively. The K_d values are given by

$$K_d = \frac{\textit{Concentration of Tc sorbed onto soil solids (Bq·kg}^{-1}\textit{ dry soil)}}{\textit{Concentration of Tc in soil solution (Bq·l}^{-1})}$$

The anaerobic K_d values tended to increase with clay content and pH and appeared to be higher for the more humified organic soils [25].

Organic matter is obviously a geochemical sink for technetium in soils and sediments. Complexes of technetium with humic acids were shown to be quite stable and characterized by rather slow ligand exchange rates [26]. Soil organic matter will stabilize reduced pertechnetate in chelating complexes, possibly in a variety of combinations of coordinating functional groups such as amine, carboxyl, carbonyl, mercapto and hydroxyl. Local reducing conditions in soils can be generated by microbial growth. Reoxidation of humic acid technetium complexes by air may proceed in half-life values in the range of 10 to 100 days [27].

A study of the complexation of technetium with well characterized humic acid indicated the formation of technetium humate as a brownish-black precipitate after addition of Sn(II) as a reductant to a solution of pertechnetate and humic acid at pH 4 in 0.1 M $NaClO_4$. A +3 valence state of technetium in the technetium humate complex was derived from the reduction process [28].

The distribution coefficients K_d [cm^3/g] for the sorption of ^{95m}Tc by peat and the rates of sorption and desorption were determined as a function of the concentration of $CaCl_2$ as a supporting electrolyte, the concentration of dissolved oxygen, and the pH of the solution. The K_d values of Tc, added as $^{95m}TcO_4^-$, increased if the concentration of dissolved oxygen or that of $CaCl_2$ decreased. The influence of pH was negligible. The half-times for the rates of sorption and desorption were in the range of 20–60 min and 500–900 min, respectively [29].

Diffusion of ^{99}Tc and other fission products such as ^{134}Cs and ^{152}Eu as well as the actinides ^{237}Np, ^{241}Am and natural uranium was studied in a sample of a sediment from an enclosed brackish water bay of the Baltic Sea. Under oxidizing conditions TcO_4^- did not interact with the sediment to any large degree. Deeper laying sediments were depleted of oxygen and showed negative redox potentials. In this case the apparent diffusivity of ^{99}Tc $D_a = 5 \cdot 10^{-13}$ $m^2 \cdot s^{-1}$ was low compared to compacted clay with $D_a = 8 \cdot 10^{-11}$ $m^2 \cdot s^{-1}$, indicating a reduction of TcO_4^- [30].

The biosorption of ^{99}Tc by natural bottom sediments of the eutrophic Lake Beloye, one of the Kosino Lakes near Moscow, was also studied. The initial concentration of ^{99}Tc in samples of the lake water was 25 mg/l. The bottom sediments sorbed 98 % of ^{99}Tc within 4.5 months at room temperature. The samples of the sediments and the benthonic water were withdrawn at a depth of 9 m. The ratio between the volumes of suspended particles of the sediment and water was 1:3. The pH 7 of the lake water was practically unchanged by addition of ^{99}Tc as $NaTcO_4$. The sorption of ^{99}Tc is explained by sulfate reducing bacteria generating H_2S, which reduces TcO_4 [31].

Investigations on the transfer of $^{99}TcO_4^-$ from surface water to organic-rich bottom sediments in the freshwater Perch Lake, located on the Canadian Shield, revealed very low transfer rates of only 1.4 to 3.3 % of radioactivity per day. The same range of transfer rates was found for $^{125}I^-$ and $^{131}I^-$ [32].

The retention and migration of ^{99}Tc in sediments and rocks deserves much attention when considering the problem of separating long-lived radionuclides in high-level radioactive waste repositories from the biosphere. ^{99}Tc was considered to be almost not sorbed by deep geologic media, apparently on the basis of experimental data obtained with TcO_4^- under oxidizing conditions. However, mobile TcO_4^- can be reduced to less soluble compounds in the presence of igneous rocks like basalt or granite [33]. Already under the reduction potential expected for groundwater not in contact with the atmosphere, TcO_4^- is no longer a stable species. Rather, insoluble hydrated forms of TcO_2 [34] will occur. Iron(II)-containing minerals, e. g. magnetite, seem to have a reducing effect after a contact time of 24 h [35]. The degree to which geological media will influence the chemical state of ^{99}Tc was determined by the reactivity of the rocks, the contact time and the degree of weathering and oxidation of the fracture surfaces through which migration occurs [33].

TcO_4^- shows only minor interaction with inorganic solids. In aerated aqueous solutions the sorption behavior of TcO_4^- resembles that of ClO_4^-. Sorption ratios $R_s = \frac{I_0 - I_L}{I_L} \frac{V}{m}$ with the initial counting rate of the spiked groundwater I_0, the counting rate at the end of the experiment I_L, the volume of the solution V, and the mass of the sediment m, found with natural sediments from Gorleben, Germany, consisting mainly of quartz and silicates, are of the order of 0.1 ml/g. The sorption of TcO_4^- was found to be reversible and is explained by physical adsorption at the surface of the grains of the sediments. At low redox potentials (Eh), i. e. strongly anaerobic conditions, where hydrated TcO_2 is the stable species, high sorption ratios of the order of 10^3 ml/g were measured that did not depend significantly on salinity. The sorption was not reversible. When Eh is increased, the sorption ratios decreased rather sharply at about 170 mV. The difference between the sorption ratios under reducing and under oxidizing conditions was about 4 orders of magnitude [36].

4.2.2 Occurrence in rainwater, freshwater, and the atmosphere

^{99}Tc was detected early in surface waters and rain samples. In surface water samples at Argonne, Wisconsin, radiochemical determination since 1965 yielded values ranging from 0.018–1.82 Bq/l [37] which are by some orders of magnitude higher than those found in rain samples collected in 1967 at Commerce, Texas varying from $0.52 \cdot 10^{-4}$ to $6.3 \cdot 10^{-4}$ Bq/l [38]. The activities of ^{99}Tc determined in these studies are low and appear negligible, because they do not represent major environmental contamination. To measure ^{99}Tc in fallout, a neutron activation analysis procedure using the reaction $^{99}Tc(n,\gamma)^{100}Tc$ was developed [39]. The estimated detection limits with sample irradiations at a thermal neutron flux of about $5 \cdot 10^{13}$ n $\cdot$ cm$^{-2} \cdot$ s^{-1} were $5 \cdot 10^{-12}$ g ^{99}Tc ($3.1 \cdot 10^{-3}$ Bq) in filter paper samples [40].

^{99}Tc and ^{90}Sr concentrations were determined from a composite rain sample collected in 1975 in Commerce, Texas. The concentrations were $0.75 \cdot 10^{-4}$ and $1.83 \cdot 10^{-3}$ Bq/l, respectively, indicating that the ^{99}Tc/^{90}Sr activity ratio of $4 \cdot 10^{-2}$ increased since 1961, when the ratio was $1.8 \cdot 10^{-3}$. All observed ^{99}Tc/^{90}Sr values were larger than the anticipated values from the neutron-induced fission of ^{235}U or ^{239}Pu, which points to sources of ^{99}Tc other than fallout, e. g. release of ^{99}Tc to the environment by nuclear fuel reprocessing [41].

Water samples taken during 1985 and 1986 from the Rhone river exhibited ^{99}Tc radioactivities ranging from 0.1–2.1 mBq/l [42]. ^{99}Tc in rain and dry fallout were collected monthly in the summer of 1993 at Nakaminato, Japan in containers of distilled water with a collection area of 0.21 m^2. After concentration ^{99}Tc was measured by ICP-MS. Values of 0.23 and 0.36 $mBq \cdot m^{-2}$ of ^{99}Tc were observed [43].

There are only a few reports concerning ^{99}Tc concentrations in the atmosphere. Early measurements of ^{99}Tc in the surface air of Seville, Spain, where no nuclear installations existed, were done. Filter samples taken from 1965 to 1967 were analyzed. The average radioactivity of ^{99}Tc per 1000 m^3 of air yielded 1.23 mBq in 1965, 0.71 mBq in 1966 and 0.78 mBq in 1967 [44]. In 1988 a compilation of ^{99}Tc radioactivity data and ^{99}Tc/^{137}Cs activity ratios determined in rainwater and air was reported (Table 4.2.A).

Table 4.2.A ^{99}Tc activity concentrations and ^{99}Tc/^{137}Cs activity ratios determined for rainwater and air samples, (n) = number of samples [45].

Year of collection	Country	^{99}Tc		^{99}Tc/^{137}Cs Activity ratio · 10^3	
		[mBq l^{-1} (n)] Rainwater	[μBq m^{-3} (n)] Air	Rainwater	Air
1961	Arkansas, USA	66 ± 33(1)	–	1.1 ± 0.5	
1962	Arkansas, USA	1330 ± 180(1)	–	1.5 ± 0.2	–
1965	Spain	–	1.3 ± 0.5(4)	–	4
1966	Spain	–	0.7 ± 0.2(6)	–	5
1967	Texas USA, Spain	230 ± 50(13)	0.7 ± 0.6(5)	3.8 ± 1.3	10
1974	Texas USA	75 ± 25	–	25 ± 9	–
1981	Sweden	–	0.48 ± 0.07(8)	–	12.5 ± 5.0
1985 (Nov)	Monaco	20 + 5(1)	< 0.2	19 ± 5	–
1986 (Jan)	Monaco	20 ± 10(1)	–	15 ± 8	–
1986 (Mar)	Monaco	90 ± 5(1)	–	2.3 ± 0.2	–
1986 (May)	Monaco	20000 ± 2500(1)	–	0.23 ± 0.06	–
1986 (Jun)	Monaco	–	3.6 ± 0.8(1)	–	20 ± 6

4.2.3 Accumulation in plants, microorganisms, and animals

Readily soluble pertechnetate ions in soil may compete with nutrient ions for uptake by plant roots possibly leading to accumulation in foodstuffs.

Soybean (*Glycine max.*) and wheat (*Tricicum aestivum*) plants were grown in silt loam amended with $^{99}TcO_4^-$ ranging from 0.001–5 μg (0.63–3145 Bq) ^{99}Tc per gram of soil. At the 0.001 and 0.01 μg/g levels soybean plants were similar in appearance to the controls. However, at the 0.1 μg/g level, growth did not occur beyond cotyledon expansion. At the 5 μg/g level growth ceased 3 days after emergence. ^{99}Tc was mobile in the soybean plant with the highest concentrations in the cotyledon, followed by the leaves, stem, and bud. Marked enrichment in ^{99}Tc concentration up to 380 μg/g in the aerial portion of the plant occurred with increased soil concentration up to 5 μg/g [46]. Observation of mitotic figures did not reveal any chromosome aberrations, micronuclei or chromosome bridges. It is quite probable that the growth effects are due to chemical toxicity, possibly due to nutrient competition and/or substitution in uptake or metabolism. However, a radiation effect cannot completely be excluded [47].

Toxicity symptoms in wheat were also observed at the 0.1 μg/g level. The plants were stunted and there was a necrosis of the blade tips and margins. Growth did not occur at the 1.0 μg/g level. Wheat exhibited the highest ^{99}Tc concentrations in the blade [46]. The plant affinity for TcO_4^- applied to soil is high and generally exceeds that reported for other non-nutrient nuclides arising from the nuclear fuel cycle [48].

The accumulation of ^{99}Tc by tumbleweed and cheatgrass on arid soils was measured. The initial soil concentration of 10^{-12} g ^{99}Tc/g added to the soil as pertechnetate was traced by ^{95m}Tc. At the three month harvest time the uptake of the added Tc ranged from 23 to 82 % for tumbleweed and 10 to 69 % for cheatgrass [49].

Pea plants (*Pisum sativum*) were grown in diluted Hoagland nutrient solutions at pH 5.5 contaminated with different levels of $^{99}TcO_4^-$. No symptoms of toxicity were observed in the radioactivity range $63–63 \cdot 10^4$ Bq/l, only some delay in the maturation of fruits with increasing concentration of ^{99}Tc was established. The observation confirms the higher resistance of *Pisum sativum* to ^{99}Tc in comparison to other species like soybean [46]. ^{99}Tc is translocated to aerial parts. Leaves constitute the predominant repository of ^{99}Tc in the pea plant. Concentration factors (radioactivity per g fresh weight/radioactivity per ml of the nutrient solution) reached values of 10^2 for leaves [50]. The translocation of ^{99}Tc from soil to leaves of *Pisum sativum* is reduced in soils rich in organic matter, indicating some TcO_4^- modification in soils with time [51].

In order to quantify the interception and retention of Tc by herbaceous vegetation as a consequence of direct deposition and uptake from soil, field experiments were performed. A simulated rain containing a solution of $^{95m}TcO_4^-$ was applied to plots of bare soil and plots with standing vegetation. Vegetation standing during application obtained ^{95m}Tc from both direct foliar interception and root uptake. The concentrations of ^{95m}Tc in emerging vegetation decreased with time by an effective first-order rate constant of 0.016 days,$^{-1}$ equivalent to an environmental half-life of 43 days. The retention of ^{95m}Tc by vegetation receiving direct contamination varied with half-lives ranging from 15.9 to 18.7 days. The results indicate that ^{95m}Tc is removed from vegetation, regardless of whether the Tc content in vegetation is from direct deposition onto plant surfaces or root uptake from soil [52].

The uptake of $^{99}TcO_4$ by mature Swiss chard plants from sandy and peaty soils revealed that ^{99}Tc is predominantly translocated to the shoots. In sand, where the sorption capacity of the soil is negligible, ^{99}Tc uptake was four orders of magnitude higher than from peat [53].

The sorption of $^{99}TcO_4^-$ by roots of hydroponically grown soybean seedlings (*Glycine max.*) was shown to be linear from 10^{-5} M pertechnetate solutions for at least 6 h and to exhibit characteristics of carrier-mediated transport commonly associated with the sorption of nutrient ions in higher plants. Analyses of $^{99}TcO_4^-$ uptake in the presence of individual nutrient anions revealed the sorption to be competitively inhibited by sulphate, phosphate, selenate, and molybdate indicating the use of common transport mechanisms [54].

To assess the relative extent of ^{99}Tc sorption and its mobility, plants were grown for 40 days in hydroponics amended with 10^{-4} M $^{99}TcO_4$. Uptake rates in roots and leaf concentrations after 48 h were determined (Table 4.3.A).

Table 4.3.A Comparison of ^{99}Tc uptake rates and leaf concentrations in different plant species [55].

Plant	Plant uptake rate [$\mu g \cdot h^{-1} g^{-1}$ dry wt root]	Plant leaf (48 h) concentration [$\mu g \cdot g^{-1}$ dry wt]
Spanish bunch onion (*Allium cepa*)	0.57	7.7
Garden bunch onion (*Allium cepa*)	0.80	4.1
Yellow bulb onion (*Allium flavum*)	1.1	13
Garlic (*Allium sativum*)	0.16	4.6
Leek (*Allium porrum*)	0.40	5.9
Radish (*Raphanus sativus*)	4.4	62
Mustard (*Brassica juncea*)	3.7	79
Soybean (*Glycine max.*)	2.1	130
Alfalfa (*Medicago sativa*)	2.9	94
Pea (*Pisum sativum*)	0.98	46
Lettuce (*Lactuca sativa*)	1.4	12
Cabbage (*Brassica oleracea*)	2.3	28
Carrot (*Daucus sativa*)	0.87	23

Sorption rates for the 13 plants studied ranged from 0.16 to 4.4 μg ^{99}Tc h $^{1}g^{-1}$ dry wt root. Leaf concentrations ranged from 4.1 to 130 μg $^{99}Tc \cdot g^{-1}$ dry weight after 48 h. The five *Allium* species exhibited both the lowest sorption rates and the lowest leaf concentrations. Obviously, there are substantial differences in sorption rates and leaf concentrations among plant species. Frequently, greater than 90 % of the ^{99}Tc contained in the tissue is soluble in water. If the soluble fractions are further fractionated by ultrafiltration, it appears that the majority of ^{99}Tc accumulated in tissues is in a form other than TcO_4^-. The data suggest that ^{99}Tc accumulated by plants is predominantly incorporated into soluble plant macromolecules or complexed by plant metabolites [55].

When $NH_4^{99}TcO_4$ was administered in subtoxic levels to spinach plants (*Spinacea oleraces*) growing in nutrient solutions, it was shown that ^{99}Tc is transported in the plants as $^{99}TcO_4^-$, that free $^{99}TcO_4^-$ is present in growing leaves, that uptake and incorporation are directly proportional to the pertechnetate concentration of 10^{-6}–10^{-8} M in the nutrient solution and that rates of uptake and metabolization decrease with increasing age of the leaves. In the roots and petioles of spinach plants of four weeks of age about 60 % of all ^{99}Tc is present as TcO_4^-. Accumulated TcO_4^- is continuously metabolized as shown by a decrease of the TcO_4^- fraction as a function of time [56].

In the leaves ^{99}Tc is almost exclusively concentrated in the chlorophyll containing cells. In addition, fixation occurs in those cells and organs of nitrogen reducing organisms containing nitrogenase. Such observations support the idea of reduction of TcO_4^- in cell compartments which generate high reducing power. Illuminated samples of broken chloroplasts isolated from spinach plants indicate that TcO_4^- might be reduced in reactions linked to the photochemical events [57].

Isolated spinach chloroplasts, thylakoids, and purified compounds of the photosynthetic electron transport chain were incubated with $^{99}TcO_4^-$. After illumination, the quantity of reduced $^{99}TcO_4^-$ was measured with gel filtration chromatography. Isolated thylakoids showed reduction of $^{99}TcO_4^-$ in the light, suggesting direct interference of $^{99}TcO_4^-$ with the electron transport chain. $^{99}TcO_4^-$ is reported to be mainly reduced to an extractable Tc(V) compound. The stable complexes *in vivo* are supposed to originate through ligand exchange with strong complexing agents such as thiol compounds. The normal electron acceptors O_2 and $NADP^+$ (nicotinamide-adenine dinucleotide phosphate) inhibit reduction of $^{99}TcO_4^-$ [58].

Corn plants (*Zea mays*) were grown under greenhouse conditions in a nutrient solution containing 2.2–2.3 MBq $^{95m}TcO_4^-$/l. After six weeks almost 40 % of the ^{95m}Tc, biologically incorporated into corn leaves via root uptake, was present in plant tissue in forms that are not readily extractable. The bound forms of technetium in the leaves appear to be mostly complexes with proteins and polysaccharides of the plant cell walls [59].

The uptake of ^{99}Tc by trees such as red maple (*Acer rubrum*), yellow poplar (*Liriodendron tulipifera*) and elm (*Ulmus spp.*), intercepting contaminated groundwater from a radioactive waste storage site, was studied in a forest ecosystem. Although technetium was accumulated progessively over the growing season in leaves, average concentrations in wood and twigs were equal to or greater than concentrations in leaves. Tree wood was the major above-ground pool. The most important return pathway for ^{99}Tc to the forest floor was leaf fall [60]. Chromatography of the ethanol-water extract from the wood of maple tree (*Acer sp.*) and the alkaline extract from leaves demonstrated ^{99}Tc to be complexed in molecules of a molecular weight > 1000. In the leaf $^{99}TcO_4^-$ is converted to less soluble forms apparently associated with structural components of leaf cell walls [61].

Gross subcellular distributions of $^{99}TcO_4^-$ and $^{35}SO_4^{2-}$ were shown to be similar in soybean seedlings. *In vitro* assay of chloroplast-based $^{35}SO_4^{2-}$ reduction and incorporation systems showed $^{99}TcO_4^-$ to be reduced and incorporated into amino-nitrogen containing products [62].

To investigate cytological effects of ^{99}Tc, soybean seedlings were exposed to $^{99}TcO_4^-$ at various concentrations in dilute culture solutions. Reduced primary leaf midrib length was observed with 67 h exposures to $\geq$6 μM ^{99}Tc. After 43 h or longer exposure, cellular effects were observed consistently by a light microscope. Already at lower ^{99}Tc levels, abnormal cells were interspersed among cells of normal appearance. Abnormal cells displayed blockshaped nuclei that frequently demonstrated incipient plasmolysis. At levels of $\geq$13.2 μM $^{99}TcO_4^-$, cellular damage was extensive. Cells were reduced in size and were highly plasmolyzed, cell walls were distorted and intercellular spaces were reduced or became non-existent. Mitotic activity was observed at TcO_4^- concentrations $<$ 9.9 μM. The cellular effects are attributed to the alteration of membrane permeability characteristics [63].

Experiments on the transfer of $^{95m}TcO_4^-$ from soil to rice and wheat plants were carried out. The soil/plant transfer factors of ^{95m}Tc for rice plants were $\leq$ 0.005 on dry weight basis for hulled grains and 1.1 for the lower leaf blade. In contrast, much higher transfer factors were found for wheat plants, i. e. 0.027 for the hulled grains and 230 for the lower leaf blade. The level of ^{95m}Tc in the soil solution collected from the flooded soil used for rice plants was found to decrease rapidly with time. For wheat plants grown in non-flooded soil, the decrease of the ^{95m}Tc level in the soil solution was rather slow. Obviously, $^{95m}TcO_4^-$ was readily transformed under the reducing conditions in the flooded soil to insoluble forms of ^{95m}Tc, which could explain the low transfer factor for rice plants [64].

Similar experiments for evaluating transfer factors of ^{95m}Tc from soil to vegetables resulted in the following average values based on Bq of dry weight of gram of soil and vegetable (Table 4.4.A).

Table 4.4.A Transfer factors of ^{95m}Tc from soil to edible parts of vegetables [65].

Cabbage (*Brassica oleracea*)	1.3 ± 1.6
Chinese cabbage (*Brassica campestris*)	0.8 ± 0.8
Spinach(*Spinacia oleracea*)	17 ± 8
Komatsuna (*Brassica rapa*)	11 ± 9.5
Carrot (*Daucus carota*)	1.9 ± 0.2
Onion (*Allium cepa*)	0.5 ± 0.4
Sweet potato (*Ipomaea batatas*)	0.08 ± 0.01
Tomato (*Lycopersicon esculentum*)	0.3 ± 0.1

Transfer factors for leaf vegetables such as spinach or komatsuna are considerably higher than those of edible parts of non-leaf vegetables. Technetium taken up through roots was not retained in roots, but transported into the leaves [65].

The deposition, migration, and annual variation of ^{99}Tc fallout in carpets of lichen collected during the period 1956–1981 in Finland, Sweden, Iceland, Norway, Spitsbergen, and Yugoslavia were investigated. ^{99}Tc showed a shorter mean residence time in the lichen carpet than ^{137}Cs. The maximum concentration of ^{99}Tc of ca 60 mBq per kg of dry weight lichen occurred in 1967 in Sweden at the sampling site in the Lake Rogen district [66].

The biochemical effects of $^{99}TcO_4^-$ were studied in microorganisms like non-sulphur purple bacteria, blue-green algae, protozoa, diatoms, heterotrophic bacteria, red algae and green algae. Sensitivity to pertechnetate, as measured by growth, ranged from marked inhibition at 1 µg ^{99}Tc/ml for the non-sulphur purple bacteria to no effect at 600 µg ^{99}Tc/ml for green algae. The blue-green alga (*Agmenellum quadruplicatum*) bound ^{99}Tc from the medium containing 1.5 mM $^{99}TcO_4^-$ to a level of 3 µg/mg dry weight cells in the light, but little or none in the dark. TcO_4^- in the medium caused a rapid but temporary increase in ATP levels of *Agmenellum quadruplicatum* and the protozoan *Tetrahymena pyriformis*. Respiration of *Tetrahymena pyriformis* and *Bacillus subtilis* and photosynthesis of *Agmenellum quadruplicatum* were immediately slowed by the uptake of $^{99}TcO_4^-$ [67].

Bioaccumulation and chemical modification of TcO_4^-, traced with $^{95m}TcO_4^-$, by aerobically and anaerobically grown soil bacteria and by pure cultures of sulphate-reducing bacteria (*Desulfovibrio sp.*) were investigated. Aerobically grown bacteria did not accumulate Tc nor modify its chemical form. Anaerobically grown bacteria exhibited high bioaccumulation and reduced TcO_4^-. The concentration ratio values observed over a 200 h period ranged from 50 to 600. The reduction of TcO_4^- was a metabolic process. Association of Tc with bacterial polysaccharides was found only in cultures of anaerobic bacteria. Sulphate-reducing bacteria efficiently removed Tc from solution and promoted its association with organics. Up to 70 % of the total Tc in the growth medium was bioaccumulated and/or precipitated [68].

For measuring the bioaccumulation of ^{95m}Tc in fishes and snails a small experimental freshwater pond was spiked with ^{95m}Tc. The concentration factors based on the calculated body burden (fresh wt) for carps (*Caprinus carpio*), mosquitofishes (*Gambusia affinis*), and snails (*Helisoma sp.*) were 11, 75, and 121, respectively. The effective biological half-lives were 2.5, 4.3 and 21.3 d, respectively [69].

For two freshwater species, the crayfish (*Pacifastacus leniusculus*) and the snail (*Juga silicula*) whole-body concentration ratios of 1.6 and 41, respectively, were obtained when $^{95m}TcO_4^-$ was used as a tracer. Tissue distribution data showed that 79–100 % of the crayfish body burden was in the exoskeleton and digestive gland, whereas the soft tissues of the snails contained 82–96 % of the whole-body activity [70].

$^{95m}TcO_4^-$ was accumulated rapidly from a freshwater pond by periphyton, zooplankton, and algae. Aquatic insects such as adult backswimmers (*Notonectidae*), dragonfly nymphs (*Libellulidae*) and others (*Coleoptera, Diptera, Hemiptera, Odonata, Trichoptera*) concentrated ^{95m}Tc by factors of 3–8, based on wet weight. Macrophytes, e. g. *Elodea canadensis*, very rapidly reached tissue concentrations of ^{95m}Tc equivalent to the water concentrations and continued to accumulate until the concentration factor was equal to the upper range of those reported for terrestrial plants. A comparison (Table 4.5.A) of concentration factors for freshwater and marine organisms shows that, with the exception of brown algae and lobsters, the bioaccumulation of technetium by similar organisms is in relatively good agreement despite marked differences in environmental and experimental conditions [71].

Experiments with goats showed that ^{95m}Tc given orally as pertechnetate is readily sorbed from the gastrointestinal tract. Within 1 h after administration the concentration was about 0.1 % of the administered activity (5 MBq) per liter of blood plasma.

Table 4.5.A Comparison of technetium concentration factors (CF) for freshwater and marine organisms [71]. See literature cited in [71]

Freshwater	CF	Marine	CF
Periphyton		Phytoplankton	
Slide samples	40	*Heterocapsa pygmaca*	17
		Mixed flagellates	1
		Phytoflagellates	1
Algae		Algae	
Green algae	1–10	Brown algae	250–2500
		Red and green algae	1–20
Macrophytes			
Elodea canadensis	61		
Zooplankton		Zooplankton	
Diaptomus reighardi	36	*Artemia salina*	3
Difflugia		Euphausiid	1
Ostracods			
Other crustaceans		Other crustaceans	
		Shrimp crab, isopod amphipods	2–12
Crayfish		Lobster	1000–1400
Pacifastacus leniusculus	1.6	*Hormarus gammarus*	
Cambarus	30		
Molluscs		Molluscs	
Margaritifera margaritifera	0.9	*Mytilus edulis*	2
Corbicula manilensis	1	*Mytilus galloprovinciallis*	
		Mytilus californianus	
		Crassostrea gigas	
Snails		Red abalone	
Helisoma sp.	121	*Haliotis rufescens*	100–200
Juga silicula	41		
		Gastropod	
		Aporrnais pespelicana	3
Aquatic insects	3–8	Fishes	
Notonectidae		*Pleuronectes platessa*	9
Belostomatidae		*Raja clavata*	8
Chironomidae		*Blennius pholis*	2
Dytisidae			
Tricoptera			
Odonata			
Amphibians			
Taricha granulosa	11		
Fishes			
Cyprinus carpio	11		
Gambusia affinis	75		

However, the concentration fell rapidly and after 24 h it was about 0.005 %/l, thereafter the decrease was slower and the concentration was still about 0.001 %/l eight days after administration. A similar pattern was seen in milk, where as much as 1.5 %/l was seen the first 5 h after administration. After 2–3 days the concentration in milk was 0.005–0.05 %/l. In muscular tissues the measured amounts of ^{95m}Tc were often

below the detection limit, which indicates that the transfer of TcO_4^- from grazing animals via meat to humans is of minor importance [72].

The transfer of $^{95m}TcO_4^-$ from pasture to milk of goats was much lower than that for ^{131}I under identical field conditions. The transfer of ^{131}I to goat's milk was about 5600 times more than that of ^{95m}Tc after 5 d of grazing contaminated pasture. It is apparent that the food chain behavior of ^{95m}Tc is very different from that of ^{131}I. The transfer of ^{95m}Tc from pasture to milk is affected not only by the reactions in the rumen, but also by reactions with pasture vegetation. The results of this study are most applicable when aerial deposition is the main source of technetium contamination [73].

The intestinal sorption of ^{95m}Tc given as $^{95m}TcO_4^-$ was studied in female goats and swine. Only 0.1 % of the dose administered orally was found in the milk of goats, 90 % was found in feces. Swine retained ^{95m}Tc in the thyroid gland with a biological half-life of 20 h. goats with 30 h. 200 h post-administration the liver in swine contained three times as much ^{95m}Tc as the thyroid or kidneys. The conclusion of these experiments would be that the concentration of ^{95m}Tc does not present a hazard to humans from consumption of milk or meat [74].

^{95m}Tc was administered as pertechnetate to sheep. Urinary excretion amounted to only 1 % of the dose. Most ^{99}Tc was excreted within 4 days by the feces. Highest specific activities were found in thyroid followed by liver and kidney. Considerable activities were also detected in skin and wool. Wool may constitute an easily accessible indicator to assess the extent of a ^{99}Tc contamination [75].

Japanese quail (*Coturnix japonica*) are often considered suitable substitutes for commercial laying hens, because of their lower feed consumption compared to domestic chickens. Concentration ratios and transfer coefficients for this species were determined using feed containing $0.74 \cdot 10^4$ Bq $^{95m}Tc/g$. The data showed that the ^{95m}Tc content in males and females differed principally because ^{95m}Tc was preferentially deposited in oocytes and albumin. The highest ^{95m}Tc concentrations in tissues of laying quail were in oocytes, followed by the fully formed unlaid egg. The corresponding concentration ratios ($Bq \cdot g^{-1}$ wet tissue/$Bq \cdot g^{-1}$ air dry food) were 0.01 and 0.003, respectively. The shelled egg contained five times the daily ingested dose found in muscle, liver, gizzard, and heart combined. Transfer coefficients for males indicated that gizzards contained about 53 % of the total amount of ^{95m}Tc in edible tissues, followed by muscle, liver, and heart. Both the concentration ratio and the weight-based transfer coefficient show that liver, and gizzard present a greater potential for transfer by ingestion than do muscle or heart [76].

4.2.4 Occurrence in the marine environment

Only a limited number of ^{99}Tc concentration data in surface seawater are available (Table 4.6.A)

^{99}Tc can reach the sea from both fallout from nuclear weapons testing and releases from the nuclear fuel cycle. The considerably high concentrations of ^{99}Tc of 4.5 and even 108 mBq/l in the Irish Sea may originate from the Sellafield nuclear fuel reprocessing plant at Seascale, UK, with perhaps a contribution from the Capenhurst

Table 4.6.A ^{99}Tc activity concentrations in surface waters from different areas [2].

Year of collection	Sample area	^{99}Tc [mBq/l] (average)
1969	Irish Sea	4.5
1972	Irish Sea	108
1980	North Sea	0.7
1981	North Sea	3.5
1985–86	Mediterranean	0.07
1986–87	Mediterranean	0.03
1983	Baltic Sea	0.07
1986	Baltic Sea	0.04
1980	Norwegian Sea	0.36
1980	Barents Sea	0.56
1984	Davis Strait	0.04
1988	Greenland Sea	0.08

enrichment plant via the Dee Estuary [77]. Most of the ^{99}Tc activity concentrations in Table 4.6.A range between 0.03 and 0.56 mBq/l. Around Japan values of 0.1 mBq/l were measured [78].

More recently, the concentration of ^{99}Tc in coastal seawater samples collected 1993 in Fukuoka (Kyushu) Japan was determined by ICP-MS. ^{99}Tc was enriched by coprecipitation on iron hydrated oxide and separated from impurities by solvent extraction and ion exchange techniques. The ^{99}Tc concentrations found were only 1–7 μBq/l. The activity ratio of ^{99}Tc/^{137}Cs was $2.7 \cdot 10^{-4}$, which is very close to the value expected for fallout from nuclear tests [79].

Several sea sediments were analyzed for ^{99}Tc (Table 4.7.A).

The sediments exposed to weapons testing or adjacent to nuclear facilities have accommodated significant amounts of ^{99}Tc. The Bravo Crater, Eniwetok, Marshall Islands, contains calcareous debris rather rich in ^{99}Tc. The IAEA sediments were collected near the reprocessing plant at Bombay, India. There was a measurable ^{99}Tc content in the coastal sediments collected off the coasts of Peru and Chile. This might be related to the mineral phosphorite. Samples of Whitehaven Harbour sediments were taken near the Sellafield, UK, reprocessing plant outfall. ^{99}Tc was also detected in sediments from the Clyde Estuary, UK, but with no evident differences from those taken from anoxic or from oxic areas [80].

In the marine environment, green, red, and brown algae as well as phanerogams are primary producers of organic matter. The green marine alga *Acetabularia acetabulum* showed concentration ratios for $^{95m}TcO_4^-$ of some hundred (activity incorporated g^{-1}/activity ml^{-1} seawater) while for the green alga *Ulva lactuca* a concentration ratio of 11 was found. The green alga *Boergesenia forbesii*, on the contrary, appeared to be incapable of accumulating ^{95m}Tc. All studied brown algae such as *Ascophyllum nodosum, Cystoseira compressa, Ectocarpus confervoides, Fucus serratus*, and *Fucus vesiculosus* concentrated ^{95m}Tc by ratios ranging from 6 to 85 [81].

Table 4.7.A ^{99}Tc in marine sediments [80].

Sample	^{99}Tc [Bq/kg]
Bravo Crater, Eniwetok Island Marshall Islands	187 ± 6
IAEA sediment (SD-B-1)	78 ± 5
Saanich Inlet, Washington USA 0–6 cm	not detected
Santa Barbara Basin, California, USA (1960–1962)	not detected
Peru	107 ± 10
Santa Monica Basin, California, USA	not detected
Chile	7.8 ± 0.4
Soledad Basin, Mexico	not detected
Mazatlan, Mexico	not detected
Sediment dredge, San Onofre California, USA	not detected
Whitehaven Harbour, UK Surface (silt)	7.7 – 0.4
Clyde, UK Anoxic	9.2 ± 0.8

Along the east coast of Sweden ^{99}Tc activity concentrations of 1.3 Bq per kg dry weight of the brown alga *Fucus vesiculosus* were found in 1982, whereas on the south coast higher values of 4.5 Bq/kg were observed. The west coast even showed values of around 80 Bq/kg. The reason appears to be an inflow from the North Sea. Surface water activities for ^{99}Tc of 68 mBq/m^3 in the Baltic Sea result in activity concentration ratios *Fucus*/seawater of about 40000 [82].

In batch experiments the macrophytic brown algae *Sargassum vulgare, Cystoseira complexa, Dictyopteris membranacea, Dictyota dichotoma implexa*, and the macrophytic green alga *Ulva rigida* were contacted for 72 h at 20 °C with Mediterranian seawater containing $18.5 \cdot 10^3$ Bq/l $^{95m}TcO_4^-$. Concentration factors between 7 (*Ulva rigida*) and 300 (*Sargassum vulgare*) were observed demonstrating the tendency of lower pertechnetate uptake of green algae compared to brown algae [83]. Fixation of ^{95m}Tc by brown algae appears to be an active process rather than one of simple, passive sorption. The uptake is both temperature- and light-dependent with rapidly growing parts of the plant showing the highest activities per unit weight [84].

The uptake of ^{95m}Tc added to marine algae in seawater as $^{95m}TcO_4^-$ was localized by autoradiography. In the brown species (*Ascophyllum nodosum, Fucus spiralis* and *Fucus vesiculosus*) as well as in the red species (*Porphyra umbilicalis*), the distribution of ^{95m}Tc was heterogeneous. The nuclide was mostly accumulated in those parts of the algae which bore reproductive cells or contained young tissues. A close relation was suggested between active cellular metabolism and ^{95m}Tc accumulation. Since

brown algae have high concentration factors they could constitute an important link in the transfer of technetium through the food chain (Table 4.8.A) [85, 86].

Table 4.8.A Technetium uptake by green, red, and brown marine algae [85]. See literature cited in [85]. The concentration factor is defined as the ratio Bq · g $^{-1}$ algae (wet wt)/Bq · ml $^{-1}$ $^{95m}TcO_4^-$ solution.

Species	Concentration factor
Green algae	
Acetabularia acetabulum	348
Boergesenia forbesii	0.7
Bryopsis hypnoides	350
Caulerpa prolifera	0.6
Enteromorpha intestinalis	<1
Ulva lactuca	11
Ulva rigida	7
Red algae	
Chondrus crispus	4
Iridaea splendens	1
Porphyra umbilicalis	0.1–5
Rhodymenia palmata	8
Brown algae	
Ascophyllum nodosum	9000
Colpomenia sinuosa	14
Cystoseira complexa	532
Cystoseira compressa	53–85
Cystoseira sp.	2500
Dictyota dichotoma	31
Dictyopteris membranacea	21
Ectocarpus Confervoides	30–49
Fucus serratus	12000
Fucus spiralis	51000
Fucus sp.	88000
Fucus vesiculosus	100000
Fucus virsoides	1100
Laminaria digitata	400–800
Nereocystis pyrifera	1000
Sargassum vulgare	1300

Brown algae from Iki Island, Nagasaki Prefecture, Japan, showed ^{99}Tc concentrations of $1.2 \cdot 10^{-3}$ to $5.8 \cdot 10^{-2}$ Bq/kg wet algae and concentration factors ranging between 13 and 583 [78].

$^{95m}TcO_4^-$ was added in picomolar quantities to monocultures of seven species of marine phytoplankton, including a green alga (*Dunaliella tertiolecta*), a diatom (*Thalassiosira pseudonana*), a blue-green alga (*Oscillatoria woronichinii*), a prasinophyte (*Tetraselmis chuii*), two haptophytes (*Emiliania huxleyi* and *Cricosphaera carterae*), and a dinoflagellate (*Heterocapsa pygmaea*). None of the species appreciably concentrated ^{95m}Tc in 4 days. Wet weight concentration factors never exceeded 20 for any species. The results indicate that phytoplankton are likely to have negligible influence on the cycling of technetium in marine systems [87].

The aquatic microorganisms *Flavobacterium halmephilum*, *Uronema marinum*, *Chlamydomonas reinhardtii*, and *Dunaliella bioculata* are capable of fixing ^{95m}Tc or

^{99}Tc. In spite of the fact that both *Chlamydomonas reinhardtii* and *Dunaliella bioculata* are wall-less, the first microalga accumulates Tc with a concentration factor of 90, whereas the second one concentrates Tc with a factor of only 0.3. On the other hand, the cell wall appears not to be a barrier to the penetration of Tc inside algal cells, because the unicellular alga *Acetabularia*, which possesses a thick cell wall, strongly accumulates Tc up to a concentration factor of 400 [88].

For three species of mussel, *Mytilus edulis*, *Mytilus galloprovincialis*, and *Mytilus californianus*, steady state concentration factors for ^{95m}Tc, following uptake of $^{95m}TcO_4$ from labelled seawater, never exceeded a value of 2. The same low value applies for the oyster *Crassostrea gigas*. Other members of the phylum Mollusca do not show the same low concentration factors [89]. For the red abalone *Haliotis rufescens*, the whole-body concentration factors for ^{95m}Tc ranged from 135 to 205 and the biological half-life was 60 days. The highest activities were in the order of digestive gland > gill > kidneys > heart > gonad > columnar muscle. The total radioactivity was partitioned nearly equally between soft tissue and shell [90, 91].

Pronounced differences have been observed in the uptake behavior of Tc in crustaceans, i. e. shrimps, crabs, isopods, and amphipods in contrast to lobsters. With the exception of lobsters, all the species mentioned exhibited whole body concentration factors that range between 2 and 12. For lobsters, values between 1000 and 1400 were recorded [92]. Particularly high concentration factors of 10^4 occur in the lobster *hepatopancreas* [89].

Among the invertebrates, seastars display a particularly marked ability to assimilate and retain a variety of heavy elements such as vanadium, plutonium, americium, and californium. The subcellular distribution of ^{95m}Tc was studied in the seastar *Marthasterias glacialis*, the food of which was labelled with $^{95m}TcO_4$. The majority (96 %) of ^{95m}Tc was taken up and retained in the pyloric caeca, the gland responsible for digestive and food storage processes. In the pyloric caeca ^{95m}Tc was largely associated with the lysosomes. Chromatography indicated the presence of two distinct protein compounds which were responsible for binding virtually all of the technetium in the soluble fraction. The anionic protein may play a role in metal detoxification at the cellular level [93].

Within the phylum Annelida, polychaetes have shown a variation in their biokinetic behavior of Tc not unlike that observed for molluscs and arthropods. Three species of polychaetes exposed to $^{95m}TcO_4^-$ in seawater for a period of 40 d exhibited concentration factors ranging between 10 for *Arenicola marina* and 1100 for *Perinereis cultrifera*. *Nereis diversicolor* showed intermediate values of 100 and *Nereis sp.* concentration factors of more than 500 [89, 92].

Few experiments that deal with uptake of technetium in marine fishes have been reported. The plaice *Pleuronectes platessa* showed an equilibrium concentration factor of around 9 after 61 days, when $^{95m}TcO_4$ was added to seawater. The highest concentrations were attained by kidney and the lowest by muscle. A mean biological half-life of 46 days was observed [92]. The thornback ray *Raja clavata* attained equilibrium concentration factors near 8. The distributions of ^{95m}Tc at the organ/tissue level in these two species of fish were remarkably similar for both the direct water uptake and the labeled food experiments. The data may be compared with the concentration fac-

tor of 2 observed in the blenny (*Blennius pholis*) following 40 d of exposure to $^{95m}TcO_4^-$ labeled seawater. The seabass *Dicentrarchus labrax* fed with ^{95m}Tc labeled worms (*Marphysa bellii*) over a period of 18 days exhibited an activity retention of 22 %. 48 % of the incorporated isotope was lost during a period of only 1.1 d [89]. The marine fish *Serranus cabrilla* treated in seawater with $^{99}TcO_4^-$ showed a concentration factor of only 0.2. However, when the fishes were fed with labeled molluscs, 20 % of the ingested ^{99}Tc was assimilated [94].

A graphical represention of concentration factor data for some marine organisms is given in Fig. 4.3.A. The data relate to direct uptake of $^{95m}TcO_4^-$ from seawater. It is evident that sentinel organisms for monitoring the change of $^{99}TcO_4^-$ levels in seawater would be relegated to brown macroalgae, certain species of polychaetes and lobsters. Of these target materials, brown macroalgae appear to be the logical candidate [89].

4.2.5 Conclusion

Technetium-99, produced at high yield by nuclear fission, is often thought to be a significant long-term risk to humans. It spreads more readily in the environment than many other radionuclides. TcO_4^- is highly soluble and will not be sorbed in significant quantities on soil and sediments without reduction. It was shown to be mobile in soil and water and available for uptake by biota. Information is scanty on ^{99}Tc toxicity to humans and animals, even though this is the decisive criterion for assessing the consequences of the occurrence of ^{99}Tc in the environment. Studies on rats given relatively large amounts of $NH_4^{99}TcO_4$ for several months, revealed that thyroid damage as well as effects on pregnancy could be observed only after 10 µg ^{99}Tc per gram of food was administered; 1 µg ^{99}Tc per gram of food yielded no changes. The radiological toxicity of ^{99}Tc might be even less than its chemical toxicity. It appears unlikely that ^{99}Tc contamination levels in the environment would ever reach levels that could lead to serious effects, even in developing organisms [95].

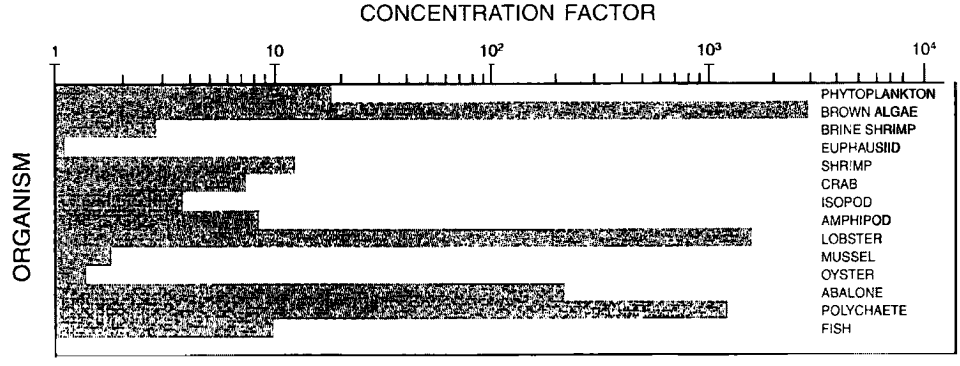

Fig. 4.3.A Maximum concentration factors for ^{95m}Tc in marine organisms [89].

The use of ^{99m}Tc, the short-lived metastable isomer of ^{99}Tc, in nuclear medicine for diagnostic organ imaging has dramatically increased over the past two decades. Already in 1973 concern was expressed about the impact of ^{99m}Tc disposal on the environment [96]. The release of medically used ^{99m}Tc can come from the wastes of laboratories and from the excreta of patients. The diagnostic doses of ^{99m}Tc are in the range of 20–1000 MBq. It is assumed that more than half of the radioactivity excreted by patients can enter the sewage system. An inventory of the use of ^{99m}Tc by the major hospitals in the sampling area of Cincinnati, Ohio, for example, showed that already in the early 1970s in a typical week about $7 \cdot 10^{10}$ Bq was administered to patients and that around $1.1 \cdot 10^{10}$ Bq per week was released to the Ohio River [97, 98]. However, the amount of long-lived ^{99}Tc produced from the decay of ^{99m}Tc is governed by the ratio of the decay constants and would be, even now, negligible.

4.3 References

[1] UNSCEAR, Ionizing Radiation: Sources and Biological Effects, New York, United Nations (1982), p. 773
[2] E. Holm, Radiochim. Acta *63*, 57–62 (1993)
[3] E. H. Schulte and P. Scoppa, The Science of the Total Environment *64*, 163–179 (1983)
[4] F. Luykx in: Technetium in the Environment (G. Desmet and C. Myttenaere, eds.), Elsevier, Appl. Sci. Publ. (1986), pp. 21–27
[5] Atomwirtschaft, Juni 1994, 398–400 (1994)
[6] J. E. Till in: Technetium in the Environment (G. Desmet and C. Myttenaere, eds.), Elsevier, Appl. Sci. Publ. (1986), pp. 1–20
[7] K. H. Lieser, Chem. Ztg. *110*, 215–231 (1986)
[8] A. Huber, F. Baumgärtner, R. Henkelmann, and A. Gauthier, KFK Karlsruhe, Pt UB 15, 355 (1986)
[9] K. H. Lieser, Radiochim. Acta *63*, 5–8 (1993)
[10] D. J. Pruett, Sep. Sci. Technol. *16*, 1157–1179 (1981)
[11] N. Boukis, The chemistry of technetium under Purex process conditions, KFK 4362, Karlsruhe (1988)
[12] J. Vida, Zum chemischen Verhalten des Technetiums bei der Behandlung des hochradioaktiven Abfalls, KFK 4642, Karlsruhe (1989)
[13] J. M. Storton, Ion exchange as a technique to remove technetium, in: Management of Low-Level Radioactive Waste, Vol. 1 (M. W. Carter, A. A. Moghissi and B. Kahn, eds.), Pergamon Press, New York (1977), pp. 411–418
[14] K. H. Lieser, C. Bauscher, and T. Nakashima, Radiochim. Acta *42*, 191–200 (1987)
[15] S. Magirius, W. T. Carnall, and J. I. Kim, Radiochim. Acta *38*, 29–32 (1985)
[16] K. H. Lieser, P. P. Coetzee, and M. Förster, Radiochim. Acta *38*, 33–35 (1985)
[17] B. Torstenfelt, B. Allard, K. Andersson, and U. Olofsson, Technetium in the geologic environment – A literature survey, Report Prav. 4.28 (1981)
[18] R. E. Wildung, K. M. McFadden, and T. R. Garland, J. Environ. Qual. *8*, 156–161 (1979)
[19] R. E. Wildung, R. C. Routson, R. J. Serne, and T. R. Garland, USERDA Rep. BNWL-1950, Part 2, Natl. Tech. Inf. Serv., Springfield, Va (1974), pp.37–41
[20] G. A. Bird and W. J. Schwartz, Wat. Res. *31*, 1673–1678 (1997)
[21] E. R. Landa, L. Thorvig, and R. T. Gast, J. Environ. Qual. *6*, 181–187 (1977)
[22] K. Tagami and S. Uchida, Environmental Pollution *95*, 151–154 (1997)
[23] J. C. Balogh and D. F. Grigal, Soil Science *130*, 278–282 (1980)
[24] R. E. Wildung, T. R. Garland, K. M. McFadden, and C. E. Cowan in: Technetium in the Environment (G. Desmet and C. Myttenaere, eds.), Elsevier, Appl. Sci. Publ. (1986), pp. 115–129
[25] S. C. Sheppard, M. I. Sheppard, and W. G. Evenden, J. Environ. Radioactivity *11*, 215–233 (1990)
[26] M. Stalmans, A. Maes and A. Cremers in: Technetium in the Environment, (G. Desmet and C. Myttenaere, eds.), Elsevier, Appl. Sci. Publ. (1986), pp. 91–113

[27] L. Van Loon, M. Stalmans, A. Maes, A. Cremers, and M. Cogneau in: Technetium in the Environment, (G. Desmet and C. Myttenaere, eds.), Elsevier, Appl. Sci. Publ. (1986), pp. 143–153
[28] T. Sekine, A. Watanabe, K. Yoshihara, and J. I. Kim. Radiochim. Acta *63*, 87–90 (1993)
[29] C. Wolfrum and K. Bunzl, J. Radioanal. Nucl. Chem., Art. *99*, 315–323 (1986)
[30] K. Andersson, S. Evans, and Y. Albinsson. Radiochim. Acta *58/59*, 321–327 (1992)
[31] V. F. Peretrukhin, T. V. Khizhnyak, N. N. Lyalikova, and K. E. German, Radiochemistry *38*, 440–443 (1996)
[32] G. M. Milton, R. J. Cornett, S. J. Kramer, and A. Vezina, Radiochim. Acta *58/59*, 291–296 (1992)
[33] F. A. Bondietti and C. W. Francis. Science *203*, 1337–1340 (1979)
[34] R. E. Meyer, W. D. Arnold, F. I. Case, and G. D. O'Kelly, Radiochim. Acta *55*, 11–18 (1991)
[35] B. Allard, H. Kigatsi, and B. Torstenfelt, Radiochem. Radioanal. Letters *37*, 223–230 (1979)
[36] K. H. Lieser and C. Bauscher, Radiochim. Acta *42*, 205–213 (1987)
[37] N. W. Golchert and J. Sedlet, Anal. Chem. *41*, 669–671 (1969)
[38] M. Attrep, J. A. Enochs, and L. D. Broz, Environ. Sci. Technol. *5*, 344–345 (1971)
[39] S. Foti, F. Delucchi, and V. Akamian, Anal. Chim Acta *60*, 261–268 (1972)
[40] S. Foti, E. Delucchi, and V. Akamian, Anal. Chim Acta *60*, 269–276 (1972)
[41] K. C. Ehrhardt and M. Attrep, Jr., Environ. Sci. Technol. *12*, 55–57 (1978)
[42] S. Ballestra, G. Barci, F. Holm, J. Lopez, and J. Gastaud, J. Radioanal. Nucl. Chem., Art. *115*, 51–58 (1987)
[43] K. Tagami and S. Uchida, J. Radioanal. Nucl. Chem., Art. *197*, 409–416 (1995)
[44] M. Garcia-Leòn, J. Radioanal. Nucl. Chem., Art. *138*, 171–179 (1990)
[45] F. Holm, J. Rioseco, S. Ballestra, and A. Walton, J. Radioanal. Nucl. Chem., Art. *123*, 167–179 (1988)
[46] R. E. Wildung, T. R. Garland, and D. A. Cataldo, Health Phys. *32*, 314–316 (1977)
[47] G. P. Berlyn, S. S. Dhillon, and E. E. Koslow, Environmental Management *4*, 149–156 (1980)
[48] R. G. Menzel, Health Phys. *11*, 1325–1332 (1965)
[49] R. C. Routson and D. A. Cataldo, Health Phys. *34*, 685–690 (1978)
[50] J. M. Mousny, P. Roucoux, and C. Myttenaere. Environm. Exp. Bot. *19*, 263–268 (1979)
[51] J. M. Mousny and C. Myttenaere, Plant and Soil *61*, 403–412 (1981)
[52] F. O. Hoffman, C. T. Garten, Jr., J. W. Huckabee, and D. M. Lucas, J. Environ. Qual. *11*, 134–141 (1982)
[53] M. I. Sheppard, T. T. Vandergraaf, D. H. Thibault, and J. A. K. Reid, Health Phys. *44*, 635–643 (1983)
[54] D. A. Cataldo, R. E. Wildung, and T. R. Garland Plant Physiol. *73*, 849–852 (1983)
[55] D. A. Cataldo, T. R. Garland, and R. E. Wildung in: Technetium in the Environment, (G. Desmet and C. Myttenaere, eds.), Elsevier, Appl. Sci. Publ. (1986), pp. 265–280
[56] J. F. M. M. Lembrechts and G. M. Desmet in: Technetium in the Environment, (G. Desmet and C. Myttenaere, eds.), Elsevier, Appl. Sci. Publ. (1986), pp. 265–280
[57] J. F. Lembrechts and G. M. Desmet, Plant Physiol. *81*, 1003–1007 (1986)
[58] J. F. Lembrechts and G. M. Desmet, Health Phys. *57*, 255–262 (1989)
[59] C. T. Garten, Jr., C. Myttenaere, C. M. Vandecasteele, R. Kirchmann, and R. Van Bruwaene in: Technetium in the Environment, (G. Desmet and C. Myttenaere, eds.), Elsevier, Appl. Sci. Publ. (1986), pp. 319–332
[60] C. T. Garten, Jr., C. S. Tucher, and B. T. Walton, J. Environ. Radioactivity *3*, 163–188 (1986)
[61] C. T. Garten, Jr., and R. D. Lomax, Health Phys. *57*, 299–307 (1989)
[62] D. A. Cataldo, T. R. Garland, R. E. Wildung, and R. J. Fellows, Health Phys. *57*, 281–287 (1989)
[63] J. W. Neel and M. A. Onasch, Health Phys. *57*, 289–298 (1989)
[64] K. Yanagisawa, Y. Muramatsu, and H. Kamada, Radioisotopes *41*, 397–402 (1992)
[65] K. Yanagisawa and Y. Muramatsu, Radiochim. Acta *63*, 83–86 (1993)
[66] E. Holm and J. Rioseco, J. Environ. Radioactivity *5*, 343–357 (1987)
[67] P. Gearing, C. Van Baalen, and P. L. Parker, Plant Physiol. *55*, 240–246 (1975)
[68] J. Henrot, Health Phys. *57*, 239–245 (1989)
[69] N. H. Blaylock, M. L. Frank, and D. L. DeAngelis, Health Phys. *42*, 257–266 (1982)
[70] D. L. Willis and M. McKenzie-Carter, Health Phys. *47*, 209 (1984)
[71] B. G. Blaylock, M. L. Frank, F. O. Hoffman, and D. L. DeAngelis in: Technetium in the Environment, (G. Desmet and C. Myttenaere, eds.), Elsevier, Appl. Sci. Publ. (1986), pp. 79–89
[72] B. Jones, Int. J. Appl. Radiat. Isot. *34*, 837–839 (1983)
[73] F. A. Bondietti and C. T. Garten, Jr., in: Technetium in the Environment, (G. Desmet and C. Myttenaere, eds.), Elsevier, Appl. Sci. Publ. (1989), pp. 339–347

[74] B.-E. V. Jones, Health Phys. *57*, 331–336 (1989)
[75] R. Van Bruwaene, G. B. Gerber, R. Kirchmann, C. T. Garten, Jr., J. Vankerkom, S. Bonotto, T. Mathieu, and M. Cogneau in: Technetium in the Environment (G. Desmet and C. Myttenaere, eds.), Elsevier, Appl. Sci. Publ. (1986), pp. 333–338
[76] J. M. Thomas, L. L. Cadwell, D. A. Cataldo, and T. R. Garland in: Technetium in the Environment (G. Desmet and C. Myttenaere, eds.), Elsevier, Appl. Sci. Publ. (1986), pp. 349–357
[77] J. P. Riley and S. A. Siddiqui, Marine Pollution Bulletin *17*, 229 (1986)
[78] N. Matsuoka, T. Umata, M. Okamura, N. Shiraishi, N. Momoshima, and Y. Takashima, J. Radioanal. Nucl. Chem. Art. *140*, 57–73 (1990)
[79] N. Momoshima, M. Sayad, and Y. Takashima, J. Radioanal. Nucl. Chem. Art. *197*, 245–251 (1995)
[80] M. Koide and E. D. Goldberg, J. Environ. Radioactivity *2*, 261–282 (1985)
[81] S. Bonotto, G. B. Gerber, M. Cogneau, and R. Kirchmann, Ann. Ass. Belge Radioprotection *8*, 237–243 (1983)
[82] E. Hohn, J. Rioseco, and S. Mattsson in: Technetium in the Environment, (G. Desmet and C. Myttenaere, eds.), Elsevier, Appl. Sci. Publ. (1986), pp. 61–68
[83] L. Benco, S. Cannarsa, I. Ceppodomo, and A. Zattera in: Technetium in the Environment, (G. Desmet and C. Myttenaere, eds.), Elsevier, Appl. Sci. Publ. (1986), pp. 217–227
[84] S. Topcuoglu and S. W. Fowler, Mar. Env. Res. *12*, 25–43 (1984)
[85] S. Bonotto, V. Robbrecht, G. Nuyts, M. Cogneau, and D. van der Ben, Marine Pollution Bulletin *19*, 61–65 (1988)
[86] C. Hurtgen, G. Koch, D. van der Ben, and S. Bonotto, Sci. Total Environ. *70*, 131–149 (1988)
[87] N. S. Fisher, Environ. Sci. Technol. *16*, 579–581 (1982)
[88] B. Mania, Z. Moureau, D. van der Ben, J. van Baelen, C. Verthé, J. M. Bouquegneau, M. Cogneau, S. Bonotto, C. M. Vandecasteele, L. Pignolet, and C. Myttenaere in: Technetium in the Environment, (G. Desmet and C. Myttenaere, eds.), Elsevier, Appl. Sci. Publ. (1986), pp. 229–244
[89] T. M. Beasley and H. V. Lorz, J. Environ. Radioactivity *3*, 1–22 (1986)
[90] R. B. Spies, Health Phys. *29*, 695–699 (1975)
[91] T. M Beasley, H. V. Lorz, and J. J. Gonor, Health Phys. *43*, 501–507 (1982)
[92] R. J. Pentreath in: Impacts of radionuclide releases into the marine environment, Vienna, International Atomic Energy Agency, IAEA-SM-248/102 (1981), pp. 241–272
[93] F. Gondard, J. Galey, J. Pieri, S. W. Fowler, S. Heussner, and J. La Rosa, Mar. Biol. *85*, 43–50 (1985)
[94] C. Verthé, Z. Moureau, B. Mania, J. van Baelen, D. van der Ben, M. Cogneau, C. M. Vandecasteele, J. M. Bouquegneau, C. Myttenaere, and S. Bonotto in: Technetium in the Environment, (G. Desmet and C. Myttenaere, eds.), Elsevier, Appl. Sci. Publ. (1986), pp. 245–250
[95] G. B. Gerber, M. Hegela, J. Vankerkom, R. Kirchmann, J. R. Maisin, and M. Lambiet-Collier, Health Phys. *57*, 345–350 (1989)
[96] C. F. Moss, Health Phys. *25*, 197–198 (1973)
[97] V. J. Sodd, R. J. Velten, and E. L. Saenger, Health Phys. *28*, 355–359 (1975)
[98] J. L. Birks, Nature *255*, 621–622 (1975)

5 Isotopes and isomers

At present 22 isotopes and 9 isomers of technetium are known, and are summarized in Table 5.1.A. The half-lives range from 0.3 s to 4.2 million years. As expected, long half-lives are observed in the range of mass numbers where electron capture decay turns to β^--decay. Long-lived isotopes are ^{97}Tc ($2.6 \cdot 10^6$ a), ^{98}Tc ($4.2 \cdot 10^6$ a), and ^{99}Tc ($2.1 \cdot 10^5$ a). In this range of mass numbers, stable isobars of the neighboring elements molybdenum and ruthenium are known. Thus, according to Mattauch's rule [6], no stable technetium nuclide should exist (Fig. 5.1.A). An explanation for the absence of β-stable isotopes of technetium regarding the odd number (43) of protons was given as early as 1951 [7].

Table 5.1.A Isotopes and isomers of technetium [1–5]. Spin values not determined experimentally are put in parentheses.

Nuclide	Production	Atomic mass [a.m.u.]	Spin and Parity [h/2π]	Half-life	Mode and energy [keV] of decay
^{90}Tc	^{97}Mo(p,3n)	89.923810	1+	8.7 s	β^+7900; 6950; γ948
^{90m}Tc	^{97}Mo(p,3n)		6+	49.2 s	β^+; γ1054; 948; 945; ...
^{91}Tc	^{92}Mo(p,2n)	90.918430	(9/2)+	3.14 min	β^+; γ2451; 1639; 1605; ...
^{91m}Tc	^{92}Mo(p,2n)		(1/2)−	3.3 min	β^+; γ653; 503; 928; ...
^{92}Tc	^{92}Mo(d,2n) ^{92}Mo(p,n)	91.915257	(8)−	4.23 min	β^+4300; 4100; γ1510; 773; 329; ...
^{93}Tc	^{92}Mo(d,n) ^{93}Mo(p,γ)	92.910246	9/2+	2.75 h	β^+807; ε; γ1363; 1522; 1478; ...
^{93m}Tc	^{93}Mo(d,n) ^{92}Mo(p,γ) ^{93}Nb(α,4n)		1/2−	43.5 min	IT392; ε; γ2645; 3129; 3221; ...
^{94}Tc	^{93}Nb(α,3n) ^{94}Mo(d,2n) ^{94}Mo(p,n) ^{93}Nb(^{3}He,2n)	93.909654	7+	4.883 h	ε; β^+800; γ871; 850; 916; ...
^{94m}Tc	^{93}Nb(α,3n) ^{94}Mo(d,2n) ^{94}Mo(p,n)		(2)+	52.0 min	β^+2420; γ871; 1869; 1522; ...
^{95}Tc	^{95}Mo(p,n) ^{94}Mo(d,n) ^{95}Mo(d,2n)	94.907657	9/2+	20.0 h	ε; γ766; 1074; 948; ...
^{95m}Tc	^{95}Mo(p,n) ^{94}Mo(d,n) ^{95}Mo(d,2n)		1/2−	61 d	ε; β^+700; 492; IT; γ204; 582; 835; ...
^{96}Tc	^{93}Nb(α,n) ^{96}Mo(p,n) ^{96}Mo (d,2n)	95.907870	7+	4.28 d	ε; γ778; 850; 813; ...
^{96m}Tc	^{93}Nb (α,n) ^{96}Mo (p,n) ^{96}Mo (d,2n)		4+	51.5 min	IT34; ε; γ778; 1200; 481; ...

Nuclide	Production	Atomic mass [a.m.u.]	Spin and Parity [h/2π]	Half-life	Mode and energy [keV] of decay
^{97}Tc	daughter ^{97}Ru ^{97}Mo(d,2n)	96.906364	9/2+	$2.6 \cdot 10^6$ a $(4.0 \cdot 10^6$ a)[5]	ε
^{97m}Tc	^{96}Mo(d,n) ^{97}Mo(p,n) ^{97}Mo(d,2n)		1/2	90.1 d	IT 97
^{98}Tc	^{98}Mo(p,n)	97.907215	(6)+	$4.2 \cdot 10^6$ a	β⁻397; γ745; 652
^{99}Tc	fission, daughter ^{99}Mo	98.906254	9/2+	$2.13 \cdot 10^5$ a	β 292; 203
^{99m}Tc	daughter ^{99}Mo		1/2−	6.006 h	IT140; 143; β ,e ,γ322; 233
^{100}Tc	^{99}Tc(n,γ) ^{100}Mo(p,n) ^{103}Rh(n,z)	99.907657	1+	15.8 s	β⁻3380; 2880; γ540; 591; 1512; ...
^{101}Tc	daughter ^{101}Mo	100.907327	9/2	14.22 min	β⁻1320; 1070; γ307; 545; 127; ...
^{102}Tc	daughter ^{102}Mo	101.909208	1+	5.28 s	β 4150; 3400; 2200; γ475; 105; 628; ...
^{102m}Tc	^{102}Ru(n,p) fission		(4,5)	4.35 min	β 1600; 3200; γ475; 628; 630; ... ; IT
^{103}Tc	fission ^{104}Ru(n,np) ^{103}Ru(γ,p)	102.909172	5/2+	54.2 s	β⁻2200; 2000; γ136; 346; 210; ...
^{104}Tc	fission ^{104}Ru(n,p)	103.911460	(3+)	18.3 min	β⁻ 5100; ... ; γ358; 531; 535; ...
^{105}Tc	fission	104.911820		7.7 min	β 3400; γ143; 108; 159; ...
^{106}Tc	fission	105.914510	(1,2)	36 s	β⁻; γ270; 2239; 1969; ...
^{107}Tc	fission	106.915230		21.2 s	β ; γ103; 106; 177; ...
^{108}Tc	fission	107.918420	(2−,3)	5.17 s	β⁻; γ242; 732; 708; ...
^{109}Tc	fission	108.919580		0.86 s	β⁻
^{110}Tc	fission			0.92 s	β ; γ241
^{111}Tc				0.30 s	β

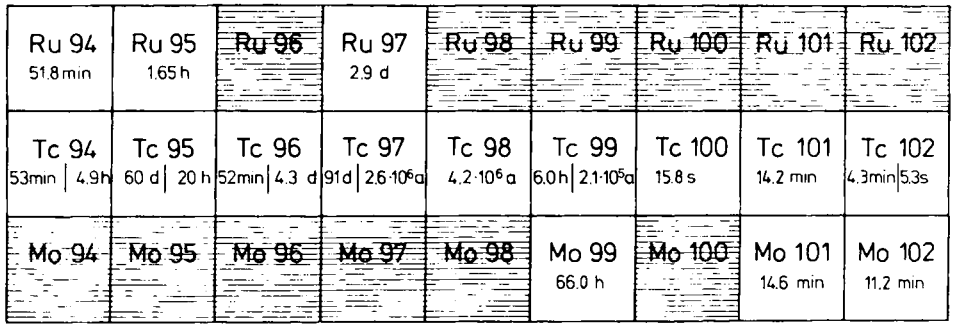

Fig. 5.1.A A modified section of the nuclide chart of some technetium isotopes and isotopes of ruthenium and molybdenum. The stable isotopes are indicated by the hatched squares.

5.1 Production and isolation of ^{99}Tc

Small quantities (μg) of the three long-lived technetium isotopes ^{97}Tc, ^{98}Tc, and ^{99}Tc were produced for the first time by bombarding molybdenum metal with 22 MeV protons [8]. Small amounts of ^{97}Tc are also accessible by neutron irradiation of ruthenium [4]:

$$^{96}Ru(n,\gamma)^{97}Ru \xrightarrow[2.88d]{\varepsilon} {}^{97m}Tc \xrightarrow[90d]{IT} {}^{97}Tc$$

^{99}Tc can be obtained in milligram quantities by prolonged neutron irradiation of purified natural molybdenum [9,10]:

$$^{98}Mo(n,\gamma)^{99}Mo \xrightarrow[66h]{\beta^-} {}^{99m}Tc \xrightarrow[6.0h]{IT} {}^{99}Tc$$

To produce quantities of ^{99}Tc sufficient for chemical studies, 5.7 kg of pure natural molybdenum metal powder was irradiated for one year in an average thermal neutron flux of $5 \cdot 10^{11}$ n cm^{-2} s^{-1}. The irradiated molybdenum was dissolved in conc. sulphuric acid and distilled. The distillate was diluted to 4 M, heated to boiling and treated with bromine water. Platinum sulphide was precipitated to co-precipitate ^{99}Tc. The precipitate was dissolved in ammonia containing hydrogen peroxide. This solution was evaporated to dryness, the residue taken up in conc. H_2SO_4 or $HClO_4$, and ^{99}Tc was separated from the platinum by distillation. Since the original molybdenum powder contained 3 ppm of rhenium, which was concentrated together with technetium, the two metals were separated by ion-exchange chromatography using strong base anion exchangers. The overall yields ranged from 30–65 % of the theoretically expected 2.8 mg of ^{99}Tc [11].

However, gram and kilogram amounts can be obtained by fission of ^{235}U with thermal neutrons in the high, cumulative fission yield of 6.13 atom% [12]. This fission yield results in the production of about 1 kg of ^{99}Tc from 1 ton of uranium (3 % enriched in ^{235}U) after burnup in a nuclear reactor [13]. Reactors with a power of 100 MW produce about 2.5 g of ^{99}Tc per day [14]. ^{99}Tc is also formed in high yield (atom%) from thermal neutron fission of ^{233}U (4.8), ^{239}Pu (5.9), and fast neutron fission of ^{239}Pu (5.9), ^{238}U (6.3) and ^{232}Th (2.7) [15]. Compared to the high fission yield of 6.13 atom% for ^{99}Tc, the fission yield for ^{98}Tc by fission of ^{235}U with thermal neutrons is only $8.7 \cdot 10^{-7}$ atom% [12].

During recycling of the fuel, ^{99}Tc follows the majority of the other fission products into the waste solution. The ^{99}Tc content in solutions to be processed amounts to 5–100 mg/l. After storage for several years, the level of radioactivity in the waste solutions falls sufficiently to allow the extraction of long-lived fission products including ^{99}Tc. The first 18 g of ^{99}Tc was isolated in 1952 [16]. $[AsPh_4]TcO_4$ was precipitated in the presence of perchlorate as a carrier. The mixed salts were dissolved in conc. H_2SO_4 and the solution was electrolyzed at platinum electrodes. The black deposit obtained (TcO_2) was dissolved in $HClO_4$, and Tc_2O_7 distilled out of the solution. The element was finally isolated by precipitation of Tc_2S_7 which can be reduced by hydrogen to the metal. The disadvantages of using $[AsPh_4]Cl$ for precipitation are the high cost of the reagent and its high rate of consumption, since the electrolysis procedure decomposes the $[AsPh_4]^+$ ions. In order to recover $[AsPh_4]Cl$, the tetraphenylarsonium pertechnetate/perchlorate precipitate was dissolved in ethanol and the solution passed through the bed of a strong basic anion exchanger in the chloride form. TcO_4^- / ClO_4^- are strongly absorbed and finally eluted with 2M $HClO_4$. $[AsPh_4]Cl$ in the effluent could be isolated and purified by recrystallization [10].

The extraction of TcO_4^- with pyridine [17] appears to be one of the most suitable processes of recovering ^{99}Tc from the waste solutions of the nuclear fuel cycle. The

scheme described in Fig. 5.2.A was used at Oak Ridge National Laboratory for the extraction of ^{99}Tc from the wastes of the Purex process. The composition of typical metal recovery waste solutions after the refining of nuclear fuel in the Purex process is given in Table 5.2.A.

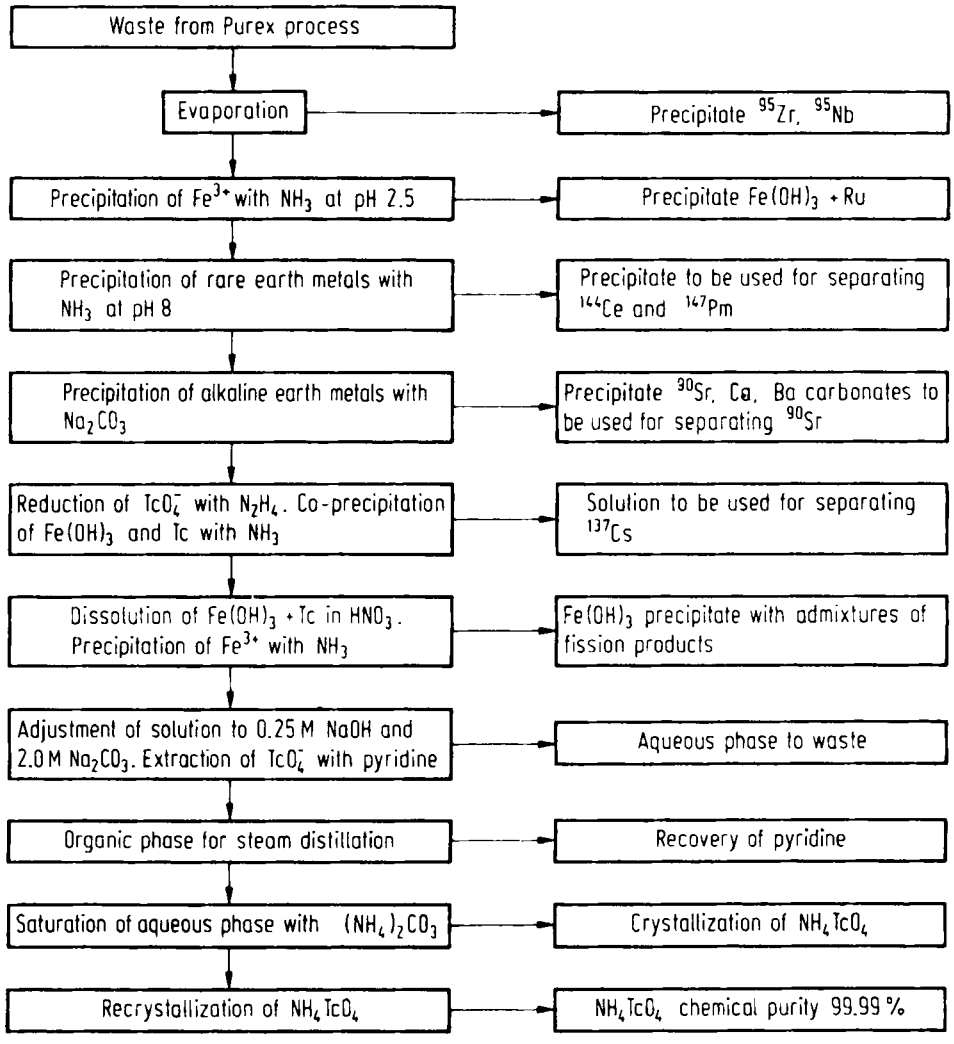

Fig. 5.2.A Scheme of the extraction of ^{99}Tc from a Purex process waste solution [18].

The waste solution (Fig. 5.2.A) is evaporated and the cake containing ^{95}Zr and ^{95}Nb is removed. To separate Ru, iron(III) hydrated oxide is precipitated with ammonia. Rare earth metal ions are removed by precipitation of the hydrated oxides with ammonia. Thereafter, alkaline earth metal ions including ^{90}Sr are precipitated by add-

Table 5.2.A Composition of a metal recovery waste solution (3.9 M HNO_3) remaining from the Purex process [10].

^{137}Cs	4.4 Ci(163 GBq)/l	~ 73 mg/l
^{90}Sr	4.6 Ci(170 GBq)/l	~ 48 mg/l
^{106}Ru	9.0 Ci(333 GBq)/l	~ 4 mg/l
^{144}Ce	88.7 Ci(3280 GBq)/l	~ 40 mg/l
^{147}Pm	17.0 Ci(629 GBq)/l	~ 26 mg/l
^{99}Tc	$7.0 \cdot 10^{-1}$ Ci(0.026 GBq)/l	~ 41 mg/l

ing Na_2CO_3. To concentrate ^{99}Tc, TcO_4^- is reduced with 0.1 M hydrazine and TcO_2-hydrate co-precipitated with iron(III) hydrated oxide by adding NH_3. The precipitate is dissolved in nitric acid and a second precipitation of Fe(III) follows, which does not co-precipitate ^{99}Tc because of its oxidation by nitric acid to TcO_4^-. The TcO_4^- solution is neutralized and then adjusted to 0.25 M NaOH and 2.0 M Na_2CO_3 for extraction of TcO_4^- with pyridine. Under these conditions the partition coefficient of TcO_4^- amounts to 740. The pyridine phase is steam-distilled, pyridine is distilled off and the aqueous solution containing TcO_4^- is saturated with $(NH_4)_2CO_3$ and cooled to 0 °C for crystallization of NH_4TcO_4. After three recrystallizations NH_4TcO_4 exhibits a radiochemical purity of over 99.998 % and chemical purity of more than 99.99 % [18].

There have been brief communications concerning a method of obtaining ^{99}Tc during processing of spent nuclear fuel in gaseous diffusion plants. TcF_6 is formed along with UF_6 during fluorination of uranium. By adsorbing TcF_6 on a bed of magnesium fluoride, technetium can be concentrated and separated from uranium [19]. In another procedure pertechnetate is extracted with 2,4-dimethyl pyridine, steam distillation of which leaves behind pertechnetate, which is then extracted with trioctylamine in benzene to remove organic impurities. Pure NH_4TcO_4 is isolated from an aqueous solution of NH_4NO_3 by means of a series of crystallizations. Reduction with hydrogen at 400–500 °C gives technetium metal of more than 99.9 % purity [20]. The use of these methods was reported to reduce the cost of isolating technetium and to increase its production [19,20].

5.2 Nuclear properties of ^{99}Tc

^{99}Tc is a weak β emitter of 292 KeV β^--energy. In addition the nuclide emits 203 keV β rays, however, with a very low probability of only $1.2 \cdot 10^{-5}$ % [21] (Table 5.3.A).

Table 5.3.A Nuclear data of ^{99}Tc

Atomic mass	98.906254 amu
Decay mode	β ,no γ
β -energy	292; 203 ($1.2 \cdot 10^{-5}$ %) keV [21]
Half-life	$2.13 \cdot 10^5$ a
Spec. activity	17.0 mCi(629 MBq)/g
Cross-section (n_{therm},γ)	20 barn [24]
Nuclear spin	9/2 h/2π
Nuclear magn. moment	+5.6847 nucl. magneton [24]
Elect. quadrupole moment	0.129 barn [24]

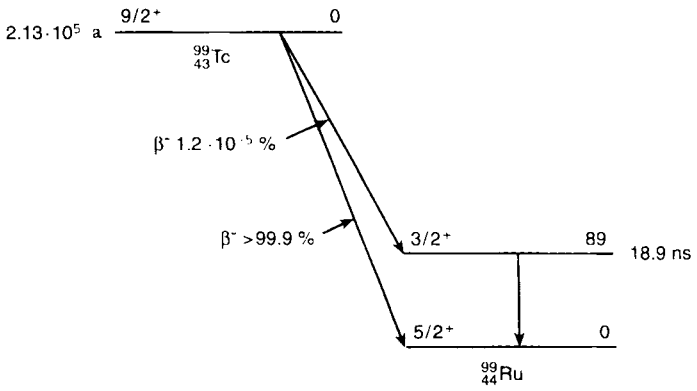

Fig. 5.3.A Decay scheme of ^{99}Tc. Energies in keV [21].

The β^- emission of ^{99}Tc is not accompanied by γ-radiation. An 89 keV γ-line belongs to the 89 keV level 3/2+ of ^{99}Ru (Fig. 5.3.A). With the half-life of $2.13 \cdot 10^5$ a, ^{99}Tc decays into the stable nuclide ^{99}Ru. The nuclear spin of 9/2 h/2π [22] can also be derived from 10 hyperfine structure lines in the EPR spectra of paramagnetic ^{99}Tc complexes [23].

5.3 Laboratory handling of technetium nuclides

The handling of ^{99}Tc on a small scale (<20 mg) does not present a danger to health provided some elementary precautions are taken. The walls of ordinary laboratory glassware give adequate protection against the weak β^- emissions. Small amounts of very soft X-rays are produced by the action of the β^- rays on glass. Therefore the operator should maintain a distance of at least 30 cm from the working area. Moreover, it is advisable to wear glasses as a protection against β^- and X-rays, which may cause clouding of the eye lenses.

Technetium can be handled in a well ventilated fume hood; glove boxes are usually not required. Nothing unnecessary is placed into the hood. Standard semimicro techniques are easily adapted for experimental work. Evaporations of solutions should be carried out using a rotation evaporator; however, it is advisable to evaporate concentrated solutions to dryness in a desiccator. The vessel containing a technetium solution is covered by a watch glass or an inverted beaker to avoid contamination by spraying. Above all, operations that might introduce Tc-containing fumes or dusts into the atmosphere must be rigorously avoided. Incorporation of Tc, which constitutes the main health hazard, could result from inhalation; in addition, extensive contamination could occur. For example, care must be taken in evaporating solutions of pertechnetic acid to prevent volatilization. The transfer of powdery dry solids should be performed carefully without the formation of dusts; sometimes it may be necessary to transfer a powder as a slurry in benzene or ether. If reactions of technetium cannot be carried out in closed systems, radioactive

material carried along with a gas current has to be absorbed in scrubbers containing oxidizing alkaline solutions. The working area should be monitored from time to time by means of a counter provided with a thin window. Finally, workers should be familiar with safety regulations for protection of persons exposed to ionizing radiation [25].

^{99}Tc and other isotopes and isomers of technetium are nuclides of medium radiotoxicity [26]; licensing limits, annual limits of intake and maximum permitted air concentrations are compiled in Table 5.4.A.

Table 5.4.A Licensing limits, intake limits, and maximum permitted air concentrations of technetium nuclides [27].

Nuclide	Licensing limit	Annual intake limit		Controlled area
		inhalation	ingestion	max. perm. air concentr.
	[Ci(Bq)]	[Ci(Bq)]	[Ci(Bq)]	[Ci(Bq)/cm^3]
^{96m}Tc	$1.0 \cdot 10^{-4}(3.7 \cdot 10^6)$	$4.4 \cdot 10^{-4}(1.6 \cdot 10^7)$	$4.8 \cdot 10^{-4}(1.8 \cdot 10^7)$	$2.9 \cdot 10^{-11}(1.1)$
^{96}Tc	$1.0 \cdot 10^{-5}(3.7 \cdot 10^5)$	$3.6 \cdot 10^{-6}(1.3 \cdot 10^5)$	$2.3 \cdot 10^{-6}(8.5 \cdot 10^4)$	$2.4 \cdot 10^{-13}(5.6 \cdot 10^{-3})$
^{97m}Tc	$1.0 \cdot 10^{-5}(3.7 \cdot 10^5)$	$2.3 \cdot 10^{-6}(8.5 \cdot 10^4)$	$8.4 \cdot 10^{-6}(3.1 \cdot 10^5)$	$1.5 \cdot 10^{-13}(5.6 \cdot 10^{-3})$
^{97}Tc	$1.0 \cdot 10^{-5}(3.7 \cdot 10^5)$	$4.4 \cdot 10^{-6}(1.6 \cdot 10^5)$	$3.8 \cdot 10^{-5}(1.4 \cdot 10^6)$	$2.9 \cdot 10^{-13}(1.1 \cdot 10^{-2})$
^{99m}Tc	$1.4 \cdot 10^{-4}(5.0 \cdot 10^6)$	$8.1 \cdot 10^{-2}(3.0 \cdot 10^9)$	$5.4 \cdot 10^{-7}(2.0 \cdot 10^9)$	$1.4 \cdot 10^{-11}(5.2 \cdot 10^{-1})$
^{99}Tc	$1.4 \cdot 10^{-4}(5.0 \cdot 10^6)$	$2.4 \cdot 10^{-4}(9.0 \cdot 10^6)$	$1.1 \cdot 10^{-3}(4.0 \cdot 10^7)$	$5.9 \cdot 10^{-14}(2.2 \cdot 10^{-3})$

For β emitting nuclides that are not included in Table 5.4.A the licensing limits depend on the half-life $t_{1/2}$, being 10^{-4} Ci ($3.7 \cdot 10^6$ Bq) for $t_{1/2} \leq 1$ h and 10^{-6} Ci ($3.7 \cdot 10^4$ Bq) for $t_{1/2} > 1$ h. The annual inhalation and ingestion intake limits are $5.7 \cdot 10^{-8}$ Ci ($2.1 \cdot 10^3$ Bq) and $1.1 \cdot 10^{-7}$ Ci ($4.1 \cdot 10^3$ Bq), respectively. The maximum permitted concentration of these nuclides in the controlled area air is confined to $3.7 \cdot 10^{-15}$ Ci ($1.4 \cdot 10^{-4}$ Bq)/cm^3.

The maximum permitted body burdens of technetium nuclides are given in Table 5.5.A.

Table 5.5.A Maximum permitted body burdens of some technetium nuclides [28].

Organ	Maximum permitted body burden [Ci(Bq)]					
	^{96m}Tc	^{96}Tc	^{97m}Tc	^{97}Tc	^{99m}Tc	^{99}Tc
Kidneys	$6 \cdot 10^{-5}(2.2 \cdot 10^6)$	$10^{-5}(3.7 \cdot 10^5)$	$2 \cdot 10^{-5}(7.4 \cdot 10^5)$	$6 \cdot 10^{-5}(2.2 \cdot 10^6)$	$8 \cdot 10^{-4}(3.0 \cdot 10^7)$	$10^{-5}(3.7 \cdot 10^5)$
Liver	$8 \cdot 10^{-4}(3.0 \cdot 10^7)$	$2 \cdot 10^{-4}(7.4 \cdot 10^6)$	$2 \cdot 10^{-4}(7.4 \cdot 10^6)$	$8 \cdot 10^{-4}(3.0 \cdot 10^7)$	$10^{-2}(3.7 \cdot 10^8)$	$2 \cdot 10^{-4}(7.4 \cdot 10^6)$
Lungs	$2 \cdot 10^{-3}(7.4 \cdot 10^7)$	$5 \cdot 10^{-4}(1.8 \cdot 10^7)$	$2 \cdot 10^{-3}(7.4 \cdot 10^7)$	$9 \cdot 10^{-3}(3.3 \cdot 10^8)$	$2 \cdot 10^{-2}(7.4 \cdot 10^8)$	$2 \cdot 10^{-3}(7.4 \cdot 10^7)$
Bone	$10^{-7}(3.7 \cdot 10^8)$	$2 \cdot 10^{-3}(7.4 \cdot 10^7)$	$7 \cdot 10^{-4}(2.6 \cdot 10^7)$	$6 \cdot 10^{-3}(2.2 \cdot 10^8)$	$2 \cdot 10^{-1}(7.4 \cdot 10^9)$	$5 \cdot 10^{-4}(1.8 \cdot 10^7)$
Skin	$2 \cdot 10^{-7}(7.4 \cdot 10^8)$	$10^{-2}(3.7 \cdot 10^8)$	$5 \cdot 10^{-4}(1.8 \cdot 10^7)$	$3 \cdot 10^{-2}(1.1 \cdot 10^9)$	$10^{-1}(3.7 \cdot 10^9)$	$4 \cdot 10^{-4}(1.5 \cdot 10^7)$
Total body	$7 \cdot 10^{-5}(2.6 \cdot 10^6)$	$10^{-5}(3.7 \cdot 10^5)$	$2 \cdot 10^{-4}(7.4 \cdot 10^6)$	$10^{-3}(3.7 \cdot 10^7)$	$2 \cdot 10^{-4}(7.4 \cdot 10^6)$	$2 \cdot 10^{-4}(7.4 \cdot 10^6)$

5.4 References

[1] E. Browne and R. B. Firestone, Table of Radioactive Isotopes, (V. S. Shirley, ed.), Wiley, New York (1986)

[2] J. K. Tuli and M. J. Martin (eds.), Nuclear Data Sheets, Vol. 60–70, Academic Press, INC, San Diego (1990–1993)

[3] A. H. Wapstra and G. Audi, Nuclear Physics *A432*, 1–54 (1985)
[4] K. H. Lieser, Einführung in die Kernchemie, 3. Auflage, VCH-Verlagsgesellschaft, Weinheim (1991)
[5] T. Kobayashi, K. Sueki, M. Ebihara, H. Nakahara, M. Imamura, and A. Masuda, Radiochim. Acta *63*, 29–31 (1993)
[6] J. Mattauch, Z. Physik *91*, 361–371 (1934)
[7] H. E. Suess, Phys. Rev. *81*, 1071 (1951)
[8] G. E. Boyd, J. R. Sites, Q. V. Larson, and C. R. Baldock, Physic. Rev. *99*, 1030–1031 (1955)
[9] E. E. Motta, G. E. Boyd, and Q. V. Larson, Phys. Rev. *72*, 1270 (1947)
[10] G. E. Boyd, J. Chem. Educ. *36*, 3–14 (1959)
[11] G. E. Boyd, Q. V. Larson, and E. E. Motta, J. Amer. Chem. Soc. *82*, 809–815 (1960)
[12] B. F. Rider and M. E. Meek, NEDO-12154-2(E) (1978)
[13] K. H. Lieser, Radiochim. Acta *63*, 5–8 (1993)
[14] K. Schwochau, Angew. Chem. *76*, 9–19 (1964)
[15] J. E. Till in: Technetium in the Environment, (G. Desmet and C. Myttenaere, eds.), Elsevier, Appl. Sci. Publ. (1986), pp. 1–20
[16] G. W. Parker and W. J. Martin, Oak Ridge National Laboratory, Declassified Report ORNL-1116, (1952), pp. 26–27
[17] S. J. Rimshaw and G. F. Malling., Anal. Chem. *33*, 751–754 (1961)
[18] K. V. Kotegov, O. N. Pavlov, and V. P. Shvedov, Adv. Inorg. Chem. Radiochem. *2*, 1–90 (1968)
[19] Chem. Eng. News *39*, 52 (1961)
[20] Sci. News Letter *83*, 264 (1963)
[21] C. E. Engelke and J. D. Ullman, Phys. Rev. C. *9*, 2358–2362 (1974)
[22] K. G. Kessler and R. E. Trees, Phys. Rev. *92*, 303–307 (1953)
[23] G. Römelt and K. Schwochau, Z. Naturforschg. *22a*, 519–522 (1967)
[24] CRC Handbook of Chemistry and Physics (D. R. Lide and H. P. R. Frederikse, eds.), CRC Press, 75th Edition (1994/95), Chapter 11, p. 60
[25] K. Schwochau, Handling of technetium, in: Gmelin Handbook of Inorganic Chemistry, 8th ed., Vol. 1, (H. K. Kugler and C. Keller, eds.), Springer, Berlin (1982), p.210
[26] Office of the European Communities, Off. Bull. Eur. Com. L23, No. 246 (1980)
[27] Government of the German Federal Republic, Strahlenschutzverordnung [StSVO], Bundesgesetzblatt I No. *125*, 2941 (1976) and No. *34*, 1358 (1989)
[28] Government of the German Federal Republic, Schriftenr. Bundesminist. Wiss. Forsch. Ger. Strahlenschutz No. *27*, 76–77, 200–203 (1967)

6 Some fundamentals of technetium chemistry

The chemical behavior of technetium, a true second-row transition element, closely resembles that of the third-row congener rhenium, due to the prolonged effects of the lanthanide contraction, whereas the chemical properties of both elements differ considerably from those of manganese. As a consequence of the lanthanide contraction, the atomic radius of technetium of 1.358 Å proved to be only 0.015 Å smaller than the radius of rhenium, while the difference between the atomic radii of technetium and manganese is almost 0.1 Å. Technetium and rhenium often form compounds of analogous composition and only slightly differing properties. Corresponding compounds were frequently shown to be isostructural. However, technetium compounds appear to be more easily reduced than analogous rhenium compounds and, according to present knowledge, technetium compounds are frequently more reactive than their rhenium analogues. Technetium differs from manganese, for example, in the high stability of the +7 oxidation state, in particular in the form of pertechnetate, compared to permanganate. Furthermore, divalent technetium exists in strong complexes, but not like Mn^{2+} as a hydrated ion.

The electronic configuration of neutral, gaseous technetium atoms in the ground state is [Kr]$4d^5 5s^2$ [1] with the term symbol $^6S_{5/2}$. The valence electron configuration corresponds to those of the congeners manganese and rhenium. Several reviews, however, presented the assignment [Kr] $4d^6\ 5s^1$ for technetium, obviously caused by misinterpretation of some publications [2, 3]. In the first detailed spectrum of TcI, the ground state of the valence electrons of neutral atomic technetium was given as $4d^5 5s^2(^6S_{5/2})$ and the first metastable state by $4d^6 5s^1$ ($^6D_{9/2}$), only 2573 cm^{-1} higher [4]. In addition, the $4d^5 5s^2$ configuration was more recently predicted by *ab initio* effective core potential calculations to be lower in energy than the $4d^6 5s^1$ configuration [5].

A total of seven valence electrons are available for bonding. Compounds of technetium in the formal oxidation states from +7 to −1 have been synthesized. Tc^{+7} (d^0) is verified for example by TcO_4^-. An example of the −1 oxidation state is the pentacarbonyl anion $[Tc(CO)_5]^-$ [6], but no structure determination or magnetic susceptibility measurement have been reported.

Some redox potentials of manganese, technetium, and rhenium are compared in Table 6.1.A.

The potentials of the couples TcO_4^-/TcO_2 and TcO_4^-/Tc are intermediate between those of the corresponding couples of manganese and rhenium; however, they are drastically lower than those of the manganese couples, indicating the higher stability of pertechnetate compared to permanganate. TcO_4^- is only a weak oxidizing agent, although somewhat stronger than ReO_4^-. On the other hand, the potential of the

TcO_2/Tc couple turns out to be somewhat higher than those of the corresponding couples of manganese and rhenium.

Table 6.1.A Redox potentials Eh [V] of the VII subgroup elements in acidic aqueous solutions [8–10]

Manganese	Eh[V]	Technetium	Eh[V]	Rhenium	Eh[V]
MnO_4^-/MnO_2	+1.679	TcO_4/TcO_2	+0.747	ReO_4^-/ReO_2	+0.510
MnO_4^-/Mn	+1.781	TcO_4^-/Tc	+0.477	ReO_4^-/Re	+0.368
MnO_2/Mn	+0.115	TcO_2/Tc	+0.281	ReO_2/Re	+0.251

6.1 Electrochemistry

In view of the numerous oxidation states, an extensive oxidation-reduction chemistry of technetium is expected. Polarographic reductions of pertechnetate in aqueous and in non-aqueous solutions, supplemented by coulometric and cyclic voltammetric measurements, were conducted to study the electrochemical behavior of technetium, to identify some oxidation states and to synthesize new technetium compounds. Electrode reactions frequently proved to be irreversible and therefore not adequate for calculating thermodynamic data. The electrochemistry of technetium is reported in detail in several review articles [11–13].

The polarography of pertechnetate in acidic aqueous solutions often revealed ill-defined, irreversible waves and led to conflicting results [14–17]. In general, the current gradually increased up to the hydrogen discharge. Conflicting results may be explained by rapid chemical reduction of strongly acidic pertechnetate solutions in contact with metallic mercury [18,19]. Taking precautions to overcome the chemical reduction by mercury, the polarographic reduction of pertechnetate appears to proceed in acidic media in two main steps. Both steps were observed as irreversible and more or less pH dependent waves. The first half-wave potential $E_{1/2}$ appeared at –0.17 V *vs* SCE and corresponds to a four-electron process, the second wave at –0.73 V, which probably involves a three-electron step producing a deposit of technetium metal on the mercury drop [20].

The polarographic reduction of pertechnetate in neutral aqueous solutions resulted in two discernible waves. The first wave at $E_{1/2}$=–0.8 V *vs* SCE showed an alternating current efficiency of 70–90 %, demonstrating a relatively high reversibility of the corresponding electrode reaction which involves the reduction of Tc(VII) to Tc(V) [21]. The second ill-defined wave at $E_{1/2} \approx -1.2$ V may be partially attributed to catalytic hydrogen discharge [21] probably arising from the lowering of the overpotential of mercury due to the deposition of metallic technetium [11, 17].

In aqueous alkaline solutions containing 0.1 to 1.0 M alkaline hydroxide, the polarograms revealed four waves. The first wave at $E_{1/2} \approx -0.8$ V *vs* SCE exhibited an alternating current efficiency of nearly 90 % [21] and can be attributed to a two-electron change [14, 21, 22]. The second wave at $E_{1/2} \approx -1.1$ V was found to be well separated from the first wave and corresponded to a three-electron process of low reversibility.

The third and fourth wave commencing at ≈ –1.2 and ≈ –1.4 V, respectively, are ill-defined and affected by catalytic hydrogen discharge [21].

To assess the number of electrons transferred in a polarographic reduction step, the Ilkovič equation is used which, however, contains the frequently unknown diffusion coefficient. The diffusion coefficient of TcO_4^- at infinite aqueous dilution $D°=1.48 \cdot 10^{-5}$ cm$^2 \cdot$ s^{-1} was calculated from the limiting ionic equivalent conductance of TcO_4 to $l°=55.5\ \Omega^{-1} \cdot cm^2$ at 25 °C. As expected, $D°(ReO_4^-)=1.456 \cdot 10^{-5}$ cm$^2 \cdot$s^{-1} was found to be only slightly smaller than $D°(TcO_4^-)$ [23, 24]. In addition, self-diffusion coefficients D of TcO_4 were determined in the presence of different supporting electrolytes using the capillary method, in order to evaluate the influence of the supporting electrolytes on the diffusion and the electron transfers found for the polarographic reduction of TcO_4. The D values of 10^{-3} M TcO_4^- in 1 M NaOH and 1 M LiCl at 25 °C are $1.27 \cdot 10^{-5}$ and $1.24 \cdot 10^{-5}$ cm$^2 \cdot$s^{-1}, respectively. Whereas the supporting electrolytes obviously affect the self-diffusion of TcO_4, the changes of the electron transfers hereby induced can be neglected [25].

The polarographic reduction of pertechnetate in aqueous solutions was supplemented by controlled-potential coulometric studies [14, 18, 19, 20, 22, 26, 27, 28] and cyclic voltametry [22, 28]. Controlled-potential electrolytic reduction of aqueous pertechnetate solutions on metallic cathodes is generally accompanied by deposition of surface films, probably of TcO_2-hydrate or, at more negative potentials, of metallic technetium [29]. Such films seriously interfere with the coulometric determination of reduction steps [13].

When pertechnetate is electrochemically reduced in aqueous alkaline solution in the presence of gelatin using the techniques of controlled-potential coulometry, chronoamperometry, and double potential step chronoamperometry, at the mercury electrode surface the technetate ion TcO_4^{2-} is reported to be produced:

$$TcO_4^- \xrightarrow{e^-} TcO_4^{2-} .$$

TcO_4^{2-} undergoes rapid disproportionation:

$$2TcO_4^{2-} \longrightarrow TcO_4^- - TcO_4^{3-} .$$

However, gelatin seems to block the electrode reaction:

$$TcO_4^{2-} \xrightarrow{e} TcO_4^{3-} .$$

The dependence of the disproportionation rate constant on ionic strength confirmed that the reacting species is doubly charged [30].

In acetonitrile or dimethylsulphoxide the polarographic and controlled-potential coulometric reduction of the tetramethylammonium salts of permanganate, pertechnetate, and perrhenate yielded as the first reduction step a one-electron transfer; the half-wave potentials *vs* SCE observed in solutions of acetonitrile are $E_{1/2}$=–0.60 V, –1.74 V and –2.30 V, respectively (Fig. 6.1.A). The limiting ionic equivalent conductance of TcO_4^- was determined in acetonitrile and dimethylsulphoxide to be $l°=127.5$

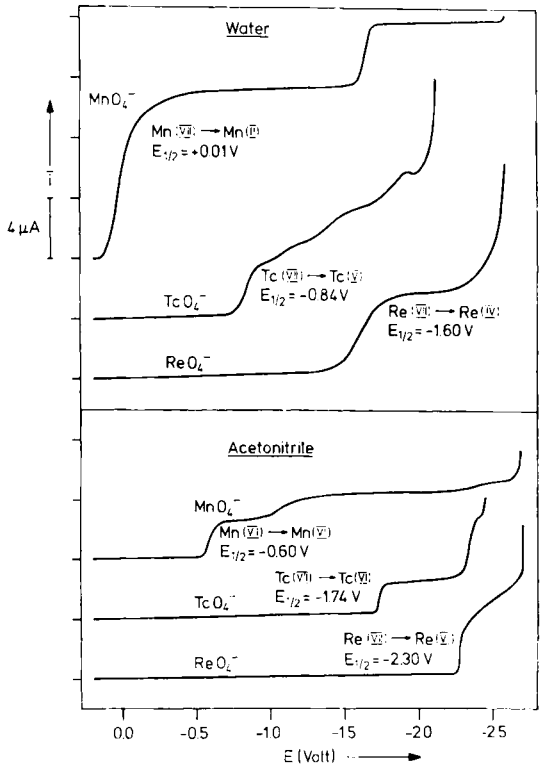

Fig. 6.1.A D.C. polarograms of 10^{-3} M MnO_4^-, TcO_4^-, and ReO_4^- in water and acetonitrile. Supporting electrolyte 0.05 M $(CH_3)_4NClO_4$, drop time 0.5 s, flow rate of mercury 0.923 mg/s, temperature 25 °C [31].

and $l°$=26.2 $\Omega^{-1} \cdot cm^2$, respectively, at 25 °C, and the corresponding diffusion coefficients of TcO_4^- are $D°=3.40 \cdot 10^{-5}$ and $0.70 \cdot 10^{-5}$ $cm^2 \cdot s^{-1}$ [31]. The slightly soluble tetramethylammonium salts of dark green manganate(VI), violet technetate(VI), and olive green rhenate(VI) were prepared most purely with a yield of more than 90 % by controlled-potential electrolytic reduction of MnO_4^-, TcO_4^-, and ReO_4^- at a platinum electrode in deaerated acetonitrile containing 0.04 M $[(CH_3)_4N]ClO_4$. Tetraoxotechnetate(VI) and -rhenate(VI) proved to be considerably more sensitive to oxygen and moisture than tetraoxomanganate(VI). TcO_4^{2-} was shown to undergo rapid disproportionation [31] to pertechnetate and a Tc(+5) species according to

$$2\,Tc(+6) \rightarrow Tc(+7) + Tc(+5)$$

Some years later the detection and production of transient hexavalent technetium in aqueous alkaline media by pulsed radiolysis and very fast scan cyclic voltammetry were reported [32]. More recently, the mechanism of the stepwise reduction of TcO_4^- to Tc(+6), Tc(+5) and Tc(+4) in alkaline solution was reinvestigated in detail by pulsed and dc polarography [33].

Some standard oxidation/reduction electrode potentials of fundamental technetium couples are summarized in Table 6.2.A

Table 6.2.A Redox potentials Eh[V] of some technetium couples in aqueous solution at 25 °C.

Reaction	Potential Eh[V]	References
$TcO_4^- + 4H^+ + 3e^- \leftrightarrow TcO_2 + 2H_2O$	+0.747	[9]
	+0.738	[34]
	+0.782	[35]
	+0.769	[36]
$TcO_4^- + 8H^+ + 7e^- \leftrightarrow Tc + 4H_2O$	+0.472	[35]
	+0.477	[8]
$TcO_2 + 4H^+ + 4e^- \leftrightarrow Tc + 2H_2O$	+0.272	[34]
	+0.240	[35]
	+0.281	[8]
$TcO_4^- + e^- \cdot TcO_4^{2-}$	+0.61	[32]
	+0.65	[8]

Only potentials that refer to couples of chemically defined species are quoted. Couples containing compounds or ions like TcO_3, Tc [8], TcO_3^-, TcO_5^{2-} [12] or other hypothetical species like Tc_3O_4, Tc_4O_7, and hydrous oxides of low-valent technetium [37], the existence of which has not been proved till now, are neglected.

6.2 Thermodynamic data

Soon after the first isolation of milligram amounts of technetium, thermodynamic properties of the element and of several technetium compounds were determined [8]. Currently known thermodynamic data on enthalpies $\Delta H°_f$, entropies $S°$, and Gibbs free energies $\Delta G°_f$ are compiled in Table 6.3.A.

Technetium metal melts at 2413 ± 20 K [45]. The melting point is near those of other elements in the same period of the periodic system, e.g., molybdenum (2893 K) or ruthenium (2723 K). Rhenium melts more than 1000° higher (3453 K) than technetium, while the melting point of manganese (1533 K) is considerably lower. The heat of melting of technetium was estimated to be 5.5 kcal · mole^{-1} [37], the entropy of fusion $\Delta_f S$ to be 3.3 cal · mole^{-1} · K^{-1} [38], the heat of sublimation at 298.15 K as 152 ± 2 kcal · mole^{-1} [47], the normal boiling point at 4900 K and the accompanying heat of vaporization is 138 kcal · mole^{-1} [37]. The heat capacity of technetium metal increases slightly from 6.87 cal · mole^{-1} · K^{-1} at 1000 K to 7.34 cal · mole^{-1} · K^{-1} at 1600 K [46], the liquid heat capacity was calculated as 11.2 cal · mole^{-1} · K^{-1} [38], and the heat capacity for monoatomic technetium vapor as 4.98 cal · mole^{-1} · K^{-1} at 298 K [37].

TcO_2 does not decompose up to 1400 K and sublimes *in vacuo* at temperatures above 1300 K [48]. For the dissociation $TcO_2(g) \leftrightarrow Tc(g) + 2\,O(g)$ the enthalpy ΔH at 298 K is estimated to be 255 ± 14 kcal/mole [49].

The melting point of Tc_2O_7 was determined to be 392.6 ± 0.1 K [50]. Extrapolation of the vapor pressure of liquid Tc_2O_7 yielded a boiling point of 584 ± 2 K [51]. The vapor pressure of crystalline and liquid Tc_2O_7 follows a two-term equation between 298 and 533 K [51]:

Table 6.3.A Thermodynamic data of elemental technetium and some of its compounds at 298.15 K.

Substance	Enthalpy ΔH°_f [kcal·mole^{-1}]	Entropy S° [cal·mole^{-1}·K^{-1}]	Gibbs free energy ΔG°_f [kcal·mole^{-1}]	Method	References
Tc (cryst)	0.0	7.4 ± 0.2	0.0	–	[8]
	—	8.0	—	estim.	[37]
	-	7.89 ± 0.08	—	calc.	[38]
Tc (gaseous)	-	43.26 ± 0.01		calc.	[8,37]
TcO_2 (cryst)	−109 ± 1	13.0	−96 ± 2	calor.	[39,40]
	−104 ± 2	14.9 ± 0.5	−91 ± 2	potentiom.	[8,35]
	-101	–	−88	potentiom.	[34]
TcO_3 (cryst)	−129 ± 5	17.3 ± 0.6	−110 ± 5	estim.	[8,35]
Tc_2O_7 (cryst)	−266 ± 3	46 ± 2	-224 ± 3	calor.	[8,35]
	−270 ± 2	—	—	calor.	[41]
Tc_2O_7 (gaseous)	-236 ± 2	108 ± 3	−213 ± 4	calc.	[42]
$HTcO_4$ (cryst)	−167 ± 1	33 ± 2	−141 ± 1	calor.	[8,35]
$KTcO_4$ (cryst)	−243 ± 2	39.7 ± 0.1	−219 ± 2	calc.	[8,35]
	-245 ± 1	39.38	−220 ± 2	calor.	[42,43]
TcO_4^- (aq)	−173 ± 1	46.0 ± 0.1	−151 ± 1	calor.	[8,35]
	-	47.2 ± 0.3	—	calor.	[43]
	−171 ± 1	47.6 ± 0.3	-149 ± 2	calc.	[42]
TcF_6 (cryst)	—	60.65 ± 0.06		calor.	[44]
$K_2[TcCl_6]$ (cryst)	-	80 ± 1	—	—	[8]

Crystalline Tc_2O_7: $\log P$ [mmHg] $= -\frac{7205}{T} \pm 18.279$

Liquid Tc_2O_7: $\log P$ [mmHg] $= -\frac{3571}{T} \pm 8.999$

The enthalpy of solution of crystalline Tc_2O_7 in water was measured calorimetrically. The value ΔH° (solution) at 298.15 K is 11.0 ± 0.3 kcal · mole^{-1} [41].

$KTcO_4$ melts at 813 K and sublimes without decomposition at about 1300 K [52]. The heat capacity of $KTcO_4$ was determined over the temperature range of 10 to 310 K. The standard heat capacity C_p° at 298.15 K is 29.47 cal · mole^{-1} · K^{-1} [43].

TcF_6 melts at 310.6 K to a yellow liquid that boils at 328.5 K [53]. The heat capacity C_p° of TcF_6 was found to be 37.76 cal · mole^{-1} · K^{-1} at 298.15 K [44]. At the melting point the heat of sublimation is 8.555 kcal · mole^{-1}, the heat of vaporization 7.427 kcal · mole^{-1}, the heat of fusion 1.128 kcal · mole^{-1}, and the entropy of fusion 3.63 cal · deg^{-1} · mole^{-1} [53].

TcO_3F has its melting point at 291.5 K, the boiling point of the yellow liquid is about 373 K, as extrapolated from vapor-pressure measurements. The heat of fusion is 5.377 kcal · mole^{-1}, the heat of sublimation of the solid 14.832 kcal · mole^{-1}, and the heat of vaporization of the liquid 9.453 kcal · mole^{-1} [54].

$TcOF_4$ melts at 407 K and has a boiling point of 438 K. Its heat of fusion is 6.7 kcal · mole $^{-1}$, the heat of vaporization 11.6 kcal · mole^{-1}, the heat of sublimation above 357.5 K is 18.3 kcal · mole $^{-1}$, and the vaporization enthropy 26.5 cal · deg^{-1} · mole $^{-1}$ [55].

6.3 Stability and reactivity of technetium compounds

Thermodynamic stability, bonding strength, and kinetic lability of technetium compounds are highly significant for characterizing technetium chemistry, in particular to compare with the chemistry of the congener rhenium. Such characterizations are of special concern for the development of ^{99m}Tc and $^{186/188}$Re radiopharmaceuticals and their application in nuclear medicine. Qualitatively, there is some experimental evidence that under similar conditions the compounds of technetium frequently appear to be more reactive than the corresponding rhenium compounds. However, only a few quantitative results on stability, bond strengths and reactivity are available to date [56]. Already more than 30 years ago comparative studies were first accomplished on hexahalide complexes of Tc(IV) and Re(IV) (Tables 6.4.A and 6.5.A).

Table 6.4.A Formation constants, force constants, and crystal field stabilization energies of Tc(IV) and Re(IV) hexahalide complexes [57–59].

Parameter	$[TcCl_6]^{2-}$	$[ReCl_6]^{2-}$	$[TcBr_6]^{2-}$	$[ReBr_6]^{2-}$
Formation constant k_6 [10^4 · mole $^{-1}$ · l]	4.6	220	0.38	18
Stretching force constant f_r [mdyne · Å^{-1}]	1.44	1.62	1.31	1.35
Crystal field stabilization energy C.F.S.E [kcal · mole^{-1}]	–83.6	–98.4	–64.1	–72.0

The stepwise formation constants k_6 of hexachloro- and hexabromotechnetate(IV) and -rhenate(IV) were measured potentiometrically in 3M $HClO_4$ solutions at 15 °C. The easy decomposition of the complexes by hydrolysis required strongly acidic solutions. The formation constants of both the chloride and bromide complexes of Tc(IV) turn out to be lower by almost a factor of 50 compared with the formation constants of the corresponding rhenium compounds, thus demonstrating the considerably lower stability of the Tc complexes under the same conditions [57]. The metal–halogen stretching force constants of the complexes were calculated in the valence force field on the basis of the vibrational frequencies measured by IR and Raman spectroscopy in the range 1000–45 cm^{-1} [58]. The chlorine bond and the bromine bond of technetium are weaker than the analogous bonds in rhenium complexes, yet less so for the bromide complexes. The formation constants k_6 and the stretching force constants f_r suggest lower bond energies for the technetium complexes, which may be partially related to the lower crystal field stabilization energies (C.F.S.E.) [57]. For octahedral d^3 complexes the stabilization energy is –12 Dq. The crystal field splitting parameters 10 Dq were derived from the polarized electronic absorption spectra of the Tc(IV) and Re(IV) hexahalide complexes [59].

The rate of isotopic exchange by ligand substitution is the most useful estimate of the lability of complexes. An isotopic exchange reaction essentially involves no overall enthalpy change and the Gibbs free energy is given by the entropy of isotopic mixing. The ligand exchange rate of 10^{-2}M solutions of the hexachloride and hexabromide complexes of Tc(IV) and Re(IV) in corresponding 8 M hydrohalic acids was measured at 60 °C after the complexes were labeled with the β^--emitter ^{36}Cl and the β -, γ-emitter ^{82}Br, respectively (Table 6.5.A).

Table 6.5.A Exchange rates R and activation energies E_a of chloride and bromide isotopic exchange in Tc(IV) and Re(IV) hexahalide complexes [57].

Ligand exchange reactions	R(60 °C) [10^{-4} mole·l^{-1}·h^{-1}]	E_a kcal·mole^{-1}
$[TcCl_5{}^{36}Cl]^{2-}+Cl^- \rightarrow [TcCl_6]^{2-}+{}^{36}Cl^-$	29.0	28.4
$[ReCl_5{}^{36}Cl]^{2-}+Cl^- \rightarrow [ReCl_6]^{2-}+{}^{36}Cl^-$	1.29	30.3
$[TcBr_5{}^{82}Br]^{2-}+Br^- \rightarrow [TcBr_6]^{2-}+{}^{82}Br^-$	5030	22.8
$[ReBr_5{}^{82}Br]^{2-}+Br^- \rightarrow [ReBr_6]^{2-}+{}^{82}Br^-$	81.6	27.5

The isotopic exchange rate R is defined by the expression [60]

$$R = -\ln(1-F)\,\frac{a\cdot b}{a+b}\cdot\frac{1}{t}$$

where F is the degree of exchange, a the complex concentration, b the free ligand concentration, and t the time. The radioactivity of $^{36}Cl^-$ and $^{82}Br^-$ in the hydrohalic acid solutions was measured as a function of time after precipitation of the complexes with Cs^+. Under the same conditions the ligand exchange rate R of $[TcCl_6]^{2-}$ was found to be more than 20 times higher than the exchange rate of $[ReCl_6]^{2-}$. For the bromide complexes the rates even differ by a factor of more than 60. Obviously the technetium hexahalide complexes exhibit a considerably higher reactivity [57], which may qualitatively be understandable in view of the lower crystal field activation energy (C.F.A.E.) [68, 69].

Another example demonstrating that technetium compounds are more reactive than the analogous compounds of rhenium is the racemization of the penicillamine complexes of Tc(V) and Re(V). The complexes are six-coordinate in solution with one tridentate and one bidentate penicillamine (pen) and one oxo ligand. Both mixed ligand anionic complexes [(*D*-pen)(*L*-pen)TcO]$^-$ and [(*D*-pen)(*L*-pen)ReO]$^-$ undergo a unimolecular racemization by exchange of carboxylates at the site *trans* to the oxo ligand:

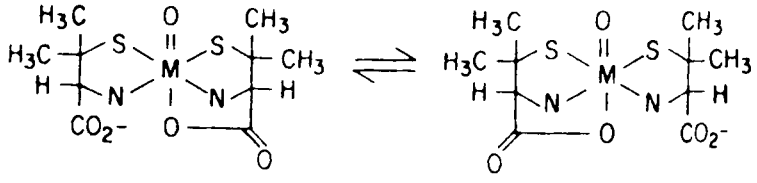

M = Tc: k=940 s^{-1}, E_a=13.4 kcal/mole

M = Re: k=15.5 s^{-1}, E_a=18.5 kcal/mole

The kinetics of these processes were measured at 25 °C by complete line-shape analysis of the ^1H NMR spectra. The racemization reaction of $[(D\text{-pen})(L\text{-pen})TcO]^-$ proceeds nearly 60 times faster than the racemization of the corresponding complex of rhenium [61].

The displacement of water in the analogous complexes *trans*-$[Tc^VO(OH_2)(CN)_4]$ and *trans*-$[Re^VO(OH_2)(CN)_4]$ by NCS^- ions in an aqueous medium was monitored spectrophotometrically [62] using a stopped-flow technique [63]. The substitution of water by thiocyanate can be represented by the bimolecular reaction:

$$[MO(OH_2)(CN)_4] + NCS^- \leftrightarrow [MO(NCS)(CN)_4]^{2-} + H_2O,\ M=Tc \text{ or } Re$$

IR and X-ray structural analyses [64] established the N-bonding of the NCS^- ligand in both complexes. The rate constant k(Tc) for the reaction of *trans*-$[TcO(OH_2)(CN)_4]^-$ with thiocyanate at 25 °C was found to be 22.2 mole$^{-1} \cdot s^{-1}$, while k(Re), evaluated under the same conditions, was only $35 \cdot 10^{-4}$ mole$^{-1} \cdot s^{-1}$ [62,65]. The rate constant k(Tc) turns out to be over 6000 times higher than k(Re) of the rhenium complex.

The kinetics of pyridine (py) exchange on the cations *trans*-$[Tc^VO_2(py)_4]^+$ and *trans*-$[Re^VO_2(py)_4]^+$ were followed by ^1H NMR in deuterated nitromethane using deuterated pyridine as the reacting ligand (Table 6.6.A).

Table 6.6.A Exchange rates of pyridine in Tc(V) and Re(V) *trans*-dioxopyridine complexes [66].

Ligand exchange reactions	Rate constant k (25 °C) [$10^{-6} \cdot s^{-1}$]
$[TcO_2(py)_4]^+ + 4py\text{-}d_5 \xrightarrow{CD_3NO_2} [TcO_2(py\text{-}d_5)_4]^+ + 4py$	40.000
$[ReO_2(py)_4]^+ + 4py\text{-}d_5 \xrightarrow{CD_3NO_2} [ReO_2(py\text{-}d_5)_4]^+ + 4py$	5.5

The rate law for pyridine exchange was first-order in both complexes and zero-order in pyridine (py-d_5). The rate-determining step in the exchange reactions is a dissociative mechanism. The ratio of the pyridine exchange rate constants k(Tc)/k(Re) at 25 °C was found to be more than 7000 [66].

These examples also demonstrate the higher reactivity of the technetium complexes with respect to the analogous compounds of rhenium. Qualitatively, the results seem to be independent of the anionic or cationic character of the complexes, the oxidation state of the central atoms, the presence or absence of an MO^{3+} or MO_2^+ core, and the reaction order. However, it was recently reported that the exchange of oxygen between water and the oxo core complexes $[Tc^VO(DBDS)]$ and $[Re^VO(DBDS)]$ {DBDS=N,N′-bis(mercaptoacetyl)butane-1,4-diamine}:

$$[M^VO(DBDS)] + {}^{17}OH_2 \xrightarrow{d_6\text{-DMSO}} [M^V\,{}^{17}O(DBDS)] + H_2O$$

yields rate constants at 25 °C of $7.1 \cdot 10^{-4}$ mole$^{-1} \cdot s^{-1}$ for $[Tc^VO(DBDS)]^+$ and $7.5 \cdot 10^{-3}$ mole$^{-1} \cdot s^{-1}$ for $[Re^VO(DBDS)]^+$, demonstrating a rate constant ratio k(Tc)/k(Re) < 1 ≈ 0.1. These oxygen exchange reactions are base catalyzed and no exchange was detected without the addition of base. Sodium methoxide was used as a catalyst and

d_6-DMSO as the solvent. The rate of water exchange was measured with ^{17}O NMR. The rate law can be expressed as

$$R = k[M^{V}O(DBDS)]\,[CH_3O^-]\,.$$

This rate law is consistent with an associative mode of activation. Base attack on the metal center leads to the expansion of the coordination number of the metal from 5 to 6. The supposed stronger Tc=O bond generates larger kinetic *trans* effects and makes associative attack by CH_3O^- less favorable than the somewhat weaker Re=O bond. The six-coordinate complexes mentioned above may react by a dissociative activation mode [67].

Additional results for comparing analogous compounds of technetium and rhenium with respect to both reactivity and thermodynamic stability would be desirable, taking into account electron configurations, molecular structures, and strength of bonding and of ligand fields.

6.4 References

[1] J. A. Rard, M. H. Rand, J. R. Thornback, and H. Wanner, J. Chem. Phys. *94*, 6336–6337 (1991)
[2] K. G. Kessler and R. E. Trees, Phys. Rev. *92*, 303–307 (1953)
[3] D. O. Van Ostenburg, H. Trapp, and D. J. Lam, Phys. Rev. *126*, 938–940 (1962)
[4] W. F. Meggers, J. Res. Natl. Bur. Stand. *47*, 7–14 (1951)
[5] P. J. Hay and W. R. Wadt, J. Chem. Phys. *82*, 270–283 (1985)
[6] J. C. Hileman, D. K. Huggins, and H. D. Kaesz, Inorg. Chem. *1*, 933–938 (1962)
[7] K. Schwochau, Some fundamental aspects of technetium chemistry in: Technetium in Chemistry and Nuclear Medicine 2, (M. Nicolini, G. Bandoli, U. Mazzi, eds.), Cortina International, Verona, Raven Press, New York (1986), pp. 13–23.
[8] G. E. Boyd, J. Chem. Educ. *36*, 3–14 (1959)
[9] R. E. Meyer and W. D. Arnold, Radiochim. Acta 55, 19–22 (1991)
[10] D. R. Lide and H. P. R. Frederikse (eds.), CRC Handbook of Chemistry and Physics, CRC Press, 75th Edition (1994/95), pp. 11–59
[11] R. J. Magee and T. J. Cardwell in: Encyclopedia of Electrochemistry of the Elements, Vol. II (A. J. Bard, ed.), Marcel Dekker, New York (1974), pp. 125–189
[12] M. Jovtschev, H. Koch, and H. Kupsch, Isotopenpraxis *11*, 369-378 (1975)
[13] C. D. Russell, J. Appl. Radiat. Isot. *33*, 883–889 (1982)
[14] H. H. Miller, M. T. Kelley, and P. F. Thomason, Advan. Polarog. *2*, 716-726 (1959)
[15] R. J. Magee, J. A. P. Scott, and C. L. Wilson, Talanta *2*, 376–379 (1959)
[16] R. Colton, J. Dalziel, W. P. Griffith, and G. Wilkinson, J. Chem. Soc. 71-78 (1960)
[17] A. F. Kuzina, S. I. Zhadanov, and V. I. Spitsyn, Dokl. Akad. Nauk. SSSR *144*, 836 (1962)
[18] G. B. S. Salaria, C. L. Rulfs, and P. J. Elving, J. Chem. Soc. 2479-2484 (1963)
[19] G. B. S. Salaria, C. L. Rulfs, and P. J. Elving, Anal. Chem. *35*, 979-982 (1967)
[20] C. L. Rulfs, R. Pacer, and A. Anderson, J. Electroanal. Chem. *15*, 61–66 (1967)
[21] L. Astheimer and K. Schwochau, J. Electoanal. Chem. *8*, 382-389 (1964)
[22] J. Grassi, J. Devynck, and B. Trémillon, Anal. Chim. Acta *107*, 47–58 (1979)
[23] K. Schwochau and L. Astheimer, Z. Naturforschg. *17a*, 820 (1962)
[24] V. P. Shvedov and K. V. Kotegov, Soviet Radiochem. 5, 342-345 (1963)
[25] L. Astheimer, K. Schwochau, and W. Herr, J. Electroanal. Chem. *14*, 161–167 (1967)
[26] A. A. Terry and H. E. Zittel, Anal. Chem. *35*, 614–618 (1963)
[27] J. Grassi, P. Rogelet, J. Devynck, and B. Trémillon, J. Electroanal. Chem. *88*, 97-103 (1978)
[28] G. A. Mazzocchin, F. Magno, U. Mazzi, and R. Portanova, Inorg. Chim. Acta 9, 263–268 (1974)

[29] V. I. Spitsyn, A. F. Kuzina, A. A. Oblova, M. I. Glinkina, and L. I. Stepovaya, J. Radioanal. Chem. *30*, 561–566 (1976)
[30] G. Kissel and S. W. Feldberg, J. Phys. Chem. *73*, 3082–3088 (1969)
[31] L. Astheimer and K. Schwochau, J. Inorg. Nucl. Chem. *38*, 1131–1134 (1976)
[32] F. Deutsch, W. R. Heineman, R. Hurst, J. C. Sullivan, W. A. Mulac, and S. Gordon, J. Chem. Soc. Chem. Commun. 1038–1040, (1978)
[33] A. Founta, D. A. Aikens, and H. M. Clark, J. Electroanal. Chem. *219*, 221–246 (1987)
[34] G. H. Cartledge and W. T. Smith, Jr., J. Phys. Chem. *59*, 1111–1112 (1955)
[35] J. W. Cobble, W. T. Smith, Jr., and G. E. Boyd, J. Am. Chem. Soc. *75*, 5777–5782 (1953)
[36] I. Liebscher and R. Münze, Zentralinstitut für Kernforschung, Rossendorf/Dresden, ZfK-294 (1975) pp.140–143
[37] D. R. Stull and G. C. Sinke in: Thermodynamic Properties of the Elements. Advances in Chemistry. Series 18. ACS, Washington, D.C. (1956)
[38] A. F. Guillermet and G. Grimvall, J. Less-Common. Met. *147*, 195–211 (1989)
[39] K. B. Burnett, A. B. Campbell, D. J. Jobe, R. J. Lemire, and P. Taylor, Radiochim. Acta *69*, 241–249 (1995)
[40] R. J. Lemire, P. P. S. Saluja, and A. B. Campbell, J. Soln. Chem. *21*, 507 (1992)
[41] K. H. Gayer, A. Y. Herrell, and R. H. Busey, J. Chem. Thermodynamics *8*, 959–964 (1976)
[42] J. A. Rard in: Critical Review of the Chemistry and Thermodynamics of Technetium and Some of its Inorganic Compounds and Aqueous Species, UCRL-53440, Lawrence Livermore National Laboratory (1983)
[43] R. H. Busey, R. B. Bevan, Jr., and R. A. Gilbert, J. Chem. Thermodynamics *4*, 77–84 (1972)
[44] D. W. Osborne, F. Schreiner, K. Otto, J. G. Malm, and H. Selig, J. Chem. Phys. *68*, 1108–1118 (1978)
[45] G. W. Parker, G. E. Creek, W. J. Martin, G. M. Herbert, and P. M. Lantz, Oak Ridge National Laboratory Rep. ORNL-1260, (1952) p. 29
[46] V. I. Spitsyn, V. E. Zinovev, P. V. Gel'd, D. A. Balakhovskii, Dokl. Akad. Nauk SSSR *221*, 145–148 (1975)
[47] R. G. Behrens and G. H. Rinehart, J. Less-Common. Met. *75*, 241–254 (1980)
[48] C. M. Nelson, G. E. Boyd, and W. T. Smith, Jr., J. Am. Chem. Soc. *76*, 348–352 (1954)
[49] L. Brewer and G. M. Rosenblatt, Chem. Rev. *61*, 257–263 (1961)
[50] G. E. Boyd, J. W. Cobble, C. M. Nelson, and W. T. Smith, Jr., J. Am. Chem. Soc. *74*, 556–557 (1952)
[51] W. T. Smith, Jr., J. W. Cobble, and G. E. Boyd, J. Am. Chem. Soc. *75*, 5773–5776 (1953)
[52] E. Anders, Ann. Rev. Nucl. Sci. *9*, 203–216 (1959)
[53] H. Selig and J. G. Malm, J. Inorg. Nucl. Chem. *24*, 641–644 (1962)
[54] H. Selig and J. G. Malm, J. Inorg. Nucl. Chem. *25*, 349–351 (1963)
[55] R. D. Peacock, Comprehensive Inorg. Chem. *3*, 891 (1973)
[56] K. Schwochau and U. Pleger, Radiochim. Acta *63*, 103–110 (1993)
[57] K. Schwochau, Z. Naturforschg. *20a*, 1286–1289 (1965)
[58] K. Schwochau and W. Krasser, Z. Naturforsch. *24a*, 403–407 (1969)
[59] H. J. Schenk and K. Schwochau, Z. Naturforsch. *28a*, 89–97 (1973)
[60] H. A. C. McKay, Nature *142*, 997–998 (1938)
[61] D. L. Johnson, A. R. Fritzberg, B. L. Hawkins, S. Kasina, and D. Eshima, Inorg. Chem. *23*, 4204–4207 (1984)
[62] K. Libson, L. Helm, A. Roodt, C. Cutler, A.E. Merbach, J.C. Sullivan, and E. Deutsch in: Technetium and Rhenium in Chemistry and Nuclear Medicine 3, (M. Nicolini, G. Bandoli, and U. Mazzi, eds.), Cortina International, Verona, Raven Press, New York (1990), pp. 31–33
[63] M. N. Doyle, K. Libson, M. Woods, J. C. Sullivan, and E. Deutsch, Inorg. Chem. *25*, 3367–3371 (1986)
[64] A. Roodt, J. G. Leipoldt, E. A. Deutsch, and J. C. Sullivan, Inorg. Chem. *31*, 1080–1085 (1992)
[65] W. Purcell, A. Roodt, S.S. Basson, and J.G. Leipoldt, Transition Met. Chem. *14*, 224–226 (1989)
[66] L. Helm, K. Deutsch, E. A. Deutsch, and A. E. Merbach, Helv. Chim. Acta *75*, 210–217 (1992)
[67] B. Chen, M. J. Heeg, and E. Deutsch, Inorg. Chem. *31*, 4683–4690 (1992)
[68] K. Schwochau, Zur Komplexchemie und Polarographie des Technetiums, Bericht der Kernforschungsanlage Jülich, Institut für Radiochemie, JÜL-465-RC (1967)
[69] F. Basolo and R. G. Pearson, Mechanisms of Inorganic Reactions. A Study of Metal Complexes in Solution. 2nd ed., John Wiley & Sons, Inc., New York (1967)

This Page Intentionally Left Blank

7 Analytical chemistry

Progress in technetium chemistry obviously depends on sensitive analytical methods to detect this radioelement, to efficiently separate it, and to determine technetium accurately. Several reviews on the analytical chemistry of technetium have been published [1–7]. Even the discovery of technetium was conclusive only because separation techniques known at the time for the homologous element rhenium were used [8]. Furthermore, the detection of naturally occurring technetium or the determination of the element in the environment presupposed the application of highly sensitive methods. The effective extraction of pertechnetate into organic solvents for the isolation of technetium from fission product waste solutions is, in addition, an example of the significance of appropriate techniques in analytical chemistry.

7.1 Determination methods

7.1.1 Radiometry

An obvious method for the detection and determination of Tc is based on the β^- activity of ^{99}Tc whose specific activity amounts to $3.7698 \cdot 10^4$ disintegrations per minute and microgram. ^{99}Tc emits only β^- particles and no γ quanta. However, the low energy of the β^- particles (E_{max}=292 keV) imposes several difficulties on the quantitative determination, caused by self-absorption in the sample, back scattering of β particles, and the geometry of counting. In order to avoid errors, the sample should be carefully prepared for counting. Preparations like electrodeposition are recommended to form thin layers on a film of mica or collodion. The film is rendered conductive by vacuum evaporation of gold onto the surface [9]. In practice, ordinary end-window counters with a thin mica window can determine about 0.1 µg of ^{99}Tc. The use of special low-background apparatus permits one to raise the sensitivity by another two or three orders of magnitude [5]. For example, low background β^- counter was employed to count ^{99}Tc fractions isolated from pitchblende. The background was about 0.7 counts per min [10].

Low background β^- counting was also used to determine ^{99}Tc in seawater. The nuclide was preconcentrated from seawater by adsorbing $^{99}TcO_4^-$ on an anion exchanger. It was purified from other radionuclides by scavenging with iron(III)-oxide hydrate and extracting from sodium hydroxide solution into methyl ethyl ketone.

Finally, ^{99}Tc was electrodeposited from an oxalic acid medium onto a bronze disc and counted. The overall recovery was >90 % and the precision ±0.2 pCi ($7.4 \cdot 10^{-3}$ Bq) at a technetium level of 0.6–1.0 pCi/l seawater [11].

To recover and measure $^{99}TcO_4^-$ from a variety of types of water, a method was developed that is based on the elution of $^{99}TcO_4^-$ from an ion-exchange column using thiocyanate, extraction of the formed thiocyanate complex into butane-2-one, evaporating the solution onto a planchet and counting the ^{99}Tc β^- emission with a Geiger-Müller tube. The method recovered as little as 10 ^{15}g of ^{99}Tc in 500 ml of seawater [12].

High counting efficiencies can be achieved by using gas-flow counters, while liquid scintillation counters are most suitable when the samples are soluble in the scintillation liquid [13]. The determination of ^{99}Tc in urine gave a better limit of detection with a gas proportional counter than with liquid scintillation methods. The recovery of ^{99}Tc using a gas proportional counter was 80 % and the detection limit 20 mBq, having a counting time of 20 minutes, a counting efficiency of 24 % and a background of 1.3 counts per minute [14]. For the determination of ^{99}Tc in environmental samples like rainwater, riverwater, seawater, biota, soils, and sediments, using anti-coincidence shielded Geiger-Müller-gas flow counters, the background could be reduced to 3 mBq and the counting efficiency enhanced to 42 %, which results in a detectable activity of 1.4 mBq for 1400 min counting [15,16]. ^{99}Tc activities measured with a gas-flow proportional counter in air samples from 1965–1967 ranged between 2.6 and 0.2 μBq/m^3 [17].

^{99}Tc was determined in vegetation with a scintillation counter. The samples were wet-ashed without significant loss of technetium, which was separated by co-precipitation with $CaCO_3$, purified by anion-exchange chromatography and electrodeposition. The detection limit for ^{99}Tc in a sample weighing about 10g was 3.7 mBq for a 3000 min count [18]. Liquid scintillation counting was also used to determine ^{99}Tc in effluents from nuclear plants [19] and in soil samples [20]. To determine ^{99}Tc in urine by liquid scintillation counting the nuclide was co-precipitated with tetraphenylarsonium perchlorate. The limit of detection was about 74 mBq in 50 ml of urine. The procedure did not require any concentration of urine samples and gave reproducible yields near 100 % [21].

A highly sensitive method for the determination of trace amounts of ^{99}Tc is neutron activation analysis. The sample containing ^{99}Tc is irradiated with thermal neutrons after separation of interfering nuclides. The radioactive isotope ^{100}Tc with a half-life of only 15.8 s is formed by the reaction

$$^{99}\mathrm{Tc}(n,\gamma)^{100}\mathrm{Tc}.$$

The relatively large cross section of ^{99}Tc for thermal neutrons is σ=19 barn [22]. With a probability of about 94 % ^{100}Tc decays through 3.38 MeV β rays to the stable ^{100}Ru. Most of the remaining 6 % decays through 2.88 MeV β rays, followed by the 0.59–0.54 MeV γ-γ cascade [23,24].

A procedure for the determination of trace amounts of ^{99}Tc in filter paper and vegetation samples by neutron activation analysis has been developed. The procedure

consists of the separation of ^{99}Tc from the sample, irradiation with thermal neutrons at a flux of about $5 \cdot 10^{13}$ n · cm $^{-2} \cdot s^{-1}$ to produce ^{100}Tc, post-irradiation separation and purification of ^{100}Tc from other activated nuclides, and the counting of ^{100}Tc in a low-background β^- counter. The detection limits were $5 \cdot 10^{-12}$ g ^{99}Tc in filter paper samples and $9 \cdot 10^{-12}$ g ^{99}Tc in vegetation samples [24,25].

Using the γ-γ cascade of 0.59–0.54 MeV emitted by ^{100}Tc, ^{99}Tc was determined in samples of 1–2 mg of technetium complex compounds by neutron activation analysis. Moderate sample activities were obtained after an irradiation time of 20 s at a neutron flux of about 10^{12} cm $^{-2} \cdot s^{-1}$. Good agreement between expected and found ^{99}Tc contents was observed. The uncertainty of the mean value could be restricted to less than 1 % [26].

Recently, the determination of ^{99}Tc in mixed fission products by neutron activation was reported. $^{99}TcO_4^-$ was separated from the bulk of fission products and other elements in dissolved nuclear fuel by an iron(III)-oxide-hydrate precipitation. The filtrate containing $^{99}TcO_4^-$ was loaded on an anion exchange resin and ^{99}Tc bonded on the resin was exposed to a neutron flux in a nuclear reactor for only one minute. The counting of the 539 keV γ-rays of ^{100}Tc was performed with a germanium detector and a multichannel analyzer. The minimum detectability was 0.3 µg ^{99}Tc limited by resin impurities and capsule materials [27].

A disadvantage of the above mentioned neutron activation analysis is the rather short ^{100}Tc half-life of 15.8 s. Therefore, other activation reactions were proposed for the determination of ^{99}Tc. When ^{99}Tc was irradiated by fast reactor neutrons in a flux of $5.5 \cdot 10^{12}$ cm$^{-2} \cdot$ s^{-1}, the reaction

$$^{99}\text{Tc}(n,n')^{99m}\text{Tc}$$

was observed. The cross section of the excitation reaction was found to be 0.24 barn [28,29] which is in good agreement with recent evaluations [30]. The half-life of ^{99m}Tc of 6.0 h allows a more convenient elimination of interfering radionuclides than the 15.8 s half-life of ^{100}Tc. The method was applied to the determination of ^{99}Tc in a ^{99m}Tc generator after decay of ^{99m}Tc and ^{99}Mo. The detection limit for ^{99}Tc was calculated to be about 2 Bq, when the 140 keV activity of ^{99m}Tc was measured for a period of 3000 s by a Ge(Li) detector [28].

In addition the nuclear excitation process

$$^{99}\text{Tc}(\gamma,\gamma')^{99m}\text{Tc}$$

was used for the activation analysis of ^{99}Tc. Bremsstrahlung of a maximum energy of 50 MeV, produced by converting electrons from a linear electron accelerator, was irradiating ^{99}Tc compounds such as $[Bu_4N][TcOCl_4]$ at a temperature below −100 °C. The production rate of ^{99m}Tc per µg ^{99}Tc was linearly correlated with the flux of bremsstrahlung. The detection limit was estimated to be on the order of 10^{-9}g of ^{99}Tc under the optimum irradiation conditions [31]. The determination of ^{99}Tc by nuclear excitation must take into consideration the interference of the following nuclear reactions:

$$^{100}Mo(\gamma,n)^{99}Mo \xrightarrow{\beta} {}^{99m}Tc,$$

$$^{100}Ru(\gamma,p)^{99m}Tc,$$

and $$^{92}Mo(\gamma,2n)^{90}Mo \xrightarrow{\beta^+} {}^{90}Nb$$

The last reaction forms ^{90}Nb which emits γ quanta of 141 keV and cannot be readily discriminated from the 140 keV quanta of ^{99m}Tc [32].

For routine determination of ^{99}Tc in solutions a fast and convenient method was reported that uses the measurement of bremsstrahlung emitted by conversion of ^{99}Tc β particles at the wall of a vial containing the ^{99}Tc compound in a suitable solvent. A sample of 0.1–0.5 mg ^{99}Tc in 5 ml solution was transferred to a vial and measured within a well-type γ-ray NaI(Tl) scintillation detector. The background was about 1000 counts/min, the counting efficiency 39.4 counts/min for 1 µg of ^{99}Tc. The elemental composition of the sample and the solution density did not affect the determination [33].

7.1.2 Spectrometry

The arc and spark emission spectra of technetium are uniquely characteristic of the element. The measured wavelengths range from 2261.30 (ultraviolet) to 8829.80 Å (near infrared). More than 2300 lines that are characteristic of Tc atoms, TcI, or unipositively charged Tc^+ ions, TcII, were recorded. The strongest TcI lines have the wavelengths 4297.06, 4262.26, 4238.19, 4031.63, and 3636.10 Å. The strongest TcII lines are observed at 2543.24, 2610.00, and 2647.02 Å [34–37]. Several lines are free from ruthenium or rhenium interferences [38] and are useful for detecting ^{99}Tc in concentrations of the order of 10^{-7} [35]. As little as 0.1 µg of technetium electroplated onto copper electrodes may be detected by using the line at 4031.63 Å [36].

The three strong TcII lines were used as sensitive emission lines for the determination of ^{99}Tc by inductively coupled plasma optical emission spectrometry (ICP-OES), which achieves a detection limit of around 4 µg $^{99}Tc/l$. The convenience of this approach makes it particularly suitable for on-line HPLC detection in speciation studies at enhanced environmental technetium levels [39]. Examples of this type of procedure for the determination of elements are described in reviews [40,41].

The determination of technetium by atomic absorption spectrophotometry was studied with a ^{99}Tc hollow-cathode lamp as a spectral line source. The sensitivity for technetium in aqueous solution was $3 \cdot 10^{-6}$ g/ml in a fuel-rich acetylene-air flame for the unresolved 2614.23–2615.87 Å doublet. Cationic interferences were eliminated by adding aluminum to the sample solutions. The applicability of atomic absorption spectrophotometry to the determination of technetium in uranium and a uranium alloy was demonstrated [42]. A detection limit of $6 \cdot 10^{-11}$ g was achieved for measuring technetium by graphite furnace atomic absorption spectrometry. In using the same doublet and both argon and neon as fill gases for the lamp, $6 \cdot 10^{-11}$ to $3 \cdot 10^{-9}$ g of technetium was found to be the range of applicability [43].

Several X-ray fluorescence spectrometric determinations of technetium were reported. The lines $K_{\alpha 2}$=0.67927 Å, $K_{\alpha 1}$=0.67493 Å, $K_{\beta 1}$=0.60141 Å, and $K_{\beta 2}$= 0.59018 Å can be used for detection and determination of the element [30,31]. From neutron irradiated molybdenum milligram quantities of ^{99}Tc could be isolated and detected by the $K_{\alpha 1}$ and $K_{\beta 1}$ lines [46]. Because of its simplicity and selectivity, an X-ray fluorescence method was developed for the determination of technetium in solution. At concentrations of less than 1.0 mg ^{99}Tc per ml no interelement effects were observed. Therefore, it is possible to ascertain technetium in its compounds without their prior decomposition, provided the compounds are soluble in water or dioxane. The detection limit is about $4 \cdot 10^{-6}$ g ^{99}Tc [47]. For the determination of ^{99}Tc in nuclear fuel processing wastes by X-ray fluorescence, a rapid, simple, and accurate method was reported [48].

The mass spectrometric determination of technetium is a highly sensitive and frequently applied method. Tc isotopes formed upon bombardment of a molybdenum target with 22 MeV protons were identified by mass spectrometry. The technetium fraction was separated and purified by anion exchange chromatography and the isotopes (abundance) ^{95}Tc (0.5 %), ^{97}Tc (56.0 %), ^{98}Tc (17.3 %), and ^{99}Tc (26.7 %) were detected in about 1 µg technetium on a mass spectrometer for the first time (Fig. 7.1.A). As little as $5 \cdot 10^{-9}$ g of technetium could be measured by mass spectrometry [49].

An improved isotope dilution mass spectrometric technique was developed for the analysis of ^{99}Tc in environmental samples. ^{99}Tc is isolated from the sample, after spiking with ^{97}Tc as a yield tracer, by ion-exchange chromatography and solvent extraction. Technetium is then concentrated onto a pair of anion exchange beads of 0.3 mm in diameter. Determination of 10^{-12} g of technetium was achieved through the enhanced ionization efficiency afforded by the resin bead source [50]. Spark source mass spectrometry was

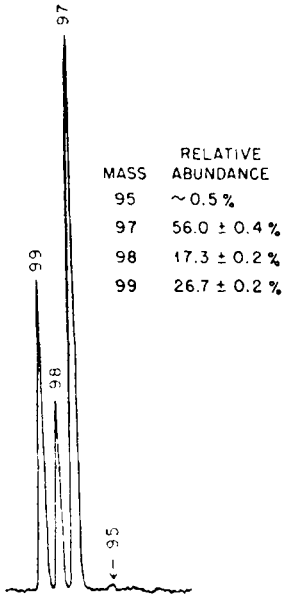

Fig. 7.1.A Mass spectrogram of technetium produced by the irradiation of molybdenum metal with 22 MeV protons [49].

used for survey elemental analyses on compounds of ^{99}Tc. The method allowed the simultaneous detection of numerous elements within the ppb range [51].

Recently, inductively coupled plasma mass spectrometry (ICP-MS) was proven to be an extremely sensitive method of high resolution, high precision, and short measuring time [52]. It was used for the detection and determination of technetium [53] in environmental materials. To determine ^{99}Tc by ICP-MS the sample has to be completely purified from ^{99}Ru. Technetium was efficiently extracted as pertechnetate from 1 M K_2CO_3 by cyclohexanone; the decontamination factor for ruthenium was found to be $7 \cdot 10^4$, when the sample was pretreated with hydrogen peroxide [54]. Several methods were studied for the separation of technetium from ruthenium [55]. Soil and sediment samples were analyzed [56,57]. The detection limit of $1.73 \cdot 10^{-12}$ g was found to be lower than for liquid scintillation or low background gas flow counting [54]. ^{99}Tc was determined by ICP-MS in coastal seawater after reduction of TcO_4^- and enrichment of Tc by co-precipitation with iron(III)-oxide hydrate. A detection limit of 1.1 µBq/l ($1.73 \cdot 10^{-15}$ g/l) ^{99}Tc was achieved [58]. Technetium analysis at the ultra-trace level was performed with high-resolution inductively coupled plasma mass spectrometry (HR-ICP-MS). By means of a double focusing analyzer the mass resolution was improved and the background reduced, since no photons reach the detector due to a longer and more complicated ion flight path and the use of narrow slits [59]. Intertidal coastal and estuarine sediments of the Irish Sea were analyzed by HR-ICP-MS for ^{99}Tc and other radionuclides discharged from the Sellafield nuclear fuel reprocessing plant [60]. By using HR-ICP-MS in combination with an ultrasonic nebulizer a detection limit for ^{99}Tc of $8 \cdot 10^{-15}$ g/ml was reported [61].

In addition, laser resonance ionization mass spectrometry (RIMS) was employed for the detection of trace amounts of technetium. Three-step laser resonance photoionization combined with a mass measurement results in an almost unambiguous element and isotope assignment. A detection limit of 10^7 atoms can be reached if the ionization is performed via an autoionizing state and the mass measurement with a conventional time-of-flight mass spectrometer [62]. A reflectron time-of-flight spectrometer enhances the efficiency of RIMS by about one order of magnitude, enabling the detection of about 10^6 atoms ($1.6 \cdot 10^{-16}$ g of ^{99}Tc) [59]. A chemical procedure for the isolation of ^{99}Tc from environmental aqueous samples and its detection by RIMS has been presented [62]. Negative thermal ionization was shown to be a possible means of performing high ionization efficiency mass spectrometry. Technetium was measured as the TcO_4^- ion. Samples of technetium from 10^{-9} down to 10^{-15} g were successfully analyzed with ionization efficiencies of more than 2 %. Such sensitivity simplifies the determination of ^{99}Tc in environmental samples, because the sample weight requirement may be reduced to a few grams [63].

7.1.3 Spectrophotometry

The spectrophotometric methods developed for the determination of technetium are, in general, less sensitive than the sophisticated spectrometric techniques. However, spectrophotometry is often simple and rapid.

Aqueous solutions of pertechnetate display rather strong absorptions in the UV range. A simple method of ascertaining technetium involves the measurement of the optical density of aqueous TcO_4^- solutions at the absorption maxima of 244 nm ($40.98 \cdot 10^3$ cm^{-1}) and 287 nm ($34.84 \cdot 10^3$ cm^{-1}) with molar absorbance indices of 5690 and 2170 mole$^{-1} \cdot l \cdot cm^{-1}$, respectively [5, 64]. Beer's law is obeyed up to a concentration of 10^{-3} mole $\cdot l^{-1}$. Thus, less than 1 µg of technetium can easily be determined spectrophotometrically. This method is particularly advantageous in the simultaneous determination of technetium and rhenium. The spectrum of TcO_4^- bears a remarkable resemblance to those of the isoelectronic species ReO_4^- and MnO_4^-, which display a shift to higher and lower wavenumbers, respectively [38,64].

$[TcCl_6]^{2-}$, $[TcBr_6]^{2+}$ and $[TcI_6]^{2-}$ dissolved in the corresponding hydrohalide acids have higher molar absorbance indices [65]. However, a disadvantage of these complexes is their easy hydrolytic decomposition. A procedure for determining technetium spectrophotometrically was developed using $[TcCl_6]^{2-}$. It is based on reducing pertechnetate with conc. HCl to hexachlorotechnetate(IV) and measuring the absorbance at 338 nm, where less than 1 µg Tc/ml may be determined in the presence of microgram amounts of rhenium or molybdenum [66]. The cited molar absorbance index ε(338 nm)=32000 should be corrected to 10600 mole$^{-1} \cdot l \cdot$ cm^{-1} [65].

Pertechnetate, reduced in acidic aqueous solution in excess thiocyanate, forms a red-violet and simultaneously a yellow complex [67]. The red-violet complex $[Tc^{IV}(NCS)_6]^{2-}$ and the yellow complex $[Tc^{III}(NCS)_6]^{3-}$ [68] are coupled in a redox system, the potential of which was found to be Eh = +0.53 V at 25 °C in 1 M H_2SO_4 [69]. The molar absorbance indices of $[Tc^{IV}(NCS)_6]^{2-}$ and $[Tc^{III}(NCS)_6]^{3-}$ in aqueous solutions are ε(503 nm) = $2.7 \cdot 10^4$ mole$^{-1} \cdot l \cdot$ cm^{-1} and ε(403 nm) = $1.7 \cdot 10^4$ mole$^{-1} \cdot l \cdot$ cm^{-1}, respectively [69]. The disadvantages of this spectrophotometric method are the long reaction time, the simultaneous formation of two complexes and the interference of Mo, U, and Fe. An improved technique was used for the determination of Tc in uranium materials [70] and in nuclear fuel solutions [71]. Laser induced photoacoustic spectroscopy (LPAS) was used to determine Tc in solution by formation of $[Tc(NCS)_6]^{2-}$. The determination limit could be improved down to a concentration of 10^{-9} mole $\cdot l^{-1}$ [72].

Microgram amounts of TcO_4^- can be ascertained by measuring the absorbance of the colored complex, formed with toluene-3,4-dithiol in 2.5 M HCl, after extraction into carbon tetrachloride. One hour must be allowed for the development of the color. The molar absorbance index at 450 nm is $1.5 \cdot 10^4$ mole$^{-1} \cdot l \cdot$ cm^{-1}. Beer's law is followed over the range of 1.5 to 16.5 µg Tc/ml. Because many cations interfere, an initial separation of technetium is necessary [73]. The same complex was used for the determination of technetium in uranium fission element alloys after separation of Tc by distillation from sulphuric acid [74]. The complex formation of technetium, rhenium, and molybdenum with toluene-3,4-dithiol and its analytical application have been studied in detail [75].

Thioglycolic acid reacts with pertechnetate at pH 8.0 to a green complex which is determined by measuring the absorbance at 655 nm. Beer's law is obeyed over the range of 2 to 40 µg Tc/ml. The molar absorbance index at 655 nm is estimated to be of the order of 1800. A tenfold excess of F^-, Cl^-, Br^-, I^-, PO_4^{3-}, SO_4^{2-}, WO_4^{2-}, and ReO_4^-

does not disturb the measurements. Significant interferences have only been observed in the case of molybdate, dichromate, and ruthenate [76].

4-thiocresol reduces TcO_4^-, presumably to Tc(V), in acetic acid solution and forms a yellow-brown complex that is readily extracted by chloroform, carbon tetrachloride, benzene, and ether. Unless the concentration of 4-thiocresol is >0.1 % and the concentration of acetic acid is high, ReO_4^- is not reduced. The absorbance of the technetium complex was measured at 410 nm, where the molar absorbance index is about 7350. The elements of the platinum group Ru, Pd, Pt, and Rh interfere and must be removed [77].

Spectrophotometric studies on technetium and rhenium were carried out with $K_4[Fe(CN)_6]$, sulphosalicylic acid, and α-picolinic acid using pertechnetate or perrhenate as starting compounds and bismuth amalgam, $SnCl_2$ or ascorbic acid as reducing agents [78].

α-Furildioxime dissolved in acetone forms a raspberry colored technetium complex, when TcO_4^- is reduced with $SnCl_2$ in hydrochloric acid solution. After 2.5 h the molar absorbance index attains a maximum of $1.3 \cdot 10^4$ mole$^{-1} \cdot 1 \cdot$ cm^{-1} at 520 nm. Between 1 and 10 μg/ml Tc the relationship of the optical density and the Tc concentration was shown to be linear. Tenfold amounts of Mo or Re almost do not affect the photometric determination of technetium [79].

A method was developed to ascertain technetium in the range of μg/ml by reduction of TcO_4^- to Tc(IV) with 1,5-diphenylcarbohydrazide and subsequent complexation of Tc(IV) with the reagent. The absorbance was measured at 520 nm after extraction of the complex in carbon tetrachloride. The molar absorbance index was found to be $4.86 \cdot 10^4$ mole$^{-1} \cdot 1 \cdot$ cm^{-1} [80].

Around 10^{-8} g of technetium were detected by treating an acidified aqueous solution of pertechnetate with a saturated solution of potassium ethyl xanthate. An immediate pink to purple coloration was produced, which is readily extractable into chloroform or carbon tetrachloride. Re, Mn, and Ru did not react, but Mo gave a similar reaction. Pertechnetate, reduced with $SnCl_2$ in HCl, reacts with dimethylglyoxime in ethanol to give a bright green coloration that is stable even at boiling temperature. The test appears likely to be specific for technetium. The limit of identification was 0.04 μg. Aqueous thiourea solution produces by reaction with an acidified TcO_4^- solution an orange-red color, when the reaction mixture is heated for some minutes at 80 °C. Re, Mn, and Ru did not interfere. The identification limit was again 0.04 μg [81].

Microgram amounts of pertechnetate can be assessed by IR spectrophotometry. TcO_4^- is precipitated with $[AsPh_4]Cl$ in the presence of $KClO_4$ as a carrier. The precipitate is dried and mixed with KBr for preparing a disc according to the IR pellet technique. $[AsPh_4]TcO_4$ reveals a strong sharp band at 11.09 μm (901.7 cm^{-1}) which belongs to the stretching vibration $\nu_3(F_2)$. The TcO_4^- concentration is determined by plotting a calibration curve. ReO_4^- and MnO_4^- interfere with the evaluation of TcO_4^- [82].

7.1.4 Gravimetry

Weighable amounts of technetium are readily determined gravimetrically. However, none of the methods is specific. The most common procedures involve weighing of

the precipitate in the form of tetraphenylarsonium pertechnetate [83,84] or nitron pertechnetate.

The precipitation of $[AsPh_4]TcO_4$ is performed from neutral or alkaline solution at pH 8–9 by adding an excess of tetraphenylarsonium chloride. Since the precipitate is slightly soluble in water, the total volume of the solution should be kept to a minimum. In order to avoid significant losses, at least 40 mg of the precipitate is required, since solubility losses of about 1 % have to be taken into account. The solubility product of $[AsPh_4]TcO_4$ is estimated to be $8.6 \cdot 10^{-10}$ at room temperature [85]. The use of a special microtechnique [86] permitted the precipitation, weighing, and determination of about 2 µg of technetium with a standard deviation of ±0.08 µg. The precipitate is filtered, washed with ice-cold water, dried at 110 °C, and weighed as $[AsPh_4]TcO_4$. Perrhenate, permanganate, perchlorate, periodate, iodide, fluoride, bromide, and thiocyanate anions as well as vanadyl cations and nitrate concentrations above 0.5 M interfere with the determination. $[AsPh_4]TcO_4$ is soluble in alcohol.

According to the gravimetric procedure for the determination of rhenium as nitron perrhenate [87], technetium may be ascertained as nitron pertechnetate. The precipitation is carried out in slightly sulphuric or acetic acid solution using a 10 % nitron {1,4-diphenyl-3-(phenylamino)-1H-1,2,4-triazoliumhydroxide} acetate solution. $C_{20}H_{17}N_4TcO_4$ is appreciably soluble in water, thus the volume is kept again to a minimum and before filtration the solution is cooled in ice. The precipitate is washed successively with nitron acetate solution, saturated nitron pertechnetate solution and finally with a little iced water. The precipitate is dried at 110 °C. Perrhenate, permanganate, perchlorate, periodate, nitrate, chloride, bromide, and iodide ions interfere. Technetium can be recovered as NH_4TcO_4 by dissolving nitron pertechnetate in ethyl acetate and shaking the solution with dilute ammonia. Pertechnetate passes into the aqueous layer, but nitron remains in the ester [88].

Finally, the gravimetric determination of metallic technetium may be taken into consideration. Several compounds are easily reduced to metallic technetium in a stream of hydrogen at temperatures of 900–1000 °C. However, this method excludes any compounds that do not decompose and/or volatilize under the conditions of the reduction [1].

7.1.5 Electrochemical methods

The existence of various oxidation states of technetium indicates the possibility of using polarographic, coulometric, and potentiometric techniques for its determination.

7.1.5.1 Polarography

The polarographic reduction of TcO_4^- at a dropping mercury electrode was studied in several supporting electrolytes.

Pertechnetate in 4 M HCl was found to undergo reduction to Tc(IV). A double wave was observed corresponding to a one- and a two-electron transfer. The corre-

sponding half-wave potentials ($E_{1/2}$) of the irreversible and poorly defined waves are –0.52 and –0.68 V *vs* SCE [89]. The polarographic reduction of TcO_4^- in 0.01–4 M $HClO_4$ appeared in two stages. $E_{1/2}$ of the more positive wave shifted from –0.17 to +0.10 V vs SCE with increasing perchloric acid concentration, and coulometric measurements indicated a four-electron process. The second wave at –0.73 V seemed to involve a three-electron step for the reduction of Tc(III) to Tc(O) [90].

In neutral and acidic sulphate solutions TcO_4^- is reduced to Tc(IV), in alkaline medium in a one-electron step to TcO_4^{2-} [91]. In a 0.5 M KCl solution, acidified to pH 2 by adding HCl, TcO_4^- exhibited three diffusion-controlled waves with $E_{1/2}$ –0.14, –0.91, and –1.12 V *vs* SCE. For the first wave the diffusion current constant proved to be rather constant in the range of 0.01–0.2 mM TcO_4^-, suggesting that Tc in concentrations as low as 0.01 mM can be estimated with an accuracy of ±0.8 % [92,93]. 1 M LiCl and 1 M NaOH solutions of TcO_4^- in the concentration range of 10^{-3}–10^{-4} M were studied with direct and alternating current polarography. Four waves were observed. The first two waves with $E_{1/2}$ –0.85 and –1.15 V *vs* SCE are clearly recognizable only in alkaline solution (Fig. 7.2.A). They correspond to the electron transitions n=2 and n=3 and can be used for the determination of technetium. The third and fourth wave are not diffusion controlled [94,95]. For the wave at $E_{1/2}$ = –0.85 V alternating current efficiencies of 70–90 % were obtained depending on the type and concentration of the supporting electrolyte. Thus, technetium may also be determined by alternating current polarography, which is advantageous on account of its higher separation capacity compared with direct current polarographic methods [94]. In the range $5 \cdot 10^{-6}$–$8 \cdot 10^{-5}$ M TcO_4^- the element could be ascertained by employing the polarographic wave at $E_{1/2}$ = –0.8 V *vs* SCE, which was observed in 1 M $NaClO_4$ [96].

For direct current polarographic determination of TcO_4^- in the concentration range 0.1–1.1 ppm in fission product solutions, a phosphate buffer of pH 7 was recommended. $E_{1/2}$ of the wave used was –0.68 V *vs* SCE. Neither rhenium nor ruthenium nor other fission products interfered. However, $[AsPh_4]Cl$, present in certain fission product solutions, must be separated out [97]. A rapid method was developed for the determination of ^{99m}Tc in fission product mixtures. It consists of a selective reduction of $^{99m}TcO_4^-$ at a dropping mercury electrode at –1.55 V *vs* SCE in a medium of 1 M

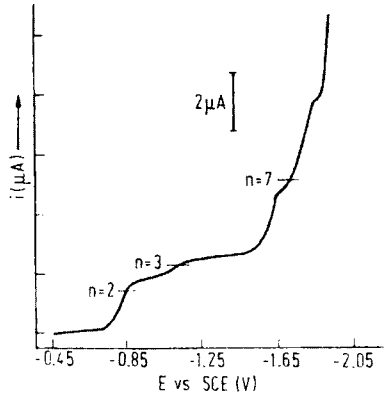

Fig. 7.2.A Polarogram of $0.206 \cdot 10^{-3}$ M $KTcO_4$ in 1.0 M NaOH [94].

sodium citrate and 0.1 M NaOH. $^{99m}TcO_4$ is probably reduced to ^{99m}Tc metal, which is soluble in mercury. The mercury [90] was removed from the solution of fission products and the amount of ^{99m}Tc determined in nitric acid solution of mercury by γ-counting. The precision obtained for ^{99m}Tc was about 1 % and the decontamination factor from other fission products about 10^5 [98].

7.1.5.2 Stripping voltammetry

One of the most sensitive electroanalytical methods, stripping voltammetry, was used to determine low technetium concentrations in the presence of molybdate or perrhenate ions. Technetium was concentrated, probably as TcO_2 hydrate, on a hanging mercury drop electrode from alkaline solutions of $6.0 \cdot 10^{-5}$ M $KTcO_4$ by electrolysis at a potential of –1.0 V *vs* SCE. Anodic stripping yielded a characteristic stripping curve. The height of the peak current at –0.38 V proved to be linearly dependent on the concentration of technetium in the range of 10^{-4}–$3 \cdot 10^{-7}$ M. Tc could be detected with an accuracy of ±4 %. The determination of 0.5 µg of Tc was feasible in a 10^4 fold molar excess of ReO_4^- or MoO_4^{2-} [99].

Pertechnetate and Tc(IV) could be more sensitively analyzed in acidic media in the presence of thiocyanate by adsorption stripping voltammetry at the hanging mercury drop electrode using the differential pulse mode. Determinations down to $5 \cdot 10^{-11}$ g Tc per ml were feasible. An intense current signal at –1.32 V vs SCE was observed if only technetium and thiocyanate were present in the solution. Larger quantities of salts, e.g. chlorides and sulphates, decreased the sensitivity of the method considerably. This, however, could easily be avoided if, after electrodeposition was completed, the primary electrolyte was replaced by a pure solution of dilute acid for the stripping voltammetric step [100].

The stripping voltammetric determination of pertechnetate by means of a glassy carbon electrode, chemically modified with a tetraphenylarsonium chloride loaded copolymer film, was reported. A detection limit of 10^{-8} M TcO_4^- was achieved after a 5 min enrichment time [101].

7.1.5.3 Titration techniques

A controlled potential coulometric titration has also been developed for the determination of technetium. Pertechnetate was titrated in an acetate buffered (pH 4.7) aqueous solution of sodium tripolyphosphate ($Na_5P_3O_{10}$) at a potential of –0.70 V vs SCE. Under these conditions TcO_4^- was found to be quantitatively reduced to Tc(III). In the range of 0.5–5 mg of titrated TcO_4, the relative error of the method was about ±1 % and the relative standard deviation 0.5 %. The ions Fe(III), Mo(VI), Ru(IV), U(VI), V(IV), F^-, and NO_3^- interfere strongly. Technetium can be removed from these ions by distillation from conc. sulphuric acid solution [102].

Several titration methods were studied for determining Tc(IV) or Tc(VII) in the concentration range of 10^{-4}–10^{-5} M. Tc(IV) was titrated volumetrically with Ce(IV) using potentiometric, biamperometric, and bipotentiometric detection of the equivalence point. The most precise results were obtained by coulometric titration of TcO_4^-

with electrogenerated Sn(II). The supporting electrolyte was a mixture of 2.5 M NaBr, 0.15 M $SnCl_4$, and 0.2 M HCl. The titration reaction was very fast and currents of up to 40 mA could be readily employed for the detection of the equivalence point. In addition, a conductometric titration of TcO_4 based on the precipitation of $[AsPh_4]TcO_4$ or $[PPh_4]TcO_4$ was proposed [103].

7.2 Separation methods

7.2.1 Volatilization

Owing to the volatility of Tc_2O_7 and pertechnetic acid, Tc(VII) may be co-distilled with oxidizing strong acids [46,104] (Fig. 7.3.A). The use of $HClO_4$ results in superior yields. About 75 wt% of technetium is co-distilled with the first 20 wt% of perchloric acid. With nitric acid, aqua regia, sulphuric acid, and fuming sulphuric acid the distillation of technetium proves to be incomplete. The addition of oxidants like $KBrO_3$, $K_2Cr_2O_7$, $Na_2S_2O_8$ or $KMnO_4$ to the acids such as H_2SO_4 or H_3PO_4 considerably increases the extent of co-distillation. HCl, HBr, and HI do not volatilize technetium, because these acids reduce Tc(VII) to form non-volatile hexahalide complexes of Tc(IV). However, a more detailed study of the co-distillation with sulphuric acid revealed that technetium can be distilled quantitatively with H_2SO_4, provided the acid, the sweep gas, and the distillation apparatus are free from contaminations. Reducing agents only inhibit the distillation, but do not affect the complete separation of technetium. If, for instance, reducing bromide is present, the technetium distillation begins at 155 °C instead of 110 °C, because it is reoxidized by sulphuric acid [74].

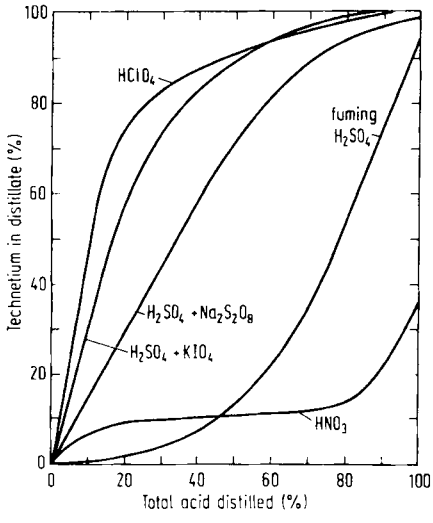

Fig. 7.3.A Co-distillation of technetium with acids [46].

The property of pertechnetate to be reduced by hydrochloric acid can be used for separating ReO_4 from reduced TcO_4^- by distillation in a mixture of H_2SO_4 and HCl at 180 °C [8]. Under these conditions most of rhenium passes into the distillate, but almost all the technetium remains in solution. Another distillation procedure involves reduction of TcO_4 by hydroxylamine. Perrhenic acid is distilled with steam from sulphuric acid. Up to 10 mg of rhenium can be separated quantitatively from traces of technetium [105]. Partial separation of TcO_4^- from ReO_4 is achieved by distillation from perchloric acid, because the first fraction is enriched by technetium. However, ruthenium is oxidized by perchloric acid to RuO_4 and volatilizes together with technetium [104]. Due to considerable differences in vapor pressures of $HTcO_4$ and $HReO_4$, technetium may be almost quantitatively separated from rhenium by alternate evaporation with nitric and hydrochloric acid [106].

For separating technetium produced by neutron irradiation of molybdenum, the distillation method using sulphuric acid proved to be efficient. For each gram of molybdenum 6 ml of conc. sulphuric acid was added and distilled leading to a yield of 75 wt% of Tc in the distillate. When double the amount of acid was added, about 90 wt% of Tc was recovered on distilling to a dry molybdic oxide residue. More than 98 wt% of Tc was extracted after two distillations [46]. $HTcO_4$ may also be distilled at 120–200 °C from a mixture of $HClO_4/H_3PO_4$. Phosphoric acid forms a phosphomolybdate complex, tending to hold the molybdenum in solution [107,108].

Dry distillation and gas phase separation of technetium oxides from oxides of rhenium, osmium, iridium, and ruthenium by temperature-programmed gas chromatography using O_2 as reactive gas was reported [109]. Furthermore, the separation of technetium chloride ($TcCl_4$) from volatile chlorides of numerous elements by thermochromatography combined with complex formation was investigated. The separation tube had a temperature gradient from 600 to 25 °C and was coated with KCl, CsCl, NaCl, and $BaCl_2$ [110].

7.2.2 Solvent extraction

The extraction of technetium with organic solvents was extensively used in numerous separation and concentration procedures. Technetium is extracted as pertechnetate, predominantly in the form of large organic cation salts, or in lower oxidation states in the form of complex compounds.

7.2.2.1 Pertechnetate

The principal disadvantage of the extraction methods is the introduction of organic compounds which may reduce TcO_4^- and cause difficulties in subsequent steps. Therefore, it is advisable to have some small amounts of an oxidizing agent, such as hydrogen peroxide, present during the extraction. The extraction of TcO_4^- from aqueous acid, neutral salt, and alkaline solutions by a wide variety of organic liquids, including alcohols, ethers, esters, nitro-compounds, nitriles, amines, hydrocarbons, chlorinated

hydrocarbons, organo-phosphorus and organo-nitrogen compounds, dissolved in non-polar liquids, was studied in detail. The general conclusions are [111]:

- The extraction of pertechnetate from aqueous solutions by aliphatic, aromatic, and chlorinated hydrocarbons is negligible, even when the latter possess relatively large dielectric constants.
- A necessary but not sufficient condition for efficient extraction by a pure liquid appears to be the presence of an electron donor atom, e.g. a basic oxygen or nitrogen atom. The possession of an appreciable dielectric constant favors extraction by a liquid even when only weak donor atoms are present.
- The extraction of pertechnetate decreases within a homologous series on increasing the hydrocarbon character of the molecules of the extracting agent.
- As a rule, extraction is more efficient from acid than from neutral salt or alkaline aqueous solutions.

The dependence of the pertechnetate extraction with cyclohexanol on the concentration of acid, initially in the aqueous phase, demonstrates the rapid extraction increase upon the addition of small amounts of acid. After a maximum extraction coefficient is reached, an exponential decrease sets in (Fig. 7.4.A). Curves similar to those in Fig. 7.4.A were also observed with cyclohexanone, tri-*n*-butyl phosphate (TBP), and with solutions of TBP in a liquid hydrocarbon.

In general, tertiary alcohols are more powerful extractants than secondary or primary alcohols of the same oxygen-to-carbon ratio. Aromatic or alicyclic alcohols reveal higher extraction coefficients than straight-chain alcohols of the same oxygen-to-carbon ratio. Among a series of isomeric ketones methyl ketones have the largest and symmetric ketones the smallest extraction efficiency. Aromatic or alicyclic ketones show higher extraction coefficients than *n*-aliphatic ketones of the same oxygen-to-carbon ratio. Polyethers are more effective extractants than normal ethers of the same O:C atom ratio. Compared with tri-*n*-butyl phosphate at equal concentra-

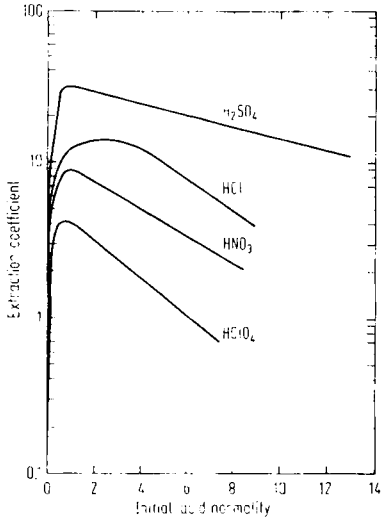

Fig. 7.4.A Extraction of TcO_4^- from aqueous solutions with cyclohexanol as a function of acid concentration [111].

tions in an inactive solvent, the more stongly basic tri-*n*-alkyl-phosphine oxides are substantially more effective. In going from primary to secondary and tertiary amine solutions in cyclohexane the extraction from acid solutions increases. Among the tertiary amines extraction coefficients decrease with decreasing basicity. Quaternary ammonium salts dissolved in inert solvents ensure efficient extraction not only from acid but also from neutral and alkaline solutions [111].

The dependence of the extraction coefficient of pertechnetate on the salt concentration and on the kind of anions being in the aqueous solutions is shown in Fig. 7.5.A, the data are for TBP as the extractant. With all solvents studied including cyclohexanol, methyl ethyl ketone, and cyclohexane, pertechnetate is extracted most efficiently from Na_2SO_4 and least from $NaClO_4$ [111]. The slight extractability of TcO_4^- from perchlorate solutions and the almost non-extractability by non-polar solvents may be used for the re-extraction of TcO_4^- into the aqueous phase by either shaking the organic phase with perchlorate solution or by diluting the extractant with a non-polar solvent [112].

TcO_4^- can be extracted by the following main types of reactions:

$$TcO_4(aq) + H^+(aq) \leftrightarrow HTcO_4(org) \quad (1)$$

$$TcO_4^-(aq) + M^+(aq) \leftrightarrow MTcO_4(org) \quad (2)$$

$$TcO_4^-(aq) + MX(org) \leftrightarrow MTcO_4(org) + X^-(aq) \quad (3)$$

In process (1) solvents like cyclohexanol or TBP containing a donor group have been used. In process (2) large cations M^+ such as $[N(But)_4]^+$, $[PPh_4]^+$ or $[AsPh_4]^+$ with hydrophobic groups can be employed together with organic solvents like chloroform. In process (3) the cation M^+ has such large hydrophobic groups (e.g. trilaurylammonium ions) that it is insoluble in the aqueous phase. The extraction will then take place through an ion exchange reaction [113].

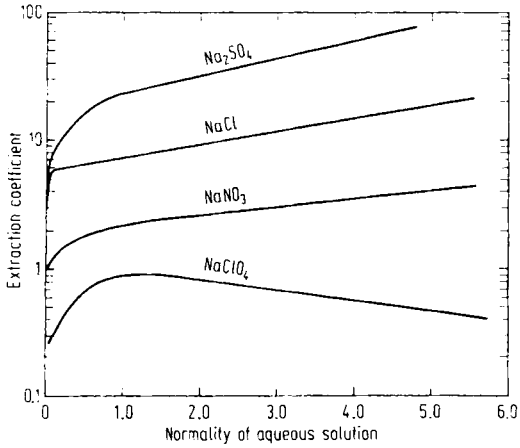

Fig. 7.5.A Extraction of TcO_4^- from aqueous salt solutions with TBP [111].

Tri-*n*-butyl phosphate (TBP)

The solvent extraction of $KTcO_4$ from aqueous nitric or hydrochloric acid solutions by TBP dissolved in *n*-dodecane was studied over a wide range of TBP, HNO_3 or HCl concentrations at 25, 40, and 60 °C. The extraction [114,116] was found to proceed according to the reaction:

$$3TBP(org) + H^+(aq) + TcO_4^-(aq) \leftrightarrow [HTcO_4 \cdot 3TBP](org)$$

The composition of the extracted complex is in agreement with the results of former investigations [118]. In the absence of HNO_3 pertechnetic acid is reported to be coordinated with 4TBP [119]. The distribution coefficients $D_{Tc}=[Tc]_{organic}/[Tc]_{aqueous}$ at 25 °C as a function of nitric or hydrochloric acid concentration and the vol% of TBP in *n*-dodecane are plotted in Figs. 7.6.A and 7.7.A. D_{Tc} increases with increasing acidity and increasing TBP concentration. However, for the HNO_3-TBP system (Fig. 7.6.A) D_{Tc} passes through a maximum near 0.8 M HNO_3 [115,117] and decreases rapidly at higher nitric acid concentrations, while D_{Tc} in the HCl-TBP system (Fig. 7.7.A) was found to increase smoothly. The difference in behavior can be attrib-

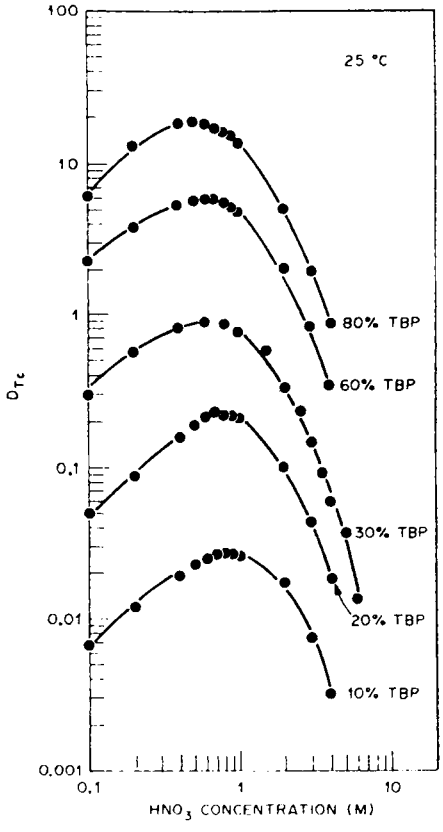

Fig. 7.6.A D_{Tc} as a function of HNO_3 and TBP concentration at 25 °C [114].

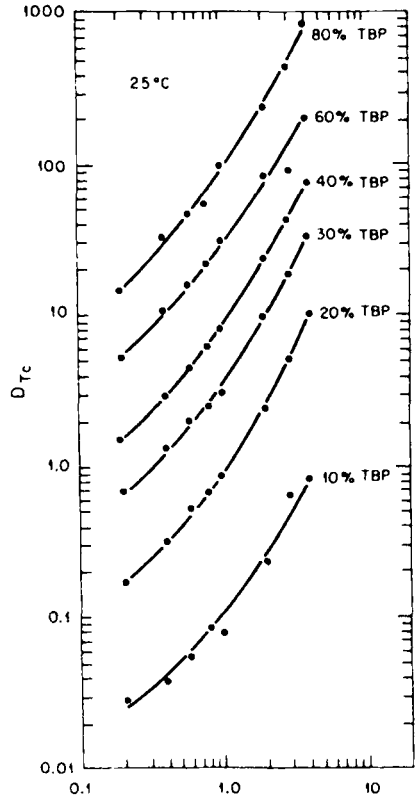

Fig. 7.7.A D_{Tc} as a function of HCl and TBP concentration at 25 °C [116].

uted to the relatively large amounts of TBP bonded to HNO_3 that reduce the amount of free TBP available to extract pertechnetate. The amounts of TBP bonded to HCl are negligible over the range of conditions studied. D_{Tc} decreases in both systems HNO_3-TBP and HCl-TBP with increasing temperature. D_{Tc} proves to be considerably higher for the latter at 25 °C under similar conditions of acid concentrations and TBP vol% [114, 116].

In addition, the extraction of $MTcO_4$ (M=H, Li, Na, K, Rb, or NH_4) by TBP from aqueous solutions of MCl was examined as a function of temperature and concentration. The distribution of the pertechnetate salts to the organic phase increased in the order Rb<K<Na<NH_4<Li<H. The stoichiometry of the extraction reaction was determined [120] to be

$$M^+(aq) + TcO_4^-(aq) + 3TBP(org) \rightarrow MTcO_4 \cdot 3TBP(org).$$

Uranyl nitrate substantially increases the distribution coefficient D_{Tc}. This was explained by the formation of a mixed nitrato-pertechnetato-TBP complex of UO_2^{2+} [121,122] according to the equilibrium:

$$[UO_2(NO_3)_2 \cdot 2TBP](org) + TcO_4(aq) \leftrightarrow [UO_2(NO_3)(TcO_4) \cdot 2TBP](org) + NO_3\ (aq)$$

A technique for the separation of pertechnetate from mixed fission products by solvent extraction with TBP was described. The extraction was almost quantitative from a sulphuric acid solution. Sodium fluoride was used to provide the zirconium-niobium decontamination and a cation exchange column ensured the decontamination from metallic ions. ^{99}Tc yields of 92 % were obtained [123].

Distribution coefficients of pertechnetate in some other organo-phosphorus compounds are given in Table 7.1.A.

Table 7.1.A Distribution coefficients D_{Tc} for the extraction of pertechnetate from aqueous 1 M HNO_3 with organo-phosphorus compounds [124].

Extractant		D_{Tc}
Trichloroethyl phosphate		3.9
Diisoamyl methylphosphonate (50 %)	in decane	117
0.2 M Tri*iso*hexylphosphine oxide	in decane	5.7
0.5 M Tri-*n*-octylphosphine oxide	in decane	27
0.2 M Dioctylphenylphosphine oxide	in decane	4.3

Ketones

Pertechnetate is extractable from a basic aqueous solution of 2–6 M NaOH with acetone. The NaOH concentration provides a separation of the acetone and the aqueous phase. In 4 M NaOH a distribution coefficient D_{Tc}=10 was achieved at room temperature, 92 % of TcO_4^- was extracted into the acetone phase. Almost the same distribution coefficient was observed when the basic aqueous solution contained 75 g/l Na_2MoO_4. This procedure allows the extractive separation of TcO_4^- from neutron-irradiated molybdenum [125].

Using methyl ethyl ketone as the extracting agent, D_{Tc} values up to about 400 were obtained in the presence of 6 N K_2CO_3 and after addition of 190 g/l Mo as molybdate to the aqueous solution. Without addition of molybdate, D_{Tc} decreased to 300, while 6 N KOH resulted in a D_{Tc} of less than 100. The distribution coefficient of molybdate studied at concentrations between 10^{-6} and 2 M MoO_4^{2-} did not exceed $5 \cdot 10^{-4}$, demonstrating again the possibility of separating TcO_4 efficiently [126]. Detailed separation procedures for ^{99m}Tc production based on the extraction with methyl ethyl ketone have been communicated [127,128]. Furthermore, isobutyl methyl ketone can be used to extract $^{99m}TcO_4^-$ from $^{99}MoO_4^{2-}$ in the wide pH range of 0.5–13.0 almost quantitatively [129].

The extraction of TcO_4^- with cyclohexanone proved to be an unusually rapid, efficient, and selective method. More than 95 % of TcO_4^- was extracted from 0.2 N to 7 N H_2SO_4 solutions in a single equilibration that is achieved in about 5 minutes. At higher acidities the phase volume ratio changed drastically because of increasing solubility of cyclohexanone in the aqueous phase. The separation was applied in the determination of the number of fissions occurring in a short neutron irradiation of

uranium by measurement of ^{99m}Tc, and to the separation of ^{99}Tc from long-lived fission products for burnup analysis [130]. Also for determining ^{99}Tc in environmental samples, an extraction of TcO_4^- with cyclohexanone was used. In the concentration range from 0.2 to 4.0 N H_2SO_4 distribution coefficients D_{Tc} from 82 to 200 were achieved [131].

Organo-nitrogen compounds

As already described in Sect. 5.1, pertechnetate is efficiently extracted by pyridine from alkaline solutions. Pyridine extracts TcO_4^- almost quantitatively from 4 M NaOH with a distribution coefficient $D_{Tc}= 7.78 \cdot 10^2$ at room temperature [132]. Pyridine and methyl-substituted derivatives were applied as extractants in the isolation and purification of technetium from aqueous NaOH, Na_2CO_3, and $NaNO_3$ solutions. D_{Tc} was found to increase with increasing NaOH concentration, while nitrate decreased the distribution coefficient. Methyl-substituted derivatives of pyridine are useful in separating TcO_4^- from appreciable amounts of nitrate ions. D_{Tc}=110 of aqueous solutions of TcO_4^- containing 0.25 M NaOH/2.0 M Na_2CO_3 and 0.25 M $NaNO_3$ allows the ready decontamination of TcO_4^- from other fission products like ^{137}Cs, ^{106}Ru, ^{95}Zr, ^{95}Nb, $^{152,155}Eu$, and ^{90}Sr [133]. Later, 2,4-dimethylpyridine and 2-methyl-5-ethylpyridine were recommended to extract TcO_4^- from alkaline solutions. 2-methylpyridine appeared to be less suitable with respect to its solubility in aqueous alkaline solutions. Table 7.2.A summarizes some distribution coefficients.

Table 7.2.A D_{Tc} values for the extraction of pertechnetate from alkaline solutions by pyridine bases at room temperature [134].

Composition of the aqueous phase	pyridine	2-methyl-pyridine	2,4-dimethyl-pyridine	2-methyl-5-ethylpyridine	quinoline
1 M NaOH	180	474	314	470	150
1 M LiOH	–	–	1280	1130	–
3 M NaOH	239	1970	1670	930	356
1 M NaOH + 2 M $NaNO_3$	–	78	146	143	49
0.5 M NaOH + 1 M Na_2CO_3	150	1840	700	1000	236
1 M NH_4OH + 1M $(NH_4)_2CO_3$	–	286	405	708	522

The best conditions for the extraction of TcO_4^- by 2,4-dimethyl- and 2-methyl-5-ethylpyridine are provided by 1 M LiOH and 3 M NaOH [134].

The extractant 4-(5-nonyl)pyridine in benzene displays considerable advantage over pyridine and methyl-substituted pyridines in that its solubility in water is almost negligible. However, the distribution coefficients proved to be rather low.

In various nitric acid concentrations the maximum D_{Tc} value at 25 °C was found to be around 10 at 0.5 M HNO_3 [135]. More recently D_{Tc} =60 was reported for a 0.5 M HNO_3 solution of pertechnetate using a 0.1 M solution of 4-(5-nonyl)pyridine in benzene [136].

Early extractions of pertechnetate, dissolved in 1 N H_2SO_4, with a 0.1 M solution of tri-*n*-octylamine (TOA) in cyclohexane resulted in distribution coefficients of D_{Tc}=110 at 25 °C [111]. Recently, D_{Tc} was determined as a function of the nitric acid concentration using 0.01 and 0.1 M solutions of tri-*n*-octylamine in benzene. The distribution coefficients increased with increasing acidity until a maximum was reached near 0.1 M HNO_3. At higher concentrations of nitric acid, D_{Tc} fell rapidly because of competition from the simultaneously extracted nitric acid, which reduces the concentration of free tri-*n*-octylamine available to extract TcO_4^- (Fig. 7.8.A). The extraction is considerably affected by the temperature. A linear relation is obtained between D_{Tc} and the concentration of TOA. The slope of 1.0 indicates an extractant:Tc ratio of 1:1. The extraction of pertechnetate from aqueous HNO_3 solution may be represented by the equation [117]:

$$H^+(aq) + TcO_4^-(aq) + TOA(org) \leftrightarrow [HTcO_4 \cdot TOA](org)$$

A mixture of tri-*n*-octylamine and xylene (30 %v/v) was used for extracting TcO_4 from mineralized seaweeds collected at the coast of the Ibaraki Prefecture in Japan. A specific activity of ^{99}Tc in the fresh seaweed *Eisenia bicyclis* of 503 mBq/kg was determined [137].

The distribution coefficient of TcO_4^- for the extraction with 0.1 M tri-*iso*octylamine (TIOA) in cyclohexane from 1 N H_2SO_4, D_{Tc} =72 at 25 °C, is somewhat lower than that of tri-*n*-octylamine (TOA) under identical conditions [111]. A procedure for the separation of $^{99m}TcO_4^-$ from neutron irradiated MoO_3 by extraction with TIOA was described. MoO_3 was dissolved in 1 M NaOH and ^{99m}Tc extracted from 1 M HCl into a solution of TIOA in 1,2-dichloroethane. At a concentration

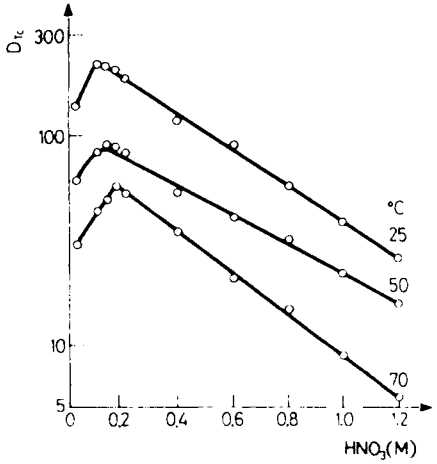

Fig. 7.8.A D_{Tc} as a function of HNO_3 concentration for 0.1 M TOA at 25, 50, and 70 °C [117].

of $3 \cdot 10^{-3}$ M TIOA, a distribution coefficient D_{Tc} =50 was obtained. Less than 0.5 % of ^{99}Mo was found in the organic phase [138]. For environmental studies TcO_4^- was extracted from aqueous sulphuric acid solutions with 5 % TIOA/xylene. Unexpectedly high distribution coefficients D_{Tc} were measured, decreasing from $4.7 \cdot 10^3$ to $1.6 \cdot 10^3$ in the concentration range of 0.5 to 4.0 N H_2SO_4. Almost 100 % of the pertechnetate could be extracted when the aqueous and the organic phase were shaken for only 1 min [131].

$5 \cdot 10^{-2}$ M N-Benzoyl-N-phenylhydroxylamine (BPHA) in chloroform extracts pertechnetate from 4–7 M aqueous solutions of $HClO_4$ with distribution coefficients D_{Tc} between 2 and 500 at 25 °C. D_{Tc} strongly increases with increasing $HClO_4$ concentration. The extraction is represented by the reaction [139]:

$$2H^+(aq) + TcO_4(aq) + BPHA(org) \rightarrow [HTcO_4 \cdot HBPHA](org)$$

The distinctly lower distribution coefficient of ReO_4^- provides a method for separating TcO_4^- and ReO_4 [140].

Pertechnetate is efficiently extracted from aqueous solutions by rhodamine-B hydrochloride (RH^+Cl^-) in nitrobenzene. At pH 4.7 and 28 °C an extraction coefficient of $7.96 \cdot 10^3$ was reported when 10 ml of the organic phase contained 5 mg of RH^+Cl^-. The extraction equilibrium was reached within 2 min and the separation of the two phases was rapid. The extraction process may be formulated as

$$TcO_4^-(aq) + (RH^+Cl^-)(org) \rightarrow (RH^+TcO_4^-)(org) + Cl^-(aq)$$

Separation factors greater than 10^7 could be achieved for Ni(II), Mn(II), Zn(II), Sn(IV), and Sb(III) [141].

Alkyl- and arylammonium salts

Tetra-*n*-butyl, -pentyl, -hexyl, and -heptyl ammonium iodides, dissolved in benzene or chloroform, can be used to extract TcO_4^- from aqueous solutions. Such cations act as liquid anion exchangers. Distribution coefficients are compared in Table 7.3.A.

Table 7.3.A Distribution coefficients D_{Tc} for the extraction of 10^{-4} M pertechnetate at pH 5 with 10^{-3} M tetraalkylammonium iodide in chloroform [142].

Alkylammonium iodide	$[But_4N]I$	$[Pent_4N]I$	$[Hex_4N]I$	$[Hept_4N]I$
D_{Tc}	3.40	9.29	9.10	9.89

The two phases were equilibrated in a separating funnel for 15 min. The expected reaction is

$$TcO_4^-(aq) + [(alkyl)_4N]I(org) \rightarrow [(alkyl)_4N]TcO_4(org) + I^-(aq)$$

The separation of TcO_4^- from MoO_4^{2-} was carried out at pH 10.5 with tetra-*n*-heptylammonium iodide dissolved in benzene. The separation factor D_{Tc}/D_{Mo} of 14 requires only a few cycles to efficiently separate both anions [142].

The chief decontamination step for the radiochemical separation of pertechnetate from mixed fission products was the extraction of TcO_4^- from a 4 M NaOH solution into a tetrapropylammonium hydroxide/bromoform mixture in only 30 s [143]. This rapid and quantitative extraction was proposed for the separation of Tc from the fission products Mo, Ru, Rh, and Pd. D_{Tc} values of 10^2 were obtained for the concentration of 0.12 M tetrapropylammonium hydroxide in 4 M NaOH, whereas the distribution coefficients of the other fission products were only around 10^{-3} [144].

Extraction with a 0.15 M solution of methyltricaprylammonium chloride in chloroform results in the quantitative isolation of pertechnetate from aqueous media, ranging from 4M sulphuric acid or 9 M hydrochloric acid to pH 13. The formation of a 1:1 organic cation-pertechnetate salt appears to be requisite for the extraction at any pH:

$$TcO_4^-(aq) + [CH_3(C_7H_{15})_3N]Cl(org) \leftrightarrow [CH_3(C_7H_{15})_3N]TcO_4(org) + Cl^-(aq)$$

Depending on the concentration of H_2SO_4, HCl or KOH, distribution coefficients D_{Tc} between 7 and 175 at 24 °C were reported. ReO_4^- follows TcO_4^- so closely that their separation from each other appears to be difficult [145].

Pertechnetate is efficiently extracted from aqueous solutions of HNO_3 and $LiNO_3$ by trilaurylammonium nitrate dissolved in 2-xylene according to the anion exchange reaction:

$$TcO_4^-(aq) + [(C_{12}H_{25})_3NH]NO_3(org) \leftrightarrow [(C_{12}H_{25})_3NH]TcO_4(org) + NO_3^-(aq)$$

D_{Tc} decreases from 156 at 10^{-3} M HNO_3 to 1.8 at 0.9 M HNO_3 and from 140 at $5 \cdot 10^{-3}$ M $LiNO_3$ to 2.6 at 0.9 M $LiNO_3$ using a concentration of $1.5 \cdot 10^{-2}$ M trilaurylammonium nitrate at a temperature of 25 °C [113].

Distribution coefficients D_{Tc} of 10^3 can be achieved when pertechnetate in 1 M H_2SO_4 is extracted with triphenylguanidinium chloride dissolved in β,β-dichlorodiethyl ether. D_{Tc} decreases with increasing H_2SO_4 concentration, similar to D_{Re}. The separation of TcO_4^- from ReO_4^- and even from MoO_4^{2-} is not possible by a single-stage extraction [146].

Tetraphenylarsonium salts

The extraction of $[(C_6H_5)_4As]TcO_4$ into chloroform and the application of the extraction procedure to separate TcO_4^- produced from molybdenum or uranium were studied very early. The extraction proceeds according to the equation [147]:

$$[(C_6H_5)_4As]^+(aq) + TcO_4^-(aq) \leftrightarrow [(C_6H_5)_4As]TcO_4(org)$$

The distribution coefficient D_{Tc} increased with decreasing concentrations of mineral acids, while the extraction of molybdate was negligible. Using 0.05 M solutions of tetraphenyl arsonium chloride in chloroform $D_{Tc}>10^3$ are reported for <0.1 M concentrations of H_2SO_4 or HCl. At high supporting acid concentrations the decrease in TcO_4 extraction may be attributed to the depressed dissociation of $HTcO_4$. At low acidities TcO_4^- could be separated from neutron-irradiated Mo with very high selectivity. Use of 0.05 M H_2SO_4 results in a separation factor of 10^6 for technetium and molybdenum [148].

D_{Tc} strongly depends on the concentration of $[(C_6H_5)_4As]Cl$ in chloroform. For the extraction of pertechnetate from 3 M HNO_3 a distribution coefficient of around 100 is attained when the concentration of tetraphenylarsonium chloride in chloroform is raised to 1 M. TcO_4 can be separated from 3 M HNO_3 by extraction with $\geq$0.1 M $[(C_6H_5)_4As]Cl$ in chloroform, whereas $[TcCl_6]^{2-}$ is not extracted under the same conditions [149]. Dilute solutions of $[(C_6H_5)_4As]Cl$ ($<10^{-2}$ M) in $CHCl_3$ extract TcO_4 at pH values from the alkaline to the weakly HCl acid range with a high distribution ratio of more than 10^2 [150]. Even from saturated NaCl solutions pertechnetate can be extracted almost quantitatively [151].

7.2.2.2 Complex compounds

In strongly acidic media, cupferron, the ammonium salt of N-nitroso-N-phenylhydroxylamine, seems to form with TcO_4^- the adduct $[(Cupf)^+(TcO_4)^-]$ or an adduct with pertechnetic acid, which can be extracted from 6 M HCl into ether by 99 %. The occurrence of any significant reduction was not observed. Tc(III), prepared by coulometric reduction of pertechnetate, was extracted as a cupferrate into ether up to 26 % [152].

Potassium xanthate reduces pertechnetate and forms a technetium complex in a 1.5 N aqueous solution of HCl, H_2SO_4 or $HClO_4$, from which more than 99 % of technetium could be extracted into carbon tetrachloride at 20 °C. The concentration of potassium xanthate was 0.1 M. Perrhenate remained entirely in the aqueous phase, thus separation from technetium could be readily achieved. Instead of carbon tetrachloride, other extractants like chloroform, 1,1,1-trichloroethane, xylene or isopropyl ether are also suitable [153].

In addition, tetramethylenedithiocarbamate was used for reduction of TcO_4^-, chelation, and extraction of the complex into chloroform from hydrochloric acid solution. More than 99 % of the technetium can be extracted into chloroform when the HCl concentration is $\geq$0.01 M. In contrast to technetium most of the accompanying radionuclides in low-level radioactive wastes are not extracted into the organic phase at high HCl concentrations, e.g. 4 M HCl, except ^{60}Co and ^{110m}Ag. The suitable concentration of tetramethylenedithiocarbamate ranged between $1 \cdot 10^{-4}$ and $1.5 \cdot 10^{-2}$ M [154].

Potassium thiocyanate reduces pertechnetate in aqueous hydrochloric acid solution and forms thiocyanato complexes of technetium that are extractable by a solution of 0.1 M 2-hexylpyridine in benzene. Also Mo(VI), Au(III), As(III), Fe(III), Zn(II), and Hg(II) are extracted under similar conditions. The equilibrium is attained in about 3

min. Around 70 % of technetium can be extracted at 5 M HCl in the presence of 0.02 M KSCN [155].

Tc(IV), obtained by reduction of TcO_4^- with hydrazine in 0.5 to 3 M HNO_3, was extracted with a solution of 15 vol% of dibutyl phosphoric acid. Distribution coefficients only between 2 and 3 were observed for 1–2 M HNO_3. Somewhat higher coefficients (D_{Tc}=8.5) could be achieved when Tc(IV) was extracted with thenoyltrifluoroacetone from aqueous solutions of pH 6.5 to 9. Under these conditions more than 90 % of Tc(IV) was extracted in a single equilibration step [156]. Some systematic studies on the extraction of Tc(IV) with several complexing extractants have been reported [157].

To conclude Sect. 7.2.2, Table 7.4.A summarizes the significant distribution coefficients D_{Tc} for the solvent extraction of pertechnetate from aqueous solutions.

Table 7.4.A Solvent extraction of pertechnetate from aqueous solutions

Extractant	Aqueous phase	Distribution coefficient D_{Tc}		References
3-Pentanol	1 N H_2SO_4	9.5	(25 °C)	[111]
2-Methyl-2-butanol	1 N H_2SO_4	10.4	(25 °C)	[111]
Cyclohexanol	1 N H_2SO_4	32	(25 °C)	[111]
Acetone	4 N NaOH	10	(room temp.)	[125]
Methyl ethyl ketone	6 N K_2CO_3 + 190g/l Mo	400	(room temp.)	[126]
Cyclohexanone	1 N H_2SO_4	93	(25 °C)	[111]
2-Pentanone	1 N H_2SO_4	38	(25 °C)	[111]
3-Pentanone	1 N H_2SO_4	35	(25 °C)	[111]
Tri-*n*-butyl phosphate (80 vol% in *n*-dodecane)	4 N HCl	900	(25 °C)	[116]
Trichloroethyl phosphate	1 N HNO_3	3.9	(room temp.)	[124]
Di-*iso*-amylmethyl phosphonate (50 vol% in decane)	1 N HNO_3	117	(room temp.)	[124]
0.2 M Tri-*iso*-hexylphosphine oxide (in decane)	1 N HNO_3	5.7	(room temp.)	[124]
0.1 M Trihexylphosphine oxide (in cyclohexane)	1 N H_2SO_4	46	(25 °C)	[111]
0.1 M Trioctylphosphine oxide (in cyclohexane)	1 N H_2SO_4	41	(25 °C)	[111]
0.2 M Dioctylphenylphospine oxide (in decane)	1 N HNO_3	4.3	(room temp.)	[124]
0.1 M Tridecylphosphine oxide (in cyclohexane)	1 N H_2SO_4	49	(25 °C)	[111]
Pyridine	4 N NaOH	778	(room temp.)	[132]
2-Methylpyridine	3 N NaOH	1970	(room temp.)	[134]
2,4-Dimethylpyridine	3 N NaOH	1670	(room temp.)	[134]

Table 7.4.A Continued

Extractant	Aqueous phase	Distribution coefficient D_{Tc}		References
2-Methyl-5-ethylpyridine	1 N LiOH	1130	(room temp.)	[134]
4-(5-nonyl)pyridine	0.5N HNO_3	60	(room temp.)	[136]
Quinoline	3 N NaOH	356	(room temp.)	[134]
0.1 M Tri-*n*-octylamine (in cyclohexane)	1 N H_2SO_4	110	(25 °C)	[111]
$5 \cdot 10^{-2}$ M N-Benzoyl-N-phenyl-hydroxylamine (in chloroform)	7 N $HClO_4$	500	(25 °C)	[139]
$5 \cdot 10^{-2}$ % Rhodamino-B hydrochloride (in nitrobenzene)	pH 4.7	7961	(28 °C)	[141]
0.1 M Cetyl-dimethyl-benzyl-ammonium chloride (in toluene)	1 N H_2SO_4	105	(25 °C)	[111]
0.1 M Dimethyl-didodecenylammonium chloride (in toluene)	1 N H_2SO_4	100	(25 °C)	[111]
0.12 M Tetrapropylammonium hydroxide (in bromoform)	4 N NaOH	100	(room temp.)	[144]
10^{-3} M Tetrabutylammonium iodide (in chloroform)	pH 5	3.40	(room temp.)	[142]
10^{-3} M Tetrapentylammonium iodide (in chloroform)	pH 5	9.29	(room temp.)	[142]
10^{-3} M Tetrahexylammonium iodide (in chloroform)	pH 5	9.10	(room temp.)	[142]
10^{-3} M Tetraheptylammonium iodide (in chloroform)	pH 5	9.89	(room temp.)	[142]
0.15 M Methyltricaprylammonium chloride (in chloroform)	6 N HCl	175	(24 °C)	[145]
$1.5 \cdot 10^{-2}$ M Trilaurylammonium nitrate (in xylene)	10^{-3} N HNO_3	156	(25 °C)	[113]
Triphenylguanidinium chloride (in β,β-dichlorodiethyl ether)	2 N H_2SO_4	1000	(room temp.)	[146]
0.05 M Tetraphenylarsonium chloride (in chloroform)	1 N H_2SO_4	>1000	(room temp.)	[148]

7.2.3 Chromatography

7.2.3.1 Ion exchange chromatography

Pertechnetate is strongly adsorbed by strong-base anion exchangers and can be eluted only by ions with a high affinity for the resin, such as ClO_4^-. Recently, the adsorption behavior of pertechnetate on the anion exchanger Dowex 1-X8 was studied as a function of the acid concentration in chloride, nitrate or perchlorate solutions at constant ionic strength and also in dependence on the hydroxide concentration, demonstrating the pro-

minent eluting properties of perchloric acid [158]. Using Dowex 1-X8, various factors such as quantity of the resin, eluant concentration, and elution flow rate for the separation of TcO_4 from environmental waters were optimized. The average recovery was 91 % of TcO_4 when the resin was eluted with 12 M HNO_3 [159].

Perrhenate is almost as strongly adsorbed as pertechnetate, but the separation of both anions can be carried out if a strong base exchanger is used [160]. Early, pertechnetate and perrhenate were separated on a Dowex-2 resin using as the eluent a mixture of 0.1 M $(NH_4)_2SO_4$ and 0.1 M NH_4SCN adjusted to pH 8.3–8.5. The two elution peaks were only partially resolved. In spite of some cross contamination, pertechnetate was obtained in a purity of over 99 % [161]. A better separation of TcO_4^- and ReO_4^- was attained (Fig. 7.9.A) when perchlorate solutions were used as eluents [160–164]. Maximum separation factors of 10^4–10^5 could be achieved on a Dowex 1-X4 resin of 200–400 mesh. At high perchloric acid concentrations (0.1 M), a broadening and distortion of the technetium peaks was observed, indicating reduction of pertechnetate by the resin [164].

To separate manganese, technetium, and rhenium, MnO_4^- is reduced with hydrogen peroxide to Mn^{2+} which is not adsorbed on the anion exchange resin Amberlite IRA-400. Mixtures of TcO_4^- and ReO_4^- in 0.1–0.3 M HCl are passed through the Amberlite and both anions are adsorbed. Rhenium is eluted with a 5 wt% solution of NH_4SCN in 0.1–0.2 M HCl. After washing the column with water, technetium is eluted with 0.1 M HNO_3. The separation is reported to be most satisfactory. 10 µg of technetium can be separated from 15 mg of manganese and 0.8 mg of rhenium, however, the elution of the three elements requires a total time of about 24 h [165].

Again the thiocyanate-hydrochloric acid medium was applied to separate by anion exchange perrhenate from molybdate and pertechnetate. Rhenium is first eluted with a 0.5 M NH_4SCN/0.5 M HCl solution while MoO_4^{2-} and TcO_4 remain strongly adsorbed on the anion exchanger Dowex 1-X8. Molybdate is then removed quantitatively by passing a 2.5 M NH_4NO_3 solution through the column. Pertechnetate is eluted with 4 M HNO_3. Microgram to a few milligram quantities of perrhenate can be quantitatively separated from tracer quantities of pertechnetate [166].

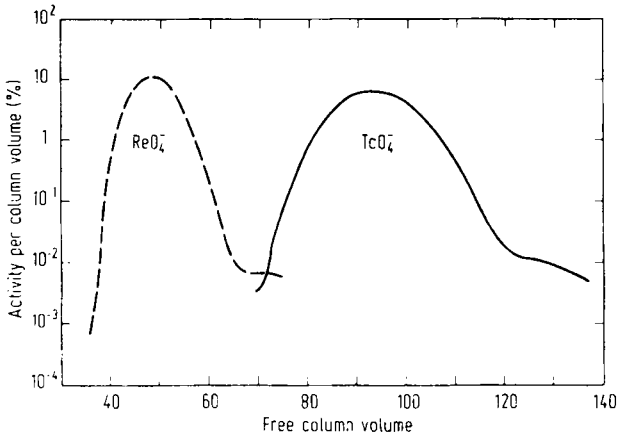

Fig. 7.9.A Anion exchange separation of TcO_4^- and ReO_4^-. Dowex 1-X4, ClO_4^- form, column eluted with 0.1 M NH_4ClO_4 [164].

The separation of $^{99}TcO_4^-$, formed by neutron bombardment of molybdenum, from its molybdenum matrix, was accomplished by means of the Amberlite anion exchange resin IRA-400. Irradiated molybdenum was dissolved in $NH_4OH + H_2O_2$ and molybdate was eluted from the anion exchanger with a mixture of potassium oxalate and potassium hydroxide, while the elution of pertechnetate was achieved with 0.5 M NH_4SCN. 80 to 93 % of the calculated ^{99}Tc could be recovered from the irradiated molybdenum [167].

For the anion-exchange separation with Dowex-1, the distribution coefficients of pertechnetate, molybdate, perrhenate, and tungstate were determined in hydrochloric acid (Fig. 7.10.A). The results indicate that the best separation of TcO_4 and MoO_4^{2-} should occur in about 1 M HCl. Molybdate is removed from the anion-exchange column with 1 M HCl, then pertechnetate with 4 M HNO_3. The recovery of pertechnetate in the first 4.4 ml of nitric acid was 98 %. A drawback of this separation might be the isolation of pertechnetate from the rather strong nitric acid [168].

The cationic thiourea complex of technetium is adsorbed from nitric and perchloric acid on the cation-exchanger Dowex 50WX4. In dilute HNO_3 and $HClO_4$ (pH 1) distribution coefficients of 10^3 and $>10^4$, respectively, were observed. Technetium was eluted with 8 M HCl or a mixture of 5 M HNO_3 and 10 % H_2O_2 [169].

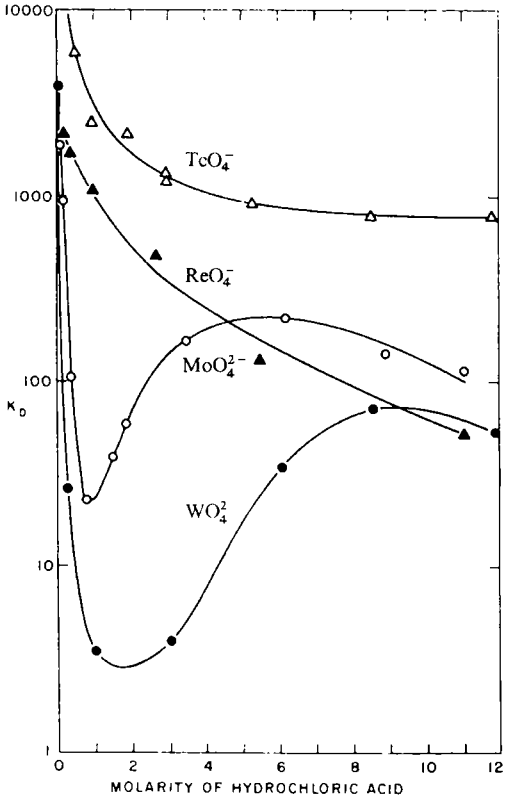

Fig. 7.10.A Dependence of the distribution coefficient K_D at 25 °C on the HCl concentration with Dowex-1 [168].

7.2.3.2 Adsorption chromatography

Paper chromatography can be employed for separating pertechnetate from perrhenate and molybdate. Using Whatman No.1 paper the separation of TcO_4^- and ReO_4^- is rather satisfactory, in a mixture of butanol and conc. HCl (50/50 vol%) as the mobile phase. Hydrochloric acid causes selective reduction of TcO_4^- with the formation of a chloride complex that is less mobile in this system. The R_f values of technetium and rhenium are 0.70 and 0.77, respectively [170]. The solution chemistry of pertechnetate and reduced species in different concentrations of hydrochloric or hydrobromic acid was studied by paper chromatography [171–173]. Another paper chromatographic method uses the formation of a technetium complex with thiourea in nitric acid. TcO_4^- is reduced by this reagent, in contrast to ReO_4^- [174]. Pertechnetate and molybdate are separated by high-voltage electromigration in paper using a 0.15 % solution of CH_3COONH_4 and a gradient of 60 V/cm [175].

To extract ^{99m}Tc from molybdenum irradiated by neutrons or separated from uranium fission products, inorganic adsorbents, in particular aluminum oxide, were widely used. In preparing a ^{99m}Tc generator, irradiated MoO_3 was dissolved in conc. HNO_3, the solution was diluted and passed through a column of acid aluminum oxide. The column was then eluted by 0.2 N H_2SO_4 to extract ^{99m}Tc [176]. If molybdatophosphate instead of molybdate is adsorbed by aluminum oxide, the exchange capacity increases from 1.2 to 8 g per 100 g of Al_2O_3 [177]. In order to obtain ^{99m}Tc in high specific activities, carrier-free ^{99}Mo, produced by fission of ^{235}U, is passed in dilute nitric acid of pH 1–2 through a column of chromatographic aluminum oxide. ^{99m}Tc can be easily eluted with 0.1 M HNO_3, while molybdate is retained on the column. The radiochemical purity of $^{99m}TcO_4^-$ was >99.99 % [178]. Instead of Al_2O_3, kieselgur supported with di-2-ethylhexylphosphoric acid (30 %w/w) was proposed for an easy and rapid separation of ^{99}Mo and $^{99m}TcO_4^-$ [179].

In addition, thin-layer chromatography was employed for the separation of technetium and molybdenum. Neutron-irradiated molybdate was separated from produced $^{99m}TcO_4^-$ on cellulose MN 300 using butanol saturated with 1 M HCl [180]. Molybdate was identified in pertechnetate solutions by means of thin layers of silica gel or Al_2O_3 with mixtures of 1 M HCl/methanol or 1 M HCl/ethanol as solvents. The TcO_4^- spot revealed a higher mobility than the MoO_4^{2-} spot [181].

To rather selectively separate pertechnetate, with more than 90 % yield, from solutions of acid fission products it was proposed to use finely divided cadmium sulphide. The overall yield of the radionuclide pure ^{99}Tc, finally extracted as $[(C_6H_5)_4As]TcO_4$, was 68 % [182,183]. In addition, activated carbon was used to efficiently separate pertechnetate from high-level liquid waste. Distribution coefficients of more than 500 were observed when pertechnetate was separated with activated carbon from a 2 M HNO_3 solution [184]. Effective separation and recovery of $^{99}TcO_4^-$ from contaminated groundwater with activated carbon have been reported very recently [185].

Studies on the sorption of technetium by various minerals demonstrate that only a few percent of pertechnetate are sorbed by tuff and basalt and that granite, dolomite, and shale sorbed only small amounts (≤10 %). However, minerals containing copper, lead or iron sulphide, e.g. bournonite, galena, and chalcopyrite, sorbed pertechnetate

strongly up to more than 99 %. Reduction of TcO_4^- may occur by minerals containing Cu^+, Pb^{2+} or Fe^{2+} ions [186].

7.3 References

[1] J.W. Cobble, Treatise Anal. Chem. II *6*, 407–434 (1964)
[2] A.A. Pozdnyakow, Russ. Chem. Rev. *34*, 129–141 (1965)
[3] C.L. Rulfs, Crit. Rev. Anal. Chem. *1*, 335–375 (1970)
[4] H. Kupsch and M. Jovtschev, Isotopenpraxis *15*, 1–9 (1979)
[5] K. Schwochau, Top. Curr. Chem. *96*, 109–147 (1981)
[6] S. Möbius in: Gmelin Handbook of Inorganic Chemistry, 8th ed., Suppl. Vol. 1, (H. K. Kugler and C. Keller, eds.), Springer, Berlin (1982), pp. 212–245
[7] S.E. Long and S.T. Sparkes, AERE-R12742, (1988) pp. 1–33
[8] C. Perrier and E. Segrè, J. Chem. Phys. *5*, 712–716 (1937)
[9] G. Goldstein, Diss. Abstr. *26*, 1888–1889 (1965)
[10] B.T. Kenna and P.K. Kuroda, J. Inorg. Nucl. Chem. *26*, 493–499 (1964)
[11] J.P. Riley and S.A. Siddiqui, Anal. Chim. Acta *139*, 167–176 (1982)
[12] P. Robb, P. Warwick, and D.J. Malcolme-Lawes, J. Radioanal. Nucl. Chem. Art. *89*, 323–329 (1985)
[13] K. Baechmann in: Messung radioaktiver Nuklide, Topical Presentation in Nuclear Chemistry, Vol. 2, (K.H. Lieser, ed.) Verlag Chemie, Weinheim 1970, pp. 84–85
[14] G.H. Kramer, Can. J. Chem. *61*, 1949–1951 (1983)
[15] E. Holm, J. Rioseco, and M. García-León, Nucl. Instr. Methodes *223*, 204–207 (1984)
[16] S. Ballestra, G. Barci, E. Holm, J. Lopez, and J. Gastaud, J. Radioanal. Nucl. Chem. Art. *115*, 51–58 (1987)
[17] M. García-León and C.I. Sánchez-Angulo, J. Radioanal. Nucl. Chem. Art. *115*, 377–388 (1987)
[18] N.Y. Chu and J. Feldstein, Talanta *31*, 809–813 (1984)
[19] H.J. Luxenburger, H. Schüttelkopf, and B. Bohn, Kernforschungszentrum Karlsruhe, Report KFK 3784 (1984)
[20] M. Otsuji, R. Seki, and N. Ikeda, Radioisotops *36*, 473–474 (1987)
[21] S. Cattarin, L. Doretti, and U. Mazzi, Health Phys. *49*, 795–804 (1985)
[22] W. Seelmann-Eggebert, G. Pfennig, H. Münzel, and H. Klewe-Nebenius, Chart of the nuclides, 5th edition (1981), Gersbach und Sohn, München
[23] M.E. Bunker and J.W. Starner, Bull. Amer. Phys. Soc. 7, 342 (1962)
[24] S. Foti, E. Delucchi, and V. Akamian, Anal. Chim. Acta *60*, 261–268 (1972)
[25] S. Foti, E. Delucchi, and V. Akamian, Anal. Chim. Acta *60*, 269–276 (1972)
[26] W. Görner and H. Spies, Anal. Chem. *58*, 1261–1263 (1986)
[27] B.J. Mincher and J.D. Baker, J. Radioanal. Nucl. Chem. Art. *139*, 273–276 (1990)
[28] N. Ikeda, R. Seki, M. Kamemoto, and M. Otsuji, J. Radioanal. Nucl. Chem. Art. *131*, 65–71 (1989)
[29] N. Ikeda, R. Seki, M. Kamemoto, and M. Otsuji, Radioisotopes *37*, 414–415 (1988)
[30] I. Yamagishi, M. Kubota, T. Sekine, and K. Yoshihara, Radiochim. Acta *63*, 33–36 (1993)
[31] T. Sekine, K. Yoshihara, Z. Németh, L. Lakosi, and A. Veres, J. Radioanal. Nucl. Chem. Art. *130*, 269–278 (1989)
[32] M. Yagi, T. Sekine, and K. Yoshihara, J. Radioanal. Nucl. Chem. Lett. *155*, 435–443 (1991)
[33] R. Muenze and B. Grossmann, Int. J. Appl. Radiat. Isot. *35*, 1073–1074 (1984)
[34] W.F. Meggers and B.F. Scribner, J. Res. Nat. Bur. Stand. *45*, 476–489 (1950)
[35] W.F. Meggers, Spectrochim. Acta *4*, 317–326 (1951)
[36] G.E. Boyd and Q.V. Larson, J. Phys. Chem. *60*, 707–715 (1956)
[37] D.L. Timma, J. Optical Soc. Amer. *39*, 898–902 (1949)
[38] G.E. Boyd, J. Chem. Educ. *36*, 3–14 (1959)
[39] R.M. Brown and C.J. Pickford, Analyst *109*, 673–674 (1984)
[40] J.C. Van Loon, Anal. Chem. *51*, 1139A-1150A (1979)
[41] K.J. Irgolic, R.A. Stockton, D. Chakraborti, and W. Beyer, Spectrochim. Acta *38B*, 437–445 (1983)

[42] W.A. Hareland, E.R. Ebersole, and T.P. Ramachandran. Anal. Chem. *44*, 520–523 (1972)
[43] J.H. Kaye and N.E. Ballou, Anal. Chem. *50*, 2076–2078 (1978)
[44] L.E. Burkhart, W.F. Peed, and B.G. Saunders. Phys. Rev. *73*, 347–349 (1948)
[45] G.L. Rogosa and W.F. Peed. Phys. Rev. *100*, 1763 (1955)
[46] G.E. Boyd, Q.V. Larson, and E.E. Motta, J. Amer. Chem. Soc. *82*, 809–815 (1960)
[47] F. Lux, F. Ammentorp-Schmidt, and W. Opavsky. Z. Anorg. Allgem. Chem. *341*, 172–182 (1965)
[48] S.G. Metcalf, Anal. Chim. Acta *93*, 297–299 (1977)
[49] G.E. Boyd, J.R. Sites, Q.V. Larson, and C.R. Baldock, Phys. Rev. *99*, 1030–1031 (1955)
[50] T.J. Anderson and R.L. Walker, Anal. Chem. *52*, 709–713 (1980)
[51] H.-J. Dietze and S. Becker, Isotopenpraxis *20*, 279–281 (1984)
[52] S. Morita, K. Tobita, and M. Kurabayashi. Radiochim Acta *63*, 63–67 (1993)
[53] J.S. Crain and D.L. Gallimore, Appl. Spectroscopy *46*, 547–549 (1992)
[54] S. Morita, C.K. Kim, Y. Takaku, R. Seki, and N. Ikeda. Appl. Radiat. Isot. *42*, 531–534 (1991)
[55] Ihsanullah, Sep. Sci. Technol. *29*, 781–797 (1994)
[56] K. Tagami and S. Uchida, Radiochim. Acta *63*, 69–72 (1993)
[57] C.-K. Kim, M. Otsuji, Y. Takaku, H. Kawamura, K. Shiraishi, Y. Igarashi, S. Igarashi, and N. Ikeda, Radioisotopes *38*, 151–152 (1989)
[58] N. Momoshima, M. Sayad, and Y. Takashima, Radiochim. Acta *63*, 73–78 (1993)
[59] N. Trautmann, Radiochim. Acta *63*, 37–43 (1993)
[60] C.-K. Kim, S. Morita, R. Seki, Y. Takaku, N. Ikeda, and D.J. Assinder, J. Radioanal. Nucl. Chem. Art. *156*, 201–213 (1992)
[61] C.-K. Kim, R. Seki, S. Morita, S. Yamasaki, A. Tsumura, Y. Takaku, Y. Igarashi, and M. Yamamoto. J. Anal. At. Spectrom. *6*, 205–209 (1991)
[62] P. Sattelberger, M. Mang, G. Herrmann, J. Riegel, H. Rimke, N. Trautmann, F. Ames, and H.-J. Kluge, Radiochim. Acta *48*, 165–169 (1989)
[63] D.J. Rokop, N.C. Schroeder, and K. Wolfsberg. Anal. Chem. *62*, 1271–1274 (1990)
[64] P. Mullen, K. Schwochau, and C.K. Jørgensen, Chem. Phys. Lett. *3*, 49–51 (1969)
[65] C.K. Jørgensen and K. Schwochau, Z. Naturforschg. *20a*, 65–75 (1965)
[66] A.A. Pozdnyakov, J. Anal. Chem. [USSR] *20*, 439–441 (1965)
[67] C.E. Crouthamel, Anal. Chem. *29*, 1756–1760 (1957)
[68] H.S. Trop, A. Davison, A.G. Jones, M.A. Davis, D.J. Szalda, and S.J. Lippard, Inorg. Chem. *19*, 1005–1010 (1980)
[69] K. Schwochau, L. Astheimer, and H.J. Schenk, J. Inorg. Nucl. Chem. *35*, 2249–2257 (1973)
[70] O.H. Howard and C.W. Weber, Anal. Chem. *34*, 530–533 (1962)
[71] R.E. Foster, Jr., W.J. Maeck, and J.E. Rein, Anal. Chem. *39*, 563–566 (1967)
[72] T. Fujita, T. Sekine, H. Hiraga, K. Yoshihara, A. Mutalib, R. Alberto, and J.I. Kim, Radiochim. Acta *63*, 45–47 (1993)
[73] F.J. Miller and P.F. Thomason, Anal. Chem. *33*, 404–406 (1961)
[74] R.J. Meyer, R.D. Oldham, and R.P. Larsen, Anal. Chem. *36*, 1975–1979 (1964)
[75] M. Koyama, K. Emoto, M. Kawashima, and T. Fujinaga, Chemia Analit. *17*, 679–690 (1972)
[76] F.J. Miller and P.F. Thomason, Anal. Chem. *32*, 1429–1430 (1960)
[77] M. Al-Kayssi and R.J. Magee, Talanta *10*, 1047–1053 (1963)
[78] M. Al-Kayssi, R.J. Magee, and C.L. Wilson, Talanta *9*, 125–132 (1962)
[79] A.F. Kuzina, J. Anal. Chem. [USSR] *17*, 487–489 (1962)
[80] F.J. Miller and H.F. Zittel, Anal. Chem. *35*, 299–301 (1963)
[81] F. Jasim, R.J. Magee, and C.L. Wilson, Talanta *2*, 93–95 (1959)
[82] R.J. Magee and M. Al-Kayssi, Anal. Chim. Acta *27*, 469 (1962)
[83] G.W. Parker and W.J. Martin, Oak Ridge National Laboratory, Declassified Report ORNL-1116, (1952) p. 26
[84] S. Tribalat and J. Beydon, Anal. Chim. Acta *6*, 96–97 (1952)
[85] R.A. Pacer, Talanta *27*, 689–692 (1980)
[86] F. Jasim, R.J. Magee, and C.L. Wilson, Mikrochim. Acta *5–6*, 721–728 (1960)
[87] W. Geilmann and A. Voigt, Z. Anorg. Allgem. Chem. *193*, 311 (1930)
[88] R.D. Peacock, The Chemistry of Technetium and Rhenium, Elsevier Publishing Company (1966)
[89] R. Colton, J. Dalziel, W.P. Griffith, and G. Wilkinson. J. Chem. Soc. *1960*, 71–78
[90] C.L. Rulfs, R. Pacer, and A. Anderson, J. Electroanal. Chem. *15*, 61–66 (1967)
[91] S.I. Zhadanov, A.F. Kuzina, and V.I. Spitsyn, Russ. J. Inorg. Chem. *15*, 803–806 (1970)
[92] G.B.S. Salaria, C.L. Rulfs, and P.J. Elving, Anal. Chem. *35*, 979–982 (1963)

[93] G.B.S. Salaria, C.L. Rulfs, and P.J. Elving, J. Chem. Soc. 2479–2484 (1963)
[94] L. Astheimer and K. Schwochau, J. Electroanal. Chem. *8*, 382–389 (1964)
[95] V.I. Spitsyn, A.F. Kuzina, S.I. Zhadanov, and I.V. Kaimin, Russ. J. Inorg. Chem. *15*, 662–664 (1970)
[96] A.F. Kuzina, S.I. Zhdanov, and V.I. Spitsyn, Proc. Acad. Sci. USSR, Phys. Chem. Sect. *142/147*, 442–445 (1962)
[97] H.H. Miller, M.T. Kelley, and P.F. Thomason in: Advances in Polarography, Vol. 2 (I.S. Longmuir, ed.), Pergamon Press, New York (1960), pp. 716–726
[98] D.L. Love and A.E. Greendale, Anal. Chem. *32*, 780–786 (1960)
[99] L. Astheimer and K. Schwochau, J. Electroanal. Chem. *14*, 240–241 (1967)
[100] M. Friedrich and H. Ruf, J. Electroanal. Chem. *198*, 261–268 (1986)
[101] R. Dick, H. Ruf, and H.J. Ache, Kernforschungszentrum Karlsruhe, KfK 4524 (1989)
[102] A.A. Terry and H.E. Zittel, Anal. Chem. *35*, 614–618 (1963)
[103] G.-A. Mazzocchin, U. Mazzi, R. Portanova, and O. Traverso, J. Inorg. Nucl. Chem. *36*, 3783–3788 (1974)
[104] E. Anders, The Radiochemistry of Technetium, National Academy of Sciences, Nuclear Science Series, NAS-NS 3021, National Research Council (1960)
[105] M. Koyama, Bull. Chem. Soc. Japan *34*, 1766–1769 (1961)
[106] N.Sugarman and H. Richter, Phys. Rev. *73*, 1411–1412 (1948)
[107] J.W. Mihelich, M. Goldhaber, and E. Wilson, Phys. Rev. *82*, 972–973 (1951)
[108] K.T. Bainbridge, M. Goldhaber, and E. Wilson, Phys. Rev. *90*, 430–439 (1953)
[109] A. Steffen and K. Bächmann, Talanta *25*, 551–556 (1978)
[110] S. Tsalas and K. Bächmann, Anal. Chim. Acta *98*, 17–24 (1978)
[111] G.E. Boyd and Q.V. Larson, J. Phys. Chem. *64*, 988–996 (1960)
[112] J.J. Pinajian, Oak Ridge National Laboratory, ORNL-TM-1058 (1965)
[113] A. Beck, D. Dyrssen, and S. Ekberg, Acta Chem. Scand. *18*, 1695–1702 (1964)
[114] D.J. Pruett, Radiochim. Acta *28*, 153–157 (1981)
[115] K.H. Lieser, A. Krüger, and R.N. Singh, Radiochim. Acta *28*, 97–101 (1981)
[116] D.J. Pruett, Radiochim. Acta *29*, 107–111 (1981)
[117] A.M. El-Kot, J. Radioanal. Nucl. Chem. Art. *163*, 363–373 (1992)
[118] I. Spitsyn, A.F. Kuzina, N.N. Zamoshnikova, and T.S. Tagil, Dokl. Chem. Proc. Acad. Sci. USSR *142/144*, 540–542 (1962)
[119] B. Kanellakopulos and C.P. König, Radiochim. Acta *33*, 169–175 (1983)
[120] D.J. Pruett and D.R. McTaggart, Radiochim. Acta *34*, 203–206 (1983)
[121] F. Macásek, Radiochem. Radioanal. Lett. *22*, 175–183 (1975)
[122] D.J. Pruett, Sep. Sci. Technol. *16*, 1157–1179 (1981)
[123] M.H. Campbell, Anal. Chem. *35*, 2052–2054 (1963)
[124] A.A. Zaitsev, I.A. Lebedev, S.V. Pirozhkov, and G.N. Yakovlev, Soviet Radiochem. *6*, 423–427 (1964)
[125] A.F. Kuzina, T.S. Tagil, N.N. Zamoshnikova, and V.I. Spitsyn, Proc. Acad. Sci. USSR, Chem. Sect. *142/147*, 569–571 (1962)
[126] M.S. Faddeeva, O.N. Pavlov, and V.V. Bakunina, Russ. J. Inorg. Chem. *3*, 251–254 (1958)
[127] E.P. Belkas and D.C. Perricos, Radiochim. Acta *11*, 56–57 (1969)
[128] D.V.S. Narasimhan and R.S. Mani, J. Radioanal. Chem. *33*, 81–100 (1976)
[129] N.K. Baishya, R.B. Heslop, and A.C. Ramsey, Radiochem. Radioanal. Lett. *4*, 15–20 (1970)
[130] G. Goldstein and J.A. Dean, Radiochim. Acta *5*, 18–20 (1966)
[131] Q.-J. Chen, A. Aarkrog, H. Dahlgaard, S.P. Nielsen, E. Holm, H. Dick, and K. Mandrup, J. Radioanal. Nucl. Chem. Art. *131*, 171–187 (1989)
[132] W. Goishi and W.F. Libby, J. Amer. Chem. Soc. *74*, 6109 (1952)
[133] S.J. Rimshaw and G.F. Malling, Anal. Chem. *33*, 751–754 (1961)
[134] A.A. Zaitsev, I.A. Lebedev, S.V. Pirozhkov, and G.N. Yakovlev, Soviet Radiochem. *6*, 428–431 (1964)
[135] M. Iqbal and M. Ejaz, J. Radioanal. Chem. *23*, 51–62 (1974)
[136] M. Ejaz and A.M. Mamoon, J. Radioanal. Nucl. Chem. *125*, 419–430 (1988)
[137] S. Hirano, M. Matsuba, and H. Kamada, Radioisotopes *38*, 186–189 (1989)
[138] C. Klofutar, V. Stular, and F. Krasovec, Z. Analyt. Chem. *214*, 27–33 (1965)
[139] K.F. Fouché, J. Inorg. Nucl. Chem. *33*, 857–861 (1971)
[140] F. Sebesta, S. Posta, and Z. Randa, Radiochem. Radioanal. Lett. *11*, 359–365 (1972)
[141] Z.R. Turel, P.M. Shanbhag, and B.C. Haldar, J. Indian Chem. Soc. *52*, 413–415 (1975)
[142] R. Shanker, K.S. Venkateswarlu, and J. Shankar, J. Less-Common Metals *15*, 311–316 (1968)
[143] D.L. Swindle and P.K. Kuroda, Radiochem. Radioanal. Lett. *7*, 229–234 (1971)

[144] H. Feuerstein, Kernforschungszentrum Karlsruhe, KFK 358 (1965)
[145] G.B.S. Salaria, C.L. Rulfs, and P.J. Elving, Anal. Chem. *35*, 983–985 (1963)
[146] A.A. Pozdnyakov, N.N. Basargin, and Y.B. Gerlit, Doklady Akademii Nauk SSSR *144*, 861–863 (1962)
[147] S. Tribalat and J. Beydon, Anal. Chim Acta *8*, 22–28 (1953)
[148] N. Souka and A. Sayed Ali, J. Radioanal. Chem. *26*, 271–277 (1975)
[149] R.N. Singh, A. Krüger, and K.H. Lieser, Radiochim. Acta *26*, 197–198 (1979)
[150] H. Kupsch and H. Koch, Isotopenpraxis *17*, 2–6 (1981)
[151] B. Kanellakopulos, Kernforschungszentrum Karlsruhe, KFK 3679 (1984)
[152] G.B.S. Salaria, C.L. Rulfs, and P.J. Elving, Anal. Chem. *36*, 146–149 (1964)
[153] T. Kiba, K. Terada, N. Ōkawa, and S. Ōsaki, Talanta *13*, 1385–1388 (1966)
[154] J.-H. Chiu, T.-C. Chu, and P.-S. Weng, Anal. Chim. Acta *256*, 293–299 (1992)
[155] I. Hanif, S.M. Hasany, and M. Ejaz, Radiochim. Acta *24*, 19–20 (1977)
[156] N. Boukis and B. Kanellakopulos, Radiochim. Acta *49*, 141–145 (1990)
[157] M. Jowtscheff and H. Koch, Isotopenpraxis *12*, 314–320 (1976)
[158] M. Kawasaki, T. Omori, and K. Hasegawa, Radiochim. Acta *63*, 53–56 (1993)
[159] Ihsanulla, Sep. Sci. Techn. *29*, 239–247 (1994)
[160] E. Anders, The Radiochemistry of Technetium, National Academy of Sciences, National Research Council (1960)
[161] R.W. Atteberry and G.E. Boyd, J. Amer. Chem. Soc. *72*, 4805–4806 (1950)
[162] E.A. Alperovitch and J.M. Miller, Nature *176*, 299–301 (1955)
[163] G.E. Boyd and Q.V. Larson, J. Phys. Chem. *60*, 707–715 (1956)
[164] R.N. Sen Sarma, E. Anders, and J.M. Miller, J. Phys. Chem. *63*, 559–565 (1959)
[165] M. Pirs and R.J. Magee, Talanta *8*, 395–399 (1961)
[166] H. Hamaguchi, K. Kawabuchi, and R. Kuroda, Anal. Chem. *36*, 1654–1656 (1964)
[167] N.F. Hall and D.H. Johns, J. Amer. Chem. Soc. *75*, 5787–5791 (1953)
[168] E.H. Huffman, R.L. Oswalt, and L.A. Williams, J. Inorg. Nucl. Chem. *3*, 49–53 (1956)
[169] R. Kopunec, F. Macásek, P. Rajec, and D. Hudecová, J. Radioanal. Chem. *51*, 401–405 (1957)
[170] M. Levi and M. Lederer, J. Inorg. Nucl. Chem. *4*, 381–382 (1957)
[171] L. Ossicini, F. Saracino, and M. Lederer, J. Chromatog. *16*, 524–537 (1964)
[172] S.K. Shukla, J. Chromatog. *21*, 92–97 (1966)
[173] S.K. Shukla, Ric. Sci. *8*, 725–728 (1966)
[174] T.J. Beckmann and M. Lederer, J. Chromatog. *5*, 341–350 (1961)
[175] R.A. Bailey and L. Yaffe, Can. J. Chem. *38*, 1871–1889 (1960)
[176] K.E. Scheer and W. Maier-Borst, Nucl. Med. *3*, 214–217 (1962)
[177] N.B. Mikheev, M. El Garhy, and Z. Moustafa, Atompraxis *10*, 263–264 (1964)
[178] W.D. Tucker, M.W. Greene, and A.P. Murrenhoff, Atompraxis *8*, 163–167 (1962)
[179] W. D'Olieslager, J. Indesteege, and M. D'Hont, Talanta *22*, 395–399 (1975)
[180] H. Seiler, Helv. Chim. Acta *52*, 319–322 (1969)
[181] L. Oniciu and G.B. Cook, J. Radioanal. Chem. *13*, 247–254 (1973)
[182] K.H. Lieser, Z. Anal. Chem. *273*, 189–192 (1975)
[183] G. Zuber and K.H. Lieser, Radiochim. Acta *21*, 60–62 (1974)
[184] I. Yamagishi and M. Kubota, J. Nucl. Sci. Technol. *26*, 1038–1044 (1989)
[185] B. Gu, K.E. Dowlen, L. Liang, and J.L. Clausen, Sep. Technol. *6*, 123–132 (1996)
[186] R. Strickert, A.M. Friedman, and S. Fried, Trans. Am. Nucl. Soc. *28*, 365–366 (1978)

8 Uses of technetium-99

Among the technetium isotopes, only ^{99}Tc, a pure β^- emitter (E_{max}=0.29 MeV) with a half-life of 213 000 a, can be obtained (Sect. 5.1) in amounts adequate for studying the technical applicability of the element and its compounds. However, the widespread use of technetium is necessarily restricted by its radioactivity. The application of the metastable isotope ^{99m}Tc in nuclear medicine has quite superior significance and will be described in detail in Part B.

8.1 Radiation source

The decay characteristics of ^{99}Tc, in particular the absence of γ radiation and its long half-life, suggest the application of this isotope as a standard source of weak β^- radiation. Its specific activity of 17.0 μCi/mg or 629 kBq/mg remains practically independent of time. ^{99}Tc can be isolated to a high degree of chemical and radiochemical purity, for instance by cathodic electrodeposition of $^{99}TcO_2$-hydrate on a thin silver foil of 0.005 mm thickness from 2 M NaOH solutions of pertechnetate at –0.75 V *vs* SCE. The self-scattering and self-absorption characteristics are such that ^{99}Tc makes an excellent β standard [1]. Another procedure utilizes the solubility of some pertechnetates in organic solvents, e.g. in acetone, for preparing film sources containing ^{99}Tc. When a film forming substance is added to the solution, a film with a uniform distribution of $^{99}TcO_4$ is obtained after drying or polymerization [2].

Metallic ^{99}Tc foils of 23 μm thickness and 15 × 20 cm^2 surface coated with a thin layer of acryl lacquer were used for β-radiography [3]. In the determination of heavy elements by X-ray fluorescence, ^{99}Tc was proposed as radiation source for the excitation of the *K*-fluorescence radiation [4]. In addition, ^{99}Tc was considered as radiation source for ionization detectors in gas chromatography [5].

8.2 Catalyst

In view of the excellent catalytic properties of rhenium and the related platinum metals, it was expected that technetium metal and compounds of technetium would also be qualified to be specific catalysts [6].

As early as 1968 the specific catalytic activities of a ^{99}Tc metal catalyst supported on silica or γ-alumina at a concentration of 1 wt% were studied in detail for the reactions of benzene with hydrogen in the temperature range of 100–235 °C. Both technetium and rhenium metal revealed catalytic activity in hydrogenation of benzene to cyclohexane. At temperatures above 130–200 °C both metals, like ruthenium, also catalyze benzene hydrogenolysis resulting in saturated normal aliphatic C_1–C_6 hydrocarbons. The catalytic activities of the metals for hydrogenation and hydrogenolysis decrease in the order Ru>Pt>Tc ≈ Pd>Re and Ru>Tc>Re, respectively. The apparent activation energies were found to be 7–11 kcal/mole for hydrogenation and 29–32 kcal/mole for hydrogenolysis. The activity of technetium for hydrogenation in the case of a γ-alumina carrier proved to be four times higher, the selectivity, however, six times lower than in the case of silica supported catalysts [7].

Later on, the reverse reaction, e.g., the dehydrogenation of cyclohexane, on technetium metal supported on γ-alumina was investigated between 260 and 500 °C. Benzene was formed with high selectivity. The apparent activation energy of the reaction was 13.1 kcal/mole. At temperatures higher than 410 °C cracking processes increasingly dominated. The dehydrocyclization of *n*-hexane yielded around 15 wt% of benzene and, in addition, rather high concentrations of toluene and xylene at 510 °C [8].

Similar studies were carried out on the aromatization of *n*-hexane and *n*-heptane on technetium metal catalysts supported by γ-Al_2O_3, MgO, Y_2O_3, SiO_2 or activated carbon. With an increase in the content of supported technetium (1 to 5 wt%) the yield of benzene (1.5 to 17.0 wt%) for the dehydrogenation reaction of *n*-hexane and the yield of toluene (2.0 to 22.8 wt%) for the reaction of *n*-heptane generally increased in the temperature range from 450 to 600 °C [10].

Aluminum oxide containing 0.16–0.27 wt% of metallic technetium also catalyzes the dehydrogenation of aliphatic alcohols to the corresponding aldehydes or ketones in the temperature range of 150 to 300 °C. The catalyst activity was constant over 10 h of continuous operation. CH_3OH, C_2H_5OH and $CH_3CH(OH)CH_3$ decomposed without any side reactions. The highest rate and the lowest temperature (150 °C) for initiation of the reaction were observed for the dehydrogenation of isopropyl alcohol to form acetone:

$$CH_3CH(OH)CH_3 \xleftarrow[0.5g\ (Tc/Al_2O_3)]{150\ \ 240\ ^\circ C} H_3CCOCH_3 + H_2$$

The most active Tc metal catalyst was obtained at the lowest temperature used for the reduction of TcO_2 to Tc metal. The apparent activation energy for the dehydrogenation process was 13.7 kcal/mole. At 220 °C 30 % of isopropyl alcohol was converted to acetone. The activity of the technetium metal catalyst for the dehydrogenation of isopropyl alcohol is superior to that of manganese and close to that of metallic rhenium when, however, the content of rhenium in the catalyst was 30 wt% instead of around 0.2 wt% of technetium [11].

In addition, the dehydrogenation of isopropyl alcohol was studied using technetium metal supported on the oxides Y_2O_3, Pr_4O_7, Nd_2O_3 or Yb_2O_3. Table 8.1.A. summarizes the results.

Table 8.1.A Catalysts and activity for dehydrogenation of isopropyl alcohol [12].

Catalyst		Degree of Conversion [%]		Dehydrogenation selectivitiy [%]	
Oxide	**Tc (%)**	**300 °C**	**370 °C**	**300 °C**	**370 °C**
Y_2O_3	0	0	22		7
	0.016	10	24	95	47
	0.030	28	64	100	100
	0.057	33	82	100	100
Pr_4O_7	0	0	12	–	75
	0.045	19	36	100	100
Nd_2O_3	0	0	36		92
	0.08	40	95	100	100
Yb_2O_3	0	0	21	–	25
	0.12	40	95	100	100

The outstanding catalytic properties of technetium metal compared to rhenium and palladium are illustrated in Fig. 8.1.A. On the ordinate the conversion rate of isopropyl alcohol in ml/min is plotted. According to Table 8.1.A the catalytic properties of the supporting oxides are substantially changed by adding even small amounts of technetium. The activity of the catalysts increases with increasing wt% of technetium. In particular, the selectivity of the dehydrogenation attains 100 % [12].

For reforming naphtha to gasoline by hydrogenation a Pt-Tc/Al_2O_3 catalyst containing 0.1 to 10 wt% Tc and 0.6 wt% Pt was employed at a pressure of 160 psig in the temperature range of 66 to 220 °C. The Pt-Tc catalyst exhibited greater stability than did one containing only Pt [13,14].

A technetium catalyst prepared by reduction of an aqueous solution of $HTcO_4$ with hydrogen at 200 °C under a pressure of 23 MPa was used for hydrogenation of succi-

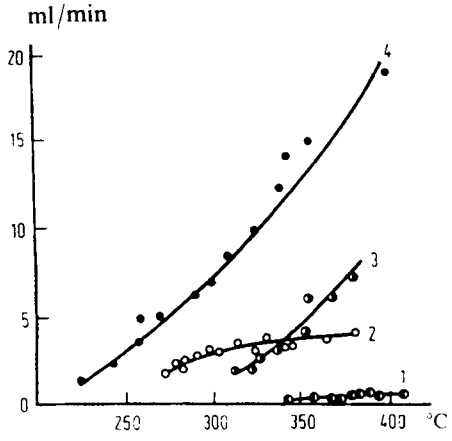

Fig. 8.1.A Dehydrogenation rate of isopropyl alcohol on catalysts. Y_2O_3(1), Y_2O_3+0.06 % Re(2), Y_2O_3+ 0.06 % Pd(3), Y_2O_3+0.06 % Tc(4) [12].

nic anhydride, 2,2-dimethyl succinic anhydride, and glutaric anhydride in an autoclave under the conditions of the catalyst preparation. The hydrogenation of succinic anhydride resulted predominantly (66 wt%) in the formation of γ-butyrolacton, in contrast to the reaction catalyzed by rhenium which mainly promoted the formation of tetrahydrofuran (78 wt%). The hydrogenation of glutaric anhydride yielded prevailingly tetrahydropyran, independent of the use of the technetium or the rhenium catalyst [15].

The catalytic properties of chlorophosphine complexes of technetium such as $[TcCl_4(Ph_3P)_2]^\circ$ for the hydrogenation of cyclohexene and octene-1, dissolved in benzene, were studied in the presence of sodium amalgam and/or 0.1 MPa H_2. The catalytic activity of the technetium complexes was shown to be evident but low as compared to the most active complexes of Ru, Rh or Ir [16].

The catalytic activity of various complex compounds of technetium was tested in the metathesis of olefins [17], epoxide ring opening reactions [18], epoxide ring formation by reaction of cyclohexene with *tert*-butylhydroperoxide [19,20], and the preferred production of *trans*-epoxides in the liquid phase oxidation of *cis/trans-n*-alkenes [21].

The technetium carbonyl catalysts, $[Tc_2(CO)_{10}]^\circ$ and $[Tc_2(CO)_{10}]^\circ/P(n\text{-}C_4H_9)_3$ promote the hydroformylation reactions of cyclohexene, propene, and 1-octene in solution at 235 °C and a pressure of 20 MPa. $[Tc_2(CO)_{10}]^\circ/P(n\text{-}C_4H_9)_3$ showed the best results in activity and selectivity within the anologous subgroup VII complexes studied, but proved to be a rather poor catalyst compared with the cobalt or rhodium carbonyl compounds [22].

In hydrogenation of carbon monoxide over supported catalysts of technetium metal between 270 and 500 °C in a helium flow, predominantly methane was formed. The conversion of CO into methane increased with increasing temperature. Conversion yields up to 100 vol% of CH_4 were obtained over a $Tc/\gamma\text{-}Al_2O_3$ catalyst [23].

Technetium in different oxidation states appears to catalyze the oxidation of hydrazine by nitric acid, a reaction which is otherwise very slow except at elevated temperatures and acidities. The reaction between TcO_4 and hydrazine in acidic nitrate media has attracted interest as a reaction occurring in the reprocessing of spent nuclear fuel. The hydrazine oxidation displays an induction period followed by rapid reaction. The induction period covers a slow reduction of Tc(VII) to Tc(IV) by hydrazine followed by a Tc(IV)-catalyzed reduction of Tc(VII) by hydrazine. The rapid reaction commences when Tc(VII) has been substantially reduced to Tc(IV). The mechanism of the rapid reaction is considered to be the oxidation of Tc(IV) to Tc(VI) by nitrate followed by reduction of Tc(VI) to Tc(IV) by hydrazine. On completion of the reaction, technetium is present predominantly as pertechnetate [24–27]. In addition, the oxidation of hydrazine by an aqueous acid perchlorate medium is catalyzed by pertechnetate. The reaction again shows an induction period followed by a fast stage of N_2 evolution, but no residue of unreacted hydrazine is left, in contrast to the nitrate system. The concentration of Tc(IV) in the perchlorate system goes through two maxima as the reaction proceeds [28]. The elucidation of the highly complex oxidation mechanisms of hydrazine needs further investigation.

8.3 Technetium(VII) as an oxidizing agent

The trioxo complexes of technetium in the oxidation state +7, $[TcO_3Cl(phen)]^\circ$, $[TcO_3Cl(bpy)]^\circ$, $[TcO_3Cl(5\text{-}NO_2\text{-}phen)]^\circ$, $[TcO_3Cl(3,4,7,8\text{-tetramethyl-phen})]^\circ$ [eq.(1)], and [TcO_3-hydrotris(1-pyrazo-lyl)borate]$^\circ$ [eq.(2)] clearly oxidize olefins forming, in high yields, the corresponding oxotechnetium(V) diolate complexes [29,30]:

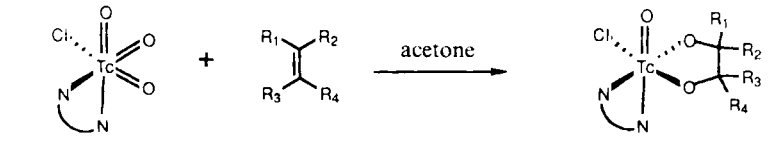

(1)

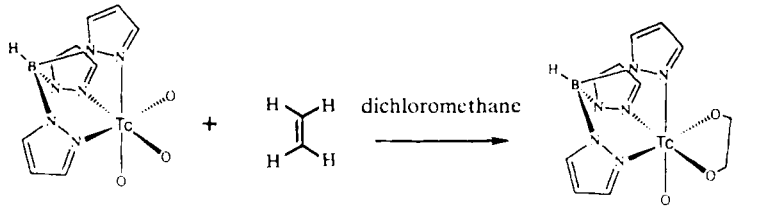

(2)

From the diolate complexes the free diols can be released by hydrolysis with hydrochloric acid. The diols reveal *cis*-addition of the two hydroxyl groups. The rhenium complex $[ReOCl(OCH_2CH_2O)(phen)]^\circ$ undergoes the reverse reaction by thermolysis, releasing ethylene and producing $[ReO_3Cl(phen)]^\circ$. The results are consistent with the periodic trends for second and third row transition elements of similar environments in which the second row elements are more easily reduced and the third row elements are more easily oxidized [29].

Methyltrioxotechnetium(VII), CH_3TcO_3, is also capable of adding olefins such as cyclohexene and forming the glycolate complex of Tc(V) that releases, by hydrolysis in the presence of acids, the 1,2-diols. When cyclohexene was added, the stereospecific production of *cis*-1,2-cyclohexanediol was observed [31].

8.4 Pertechnetate as an inhibitor of corrosion

Already in 1952 the effectiveness of TcO_4^- ions in aqueous solutions for the corrosion inhibition of iron and carbon steels was discovered [32,33]. A specimen of steel was efficiently protected against corrosion at temperatures of up to at least 250 °C in aerated distilled water containing $5 \cdot 10^{-5}$M TcO_4^-, one-tenth of the concentration required for corrosion inhibition by CrO_4^{2-}. The test specimen remained bright and unchanged in weight after being exposed for 20 years in the aqueous TcO_4^- solution at pH ~ 6. To achieve inhibition under very corrosive conditions not more than $2.2 \cdot 10^{14}$ technetium atoms per cm^2 must be deposited on the surface of the specimen, about a tenth of a monolayer. However, an inhibited specimen corroded at once when

removed from the pertechnetate solution, or when the solution was diluted below the limiting concentration of $5 \cdot 10^{-5}$ M [34,35]. Perrhenate does not inhibit corrosion, in spite of the close resemblance between the properties of perrhenate and pertechnetate. Also permanganate fails to inhibit corrosion except at relatively high concentrations of 10^{-1} M [36]. The inhibition of TcO_4^- depends on a labile state at the interface that is quickly responsive to changes in the composition of the solution by adding electrolytes. Addition of sulphate ions in a concentration of $2.5 \cdot 10^{-3}$ M disturbs the inhibition much more than perrhenate ions at the same concentration [37].

In the initial passivation process hydrous technetium oxide is produced and a film of mixed hydrous iron and hydrous technetium oxide is formed [38], but the inhibition cannot be ascribed to such a film in the absence of TcO_4^- [39]. The potential of the passivated iron electrode immersed in TcO_4^- solutions was found to be +0.157 V *vs* SCE at a TcO_4^- concentration of $4.7 \cdot 10^{-4}$ M and a pH of 6.4 in aerated aqueous solution, showing the iron electrode more noble than the Flade potential in the presence of dissolved air [40]. ReO_4^- has a less ennobling effect than TcO_4^- [41]. The passivation effect appears to be a combined action of oxygen and adsorbed pertechnetate and arises from some intra-ionic property of the TcO_4^- ion. It suggests a degree of internal polarity sufficient to induce a short-range electrostatic polarization at the interface, whereby the activation energy of the corrosion process is increased [35]. But there is still no complete understanding of the corrosion inhibition of iron by pertechnetate.

Of course, the actual application of pertechnetate ions to corrosion inhibition of iron and carbon steels will obviously be a great problem because of the radioactivity of ^{99}Tc, even in dilute solutions of $^{99}TcO_4^-$. A pertechnetate concentration of $5 \cdot 10^{-5}$ M corresponds to a specific radioactivity of 84.15 μCi/l or $3.11 \cdot 10^6$ Bq/l. Nevertheless, the corrosion inhibiting property of $^{99}TcO_4^-$ was proposed to be used in steam-generating nuclear reactors [42,43].

8.5 References

[1] M. Matsuura and H. Yumoto, Radioisotopes *8*, 32–33 (1959)
[2] K.V. Kotegov, O.N. Pavlov, and V.P. Shvedov, Advan. Inorg. Chem. Radiochem. *11*, 1–90 (1968)
[3] V.I. Spitzin, Z. Chem. [Leipzig] *21*, 131–136 (1981)
[4] K.H. Neeb, H. Neidl, and H.J. Weisse, Ger. Offen. 2, 140, 794, Feb. 1973, C.A. 78 (1973) No. 131766
[5] G.R. Shoemake, D.C. Fenimore, and A. Zlatkis, J. Gas Chromatog. *3*, 285–286 (1965)
[6] K. Schwochau, Angew. Chem. *76*, 9–19 (1964)
[7] H. Kubicka, J. Catalysis *12*, 223–237 (1968)
[8] J.L. Palmer, Brigham Young University, Diss. Abstr. Intern. *B35*, 2644 (1974)
[9] F. Bauer and C. Riedel, Chem. Techn. (Leipzig) *37*, 67–70 (1985)
[10] V.I. Spitsyn, G.N. Pirogova, R.I. Korosteleva, and G.E. Kalinina, Dokl. Akad. Nauk. SSSR, *298*, 149–151 (1988)
[11] V.I. Spitsyn, G.N. Pirogova, and R.I. Korosteleva, Dokl. Chem. Proc. Acad. Sci. USSR *208/13*, 104–105 (1973)
[12] V.I. Spitsyn, G.N. Pirogova, R.I. Korosteleva, and T.A. Lagutina, Bull. Acad. Sci. USSR, Div. Chem. Sci *1978*, 1677–1678
[13] M.M. Holm, Chevron Research Co., U.S. 3, 968, 025, July 6 (1976)
[14] M.M. Holm, Chevron Research Co., U.S. 4, 018, 667, Apr. 19 (1977)

[15] B. Bayerl and M. Wahren, Z. Chem. *21*, 149 (1981)
[16] L. Kaden, B. Lorenz, and M. Wahren, Isotopenpraxis *18*, 400–403 (1982)
[17] B. Lorenz, H. Rommel, and M. Wahren, Z. Chem. *22*, 224 (1982)
[18] S. Rummel, D. Schnurpfeil, and L. Willecke, Z. Chem. *25*, 150 (1985)
[19] S. Rummel and B. Lorenz, Isotopenpraxis *22*, 36–37 (1986)
[20] S. Rummel and D. Schnurpfeil, Oxidation Commun. *6*, 319–329 (1984)
[21] S. Rummel and D. Schnurpfeil, J. Prakt. Chem. *329*, 10–18 (1987)
[22] L. Kaden, B. Lorenz, and M. Wahren, J. Prakt. Chem. *328*, 407–412 (1986)
[23] N.M. Panich, T.A. Lagutina, and G.N. Pirogova, Izv. Akad. Nauk, Ser. Khim, 1507–1511 (1992)
[24] G.A. Akopov, A.P. Krinitsyn, and A.F. Tsarenko, Sov. Radiochem. *24*, 442–444 (1982)
[25] J. Garraway and P.D. Wilson, J. Less Common Met. *97*, 191–203 (1984)
[26] A.M. Thyer, Diss. Abstr. Int. B, *52* (11), 5820 (1992)
[27] T.J. Kemp, A.M. Thyer, and P.D. Wilson, J. Chem. Soc. Dalton Trans. 2601–2605 (1993)
[28] T.J. Kemp, A.M. Thyer, and P.D. Wilson, J. Chem. Soc. Dalton Trans. 2607–2611 (1993)
[29] R.M. Pearlstein and A. Davison, Polyhedron 7, 1981–1989 (1988)
[30] J.A. Thomas and A. Davison, Inorg. Chim. Acta *190*, 231–235 (1991)
[31] W.A. Herrmann, R. Alberto, P. Kiprof, and F. Baumgärtner, Angew. Chem. *102*, 208–210 (1990)
[32] G.H. Cartledge, Corrosion *29*, 361–362 (1973)
[33] G.H. Cartledge, J. Am. Chem. Soc. *77*, 2658–2659 (1955)
[34] G.H. Cartledge, J. Phys. Chem. *59*, 979–984 (1955)
[35] G.H. Cartledge, Corrosion *11*, 335t–342t (1955)
[36] G.H. Cartledge, J. Electrochem. Soc. *114*, 39–42 (1967)
[37] G.H. Cartledge, J. Phys. Chem. *60*, 28–32 (1956)
[38] G.H. Cartledge, Isotopes and Radiation Technology *1*, 125–129 (1963/64)
[39] G.H. Cartledge, Brit. Corros. J. *1*, 293–302 (1966)
[40] R.F. Sympson and G.H. Cartledge, J. Phys. Chem. *60*, 1037–1043 (1956)
[41] G.H. Cartledge, J. Phys. Chem. *60*, 32–36 (1956)
[42] Chem. Eng. News *39*, No. 9, 52 (1961)
[43] Sci. News Lett. *83*, 264 (1963)

9 Technetium metal

9.1 Preparation

Technetium metal is obtained by hydrogen reduction of ammonium pertechnetate. The initial reaction at 200–300 °C produces black technetium dioxide which prevents the loss of ammonium pertechnetate by sublimation [1]. At a temperature of 500–600 °C or, even better, 700–900 °C [2] the metal is left behind as a silver-grey spongy mass according to the reaction:

$$NH_4TcO_4 + 2H_2 \rightarrow Tc + 4H_2O + 1/2\ N_2$$

Heating of ammonium hexachlorotechnetate(IV) in an inert atmosphere, e.g. nitrogen, at a dull red heat, also yields technetium metal. The complex salt does not melt, but decomposes under these conditions to leave technetium metal as a fine silver-grey powder [3]:

$$(NH_4)_2[TcCl_6] \rightarrow Tc + 2NH_3 + 2HCl + 2Cl_2$$

In addition, hydrogen reduction of tetraphenylarsonium pertechnetate at 900–1000 °C produces technetium as a light grey powder with the characteristic metallic luster [5].

Films of technetium metal 5 mg/cm^2 thick can be electrodeposited on to a copper cathode, using a plating bath of 0.2 wt% technetium as NH_4TcO_4 in 1 M H_2SO_4, and a platinum anode. Agitation was by means of a circulating pump and gave a flowrate of 50 ft/min across the electrodes, and the bath was initially at room temperature, rising during the electrodeposition to about 40 °C. Technetium metal plates as a bright silver deposit, but the deposition stops after about a quarter of the total technetium has been deposited. This appears to be due to the accumulation of technetium dioxide hydrate formed by reduction of TcO_4^-. Complete deposition of technetium metal can be obtained by the continuous addition of small quantities of H_2O_2 just sufficient to oxidize the brown-black TcO_2-hydrate back to pertechnetate [3,4].

Technetium metal is also electrodeposited almost quantitatively from dilute solutions of TcO_4^- in acidic ammonium oxalate solutions. Films up to 18 mg/cm^2 were deposited as dense adherent coatings on copper, gold, silver, and platinum cathodes at a current density of 1.3 A/cm^2. At an oxalate concentration of 0.7 M, the molarity of H_2SO_4 required for the deposition of technetium metal varied between 0.45 M with a copper cathode and 1.90 M with a platinum cathode. At lower molarities of H_2SO_4 technetium was deposited as oxide (Table 9.1.A).

The technetium metal deposits had a purity of about 99 % under optimal conditions. Technetium was deposited on the cathodes in the form of microscopic spheres and could easily be removed from the cathode when dried [6].

Table 9.1.A Molarity of H_2SO_4 required for deposition of ^{99}Tc at an oxalate concentration of 0.7 M [6].

Cathode	as metal	as oxide
Copper	0.45	0.32
Nickel	0.87	0.58
Aluminum	1.14	0.71
Silver	1.41	0.87
Gold	1.41	0.87
Stainless Steel	1.411	0.87
Platinum	1.90	1.14

9.2 Physical properties

Technetium metal powder pressed into pellets at room temperature and a pressure of 20 kg/mm^2 [7] can be transformed to the compact metal by arc melting under an argon-helium mixture [8] or by electron beam melting in a vacuum of 10^{-6} torr [5,9]. Technetium is a bright silvery grey metal which is reported to tarnish slowly in a moist atmosphere [10]. Although technetium is brittle it can be formed into rod, foil, plate, and wire by using cold treatments and annealings. Cold-worked technetium has the greatest strength while recrystallized technetium the greatest plasticity. Cold-rolled technetium exhibits appreciably anisotropic mechanical properties. With increasing deformation, technetium metal displays a relatively strong increase of temper [11,12].

Three determinations of the melting point of technetium metal are in reasonably good agreement: 2140 ± 20 °C [13], 2200 ± 50 °C [14], and 2162 ± 40 °C [15]. The average melting point of 2167 °C is near those of neighboring elements in the same period—molybdenum (2610 °C) and ruthenium (2310 °C)—but almost 1000 °C lower than that of rhenium [14]. The boiling point of technetium metal was estimated as 4900 K [16]; no experimental value seems to be available.

For an ingot of arc-melted technetium metal, weighing approximately 70 g, the immersion density was found to be 11.47 g/cm^3 [7]. An electron-beam melted sample showed a density of 11.492 g/cm^3 [17]. The X-ray density, calculated with the lattice parameters a=2.7407 Å, c=4.3980 Å [18] and the nuclide mass of 98.906 g, yields 11.481 g/cm^3, which is just a little higher than that of lead.

Technetium, like rhenium, ruthenium, and osmium, crystallizes in the hexagonal close-packed arrangement, whereas manganese forms a cubic lattice at room temperature. The lattice constants [18–20] a=2.7407 ± 0.0001 and c=4.3980 ± 0.0001 Å at 298 K decrease smoothly to a=2.7364 and c=4.3908 at 4.2 K [18]. No change in the symmetry of the lattice nor any unusual changes in the expansion coefficients were found in this range of temperature. The expansion coefficients between 150 and 298 K are $\alpha_a = 7.04 \cdot 10^{-6}$ K^{-1} and $\alpha_c = 7.06 \cdot 10^{-6}$ K^{-1}. The axial ratio is remarkably constant only increasing from 1.6046 at 4.2 K to 1.6048 at 298 K [18]. No change of the crystal struc-

ture of technetium metal could be observed from shearing experiments up to a pressure of $6 \cdot 10^4$ kp/cm^2 [20].

The high superconducting transition temperature of technetium metal, the highest for a hexagonal metal and the second-highest transition temperature for any element, being exceeded only by niobium, has received much attention. The transition temperature was reported as 11.2 K for technetium powder of greater than 99.9 % purity [22], and as 9.3 K for material melted in an arc furnace in an argon atmosphere [23]. Technetium, melted several times by induction under a vacuum of 10^{-6} torr until there was no further evolution of vapor detected, had a superconducting transition temperature of 8.22 ± 0.01 K in zero magnetic field. The purity of the specimen was greater than 99.995 % [24]. Also in subsequent studies transition temperatures were observed to decrease apparently with increasing purity of the technetium metal [25,26]. Technetium cylindrical single crystals with axis parallel to [10$\bar{1}$0] had a transition temperature of 7.46 ± 0.04 K [27]. The pressure dependence of the transition temperature up to a pressure of 15 kbar was found to be $(-1.25 \pm 0.05) \cdot 10^{-5}$ K/bar [28].

The electrical resistivity of arc-melted technetium metal was determined from its superconducting transition temperature of 7.5 K to 1700 K. Above 77 K the resistivity can be described by ρ (in $\mu\Omega \cdot$ cm)= $-3.191 + 7.844 \cdot 10^{-2}T - 2.816 \cdot 10^{-5}T^2 + 4.038 \cdot 10^{-9}T^3$. From the electrical resistivity data a Debye temperature for technetium was calculated to be 411 K [7].

The thermal diffusivity of technetium was measured from room temperature to 575 °C by the flash method [29,30]. The thermal conductivity was calculated from the thermal diffusivity data [17]. Later on, the thermal diffusivity measurements were extended from 80 to 1800 K [31]. The specific heat (Cp) of technetium was determined in the temperature range 1000 to 1600 K. The metal investigated contained approximately 0.08 wt% of impurities. Cp increases slightly from 0.29 $J \cdot g^{-1} \cdot K^{-1}$ at 1000 K to 0.31 $J \cdot g^{-1} \cdot K^{-1}$ at 1600 K [31–33]. The heat capactiy was measured in zero-field between 3 and 15 K using a heat-pulse method designed for use with self-heating samples. The decay of ^{99}Tc by β^- emission results in a self-heating power of ≈15 μW/g. The electronic heat capacity coefficient and the zero-degree Debye temperature are 4.30 mJ · mole$^{-1} \cdot K^{-2}$ and 454 K, respectively [34]. The thermo-emf of technetium metal was studied by a contact-potentiometric method in a vacuum of 10^{-6} torr, with technetium coupled with platinum (Fig. 9.1.A) [31].

Some physical property data of technetium metal are summarized in Table 9.2.A.

Table 9.2.A Physical properties of technetium metal.

Property	Value	References
Melting point	2413 ± 20 K	[13]
Density (immersion)	11.47 g · cm^{-3}	[7]
Crystal structure	hexagonal close-packed	[18]
Lattice dimensions (298 K)	a = 2.7404 Å, c = 4.3980 Å	[18]
Superconducting transition temperature	7.73 ± 0.02 K	[25]
Debye temperature (zero-degree)	454 ± 4 K	[34]
Entropy (298.15 K)	33.0 ± 0.3 J · mole^{-1} · K^{-1}	[35]
Magnetic susceptibility (298 K)	$2.7 \cdot 10^{-6}$ cm$^3 \cdot$ g^{-1}	[36]
Specific heat Cp (1000 K)	0.29 J · g$^{-1} \cdot$ K^{-1}	[31]
Work function	4.88 ± 0.05 eV	[37]

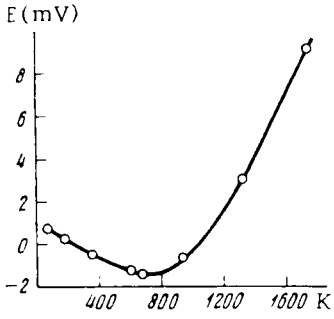

Fig. 9.1.A Integral thermo-emf of Tc metal coupled with Pd metal as a function of temperature [31].

9.3 Chemical properties

Massive technetium metal tarnishes slowly in a moist atmosphere. In sponge or powder form it is readily oxidized to the volatile heptoxide when heated in air. The metal dissolves in dilute or conc. nitric acid, in conc. sulphuric acid [38], and in chlorine or bromine water, but not in hydrochloric acid. Technetium dissolves slowly in neutral, ammoniacal or acid hydrogen peroxide solution. The solvents mentioned above oxidize technetium to pertechnetate, in the case of chlorine and bromine water the partial formation of $[TcCl_6]^{2-}$ and $[TcBr_6]^{2-}$, respectively, is expected.

Technetium burns in oxygen at 400–600 °C to Tc_2O_7 [38,39] and in fluorine to a mixture of the penta- and hexafluorides [40]. In the temperature range of 325 to 525 °C the oxidation of technetium to the heptoxide resulted in the activation energy of 90 kJ · mole $^{-1}$ [41]. Technetium reacts with chlorine at 300–550 °C to $TcCl_4$. In addition, $TcOCl_4$ and TcO_3Cl are produced if the chlorine contains some oxygen [42]. Technetium is reported to form a hydride of the composition $TcH_{0.73}$ at 300 °C under a hydrogen pressure of 19 kbar [43,44]. Sulphur combines at elevated temperatures to give the disulphide, and carbon to give TcC [40]. Melts of $LiClO_4$ react with technetium metal powder at 250–300 °C to form pertechnetate [45].

9.4 Intermetallic compounds

Much attention was paid to structures, superconducting properties, magnetic susceptibilities, Knight shifts, and specific heats of intermetallic compounds of technetium. Their structure types and lattice constants are presented in Table 9.3.A.

The $TcAl_6$ phase was shown to be isostructural with $MnAl_6$ and $ReAl_6$. $TcAl_{12}$ exhibits the same structure as $MoAl_{12}$ and $ReAl_{12}$ [51]. No new intermediate phases were found to exist in alloys of technetium with rhodium, palladium or platinum. The solubility of technetium in these metals increases in the given sequence [71]. The group VIII transition elements Co, Ni, Rh, Pd, Ir, and Pt show extensive solid solubility in technetium metal at 1050 °C [72]. The solid solubility of technetium in nickel is

Table 9.3.A Intermetallic compounds and alloys of technetium.

Phase Composition	Structure	Lattice constants [Å]	References
$TcBe_{22}$	$ZrZn_{22}$(fcc)	–	[46]
Tc_3B	*Cmcm*	$a = 2.891$ $b = 9.161$ $c = 7.246$	[47]
Tc_7B_3	$P6_3mc$	$a = 7.417$ $c = 4.777$	[47]
TcB_2	P6/mmc	$a = 2.892$ $c = 7.453$	[47]
Tc_2Al	$MoSi_2$	$a = 2.977$ $c = 9.476$	[48]
Tc_2Al_3	Ni_2Al_3 (trigonal)	$a = 4.16$ $c = 5.13$	[49]
$TcAl_4$	monoclinic	$a = 5.1$ $b = 17.0$ $c = 5.1$ $\beta = 100°$	[49]
$TcAl_6$	*Ccmm*	$a = 6.5944$ $b = 7.629$ $c = 9.0011$	[50,51]
$TcAl_{12}$	WAl_{12}(bcc)	$a = 7.528$	[48,49,52]
Tc_4Si	$W(A_2)$	$a = 3.009$	[48]
Tc_3Si	Fe_3Zn_{10}	$a = 9.014$	[48]
Tc_5Si_3	W_5Si_3	$a = 9.403$ $c = 4.849$	[48]
TcSi	FeSi	$a = 4.755$	[48]
Tc_7Sc	α-Mn	$a = 9.509$	[53]
Tc_2Sc	$MgZn_2$	$a = 5.223$ $c = 8.571$	[54]
Tc_7Ti	α-Mn	$a = 9.579$	[53]
Tc_3Ti	bcc	–	[55]
Tc_2Ti	CsCl	$a = 3.083$	[55]
TcTi	CsCl	$a = 3.091$	[54,55]
$TcTi_3$	bcc	$a = 3.181$	[55]
Tc_7V_3	CsCl	$a = 3.036$	[56]
Tc_3V_2	CsCl	$a = 3.027$	[56]
TcV	CsCl	$a = 3.025$	[54,56,57,58]
Tc_2V_3	CsCl	$a = 3.015$	[56]
TcV_3	bcc	$a = 3.026$	[57]
Tc_3Cr	σ(tetr.)	$a = 9.290$ $c = 4.846$	[54]

Table 9.3.A Continued.

Phase Composition	Structure	Lattice constants [Å]	References
Tc_3Cr_2	σ(tetr.)	$a = 9.271$ $c = 4.803$	[54]
Tc_3Mn_2	σ(tetr.)	$a = 9.15$ $c = 4.80$	[54]
Tc_3Fe_2	σ(tetr.)	$a = 9.130$ $c = 4.788$	[54]
TcFe	σ(tetr.)	$a = 9.077$ $c = 4.756$	[54]
Tc_2Fe_3	σ(tetr.)	$a = 9.010$ $c = 4.713$	[54]
$TcZn_6$	fcc	$a = 7.588$	[59]
Tc_2Y	$MgZn_2$	$a = 5.373$ $c = 8.847$	[60]
Tc_6Zr	α-Mn	$a = 9.637$	[23,54]
Tc_2Zr	$MgZn_2$	$a = 5.219$ $c = 8.655$	[54,61]
Tc_6Nb	α-Mn	$a = 9.547$	[54,62]
Tc_3Nb	α-Mn	$a = 9.625$	[23]
Tc_7Mo_3	σ(tetr.)	$a = 9.509$ $c = 4.945$	[54,63,68]
Tc_3Mo_2	Cr_3O	$a = 4.934$	[18,54,64–67]
Tc_2Gd	$MgZn_2$	$a = 5.397$ $c = 8.883$	[60]
Tc_2Tb	$MgZn_2$	$a = 5.375$ $c = 8.843$	[60]
Tc_2Dy	$MgZn_2$	$a = 5.365$ $c = 8.830$	[60]
Tc_2Ho	$MgZn_2$	$a = 5.353$ $c = 8.813$	[60]
Tc_2Er	$MgZn_2$	$a = 5.340$ $c = 8.792$	[60]
Tc_2Tm	$MgZn_2$	$a = 5.334$ $c = 8.775$	[60]
Tc_2Lu	$MgZn_2$	$a = 5.309$ $c = 8.739$	[60]
Tc_7Hf	α-Mn	$a = 9.603$	[53]
Tc_2Hf	$MgZn_2$	$a = 5.200$ $c = 8.616$	[54,61]
TcHf	CsCl	$a = 3.270$	[54]
Tc_5Ta	α-Mn	$a = 9.565$	[53,54]
TcTa	CsCl	$a = 3.172$	[54]

Table 9.3.A Continued.

Phase Composition	Structure	Lattice constants [Å]	References
Tc_3W	σ(tetr.)	$a = 9.479$ $c = 5.166$	[54,63]
Tc_3W_2	bcc	$a = 3.117$	[68]
TcW	bcc	$a = 3.117$	[68]
Tc_2W_3	bcc	$a = 3.126$	[68]
TcW_4	bcc	$a = 3.147$	[68]
Tc_2Th	$MgZn_2$	$a = 5.394$ $c = 9.222$	[61,69]
TcU_2	U_2Ru	$a = 13.407$ $b = 3.271$ $c = 5.213$ $\beta = 96°23'$	[69,70]

17 atom% at 1300 °C, widening somewhat at higher temperatures. The solubility of nickel in technetium is approximately 40 atom% at 1300 °C [73]. The peritectic Ni-Tc compound is reported to contain ~43 atom% Tc at 1495 °C [74].

9.5 Superconducting intermetallic compounds and alloys of technetium

Numerous investigations deal with the superconductivity of intermetallic compounds and alloys of technetium, essentially for raising the superconducting transition temperature by preparing various intermediate phases of technetium, mainly with transition metals, and for gaining a better understanding of superconductivity of type-II superconductors. In Table 9.4.A superconducting transition temperatures T_c of intermetallic technetium compounds and alloys are given.

The addition of small amounts of titanium to technetium increases the transition temperature T_c in the hcp solid solution. The highest T_c of 10.89 K occurs here in the solid solution containing 3 atom% Ti. The Tc-Ti α-Mn phase has a transition temperature range of 8–10 K, which is among the highest T_c of transition metal α-Mn phases. The bcc Ti-rich alloys exhibit low transition temperatures down to 1.70 K [55]. The transition temperature of technetium-rich hcp vanadium alloys increases with vanadium concentration to a maximum of 11.3 K at the limit of 6.5 atom% of vanadium solubility and decreases with increasing vanadium content in the CsCl structure. At compositions in the 50 to 80 atom% V interval no evidence of superconductivity is observed [77]. For technetium-niobium alloys the α-Mn phase is superconducting over the range from $Tc_{0.76}Nb_{0.24}$ to $Tc_{0.58}Nb_{0.42}$ with the transition temperature varying from 12.9 to 10.9 K. T_c of the Tc-Nb alloys in the hcp structure increases rapidly from

Table 9.4.A Superconducting transition temperatures of intermetallic technetium phases.

Phase composition	Structure	Transition temperature T_c [K]	References
$TcBe_{22}$	$ZrZn_{22}$	5.21	[46]
Tc_3Ti	bcc	4.2–6.0	[55]
Tc_3V	hcp+CsCl	11.24	[77]
Tc_6Zr	α-Mn	9.7	[23]
Tc_2Zr	$MgZn_2$	7.6	[61]
Tc_3Nb	α-Mn	12.9,10.5	[23,75]
Tc_9Mo_2	hcp	13.7	[76]
Tc_3Mo	hcp	16.0,14.3	[23, 67]
Tc_3Mo_2	Cr_3O	14.8,13.4,13.2	[23,64,66]
Tc_3Mo_5	bcc	12.7	[66]
TcMo	–	12.6	[78]
Tc_2Hf	$MgZn_2$	5.6	[61]
Tc_9W		10.4	[79]
Tc_3W_2	bcc	7.88	[68]
TcW	bcc	7.52	[68]
Tc_2W_3	bcc	7.18	[68]
Tc_4Re	–	5.31	[80]
Tc_2Th	$MgZn_2$	5.3	[61]

7.9 to 12.8 K after adding 0.03–0.06 atom% Nb to technetium [75]. In technetium based hcp solid solution alloys generally V, Nb, and Mo raise the transition temperature, while Cr, Fe, Co, Ni, and Ru lower T_c relative to pure technetium [81]. In the technetium-tungsten system T_c is raised by increasing the atom% of Tc. The transition temperature attains a maximum of 10.4 K at 90 atom% of Tc and decreases at still higher technetium contents [79]. The superconducting transition temperature of technetium-rhenium alloys increases monotonically with increasing technetium content. Rhenium does not result in an increase of T_c above that for pure technetium in the entire range of concentration; the pertinent lattice parameters of the hcp solid solutions vary continuously [82].

9.6 References

[1] J.W. Cobble, C.M. Nelson, G.W. Parker, W.T. Smith, Jr., and G.E. Boyd, J. Am. Chem. Soc. *74*, 1852 (1952)

[2] K. Schwochau in: Handbuch der Präparativen Anorganischen Chemie, Vol. 3, (G. Brauer, ed.), Enke, Stuttgart (1981), p. 1598

[3] J.D. Eakins and D.G. Humphries, J. Inorg. Nucl. Chem. *25*, 737 (1963)
[4] R.E. Voltz and M.L. Holt, J. Electrochem. Soc. *114*, 128–131 (1967)
[5] V.I. Spitsyn, A.F. Kuzina, A.F. Tsarenko, A.A. Oblova, O.A. Balakhovskii, P.N. Kodochigov, M.P. Glazunov, and I.V. Kaimin, Radiokhimiya *12*, 617–621 (1970)
[6] W.D. Box, Nucl. Appl. *1*, 155–157 (1965)
[7] C.C. Koch and G.R. Love, J. Less-Common Metals *12*, 29–35 (1967)
[8] J.B. Darby, Jr., D.J. Lam, L.J. Norton, and J.W. Downey, J. Less-Common Metals *4*, 558–563 (1962)
[9] A.L. Giorgi and E.G. Szklarz, J. Less-Common Metals *11*, 455–456 (1966)
[10] R.D. Peacock, The Chemistry of Technetium and Rhenium, Elsevier, London (1966)
[11] V.I. Spitsyn, Y.N. Golovanov, O.A. Balakhovskii, and A.A. Tsvetaev, Dokl. Akad. Nauk SSSR *205*, 1421–1424 (1972)
[12] V.I. Spitsyn, Z. Chem. [Leipzig] *21*, 131–136 (1981)
[13] G.W. Parker, G.E. Creek, W.J. Martin, G.M. Hebert, and P.M. Lantz, Oak Ridge National Laboratory Rep. ORNL-1260, (1952) p. 29
[14] E. Anderson, R.A. Buckley, A. Hellawell, and W. Hume-Rothery, Nature *188*, 48–49 (1960)
[15] R.G. Behrens and G.H. Rinehart, J. Less-Common Metals *75*, 241–254 (1980)
[16] D.R. Stull and G.C. Sinke, Thermodynamic Properties of the Elements, Advances in Chemistry, Series 18, ACS, Washington, D.C. (1956)
[17] D.E. Baker, J. Less-Common Metals *8*, 435–436 (1965)
[18] J.A.C. Marples and C.C. Koch, Phys. Lett. *41A*, 307–308 (1972)
[19] R.C.L. Mooney, Acta Cryst. *1*, 161–162 (1948)
[20] D.J. Lam, J.B. Darby, Jr., J.W. Downey, and L.J. Norton, Nature *192*, 744 (1961)
[21] P.W. Bridgeman, Proc. Am. Acad. Arts Sci. *84*, 111–129 (1955)
[22] J.G. Daunt and J.W. Cobble, Phys. Rev. *92*, 507–508 (1953)
[23] V.B. Compton, E. Corenzwit, J.P. Maita, B.T. Matthias, and F.J. Morin, Phys. Rev. *123*, 1567–1568 (1961)
[24] M.L. Picklesimer and S.T. Sekula, Phys. Rev. Lett. *9*, 254 (1962)
[25] S.T. Sekula, R.H. Kernohan, and G.R. Love, Phys. Rev. *155*, 364–369 (1967)
[26] M. Kurakado, T. Takabatake, and H. Mazaki, Bull. Inst. Chem. Res., Kyoto Univ. *55*, 38–45 (1977)
[27] G. Kostorz and S. Mihailovich, Proc. XIII. Intern. Conf. on Low Temperature Physics CONF-700921 (1971), pp. 341–343
[28] C.W. Chu, W.E. Gardner, and T.F. Smith, Phys. Lett. *26A*, 627–628 (1968)
[29] W.J. Parker, R.J. Jenkins, C.P. Butler, and G.L. Abbott, J. Appl. Phys. *32*, 1679–1684 (1961)
[30] R.L. Rudkin, R.J. Jenkins, and W.J. Parker, Rev. Sci. Instr. *33*, 21–24 (1962)
[31] V.I. Spitsyn, V.E. Zinovev, P.V. Gel'd, and A.O. Balakhovskii, Dokl. Phys. Chem. Proc. Acad. Sci. USSR *220/225*, 225–228 (1975)
[32] L.P. Gel'd and V.E. Zinov'ev, Teplofiz. Vys. Temp. *10*, 656 (1972)
[33] I.G. Korshunov and V.E. Zinov'ev, Trudy Uralsk. Politekhn. Inst. *231*, 119 (1974)
[34] R.J. Trainor and M.B. Brodsky, Phys. Rev. *B12*, 4867–4869 (1975)
[35] A.F. Guillermet and G. Grimvall, J. Less-Common Metals *147*, 195–211 (1989)
[36] C.M. Nelson, G.E. Boyd, and W.T. Smith, Jr., J. Am. Chem. Soc. *76*, 348–352 (1954)
[37] S. Trasatti, Surface Sci. *32*, 735–738 (1972)
[38] G.E. Boyd, J. Chem. Educ. *36*, 3–14 (1959)
[39] G.E. Boyd, J.W. Cobble, C.M. Nelson, and W.T. Smith, Jr., J. Am. Chem. Soc. *74*, 556–557 (1952)
[40] R.D.W. Kemmitt and R.D. Peacock, The Chemistry of Manganese, Technetium and Rhenium, Pergamon, Oxford (1973)
[41] V.I. Spitsyn, K.G. Bukov, A.M. Emel'yanenko, L.N. Fedotov, and T.K. Titova, Russ. J. Inorg. Chem. *33*, 1403–1405 (1988)
[42] A. Guest and C.J.L. Lock, Can. J. Chem. *50*, 1807–1810 (1972)
[43] V.I. Spitsyn, Z. Chem. *21*, 131–136 (1981)
[44] V.I. Spitsyn, E.G. Ponyatovskii, V.E. Antonov, I.T. Belash, and O.A. Balakhovskii, Dokl. Akad. Nauk SSSR *247*, 1420–1423 (1979)
[45] D. Cohen, S. Fried, and H. Selig, J. Inorg. Nucl. Chem. *33*, 2687–2688 (1971)
[46] E. Bucher and C. Palmy, Phys. Lett. *A24*, 340–341 (1967)
[47] W. Trzebiatowski and J. Rudzinski, J. Less-Common Metals *6*, 244–245 (1964)
[48] J.B. Darby, Jr., J.W. Downey, and L.J. Norton, J. Less-Common Metals *8*, 15–19 (1965)

[49] L.M. D'Alte Da Veiga and L.K. Walford, Phil. Mag. *8*, 349 (1963)
[50] L.M. D'Alte Da Veiga, Phil Mag. 7. 1247–1248 (1962)
[51] C. Wilkinson, Acta Cryst. *22*, 924–926 (1967)
[52] L.K. Walford, Acta Cryst. *17*, 57–59 (1964)
[53] D.L. Lam, J.B. Darby, Jr., J.W. Downey, and L.J. Norton, Nature *192*, 744 (1961)
[54] J.B. Darby, Jr., D.J. Lam, L.J. Norton, and J.W. Downey, J. Less-Common Metals *4*, 558–563 (1962)
[55] C.C. Koch, J. Less-Common Metals *44*, 177–181 (1976)
[56] C.C. Koch and G.R. Love, J. Less-Common Metals *15*, 43–58 (1968)
[57] D.O. Van Ostenburg, D.J. Lam, H.D. Trapp, and D.E. MacLeod, Phys. Rev. *128*, 1550–1554 (1962)
[58] D.O. Van Ostenburg, H. Trapp, and D.J. Lam, Phys. Rev. *126*, 938–940 (1962)
[59] M.G. Chasanov, I. Johnson, and R.V. Schablaske, J. Less-Common Metals *7*, 127–132 (1964)
[60] J.B. Darby, Jr., L.J. Norton, and J.W. Downey, J. Less-Common Metals *6*, 165–167 (1964)
[61] A.L. Giorgi and E.G. Szklarz, J. Less-Common Metals *22*, 246–248 (1970)
[62] D.O. Van Ostenburg and D.J. Lam, J. Phys. Soc. Japan *18*, 1744–1754 (1963)
[63] J. Niemiec, Nukleonica *1965*, 23–29 (1966)
[64] J.B. Darby, Jr., and S.T. Zegler, J. Phys. Chem. Solids *23*, 1825–1827 (1962)
[65] N.E. Alekseevskii, O.A. Balakhovskii, and I.V. Kirillov, Fiz. Met. Metalloved *40*, 50–54 (1975)
[66] G.R. Stewart and A.L. Giorgi, Phys. Rev. *B17*, 3534–3540 (1978)
[67] A.L. Giorgi and B.T. Matthias, Phys. Rev. *B17*, 2160–2162 (1978)
[68] S.H. Autler and J.K. Hulm, Phys. Rev. *A140*, 1177–1180 (1965)
[69] J.B. Darby, Jr., A.F. Berndt, and J.W. Downey, J. Less-Common Metals *9*, 466–468 (1965)
[70] A.F. Berndt and A.E. Dwight, Trans. Met. Soc. AIME *233*, 2075–2078 (1965)
[71] J. Niemiec, Bull. Acad. Polon. Sci. Ser. Sci. Chim. *11*, 665–669 (1963)
[72] J.B. Darby, Jr., L.J. Norton, and J.W. Downey, J. Less-Common Metals *5*, 397–402 (1963)
[73] P. Nash, Bull. Aloy Phase Diagrams *6*, 124–125 (1985)
[74] V.I. Spitsyn, S.P. Grishina, O.A. Balakhovskii, and A.I. Krasovskii, Izv. Akad. Nauk SSSR, Met. 196–198 (1975)
[75] A.L. Giorgi and E.G. Szklarz, J. Less-Common Metals *20*, 173–175 (1970)
[76] G.R. Stewart and A.L. Giorgi, Solid State Commun. *28*, 969–972 (1978)
[77] C.C. Koch, R.H. Kernohan, and S.T. Sekula, J. Appl. Phys. *38*, 4359–4364 (1967)
[78] F.J. Morin and J.P. Maita, Phys. Rev. *129*, 1115–1120 (1963)
[79] E. Trojnar and J. Niemiec, Bull. Acad. Polon. Sci. Ser. Sci. Chim. *14*, 565–567 (1966)
[80] T. Ishida and H. Mazaki, Physica *112B*, 411–415 (1982)
[81] R.N. Shelton, T.F. Smith, C.C. Koch, and W.E. Gardner, J. Phys. F: Metal Phys. *5*, 1916–1930 (1975)
[82] J. Niemiec and E. Trojnar, Phys. Status Solidi *17*, K89–K90 (1966)

10 Binary compounds and oxide halides

10.1 Hydrides

A foil of ^{99}Tc saturated with hydrogen at 300 °C under a hydrogen pressure $p(H_2)$=19 kbar showed the composition $TcH_{0.73}$, which represents a single phase of the hcp lattice of technetium metal. The lattice constants of $TcH_{0.73}$, a = 2.805 Å and c = 4.455 Å, are distinctly enhanced compared to those of the Tc-metal. A jump-like increase in the solubility of hydrogen in technetium is observed between 10 and 15 kbar H_2 [1]. The superconducting transition temperature of the technetium-hydrogen system was found to decrease stepwise with increasing hydrogen content [2,5].

Neutron diffraction investigations of the structure of technetum hydrides were performed at atmospheric pressure in the temperature range of 120–300 K. $TcH_{0.45}$ exhibits an octahedral superstructure of the anti-CdI_2 type with the M_2X stoichiometry, typical of some carbides and nitrides of transition metals. The Tc-H distance is 2.07 Å corresponding to an atomic hydrogen radius of 0.70 Å. The interstitial atoms in this structure form layers that are parallel to the close-packed metal layers and only every second layer of the octahedra is filled with hydrogen. Consequently, the metal atom layers separated by the hydrogen atoms move apart, whereas the metal layers between which there are no hydrogen atoms move closer together [3]. The layer superstructure of the anti-CdI_2 type was also observed for the manganese hydride near the Mn_2H composition [4].

A solid solution of hydrogen in technetium metal is formed during the electrodeposition of technetium from acid aqueous solutions of pertechnetate. The maximum hydrogen content of the amorphous phase corresponded to $TcH_{0.27}$ [6].

10.2 Borides

Technetium-boron compounds were prepared by mixing powdered technetium metal and powdered crystalline boron, pressing into pellets, and sintering in vacuum at 1100–1200 °C for 120–200 h. Among several existing compounds Tc_3B, Tc_7B_3, and TcB_2 were identified. Tc_3B crystallizes in the orthorhombic system with the lattice constants a = 2.891, b = 9.161, and c = 7.246 Å. It is isostructural with Re_3B. The unit cell contains four Tc_3B molecules and belongs to the space group $Cmcm$. Tc_7B_3, indexed in the hexagonal symmetry with a = 7.417 and c = 4.771 Å, crystallizes in the Th_7Fe_3 type, as found in the corresponding borides of ruthenium, rhodium, and rhenium. The unit cell contains two molecules and has the space group $P6_3mc$. Also TcB_2 proved to be hexagonal with a = 2.892 and c = 7.453 Å

and isostructural with ReB_2. The unit cell contains two TcB_2 molecules and belongs to the *P6mmc* space group. This phase exhibits a composition varying from the stoichiometric ratio towards higher content of boron [7]. The atomic volume of diborides indicates that semiconducting properties may occur in TcB_2 as in ReB_2, OsB_2, and RuB_2 [8]. The electronic band structures of TcB_2 and ReB_2 were calculated along all the main symmetry directions in the Brillouin zone. Comparison with the band structures of the metal and the B_2 species yielded information regarding the metal-B interactions [9].

Some ternary borides, synthesized from the elements by argon arc melting, were characterized by X-ray powder diffraction data (Table 10.1.A).

Table 10.1.A Crystallographic data for ternary borides of technetium [10].

Compound	Structure type	Space Group	Unit cell dimensions [Å]		
			a	*b*	*c*
$GdTcB_4$	y(yttrium)CrB_4	*Pbam*	5.984	11.589	3.617
$ThTcB_4$	$ThMoB_4$	*Cmmm*	7.441	9.584	3.727
$UTcB_4$	$ThMoB_4$	*Cmmm*	7.297	9.357	3.598
U_2TcB_6	Y_2ReB_6	*Pbam*	9.288	11.392	3.637

10.3 Carbide

Technetium metal embodies about 1 wt% carbon in its lattice at 910 °C, whereby the unit cell dimensions of technetium increase to $a = 2.812$ and $c = 4.470$ Å. At a carbon content between 1.4 and 9 wt%, a heterogeneous mixture was observed that consisted of carbon-rich metal and a bcc phase with the lattice constant $a = 3.982$ Å. The composition of the bcc phase corresponded to the formula TcC. Its density was found to be about 11.5 g/cm^3 [11].

A sample of technetium carbide was prepared by heating technetium metal inductively to its melting point in a graphite crucible under vacuum. The resulting pellet was ground to a fine mesh, excess purified graphite powder was added and the mixture compressed to a pellet in a steel die under 100,000 psi. The pellet was again placed in a graphite crucible and heated under vacuum to its melting point. The melting point of the carbon-rich technetium carbide was found to be 1835 ± 50 °C. The lattice parameter $a = 3.985 \pm 0.002$ Å is in excellent agreement with that of the carbide mentioned before [11], indicating that the composition of both materials is the same. Magnetic susceptibility studies on the material showed it to be superconducting with a transition temperature of 3.85 K [12].

Bond energies of RuC(g) and RhC(g) suggest that TcC(g) is a thermodynamically stable molecule present in significant amounts in the equilibrium vapor of the technetium-carbon system at temperatures above 2000 K. A graphite effusion cell was used to vaporize the technetium carbide into a quadrupole mass spectrometer. The TcC(g) molecule was observed above a liquid technetium carbide phase. A bond energy of 148 ± 2 kcal · mole $^{-1}$ at 2450 K was derived for TcC(g) [13].

10.4 Nitride

By heating of NH_4TcO_4 in ammonia at 900–1100 °C an fcc phase was detected with a lattice constant varying from 3.980 to 3.985 Å depending on the nitrogen content. The maximum nitrogen content reached the composition $TcN_{0.76}$. Probably, the nitride phase corresponds to TcN having an NaCl structure [7,14].

A technetium nitride of the composition $TcN_{0.75}$ is obtained by thermal decomposition of $(NH_4)_2[TcCl_6]$ or $(NH_4)_2[TcBr_6]$ at 380 °C in an atmosphere of argon. The product, obviously almost identical to that mentioned before [7], also had a face-centered cubic lattice with the parameter $a = 3.980$ Å. It is a black, brittle substance, insoluble in alkaline 30 % H_2O_2, soluble in conc. HNO_3. Above 500 °C, $TcN_{0.75}$ decomposes and the solid phase is reported to consist of a polymorphic modification of metallic technetium with a face-centered cubic lattice, stable up to 800 °C [15].

10.5 Phosphides

Several phosphides of technetium were prepared by reaction of technetium metal powder with red phosphorus at 1220 K using the tin-flux technique or iodine as a mineralizer. The preparation was carried out in evacuated, sealed silica tubes.

Tc_3P crystallizes in the tetragonal Fe_3P-type structure. The lattice constants of Tc_3P are $a = 9.568$ and $c = 4.736$ Å. Tc_3P proved to be isostructural with Mn_3P, Cr_3P, and Ni_3P and shows a high coordination number for all atoms, which is typical for intermetallic compounds and other electron-deficient compounds with high metal content. With $Z = 8$ formula units in the cell, the calculated density is 10.04 $g \cdot cm^{-3}$ [16].

TcP_4 adopts the orthorhombic ReP_4-type structure with $a = 6.238$, $b = 9.215$, and $c = 10.837$ Å and low coordination numbers for all atoms, where near neighbor interactions can be rationalized with classical two-electron bonds. The Tc atoms form pairs with a Tc-Tc bonding distance of 3.00 Å. The compound is expected to be diamagnetic and semiconducting as was discussed for the isoelectronic and isostructural ReP_4. The calculated density of TcP_4 is 4.75 $g \cdot cm^{-3}$ assuming $Z = 8$ formula units in the cell [16].

TcP_3 was shown to crystallize in a new structure type with four formula units per cell in the orthorhombic space group *Pnma*. The lattice constants are $a = 15.359$, $b = 3.092$, and $c = 5.142$ Å. TcP_3 is isostructural with ReP_3. The metal atoms are octahedrally surrounded by phosphorus atoms. Each metal atom forms two metal-metal bonds across the common edges of adjacent octahedra (Fig. 10.1.A). Thus all spins are compensated in agreement with the diamagnetism observed for ReP_3. The TcP_6 octahedra are linked via corners and edges to form two-dimensionally infinite, puckered sheets perpendicular to the a axis [17].

Tc_2P_3 crystallizes in the triclinic space group $P\bar{1}$ with the lattice constants a=6.266, b=6.325, and c=7.683 Å, α=95.79, β=101.76, and γ=104.34°. Tc_2P_3 is isostructural with Tc_2As_3 that has a superstructure of Mo_2As_3. The superstructure arises through differences in metal-metal bonding. The structure of Tc_2P_3 is intermediate between those of transition metal phosphides with high coordination number for all atoms, and those

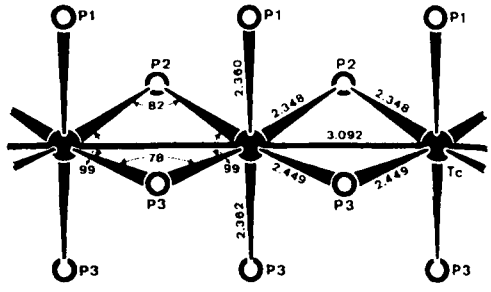

Fig. 10.1.A Near-neighbor environment of the Tc atoms in TcP_3 [17].

of phosphides whose structure can be rationalized on the basis of classical two-electron bonds [18].

10.6 Arsenides

So far two technetium arsenides, Tc_3As_7 and Tc_2As_3, have been synthesized upon reacting the powdered elements in various ratios at 600–900 °C and annealing the samples at 900 to 950 °C.

Tc_3As_7 is reported to crystallize in the cubic $D8_f$ structure with the lattice constant a=8.702 Å and to be isostructural with Re_3As_7, which is diamagnetic and shows nonmetallic behavior. From density measurements the unit cell of Re_3As_7 was found to contain four formula units [19].

Tc_2As_3 crystallizes in the triclinic space group $P\bar{1}$ with the lattice constants a=6.574, b=6.632, c=8.023 Å, α=95.69, β=102.03, γ=104.31°, and four formula units per cell. The compound is isostructural with Tc_2P_3, as mentioned before. The structure is closely related to the monoclinic structure of Mo_2As_3, from which it can be derived by distortion and by doubling of one translation period [20].

10.7 Oxides

Of the binary oxides only TcO_2 and Tc_2O_7 could hitherto be identified unambiguously.

Attempts have been made to synthesize an oxide that is intermediate in composition between Tc and TcO_2. Mixtures of Tc and TcO_2 were prepared in different ratios, wrapped in platinum foil, vacuum-sealed into Vycor tubes, and heated at about 970 °C for 4.5 days. The distorted rutile structure of TcO_2 was noted in all X-ray patterns. In addition, one new phase was found in several samples, which could be indexed on the basis of a primitive pseudocubic unit cell with a=9.45 Å. The same new pseudocubic phase was obtained when a mixture of Tc and TcO_2 corresponding to the composition $TcO_{0.10}$ was heated in a sealed silica tube up to 1250 °C over a

period of 12 h and kept at this temperature for another 12 h. However, the stoichiometry and structure of this pseudocubic phase are still unknown [21].

10.7.1 Technetium dioxide

Hydrous technetium dioxide $TcO_2 \cdot aq$ is a frequently observed precipitate when the chemistry of technetium in aqueous solution is studied. It precipitates as a dark brown solid by hydrolysis of Tc(IV) compounds [22], e.g. $[TcX_6]^{2-}$, X=Cl, Br, I [23,24,25]. The precipitation of $TcO_2 \cdot aq$ from aqueous solutions of $[TcCl_6]^{2-}$ with ammonia often leads to the formation of a light red to dark violet alkaline solution above the precipitate. The solution displays an absorption band at 475 nm. The remarkable color may be explained by the formation of a colloidal solution of $TcO_2 \cdot aq$ [24]. Relatively pure deposits of $TcO_2 \cdot aq$ are obtained by the cathodic reduction of neutral or alkaline pertechnetate solutions between platinum electrodes [26–28]. $TcO_2 \cdot aq$ can also be produced by reduction of TcO_4^- with hydrazine hydrate in perchloric acid solution [29] or with metallic zinc in hydrochloric acid [30]. The latter procedure appears to yield, in addition, technetium metal [24]. The stoichiometrically undefined hydrate is dehydrated in a nitrogen stream at 400 °C [23] or at 250 °C in vacuum [25], leading to black defined TcO_2. $TcO_2 \cdot aq$ seems to be amphoteric and dissolves not only in acids, but also in conc. solutions of alkali hydroxide [24].

The status of Tc(IV) ions in aqueous solution, obtained by dissolution of $TcO_2 \cdot aq$ in diluted $HClO_4$, was studied by electrophoresis. On the basis of ionic mobilities the existence of the species TcO^{2+} and $TcO(OH)^+$ at pH 1 and pH 2, respectively, was assumed according to the equilibria

$$TcO^{2+} + H_2O \leftrightarrow TcO(OH)^+ + H^+ \quad (1)$$

and

$$TcO(OH)^+ + H_2O \leftrightarrow TcO(OH)_2 + H^+ \quad (2)$$

$TcO(OH)_2$ precipitates as $TcO_2 \cdot H_2O$. The pertinent hydrolysis constants were evaluated as

$$K_{(1)} = (4.3 \pm 0.4) \cdot 10^{-2}$$

and

$$K_{(2)} = (3.7 \pm 0.4) \cdot 10^{-3}$$

at an ionic strength of 0.1 [29].

Anhydrous technetium dioxide, TcO_2, can be directly prepared by the thermal decomposition of NH_4TcO_4 in a nitrogen stream at 700–800 °C [21,23]:

$$NH_4TcO_4 \rightarrow TcO_2 + 2H_2O + 1/2\ N_2$$

TcO_2, like ReO_2, adopts the molybdenum dioxide structure, a distorted rutile structure type [31] of the space group $P2_1/c$. The approximate cell dimensions of the mono-

clinic structure of TcO_2 are reported to be a~5.53, b~4.79, and c~5.53 Å, β~120° [31]. Precise unit cell parameters seem to be still lacking. The density of TcO_2 is 6.9 g · cm ^{3} [26], which is in good agreement with the X-ray density of 6.856 g · cm^{-3} calculated on the basis of the cell parameters given before. More recently, powder diffraction patterns yielded cell parameters a=5.52, b=4.99, c=5.57 Å, and β=121.9° [32]. TcO_2 starts sublimating at 900 °C [30] and disproportionates above 1100 °C into Tc and Tc_2O_7 [22]. The dioxide is readily oxidized to Tc_2O_7 with oxygen, is reduced to the metal by hydrogen at 500 °C and reacts with fluorine, chlorine or bromine to give oxide halides [33]. In acid aqueous solutions TcO_2 will be oxidized easily to TcO_4^- using Ce(IV) or in alkaline solutions using H_2O_2 [26]. In view of the possible environmental impact of nuclear waste, the dissolution of TcO_2 as a function of salinity, pH, temperature, and oxygen concentration of aqueous solutions has been studied in detail [32].

10.7.2 Ditechnetium pentaoxide and technetium trioxide

The combustion of technetium metal in oxygen appears to be a complex reaction, leading to some side products in addition to technetium heptaoxide, Tc_2O_7. The initial product subliming in the combustion tube out of the furnace during the oxidation is a highly volatile red oxide, somewhat more volatile than Tc_2O_7 and tending to collect farthest from the furnace. The red oxide can be produced in apparently pure form by low-temperature oxidation of technetium. A sample of technetium was heated in oxygen at 150 °C for approximately three months, during which time a significant amount of a volatile red oxide had collected. The compound is reported to be probably Tc_2O_5 [34,35]. The identity of the product has still to be established. When a technetium oxide material of undefined actual composition was exposed to low pressures (~10 Pa) of oxygen and heated in a platinum Knudsen cell reactor to 900 °C, Tc_2O_5 was identified mass spectrometrically as an important vapor species among other volatile products. It was speculated that solid Tc_2O_5 should be a stable compound [36] like the well-known blue Re_2O_5.

TcO_3 is reported to be formed as a volatile oxide by oxidation of technetium metal in oxygen at 400–600 °C. Surprisingly no generation of Tc_2O_7 was mentioned [37]. However, TcO_3 could successfully be produced by reduction of Tc_2O_7 with sulphur dioxide. ReO_3 may be prepared by reducing Re_2O_7 with CO at 175–280 °C. When this method was tried for producing TcO_3, only technetium metal resulted. Obviously a milder reducing agent is required. Technetium trioxide appears black, but under certain conditions, e.g. in thin films, it has a reddish-purple color. The oxidation state was established by ceric perchlorate titration, and the Tc content was confirmed spectrophotometrically after oxidation to TcO_4. In some oxidations of technetium metal, a small amount of trioxide along with the red oxide (Tc_2O_5?) was obtained as a side product of Tc_2O_7 [34]. It was suggested that the darkening in color of the Tc_2O_7, usually obtained by oxidation of technetium metal, is caused by reaction of Tc_2O_7 with Tc_2O_5 impurity to give black TcO_3 [35]. According to gas chromatographic studies of fission product oxides and hydroxides, TcO_3 is reported to be formed in an oxygen stream at 1500 °C and to decompose continuously in the column to TcO_2. However, the chemical composition of these oxides could not be proved [38,39].

TcO_3 was identified from the mass spectra as a significant vapor species, present in substantial concentrations, when undefined technetium oxide material was exposed to low pressures of oxygen and heated to 900 °C [36].

The entire identification, the X-ray structural analysis and the spectrometric characterization of solid Tc_2O_5 and TcO_3 are still an important challenge to inorganic chemists, all the more as the corresponding rhenium compounds are known to be stable under normal conditions. The dark red ReO_3 crystallizes in a cubic lattice in the space group *Pm3m*, forming a prototype [40,41].

10.7.3 Ditechnetium heptaoxide

The light yellow crystalline Tc_2O_7 may be prepared by burning technetium metal in dry oxygen at 400–600 °C [35,42]. However, the oxidation of the metal is a complex reaction. The initial volatile product formed at 450 °C may be the red ditechnetium pentaoxide Tc_2O_5. In addition, the formation of small quantities of another volatile compound, possibly TcO_3 or $HTcO_4$, was observed (Sect. 10.7.2). Technetium metal powder, which had previously been degassed at 900 °C on a vacuum line, was transferred to a porcelain boat and placed in a Pyrex combustion tube. The system is evacuated to a pressure of $<10^{-6}$ torr, and the combustion tube is flamed to remove final traces of moisture. The combustion system is filled with dried oxygen, and technetium metal is oxidized at 450–500 °C for a period of several hours. The products that sublime out of the heated zone and condense in the cold region of the combustion tube are resublimed in excess oxygen, until the side products are completely oxidized to Tc_2O_7 [23,35].

Ditechnetium heptaoxide melts at 119.5 °C [42] and boils at 311 °C [43]. It is very hygroscopic, dissolves in water to form pertechnetic acid [42], and dissolves in dioxane [26]. Tc_2O_7 exerts a vapor pressure of about 0.6 mm Hg at 100 °C. Solid Tc_2O_7 is found to be a fair electrical conductor at temperatures near its melting point, while the liquid compound is not. Rhenium heptaoxide exhibits just the opposite behavior [43]. Tc_2O_7 showed a slight, temperature independent paramagnetism like Re_2O_7 [30]. It is a stronger oxidant than Re_2O_7 and is readily reduced by vapors of organic substances, including vacuum stopcock grease [44]. Tc_2O_7 reacts at 220 °C with carbon monoxide under a pressure of 5100 psig to technetium carbonyl $Tc_2(CO)_{10}$ [45].

Single crystal structure analysis of thin plates of Tc_2O_7 revealed ditechnetium heptaoxide to crystallize in the orthorhombic space group *Pbca* with a=13.756, b=7.439, c=5.617 Å, and Z=4. The crystals contain isolated centrosymmetric Tc_2O_7 molecules with tetrahedral coordination of the Tc atoms and a linear Tc–O–Tc bridge [46–48]. The Tc–O bond lengths are 1.840 (bridge), 1.658, 1.684, and 1.706 Å. The structure is more closely related to CrO_3, RuO_4, and OsO_4 than to Re_2O_7. The structure of Re_2O_7 consists of strongly distorted ReO_6 octahedra and fairly regular ReO_4 tetrahedra that are connected through corners to form polymeric double layers in the *ac* plane. Fig. 10.2.A compares the structures of Tc_2O_7 and Re_2O_7.

The Raman spectra of solid, liquid, and gaseous ditechnetium heptaoxide were recorded and compared with those of dirhenium heptaoxide [49,50]. Frequencies and assignments are summarized in Table 10.2.A.

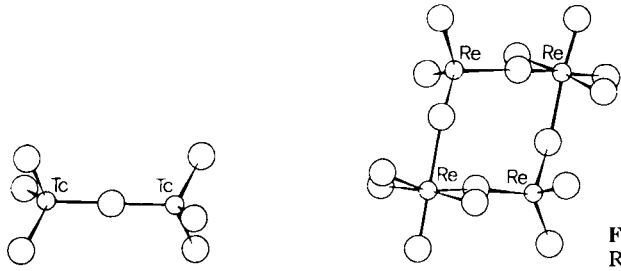

Fig. 10.2.A Structure of Tc_2O_7 and Re_2O_7 [48].

Table 10.2.A Raman spectra of Tc_2O_7 and gaseous Re_2O_7 [49,50].

Tc_2O_7						Re_2O_7		
Solid		**Liquid**		**Gas**		**Gas**		**Assignment**
964	m							
956.2	vs	952.5	vs(p)	957.3	vs(p)	1009	vs(p)	ν (MO_3)
950	w	943	m	955	m	972	m	ν (MO_3)
946	vw							
941	m							
934.3	s							
925	s							
		423	vw(p)	466	vw(p)	456	vw(p)	ν_s (MOM)
395	vw							
362	m							
352.6	m			357	m	341	m	δ (MO_3)
348	mw	348	s	340	m	322	wsh	δ (MO_3)
332								
211	m	195	m	185	s	185	ms	ρ_r (MO_3)
191	m	188	m	178	m	177	wsh	ρ_r (MO_3)
65	m			60	ms(p)	50	m(p)	δ (MOM)

The liquid and vapor of Tc_2O_7 appear to have similar structure, which is quite different from that of the solid phase. The spectra of Tc_2O_7 and Re_2O_7 look very similar to those of pyramidal MO_3 species. Gaseous, monomeric Tc_2O_7 can be assumed to have the same structure as Re_2O_7 as suggested by analogy with the structure of aqueous $Cr_2O_7^{2-}$ [50] and, on the basis of normal coordinate calculations, to have the symmetry C_{2v}. The molecules behave as if they consist of MO_3 pyramids, weakly coupled via an oxygen bridge.

The principal force constants for Tc_2O_7 and Re_2O_7 in the gas phase were calculated using a simplified molecular model (Table 10.3.A).

Most of the force constants calculated for Tc_2O_7 turn out to be smaller than the corresponding force constants calculated for Re_2O_7. Smaller bond-stretching force constants were also found for $[TcCl_6]^{2-}$ and $[TcBr_6]^{2}$ than for the analogous complexes of rhenium [52].

Table 10.3.A Force constants for Tc_2O_7 and Re_2O_7 [51]. R and r are related to the M–O′ (O′=bridged oxygen) and M–O bonds, respectively, α to the OMO angle, rr and $\alpha\alpha$ to bond/bond and angle/angle interactions, respectively, and ρ to the OMO′ angle.

Force constants [mdyne/Å]	Tc_2O_7 (gaseous)	Re_2O_7 (gaseous)
f_R	3.23	3.44
f_r	7.40	8.42
f_{rr}	0.36	0.45
f_α	0.51	0.50
f_ρ	0.13	0.13
$f_{\alpha\alpha}$	0.13	0.14

Mass spectrometry was recently used to identify the technetium-rhenium mixed oxides $TcReO_7$ and $TcReO_5$ by heating a combination of TcO_x and ReO_2 at 700–800 °C in a gaseous mixture of oxygen and iodine in a Knudsen cell reactor [53].

10.8 Sulphides

At present only two binary sulphides of technetium are known, TcS_2 and Tc_2S_7, which closely resemble the analogous compounds of rhenium.

10.8.1 Technetium disulphide

Amorphous TcS_2 is formed by the thermal decomposition of Tc_2S_7. To prepare crystalline TcS_2, a mixture of precipitated Tc_2S_7 and excess sulphur is heated in a bomb for 24 h at 1000 °C. Afterwards unreacted sulphur is removed by sublimation in vacuum [23,26]. Single crystals were prepared by chemical transport reactions. TcS_2 was obtained in the form of very thin and soft crystal slices [54].

TcS_2 is a black solid, crystallizing in a primitive triclinic lattice with the unit cell dimensions a=6.456, b=6.375, c=6.659 Å, α=103.61°, β=62.97°, and γ=118.96°. The calculated density is 5.066 g · cm^{-3}. ReS_2 is also triclinic, but its structure differs from that of TcS_2. The shape of the unit cell of TcS_2 may be described as a distortion of a $Cd(OH)_2$-type cell. There are no indications of a structure transition in TcS_2 between −180° and 1150 °C. TcS_2 and ReS_2 are semiconductors, their absorption edges were found to be at 1.00 and 1.33 eV, respectively [54].

10.8.2 Ditechnetium heptasulphide

When hydrogen sulphide is passed through a solution of TcO_4^- in 4 M HCl or 4 M H_2SO_4 the highly insoluble, dark-brown Tc_2S_7 precipitates [55,56]. Usually the preci-

pitate contains free sulphur that must be removed by careful washing with carbon disulphide [26]. Tc_2S_7 is not precipitated by H_2S from 9 M HCl, permitting its isolation from Re_2S_7, which is insoluble in this medium [57]. Tc_2S_7 seems to be insoluble in alkaline polysulphide [22]; it dissolves in ammoniacal hydrogen peroxide [57]. Hydrogen reduces Tc_2S_7 to technetium metal at 1000 °C [56]. Until now no information on the structure of Tc_2S_7 and Re_2S_7 is available.

10.9 Selenides and tellurides

Crystalline samples of $TcSe_2$ and $TcTe_2$ may be prepared by heating intimate mixtures of the elements in evacuated quartz-glass tubes at about 1000 °C. Single crystals were obtained by chemical transport reactions. Best results were achieved with temperature gradients of about 1080 → 1000 °C for the $TcSe_2$ and 980 → 840 °C for $TcTe_2$. The crystals obtained showed pronounced plate-like habit. The diffraction patterns of $TcSe_2$ closely resemble those of the disulphide, indicating both compounds to be isostructural. However, the rather diffuse diffraction lines did not allow the determination of the unit-cell dimensions. Crystals of $TcTe_2$ exhibited monoclinic symmetry. The unit cell dimensions are a=12.522, b=7.023, c=13.828 Å, and β=101.26°. The calculated density is 7.890 g · cm^{-3}. $ReTe_2$ crystallizes in the orthorhombic system. The absorption edges of the semiconductors $TcSe_2$ and $ReSe_2$ are 0.88 and 1.15 eV, respectively [54].

10.10 Halides and oxide halides

The halides and oxide halides of technetium known thus far [58] are collected in Table 10.4.A, and compared with the known compounds of rhenium. Several halides and oxide halides that are well established for rhenium are still lacking for technetium and are waiting to be discovered.

Table 10.4.A Halides and oxide halides of technetium and rhenium.

Formal Oxidation state	Fluorides and Oxide Fluorides		Chlorides and Oxide Chlorides		Bromides and Oxide Bromides		Iodides and Oxide Iodides	
I	–	–		–	–	–	–	ReI
II	–		–	–	–			ReI_2
III			Tc_3Cl_9	Re_3Cl_9		Re_3Br_9	–	Re_3I_9
IV	–	ReF_4	$TcCl_4$	$ReCl_4$	$TcBr_4$	$ReBr_4$	–	ReI_4
	–		Tc_3Cl_{12}	–	–			–
V	TcF_5	ReF_5	–	$ReCl_5$		$ReBr_5$	–	–
	–	$ReOF_3$	$TcOCl_3$	$ReOCl_3$ (?)	$TcOBr_3$	$ReOBr_3$ (?)	–	–
VI	TcF_6	ReF_6	$TcCl_6$ (?)	$ReCl_6$				–
	$TcOF_4$	$ReOF_4$	$TcOCl_4$	$ReOCl_4$		$ReOBr_4$		–
VII		ReF_7		–	–		–	
	$TcOF_5$	$ReOF_5$		–	–		–	
	TcO_3F	ReO_3F	TcO_3Cl	ReO_3Cl	TcO_3Br	ReO_3Br	TcO_3J	ReO_3J
	TcO_2F_3	ReO_2F_3	–				–	–

10.10.1 Fluorides and oxide fluorides

Technetium pentafluoride is formed as a by-product of technetium hexafluoride when technetium metal powder is heated to 350 °C in an F_2/N_2 stream [59], or by the action of I_2 on TcF_6 in IF_5 solution [60]:

$$I_2 + 10\,TcF_6 \xrightarrow{IF_5} 10\,TcF_5 + 2\,IF_5$$

TcF_5 is purified by vacuum sublimation [61]. It is a yellow solid that melts at 50 °C and begins to decompose at 60 °C. Single crystal X-ray diffraction studies showed the lattice to be orthorhombic and isostructural with CrF_5 [59], VF_5, and ReF_5. The structural unit consists of two crystallographically different octahedra, which are linked through *cis*-bridging fluorine atoms to form endless chains parallel to the *a* axis. The octahedra are only slightly distorted. The unit cell dimensions are a=5.76, b=17.01, c=7.75 Å, and Z=8; the space group is *Pmcn* [61]. The Raman spectrum of liquid TcF_5 is quite similar to those of other *cis*-F bridged polymers, which are characterized by two intense strongly polarized bands. For TcF_5 the strongly polarized bands are at 749 and 693 cm^{-1} and the weaker bands are at 669, 282, 225, and 139 cm^{-1}. Spectra obtained between 80 and 100 °C do not differ substantially from those at room temperature. In the solid at –50 °C the bond stretching region is dominated by three strong and sharp bands at 698, 750, and 775 cm^{-1} in addition to several weak bands. Magnetic susceptibility measurements yielded a magnetic moment of 3.00 B.M. and a Weiss constant of 156°. The magnetic moment is close to the spin-only value for two unpaired electrons [60].

Technetium hexafluoride can be prepared by reaction of technetium metal powder with excess fluorine gas in a closed nickel can at 400 °C. The volatile golden-yellow solid was purified by fractional sublimation at reduced pressure. The yield of purified TcF_6 was greater than 90 % [63]. Lower conversions are obtained by treating finely divided technetium metal at 350 °C with a F_2/N_2 mixture in a flow stream. TcF_6 melts at 37.4 °C, boils at 55.3 °C, and undergoes a solid-solid transition at –4.54 °C from the low temperature orthorhombic to the bcc modification at room temperature [64]. More recently the transition temperature of 268.335 K was reported [67].

The vapor pressures are given by the equations

$$\log P_{solid}(-16.32 \text{ to } -5.3\ ^\circ C) = -(3564.8/T) - 10.787 \log T + 41.1252$$
$$\log P_{solid}(-5.3 \text{ to } 37.4\ ^\circ C) = -(2178.0/T) - 2.295 \log T + 15.33427$$
$$\log P_{liquid}(37.4 \text{ to } 51.67\ ^\circ C) = -(2404.9/T) - 5.8036 \log T + 24.8087$$

Temperatures T are given in Kelvin and pressures in mm Hg at 0 °C. The calculated triple point is 37.36 °C [65].

It should be pointed out that the vapor pressure data and infrared spectra of TcF_6 did not show any evidence for the existence of TcF_7 [64]. ReF_7 is formed by the action of fluorine at 250 torr on rhenium metal at 300–400 °C. The product is always a mixture of ReF_7 and ReF_6. As it is almost impossible to separate the two fluorides, the mixture was heated with fluorine at 3 atm pressure at 400 °C for sev-

eral hours, the hexafluoride being thus converted quantitatively into the heptafluoride. ReF_7 is a thermally stable, yellow solid [65,66]. In contrast, the existence of TcF_7 could not be established so far. Obviously, compounds of technetium in the higher oxidation states are less stable than those of rhenium. To make TcF_7 it may be advised to try reactions of technetium powder with fluorine at varying pressure and temperature conditions.

Powder X-ray diffraction data of technetium hexafluoride and rhenium hexafluoride modifications are compiled in Table 10.5.A.

Table 10.5.A X-ray diffraction data of TcF_6 and ReF_6 modifications [68].

Substance	Temp. [°C]	Lattice symmetry	Z	Cell dimensions [Å]	Calcd. density [g·cm^{-3}]
TcF_6	+10	bcc	2	$a = 6.16$	3.02
TcF_6	−19	orthorhombic	4	$a = 9.55$	3.38
				$b = 8.74$	
				$c = 5.02$	
ReF_6	+10	bcc	2	$a = 6.26$	4.06
ReF_6	−22	orthorhombic	4	$a = 9.61$	4.68
				$b = 8.76$	
				$c = 5.06$	

Other transition metal hexafluorides like MoF_6, RuF_6, RhF_6, WF_6, OsF_6, IrF_6, and PtF_6 also exhibit a bcc phase near room temperature and a phase of lower symmetry, probably orthorhombic, at reduced temperatures [68].

The magnetic susceptibility of TcF_6 between 295 and 14 K was found to vary linearly with $1/T$. The molar susceptibility is given by the equation

$$\chi_M = 254 \cdot 10^{-4}/T + 4.39 \cdot 10^{-4}\ \text{cm}^3 \cdot \text{mole}^{-1}$$

The magnetic moment was reported to be 0.45 B.M. [69], which is drastically lower than expected for a d^1 system of octahedral symmetry.

For gaseous TcF_6 the IR spectrum was measured in the range from 6 to 43 μm [70] and the Raman spectrum using laser excitation [71]. The spectra were interpreted in terms of the octahedral point group O_h [72]. Considerable broadening of the E_g and F_{2g} fundamentals was observed for TcF_6 and ReF_6. This broadening was attributed to dynamic Jahn-Teller coupling. The values of fundamental frequencies for technetium and rhenium hexafluoride are given in Table 10.6.A.

Table 10.6.A Fundamental frequencies [cm^{-1}] of gaseous TcF_6 and ReF_6 [71].

Molecule	$\nu_1(A_{1g})$	$\nu_2(E_g)$	$\nu_3(F_{1u})$	$\nu_4(F_{1u})$	$\nu_5(F_{2g})$	$\nu_6(F_{2u})$
TcF_6	712.9	639	748	265	297	145
ReF_6	753.7	671	715	257	295	147

Based on the vibrational frequencies for TcF_6 [70] and ReF_6 [73] the force constants of both molecules were calculated using the force field of the general valence type (Table 10.7.A).

Table 10.7.A Force constants of TcF_6 and ReF_6 [mdyne/Å] [74].

Molecule	$f_r+f_{rr'}$	f_{rr}	$f_{r\alpha}$	f_α	$f_{\alpha\alpha}$	$f_{\alpha\alpha'}$
TcF_6	4.118	0.361	1.001	0.726	0.272	0.262
ReF_6	4.775	0.401	0.650	0.418	0.105	0.125

Technetium hexafluoride can be stored unchanged in nickel or dry Pyrex vessels for extended periods of time. It yields a black precipitate ($TcO_2 \cdot aq$) by disproportionation upon hydrolysis with aqueous NaOH solution [63]. TcF_6 reacts with iodine in iodine pentafluoride to form quantitatively TcF_5 [60]. The action of solutions of alkali chlorides on TcF_6 in IF_5 as solvent gives hexafluorotechnetates(V) [59,75]. Reactions of technetium hexafluoride with nitric oxide, nitrosyl fluoride, and nitryl fluoride result in the compounds $NO[TcF_6]$, $(NO)_2[TcF_8]$, and $NO_2[TcF_7]$, respectively [76]. TcF_6 in hydrogen fluoride reacts with hydrazinium(+2) fluoride to form $N_2H_6[TcF_6]_2$ or $N_2H_6[TcF_6]$, depending on which reactant was used in excess [77].

Technetium oxide tetrafluoride like the pentafluoride is formed as a by-product of TcF_6 in the fluorination of technetium metal [59,78,79]. $TcOF_4$ forms two phases that may be separated from TcF_5 and from one another by vacuum sublimation. One phase of $TcOF_4$ forms blue needles, has a chain structure, and is isostructural with its rhenium analogue. The other modification is a more volatile green compound of trimeric structure [78,79].

The blue phase melts at 134 °C to a blue liquid. Vapor pressure measurements indicate a phase change at 84.5 °C. The extrapolated boiling point of the blue phase is 165 °C [61]. The magnetic moment of μ=1.76 B.M., Θ=9°, is of the expected order for a d^1 compound in octahedral symmetry [59]. Blue $TcOF_4$ crystallizes isostructurally with $ReOF_4$ in the monoclinic system with the lattice constants a=18.83, b=5.49, c=14.43 Å, β=114.0°, Z=16. The structure consists of distorted octahedral groups, linked into endless chains parallel to the c-axis by *cis*-bridging of the fluorine atoms. The structural unit consists of two crystallographically distinct octahedra. A significant feature of the structure is the very short terminal oxygen bond length of about 1.65 Å in each octahedron. The bridge bond length opposite to this oxygen atom is considerably longer (2.31 Å) than that opposite to a fluorine atom [80].

The green, trimeric modification of $TcOF_4$ crystallizes in the hexagonal system with the lattice constants a=9.00 and c=7.92 Å, Z=6. The space group is $P6_3/m$. The structure consists of discrete trimeric units with the three Tc atoms forming a triangle, linked asymmetrically by *cis*-bridging fluorine atoms. The almost undistorted octahedral arrangement is completed by the oxygen atom *trans* to the longer bridge bond, and two terminal fluorine atoms. The distortion in the coordination can be correlated with a displacement of the technetium atom from the center of the octahedron by 0.36 Å towards the oxygen atom (Fig. 10.3.A). The green modification of $TcOF_4$ appears unlikely to be the high-temperature of blue $TcOF_4$, because its high- and low-

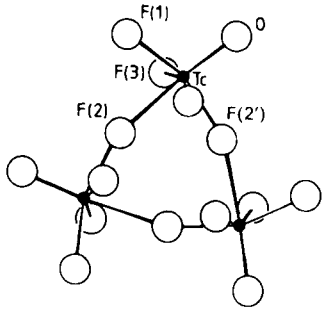

Fig. 10.3.A The trimer unit of green $TcOF_4$. Bond distances: Tc-O 1.66, Tc-F(1) 1.82, Tc-F(2) 2.26, Tc-F(3) 1.80 Å. Bond angles: F(1)-Tc-F(2) 78.0, F(1)-Tc-O 106.0, F(1)-Tc-F(3) 89.1, F(2)-Tc-O 175.9° [79].

temperature forms show no difference in color [79]. Both forms of technetium oxide tetrafluoride are moisture sensitive and are hydrolyzed completely by water to hydrofluoric acid, technetium dioxide, and pertechnetic acid [33].

Technetium trioxide fluoride was prepared by passing fluorine gas at 250 torr over TcO_2 in a nickel tube at 150 °C. The volatile product was collected downstream in a dry-ice bath and purified from hydrofluoric acid and other volatile impurities by repeated sublimations. The yield was 56 % [81]. TcO_3F is also obtained by sparing dissolution of NH_4TcO_4 in anhydrous fluoride. The reaction yields a pale yellow solution with an undissolved solid layer at the bottom [82]. TcO_3F forms yellow crystals which melt at 18.3 °C to a yellow liquid. The vapor pressures P of solid and liquid TcO_3F are given by the equations

Solid (−8.78 to 18.28 °C): $\log P = 12.448 - 3239.4/T$,
Liquid (18.28 to 51.82 °C): $\log P = 8.417 - 2064.6/T$,

when P is given in torr at 0 °C and T in Kelvin. The extrapolated boiling point is about 100 °C and the calculated triple point 18.28 °C. Technetium trioxide fluoride is stable at room temperature in nickel or monel storage vessels, but attacks even dry Pyrex or quartz fairly rapidly. With excess water TcO_3F hydrolyzes to $HTcO_4$ and HF. Upon reaction with excess fluorine gas at 400 °C and 4 atm pressure it is converted quantitatively to TcF_6 [81]. Fluoride donor properties of TcO_3F were studied in HF solution and the solid $[TcO_3]^+[AsF_6]$ was isolated [83]. IR and Raman spectra indicate the symmetry C_{3v} for TcO_3F. The fundamental vibrations of TcO_3F and ReO_3F are given in Table 10.8.A.

Table 10.8.A Fundamental frequencies [cm^{-1}] of TcO_3F and ReO_3F and their assignments [82].

Assignment	$\nu_1(A_1)$	$\nu_2(A_1)$	$\nu_3(A_1)$	$\nu_4(E)$	$\nu_5(E)$	$\nu_6(E)$
TcO_3F	696	962	317	951	347	231
ReO_3F	666	1009	321	980	403	174
Mode	ν(M–F)	$\nu_s(MO_3)$	$\delta_s(MO_3)$	$\nu_{as}(MO_3)$	$\delta_{as}(MO_3)$	ρ(F-Tc-O)

Using the fundamental vibrations of TcO_3F, the valence force constants were calculated (Table 10.9.A).

Table 10.9.A Valence force constants [mdyne/Å] for TcO_3F [84].

TcO_3F	f_R	f_r	f_{rr}	f_α	f_ρ	$f_{\alpha\alpha}$
	4.57	7.37	0.41	0.44	0.19	0.05

R and r are related to the Tc–F and Tc–O bonds, respectively, α to the O–Tc–O angle and ρ to the O–Tc–F angle, while rr and $\alpha\alpha$ are related to bond/bond and angle/angle interactions, respectively. The Tc–O force constant f_r turns out to be almost identical with the force constant f_r=7.40 mdyne/Å obtained for the terminal TcO_3 groups in ditechnetium heptoxide [51].

Technetium dioxide trifluoride was recently synthesized by reaction of Tc_2O_7 and XeF_6 in a 1:3 molar ratio in anhydrous hydrogen fluoride solution via the fluorination of TcO_3F by XeF_6:

$$Tc_2O_7 + 4\ HF \rightarrow 2TcO_3F + H_3O^+ + HF_2^-$$
$$TcO_3F + XeF_6 \rightarrow TcO_2F_3 + XeOF_4$$

The reaction resulted in a microcrystalline precipitate of TcO_2F_3. Pure TcO_2F_3 is lemon yellow and has a melting point of 200 °C. It crystallizes in the triclinic system, space group $P\bar{1}$, with a=7.774, b=7.797, c=11.602 Å, α=89.41, β=88.63, γ=84.32°. The calculated density is 3.551 g·cm^{-3} for Z=8. The structure of TcO_2F_3 consists of open chains of molecules parallel to the b-axis of the unit cell. The Tc atoms form a "zig-zag" chain linked symmetrically by fluorines which are *trans* to the oxygens. The light atoms surrounding technetium form nearly undistorted octahedra in which the Tc atoms are displaced toward the oxygen atoms (Fig. 10.4.A). The bond distances are: terminal Tc–F 1.834 Å, bridging Tc–F 2.080 Å, and Tc–O 1.646 Å. The Tc–F–Tc angle is 148.8° [85]. The structure is closely related to those of $MoOF_4$ and $ReOF_4$. The Raman spectrum of the polymeric *cis*-TcO_2F_4 unit was assigned under C_{2v} point symmetry (Table 10.10.A) and exhibits only weak vibrational coupling in the unit cell.

TcO_2F_3 reacts in anhydrous HF with excess of KrF_2 at room temperature to give **$TcOF_5$**:

$$TcO_2F_3 + KrF_2 \xrightarrow{HF} TcOF_5 + \tfrac{1}{2}\,O_2 + Kr$$

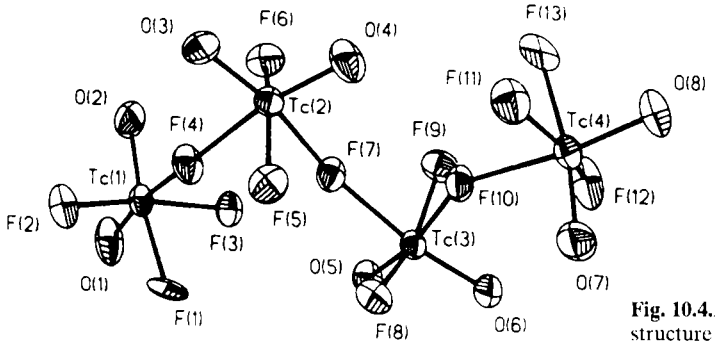

Fig. 10.4.A Asymmetric unit of the structure of TcO_2F_3 [85].

Table 10.10.A Assigned Raman frequencies of TcO_2F_3. Values in parentheses denote relative intensities [85].

Frequencies [cm^{-1}]	Assignments
974 (100)	A_1, $\nu_s(TcO_2)$
963 (27)	B_2, $\nu_{as}(TcO_2)$
958 sh	
685 (3)	B_1, $\nu_{as}(TcF_2)$ term.
670 (7)	
650 (16)	A_1, $\nu_s(TcF_2)$ term.
632 (16)	
416 sh	A_1, $\delta_{sciss}(TcO_2)$
411 (19)	
320 (22)	B_2, $\nu_{as}(TcF_2)$ bridge
295 (30)	A_1, $\nu_s(TcF_2)$ bridge
284 (24)	A_1, $\delta_{sciss}(TcF_2)$ term.

Pure $TcOF_5$ melts reversibly and without decomposition at 57–58 °C. The volatile orange solid is deep red-orange in the liquid state [86]. According to ^{19}F NMR, ^{99}Tc NMR, Raman and IR spectroscopy, the structure of the $TcOF_5$ molecule is pseudo-octahedral. The vibrational frequencies are presented in Table 10.11.A.

Table 10.11.A Vibrational frequencies and assignments for solid $TcOF_5$. Values in parentheses denote relative intensities of frequencies [86].

Frequencies [cm^{-1}]	Assignments
933 (28)	$\nu_1(A_1)$
702 (100)	$\nu_2(A_1)$
616 (8)	$\nu_5(B_1)$
601 (5)	$\nu_3(A_1)$
351 (10)	$\nu_{10}(E)$
328 (10)	$\nu_7(B_2)$
278 (5)	$\nu_4(A_1)$
206 (2)	$\nu_6(B_1)$
131 (1)	$\nu_{11}(E)$

In the reaction of technetium metal with chlorine trifluoride at 650 °C, the mixed oxide fluoride chloride molecules **$TcOF_2Cl$** and **$TcOFCl_2$** were recently identified by mass spectrometry, in addition to already known technetium oxide fluorides and oxide chlorides [87].

10.10.2 Chlorides and oxide chlorides

The hitherto only chloride of formally trivalent technetium is the trimeric compound **Tc_3Cl_9**, which was observed in a mass spectrometer when mixed phases of technetium/rhenium chlorides were heated to 300–350 °C. Other primarily vaporized molecules containing Tc were **$TcRe_2Cl_9$**, **Tc_2ReCl_9**, and the compounds **Tc_3Cl_{12}** and Tc_2ReCl_{12} of formally quadrivalent technetium. In addition, $TcCl_4$ was identified [88]. In contrast to the well defined dark-violet solid Re_3Cl_9, the compound Tc_3Cl_9 has so far not been obtained in a solid state. There is some evidence that the heating of $Ag_2[TcCl_6]$ in vacuum gives not only $TcCl_4$, but sometimes in addition a few brown flakes of possibly Tc_3Cl_9 that were extremely unstable in air. In hydrochloric acid the flakes give a dark green solution that has absorption maxima at 16200 and 11400 cm^{-1}. These bands are reminiscent of the absorption spectrum of Re_3Cl_9 in hydrochloric acid [89].

Technetium tetrachloride was synthesized by reaction of Tc_2O_7 with CCl_4 at 400 °C in a sealed glass tube. The yield of preparation was 79 % [90]. $TcCl_4$ can also be obtained by passing a stream of dry chlorine over technetium metal at 200–400 °C. The blood-red crystals may be sublimed at about 300 °C in the chlorine stream [91]. The needle-shaped crystals of $TcCl_4$ are orthorhombic, having the space group *Pbca*. The unit cell dimensions are a=11.65, b=14.06, and c=6.03 Å; Z=8. The X-ray density was calculated to be 3.26 g · cm^{-3} in good agreement with the density found experimentally [92,93]. Crystal structure analysis revealed distorted octahedral units of the composition $TcCl_6$, which are linked to form polymeric chains, each octahedral unit sharing one edge with each of the two adjacent octahedra (Fig. 10.5.A). The repeating unit of the chain is a Tc_2Cl_8 unit made up of two planar asymmetric units related to each other by a glide plane. There are three pairs

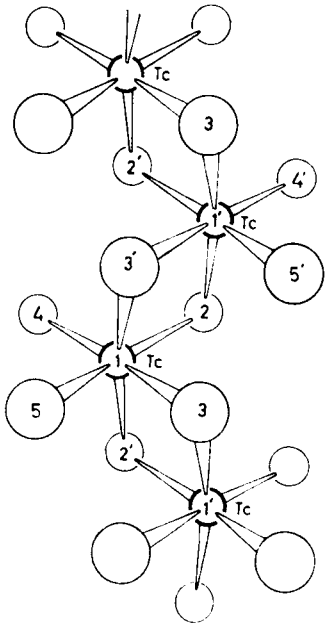

Fig. 10.5.A A section of the $(TcCl_4)_n$ chain [93].

of chemically distinct Tc–Cl bonds. The shortest bonds (2.24 Å) involve the non-bridging chlorine atoms Cl(4) and Cl(5). The longest bonds (2.49 Å) are the bridging chlorines Cl(2) and Cl(3) aligned perpendicularly to the chain length. Intermediate in length (2.38 Å) is the third pair of bonds to the bridging chlorines Cl(2′) and Cl(3′) parallel to the chain length. All bond angles are within 6° of the 90° expected for a regular octahedron [93].

Technetium tetrachloride shows a high molar magnetic susceptibility that is strongly temperature dependent. The magnetic moment μ = 3.14 B.M. and the Weiss constant Θ=–57 K were found. The moment of 3.14 B.M. appears low for 3 unpaired electrons and an almost octahedral crystal field. However, the $TcCl_6$ units are not magnetically dilute enough for exchange interactions to be negligible [94]. $TcCl_4$ is unstable in the presence of water vapor [93]. It dissolves in hydrochloric acid to give yellow solutions containing $[TcCl_6]^{2-}$. In water and alkaline solutions $TcCl_4$ is not instantly hydrolyzed [58]. In ethanolic solution it reacts with triphenylphosphine, triphenylarsine or α,α'-dipyridyl to form complexes [95]. Reaction of $TcCl_4$ with benzene, benzene derivatives or sodium cyclopentadienyl yields aromatic π-complexes [96]. In addition, reactions of $TcCl_4$ with $(CH_3)_3SiBr$, acetonitrile, *tert*-butylisonitrile, and crown ethers have been recently described [97].

Technetium oxide trichloride, $TcOCl_3$, was obtained by reaction of technetium dioxide in a chlorine stream at 300–350 °C. The brown, slightly volatile product can be sublimed at about 500 °C in vacuum. $TcOCl_3$ shows a strong band in the IR at 1017 cm^{-1}, which can be attributed to the metal-oxygen stretching mode. The compound is readily hydrolyzed and disproportionates [30,98,99]:

$$3\ TcOCl_3 + 5\ H_2O \rightarrow 2\ TcO_2 + HTcO_4 + 9\ HCl$$

Technetium hexachloride, $TcCl_6$, was claimed to be prepared by passing a stream of chlorine over technetium metal at 400 °C. A dark green product was reported to be $TcCl_6$ and melted very readily to give a green liquid [91]. However, subsequently the existence of $TcCl_6$ could not be confirmed and now appears to be doubtful [100], whereas $ReCl_6$ was obtained as a dark green to black crystalline compound by halogen exchange of ReF_6 with boron trichloride [101].

Recently, **technetium nitride trichloride**, $TcNCl_3$, was reported to be synthesized by reaction of $TcCl_4$ and IN_3 in carbon tetrachloride. The black-brown solid of $TcNCl_3$, which still has to be identified completely, dissolves in a solution of $[Ph_4As]Cl$ in dichloromethane to form $[Ph_4As][TcNCl_4]$ [102].

Technetium oxide tetrachloride, $TcOCl_4$, was separated from the mixture of the oxide chlorides, which are produced upon chlorination of technetium metal at 300 °C, by trap-to-trap distillation in vacuum in the dark. Pure $TcOCl_4$ is a purple crystalline solid that forms large crystals and melts at ~ 35 °C. It is stable at room temperature if kept out of the light, but decomposes rapidly to $TcOCl_3$ even at –78 °C, if left in sunlight or artificial fluorescent light. The chlorine produced in the photochemical reaction

$$2TcOCl_4 \xrightarrow{h\nu} 2TcOCl_3 + Cl_2$$

was identified by its ultraviolet spectrum. The Tc=O stretching frequency of $TcOCl_4$ in the IR was found at 998 cm^{-1} [98,100].

Technetium trioxide chloride, TcO_3Cl, was prepared very early by the simple procedure of adding 12 M HCl to a solution of $KTcO_4$ dissolved in 18 M H_2SO_4. Upon shaking the acid with carbon tetrachloride, chloroform or hexane, the compound is extracted into the organic phase [26,103]. Later, TcO_3Cl was obtained by vacuum distillation from the mixture of technetium oxide chlorides produced upon chlorination of technetium metal at 300 °C or by heating $TcCl_4$ with oxygen in a sealed tube to 450 °C for a few hours. TcO_3Cl is a very pale yellow liquid boiling at 25 °C. The vapor phase UV-VIS spectrum was recorded and appeared to be very similar to that of ReO_3Cl. Bands of TcO_3Cl at 192, 228 and 315 nm were reported [100]. Dynamical Jahn-Teller effects in the near UV vapor phase absorption spectra of TcO_3Cl and ReO_3Cl were observed. Calculations of the geometry in the excited state show that there is an asymmetric distortion in the metal–oxygen bond length [104]. Also the IR and Raman spectra of TcO_3Cl exhibit considerable similarity with those of ReO_3Cl. In addition, the spectra are very similar to those of the heptaoxides. Table 10.12.A summarizes the fundamental vibrations and assignments for the trioxide chlorides of technetium and rhenium, the force constants are given in Table 10.13.A.

Table 10.12.A Fundamental vibrations and assignments for TcO_3Cl and ReO_3Cl [105,106].

C_{3V}	Mode	Frequencies [cm^{-1}]		Assignments
Symmetry species		TcO_3Cl liquid	ReO_3Cl liquid	
A_1	ν_1	445	433	ν(MCl)
A_1	ν_2	950	1002	ν_s(MO)
A_1	ν_3	299	303	δ_s(OMO)
E	ν_4	932	962	ν_{as}(MO)
E	ν_5	197	197	ρ_r
E	ν_6	340	345	δ_{as}(OMO)

Table 10.13.A Force constants of TcO_3Cl and ReO_3Cl [mdyne/Å], α:OMO angle, β: OMCl angle [106].

Molecule	f_{MO}	f_{MCl}	$f_{MO/MO}$	f_{α}-$f_{\alpha\alpha}$	f_{β}-$f_{\beta\beta}$
TcO_3Cl	7.12	3.07	0.42	1.18	0.68
ReO_3Cl	8.28	3.27	0.44	1.18	0.71

The lower force constants f_{MO} and f_{MCl} of TcO_3Cl compared to the corresponding force constants of ReO_3Cl indicate again the weaker bonding strengths in the technetium compound.

10.10.3 Bromide, oxide bromides, and oxide iodide

Technetium tetrabromide, $TcBr_4$, was synthesized analogously to rhenium tetrabromide [107] by reduction of pertechnetic acid with a 46 % solution of hydrobromic acid. This procedure was repeated four times. An unstable brown-red compound was obtained which rapidly hydrolyzed in moist air. The bromine analysis was always low due to slow spontaneous loss of bromine. $TcBr_4$ dissolves in ethanol and acetone and forms complexes with 1,2-bis(diphenyl-phosphino)ethane and triphenylphosphine [89].

Technetium oxide tribromide, $TcOBr_3$, was obtained by bromination of technetium dioxide. Bromine vapor, carried in a stream of oxygen-free, dry nitrogen, reacts with TcO_2 at 300–350 °C. The grey-black crystalline product collected over a period of 4–5 h. Surprisingly, also NH_4TcO_4 or $KTcO_4$ react with bromine vapor at 350–400 °C to give $TcOBr_3$. Technetium oxide tribromide is thermally stable and sublimes at 350–400 °C. In the IR spectrum a weak absorption was observed at 770 cm^{-1} which was assigned to a Tc=O stretching mode [98].

Recently, the existence of gaseous **technetium trioxide bromide**, TcO_3Br, and **trioxide iodide**, TcO_3I, was established mass spectrometrically by heating an undefined technetium oxide, probably TcO_2, in a Knudsen cell up to 800 °C, through which the reactive gases Br_2,I_2, and O_2 were flowed. The TcO_3Br formation was found to be more facile than that of TcO_3I. Both vapor species are stable to at least 700 °C [108].

To conclude this section the synthesis and some properties of the halides and oxide halides of technetium are summarized in Table 10.14.A.

Table 10.14.A Synthesis and properties of technetium halides and oxide halides.

	Synthesis		Propterties	Refererences
$Tc+F_2/N_2$	350°C→	TcF_5	yellow, m. p. 50 °C	[59]
TcF_6+I_2/HF	→	TcF_5		[60]
$Tc-F_2$	400°C→	TcF_6	golden-yellow, m.p. 37.4 °C, b.p. 55.3 °C	[63]
$Tc+F_2/O_2$	350°C→	$TcOF_4$ $TcOF_4$	blue, m.p. 134 °C, b.p. 165 °C green, trimeric	[61] [79]
$TcO_2F_3/HF+KrF_2$	·	$TcOF_5$	red-orange, m.p. 57–58 °C	[86]
TcO_2+F_2	150°C→	TcO_3F	yellow, m.p. 18.3 °C, b.p. 100 °C	[81]
NH_4TcO_4+HF	→	TcO_3F		[82]
$Tc_2O_7/HF+XeF_6$	→	TcO_2F_3	lemon-yellow, m.p. 200 °C	[85]
Technetium chloride	300–350°C→	Tc_3Cl_9	mass spectrum	[88]
$Tc_2O_7+CCl_4$	400°C→	$TcCl_4$	blood red	[90]
$Tc+Cl_2$	200–400°C→	$TcCl_4$		[91]
Technetium chloride	300–350°C→	Tc_3Cl_{12}	mass spectrum	[88]
TcO_2+Cl_2	350°C→	$TcOCl_3$	brown	[98]
$Tc+Cl_2/O_2$	300°C→	$TcOCl_4$	purple, m.p. ~35 °C	[100]
$KTcO_4/H_2SO_4+12$ MHCl	→	TcO_3Cl	pale yellow, b.p. 25 °C	[26]
$Tc+Cl_2/O_2$	300°C→	TcO_3Cl		[100]
$TcCl_4+O_2$	450°C→	TcO_3Cl		[100]
$TcCl_4+NO_2/CCl_4$	→	$TcNCl_3$	black-brown	[102]
$HTcO_4+HBr$	·	$TcBr_4$	brown-red, unstable	[89]
TcO_2+Br_2	300–350°C→	$TcOBr_3$	grey-black	[98]
$KTcO_4+Br_2$	350–400°C→	$TcOBr_3$		[98]
TcO_2+Br_2	700°C→	TcO_3Br	mass spectrum	[108]
TcO_2+I_2/O_2	750°C→	TcO_3I	mass spectrum	[108]

10.11 References

[1] V. I. Spitsyn, E. G. Ponyatrovskii, V. E. Antonov, I. T. Belash, and O. A. Balakhovskii, Proc. Acad. Sci. USSR *244/249*, 723–726 (1979)
[2] V. I. Spitsyn, V. E. Antonov, O. A. Balakhovskii, I. T. Belash, E. G. Ponyatovskii, V. I. Rashchupkin, and V. S. Shekhtman, Dokl. Akad. Nauk SSSR *260*, 132–135 (1981)
[3] V. P. Glazkov, A. V. Irodova, V. A. Somenkov, S. S. Shil'shtein, V. E. Antonov, and E. G. Ponyatovskii, Sov. Phys. Solid State *26*, 1961 (1984)
[4] S. S. Shilstein, V. P. Glazkov, A. V. Irodova, V. A. Somenkov, V. E. Antonov, and E. G. Ponyatovskii, Z. Phys. Chem., Neue Folge *146*, 129–135 (1985)
[5] V. Y. Antonov, I. T. Belash, K. G. Bukov, O. V. Zharikov, A. V. Pal'Nichenko, and V. M. Teplinskiy, Phys. Met. Metall. *68*, 153–155 (1989)
[6] E. N. Zakharov, S. P. Bagaev, V. N. Kudryavtsev, K. S. Pedan, and V. E. Antonov, Protection of Metals *27*, 795–796 (1991)
[7] W. Trzebiatowski and J. Rudzinski, J. Less-Common Metals *6*, 244–245 (1964)
[8] I. M. Chapnik, Phys. Status Solidi *A41*, K71–K73 (1977)
[9] D. R. Armstrong, J. Less-Common Metals *67*, 191–203 (1979)
[10] A. Leithe-Jasper, P. Rogl, and P. E. Potter, J. Nucl. Mater. *217*, 194–196 (1994)
[11] W. Trzebiatowski and J. Z. Rudzinski, Z. Chem. *2*, 158 (1962)
[12] A. L. Giorgi and E. G. Szklarz, J. Less-Common Metals *11*, 455–456 (1966)
[13] G. H. Rinehart and R. G. Behrens, J. Phys. Chem. *83*, 2052–2053 (1979)
[14] I. V. Vinogradov, M. I. Konarev, L. L. Zaitseva, and S. V. Shepel'kov, Russ. J. Inorg. Chem. *23*, 977–978 (1978)
[15] I. V. Vinogradov, M. I. Konarev, L. L. Zaitseva, and S. V. Shepel'kov, Russ. J. Inorg. Chem. *23*, 639–640 (1978)
[16] R. Rühl, W. Jeitschko, and K. Schwochau, J. Solid State Chem. *44*, 134–140 (1982)
[17] R. Rühl and W. Jeitschko, Acta Cryst. *B38*, 2784–2788 (1982)
[18] L. H. Dietrich and W. Jeitschko, J. Solid State Chem. *63*, 377–385 (1986)
[19] F. Hulliger, Nature *209*, 500–501 (1966)
[20] W. Jeitschko and L. H. Dietrich, J. Solid State Chem. *57*, 59–67 (1985)
[21] O. Muller, W. B. White, and R. Roy, J. Inorg. Nucl. Chem. *26*, 2075–2086 (1964)
[22] K. Schwochau, Radiochim. Acta *32*, 139–152 (1983)
[23] K. Schwochau in: Handbuch der Präparativen Anorganischen Chemie, Vol. III (G. Brauer, ed.), Enke Verlag, Stuttgart (1981), pp. 1597–1606
[24] K. Schwochau, Diss. Univ. Köln, (1961) p.20, Report Jül-68-RC (1962)
[25] B. Kanellakopulos, Diss. Techn. Univ. Karlsruhe, (1963) p. 42
[26] G. E. Boyd, J. Chem. Educ. *36*, 3–14 (1959)
[27] G. H. Cartledge and W. T. Smith, Jr., J. Phys. Chem. *59*, 1111–1112 (1955)
[28] G. A. Mazzocchin, F. Magno, and G. Bontempelli, Inorg. Chim. Acta *13*, 209–212 (1975)
[29] B. Gorski and H. Koch, J. Inorg. Nucl. Chem. *31*, 3565–3571 (1969)
[30] C. M. Nelson, G. E. Boyd, and W. T. Smith, Jr., J. Am. Chem. Soc. *76*, 348–352 (1954)
[31] A. Magnéli and G. Andersson, Acta Chem. Scand. *9*, 1378–1381 (1955)
[32] K. H. Lieser, C. Bauscher, and T. Nakashima, Radiochim. Acta *42*, 191 (1987)
[33] R. D. Peacock in: The Chemistry of Manganese, Technetium and Rhenium, Pergamon Press, New York (1973), p. 894
[34] A. Y. Herrell and R. H. Busey, Oak Ridge National Laboratory Rep. ORNL-4791 (1972), pp. 104–105; Nucl. Sci. Abstr. *27* (1972), No. 191
[35] A. Y. Harrell, R. H. Busey, K. H. Gayer, K. Schwochau, and S. Gutzeit, Inorg. Syntheses *17*, 155–158 (1977)
[36] J. K. Gibson, Radiochim. Acta *60*, 121–126 (1993)
[37] S. Fried, A. H. Jaffey, N. F. Hall, and L. E. Glendenin, Phys. Rev. *81*, 741–747 (1951)
[38] A. Steffen and K. Bächmann, Talanta *25*, 551–556 (1978)
[39] A. Steffen and K. Bächmann, Talanta *25*, 677–683 (1978)
[40] H. Müller in: Handbuch der Präparativen Anorganischen Chemie, Vol. III (G. Brauer, ed.), Enke Verlag, Stuttgart (1981), Chapter 27
[41] H. Nechamkin, C. F. Hiskey, T. Moeller, and C. E. Shoemaker, Inorg. Syntheses *3*, 186–188 (1950)

[42] G. E. Boyd, J. W. Cobble, C. M. Nelson, and W. T. Smith, Jr., J. Am. Chem. Soc. *74*, 556–557 (1952)
[43] W. T. Smith, Jr., J. W. Cobble, and G. E. Boyd, J. Am. Chem. Soc. *75*, 5773–5776 (1953)
[44] K. V. Kotegov, O. N. Pavlov, and V. P. Shvedov, Advan. Inorg. Radiochem. *11*, Technetium (H. J. Emeléus and A. G. Sharpe, eds.). Academic Press, New York (1968), p. 21
[45] J. C. Hileman, D. K. Huggins, and H. D. Kaesz, J. Am. Chem. Soc. *83*, 2953–2954 (1961)
[46] B. Krebs, Angew. Chem. *81*, 328–329 (1969)
[47] B. Krebs, Angew. Chem. Internat. *8*, 381–382 (1969)
[48] B. Krebs, Z. Anorg. Allgem. Chem. *380*, 146–159 (1971)
[49] H. Selig and S. Fried, Inorg. Nucl. Chem. Lett. *7*, 315–323 (1971)
[50] I. R. Beattie and G. A. Ozin, J. Chem. Soc. A *1969*, 2615–2619
[51] E. J. Baran, Anales Asoc. Quim Argentina *62*, 65–70 (1974)
[52] K. Schwochau and W. Krasser, Z. Naturforsch. *24a*, 403–407 (1969)
[53] J. K. Gibson, Radiochim. Acta *62*, 127–132 (1993)
[54] J. C. Wildervanck and F. Jellinek, J. Less-Common Metals *24*, 73–81 (1971)
[55] E. E. Motta, G. E. Boyd, and Q. V. Larson, Phys. Rev. *72*, 1270 (1947)
[56] S. Fried, J. Am. Chem. Soc. *70*, 442 (1948)
[57] C. L. Rulfs and W. W. Meinke, J. Am. Chem. Soc. *74*, 235–236 (1952)
[58] J. H. Canterford and R. Colton in: Halides of the Second and Third Row Transition Metals, Wiley Interscience Publication, London (1968), pp. 272–315
[59] A. J. Edwards, D. Hugill, and R. D. Peacock, Nature *200*, 672 (1963)
[60] J. Binenboym and H. Selig, Inorg. Nucl. Chem. H. H. Hyman Mem. *1976*, 231–232
[61] R. D. Peacock in: Gmelin Handbook of Inorganic Chemistry, 8th ed., Supplement Vol. 2, (H. H. Kugler and C. Keller, eds.) Springer Verlag, Berlin (1983), pp. 78/79/84
[62] A. J. Edwards and G. R. Jones, J. Chem. Soc. A 1651–1654 (1969)
[63] H. Selig, C. L. Chernick, and J. G. Malm, J. Inorg. Nucl. Chem. *19*, 377 (1961)
[64] H. Selig and J. G. Malm, J. Inorg. Nucl. Chem. *24*, 641–644 (1962)
[65] J. G. Malm, H. Selig, and S. Fried, J. Am. Chem. Soc. *82*, 1510 (1960)
[66] J. G. Malm and H. Selig, J. Inorg. Nucl. Chem. *20*, 189–197 (1961)
[67] D. W. Osborne, F. Schreiner, K. Otto, J. G. Malm, and H. Selig, J. Chem. Phys. *68*, 1108–1118 (1978)
[68] S. Siegel and D. A. Northrop, Inorg. Chem. *5*, 2187–2188 (1966)
[69] H. Selig, F. A. Cafasso, D. M. Gruen, and J. G. Malm, J. Chem. Phys. *36*, 3440–3444 (1962)
[70] H. H. Claassen, H. Selig, and J. G. Malm, J. Chem. Phys. *36*, 2888–2890 (1962)
[71] H. H. Claassen, G. L. Goodman, J. H. Holloway, and H. Selig, J. Chem. Phys. *53*, 341–348 (1970)
[72] B. Weinstock and H. H. Claassen, Advan. Chem. Phys. *9*, 286 (1965)
[73] H. H. Claassen, J. G. Malm, and H. Selig, J. Chem. Phys. *36*, 2890–2892 (1962)
[74] R. B. Singh and D. K. Rai, Can. J. Phys. *43*, 167–169 (1965)
[75] D. Hugill and R. D. Peacock, J. Chem. Soc. A 1339–1341 (1966)
[76] J. H. Holloway and H. Selig, J. Inorg Nucl. Chem. *30*, 473–478 (1968)
[77] B. Frlec, H. Selig, and H. H. Hyman, Inorg. Chem. *6*, 1775–1783 (1967)
[78] A. J. Edwards, G. R. Jones, and R. J. C. Sills, Chem. Commun. 1177–1178 (1968)
[79] A. J. Edwards, G. R. Jones, and R. J. C. Sills, J. Chem. Soc. A 2521–2523 (1970)
[80] A. J. Edwards, G. R. Jones, and B. R. Steventon, Chem. Commun. 462–463 (1967)
[81] H. Selig and J. G. Malm, J. Inorg. Nucl. Chem. *25*, 349–351 (1963)
[82] J. Binenboym, U. El-Gad, and H. Selig, Inorg. Chem. *13*, 319–321 (1974)
[83] K. J. Franklin, C. J. L. Lock, B. G. Sayer, and G. J. Schrobilgen, J. Fluorine Chem. *21*, 36 (1982)
[84] E. J. Baran, Spectrosc. Lett. *8*, 599–603 (1975)
[85] H. P. A. Mercier and G. J. Schrobilgen, Inorg. Chem. *32*, 145–151 (1993)
[86] N. LeBlond and G. J. Schrobilgen, Chem. Commun. *1996*, 2479–2480
[87] J. K. Gibson, J. Fluorine Chem. *55*, 299–311 (1991)
[88] K. Rinke, M. Klein, and H. Schäfer, J. Less-Common Metals *12*, 497–503 (1967)
[89] J. E. Fergusson and J. H. Hickford, Aust. J. Chem. *23*, 453–461 (1970)
[90] K. Knox, S. Y. Tyree, Jr., R. D. Srivastava, V. Norman, J. Y. Bassett, Jr., and J. H. Holloway, J. Am. Chem. Soc. *79*, 3358–3361 (1957)
[91] R. Colton, Nature *193*, 872 (1962)
[92] M. Elder and B. R. Penfold, Chem. Commun. 308–309 (1965)
[93] M. Elder and B. R. Penfold, Inorg. Chem. *5*, 1197–1200 (1966)

[94] K. Knox and C. F. Coffey, J. Am. Chem. Soc. *81*, 5–7 (1959)
[95] J. E. Fergusson and J. H. Hickford, J. Inorg. Nucl. Chem. *28*, 2293–2296 (1966)
[96] E. O. Fischer and M. W. Schmidt, Chem. Ber. *102*, 1954–1960 (1969)
[97] U. Abram, R. Wollert, and W. Hiller, Radiochim. Acta *63*, 145–147 (1993)
[98] R. Colton and I. R. Tomkins, Aust. J. Chem. *21*, 1981–1985 (1968)
[99] J. H. Canterford, R. Colton, and I. B. Tomkins, Inorg. Nucl. Chem. Lett. *4*, 471–475 (1968)
[100] A. Guest and C. J. L. Lock, Can. J. Chem. *50*, 1807–1810 (1972)
[101] J. H. Canterford and A. B. Waugh, Inorg. Nucl. Chem. Lett. *7*, 395–399 (1971)
[102] U. Abram and R. Wollert, Radiochim. Acta *63*, 149–151 (1993)
[103] C. L. Rulfs, R. A. Pacer, and R. F. Hirsch, J. Inorg. Nucl. Chem. *29*, 681–691 (1967)
[104] A. Guest, H. E. Howard-Lock, and C. J. L. Lock, J. Mol. Spectrosc. *72*, 143–157 (1978)
[105] A. Guest, H. E. Howard-Lock, and C. J. L. Lock, J. Mol. Spectrosc. *43*, 273–281 (1972)
[106] A. Müller, K. H. Schmidt, E. Ahlborn, and C. J. L. Lock, Spectrochim. Acta, *29A*, 1773–1788 (1973)
[107] R. Colton and G. Wilkinson, Chem. Ind. (London) 1314–1315 (1959)
[108] J. K. Gibson, Radiochim. Acta *64*, 185–189 (1994)

11 Oxotechnetates

This chapter covers syntheses and properties of pertechnetic acid, pertechnetic acid salts, oxotechnetate(VI), ternary and quaternary oxides of technetium, and the characterization of the TcO_4^- ion.

11.1 Pertechnetic acid

The very hygroscopic Tc_2O_7 dissolves in water to give a pink solution of pertechnetic acid, $HTcO_4$, whose color disappeared with dilution. $HTcO_4$ may more conveniently be prepared by passing an aqueous solution of $KTcO_4$ through a strong-acid cation exchanger, e. g. Dowex 50-X8, in the H^+-form [7]. It is also obtained when freshly precipitated dioxide is treated with dilute hydrogen peroxide [8]. The potentiometric pH titration curve of $HTcO_4$ is characteristic of a strong monobasic acid. When a 2 M aqueous solution of $HTcO_4$ is slowly evaporated at room temperature over conc. sulphuric acid, it gradually becomes yellow, dark yellow, red, and dark red. Finally, long red-black crystals are formed, the composition of which corresponds to $Tc_2O_7 \cdot H_2O$ or to anhydrous pertechnetic acid, $HTcO_4$ [1], in contrast to perrhenic acid that is formulated as dirhenium dihydrato heptoxide $Re_2O_7(OH_2)_2$ [2].

The red-black color of $HTcO_4$ is unexpected for a compound containing Tc in the d^0 configuration [3–6]. The absorption spectrum in the visible range exhibits two bands (shoulders) in the concentration range of $0.64 \cdot 10^{-1}$ to $2.1 \cdot 10^{-1}$ mole/l, the stronger at 500 nm ($\varepsilon \sim 1.5\ l \cdot mole^{-1} \cdot cm^{-1}$), the weaker at 585 nm [5], in good agreement with measurements shown in [3]. The red color of the conc. aqueous $HTcO_4$ solution was still observed under rigorous exclusion of any reducing agent. However, the titration of the red $HTcO_4$ proved the solution to contain some reduced species, probably formed by oxygen release of conc. $HTcO_4$. The reduced species has not yet been identified [5,6]. In addition, condensation reactions of $HTcO_4$, occurring at concentrations higher than 7 M, may be responsible for the coloration observed. Because the intensity of the strong, composite Raman band of the TcO_4^- ion at 912 cm^{-1} increases linearly with the $HTcO_4$ concentration, the acid should be completely ionized [7] up to ca. 6 M.

The temperature dependence of the $HTcO_4$ dissociation equilibrium

$$HTcO_4(c) \leftrightarrow \tfrac{1}{2}H_2O(g) + \tfrac{1}{2}Tc_2O_7(c)$$

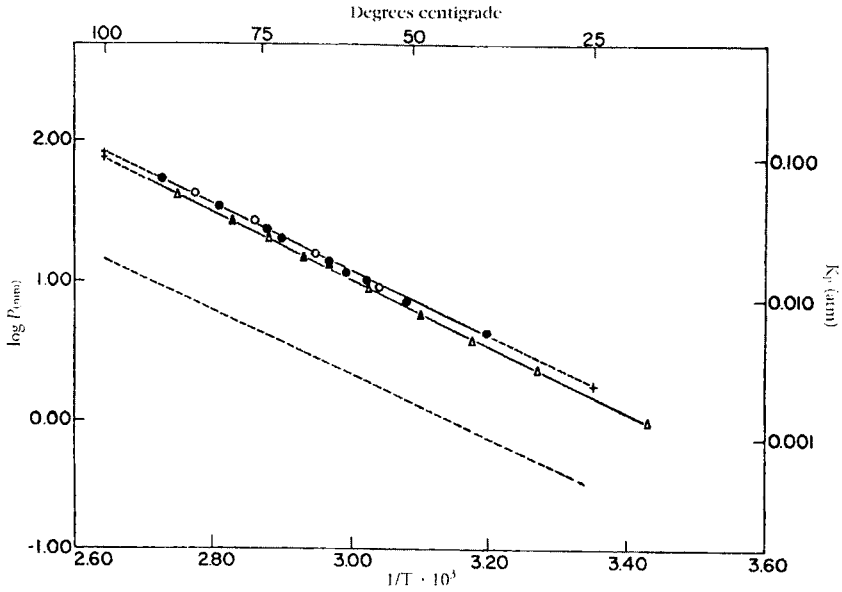

Fig. 11.1.A Temperature dependence of the vapor pressures of solid $HTcO_4$ and of saturated aqueous solution of $HTcO_4$ (upper line); open symbols on cooling. The vapor pressures for solid $HReO_4$ are represented by the dotted line [9].

was measured and is shown in Fig. 11.1.A together with the vapor pressures determined for saturated aqueous pertechnetic acid solution. Pertechnetic acid dissociates more readily than perrhenic acid to form heptoxide and water. The data for the dissociation of $HTcO_4$ could be fitted by the equation

$$\log P_{(\mathrm{mmHg})} = -2395/T + 8.207$$

The vapor pressure of the saturated aqueous solution of $HTcO_4$ was found to be only a few mm Hg higher than that of the anhydrous acid [9].

11.2 Salts of pertechnetic acid

Numerous pertechnetates have been prepared and more or less characterized. Table 11.1.A lists the salts and some of their properties.

Table 11.1.A Properties of pertechnetates.

Formula	Color	m.p. [°C]	Crystal structure and lattice constants [Å]		Solubility in water	References
$LiTcO_4$	white	365–385	isostructural with $LiReO_4$		–	[10,11]
$LiTcO_4 \cdot 2H_2O$	white	–	isostructural with $LiReO_4 \cdot 2H_2O$		extremely hygroscopic	[11]
$NaTcO_4$	white	–	$I4_1/a$	a= 5.339 c= 11.869	67.7 g/100g at 25 °C	[10,12–14]
$NaTcO_4 \cdot 4H_2O$	white	–	–	–	–	[15]
$KTcO_4$	white	540	$I4_1/a$	a= 5.630 c= 12.867	2.13 g/100 g at 25 °C	[10,16–19]
NH_4TcO_4	white	decomp. at 325 °C	$I4_1/a$	a= 5.775 c= 13.252	–	[10,17,20,62]
$RbTcO_4$	white	–	$I4_1/a$	a= 5.758 c= 13.54	1.167 g/100 ml at 20 °C	[10,17]
$CsTcO_4$	white	590	$Pnma$	a= 5.726 b= 5.922 c= 14.36	0.412 g/100 ml at 20 °C	[10,17,21,22]
$TlTcO_4$	white	530	$Pnma$	a= 5.501 b= 5.747 c= 13.45	0.072 g/100 ml at 20 °C	[10,21]
$AgTcO_4$	yellow	–	$I4_1/a$	a= 5.319 c= 11.875	0.563 g/100 ml at 20 °C	[10,12]
$[(CH_3)_4N]TcO_4$	white	–	$P2_12_12$	a= 12.142 b= 12.223 c= 5.928	2.73 g/100 ml at room temp.	[23]
$[(C_2H_5)_4N]TcO_4$	white	–	$P2_12_12$	a= 7.14 b= 7.16 c= 26.3	0.37 g/100 ml at room temp.	[23]
$[(C_4H_9)_4N]TcO_4$	white	–	$Pna2_1$	a= 15.403 b= 13.785 c= 9.864	0.17 g/100 ml at 20 °C	[23–25]
$[(C_6H_5NH)_3C]$ $TcO_4 \cdot 4H_2O$ Triphenylguanidinium pertechnetate	pale-pink	–	–	–		[26]
$[C_{20}H_{17}N_4]TcO_4$ Nitronpertechnetate	–	–	–		very low	[27]
$[(C_6H_5)_4As]TcO_4$	white	–	–		0.00164 g/ 100 ml at 24 °C	[28]
$[Fe(C_5H_5)_2]TcO_4$	–	–	$P3_121$	a= 8.967 c= 12.464	almost insoluble	[29]
$Mg(TcO_4)_2 \cdot 4H_2O$	white	.	triclinic	a= 7.44, α= 108.01° b= 7.03, β= 92.32° c= 6.46, γ= 120.45°	readily soluble	[30,31]

Table 11.1.A Continued.

Formula	Color	m.p. [°C]	Crystal structure and lattice constants [Å]	Solubility in water	References
$Mg(TcO_4)_2$	white	decomp.	hexagonal $a=$ 9.93, $c=$ 12.54	readily soluble	[30,31]
$Ca(TcO_4)_2 \cdot 2H_2O$	white		isostructural with $Ca(ReO_4)_2 \cdot 4H_2O$	—	[32,33]
$Ca(TcO_4)_2$	white	decomp. at 650 °C	isostructural with $Ca(ReO_4)_2$	—	[32,33]
$Sr(TcO_4)_2 \cdot 2H_2O$	white	—	isostructural with $Sr(ReO_4)_2 \cdot 2H_2O$	—	[32]
$Sr(TcO_4)_2$	white	decomp.	isostructural with $Sr(ReO_4)_2$		[32]
$Ba(TcO_4)_2$	white	decomp.	isostructural with $Ba(ReO_4)_2$	7.64 g/100 ml at 20 °C	[32,34]
$Co(TcO_4)_2 \cdot 4H_2O$	ruby red	—	isostructural with $Co(ReO_4)_2 \cdot 4H_2O$	readily soluble	[35]
$Ni(TcO_4)_2 \cdot 4H_2O$	green	—	isostructural with $Ni(ReO_4)_2 \cdot 4H_2O$	readily soluble	[36]
$Cu(TcO_4)_2 \cdot 4H_2O$	—	—	isostructural with $Cu(ReO_4)_2 \cdot 4H_2O$	soluble	[37]
$Zn(TcO_4)_2 \cdot 4H_2O$	white	—	isostructural with $Zn(ReO_4)_2 \cdot 4H_2O$	readily soluble	[38]
$Cd(TcO_4)_2 \cdot 2H_2O$	white	—	isostructural with $Cd(ReO_4)_2 \cdot 2H_2O$	readily soluble	[39]
$Pb(TcO_4)_2 \cdot 2H_2O$	white	—	—	soluble	[40]
$UO_2(TcO_4)_2 \cdot 2H_2O$	yellow-green	—	low symmetry	readily soluble	[41,42]
$[Pt(NH_3)_4](TcO_4)_2$	white	—	$P\bar{1}$ $a=$ 5.178, $\alpha=$ 69.33° $b=$ 7.725, $\beta=$ 79.74° $c=$ 7.935, $\gamma=$ 77.41°	slightly soluble	[43,44]
$Al(TcO_4)_3 \cdot 7H_2O$	white	—	isostructural with $Al(ReO_4)_3 \cdot 7H_2O$	readily soluble	[45]
$Sc(TcO_4)_3 \cdot 3H_2O$	white	—		readily soluble	[46]
$Y(TcO_4)_3 \cdot 4H_2O$	white	—	triclinic $a=$ 7.393, $\alpha=$ 75.65° $b=$ 8.615, $\beta=$ 96.43° $c=$ 11.819, $\gamma=$ 104.56°	readily soluble	[47,51,61]
$Fe(TcO_4)_3 \cdot 4H_2O$	reddish brown	—	—	soluble	[48]
$Ga(TcO_4)_3 \cdot 7H_2O$	white	—		readily soluble	[49]
$In(TcO_4)_3 \cdot 3H_2O$	white	—	isostructural with $In(ReO_4)_3 \cdot 3H_2O$	readily soluble	[50]
$La(TcO_4)_3 \cdot 3H_2O$	—		isostructural with $Ce(TcO_4)_3 \cdot 3H_2O$	readily soluble	[52]

Table 11.1.A Continued.

Formula	Color	m.p. [°C]	Crystal structure and lattice constants [Å]	Solubility in water	References
$Ce(TcO_4)_3 \cdot 3H_2O$	–	–	–	readily soluble	[52]
$Pr(TcO_4)_3 \cdot 4H_2O$	green	–	–	readily soluble	[53]
$Nd(TcO_4)_3 \cdot 4H_2O$	red-violet	–	isostructural with $Pr(TcO_4)_3 \cdot 4H_2O$	readily soluble	[54]
$Sm(TcO_4)_3 \cdot 3H_2O$	yellow	–	isostructural with $Eu(TcO_4)_3 \cdot 3H_2O$	readily soluble	[55]
$Eu(TcO_4)_3 \cdot 3H_2O$	pink	–	–	readily soluble	[55]
$Gd(TcO_4)_3 \cdot 3H_2O$	white	–	isostructural with $Eu(TcO_4)_3 \cdot 3H_2O$	readily soluble	[56]
$Tb(TcO_4)_3 \cdot 4H_2O$	pink	–	–	readily soluble	[57]
$Dy(TcO_4)_3 \cdot 4H_2O$	yellow	–	isostructural with $Tb(TcO_4)_3 \cdot 4H_2O$	readily soluble	[58]
$Ho(TcO_4)_3 \cdot 4H_2O$	pink	–	triclinic a= 7.157, α= 73.62° b= 8.787, β= 95.32° c= 12.278, γ= 102.55°	readily soluble	[59,61]
$Er(TcO_4)_3 \cdot 4H_2O$	reddish	–	triclinic a= 7.251, α= 73.13° b= 8.759, β= 96.07° c= 12.083, γ= 102.81°	readily soluble	[59,61]
$Tm(TcO_4)_3 \cdot 4H_2O$	green	–	triclinic a= 7.249, α= 73.94° b= 8.777, β= 96.38° c= 12.038, γ= 103.71°	readily soluble	[60,61]
$Yb(TcO_4)_3 \cdot 4H_2O$	white	–	isostructural with $Tm(TcO_4)_3 \cdot 4H_2O$	readily soluble	[60]
$Lu(TcO_4)_3 \cdot 4H_2O$	white	–	triclinic a= 7.193, α= 73.99° b= 8.686, β= 96.43° c= 11.943, γ= 102.62°	readily soluble	[47,61]

The pertechnetic acid salts are, in general, obtained by neutralization of aqueous $HTcO_4$ solution with the oxide or hydroxide of the cation. The salts are frequently isostructural with the corresponding compounds of rhenium. Alkaline pertechnetates, including ammonium salts, and alkaline earth pertechnetates are colorless (white), whereas transition metal pertechnetates are often colored. The crystal structure of many transition metal pertechnetates is still unknown. $NaTcO_4$, $KTcO_4$, NH_4TcO_4, $RbTcO_4$ and $AgTcO_4$ crystallize in the tetragonal scheelite-type structure of the space group $I4_1/a$ (Fig. 11.2.A), $CsTcO_4$ and $TlTcO_4$ in the orthorhombic space group *Pnma*, which is transformed at a transition temperature of 116 and 95 °C, respectively, into the scheelite-type structure [21]. Alkaline pertechnetates are thermally rather stable compounds, e. g. $KTcO_4$ melts at 540 °C and sublimes at ~1000 °C without decomposition [13]. The dimeric compound $(KTcO_4)_2$ was identified as a major vapor constituent by mass spectrometry at 620 °C [63]. Throughout, the pertechnetates are

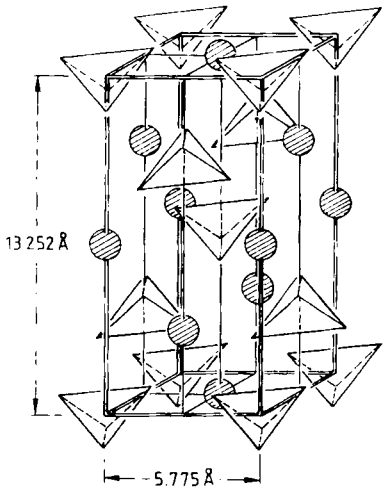

Fig. 11.2.A Crystal structure of $KTcO_4$. Scheelite type, space group $I4_1/a$.

readily soluble in water, with the exception of $[(C_6H_5)_4As]TcO_4$, nitronpertechnetate, and $TlTcO_4$. Numerous transition metal pertechnetates are reported to be easily soluble in alcohol or acetone.

The NH_4TcO_4 structure comprises discrete ammonium and pertechnetate ions held in addition together by hydrogen bonding. The cell volume of 442.0 $Å^3$ at 295 K is surprisingly larger than that of NH_4ReO_4, throughout the temperature range of 129–295 K. The observed density of NH_4TcO_4 at 295 K is 2.72 $g \cdot cm^{-3}$ [20].

Tetra-*n*-butylammonium pertechnetate dissolves in benzene without dissociation and forms ion pairs even at very low concentrations. At room temperature the formation of dimers and larger aggregates begins to occur already at concentrations of 10^{-5} mole/l [68]. This behavior resembles that of other tetraalkylammonium salts dissolved in benzene.

In $[Pt(NH_3)_4](TcO_4)_2$ the Pt atom is located on a center of symmetry at the origin. The coordination around the Pt(II) ion is square planar. The coordination around the Tc atom is tetrahedral with O-Tc-O angles ranging from 108.3 to 110.6°. The $[Pt(NH_3)_4](TcO_4)_2$ structure is stabilized by extensive hydrogen bonding between the ammine ligands and the oxygen atoms of the different layers [44].

In solid pertechnetates the TcO_4^- tetrahedra are slightly but distinctly distorted, as also known for the ReO_4^- tetrahedra. Precise interatomic Tc–O distances and O–Tc–O bond angles were derived from single crystal X-ray structure analyses of $KTcO_4$ [18], NH_4TcO_4 [29], $CsTcO_4$ [22], and $[Pt(NH_3)_4](TcO_4)_2$ [44] (Table 11.2.A)

Distortions of the TcO_4^- ion in numerous polycrystalline pertechnetates were studied by ^{99}Tc NMR measurements. Quadrupole coupling constants and asymmetry parameters of the electric field gradient of the ^{99}Tc nucleus were evaluated [82,83].

The vibrational frequencies of some crystalline pertechnetates are listed in the following tables. The factor group symmetry is C_{4h}, the anion symmetry is T_d.

Table 11.2.A Tc–O bond distances [Å] and O–Tc–O bond angles [°] of pertechnetates at room temperature [18,20,22,44].

Structure	$KTcO_4$	NH_4TcO_4	$CsTcO_4$	$[Pt(NH_3)_4](TcO_4)_2$
Space group	$I4_1/a$	$I4_1/a$	*Pnma*	$P\bar{1}$
Tc–O	1.711	1.702	1.665, 1.763, 1.716	1.710, 1.715, 1.711, 1.698
O–Tc–O	109.0–110.5	109.1–110.2		108.3–110.6

Table 11.3.A IR and Raman frequencies [cm^{-1}] of $KTcO_4$ [64–66].

IR	C_{4h}	Raman	C_{4h}	T_d
82 145	A_u+2E_u	70 104	$A_g+2B_g+3E_g$	–
313(s) 328(s)	A_u+E_u	327(m)	B_g+E_g	$\nu_4(F_2)$
351 (w)	A_u	348(w) 350(w)	A_g+B_g	$\nu_2(E)$
890 (sh)	–	–		–
908 (vs)	A_u+E_u	887(s) 920(m)	B_g+E_g	$\nu_3(F_2)$
–	–	913(vs)	A_g	$\nu_1(A_1)$

Table 11.4.A IR and Raman frequencies [cm^{-1}] of NH_4TcO_4 [20,67].

IR	T_d	Raman	T_d
317(s) 329(s)	$\nu_4(F_2)$	326(s)	$\nu_2(E)$
348(m)	$\nu_2(E)$	341(w) 352(w)	$\nu_4(F_2)$
840(w)	–	880(s)	$\nu_3(F_2)$
900(s) 925 (sh)	$\nu_3(F_2)$	908(vs)	$\nu_1(A_1)$
1390(s) 1410(s) 1790(w) 3200(s)	Site symmetry S_4 of NH_4^+	38(vw) 18(w) 77(vw) 92(w) 102(w) 116(vw)	lattice modes ?

Table 11.5.A IR frequencies [cm^{-1}] of $TlTcO_4$ [67], $AgTcO_4$ [66], $[(n\text{-}C_4H_9)_4N]TcO_4$ [65], and $[(C_6H_5)_4As]TcO_4$ [65].

$TlTcO_4$	T_d	$AgTcO_4$	T_d	$[(C_4H_9)_4N]TcO_4$	T_d	$[(C_6H_5)_4As]TcO_4$	T_d
322(s) 327(s) 332(s)	$\nu_4(F_2)$	312(s) 331(s)	$\nu_4(F_2)$	336(m)	$\nu_4(F_2)$	336(m)	$\nu_4(F_2)$
				890(s)	$\nu_3(F_2)$	895(s)	$\nu_3(F_2)$
347(m)	$\nu_2(E)$	347(w)	$\nu_2(E)$				
840(vw)	—	865(sh)	$\nu_3(F_2)$				
880(s) 905(sh) 918(sh)	$\nu_3(F_2)$	900(vs)					

Force constants of TcO_4 calculated in a modified valence field are compared with the force constants of MnO_4^- and ReO_4 in Table 11.6.A. The calculation is based on frequencies measured in aqueous solutions [64], except for the frequencies of $\nu_2(E)$ which were deduced from IR spectra of the crystalline salts. The Raman spectrum of the aqueous TcO_4^- ion shows only two lines and represents the spectrum of tetrahedral TcO_4^-, perturbed by the close association of water molecules [64].

Table 11.6.A Frequencies [cm^{-1}] and force constants [mdyne/Å] of MnO_4^-, TcO_4^-, and ReO_4 [84,85]. Frequencies recently measured and evaluated [86] are given in parentheses.

Assignment and force constants	MnO_4^-	TcO_4^-	ReO_4^-
$\nu_1(A_1)$	845	912(911)	972(972)
$\nu_2(E)$	355	347(336)	332(333)
$\nu_3(F_2)$	910	912(908)	916(919)
$\nu_4(F_2)$	395	325(323)	332(333)
f_r	5.75	6.75(6.49)	7.54(7.26)
f_{rr}	0.32	0.36(0.44)	0.45(0.55)
f_α	0.49	0.37(0.40)	0.43(0.51)
$f_{\alpha\alpha}$	0.05	0.00(0.02)	0.02(0.08)

The valence force constants f_r indicate a significant increase of the M–O bond strength from MnO_4^- via TcO_4^- to ReO_4^-.

The absorption spectra of aqueous solutions of MnO_4^-, TcO_4^-, and ReO_4, measured in the VIS and UV (Fig. 11.3.A) demonstrate for each ion essentially two band systems with pronounced vibrational structures. The band systems are shifted to higher wavenumbers from MnO_4^- via TcO_4^- to ReO_4. In addition, MnO_4^- exhibits a strong band at 52910 cm^{-1} (189 nm). Table 11.7.A summarizes the absorption maxima of TcO_4^- and ReO_4.

The polarized absorption spectrum of TcO_4^- doped in single crystals of $KClO_4$ [88] or $CsClO_4$ [89] was measured at 4.2 K and showed considerably pronounced resolution of the vibrational structure.

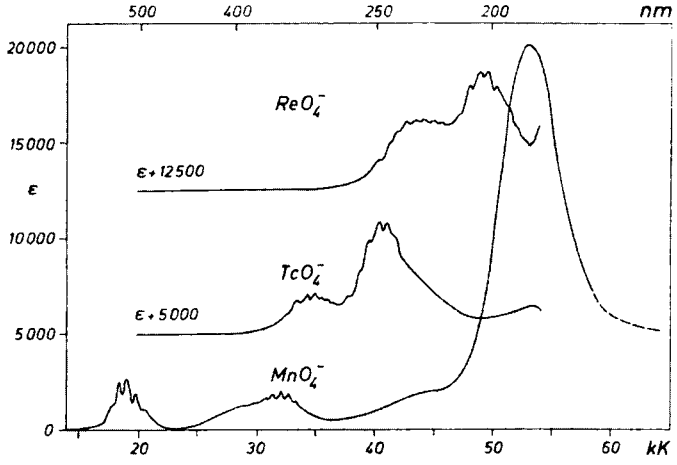

Fig. 11.3.A Absorption spectra of MnO_4^-, TcO_4^-, and ReO_4^- in aqueous solution [87]; kK = 10^3 cm^{-1}.

Table 11.7.A Absorption maxima and molar absorbance indices of TcO_4^- and ReO_4^- in aqueous solution [87]. Shoulders are given in parentheses.

TcO_4^-			ReO_4^-		
kK [$10^3 cm^{-1}$]	λ [nm]	ε [$l \cdot mole^{-1} \cdot cm^{-1}$]	*kK* [$10^3 cm^{-1}$]	λ [nm]	ε [$l \cdot mole^{-1} \cdot cm^{-1}$]
(32.36)	(309)	1070	(40.16)	(249)	1650
(33.33)	(300)	1740	(41.15)	(243)	2520
34.25	292	2130	(41.84)	(239)	3150
34.84	287	2170	(42.50)	(235)	3460
(35.59)	(281)	2010	43.42	230	3610
(36.23)	(276)	1760	44.05	227	3660
(37.88)	(264)	2070	44.84	223	3630
(38.76)	(258)	3380	(45.66)	(219)	3570
(39.53)	(253)	4830	(47.17)	(212)	4100
40.32	248	5690	47.85	209	5280
40.98	244	5690	48.78	205	6060
(41.67)	(240)	4990	49.50	202	6090
(42.37)	(236)	3900	50.25	199	5370
(43.10)	(232)	2820	(51.28)	(195)	4340
53.18	188	1370	(51.81)	(193)	3280
			(52.63)	(190)	2680
			(52.91)	(189)	2540
			(53.76)	(186)	3220

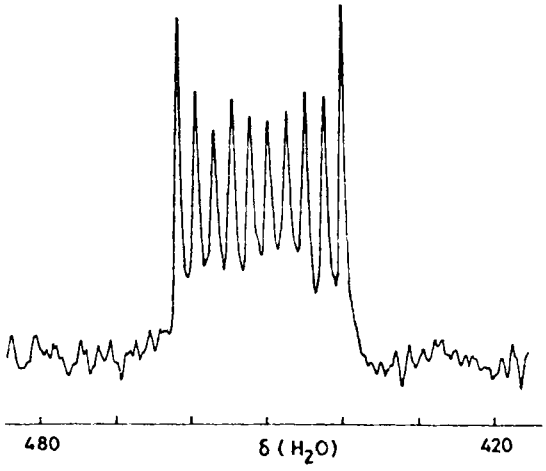

Fig. 11.4.A NMR spectrum of $^{99}TcO_4^-$ in D_2O at 54.24 MHz for natural abundance of ^{17}O [90].

The ^{99}Tc NMR spectrum of NH_4TcO_4 dissolved in D_2O exhibits 10 lines (Fig. 11.4.A) according to the nuclear spin I= 9/2 of ^{99}Tc by scalar coupling of ^{17}O to ^{99}Tc with ^1J=131.6 Hz. That the outer lines of this ^{17}O multiplet are sharper than the inner ones is expected from the finite relaxation rate of ^{99}Tc. $^{99}TcO_4^-$ gives a single resonance at 90.6 MHz at 9.4 T with the relaxation parameters T_1=0.13 s and T_2=0.10 s [90].

Some additional properties of the pertechnetate ion compared to those of the perrhenate ion are presented in Table 11.8.A.

Table 11.8.A Some physical properties of TcO_4^- and ReO_4^-.

Property	TcO_4^-	ReO_4^-	References
Equivalent conductivity at infinite dilution in water at 25 °C [$\Omega^{-1} \cdot cm^2 \cdot val^{-1}$]	55.5±0.5	54.68	[91]
Diffusion coefficient in water at 25 °C [$cm^2 \cdot s^{-1}$]	$(1.48\pm0.01) \cdot 10^{-5}$	$1.456 \cdot 10^{-5}$	[91]
Partial molar volume in water at 25 °C [$cm^3 \cdot mole^{-1}$]	47.1	48.1	[92]
Effective ionic radius in water at 25 °C [Å]	2.40±0.04	–	[92]
Molecular polarizability [$Å^3$]	47.355	33.44	[86]

11.3 Tetraoxotechnetate(VI)

The existence of the very reactive anion TcO_4^{2-} and the still more reactive ReO_4^- could be demonstrated unambiguously [69,70]. Electrochemical studies previously pointed to the formation of TcO_4^{2-} at the electrode surface [71]. Polarographic and controlled-potential coulometric reduction of permanganate, pertechnetate, and perrhenate in acetonitrile or dimethylsulphoxide yielded a one-electron transfer [72].

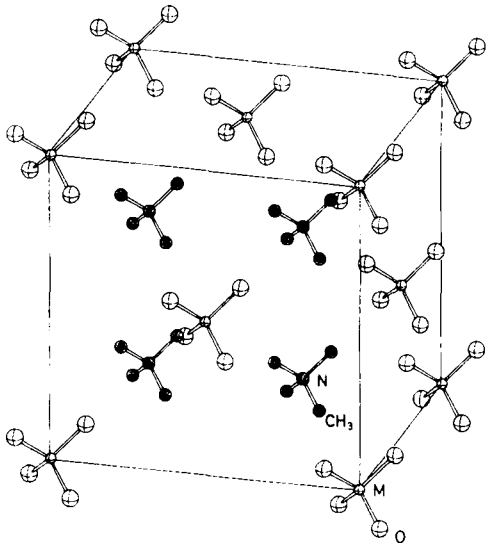

Fig. 11.5.A Face-centered cubic lattices of $[(CH_3)_4N]_2MnO_4$, $[(CH_3)_4N]_2TcO_4$, and $[(CH_3)_4N]_2ReO_4$ [73].

The syntheses of violet $[(CH_3)_4N]_2TcO_4$ and olive green $[(CH_3)_4N]_2ReO_4$ succeeded in reducing solutions of tetramethylammonium pertechnetate and perrhenate in acetonitrile at a platinum cathode. The cathodic deposits were slightly soluble crystalline products that were extremely sensitive to oxygen and atmospheric moisture causing rapid oxidation and disproportionation [72].

The tetramethylammonium salts of MnO_4^{2-}, TcO_4^{2-}, and ReO_4^{2-} crystallize in isostructural antifluorite-like cubic face centered lattices (Fig. 11.5.A) with the lattice constants a=11.09 Å, a=11.20 Å, and a=11.35 Å, respectively. The magnetic susceptibility of the compounds obeys the Curie-Weiss law over the temperature range 77–298 K (Fig. 11.6.A) with μ_{eff}=1.63 (Mn), 1.60 (Tc), and 1.47 (Re) B.M. The magnetic moments of $[(CH_3)_4N]_2TcO_4$ and $[(CH_3)_4N]_2ReO_4$ as well as the splitting and the vibrational structure of the $^2E \rightarrow {}^2T_2$ intrashell transition indicate strong Jahn-Teller distortion of TcO_4^{2-} and ReO_4^{2-} in the first excited $^2T_2$ state. Tetrahedral crystal field parameters of Δ=–11000, Δ=–17000, and Δ=–19000 cm^{-1} were derived for MnO_4^{2-}, TcO_4^{2-}, and ReO_4^{2-}, respectively. The electron transfer spectra (Table 11.9.A) reflect the lower degree of covalency of the Re–O bond in comparison to the Tc–O and Mn–O bond. In accordance with the tetrahedral structure of the oxoanions, the IR spectra exhibit two metal–oxygen vibrations, the stretching modes $\nu_3(F_2)$ between 780 and 812 cm^{-1} and the deformation modes $\nu_4(F_2)$ between 324 and 340 cm^{-1} [73].

A Tc(VI) species was reported to be prepared in aqueous solution by reduction of 1.82 mM TcO_4^- with 0.015 M N_2H_4 in 0.7 M OH^-. The reddish-brown product absorbed in the visible region at 500 nm with an absorbance index of about 200 $l \cdot mole^{-1} \cdot cm^{-1}$ [74]. This absorption maximum is in agreement with the maximum listed in Table 11.9.A for TcO_4^{2-} at 20000 cm^{-1}.

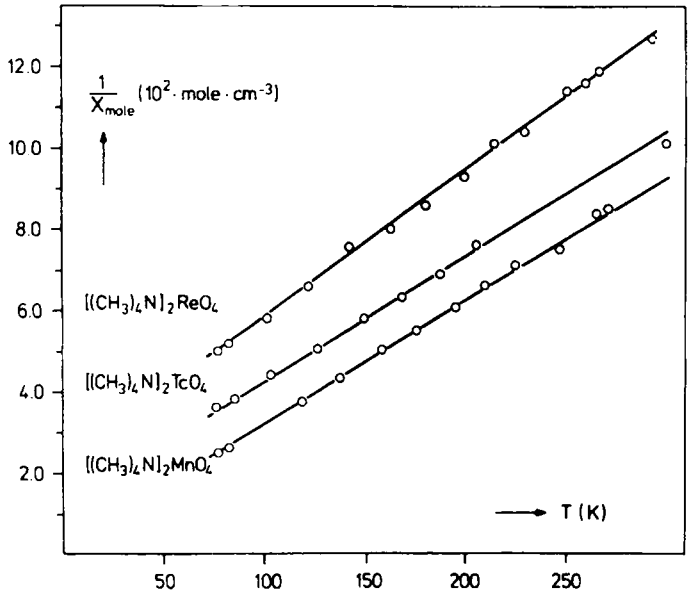

Fig. 11.6.A Reciprocal molar susceptibilities [73].

Later, several pulse radiolysis studies on aqueous solutions of pertechnetate demonstrated the formation of TcO_4^{2-}. The passage of an electron pulse through a $<5 \cdot 10^{-4}$ M solution of $KTcO_4$ developed two absorption bands, one had a maximum at 700 nm, the second at 325 nm. The band at 325 nm was related to TcO_4^{2-} that was formed by the reactions

$$TcO_4^- + e_{aq} \rightarrow TcO_4^{2-}$$

or

$$TcO_4^- + H \rightarrow TcO_4^{2-} + H^+,$$

while the band at ~700nm pertained to e_{aq}^-. In addition to the 325 nm band, a remarkably low intensity absorption at 520 nm was observed [75]. Transient hexavalent technetium, presumed to be TcO_4^{2-}, was produced in aqueous alkaline media (0.10 M NaOH) by pulse radiolysis of 10^{-4}–10^{-5} M solutions of TcO_4^-. Tc(VI) was detected and characterized by streak-camera spectra, showing a broad absorbance centered at 500 nm and a peak at 340. The life-time of the Tc(VI) species was found to be of the order of milliseconds in aqueous alkaline media [76]. The rate of decay is strongly dependent on pH. Hydrated electrons also react with perrhenate to generate a transient species that is formulated as ReO_4^{2-} and has a 100-fold higher decay rate than TcO_4^{2-} [77,78].

Table 11.9.A Absorption maxima [cm $^{-1}$] of $[(CH_3)_4N]_2TcO_4$ and $[(CH_3)_4N]_2ReO_4$ at 77 K. Shoulders are given in parentheses [73].

TcO_4^{2-}	ReO_4^{2-}	Assignment
(12400)	(12900)	
(12700)	14080	
13020	(14700)	
(13350)	15380	
13680	(16700)	$\Gamma_8[(dt_2)^1]$+ vibrational progression in $\nu_2(E)$
(14000)		
14340		
15270		
(15600)		
(15900)		
20000	22990	$\Gamma_7[(dt_2)^1]$
(27800)	(27800)	$^4T_1$, $^4T_2$?
(31500)	(34000)	
33610	37030	
35090	(40500)	$^2T_1$ and $^2T_2$ from $(\pi t_1)^5(de)^2$ and $[(\pi+\sigma)t_2]^5(de)^2$
38840		
(40500)		

11.4 Ternary and quaternary oxides

Various ternary and quaternary oxides of technetium can be prepared via solid state reactions (Table 11.10.A).

Table 11.10.A Properties and structure of ternary and quaternary oxides of technetium in the oxidation states +3 to +7.

Oxidation state	Composition	Properties	Structure	Lattice constants [Å]	References
+3	$NaTcO_2$	dark violet	-	—	[79,80]
+4	Li_2TcO_3	stable up to 900 °C	monoclinic, $LiSnO_3$ type	a=4.988 b=8.639; β=99.4° c=10.01	[79,80]
	Na_2TcO_3	olive-green, >550 °C decomp.	—	-	[79,80]
	$CaTcO_3$	black	orthorhombic	a=3.87 b=3.96 c=3.76	[32]
	$SrTcO_3$	-	cubic, $CaTiO_3$ type	a=3.949	[32,81]
	α-$BaTcO_3$	black	hexagonal, $BaTiO_3$ type	a=5.758 c=14.046	[32,81]
	β-$BaTcO_3$	black, stable up to 800 °C	cubic, perovskite type	a=8.140	[32]
	$PbTcO_3$	—	cubic, perovskite type	a=10.361	[81]
	Na_4TcO_4	brown, stable up to 800 °C, hygroscopic	isostructural with Na_4SnO_4	-	[79,80]
	Mg_2TcO_4	black	cubic, spinel type	a=8.498	[81]
	Sr_2TcO_4	-	tetragonal, K_2NiF_4 type	a=3.902 c=12.72	[32]
	Ba_2TcO_4	black, decomp. at 630 °C	tetragonal, K_2NiF_4 type	a=4.011 c=13.40	[32]
	Mn_2TcO_4	black, ferrimagnetic	cubic, spinel type	a=8.682	[81]
	Co_2TcO_4	black	cubic, spinel type	a=8.450	[81]
	$CoMnTcO_4$	black	cubic, spinel type	a=8.563	[81]
	$CoNiTcO_4$	black	cubic, spinel type	a=8.449	[81]
	$MnNiTcO_4$	black, ferrimagnetic	cubic, spinel type	a=8.551	[81]
	$NiZnTcO_4$	black	cubic, spinel type	a=8.462	[81]
	$NiCdTcO_4$	black	cubic, spinel type	a=8.786	[81]
	$Sm_2Tc_2O_7$	—	cubic, pyrochlore type	a=10.352	[81]

Table 11.10.A Continued.

	$Dy_2Tc_2O_7$	—	cubic, pyrochlore type	a=10.246	[81]
	$Er_2Tc_2O_7$	—	cubic, pyrochlore type	a=10.194	[81]
+5	α-Li_3TcO_4	black, above 950 °C	cubic, rock salt type	a=4.17	[79,80]
	β-Li_3TcO_4	black, below 950 °C	monoclinic	a=5.038 b=8.726, β=99.8° c=9.82	[79,80]
	$NaTcO_3$	black, stable up to 800 °C		—	[79,80]
+6	α-Li_4TcO_5	black, stable up to 900 °C	—	—	[79]
	β-Li_4TcO_5	blue-black	monoclinic	a=5.055 b=8.755, β=99.8° c=9.67	[79,80]
	α-Li_6TcO_6	bluish, stable 350–750 °C	—	—	[79,80]
	β-Li_6TcO_6	dark green, below 320 °C	hexagonal	a=5.05 c=14.20	[79,80]
	$Ba_3Tc_2O_9$	black	hexagonal	a=5.800 c=21.00	[32]
+7	Li_5TcO_6	stable up to 650 °C	hexagonal	a=5.04 c=14.10	[79,80]
	Na_5TcO_6	hygroscopic	isostructural with Na_5ReO_6	—	[79,80]
	$Ca_5(TcO_6)_2$	brown, stable up to 850 °C		—	[32]
	$Sr_5(TcO_6)_2$	black	hexagonal	a=5.74 c=18.98	[32]
	$Ba_5(TcO_6)_2$	dark brown, stable up to 850 °C	—	—	[32]
	$LiSr_2TcO_6$	—	pseudo cubic	a=7.84	[32]
	$NaSr_2TcO_6$	—	tetragonal	a=8.09 c=8.14	[32]
	$LiBa_2TcO_6$	—	cubic	a=8.092	[32]
	$NaBa_2TcO_6$	—	cubic	a=8.292	[32]
	K_3TcO_5	brown, hygroscopic, 500 °C decomp.	isostructural with K_3ReO_5	—	[79,80]

Table 11.10.A Continued.

Na_3TcO_5	dark brown, hygroscopic, stable up to 650 °C	isostructural with Na_3ReO_5	–	[79,80]
$Sr_3(TcO_5)_2$	black, 700 °C decomp.	–	–	[32]
$Ba_3(TcO_5)_2$	dark brown, stable up to 850 °C	isostructural with $Ba_3(ReO_5)_2$	–	[32]

11.5 References

[1] G. E. Boyd, J. W. Cobble, C. M Nelson, and W. T. Smith, Jr., J. Am. Chem. Soc. *74*, 556–557 (1952)
[2] H. Beyer, O. Glemser, and B. Krebs, Angew. Chem. *80*, 286–287 (1968)
[3] C. L. Rulfs, R. A. Pacer, and R. F. Hirsch, J. Inorg. Nucl. Chem. *29*, 681–691 (1967)
[4] C. L. Rulfs, R. F. Hirsch, and R. A. Pacer, Nature *199*, 66 (1963)
[5] U. Pozdrowicz, B. Krebs, and K. Schwochau, Unpublished Results, Master thesis of U. Pozdrowicz, University of Münster (1984)
[6] K. Schwochau, Proc. 2. Intern. Symp., in: Technetium in Chemistry and Nuclear Medicine, (M. Nicolini, G. Bandoli,and U. Mazzi, eds.), Padua, Sept. 9-11 (1985), Cortina Intern., Verona, Raven Press, New York (1986), pp. 13–23
[7] G. E. Boyd, Inorg. Chem. *17*, 1808–1810 (1978)
[8] J. A. Rard and D. G. Miller, J. Solution Chem. *20*, 1139-1147 (1991)
[9] W. T. Smith, Jr., J. W. Cobble, and G. E. Boyd, J. Am. Chem. Soc. *75*, 5773–5776 (1953)
[10] C. Keller and B. Kanellakopulos, Radiochim. Acta *1*, 107–108 (1963)
[11] L. L. Zaitseva, M. I. Konarev, and A. V. Velichko, Russ. J. Inorg. Chem. *22*, 1269–1272 (1977)
[12] K. Schwochau, Z. Naturforschg. *17a*, 630 (1962)
[13] K. Schwochau, Angew. Chem. *76*, 9-19 (1964)
[14] G. E. Boyd, J. Solution Chem. *7*, 229–238 (1978)
[15] K. E. German, S. V. Kryuchkov, and L. I. Belyaeva, Izv. Akad. Nauk SSSR, Ser. Khim. *10*, 2387 (1987)
[16] R. H. Busey and O. V. Larson, ORNL-2584, Chemistry Division, Annual Progress Report (1958), p. 5
[17] B. J. McDonald and G. J. Tyson, Acta Cryst. *15*, 87 (1962)
[18] B. Krebs and K.-D. Hasse, Acta Cryst. *B32*, 1334–1337 (1976)
[19] R. H. Busey and R. B. Bevan, Jr., ORNL-2983, Chemistry Division Annual Progress Report (1960), p. 8
[20] R. Faggiani, C. J. L. Lock, and J. Pocé, Acta Cryst. *B36*, 231–233 (1980)
[21] B. Kanellakopulos, J. Inorg. Chem. *28*, 813–816 (1966)
[22] G. Meyer and R. Hoppe, Z. Anorg. Allg. Chem. *420*, 40–50 (1976)
[23] S. V. Kryutchkov, M. S. Grigoryev, and K. E. German, Proc. 3. Intern. Symp. in: Technetium in Chemistry and Nuclear Medicine, (M. Nicolini, G. Bandoli, U. Mazzi, eds.), Montegrotto Terme, Sept. 6–8 1989, Cortina Intern., Verona, Raven Press, New York (1990) pp. 253–264
[24] K. E. German, S. V. Kryuchkov, L. L. Belyaeva, and V. I. Spitsyn, J. Radioanal. Nucl. Chem. *121*, 515–521 (1988)
[25] K. E. German, L. N. Grushevschkaya, S. V. Kryutchkov, V. A. Pustovalov, and V. V. Obruchikov, Radiochim. Acta *63*, 221-224 (1993)
[26] A. F. Kuzina, A. A. Oblova, and V. I. Spitsyn, Russ. J. Inorg. Chem. *23*, 1682–1684 (1978)
[27] C. Perrier and E. Segrè, J. Chem. Phys. *7*, 155–156 (1939)
[28] R. A. Pacer, Talanta *27*, 689–692 (1980)
[29] M. S. Grigoriev and S. V. Kryutchkov, Radiochim. Acta *63*, 187–193 (1993)
[30] L. L. Zaitseva, A. V. Velichko, and V. V. Kazakov, Russ. J. Inorg. Chem. *24*, 1132–1135 (1979)
[31] A. A. Kruglov and L. L. Zaitseva, Russ. J. Inorg. Chem. *28*, 294 (1983)

[32] C. Keller and M. Wassilopulos, Radiochim. Acta *5*, 87–91 (1966)
[33] E. G. Teterin, L. L. Zaitseva, V. F. Samsonov, and A. V. Aksenenko, Russ. J. Inorg. Chem. *31*, 1159–1161 (1986)
[34] S. K. Majumdar, R. A. Pacer, and C. L. Rulfs, J. Inorg. Nucl. Chem. *31*, 33–41 (1969)
[35] L. L. Zaitseva, A. V. Velichko, A. A. Kruglov, and V. A. Zotov, Russ. J. Inorg. Chem. *23*, 1322–1325 (1978)
[36] L. L. Zaitseva, A. V. Velichko, and V. A. Zotov, Russ. J. Inorg. Chem. *23*, 1318–1321 (1978)
[37] L. L. Zaitseva, M. I. Konarev, V. S. Romanov, and S. V. Shepel'kov, Russ. J. Inorg. Chem. *22*, 1185–1187 (1977)
[38] L. L. Zaitseva, A. V. Velichko, A. V. Demin, A. I. Sukhikh, and N. V. Morgunova, Russ. J. Inorg. Chem. *27*, 202–205 (1982)
[39] L. L. Zaitseva, M. I. Konarev, A. V. Velichko, and N. V. Morgunova, Russ. J. Inorg. Chem. *23*, 978–982, (1978)
[40] L. L. Zaitseva, M. I. Konarev, A. V. Velichko, and N. M. Morgunova,Russ. J. Inorg. Chem. *22*, 803–807 (1977)
[41] V. I. Volk and A. D. Belikov, Soviet Radiochem. *19*, 676–681 (1977)
[42] L. L. Zaitseva and A. V. Slavinskii, Russ. J. Inorg. Chem. *21* 348–350 (1976)
[43] G. F. Shakh, M. Varen, T. A. Lagutina, A. A. Gavrish, and E. Antel', Izv. Akad. Nauk SSSR, Ser. Khim. *11*, 2443–2444 (1980)
[44] F. D. Rochon, P. C. Kong, and R. Melanson, Acta Cryst. *C46*, 8–10, (1990)
[45] L. L. Zaitseva, A. V. Velichko, and S. R. Borisov, Russ. J. Inorg. Chem. *31*, 816–818 (1986)
[46] L. L. Zaitseva, A. V. Velichko, A. V. Demin, and A. I. Sukhikh, Russ. J. Inorg. Chem. *27*, 928–931 (1982)
[47] L. L. Zaitseva, A. D. Belikov, A. I. Sukhikh, A. A. Kruglov, and N. T. Chebotarev, Russ. J. Inorg. Chem. *20*, 157–159 (1975)
[48] L. L. Zaitseva, A. V. Velichko, and G. Y. Kolomeitsev, Russ. J. Inorg. Chem. *31*, 51–53 (1986)
[49] L. L. Zaitseva, A. V. Velichko, and A. V. Solomentsev, Russ. J. Inorg. Chem. *32*, 836–838 (1987)
[50] L. L. Zaitseva, A. V. Velichko, and A. V. Solomentsev, Russ. J. Inorg. Chem. *32*, 961–964 (1987)
[51] E. G. Teterin and L. L. Zaitseva, Russ. J. Inorg. Chem. *28*, 1717–1719 (1983)
[52] L. L. Zaitseva, M. I. Konarev, A. V. Velichko, A. I. Sukhikh, and N. T. Chebotarev, Russ. J. Inorg. Chem. *19*, 1285–1288 (1974)
[53] L. L. Zaitseva, A. V. Velichko, P. N. Petrov, and N. T. Chebotarev, Russ. J. Inorg. Chem. *17*, 1379–1381 (1972)
[54] L. L. Zaitseva, A. V. Velichko, and N. T. Chebotarev, Russ. J. Inorg. Chem. *17*, 1382–1384 (1972)
[55] L. L. Zaitseva, M. I. Konarev, A. V. Velichko, A. I. Sukhikh, and N. T. Chebotarev, Russ. J. Inorg. Chem. *19*, 1461–1463 (1974)
[56] L. L. Zaitseva, M. I. Konarev, A. V. Velichko, and A. I. Sukhikh, Russ. J. Inorg. Chem. *20*, 1152–1156 (1975)
[57] L. L. Zaitseva, M. I. Konarev, A. I. Sukhikh, and N. T. Chebotarev, Russ. J. Inorg. Chem. *21*, 346–348 (1976)
[58] L. L. Zaitseva, M. I. Konarev, A. I. Sukhikh, and N. T. Chebotarev, Russ. J. Inorg. Chem. *21*, 488–490 (1976)
[59] L. L. Zaitseva, M. I. Konarev, A. D. Belikov, A. I. Sukhikh, and N. T. Chebotarev, Russ. J. Inorg. Chem. *19*, 1778–1781 (1974)
[60] L. L. Zaitseva, M. I. Konarev, A. V. Velichko, A. I. Sukhikh, and N. T. Chebotarev, Russ. J. Inorg. Chem. *19*, 1625–1627 (1974)
[61] M. B. Varfolomeev, L. L. Zaitseva, A. A. Kruglov, and S. V. Mikheikin, Russ. J. Inorg. Chem. *28*, 754–755 (1983)
[62] V. I. Spitsyn, A. F. Kuzina, A. A. Oblova, G. F. Shakh, A. A. Gavrish, and L. I. Belyaeva, Russ. J. Inorg. Chem. *23*, 484–485 (1978)
[63] J. K. Gibson, Radiochim. Acta *62*, 127–132 (1993)
[64] R. H. Busey and O. L. Keller, Jr. J. Chem. Phys. *41*, 215–225 (1964)
[65] A. Müller and W. Rittner, Spectrochim. Acta *23A*, 1831–1837 (1967)
[66] M. Baluka, J. Hanuza, and B. Jezowska-Trzebiatowska, Bull. Acad. Polon. Sci. Ser. Sci. Chim. *20*, 271–278 (1972)
[67] A. Müller and B. Krebs, Z. Naturforschg. *20a*, 967 (1965)
[68] V. Neck, R. Maier, and B. Kanellakopulos, Ber. Bunsenges. Phys. Chem. *92*, 123–127 (1988)
[69] K. Schwochau, L. Astheimer, J. Hauck, and H.-J. Schenk, Ang. Chem. *86*, 350 (1974)

[70] K. Schwochau, L. Astheimer, J. Hauck, and H.-J. Schenk, Angew. Chem. Internat. Edit. *13*, 346 (1974)
[71] G. Kissel and S. W. Feldberg, J. Phys. Chem. *73*, 3082–3088 (1969)
[72] L. Astheimer and K. Schwochau, J. Inorg. Nucl. Chem. *38*, 1131–1134 (1976)
[73] L. Astheimer, J. Hauck, H. J. Schenk, and K. Schwochau, J. Chem. Phys. *63*, 1988–1991 (1975)
[74] C. L. Rulfs, R. A. Pacer, and R. F. Hirsh, J. Inorg. Nucl. Chem. *29*, 681–691 (1967)
[75] A. K. Pikaev, S. V. Kryuchkov, A. F. Kuzina, and V. I. Spitsyn,Dokl. Akad. Nauk SSSR *236*, 1155–1158 (1977)
[76] E. Deutsch, W. R. Heineman, R. Hurst, J. C. Sullivan, W. A. Mulac, and S. Gordon, J. Chem. Soc., Chem. Comm. 1038–1040 (1978)
[77] G. A. Lawrance and D. F. Sangster, Polyhedron *4*, 1095–1096 (1985)
[78] K. Libson, J. C. Sullivan, W. A. Mulac, S. Gordon, and E. Deutsch, Inorg. Chem. *28*, 375–377 (1989)
[79] B. Kanellakopulos, Dissertation, Karlsruhe (1963) KFK-197, (1964) pp. 1–73
[80] C. Keller and B. Kanellakopulos, J. Inorg. Nucl. Chem. *27*, 787–795 (1965)
[81] O. Muller, W. B. White, and R. Roy, J. Inorg. Nucl. Chem. *26*, 2075–2086 (1964)
[82] V. P. Tarasov, V. I. Privalov, S. A. Petrushin, G. A. Kirakosyan, S. V. Kryuchkov, K. E. German, and Y. A. Buslaev, Doklady Akademii Nauk SSSR *272*, 919–920 (1983)
[83] V. P. Tarasov, S. A. Petrushin, V. I. Privalov, K. E. German, S. V. Kryuchkov, and Y. A. Buslaev, Koord. Khim. *12*, 1227–1236 (1986)
[84] A. Müller and B. Krebs, *Z.* Naturforschg. *20b*, 1127–1128 (1965)
[85] A. Müller and B. Krebs, J. Mol. Spectrosc. *24*, 180–197 (1967)
[86] H. H. Eysel and B. Kanellakopulos, J. Raman Spectrosc. *24*, 119–122 (1993)
[87] P. Mullen, K. Schwochau, and C. K. Jørgensen, Chem. Phys. Lett. *3*, 49–51 (1969)
[88] H. U. Güdel and C. J. Ballhausen, Theoret. Chim. Acta *25*, 331 (1972)
[89] L. Di Sipio and G. Ingletto, Gazz. Chem. Ital. *104*, 1023 (1974)
[90] M. J. Buckingham and G. E. Hawkes, Inorg. Chim. Acta, *56*, L 41 (1981)
[91] K. Schwochau and L. Astheimer, *Z.* Naturforschg. *17a*, 820 (1962)
[92] V. Neck and B. Kanellakopulos, Radiochim. Acta *42*, 135–137 (1987)

12 Complex chemistry of technetium-99

Technetium, a true second row transition element, tends to form complex compounds. Oxidation states lower than +3 could be made with certainty only through complex stabilization. The existence of all known oxidation states of technetium from +7 to –1 has been verified in complex compounds. Coordination numbers from 4 to 9 and numerous coordination geometries have been seen. The magnetic moments of technetium complexes can be explained fairly well on the basis of crystal field considerations that show technetium to form low-spin compounds.

The intent to synthesize compounds that could be appropriate as ^{99m}Tc radiopharmaceuticals for diagnosis in nuclear medicine in selective imaging of organs has predominantly stimulated investigations on technetium complex chemistry.

This chapter includes clusters and organometallic compounds, like technetium carbonyls, but does not include oxotechnetates, which are described in the preceding chapter.

12.1 Technetium (VII)

The d^0 complexes of Tc(VII) are efficiently stabilized by trioxo-, nitrido-, and imido-groups as strong electron donors. In particular, trisimido compounds were recently shown to be resistant even to electrochemical reduction. Nitrido- and nitrido-hydrazido groups are known to occur also in structurally remarkable dinuclear complexes. Finally, the highly reactive hydridotechnetate(VII) has been the object of much attention. Altogether, the number of Tc(VII) complexes is rather limited.

12.1.1 Hydridotechnetate

For almost two decades the most interesting enneahydridotechnetate $[TcH_9]^{2-}$ was the only known complex of Tc(VII). $K_2[TcH_9]$ is obtained by reduction of ammonium pertechnetate with potassium metal in an ethylenediamine-ethanol medium [1]. X-ray powder patterns of the white solid revealed $K_2[TcH_9]$ to be isostructural with the analogous rhenium complex, the structure of which was characterized by neutron diffraction analysis [2]. Thus the Tc atom of the $[TcH_9]^{2-}$ anion is located at the center of a trigonal prism of hydrogen atoms with three additional H atoms beyond the centers of the prism faces (Fig. 12.1.A) resulting in the coordination number 9, the highest

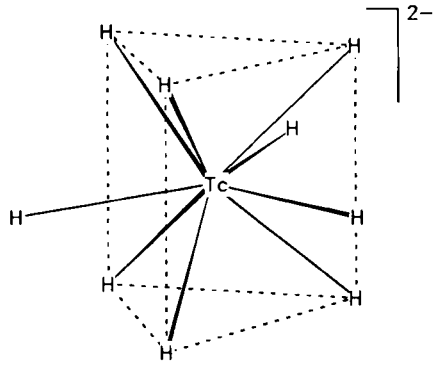

Fig. 12.1.A Expected arrangement of hydrogen atoms in $[Tc^{VII}H_9]^{2-}$ [1].

known for technetium. The lattice constants of the hexagonal unit cell are a= 9.64 and c= 5.56 Å. The high resolution ^1H MNR spectrum of $K_2[TcH_9]$ dissolved in cold alkaline D_2O showed a broad line at 18.4 ppm that is attributed to the Tc-bonded hydrogens. In the IR spectrum of the metal-hydrogen stretching region a triplet was observed at 1869, 1795, and 1779 cm^{-1}. In the metal-hydrogen bending region a single band at 689 cm^{-1} appeared. This is precisely the pattern observed in the IR spectrum of solid $K_2[ReH_9]$. $[TcH_9]^{2-}$ proved to be more reactive than $[ReH_9]^{2-}$ [1]. Later, ^{99}Tc NMR and ^1H NMR provided definite proof for the existence of the stereochemically non-rigid $[TcH_9]^{2-}$ anion [3]. It was concluded from a molecular orbital description of $[TcH_9]^{2}$ that the hydrogens are almost identical in regard to their electronic environment [4].

12.1.2 $(TcO_3)^+$-core complexes

The recently increasing number of Tc(VII) complexes containing the TcO_3^+ moiety demonstrates the stabilization of high oxidation state central atoms by oxo ligands as electron donors. Trioxohalogeno(2,2′-bipyridine)-technetium(VII), $[TcO_3Cl(bpy)]^\circ$ or $[TcO_3Br(bpy)]^\circ$ and trioxochloro(1,10-phenanthroline)technetium(VII), $[TcO_3Cl(phen)]^\circ$, could easily be synthesized by reaction of NH_4TcO_4 with bipyridine or phenanthroline and conc. HCl or HBr in a mixture of ethanol/water. The compounds precipitate as yellow or yellow orange solids that hydrolyze in water back to TcO_4^-. Complex formulation is confirmed by elemental analyses, Raman, and IR spectroscopy [5]. Furthermore, a binuclear complex of heptavalent technetium with the bridging ligand 3,6-bis(2′-pyridyl)-1,2,4,5-tetrazine(bptz), $[(\mu\text{-bptz})(TcO_3X)_2]^\circ$, (X = Cl, OCH_3, OC_2H_5) and a mononuclear complex of Tc(VII), $[TcO_3(pppz)Cl]^\circ$, {pppz = 4-phenyl-3,6-bis(2′-pyridyl)pyridazine} were prepared and characterized [6].

$[TcO_3Cl(bpy)]^\circ$, $[TcO_3Cl(phen)]^\circ$ and, in addition, $[TcO_3Cl(5\text{-}NO_2\text{-phen})]^\circ$ and $[TcO_3Cl(3,4,7,8\text{-tetramethylphen})]^\circ$ were shown to cleanly oxidize a wide variety of alkenes in acetone or dichloromethane to form, in high yields, the corresponding oxotechnetium(V) diolate complexes at room temperature [7] (Sect. 8.3). Remarkably, the oxorhenium(V) diolate complex $[ReOCl(OCH_2CH_2O(phen)]^\circ$ undergoes the

reverse reaction when thermalized at 220 °C, releasing ethylene and producing $[ReO_3Cl(phen)]^\circ$.

Another trioxotechnetium(VII) complex was recently synthesized, the hydro-tris(1-pyrazolyl-borato-trioxo-technetium(VII), which was first prepared in good yield from NH_4TcO_4 and hydro-tris(1-pyrazolyl)-borato-sodium, $[Na\{HB(pz)_3\}]^\circ$, in ethanol after addition of conc. sulphuric acid [8]. $[TcO_3\{HB(pz)_3\}]^\circ$ can also be obtained by the nitric acid oxidation of $[TcOCl_2\{HB(pz)_3\}]^\circ$ or by reaction of Tc_2O_7 with $K[HB(pz)_3]$ in THF [9]. The ^1H NMR spectrum of the pale yellow trioxo complex shows that the C_{3V} molecule has three equivalent pyrazolyl rings [10]. The structure of the compound (Fig. 12.2.A) is based on the X-ray structure analysis of the analogous rhenium complex [11,12]. Like $[TcO_3Cl(bpy)]^\circ$, $[TcO_3Cl(phen)]^\circ$ and $[TcO_3Cl$ (phen-derivatives)]° react with alkenes, the reaction of $[TcO_3\{HB(pz)_3\}]^\circ$ with ethylene yields $[Tc^VO(OCH_2CH_2O)\{HB(pz)_3\}]^\circ$. The mechanism most probably involves direct attack of ethylene to the oxo moieties of $[TcO_3\{HB(pz)_3\}]^\circ$ [10].

Furthermore, the TcO_3^+ group can be bonded to the anionic, tridentate oxygen donor ligand $[(\eta^5\text{-}C_5H_5)Co\{(POR)_2(=O)\}_3]^-$, when R is methyl, ethyl or butyl. According to the X-ray structure analysis of the corresponding complex formed with ReO_3^+, $[(\eta^5\text{-}C_5H_5)Co\{P(OCH_3)_2(=O)\}_3ReO_3]^\circ$, having the space group $P2_1/c$ [13], the same distorted octahedral geometry for $[(\eta^5\text{-}C_5H_5)Co\{P(OCH_3)_2(=O)\}_3TcO_3]^\circ$ is expected. Cyclopentadienyl-tris(dialkylphosphito)(cobaltato)-trioxotechnetium(VII) can be synthesized in excellent yield by the reaction of an aqueous solution of NH_4TcO_4, $[(\eta^5\text{-}C_5H_5)Co\{(POR)_2(=O)\}_3]^-$, and conc. HNO_3. The compounds were idendified by FAB(+) mass spectra, ^1H NMR, and IR spectra [14].

The first organometallic compound containing the TcO_3 core is methyltrioxotechnetium(VII), CH_3TcO_3, [15,16] corresponding to the previously known methyltrioxorhenium(VII) [17]. CH_3TcO_3 was synthesized by reacting Tc_2O_7 with tetramethyltin at 10 °C in a solution of tetrahydrofuran. The compound forms white needle-shaped crystals that are extremely volatile, but stable at 0 °C. CH_3TcO_3 is reported to be soluble in all solvents including water and was characterized spectroscopically. An important difference to CH_3ReO_3 is that no phenanthroline or bipyridine adduct could be precipitated. However, CH_3TcO_3 oxidizes alkenes to *cis*-diols via the formation of a diolate complex of Tc(V) [15,16].

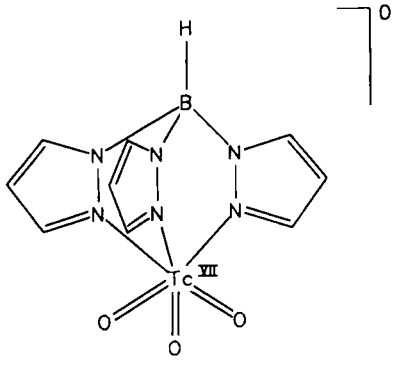

Fig. 12.2.A Hydro-tris(1-pyrazolyl)borato-trioxo-technetium (VII), $[TcO_3\{HB(pz)_3\}]^\circ$ [10,11].

The synthesis of CH_3TcO_3 by reaction of Tc_2O_7 with $(CH_3)_4Sn$ leads simultaneously to the production of the trimethylstannylester of pertechnetic acid $[TcO_3OSn(CH_3)_3]$ [15], which could be obtained as the polymer $[TcO_3OSn(CH_3)_3]_n$ in white, needle-like single crystals [18]. Polymeric trimethylstannylpertechnetate crystallizes in the monoclinic space proup $P2_1/c$; the lattice constants are a=9.616, b=7.645, c=11.901 Å, β=91.16°; Z=4. The compound is not isostructural with $[ReO_3OSn(CH_3)_3]_n$ [19], although both compounds reveal a zigzag chain structure [18].

12.1.3 $(TcN)^{4+}$-core complexes

The nitrido ligand (N^{3-}) which is isoelectronic with the oxo ligand (O^{2-}), appears also to be a powerful π-electron donor [20] efficiently stabilizing metals in high oxidation states like Tc(VII). The chloronitridoperoxo anion of heptavalent technetium $[TcN(O_2)_2Cl]^-$ was the first example of a stable transition metal nitridoperoxo complex. Reaction of $Cs_2[TcNCl_5]$ with H_2O_2 yielded $Cs[TcN(O_2)_2Cl]$ in yellow-orange crystals (Fig. 12.3.A). The coordination about the technetium central atom is a distorted pentagonal pyramid with the nitrido ligand in the apical position; the Tc≡N distance is 1.63 Å. The peroxo and chloro ligands are essentially located in a plane with the technetium atom being displaced by 0.45 Å above the plane. $Cs[TcN(O_2)_2Cl]$ is readily soluble in water. In conc. HCl the complex is converted to $[Tc^{VI}NCl_4]^-$. The relative stability of $[TcN(O_2)_2Cl]^-$ is indicative of the low oxidizing potential of the $(Tc^{VII}N)^{4+}$ core [21]. In addition to $[TcN(O_2)_2Cl]$ other technetium(VII)nitridoperoxo complexes like $[TcN(O_2)_2Br]$, $[TcN(O_2)_2(bpy)]^\circ$, and $[TcN(O_2)_2(phen)]^\circ$ were prepared. The successful synthesis of complexes containing the $TcN(O_2)_2$-core

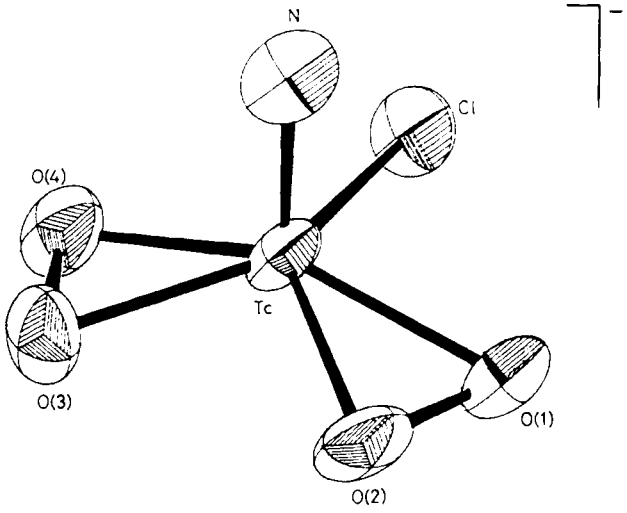

Fig. 12.3.A Nitrido-diperoxo-chlorotechnetate(VII), $[TcN(O_2)_2Cl]$ [21].

remains remarkable in view of the easy oxidation of lower valent Tc compounds by H_2O_2 to the most stable pertechnetate [22].

In addition, the dinuclear oxalate-bridged technetium(VII) nitridoperoxo complex $[TcN(O_2)_2(C_2O_4)(O_2)_2NTc]^{2-}$ was obtained by addition of oxalic acid to a solution of nitridotechnetic(VI) acid in hydrogen peroxide. $[Ph_4As]Cl$ precipitated a pale-yellow solid. Recrystallization from acetone provided single crystals of the composition $[Ph_4As]_2[TcN(O_2)_2(C_2O_4)(O_2)_2NTc]\cdot 2(CH_3)_2CO$. The structure of the anion consists of two $TcN(O_2)_2$ units bridged by a quadridentate sideways-bound oxalate. The geometry about each technetium atom is distorted pentagonal-bipyramidal with the nitrido ligand in an apical position and the peroxo ligands in equatorial positions [23].

An unusual dinuclear nitrido-hydrazido(2-)-technetium(VII) complex containing bridging thiolate ligands was sythesized by reaction of $[(n\text{-}C_4H_9)_4N][TcOCl_4]$ with 1,1-diphenylhydrazine in dichloromethylene and subsequent addition of 2,4,6-isopropyl-C_6H_2SH in methanol. After stirring and concentrating the solution followed by addition of an ether/hexane mixture, bright yellow diamagnetic crystals of $[Tc_2N_2(NNPh_2)_2(2,4,6\text{-isopropyl-}C_6H_2S)_4]\cdot 0.5(C_2H_5)_2O$ were isolated. Single crystal X-ray analysis showed the triclinic space group $P\bar{1}$ and the lattice constants a=14.422, b=16.049, c=18.918 Å, α=81.89, β=73.60, γ=86.74°, and Z=2. The coordination geometry about each Tc center may be described as distorted square pyramidal with the basal plane defined by the sulphur donors of the bridging thiolate ligands, the sulphur of the terminal thiolate and the α-nitrogen of the hydrazido(2-) ligand, while the apical position is occupied by the nitrido unit. The presence of the nitrido ligand is unexpected and must result from N-N bond cleavage of the organohydrazine reagent [24].

12.1.4 Imido complexes

Obviously, in addition to the nitrido ligand, also imido ligands are capable of stabilizing high-valent central atoms by π-electron donation. Recently, several imido complexes of Tc(VII) were identified. TcO_4^- reacts with 1,2-diaminobenzene in refluxing methanol to form, in high yield, green crystals of $[Tc(HNC_6H_4NH)_3]TcO_4$ that are stable in organic solvents without reduction of Tc(VII). The cationic complex exhibits the TcN_6 core in a trigonal-prismatic geometry (Fig. 12.4.A). The two triangular faces N(2),N(3),N(5) and N(1),N(4),N(6) are nearly parallel. The distance of Tc from the two N_3 faces is 1.24 Å and the Tc–N mean bond length is 2.00 Å. $[Tc(HNC_6H_4NH)_3]TcO_4$ crystallizes in the orthorhombic space proup $Pna2_1$ with the lattice constants a=13.869, b=12.799, c=10.851 Å, and Z=4 [25].

A series of new Tc(VII) imido complexes has been recently synthesized and characterized. When a hexamethyldisiloxane solution of $[TcO_3(OSiMe_3)]^\circ$, which can be prepared as a white solid by reaction of $AgTcO_4$ with chlorotrimethylsilane [26], is treated with 2,6-diisopropylphenylisocyanate at 100 °C, deep green $[Tc(NAr)_3(OSiMe_3)]^\circ$ (Ar = 2,6-diisopropylphenyl) is formed:

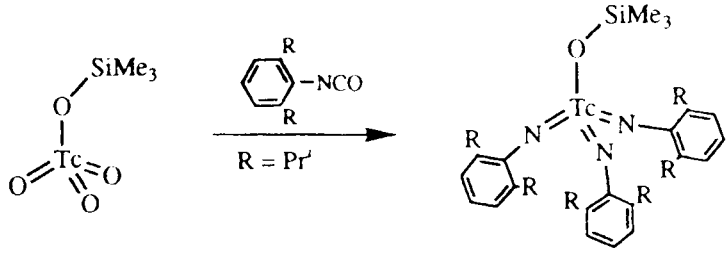

The Tc(VII) trisimido complex proved to be resistant to electrochemical reduction because of the strong π-donor ligands. ^{1}H NMR indicated free rotation of these ligands about the N–C bonds. The coordination geometry about Tc(VII) was shown by X-ray analysis to be approximately tetrahedral. The structure exhibits short Tc=N bond lengths (1.749–1.759 Å) and large Tc=N–C angles (154.3–158.5°) indicating considerable multiple bond character. The neutral complex crystallizes in the monoclinic space group *Cc* with the lattice constants a=12.077, b=19.477, c=17.914 Å, β=95.90°, and Z=4 [27].

$[Tc(NAr)_3(OSiMe_3)]^\circ$ reacts with trimethylsilyliodide in toluene to form $[Tc(NAr)_3I]^\circ$, the first example of a Tc(VII) iodide complex. The trimethylsilyl group in $[Tc(NAr)_3(OSiMe_3)]^\circ$ can be selectively removed from the trimethylsiloxy ligand by reaction with $(Ph_3P)_2NF$ in methylene chloride resulting in the oxo anion $[TcO(NAr)_3]^-$, which is a trisimido analogue of TcO_4^-. In addition, $[Tc(NAr)_3(OSiMe_3)]^\circ$ reacts quickly in THF solution at room temperature with Grignard reagents to form deep blue-green $[Tc(NAr)_3R]^\circ$, when R′ is CH_3, C_2H_5 or η^1-C_3H_5(allyl) [27,28]. When a solution of $[Tc(NAr)_3I]^\circ$ in THF is treated with 1 equivalent of potassium cyclopentadienyl (KCp), a rapid reaction occurs forming $[(\eta^1\text{-Cp})Tc(NAr)_3]^\circ$. The green complex is air- and water-stable. The η^1 nature of Cp was demonstrated by single crystal X-ray analysis (Fig. 12.5.A). Only minor deviations

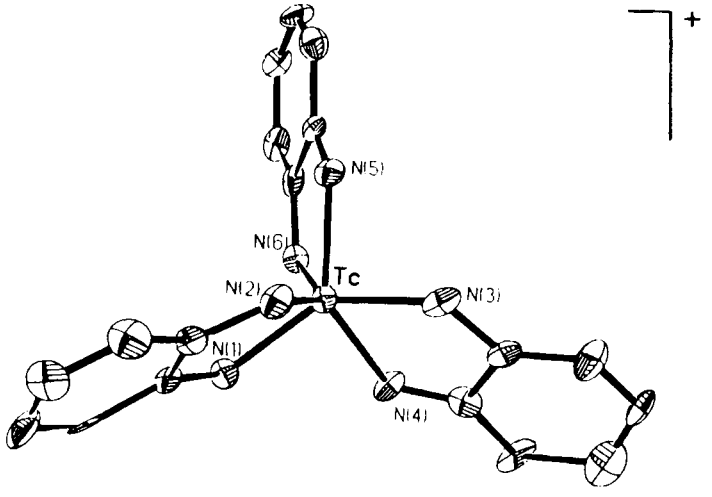

Fig. 12.4.A Tris(1,2-diimidobenzene)technetium (VII). $[Tc(HNC_6H_4NH)_3]^+$.

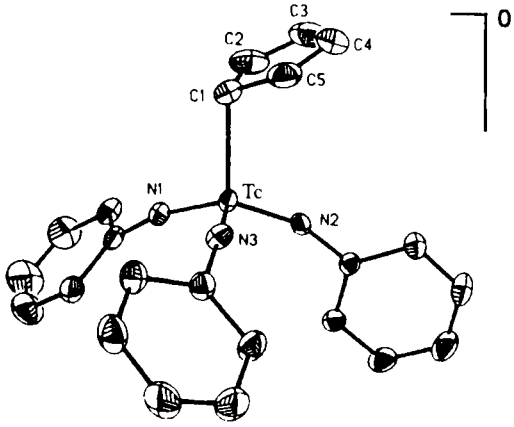

Fig. 12.5.A $[(\eta^1\text{-Cp})Tc^{VII}(NAr)_3]^\circ$ (Ar=2,6-diisopropylphenyl). The isopropyl groups are omitted [29].

from tetrahedral geometry were observed in the coordination environment of the technetium atom. The cyclopentadienyl carbons are nearly planar. When an excess of KCp is reacted with $[Tc(NAr)_3I]^\circ$, an air-sensitive blue complex is obtained that can be formulated as $K[Cp_2Tc(NAr)_3]$ [29].

Some structural data of Tc(VII) complexes are reviewed in Table 12.1.A.

Table 12.1.A Some structural data of selected Tc(VII) complexes.

Complex	Geometry	Tc–L [Å]	ν(Tc–L) IR[cm^{-1}]	References
12.1.1				
$[TcH_9]^2$	trig. prism	–	1779, 1795, 1869 (Tc–H)	[1–4]
12.1.2				
$TcO_3Cl(bpy)]^\circ$	–		980(Tc=O)	[5]
$TcO_3Br(bpy)]^\circ$	–	–	969(Tc=O)	[5]
$TcO_3Cl(phen)]^\circ$	–	–	977(Tc=O)	[5]
$[HB(pz)_3TcO_3]^\circ$	pseudo-octahedral	–	885, 898, 922 (Tc=O)	[10,11]
$[(\eta^5\text{-}C_5H_5)Co\{P(O\text{-}CH_3)_2(=O)\}_3TcO_3]^\circ$	octahedral	–	–	[13,14]
CH_3TcO_3			948(Tc=O)	[15,16]
12.1.3				
$[TcN(O_2)_2Cl]$	pentag. pyramid	1.63(Tc–N)	1063(Tc≡N) 657{$Tc(O_2)$}	[21]

Table 12.1.A Continued.

Complex	Geometry	Tc–L [Å]	ν(Tc–L) IR[cm^{-1}]	References
$[TcN(O_2)_2(bpy)]^0$	pentag. pyramid		1045(Tc≡N) 665{Tc(O_2)}	[22]
$[\mu$-$(C_2O_4)\{TcN(O_2)_2\}_2]^{2-}$	pentag. bipyramid	1.69(Tc≡N)	1051(Tc≡N) 659{(Tc(O_2)}	[23]
$[(\mu$-2,4,6-isopropyl-$C_6H_2S)_2$ {TcN(NNPh$_2$) (2,4,6-isopropyl-C_6H_2S)}$_2]^0$	square pyramid	1.64(Tc≡N)	–	[24]
12.1.4				
$[Tc(HNC_6H_4NH)_3]^+$	trig. prism	2.00(Tc–N)	418(Tc–N)	[25]
$[Tc(NAr)_3(OSiMe_3)]^-$	tetrahedral	1.749–1.759(Tc≡N)	–	[27]
$[Tc(NAr)_3I]^0$	tetrahedral	2.654(Tc–I)	–	[27]
$[Tc(NAr)_3Me]^0$	tetrahedral	2.136(Tc–CH_3)	–	[28]
$[(\eta^1$-Cp)Tc$(NAr)_3]^0$	tetrahedral	2.156(Tc–C)		[29]

12.2 Technetium(VI)

Though hexavalent technetium is known to be highly sensitive to oxydation and disproportionation, for instance in the case of tetraoxotechnetate(VI) [30], numerous complex compounds of Tc(VI) were synthesized and identified and proved to be rather stable under normal conditions. Imido and predominantly nitrido ligands frequently act in mono- and dinuclear complexes as strong stabilizing π-electron donors [31]. In fluoro complexes the coordination numbers 7 and 8 are verified. In addition catecholato and thiolato ligands form well defined compounds. EPR spectroscopy was shown to be an efficient tool to characterize the d^1 complexes.

12.2.1 Halogen containing complexes

The first complexes of hexavalent technetium were prepared by reaction of TcF_6 with nitrosyl fluoride and nitryl fluoride. At –195 °C NOF or NO_2F were condensed onto technetium hexafluoride. Reaction with nitrosyl fluoride occurred at room temperature, with nitryl fluoride at 70 °C. $(NO)_2[TcF_8]$ is an off-white, non-volatile solid, isostructural with $(NO)_2[ReF_8]$ and $(NO)_2[WF_8]$. The magnetic moment of $(NO)_2[TcF_8]$ is μ=1.72 B.M., according to the spin-only value for eight-coordinate Tc(VI). Nitrylheptafluorotechnetate(VI), $NO_2[TcF_7]$, is a yellow, non-volatile solid. Its magnetic susceptibility does not obey the Curie-Weiss law. The room temperature magnetic moment is μ_{eff}=1.62 B.M., close to the spin-only value [32].

The pentachlorooxotechnetate(VI) anion, $[TcOCl_5]^-$, was prepared by reducing a solution of $KTcO_4$ in conc. H_2SO_4 with HCl. Immediately, a deep blue solution was obtained, however, its color vanished after 1 h. The general features of the EPR spectrum recorded at 130 K are characteristic for an axially symmetric, randomly oriented $S = {}^1/_2$ system with parallel and perpendicular sets of ^{99}Tc hyperfine lines [33]. Ammonium dioxotetrachlorotechnetate(VI), $(NH_4)_2[TcO_2Cl_4]$, was synthesized by reaction of NH_4TcO_4 with thionyl chloride and isolated as its sulphuryl chloride adduct [34].

12.2.2 Imido complexes

The tris(arylimido)iodotechnetium(VII) complex $[Tc(NAr)_3I]^0$ (Ar = 2,6 diisopropylphenyl), mentioned in the last paragraph of Sect. 12.1, is reduced by elemental sodium in THF to the green dimer $[Tc_2(NAr)_6]^0$ of staggered ethane-like structure:

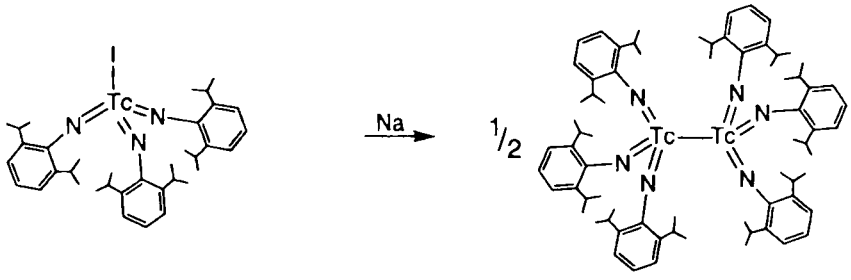

The formal oxidation state of the Tc atoms is +6 in accordance with the diamagnetic d^1–d^1 spin-paired dimer. X-ray structure analysis revealed that the Tc–Tc bond lies on a crystallographic S_6 axis, making all six imido ligands symmetry equivalent. The rather long Tc–Tc distance of 2.744(1) Å may be due to steric congestion between the imido groups around the ethane-like structure. The short Tc–N distance of 1.758(2) Å and the almost linear arrangement of the Tc–N–C units (167.6°) are to be expected. The angles N–Tc–Tc and N=Tc–N are 103.6(1)° and 114.6(1)°, respectively [35,36].

Reduction of $[Tc(NAr')_3I]^0$ (Ar' = 2,6-dimethylphenyl) by one equivalent elemental sodium in THF generates the red edge-bridged tetrahedral dimer complex $[\mu\text{-}NAr')_2Tc_2(NAr')_4]$:

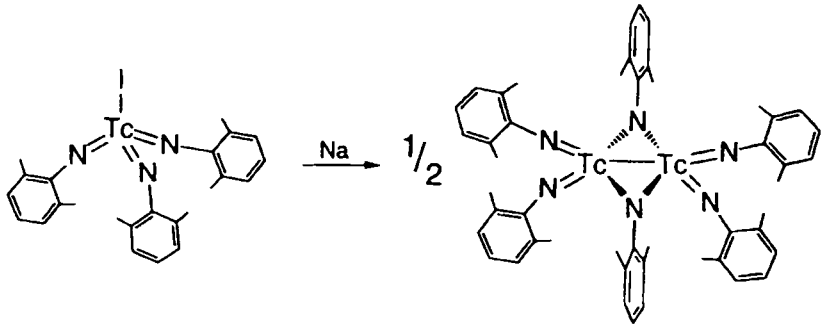

Its configuration was confirmed by X-ray structure analysis. The monoclinic space group is $P2_1/n$, the lattice constants are a=19.500(8), b=10.497(6), c=22.684(8) Å, β=110.37(3)°, and Z=4. The ditechnetium core can be formally considered to contain a Tc_2^{12+} unit, giving rise to a d^1–d^1 dimer and a Tc–Tc single bond. The average Tc–Tc bond length of 2.68 Å is consistent with this formulation and accounts for the observed diamagnetic nature. The presence of high-valent Tc metal centers and planar nitrogen atoms is suggestive of Tc–N π-bonding. The distances between technetium and the bridging nitrogen atoms (1.938–1.955 Å) are well within the range (1.88–2.14 Å) typically observed for imido technetium complexes, which are known to form Tc–N π bonds. The factors influencing the formation of either ethane-like or the more common edge-bridged tetrahedral dimer structure appear to be purely steric. Obviously, $[Tc(NAr)_3I]^\circ$ is more sterically hindered to form the edge-bridged configuration of $[(\mu\text{-}NAr')_2Tc_2(NAr')_4]^\circ$ [35,36].

Treatment of $[(\mu\text{-}NAr')_2Tc_2(NAr')_4]^\circ$ with two equivalents of MeMgCl in THF results in a deep ruby solution due to the formation of $[(\mu\text{-}NAr')_2Tc_2Me_2(NAr')_3]^\circ$ by displacement of an imido ligand. The reaction of $[(\mu\text{-}NAr')_2Tc_2Me_2(NAr')_3]^\circ$ with a further two equivalents of MeMgCl again yields the substitution of an imido ligand and the formation of $[(\mu\text{-}NAr')_2Tc_2Me_4(NAr')_2]^\circ$. Only the Z-type isomer is observed in the solid state. The dark red $[(\mu\text{-}NAr')_2Tc_2Me_4(NAr')_2]^\circ$ crystallizes in the triclinic space group $P\bar{1}$ with a=11.832(3), b=11.917(3), c=13.286(3) Å, α=75.33(2), β=71.10(2), γ=84.82(2)°, and Z=2. This complex is best described as an edge-bridged square based pyramidal dimer with the terminal imido ligands occupying the apical positions. The Tc–Tc distance is 2.733(1) Å, which is within the range for d^1–d^1 dimers [37].

12.2.3 Nitrido complexes

NH_4TcO_4, mixed with conc. hydrochloric or hydrobromic acid, reacts with an aqueous solution of NaN_3 to give an orange solution of $[TcNCl_4]^-$ or a deep violet solution of $[TcNBr_4]^-$. By addition of tetraphenylarsoniumchloride orange $[AsPh_4][TcNCl_4]$ or deep blue $[AsPh_4][TcNBr_4]$ were precipitated. Single crystal structure analysis of both complex salts revealed the square pyramidal structure (C_{4V} symmetry) of tetrachloro- and tetrabromonitridotechnetate(VI) (Fig. 12.6.A). $[AsPh_4][TcNCl_4]$ and $[AsPh_4][TcNBr_4]$ are isostructural with each other and with the corresponding compounds of Re, Mo, Ru, and Os. The crystals are tetragonal with the space group $P4/n$. The lattice constants for $[AsPh_4][TcNCl_4]$ are a=12.707(2) and c=7.793(1) Å, for $[AsPh_4][TcNBr_4]$ a=12.875(2) and c=7.992(1) Å; Z=2. In both compounds the metal-nitrogen bonds are short, corresponding to triple bonds. In $[TcNCl_4]^-$ the Tc atom is located 0.54 Å above the plane of the four chlorine atoms. The presence of sharp absorption bands in the IR at 1074–1080 cm^{-1} is characteristic of the terminal Tc≡N group. The tetrahalogenonitridotechnetate(VI) salts are surprisingly stable in air in constrast to $[AsPh_4][MoNCl_4]$, which is reported to be extremely sensitive to hydrolysis. The strong Tc≡N π bonding is consistent with the higher stretching frequencies relative to those of Tc=O (1020–996 cm^{-1}) in $[TcOX_4]^-$ (X=Cl, Br, or I) [38,39].

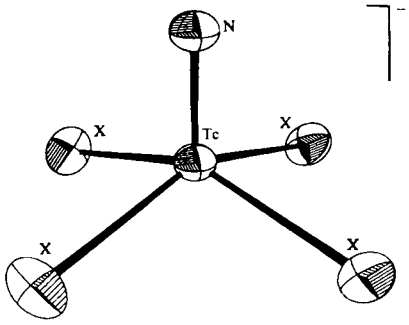

Fig. 12.6.A $[Tc^{VI}NX_4]^-$ (X=Cl,Br). Bond distances Tc Cl 2.3220(9), Tc Br 2.4816(5) Å, Tc≡N in $[TcNCl_4]^-$ 1.581(5), in $[TcNBr_4]^-$ 1.596(6) Å. Bond angles Cl Tc–Cl 86.95(1) and 153.33(6)°, Br Tc–Br 87.08(1) and 153.91(4)°, N≡Tc–Cl 103.34 (3)° and N≡Tc Br 103.04(2)° [38,39].

Tetrachloronitridotechnetate(VI) may also be obtained by reaction of $[But_4N][TcOCl_4]$, dissolved in dichloromethane, with a solution of NCl_3 in carbon tetrachloride:

$$2[TcOCl_4] + 4NCl_3 \rightarrow 2[TcNCl_4]^- + 2NOCl + 5Cl_2$$

or by reaction of $TcNCl_3$ with a solution of $[AsPh_4]Cl$ in CH_2Cl_2. From the orange-red solution $[AsPh_4][TcNCl_4]$ was isolated [40].

EPR spectroscopic studies revealed the chloride and bromide ions in $[TcNCl_4]^-$ and $[TcNBr_4]^-$ to be reactive and exchangeable. When $[AsPh_4][TcNCl_4]$ and $[AsPh_4][TcNBr_4]$ were dissolved in acetonitrile and the mixed solutions of different molar ratios boiled for 30 min, the formation of mixed-ligand complexes of the composition $[TcNBr_{4-n}Cl_n]^-$ with n=1–3 were observed. The composition could easily be determined by means of their EPR parameters [41]. In addition, equilibrium constants for the exchange reactions of $[TcNCl_4]^-$ with HBr and $[TcNBr_4]^-$ with HCl were derived, demonstrating the expected higher reactivity of $[TcNBr_4]^-$ [42]. Furthermore, both complex anions react with dialkyldithiocarbamates, diisopropyldithiophosphate, 1,2-dicyanoethene-1,2-dithiolate, thiocyanate, pyridine, and imidazole by reduction to Tc(V) nitrido complexes containing the corresponding ligands with N- and S- donor atoms, while the Tc≡N core remained unchanged, except for the oxidation state of Tc [43]. Ligand exchange reactions of $[TcNCl_4]^-$ and $[TcNBr_4]^-$ with sodium azide in acetonic solutions were studied by EPR. During the reaction time of 60 min all five complexes $[TcNX_n(N_3)_{4-n}]^-$ (n=0–4) were detected for tetrachloro- and tetrabromonitridotechnetate(VI). The EPR parameters of the individual species strongly depend on the composition of the equatorial coodination sphere. The covalent character of the equatorial Tc–N_3 bonds in $[TcN(N_3)_4]^-$ was found to be more pronounced than that in the Tc–X bonds of $[TcNX_4]^-$ [44,45].

Single-crystal EPR studies of $[AsPh_4][Tc^{15}NCl_4]$, diamagnetically diluted by the isostructural $[AsPh_4][TcOCl_4]$, were reported. The room-temperature single-crystal spectra consist of a well resolved, intense 10 line hyperfine structure multiplet due to the interaction of the unpaired $4d^1$ electron with the nuclear spin $I=9/2$ of ^{99}Tc. At low temperatures very complex $^{35,37}Cl$ and ^{15}N ligand hyperfine patterns were observed. The ^{99}Tc, $^{35,37}Cl$ and ^{15}N hyperfine data were analyzed to evaluate the electron spin delocalization. The spin density on ^{15}N was found to be zero, while 20 % of the spin

density was localized mainly in the 3*p* orbitals of the Cl atoms [46,47]. According to polarized neutron diffraction experiments on $[TcNCl_4]^-$, even 46 % of the spin density is located on the Cl atoms [48]. Single crystal EPR studies on $[(C_4H_9)_4N][TcNBr_4]$, diamagnetically diluted in $[(C_4H_9)_4N][TcOBr_4]$, established that the delocalization of the unpaired 4*d* electron to the bromine nuclei is-as expected-more pronounced than to the chlorine nuclei in $[TcNCl_4]^-$ [49]. EPR investigations on technetium complexes with respect to Tc oxidation state, coordination geometry, bonding properties, and chemical reactions have been reviewed [50,51].

The aquanitrido complexes $[TcNCl_4(OH_2)]^-$ and $[TcNBr_4(OH_2)]^-$ have also been synthesized and characterized. The acetonitrile extract prepared from the reaction of NH_4TcO_4 with NaN_3 in HCl was dissolved in 36 % HCl and $[NEt_4]Cl$ added. By addition of absolute ethanol to the orange solution, orange crystals of $[NEt_4][TcNCl_4(OH_2)]$ precipitated. Using 47 % HBr instead of HCl, refluxing the mixture for 10 min and adding $[NEt_4]Br$, blue-black crystals of $[NEt_4][TcNBr_4(OH_2)]$ were obtained that crystallize in the orthorhombic space group *Pnma* with a=11.366(1), b=12.930(2), c=11.540(1) Å, and Z=4. Tc(VI) is coordinated by the ligands to give a distorted octahedron. The water molecule position is *trans* to the nitrido ligand. The long Tc–O bond distance of 2.443(7) Å is a consequence of the strong *trans* influence of the nitrido ligand. H_2O is coordinated in an almost linear arrangement with an N≡Tc–OH_2 angle of 178.7(3)° [52].

Addition of CsCl to an orange solution of $[AsPh_4][TcNCl_4]$ in conc. HCl results in the precipitation of red-brown crystals of six-coordinate $Cs_2[TcNCl_5]$. The additional Cl^- ligand *trans* to the nitrido group caused a decrease of the Tc≡N frequency in the IR from 1076 cm^{-1} for $[TcNCl_4]^-$ to 1027 cm^{-1} for $[TcNCl_5]^{2-}$. $Cs_2[TcNCl_5]$ proved to be stable in air but is readily hydrolyzed by water [53] like $[TcNCl_4]^-$. The species $[TcNX_4]^-$, $[TcNX_4(OH_2)]^-$ and $[TcNX_5]^{2-}$ (X= Cl or Br) are interconverted by addition or removal of the *trans* ligand. In conc. HX solution the species present is most likely $[TcNX_4(OH_2)]^-$. The product isolated from solutions of the aquo-nitrido complex appears to be dependent on the nature of the added cation. Large cations R such as $[AsPh_4]^+$ or $[NBu_4]^+$ result in the precipitation of $R[TcNX_4]$, while relatively small cations like Cs^+ precipitate $Cs_2[TcNX_5]$. The intermediate-size cation $[NEt_4]^+$ allowed the isolation of $[NEt_4][TcNX_4(OH_2)]$. Crystals of $Cs_2[TcNCl_5]$ belong to the cubic space group $Fm\bar{3}m$ with a=10.211(1) Å and Z=4. The Tc≡N bond distance is 1.60 Å. The *trans* Tc–Cl distance is 2.740(5) Å, the *cis* Tc–Cl distance 2.373(5) Å. The Tc atom is displaced by 0.401(3) Å from the plane of the *cis* ligands towards the nitrido ligand. The N≡Tc–Cl angle is 99.73(8)° [52]. However, it is surprising that the EPR spectra show no direct evidence for the existence of the equilibrium

$$[TcNX_4]^- + X^- \leftrightarrow [TcNX_5]^{2-}$$

in non-aqueous and conc. aqueous acid solutions. The predominant species in solution is $[TcNX_4]^-$ [54]. In contrast, $[TcNCl_5]^{2-}$ was reported to be created by oxidation of nitrido technetate(V) complexes with chlorine, according to EPR solution studies [55]. In aqueous solutions of low HCl concentrations, $[TcNCl_4]^-$ forms dimagnetic compounds possibly containing oxygen bridges [56,57]. Brown precipitates, called

nitridotechnetic(VI) acid, dissolve in conc. hydrofluoric acid and show an EPR spectrum due to $[TcNF_4]^-$ [57].

Salts of nitridotechnetium(VI) anions with crown ether complex cations were prepared and structurally analyzed. To a suspension of $Cs_2[TcNCl_5]$ in thionylchloride 18-crown-6(1,4,7,10,13,16-hexaoxacyclooctadecane) was added. Orange-red crystals of polymeric $[Cs(18\text{-crown-}6)][TcNCl_4]$ were obtained [58]. The tetragonal unit cell, with the space group *P4/n* and Z=4, is represented by a square of 22.459(1) Å edge length and a tretragonal c-axis length of 4.275(4) Å [59]. The Cs^+ cations occupy sites at the corners of the unit cell and in the center of the square. Each 18-crown-6 molecule lies more or less in the *xy* plane with a Cs^+ cation above and below, forming a twinned infinite sandwich array with ordered and disordered infinite chains of $[TcNCl_4]^-$ anions arranged in an antiparallel fashion [58, 59].

Orange-red crystals of $[Rb(15\text{-crown-}5)_2][TcNCl_4(OH_2)]$ were grown by slow evaporation of the reaction mixture containing 15-crown-5 and $Rb_2[TcNCl_5]$ in thionyl chloride. The *trans* coordinated water molecule arises by absorption from the atmosphere. The compound crystallizes in the monoclinic space group *C2/m* with a=11.886(13), b=13.653(7), c=10.327(5) Å, β=90.33(7)°, and Z=2. The structure determination shows a lattice containing sandwich-type crown ether/alkali-metal cations and isolated anions disordered in the lattice. Also the room temperature EPR spectrum shows the presence of isolated $[TcNCl_4(OH_2)]^-$ anions with the Tc atoms separated by the relatively large distance of 9.051 Å due to the bulky $[Rb(15\text{-crown-}5)_2]^+$ cations dominating the lattice. In addition to $[Cs(18\text{-crown-}6)][TcNCl_4]$ and $[Rb(15\text{-crown-}5)_2][TcNCl_4(OH_2)]$ the complex salts $[Cs(18\text{-crown-}6)_2][TcNCl_4]$, $[Rb(18\text{-crown-}6)][TcNCl_4]$, $[Cs(18\text{-crown-}6)][TcNCl_4(OH_2)]$, and $[Cs(15\text{-crown-}5)_2][TcNCl_4(OH_2)]$ were prepared and identified [59].

The reactivity of chloride and bromide ligands in $[TcNCl_4]^-$ and $[TcNBr_4]^-$ allows their substitution by appropriate ligands containing oxygen and nitrogen donor atoms. N,N′-ethylene-bis(salicylideneiminato)nitridotechnetium(VI)

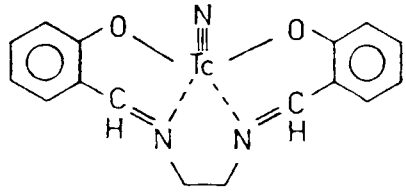

was obtained by reaction of $[But_4N](TcNCl_4]$ with the Schiff base ethylene-bis(salicylideneimine) in acetone. The complex salt crystallizes in dark green needles that are soluble in water, methanol and DMSO. According to EPR measurements, around 30 % of the spin density is localized in the ligand orbitals. The Tc≡N stretching vibration was found at 1037 cm^{-1} in the IR [60].

$[TcNCl_4]^-$ reacts in aqueous solution with Na_2H_2edta to form a red-violet precipitate of the composition $[TcN(Hedta)]^0 \cdot 3H_2O$ [61]. Later, the formation of the μ-oxo dimer complex $Na_4[Tc_2N_2(\mu\text{-}O)(edta)_2] \cdot 5H_2O$ was suggested [62] from an absorption maximum at 504 nm, because μ-oxo dimers are reported to show an intense absorp-

tion at 470–510 nm [63]. When ethylenediamine-N,N′-diacetic acid (H_2edda) reacted with $[TcNCl_4]^-$ in acetone, a purple precipitate of the reported composition $[Tc_2N_2(\mu\text{-}O)(edda)_2]\cdot 5H_2O$ was obtained [62].

The interconversion of monomeric, μ-oxo, and di(μ-oxo) dimeric nitridotechnetium(VI) species in aqueous solution was studied by EPR and VIS/UV spectrophotometry. The position of the equilibrium and the rates of interconversion of the species depend on the acidity and the coordination ability of the medium. High acidity (conc. HCl) favors the monomeric form $[TcNCl_4(OH_2)]^-$, readily established by EPR spectroscopy. The dimeric species can not be seen by EPR. The di(μ-oxo)structure was confirmed by single crystal X-ray structure determination of $[AsPh_4]_2[\{TcNCl_2\}_2(\mu O)_2]^{2-}$ (Fig. 12.7.A) [64].

The so-called nitridotechnetic acid $[TcN(OH_2)_3(\mu\text{-}O)_2TcN(OH_2)_3]^{2-}$, dissolved in 1 M toluene-4-sulphonic acid, reacts with diethyldithiocarbamate $S_2CNEt_2^-$ to give the yellow dimer $[\{Tc^{VI}N(S_2CNEt_2)\}_2(\mu\text{-}O)_2]^\circ$. The neutral complex crystallizes in the triclinic space group $P\bar{1}$ with a=8.069(2), b=9.224(2), c=14.017(3) Å, α=107.77(2), β=102.05(2), γ=93.80(2)°, Z=2. The geometry is described as two square pyramids sharing an edge. The Tc≡N distances of 1.624 Å are almost identical. The short Tc–Tc distance of 2.543 Å and the Tc–O–Tc angles of about 82° indicate a metal–metal interaction. The Tc atoms are situated 0.65 Å above the corresponding S_2O_2 basal planes [65]. The formation of the di(μ-O)bridged $[\{TcN(S_2CNEt_2)\}_2(\mu\text{-}O)_2]^\circ$ is consistent with the formulation of the di-(μ-O) nitridotechnetic acid [66].

The coordination geometry of the complex $[\{TcN(S_2CNC_4H_8)\}_2(\mu\text{-}O)_2]^\circ$, containing pyrrolidinyl groups, was found to be almost identical with that of $[\{TcN(S_2CNEt_2)\}_2(\mu\text{-}O)_2]^\circ$. In addition, the di($\mu$-O) bridged anions $[\{TcN(CN)_2\}_2(\mu\text{-}O)_2]^{2-}$ and $[\{TcN(edt)\}_2(\mu\text{-}O)_2]^{2-}$ (H_2edt = ethane-1,2-dithiol) were synthesized. The EPR spectra of solutions of $[\{TcN(S_2CNEt_2)\}_2(\mu\text{-}O)_2]^\circ$ and $[\{TcN(S_2CNC_4H_8)\}_2(\mu\text{-}O)_2]^\circ$ in $SOCl_2$ and of $[AsPh_4]_2[\{TcN(CN)_2\}_2(\mu\text{-}O)_2]$ in acetonitrile with added

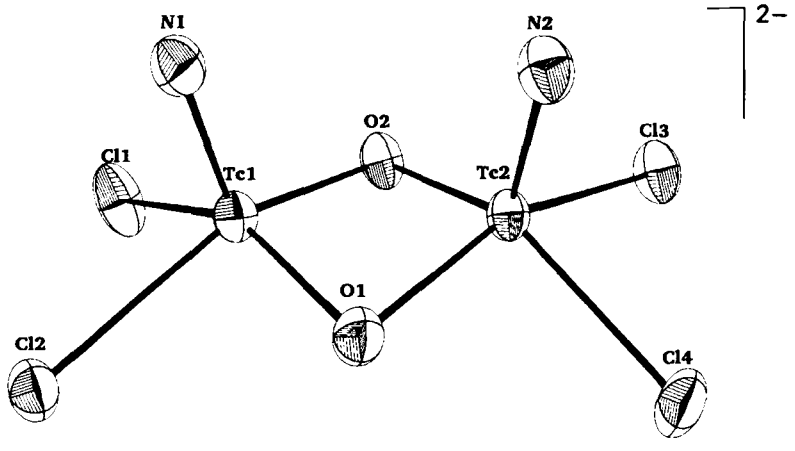

Fig. 12.7.A Bis(μ-oxo)-bis{dichloro-nitrido-technetate(VI)}, $[(\mu\text{-}O)_2(TcNCl_2)_2]^{2-}$. Bond distances Tc–Tc 2.579(1), Tc≡N 1.650(8), 1.648(8), Tc–Cl(average) 2.396 Å [56].

$[AsPh_4]Cl \cdot HCl$ revealed that cleavage of the dimers occurs to give the nitridotechnetium(VI) monomers $[TcNCl_2(S_2CNR_2)]^0$ (R = Et or C_4H_8) and $[TcNCl_2(CN)_2]^-$ [67].

A nitrido-oxalato complex of Tc(VI) of unique coordination features was synthesized by reaction of oxalic acid with $[AsPh_4][TcNCl_4]$ in aqueous acetone. The red-brown crystals of $[AsPh_4]_4[Tc_4N_4O_2(ox)_6]$ (ox = oxalate) crystallize in the monoclinic space group $P2_1/n$ with the cell parameters a=14.433(1), b=13.229(1), c=27.020(1) Å, β=92.90(1)°, and Z=4. The anion is a cyclic tetranuclear complex with C_i point symmetry. Each Tc(VI) atom is coordinated by five oxygens and one nitrogen yielding a distorted octahedron. In each half of the anion, a quadridentate oxalato ligand bridges the two octahedra. Each of the two octahedra is also linked to an adjacent octahedron by a bridging oxo ligand. Two oxygens of a bidentate oxalato ligand and one nitrido ligand complete the octahedral coordination for each Tc(VI) central atom (Fig. 12.8.A). The *trans* effect exerted by the nitrido ligands is manifested by the displacement of Tc(VI) above the plane of the four oxygen atoms by 0.36(1) Å for Tc(1) and 0.37(1) Å for Tc(2). The technetium nitrido bond lengths of 1.639(17) and 1.606(17) Å for Tc(1)–N(1) and Tc(2)–N(2), respectively, are similar to those observed in other nitrido complexes of Tc(VI). The Tc...Tc spacings of 3.586(2) and 5.756(3) Å preclude any Tc–Tc bonding. The bridging and terminal oxalato ligands are essentially planar. The complex anion represents a new oxalate-containing tetrameric coordination type with a twelve-membered macrocyclic ring. The Tc(VI) oxidation state could be confirmed by a magnetic moment of 1.64 B.M. per technetium atom, a value consistent with the presence of one unpaired *4d* electron [68].

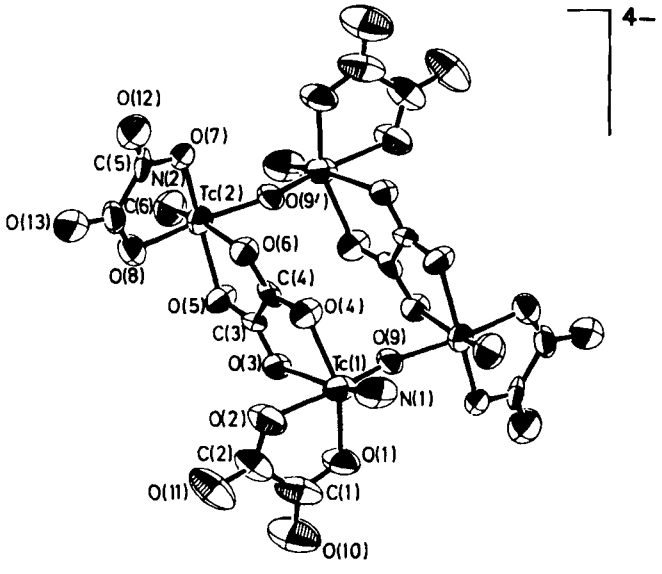

Fig. 12.8.A Cyclo-bis{μ-oxalato-(μ-oxo)-bis(nitrido-oxalato-technetate(VI)}, $[Tc_4N_4O_2(ox)_6]^{4-}$ [68].

12.2.4 Catecholato and thiolato complexes

NH_4TcO_4 reacts with an excess of 3,5-di-*tert*-butylcatechol in methanol to yield tris(3,5-di-*tert*-butylcatecholato)technetium(VI), $[Tc(dbcat)_3]^0$. Catechol serves as both a reducing agent and a chelating ligand. The neutral complex forms dark blue, air stable crystals of the monoclinic space group $P2_1/n$ and the unit cell dimensions a=15.892(3), b=15.878(4), c=16.367(3) Å, β=93.13(1)°, and Z=4. The molecule has the tris-chelated structure of C_3 symmetry. The coordination geometry of Tc(VI) is approximately octahedral. The average Tc–O bond length is 1.951 Å. The average ligand C–O bond distance of 1.334 Å is typical of values found for catecholate ligands. The magnetic moment of μ_{eff}=1.28 B.M. is considerably lower than the expected spin-only value of 1.73 B.M. Spin-orbit coupling effects may be the reason. $[Tc(dbcat)_3]^0$ exhibits a well resolved 10-line EPR spectrum in CH_2Cl_2 solution at room temperature and readily undergoes a reversible one-electron oxidation to an undefined cationic complex [69].

The unusual binuclear Tc(VI)/Tc(V) mixed-valence catecholato-hydrazido complex anion $[Tc_2(NNPh_2)_2(C_6Cl_4O_2)_4]^-$ was synthesized by reaction of $[n\text{-}(C_4H_9)_4N][Tc^{V}O(C_6Cl_4O_2)_2]$ with N,N-diphenylhydrazine in methanolic solution. Deep purple crystals of $[n\text{-}(C_4H_9)_4N][Tc_2(NNPh_2)_2(C_6Cl_4O_2)_4]\cdot CH_2Cl_2\cdot 2CH_3OH$ precipitated from dichloromethane. The substitution of the terminal oxo group may be formally described as a condensation type reaction. Since the average oxidation state of the Tc centers is 5.5, it would appear that the diphenylhydrazine serves as an oxidant as well as a ligating group. The structure of the binuclear anion consists of two distorted octahedral Tc centers bridged by two hydrazido(2-) groups (Fig. 12.9.A). The Tc–Tc bond length of 2.612(2) Å indicates a significant metal–metal interaction. The average Tc–N bond distance of 1.94(1) Å is consistent with considerable multiple-bond character. The N-N bond lengths of 1.311(13) and 1.297(13)Å are short in the Tc_2N_4 moiety. $[n\text{-}(C_4H_9)_4N][Tc_2(NNPh_2)_2(C_6Cl_4O_2)_4]\cdot CH_2Cl_2\cdot 2CH_3OH$ crystallizes in the triclinic space group $P\bar{1}$ with a=14.210(3), b=16.663(4), c=19.644(4) Å, α=76.82(2), β=80.52(2), γ=66.79(2)°, and Z=2 [70].

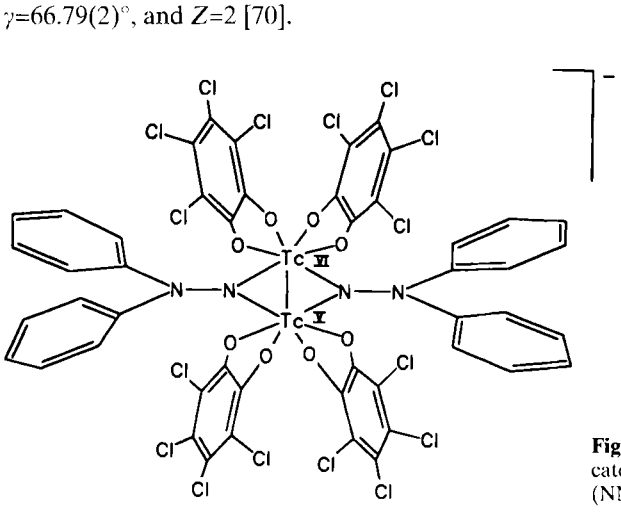

Fig. 12.9.A Binuclear Tc(V)/Tc(VI) catecholato-hydrazido complex, $[Tc_2(NNPh_2)_2(C_6Cl_4O_2)_4]^-$ [70].

The thiolato complex tris(2-aminobenzenethiolato)technetium(VI), $[Tc(NHC_6H_4S)_3]^\circ$ has attracted much attention [71–73]. The compound was prepared by reaction of NH_4TcO_4 with 2-aminobenzenethiol in aqueous 0.1 M HCl solution [71]. The green-black crystals are orthorhombic, space group $P2_12_12_1$, with a=10.696(2), b=11.363(1), c=15.220(2) Å, Z=4. The structure consists of dicrete $[Tc(NHC_6H_4S)_3]^\circ$ molecules, with the six-coordinated technetium atom bonded to the sulphur and nitrogen atoms. The complex is isostructural with the molybdenum analogue [74]. The arrangement of the 2-aminobenzenethiol ligands about Tc(VI) approximates a trigonal-prismatic geometry. The triangular faces are almost parallel. The distance of the technetium atom from the N_3 plane is 1.265(1) Å, from the S_3 plane 1.482(1) Å. The Tc–N bond distance on average is 1.995(11) Å, the average Tc–S distance 2.351(10) Å [72]. The EPR spectrum of $[Tc(NHC_6H_4S)_3]^\circ$, giving almost isotropic g values slightly greater than the free electron value and very small hyperfine coupling constants, indicate that the unpaired electron is in an orbital with mainly ligand character [71,73].

Tc(VI) complexes are reviewed in Table 12.2.A.

Table 12.2.A Some structural data of selected Tc(VI) complexes.

Complex	Geometry	Tc–L [Å]	μ_{eff} [B.M.]	References
12.2.1				
$(NO)_2[TcF_8]$	–	–	1.72	[32]
$NO_2[TcF_7]$	–	–	1.62	[32]
$[TcOCl_5]^-$	octahedral	–	–	[33]
12.2.2				
$[Tc_2(NAr)_6]^\circ$	ethane-like, staggered	2.744(Tc–Tc)	diamag.	[35,36]
$[\mu\text{-}NAr')_2Tc_2(NAr')_4]^\circ$	tetrahedral	2.673 (Tc–Tc)	diamag.	[35,36]
$[(\mu\text{-}NAr')_2Tc_2(NAr')_2Me_4]^\circ$	square pyramid	2.733 (Tc–Tc)	–	[37]
12.2.3				
$[TcNCl_4]^-$	square pyramid	1.581 (Tc≡N)	–	[38]
$[TcNBr_4]^-$	square pyramid	1.596(Tc≡N)	–	[38,39]
$[TcNCl_4(OH_2)]$	octahedral	–	–	[52]
$[TcNBr_4(OH_2)]$	octahedral	2.443 (Tc–OH_2)	–	[52]
$[TcNCl_5]^{2-}$	octahedral	2.740 (Tc–Cl_{trans})	–	[52]
$[(\mu\text{-}O)_2\{TcNCl_2\}_2]^{2-}$	square pyramid	2.579 (Tc–Tc)	diamag.	[64]
$[(\mu\text{-}O)_2\{TcN(S_2CNEt_2)\}_2]^\circ$	square pyramid	2.543 (Tc–Tc)	diamag.	[65]
$[(\mu\text{-}O)_2\{TcN(OH_2)_3\}_2]^{2+}$	octahedral	–	diamag.	[65]
$[(\mu\text{-}O)_2\{TcN(S_2CNC_4H_8)\}_2]^\circ$	square pyramid	2.542 (Tc–Tc)	diamag.	[67]
$[Tc_4N_4O_2(ox)_6]^{4-}$	octahedral	1.606–1.639 (Tc≡N)	1.64	[68]

Table 12.2.A Continued.

Complex	Geometry	Tc–L [Å]	μ_{eff} [B.M.]	References
12.2.4				
$[Tc(dbcat)_3]^0$	octahedral	1.951 (Tc–O)	1.28	[69]
$[Tc_2(NNPh_2)_2(C_6Cl_4O_2)_4]^-$	octahedral	2.612 (Tc–Tc)	paramag.	[70]
$[Tc(NHC_6H_4S)_3]^0$	trig. prism	1.995 (Tc–N) 2.351 (Tc–S)	paramag.	[71–73]

12.3 Technetium(V)

No oxidation state of technetium in complex compounds proves to be as frequently represented as Tc(V). The quite large number of publications is devoted to complexes containing the $(Tc{=}O)^{3+}$ core, followed by compounds characterized by the isoelectronic $(Tc{\equiv}N)^{2+}$. O^{2-} and N^{3-} are excellent π-electron donors that stabilize compounds of transition metals in high oxidation states, as has already been emphasized in preceding sections. In general, the coordination geometry of these complexes is defined by more or less distorted square pyramids, with the oxygen or nitrogen atom in the apical position. Oxygen was successfully replaced in a few examples by S^{2-} yielding a $(Tc{=}S)^{3+}$ core. Another characteristic core, established in numerous complex compounds, is the linear *trans*-oxo group $(O{=}Tc{=}O)^{+}$ forming distorted octahedral arrangements with ligands. In addition, several dinuclear Tc(V) complexes have been obtained, some of them contain the bridging $(O{=}Tc{-}O{-}Tc{=}O)^{4+}$ unit. Also, structurally interesting imido, hydrazido and diazenido compounds have been synthesized and identified. Hexafluorotechnetate(V) and diarsinetetrachlorotechnetate(V) are among the complexes that had been characterized already in very early investigations of technetium chemistry.

12.3.1 Hexafluoro complexes

When TcF_6, dissolved in iodine pentafluoride, is treated with an alkali chloride, reduction to Tc(V) takes place and the complex fluorides $M[TcF_6]$ (M=Na, K, Rb, Cs) crystallize from solution. The salts are bright yellow crystalline powders that are air sensitive and hydrolyzed by water. The rhombohedrally crystallizing alkali salts are reported to be not isostructural with the corresponding complex salts of rhenium, but $Na[TcF_6]$ and $K[TcF_6]$ proved to be isostructural with the analogous ruthenium salts $Na[RuF_6]$ and $K[RuF_6]$. The alkali hexafluorotechnetate(V) salts reveal magnetic moments close to those required by the Kotani theory, e.g. μ_{eff}=2.25 B.M., Θ=130°, for $Na[TcF_6]$ at 25 °C [75–77]. Hydrazinium hexafluorotechnetate(V), $[N_2H_6][TcF_6]_2$, was obtained by reduction of TcF_6 with $[N_2H_6]F_2$ in anhydrous H_2F_2 solution. It forms a yellowish orange salt [78].

12.3.2 Diarsine, benzenethiolato, and thiocarbamato complexes

The oxidation of $[Tc^{III}(diars)_2Cl_2]Cl$ {diars = 2-phenylene-bis-(dimethylarsine)} in alcoholic solution with molecular chlorine yields the corresponding eight coordinate, dark brown complex salt $[Tc^{V}(diars)_2Cl_4]Cl$. The oxidation state of Tc(V) was confirmed by titration with titanous chloride solution. The conductivity in nitrobenzene and the negligible magnetic moment (~0.9 B.M.) agree with this formulation [79]. Single crystals of $[Tc(diars)_2Cl_4]PF_6$ belong to the orthorhombic space group *Fddd*, Z=8, with a=13.821(4), b=21.159(8), c=21.227(18) Å. The structure of the $[Tc(diars)_2Cl_4]^+$ cation is shown in Fig. 12.10.A. The D_{2d} dodecahedral coordination geometry is the same as in the analogous eight-coordinate $[Ti(diars)_2Cl_4]^0$. The stability of $[Tc(diars)_2Cl_4]^+$ results mainly from the diars ligands which are known to promote high coordination numbers [80].

The blue complex salt *n*-tetrabutylammonium-(2-aminobenzenethiolate(2-)-*S,N*) tetrachlorotechnetate(V) $[n\text{-}Bu_4N][TcCl_4(abt)]$, can be isolated, when $[n\text{-}Bu_4N][TcO(abt)_2]$ is reacted with conc. HCl in the presence of methanol. The complex was found to have a magnetic moment of μ_{eff}=2.86 B.M., which corresponds to two unpaired electrons. In the IR a single N–H absorption occurs at 3252 cm^{-1}, which is consistent with the N–H proton. The molecular structure of the complex anion (Fig. 12.11.A) exhibits distorted octahedral geometry imposed by the 82.3(1)° bite angle of the abt ligand. The bond length of Tc–Cl(2) with 2.324(2) Å and Tc–Cl(3) with 2.322(2) Å are comparable to the Tc–Cl distance found for the nitrido analogue $[AsPh_4][TcNCl_4]$. All four Tc–Cl bond lengths in $[n\text{-}Bu_4N][TcCl_4(abt)]$ are shorter than the average Tc–Cl distance of 2.442(4) Å in the eight-coordinate Tc(V) complex cation $[Tc(diars)_2Cl_4]^+$ mentioned above. As a consequence of a *trans* structural effect of the thiolato ligand the longest of the four reported Tc–Cl bonds occurs for Tc-Cl(4) with 2.390(2) Å. The Tc–N bond length is 2.145(4) Å. The Tc–S distance of 2.322(2) Å falls within the range of values reported for Tc(V) square-pyramidal complexes. $[n\text{-}Bu_4N][TcCl_4(abt)]$ crystallizes in the triclinic space group $P\bar{1}$ with a=11.5154(8), b=13.6200(9), c=10.5547(8) Å, α=95.205(5)°, β=116.970(7)°, γ=76.198(4)°, and Z=2 [81].

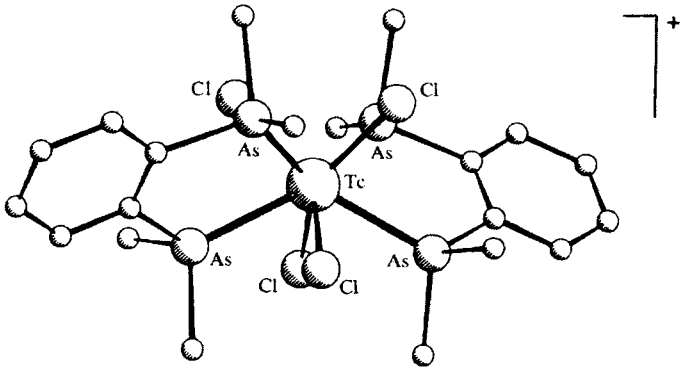

Fig. 12.10.A $[Tc^{V}(diars)_2Cl_4]^+$. Bond lengths Tc–Cl 2.442(4), Tc–As 2.578(2) Å; bond angles As–Tc–As 129.46(5), Cl–Tc–Cl 91.21(12)° [80].

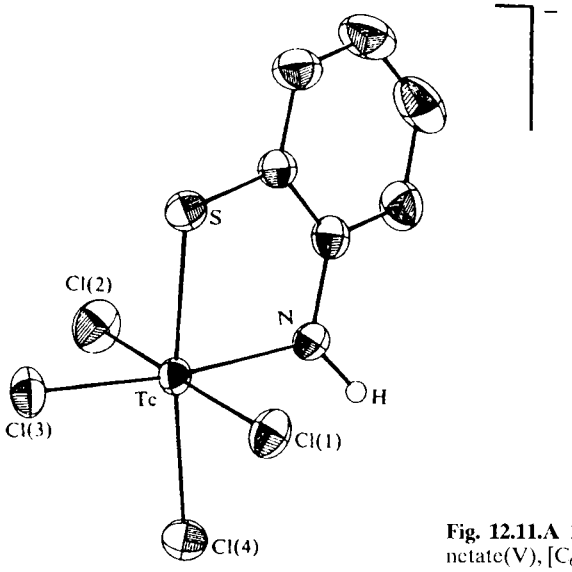

Fig. 12.11.A 2-Aminobenzenethiolato-tetrachlorotechnetate(V), $[C_6H_4SNHTeCl_4]^-$ [81].

Tris(benzene-1,2-dithiolato)technetate(V), $[Tc(bdt)_3]^-$, was synthesized by reaction of $[AsPh_4][TcNCl_4]$ with benzene-1,2-dithiol in acetone. Brown crystals of $[AsPh_4][Tc(bdt)_3]$ were isolated that crystallize in the monoclinic space group $P2_1/n$, with a=12.966(1), b=12.746(2), c=23.233(1) Å, β=92.27(8)°, and Z=4. Tc(V) is coordinated to six sulphur atoms in an almost ideal trigonal-prismatic geometry. The average angle between the TcS_2 planes of 119.4° is close to the expected value of 120°. The Tc–S distances range from 2.322(1) to 2.369(2) Å. The dithiol ligands and the TcS_2 planes are essentially coplanar [376].

Reaction of dicyclopentamethylenethiuram disulphide with $[TcOCl_4]^-$ in dichloromethane resulted in the formation of the tetrakis(cyclopentamethylenedithiocarbamate-S,S')technetium(V) cation with eight-coordinate Tc. The shape of the cation is a distorted square antiprism (Fig. 12.12.A) with Tc–S distances ranging between 2.463 and 2.494 Å. The four S–Tc–S angles are between 77.30 and 79.57°. $[Tc(C_6H_{10}NS_2)_4]Br \cdot C_3H_6O$ crystallizes in the monoclinic space group $C2/c$ with a=12.343(2), b=20.557(3), c=15.133(2) Å, β=103.42(1), and Z=4 [82].

Table 12.3.A Some structural data of Tc(V) complexes described in Sects. 12.3.1 and 12.3.2.

Complex	Geometry	Tc–L [Å]	μ_{eff} [B.M.]	References
12.3.1				
$[TcF_6]^-$	octahedral	–	2.25	[75–78]
12.3.2				
$[Tc(diars)_2Cl_4]^+$	dodecahedral	2.578(Tc-As) 2.442(Tc-Cl)	0.9	[79,80]

Table 12.3.A Continued

Complex	Geometry	Tc–L [Å]	μ_{eff} [B.M.]	References
$[Tc(abt)Cl_4]^-$	octahedral	2.145(Tc–N)	2.86	[81]
		2.322(Tc–S)		
$[Tc(bdt)_3]$	trig.prism	2.32–2.37(Tc–S)	-	[376]
$[Tc(C_6H_{10}NS_2)_4]^+$	square antiprism	2.463–2.494(Tc–S)	–	[82]

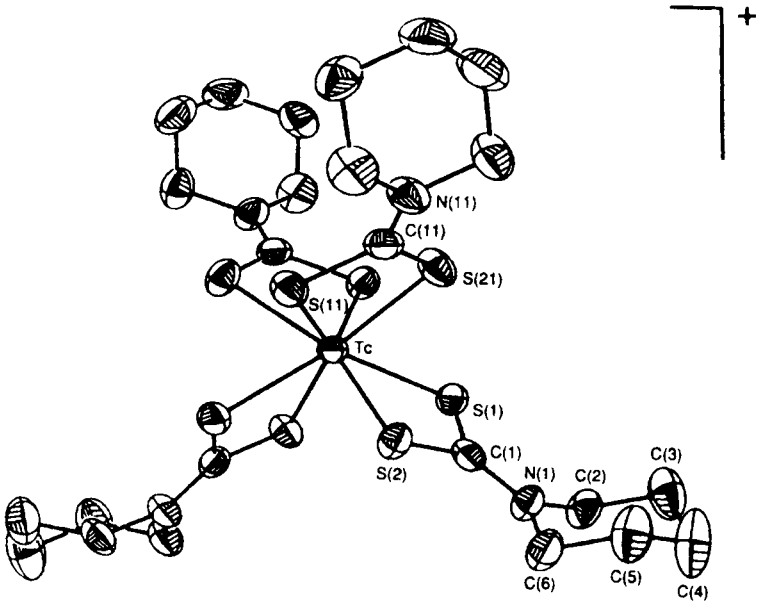

Fig. 12.12.A Tetrakis(cyclopentamethylenedithiocarbamate)technetium(V), $[Tc(C_6H_{10}NS_2)_4]^+$ [82].

12.3.3 $(TcO)^{3+}$-core complexes

12.3.3.1 Oxotetrahalogeno and oxopentahalogeno complexes

The reduction of TcO_4^- in aqueous HCl by hypophosphorous acid [83] or without H_3PO_2 in 12M HCl [84,85] yields a dark green solution of $[TcOCl_4]^-$, from which gray-green solids can be precipitated by addition of large cations like $[n\text{-}(C_4H_9)_4N]^+$ or $[(C_6H_5)_3PNP(C_6H_5)_3]^+$. $[n\text{-}(C_4H_9)_4N][TcOCl_4]$ is recrystallized from CH_2Cl_2/hexane to obtain large green plates. The complex salt dissolves readily in polar organic solvents such as methanol, acetone, dichloromethane, and acetonitrile. Upon addition of water it disproportionates rapidly to form TcO_4^- and TcO_2-hydrate [85]. The crystal structure of $[Ph_4As][TcOCl_4]$ was determined. The crys-

tals are tetragonal, space group $P4/n$, a=12.664(1), c=7.822(1) Å, and Z=2. The $[TcOCl_4]^-$ anion possesses ideal C_{4V} symmetry (Fig. 12.13.A). The Tc atom is located in a square-pyramidal arrangement with the chloro ligands occupying the basal position and the oxo ligand at the apex. The Tc=O bond length of 1.593(8) is not significantly different from the Tc≡N bond length of 1.581(5) Å in $[Ph_4As][TcNCl_4]$, but the Tc–Cl bond length of 2.309(2) is slightly shorter than that of 2.322(1) Å in the nitrido complex salt. This is indicative of a stronger electronic influence of the nitrido ligand compared with that of the oxo ligand. Conversely, the oxo ligand apparently has a larger steric requirement as shown by the O=Tc–Cl angles of 106.8(1)° and the displacement of the Tc atom of 0.67 Å from the basal plane [86,46].

$[n\text{-}(C_4H_9)_4N][TcOBr_4]$ was prepared by reaction of $[n\text{-}(C_4H_9)_4N]TcO_4$ with conc. HBr. The gold red crystals dissolve in dichloromethane, acetone, and methanol [84,87]. $[Ph_4As][TcOBr_4]$ proved to be isostructural with $[Ph_4As][TcOCl_4]$. The Tc=O length is 1.613(9), the Tc–Br distance 2.460(1) Å [88]. The square pyramid of $[TcOBr_4]^-$ can be capped by a water molecule leading to the distorted octahedron of $[TcOBr_4(H_2O)]^-$, which was obtained by reduction of NH_4TcO_4 with 48 % HBr at –5 °C. Tetraethylammonium bromide produced a dichroic green orange precipitate. $[(C_2H_5)_4N][TcOBr_4(H_2O)]$ crystallizes in the orthorhombic space group *Pnma*. X-ray diffraction analysis revealed that the four bromine atoms in $[TcOBr_4(H_2O)]^-$ define a nearly square plane to which the O=Tc–OH_2 spine stands perpendicularly. The water oxygen atom is weakly bound below the plane at a Tc–OH_2 distance of 2.317(9) Å [89].

$[n\text{-}(C_4H_9)_4N][TcOI_4]$ was obtained from the corresponding oxochloro complex by ligand exchange reaction with NaI in acetone. The reduction of TcO_4^- with conc. HI yielded products always contaminated with polyiodides. $[n\text{-}(C_4H_9)_4N][TcOI_4]$ forms dark gold-brown crystals [90].

The $[TcOX_4]^-$ anions are versatile intermediates for the synthesis of a variety of oxotechnetium(V) complexes [91].

The vibrational spectra of the tetrabutylammonium salts of $[TcOCl_4]^-$, $[TcOBr_4]^-$, and $[TcOI_4]^-$ indicate C_{4V} symmetry for the complex ions (Table 12.4.A).

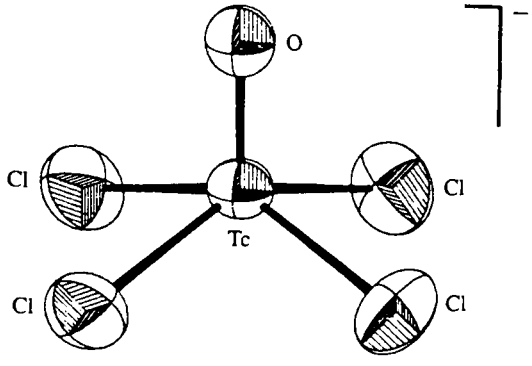

Fig. 12.13.A Tetrachloro-oxotechnetate(V), $[TcOCl_4]^-$ [86].

Table 12.4.A IR and Raman frequencies [cm $^{-1}$] of $[TcOX_4]^-$ (X=Cl, Br or I) in $[(C_4H_9)_4N][TcOX_4]$ [84,90].

	$[TcOCl_4]^-$	$[TcOBr_4]^-$	$[TcOJ_4]^-$	Assignment
ν_1	1026 Ra,p 1037	1016 Ra,p 1027	996 Ra,p	$\nu(TcO)(A_1)$
ν_1	1020 IR,vs	1015 IR,vs	993 IR,vs	$\nu(TcO)(A_1)$
ν_8	397 IR,vs	317 IR,vs	274 IR,s	$\delta(XTcO)(E)$
ν_2	361 Ra,p	237 Ra,p	179 Ra,p	$\nu_s(TcX_4)(A_1)$
ν_7	316 IR,s	215 IR,vs	157 IR,s	$\nu_{as}(TcX_4)(E)$
ν_4	312 Ra,dp	200 Ra,dp	135 Ra,dp	$\nu(TcX_4)(B_1)$
ν_9	189 IR,s	158 IR,s	101 IR,w	$\delta(XTcX)(E)$

Force constants and mean amplitudes of vibration were evaluated. The Tc=O bond proved to be by far the strongest, exhibiting force constants of more than 8 mdyne/Å [92].

When TcO_4^- is reduced by conc. HCl or HBr, the reaction solution can yield salts of either $[TcOX_4]^-$ or $[TcOX_5]^{2-}$ depending on the counterion. Addition of $[Ph_4As]^+$ or $[n\text{-}(C_4H_9)_4N]^+$ yields salts of $[TcOX_4]^-$, while addition of K^+, NH_4^+, Cs^+, or $[(C_2H_5)_4N]^+$ generates salts of $[TcOX_5]^{2-}$. Analysis of the Raman spectrum of a 12 M HCl solution containing a $[TcOCl_4]^-/[TcOCl_5]^{2-}$ equilibrium mixture leads to an estimated equilibrium constant of $(1.5\pm1.0)\cdot10^{-3}$ M^{-1} [93]. $Cs_2[TcOCl_5]$ was prepared by adding CsCl to a warm solution of $NaTcO_4$ in conc. HCl [94] or by reaction of NH_4TcO_4 with 12 M HCl at ambient temperature and addition of CsCl to the reaction solution cooled to 0 °C, yielding a light olive green precipitate [93]. Orange-red $Cs_2[TcOBr_5]$ was obtained when 48 % HBr was reacted at −8 °C with NH_4TcO_4 and the formed complex precipitated by addition of CsBr [93]. X-ray powder diffraction measurements revealed $Cs_2[TcOCl_5]$ and $Cs_2[TcOBr_5]$ to crystallize in a cubic system with the lattice constants of a=10.199(1) and a=10.672(3) Å, respectively [94].

Almost 20 years earlier the preparation of $(NH_4)_2[TcOCl_5]$ by reaction of NH_4TcO_4 with 12 M HCl was reported. The identified compound proved to be diamagnetic, which was explained as a result of splitting of the t_{2g} orbital and the formation of the non-degenerate b_{1g} ground level in the tetragonal ligand field [95,96]. The spectra of $(NH_4)_2[TcOCl_5]$, $K_2[TcOCl_5]$, and $Cs_2[TcOCl_5]$ in the UV, VIS, and IR were recorded and interpreted [97]. The Raman and IR frequencies of $[TcOCl_5]^{2-}$ and $[TcOBr_5]^{2-}$ and their tentative assignments are listed in Table 12.5.A.

Table 12.5.A Vibrational frequencies of $Cs_2[TcOCl_5]$ and $Cs_2(TcOBr_5]$ in [cm $^{-1}$]. The estimated relative Raman intensities are given in parentheses [98].

$Cs_2[TcOCl_5]$		$Cs_2[TcOBr_5]$		Tentative
Raman	IR	Raman	IR	assignment
953(3)	956 vs	931(3)	962 vs	$\nu(TcO),\nu_1(A_1)$
352(3)	339 sh	263(2)	262 sh	
341(4)	330 vs	241(4)	248 vs	$\nu(TcX),\nu_2(A_1)$,
330(1)	323 sh	230(1)	239 sh	$\nu_3(A_1),\nu_5(B_1)$,
303(1)	303 sh	220(1)	218 sh	$\nu_8(E)$

Table 12.5.A Continued

$Cs_2[TcOCl_5]$		$Cs_2[TcOBr_5]$		Tentative
Raman	**IR**	**Raman**	**IR**	**assignment**
238 (5)	230 sh	211 sh	210 sh	δ(OTcX),$\nu^9(E)$
219 (10)	222 vs	194 (7)	192 vs	
193 (1)	194 s	132 (3)	120 m	-
174 (2) 169 (2)	175 s	120 sh	115 s	δ(XTcX),$\nu_4(A_1)$,$\nu_6(B_1)$, $\nu_7(B_2)$,$\nu_{10}(E)$,$\nu_{11}(E)$
134 (2)	131 m	104 (2)	92 w	-
115 (5)	96 m	80 (1)	70 w	lattice vibrations
36 (1)	46 m	50 (0.5)	49 w	

12.3.3.2 Oxocyano and oxothiocyanato complexes

When a suspension of TcO_2-hydrate in water is reacted with a hot aqueous solution of KCN, a honey-colored solution is obtained. After addition of methanol, greenish yellow crystals of $K_2[TcO(CN)_5]\cdot 4H_2O$ were isolated which hydrolyzed in aqueous solution slowly in the absence of cyanide ions to form $K_3[TcO_2(CN)_4]$. Reaction of $[TcOCl_4]^-$ with CN^- ions in methanol produced *trans*-oxomethoxy-tetracyanotechnetate(V), $[TcO(OMe)(CN)_4]^{2-}$. Its $[n\text{-}(C_4H_9)_4N]^+$ salt formed lilac needles. The Tc=O stretch of the methoxide complex appeared at 932 cm^{-1}, while that of $[TcO(CN)_5]^{2-}$ occured at 910 cm^{-1} [99].

Oxotetracyanoaquotechnetate(V), $[TcO(OH_2)(CN)_4]^-$, was obtained in acid solution by protonation of $[TcO_2(CN)_4]^{3-}$ and precipitated with $[(CH_3)_4N]^+$ to form blue crystals of $[(CH_3)_4N][TcO(OH_2)(CN)_4]\cdot 2H_2O$. The compound crystallizes in the orthorhombic space group *Pmnn* with a=12.11, b=9.04, c=7.10 Å, and Z=2, and is isostructural with the analogous complex salt of Re(V). In $[TcO(OH_2)(CN)_4]^-$ the aquo ligand is displaced upon reaction with excess thiocyanate.

$$[TcO_2(CN)_4]^{3-} \xleftarrow{2H^+} [TcO(OH_2)(CN)_4]^- \xleftarrow{NCS^-} [TcO(NCS)(CN)_4]^{2-} + H_2O$$

By addition of 2,2'-bipyridine to the reaction solution the complex salt $(2,2'\text{-bpyH})_2[TcO(NCS)(CN)_4]$ was obtained in form of green needles, crystallizing in the monoclinic space group *C2/c* with a=18.210(4), b=19.473(1), c=15.501(3) Å, β=107.507(14)°, and Z=8. The structure consists of discrete $[TcO(NCS)(CN)_4]^{2-}$ and monoprotonated 2,2'-bipyridinium ions. The NCS^- ligand is coordinated via the nitrogen atom (Fig. 12.14.A). The coordination geometry is a distorted octahedron that is very similar to the coordination mode observed for $[ReO(NCS)(CN)_4]^{2-}$. The slightly shorter Tc=O bond length of 1.612(8) Å is accompanied by a longer *trans*-Tc–NCS bond of 2.162(9) Å reflecting the greater structural *trans* effect exerted by the stronger Tc=O linkage [100].

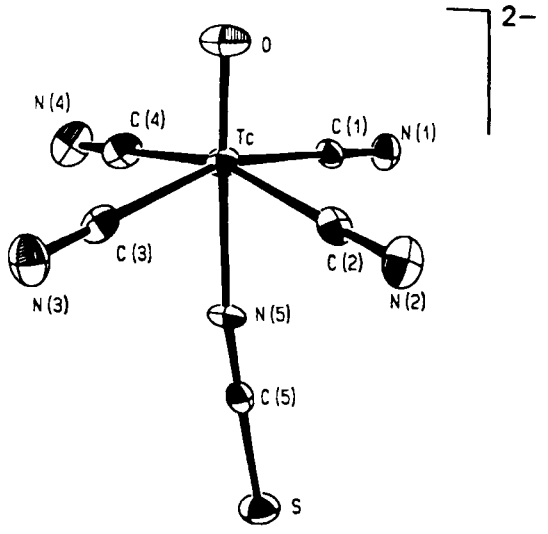

Fig. 12.14.A Tetracyano-isothiocyanato-oxotechnetate(V). $[TcO(NCS)(CN)_4]^{2-}$ [100].

Oxopentakis(isothiocyanato)technetate(V), $[TcO(NCS)_5]^{2-}$ was obtained by substitution of chloride in $[TcOCl_4]^-$ with thiocyanate ions. The reaction of a methanol solution of $[n\text{-}(C_4H_9)_4N][TcOCl_4]$ with five equivalents of NH_4SCN, followed by precipitation with $[Ph_4As]^+$, yielded a bright red microcrystalline solid of $[Ph_4As]_2[TcO(NCS)_5]$. The magnetic moment of μ_{eff}= 1.04 B.M. at 298 K is difficult to interpret. In the presence of excess SCN^-, $[TcO(NCS)_5]^{2-}$ is easily reduced to mixtures of both $[Tc(NCS)_6]^{2-}$ and $[Tc(NCS)_6]^{3-}$ [101].

12.3.3.3 $TcO(O_4)$-, $TcO(O_2Cl)$-, $TcO(O_2Cl_3)$-, and $TcO(O_5)$-core complexes

The existence of the first core was verified by the oxoglycolate complex $[TcO(OCH_2CH_2O)_2]^-$ that was prepared by reacting $[TcOCl_4]^-$ with excess ethylene glycol in an alkaline medium. $[n\text{-}(C_4H_9)_4N][TcO(OCH_2CH_2O)_2]$ forms violet crystals that are very soluble in water, alcohols, acetone or benzene, insoluble in ether and hexane. The complex is hydrolytically unstable in water and decomposes in aqueous solution at pH<10. Since the glycolate ligands are readily exchanged, the complex is useful for sythesizing new oxotechnetium(V) compounds [102,103].

Several catecholato complexes containing the $O{=}Tc(O)_4$-core have been synthesized and structurally identified. Catechol and $[TcOCl_4]^-$ react in methanol to produce a red-purple reaction mixture from which, after treating with NaOH and *n*-tetrabutylammonium chloride, golden crystals of $[n\text{-}(C_4H_9)_4N][TcO(O_2C_6H_4)_2]$ were obtained. The crystals are monoclinic, space group *C2/c*, with cell dimensions a=10.393(3), b=13.835(3), c=20.643(5) Å, β=101.74(3)°, and Z=4. The coordination geometry of the anion is square pyramidal with a short Tc=O bond of 1.648(5) Å and the longer Tc–O distances of 1.956(3) and 1.958(3) Å to the catechol groups. The Tc atom lies 0.7014(4) Å out of the plane of the four catechol oxygen atoms. Each pair of the cate-

chol oxygens is almost coplanar with their benzene ring. The rings are bent away from the oxo group, forming a dihedral angle of 162° with the base of the square pyramid. In contrast to the oxoglycolate complex, the oxocatecholate anion decomposes only minimally in pure water [102]. In order to facilitate the deprotonation of the catechol ligand, 4-nitro-1,2-catechol was used for chelating the $Tc{=}O^{3+}$ core. The coordination geometry of $[TcO(O_2C_6H_3NO_2)_2]^-$ is again square pyramidal exhibiting similar bond distances as described above for the catechol complex containing no nitro groups [104]. The same applies to the diamagnetic oxo-bis(tetrachlorocatecholatotechnetate(V), $[TcO(O_2C_6Cl_4)_2]$ [70]. Tc^VOL_4 complexes of C_{4V} symmetry are expected to be spinpaired and diamagnetic [91].

Neutral Tc(V) complexes containing the bidentate, monobasic ligands 2-methyl-3-oxy-4-pyronate (Hhmpo) or 1,2-dimethyl-3-oxy-4-pyridinonate (Hdpp) were synthesized by ligand substitution on $[TcOCl_4]^-$. The greenish yellow crystalline $[TcO(hmpo)_2Cl]^\circ$ and the red $[Tc(dpp)_2Cl]^\circ \cdot 0.5H_2O$ were identified. Depending on the reaction conditions also the complex anion $[TcO(hmpo)Cl_3]$ can be prepared. $[(n\text{-}Bu)_4N][TcO(hmpo)Cl_3]$ crystallizes in the monoclinic space group $P2_1/c$ with a=10.724(2), b=11.327(2), c=23.651(2) Å, β=101.46(1)°, and Z=4. The coordination is highly distorted octahedral. The oxo oxygen and the negatively charged oxy oxygen donor of the hmpo ligand occupy *trans* positions subtending an angle at Tc of 162.3(1)°. The three chloro ligands and the ketonic oxygen donor form an equatorial plane, out of which Tc is displaced by about 0.2 Å toward the oxo oxygen. The distortions from octahedral geometry are primarily due to the bite angle of 76.08° of the hmpo ligand. The mean Tc–Cl distance is 2.359 Å [105].

Reation of $[(n\text{-}Bu_4)N][TcOCl_4]$ with oxalic acid in aqueous acetone and addition of $[Ph_4As]Cl$ gave a pale green, crystalline, diamagnetic product of the composition $[Ph_4As]_2[Tc^VO(ox)_2(Hox)] \cdot 3H_2O$. The complex anion is unusual in that it contains the unidentate oxalato group (Hox) . The Tc atom is coordinated by six oxygen atoms to give a distorted octahedron (Fig. 12.15.A). The unidentate group Hox is coordi-

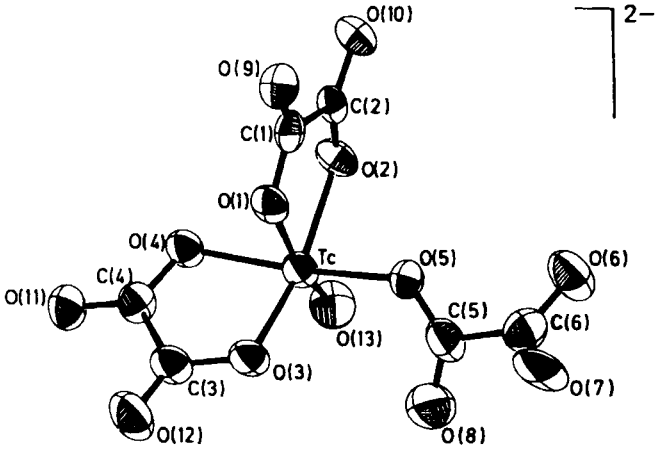

Fig. 12.15.A Hydrogenooxalato-bis(oxalato)oxotechnetate(V), $[TcO(ox)_2(Hox)]^{2-}$ [68].

nated to the Tc atom via the oxygen O(5) with the Tc–O(5) distance of 2.031(6) Å. The adjacent O(8) is not coordinated, since the Tc···O(8) spacing is 3.234(9) Å. The bond length in the Tc=O group is 1.640(6) Å. While the two bidentate oxalato ligands are essentially planar, the unidentate oxalato ligand is severely distorted from planarity. The six-coordinate structure is unexpected in view of the preference of the $(TcO)^{3+}$-core to form square-pyramidal complexes. $[Ph_4As]_2[TcO(ox)_2(Hox)]\cdot 3H_2O$ crystallizes in the monoclinic space group $P2_1/c$ with the lattice constants a=16.495(3), b=14.802(2), c=21.805(4) Å, β=98.76(1)°, and Z=4 [68].

12.3.3.4 $TcO(S_4)$-, $TcO(OS_3)$-, $TcO(O_2S_2)$-, $TcO(Se)_4$-, and $TcO(S_2Se_2)$-core complexes

The reduction of NH_4TcO_4 in ethanol with sodium borohydride in the presence of aliphatic dithiols yielded the bright orange oxo-bis(dithiolato)technetate(V) complexes $[TcO(SCH_2CH_2S)_2]$, $[TcO(SCH_2CH_2CH_2S)_2]$, and $[TcO(SCH_2CHCH_3S)_2]$, which were conveniently precipitated upon addition of $[Ph_4As]^+$. The X-ray structure of $[Ph_4As][TcO(SCH_2CH_2S)_2]$ was solved in the orthorhombic space group *Pbca* with a=19.669(3), b=18.745(4), c=15.122 Å, and Z=8. The structure of the anion shows a coordination geometry around the Tc(V) close to square pyramidal. The four sulphur atoms form a square base with the Tc atom 0.761(2) Å above the base. The average Tc–S bond distance is 2.30(1) Å. The oxygen atom constitutes the apex of the square pyramid with a Tc–O bond distance of 1.64(1) Å [106]. The oxo-bis(dithiolato)technetate(V) complexes were found to be weakly paramagnetic and to possess magnetic moments that are field-strength dependent. The complexes have been characterized by UV, VIS, IR, Raman, and NMR spectroscopy [107].

When $[n\text{-}Bu_4N]^+$ is added to the aqueous reaction mixture of thioglycolate with TcO_4^-, a yellow-brown crystalline precipitate of the thiomercaptoacetato complex salt $[n\text{-}Bu_4N][TcO(SCH_2COS)_2]$ is obtained instead of the expected corresponding thioglycolate complex. Mercaptothioacetic acid is suggested to be a significant impurity in commercial thioglycolic acid. The complex compound crystallizes in the monoclinic space group C_m with the lattice dimensions a=10.451(5), b=14.855(8), c=9.927(7) Å, β=114.88(5)°, and Z=2. The Tc atom is coordinated by the apical oxo oxygen and four sulphur atoms in a near square pyramid. The Tc=O bond distance of 1.672(8) Å is slightly greater than that in $[Ph_4As][TcO(SCH_2CH_2S)_2]$. $[n\text{-}But_4N][TcO(SCH_2COS)_2]$ was also found to be weakly paramagnetic and the effective moment of 1.2–1.5 B.M. to be field strength dependent [108].

Dithiooxalate ligands $(SCOCOS)^{2-}$ react with $[TcOCl_4]^-$ in acetone to form $[TcO(SCOCOS)_2]^-$. Addition of $[Ph_4As]^+$ yields red-brown $[Ph_4As][TcO(SCOCOS)_2]$ [109]. Crystals of the complex salt belong to the triclinic space group $P\bar{1}$ with Z=2. The lattice parameters are a=12.294(2), b=12.531(2), c=13.071(2) Å, α=115.10(1), β=114.22(1), γ=101.93(1)°. The geometry about the Tc atom is again distorted square pyramidal with the oxo oxygen occupying the apical position. The distortion arises from the large *trans* influence of the oxo ligand and is manifested by the displacement

of the Tc atom from the basal plane by 0.759 Å. The Tc=O bond distance of 1.646(4) Å and the Tc–S bond length of 2.329(1) Å are consistent with other Tc(V) complexes containing the $O=Tc(S)_4$ core [110].

The reaction of benzene-1,2-dithiol (H_2bdt) with $[Ph_4As][TcOCl_4]$ in aqueous ethanol resulted in the red-brown complex salt $[Ph_4As][TcO(bdt)_2]$ with m.p. 208–210 °C. $[Ph_4As][TcO(bdt)_2]$ crystallizes in the monoclinic space group *Cc* with a=12.652(1), b= 15.783(1), c=16.662(1) Å, β=93.03(1)°, and Z=4. The Tc atom lies 0.732(1) Å above the plane of the four sulphur atoms. The sulphur and carbon atoms are located in two different planes. The dihedral angle of 164.91(1)° between the normals of the planes renders a butterfly conformation to the complex anion [111].

$[Ph_4As][TcOCl_4]$ reacts with 1,2-dicyanoethenedithiolate $\{C_2(CN)_2S_2\}^{2-}$ in ethanol to yield red-brown crystals of $[Ph_4As][TcO\{C_2(CN)_2S_2\}_2]$ that are monoclinic and belong to the space group $P2_1/c$ with a=12.636(1), b=13.749(1), c=18.484(1) Å, β=93.49(1)°, and Z=4. The structure of the $[TcO\{C_2(CN)_2S_2\}_2]^-$ anion shows again a distorted square pyramidal core. The Tc atom is placed 0.742(3) Å above the plane of the four sulphur atoms. The anion conformation is similar to that in $[TcO(bdt)_2]$ described before [112].

Monodentate aromatic thiols ArSH {Ar = 2,4,6-$(CH_3)_3C_6H_2$, 2,4,6-$(CH_3CHCH_3)_3C_6H_2$, and 2,6-$(C_6H_5)_2C_6H_3$)} react in methanol with $[TcOCl_4]^-$ to produce the complexes $[TcO(ArS)_4]^-$ that may be precipitated with bulky organic cations. $[n\text{-}Bu_4N][TcO\{(CH_3)_3C_6H_2S\}_4]$ forms red-brown needles that crystallize in the monoclinic space group *C2/c* with a=21.909(6), b=17.366(5), c=14.348(7) Å, β=100.67(3)°, and Z=4. The $O=Tc(S)_4$ core adopts the expected square pyramidal geometry (Fig. 12.16.A). The Tc=O

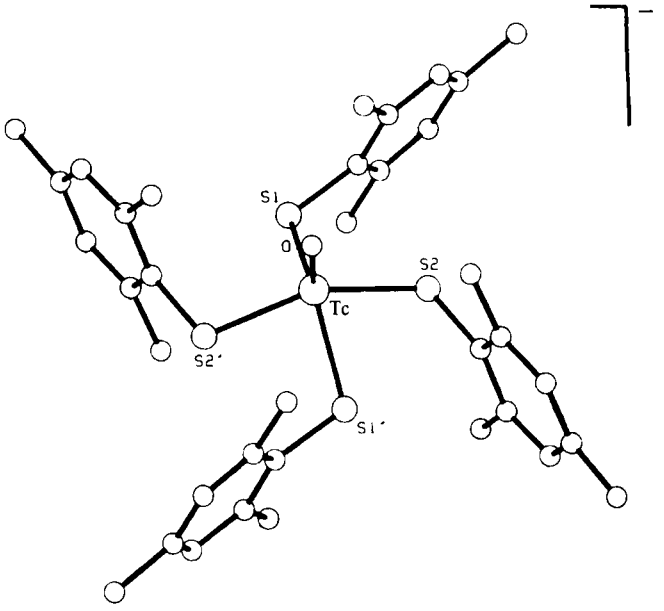

Fig. 12.16.A Tetrakis(2,4,6-trimethylbenzenethiolato)oxotechnetate(V). $[TcO(2,4,6\text{-}Me_3C_6H_2S)_4]$ [113].

distance is 1.659(11) Å and the average Tc–S distance 2.38(2) Å. The Tc atom is displaced by 0.846 Å from the basal plane towards the apical oxygen. The average *cis* S–Tc–S, *trans* S–Tc–S and O–Tc–S angles are 82.7(6), 138.4(3)°, and 110.8(4)°, respectively [113]. Another complex salt containing a monodentate aromatic thiol is the red $[Ph_4As][TcO(tmbt)_4]$ (Htmbt = 2,3,5,6-tetramethylbenzenethiol). The complex salt is readily prepared by reaction of $[Ph_4As][TcOCl_4]$ with Htmbt [114].

By reaction of TcO_4^- in 2 M HCl with reducing and complexing tetramethylthiourea (tmtu) the cationic complex $[TcO(tmtu)_4]^{3+}$ is generated which precipitates as the red-orange $[TcO(tmtu)_4][PF_6]_3$. Obviously, tetramethylthiourea ligates through the terminal sulphido groups [115]. $[TcO(tmtu)_4][PF_6]_3$ reacts in a DMF solution of bis(diphenylphosphino)ethane (dppe) to form a brown crystalline product that was identified as $[Tc^{V}O(tmtu)_2(CH_3)_2NCSS][PF_6]_2$. The complex contains a bidentate dimethyldithiocarbamate ligand produced from the rearrangement of bonded tetramethylthiourea. The crystals are monoclinic with the space group $P2_1/c$, a=9.388(4), b=26.745(20), c=11.990(3) Å, β=101.62(3)°, and Z=4. The geometry around the Tc atom is square pyramidal. The Tc–O bond distance is 1.661(6) Å. The Tc–S bond lengths are 2.328(2) and 2.343(2) Å for the tetramethylthiourea ligands and 2.349(2) and 2.353(2) Å for the dimethyldithiocarbamate ligand [116].

In addition, several Tc(V) complexes based on the $O{=}Tc(S)_4$-core have been prepared. The preparation was achieved by exchange reaction of Tc(V) gluconate with various dithiols in aqueous ethanolic solution. The oxo-dithiolatotechnetate(V) complexes were mostly precipitated as the $[Et_4N]^+$ salts. The complex compounds turned out to be diamagnetic in solution, and have probably square pyramidal structure [117,118,119]. Stereoisomeric complexes derived from *meso* and *racemic* 2,3-dimercaptosuccinic acid dimethylester were identified by ^1H NMR [120]. The kinetics of the reaction between pertechnetate and *meso*- or *racemic* dimercaptosuccinic acid in hydrochloric acid solution were studied. The reaction was found to be first order in each reactant [121]. Also the reaction of pertechnetate with para-substituted benzene thiols was followed and showed a simple second order kinetics. The reaction rate decreased when the substituent became more electron-withdrawing [122].

Because *racemic* 2,3-dimercapto-succinic acid (DMSA) by reaction with reduced $^{99m}TcO_4^-$ leads to a product that is excreted by the kidneys, whereas the ^{99m}Tc complex with *meso*-DMSA was found to be osteotropic, an important experiment was to find the molecular structure of the dimethylester of the latter complex containing long-lived ^{99}Tc. The complex anion was prepared by ligand exchange reaction of technetium(V) gluconate with *meso*-2,3-dimercaptosuccinic acid dimethylester. Red crystals of the tetraethylammonium salt were obtained, crystallizing in the monoclinic space group $P2_1/c$ with a=12.722(3), b=13.820(4), c= 18.213(5) Å, β= 107.13(4)°, and Z=4. The structure of $[TcO\{SCH(CO_2Me)CH(CO_2Me)S\}_2]^-$ confirms the nearly square pyramidal coordination geometry of Tc(V) (Fig. 12.17.A) with the sulphur atoms forming the basal plane. The Tc atom lies 0.78 Å above this plane. The Tc=O bond length is 1.672(6) Å, the average Tc–S bond distance 2.316 Å. The structure reveals the *endo* form of the *syn* isomer. The *syn* isomer has the four carboxylic groups on one side of the molecule, allowing strong interaction between the carboxylic groups and bone [123].

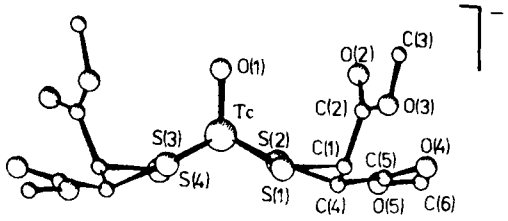

Fig. 12.17.A Bis-{1,2-di(carbomethoxy)ethane-1,2-di-thiolato}oxotechnetate(V). $[TcO\{SCH(CO_2Me)CH(CO_2Me)S\}_2]^-$, *syn-endo* form [123].

The tridentate ligand 3-thiapentane-1,5-dithiol, $HS(CH_2)_2S(CH_2)_2SH$, and thiophenol in an equimolar ratio react with Tc(V)gluconate in acetone to form a brown solid of oxo-(3-thiapentane-1,5-dithiolato)(thiophenolato)technetate(V). Spectroscopic characterization points to a $TcO(S_4)$-core [124]. In place of thiophenol other monodentate thiols were also used for complexation, and 3-thiapentane-1,5-dithiol was replaced by $HS(CH_2)_2O(CH_2)_2SH$ resulting in $TcO(OS_3)$-core complexes [125].

Instead of sulphur donor atoms the MoS_4^{2-} anion was coordinated to oxotechnetium(V). The pale yellow complex salt $[Bu_4N][Tc^VO(MoS_4)_2]$ was obtained by treating $[Bu_4N][TcOCl_4]$ in methanol with a methanolic solution of $(NH_4)_2[MoS_4]$. $[Bu_4N][TcO(MoS_4)_2]$ is diamagnetic and soluble in EtOH and DMF. It exhibits an intense IR absorption at 895 cm^{-1} that is attributed to the Tc=O stretch [126].

The substitution of sulphur by oxygen in Tc(V) complexes containing the $TcO(S)_4$-core was early demonstrated in the preparation of bis(2-mercapto-ethanolato)oxotechnetate(V). Reduction of TcO_4^- by $S_2O_4^{2-}$ in aqueous alkaline solution in the presence of 2-mercaptoethanol and subsequent addition of $[Ph_4As]^+$ yielded a metallic pink crystalline precipitate of $[Ph_4As][TcO(SCH_2CH_2O)_2]$. The X-ray structure analysis of the complex salt revealed a pseudo-square pyramidal coordination geometry for the technetium atom. The basal plane is distorted toward a trapezoid because of the difference between the average Tc–O and Tc–S distances of 1.950(4) and 2.291(2) Å, respectively. The Tc distance to the basal plane of 0.720(1) Å is considerably shorter than that in $[TcO(SCH_2CH_2S)_2]^-$. The Tc=O distance is 1.64(1) Å, the S–Tc–S and O–Tc–O angles are 86.09(7) and 79.8(2)°, respectively. Although the *cis* form of the complex was isolated, there is no doubt about the existence of the *trans* isomer. $[Ph_4As][TcO(SCH_2CH_2O)_2]$ crystallizes in the orthorhombic space group *Pbca* with a=15.039(2), b=18.510(3), c=19.196(3) Å, and Z=8 [127]. The ligand exchange reactions of $[TcO(OCH_2CH_2O)_2]^-$, $[TcO(OC_6H_4O)_2]^-$ and $[TcO(SCH_2CH_2O)_2]^-$ with two equivalents of 1,2-ethanediol in methanol ultimately yielded $[TcO(SCH_2CH_2S)_2]^-$ [128].

Metallothioneins, sulphur-rich metal-binding proteins, offer promise as carrier of ^{99m}Tc in radiolabeling of biologically active molecules. Metallothionein binds Tc(V) in a thermodynamically stable and kinetically inert thiolate complex. As demonstrated spectroscopically, the TcO^{3+}-core is bound in square pyramidal geometry to give the $TcOS_4^-$ stoichiometry [129].

Using the ligand 1,1-dicyanoethene-2,2-diselenolate, $\{(CN)_2C{=}CSe_2\}^{2-}$, for ligand exchange reaction in aqueous solution with Tc(V) gluconate, the diselenato-complex

$[TcO\{Se_2C{=}C(CN)_2\}_2]^-$ was obtained and precipitated as a brown tetraethylammonium salt. The complex demonstrates the existence of the $TcO(Se)_4$ core. X-ray analysis confirms its approximately square pyramidal geometry in which the four selenium atoms form the basal plane and the oxo oxygen occupies the apical position. The distance of the Tc atom from the basal plane is 0.88 Å towards the oxygen atom. The Tc=O bond is approximately perpendicular to this plane and its length is 1.67(2) Å. The four Tc–Se bond distances are almost equal with a mean value of 2.471 Å. $[Et_4N][TcO\{Se_2C{=}C(CN)_2\}_2]$ crystallizes in the triclinic space group $P\bar{1}$ with a=13.394(8), b=9.935(6), c=9.703(6) Å, α=107.21(7)°, β=95.12(5)°, γ=92.89(4)°, and Z=2 [130]. Reaction of $\{(CN)_2C{=}CSSe\}^2$ with Tc(V)gluconate yielded $[TcO\{SeSC{=}C(CN)_2\}_2]^-$, containing the $TcO(S_2Se_2)$-core [131].

12.3.3.5 $TcO(N_4)$-, $TcO(N_4Cl)$-, $TcO(N_3O)$-, $TcO(N_3O_2)$-, $TcO(N_2O_2)$-, $TcO(N_2O_2Cl)$-, $TcO(N_2O_3)$-, and $TcO(NO_4)$-core complexes

Pertechnetate reacts in alkaline aqueous solution with 1,2-diaminobenzene in the presence of $S_2O_4^{2-}$ as the reducing agent to form the complex anion $[TcO(HNC_6H_4NH)_2]$ that was precipitated as the orange tetrabutylammonium salt. The complex is diamagnetic. A single N–H stretching frequency at 3247 cm ^{1} indicates that each ligand contains one hydrogen per nitrogen. The Tc=O stretch at 891 cm^{-1} is unexpectedly low. The compound proved to be soluble in most organic solvents, but was unstable in solution, even in the absence of air. The complex core has square pyramidal geometry with the oxo oxygen occupying the apical position. The Tc atom lies 0.67 Å above the plane defined by the four nitrogen atoms. The Tc=O distance is 1.668(7) Å. The mean Tc–N distance of 1.98(1) Å is intermediate between the values for deprotonated (1.91Å) and amine nitrogen (2.08 Å). The bite angles of the nitrogen atoms are 78.8 and 79.0°. $[n\text{-}Bu_4N][TcO(HNC_6H_4NH)_2]$ crystallizes in the orthorhombic space group $P2_12_12_1$ with a= 11.644(3), b=15.303(4), c=16.950(5) Å, and Z=4 [25].

α-amineoxime complexes of technetium have been extensively studied in order to develop ^{99m}Tc radiopharmaceuticals for the measurement of regional cerebral blood flow. The oxo(tetradentate-amineoxime)-technetium(V) complexes of long-lived ^{99}Tc were prepared by reaction of TcO_4^- with the amineoxime ligand dissolved in 0.9 % saline, when TcO_4 was reduced with Sn(II)-tartrate. The neutral, lipophilic, orange to rust-colored complexes are extractable into ether. 3,3,9,9-tetramethyl-4,8-diazaundecane-2,10-dione dioxime forms the prototype complex with an approximate square pyramidal core (Fig. 12.18.A). The Tc atom is 0.678(1) Å above the plane determined by the nitrogen atoms. The distance to the doubly bonded apical oxygen is 1.679(3) Å. The bond lengths between the deprotonated N(imino) atoms and the Tc atom of Tc–N(3)=1.908 and Tc–N(4)=1.917 Å are much smaller than the N(oxime)–Tc bond distances of Tc–N(2)=2.086 and Tc–N(1)=2.093 Å which would indicate multiple-bond character in the Tc–N(imino) bonds. The O···O distance of 2.420(5) Å is in the range of short interactions that often have a hydrogen bond between the oxime oxygen atoms. The complex crystallizes in the monoclinic space group Pc with a=6.950(4), b=11.187(3), c=11.060(4) Å, β=104.13(5)°, and Z=2 [132].

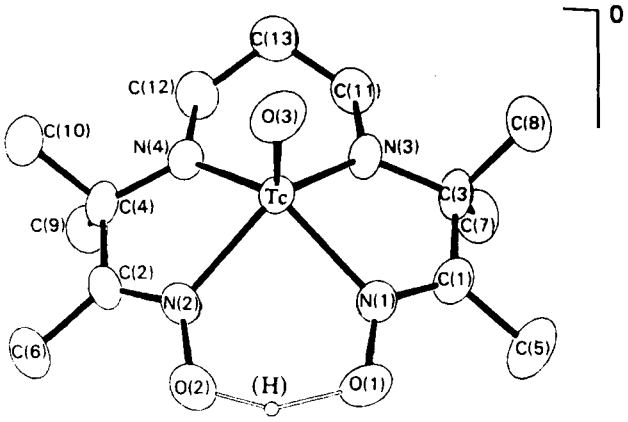

Fig. 12.18.A 3,3,9,9-Tetramethyl-4,8-diazaundecane-2,10-dione dioximato-oxotechnetium(V), $[TcO(pnao)]^0$ [132].

Other square pyramidal technetium(V) tetradentate amine oxime complexes were prepared using the ligands 3,3,9-trimethyl-, 3,9-dimethyl-, and 3,6,6,9-tetramethyl-4,8-diaza-undecane-2,10-dione dioxime or 3,3,8,8-tetramethyl-4,7-diaza-decane-2,9-dione dioxime. The IR spectra show the Tc=O stretch between 908 and 927 cm^{-1} that is at the low-energy end of the range (880–1020 cm^{-1}) thus far observed for monooxo-technetium(V) complexes. This observation can be interpreted by weakening of the Tc=O bond through the multiple bond character of the two Tc–N bonds in the basal plane. Accordingly, the average Tc=O bond distance of 1.676(8) Å is at the long end of the range (1.610–1.672 Å) found for monooxo-technetium(V) complexes [133,134].

There is some evidence for the synthesis of green oxo-octaethylporphyrinato-technetium(V) acetate, when TcO_4^- and octaethylporphyrin were reacted in glacial acetic acid under a nitrogen atmosphere. The apparently neutral product is soluble in CH_2Cl_2 and benzene. The FAB^+ mass spectrum corresponds to the cation [TcO(octaethylporphyrinate)]$^+$ [135].

The dark violet oxochloro-bis-(1,10-phenanthroline)technetium(V) cation $[TcOCl(phen)_2]^{2+}$ was prepared by controlled potential cathodic reduction or dithionite reduction of TcO_4^- in aqueous alcoholic solution containing 1,10-phenanthroline. The compound was also obtained by ligand exchange reaction of $[TcOCl_4]^-$ with phen in methanol. The strong IR absorption at 895 cm^{-1} was attributed to the Tc=O stretching vibration. The ^1H NMR spectrum of the complex displayed 16 distinct resonances that were assigned by HH-COSY experiments to the non-equivalent aromatic protons of the two phen ligands. The ^1H NMR signals suggest that the oxygen and chlorine atoms assume a *cis* configuration yielding a completely asymmetrical environment [136].

A neutral oxo-technetate(V) complex based on the core $TcO(N_3O)$ was obtained by reaction of $[TcO(OCH_2CH_2O)_2]^-$ with N-{2(1H-pyrolylmethyl)}N′-(4-pentene-3-one-2)ethane-1,2-diamine (H_3ped) in methanol. The neutral complex [TcO(ped)]^0 precipitated, yielding orange-red needles crystallizing in the orthorhombic space group $P2_12_12_1$ with the cell parameters a=11.701(1), b=14.949(2), c=7.516(1) Å, and

Z=4. The Tc=O stretch was observed at 953 cm $^{-1}$. Strong IR absorptions at 1580 and 1524 cm^{-1} were assigned to the C=N and C=O stretches, respectively. X-ray analysis confirmed the five-coordinate, distorted square pyramidal geometry of the core. The Tc=O bond length is 1.666(3) Å, the Tc–O distance 2.025(3) Å, the shortest Tc–N bond length 1.897(4) Å [137,138].

Some complexes containing the $TcO(N_3O_2)$-core with pentadentate ligands are known. The Schiff-base ligand, derived from salicylaldehyde and diethylenetriamine, reacts with $[TcO(OCH_2CH_2O)_2]^-$ in methanol to give the neutral compound N,N′-3-azapentane-1,5-diyl-bis(salicylideneiminato)oxotechnetium(V), [TcO (aps)]°. The red complex crystallizes in the monoclinic space group $P2_1/c$ with a=9.459(8), b=9.437(7), c=21.768(12) Å, β=99.08(5)°, and Z=4. The IR spectrum of the diamagnetic compound shows the Tc=O stretch at a low frequency of 888 cm $^{-1}$. The structure reveals a highly distorted octahedral coordination geometry (Fig. 12.19.A) of Tc(V). The Tc atom lies out of the mean equatorial plane by 0.30 Å towards the oxo ligand. The O(1) atom of the quinquedentate ligand is located *trans* to the Tc=O group, while the remaining four donor atoms, N_3O, occupy equatorial sites. The O(1)–Tc=O axis of 161.2(3)° is non-linear. The Tc–N(2) bond distance of 1.894(2) Å is much shorter than the Tc–N(1) bond length of 2.101(8) Å. The reason is the deprotonation of N(2). The Tc=O(3) bond length of 1.685(6) Å is at the longer end of the range expected for oxotechnetium(V) complexes. When the Schiff-base ligand is derived from salicylaldehyde and e.g. 3,3′-diamino-N-methyldipropylamine, in which the hydrogen atom of the central amine group is substituted by an alkyl group, the expected cationic oxotechnetium(V) complex is obtained [139].

A similar oxotechnetium(V) complex of highly distorted octahedral coordination geometry was prepared using the pentadentate ligand N,N′-3-azapentane-1,5-diyl-bis{3-(1-iminoethyl)-6-methyl-2H-pyran-2,4-dione} (H_3apa). The purple-red, neutral

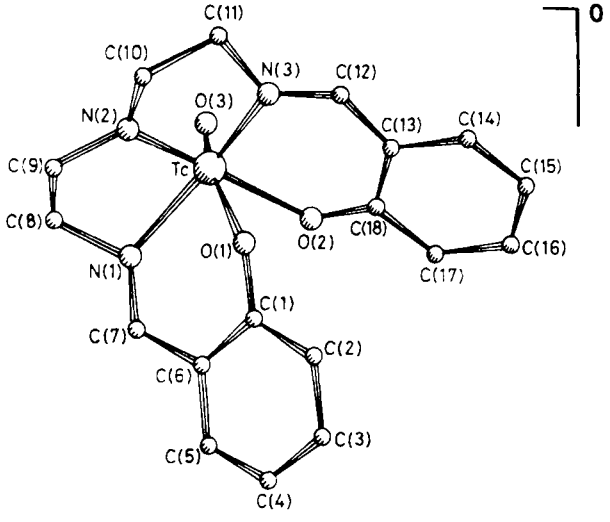

Fig. 12.19.A N,N′-3-azapentane-1,5-diyl-bis(salicylideneiminato) oxotechnetium(V), [TcO (aps)]° [139].

complex crystallizes in the orthorhombic space group *Pbca* with a=12.833(2), b=33.320(5), c=9.942(4) Å, and Z=8. One of the two oxygen donor atoms of the pentadentate ligand is located *trans* to the Tc=O bond. The distance of 1.880(2) Å between the deprotonated N atom and Tc is significantly short [140].

Cationic complexes of the core $Tc(N_3O_2)$ have been recently synthesized. The reaction of chloro{N-(2-oxidophenyl)salicylideneiminato}oxotechnetium(V) [TcOCl(ophsal)]° with neutral, bidentate, aromatic nitrogen donor ligands gave the complex salts $[TcO(ophsal)(bpy)]PF_6$, $[TcO(ophsal)(phen)]Cl \cdot H_2O$, and $[TcO(ophsal)(dpk \cdot EtOH]Cl$, where bpy=2,2′-dipyridyl, phen=1,10-phenanthroline, and dpk=bis(2-pyridyl)ketone. The dark green compounds are soluble in polar solvents. Spectroscopic and analytical results suggest terdentate coordination of $(ophsal)^{2-}$ in the equatorial plane with the bidentate nitrogen donor ligands bridging the fourth equatorial site and the position *trans* to the oxo group [141].

The $TcO(N_2O_2)$ core is represented in anionic and cationic complexes and the core $TcO(N_2O_2Cl)$ in neutral complexes. N,N′-ethylene-bis(2-phenoxyacetamide), $HOC_6H_4CONHCH_2CH_2NHCOC_6H_4OH$($H_4$epa), reacts with $[n\text{-}Bu_4N][TcOCl_4]$ in CH_2Cl_2 to form orange crystals of $[n\text{-}Bu_4N][TcO(epa)]$, in which Tc is coordinated by a distorted square pyramid. The oxo oxygen occupies the apical position and the base is defined by the two nitrogen and the two oxygen donors of the quadruply deprotonated ligand (Fig. 12.20.A). The Tc atom rests 0.65 Å above the N_2O_2 base. The Tc=O bond length is 1.648(3) Å, the average Tc–O ligand distance 1.960(4) Å, and the average Tc–N distance 1.977(6) Å. $[n\text{-}Bu_4N][TcO(epa)]$ crystallizes in the triclinic space group $P\bar{1}$ with a=12.067(3), b=12.110(4), c=12.289(3) Å, α=109.59(1), β=111.11(1), γ=92.09(1)°, and Z=2. The compound is soluble in DMF, CH_3CN or CH_2Cl_2 and proved to be diamagnetic [142].

The similar neutral complex

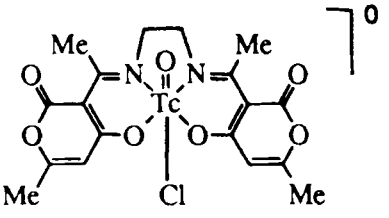

was obtained as a brown precipitate by refluxing $[(n\text{-}Bu)_4N][TcOCl_4]$ with N,N′-ethylene-diyl-bis{3-(1-iminoethyl)-6-methyl-2H-pyran-2,4(3H)-dione} in ethanol. The ν(Tc=O) frequency was found at 960 cm^{-1} [143].

The cationic complexes $[TcO(bgo)_2]^+$ and $[TcO(blo)_2]^+$, formed by reduction of TcO_4^- with $S_2O_4^{2-}$ in the presence of the bidentate, monoanionic benzimidazolylalcoholates $(bgo)^-$ and $(blo)^-$, were precipitated as the green crystalline hexafluorophosphates $[TcO(bgo)_2][PF_6] \cdot 2H_2O$ and $[TcO(blo)_2][PF_6] \cdot 2H_2O$. The green neutral compounds $[TcO(bgo)_2Cl]$° and $[TcO(blo)_2Cl]$° were synthesized by substituion of chloride in $[TcOCl_4]^-$. The four coordinating sites on the plane perpendicular to Tc=O are occupied by *trans*-N,O arrangements of the two bidentate ligands. The neutral complexes appear to have a distorted octahedral geometry around Tc(V) [144].

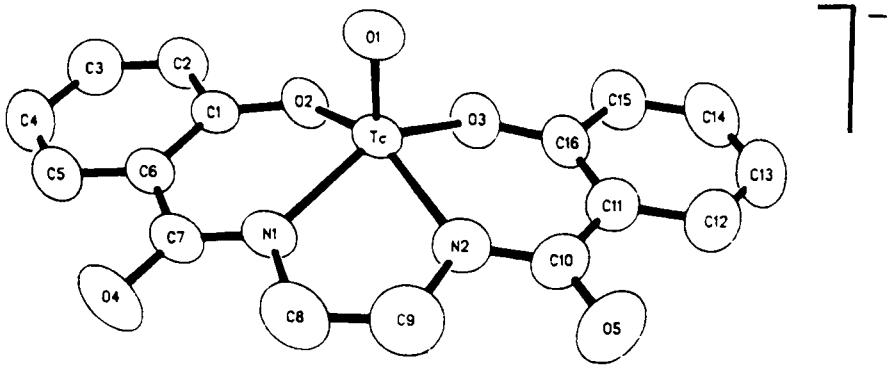

Fig. 12.20.A N,N′-ethylene-bis(2-phenoxyacetamido)-oxotechnetate(V), $[TcO(epa)]^-$ [142].

The replacement of chloride ligands on $[TcOCl_4]^-$ in ethanol by the tetradentate Schiff-base ligands N,N′-ethylene-bis(acetylacetoneimine) $\{H_2(acac)_2en\}$ and N,N′-ethylene-bis(salicylideneimine) $\{H_2(sal)_2en\}$ yielded the cationic acetylacetoneiminato complex $[TcO(H_2O)\{(acac)_2en\}]^+$ which exhibits a distorted octahedral coordination geometry containing a *trans*-oxo-aqua-technetium(V) core and the neutral N,N′-ethylene-bis(salicylideneaminato) complex $[TcOCl\{(sal)_2en\}]^\circ$, which has pseudo-octahedral arrangement of the donor atoms with a *trans*-oxo-chloro-technetium(V)-core. The latter compound crystallizes in the orthorhombic space group $P2_12_12_1$ with a=26.653(11), b=11.697(5), c=10.529(3) Å, and Z=8. The strong structural *trans* influence of the oxo oxygens results in significantly lengthened bonds, the Tc–$O(H_2O)$ bond of 2.282(2) Å and the Tc–Cl bond of 2.527(4) Å [145].

Reduced pertechnetate reacts in aqueous alcoholic solution with N-acetylanthranilic acid to form the brown anionic complex $[TcO(C_6H_4COONCOCH_3)_2]^-$ which also appears to contain the $TcO(N_2O_2)$ core [146,147].

A $TcO(N_2O_3)$-core complex is verified by the neutral compound N-(2-oxidophenyl)salicylideneiminato-8-quinolinolato-oxotechnetium(V). $[TcO(ophsal)Cl]^\circ$ was precipitated from methanolic solution upon reaction of the tridentate Schiff-base ligand with $[TcOCl_4]^-$, and subsequently, $[TcO(ophsal)Cl]^\circ$ in ethanol was reacted with 8-quinoline(quin) to form dark red crystals of $[TcO(ophsal)(quin)]^\circ$. The complex crystallizes in the monoclinic space group $P2_1/n$ with a=15.496(8), b=10.355(4), c=12.122(5) Å, β=109.03(6)°, and Z=4. The coordination (Fig. 12.21.A) around Tc is approximately octahedral. The tridentate ligand $(ophsal)^{2-}$ occupies three equatorial sites and the bidentate ligand (quin) bridges the remaining equatorial and one apical site with the oxygen occupying the sixth position *trans* to the terminal oxo oxygen. The tridentate ligand is roughly planar and nearly normal to the 8-quinolinolate mean plane. The O(1)–Tc–O(2) angle of 160.8(3)° deviates significantly from linearity. The Tc–O(2) bond length of 2.014(6) Å seems to exclude considerable *trans* weakening [148].

The electrochemistry of six-coordinate oxotechnetium(V) complexes containing Schiff-base and 8-quinolinol ligands was studied in solutions of acetonitrile and DMF. The main features of the reactions are the reduction of Tc(V) to Tc(IV), the subse-

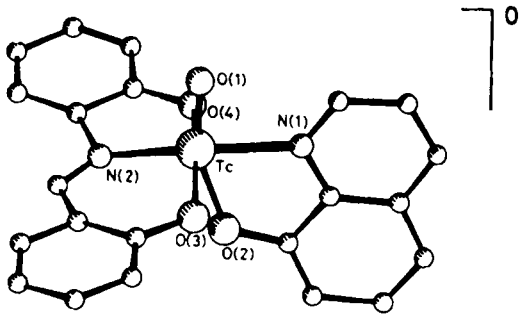

Fig. 12.21.A N-(2-oxidophenyl)salicylideneiminato-8-quinolato-oxotechnetium(V), [TcO(ophsal)(quin)]° [148].

quent loss of a ligand located *cis* to the Tc=O linkage, and the following isomerization of this unstable Tc(IV) product to a more stable complex in which the site *trans* to the Tc=O linkage is vacant [149].

An oxotechnetium(V) complex representing the $TcO(NO_4)$-core is the neutral amino-sugar-Schiff-base compound (N-salicylidene-D-glucosaminato)(salicylaldehydato)oxotechnetium(V). The complex precipitates from a conc. solution of $[TcOCl_4]^-$ in methanol after reaction with excess N-salicylidene-D-glucosamine. Probably, the coordinated salicylaldehydato moiety originates from hydrolysis of a coordinated N-salicylidene-D-glucosaminato ligand. The red, diamagnetic complex is nearly insoluble in common solvents, but slightly soluble in methanol and H_2O. The IR spectrum shows a Tc=O stretch at 970 cm^{-1}, which is at the upper limit for this bond vibration. The complex crystallizes in the orthorhombic space group $P2_12_12_1$ with a=6.533(2), b=12.649(4), c=23.675(7) Å, and Z=4. The coordination environment around the Tc atom can be described as a distorted octahedron (Fig. 12.22.A). If the axial positions are defined to be those of the oxo group and the carbonyl oxygen atom of the sali-

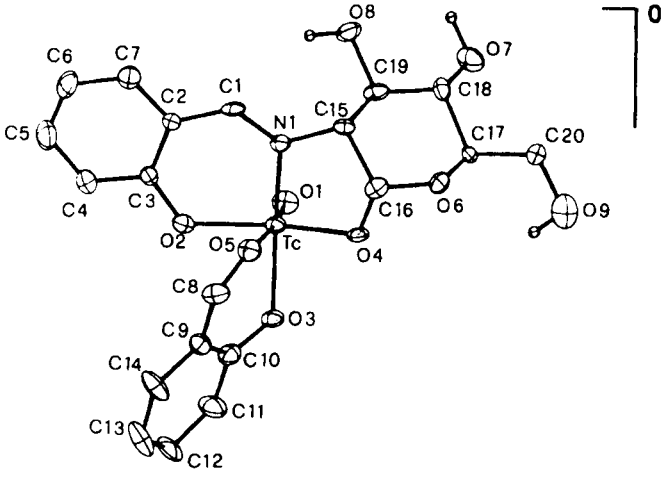

Fig. 12.22.A N-salicylidene-D-glucosaminato-salicylaldehydato-oxotechnetium(V). [TcO(gluca)(sal)]° [150].

cylaldehydato ligand, the equatorial positions are occupied by the aldimine nitrogen atom, two oxygen atoms of the tridentate ligand and by the phenolic oxygen atom of the salicylaldehydato moiety. The principal distortion from octahedral geometry is exhibited by the 0.422(1) Å displacement of Tc toward the oxo oxygen O(1) from the mean N(1), O(2), O(3), O(4) plane. The sugar ring shows its usual chair configuration. The Tc=O(1) distance of 1.656(8) Å is indicative of a strong bond. The molecule displays a long Tc–O(5) bond of 2.359 Å, which can be explained by the structural *trans* effect. Remarkably, the *trans* position is occupied by the neutral carbonyl oxygen and not by the charged phenolic oxygen atom [150].

12.3.3.6 $TcO(N_2S_2)$-, $TcO(N_3S)$-, and $TcO(NS_3)$-core complexes

TcO_4^- reacts with 2-aminobenzenethiol in alkaline aqueous solution, using $S_2O_4^{2-}$ as reducing agent, to yield the anion $[TcO(NHC_6H_4S)_2]^-$ that was precipitated as a red crystalline solid by addition of $[n\text{-}Bu_4N]^+$. The diamagnetic complex salt is indefinitely stable and soluble in acetone, chloroform, methanol, and nitromethane. $[n\text{-}Bu_4N][TcO(NHC_6H_4S)_2]$ crystallizes in the orthorhombic space group $P2_12_12_1$ with a=17.113(6), b=15.573(5), c=11.677(4) Å, and Z=4. The structure analysis confirmed the expected square pyramidal coordination geometry around Tc(V). The basal plane of the distorted square pyramid is defined by the N_2S_2 group. The N and S atoms are in *trans* position. The oxo ligand occupies the apical position. The Tc atom lies 0.72 Å above the basal plane towards the apex. An interesting phenomenon is the unusually long Tc=O bond distance of 1.73(2) Å. The average Tc–S and Tc–N distances are 2.30(1) and 2.08(2) Å, respectively. The long Tc=O bond corresponds with the low Tc=O frequency of 906 cm^{-1} in the IR [151,152].

In order to synthesize technetium complexes of kinetic inertness suitable for radiopharmaceutical purposes, tetradentate N_2S_2 ligands that bind the Tc=O group and occupy the basal position in a square pyramid were proposed. N,N′-ethylene-bis(2-mercaptoacetimido)oxotechnetate(V), $[TcO(ema)]^-$, was prepared by $S_2O_4^{2-}$ reduction of TcO_4^- in alkaline aqueous/ethanolic solution in the presence of the ligand. The thiol groups were protected as benzoyl esters. The anionic complex was separated as a yellow precipitate after addition of $[Ph_4As]^+$. The tetraphenylarsonium salt is diamagnetic, air-stable, and readily soluble in polar, non-aqueous solvents. The Tc=O stretch was found at 945 cm^{-1}. The configuration of $[TcO(ema)]^-$ containing three five-membered rings appears to be most favored [153]. The structure determination of the methyl-triphenylarsonium salt demonstrates the distorted square pyramid core of the complex with the oxygen at the apex (Fig. 12.23.A). The Tc=O bond length is 1.679(5) Å, the distance of the Tc atom above the square plane 0.771(5) Å. The distortion is reflected in the square plane. N(1) is 0.0863(6) Å above and N(2) 0.076(6) Å below the best N_2S_2 plane in which the two sulphur atoms lie. $[CH_3Ph_3As][TcO(ema)]$ has monoclinic symmetry, space group $P2_1/c$, a=10.203(2), b=13.449(2), c=16.140(4) Å, β=110.37(1)°, and Z=4 [154]. The structurally related complexes N,N′-propylene-bis(2-mercaptoacetimido)oxotechnetate(V), N,N′-ethylene-bis(3-mercaptopropionimido)oxotechnetate(V), and N,N′-2-phenylene-bis(2-mercaptoacetimido)oxotechne-

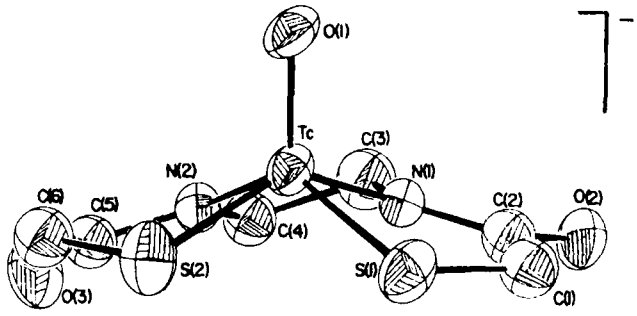

Fig. 12.23.A N,N′-ethylene-bis(2-mercaptoacetimido) oxotechnetate(V), [TcO(ema)] [154].

tate(V) have also been synthesized and characterized [153] and, in addition, a series of isomeric oxotechnetium(V) diamido dithiolato complex anions, containing the tetradentate ligand system, have been identified [155].

To develop a ^{99m}Tc radiopharmaceutical as a renal tubular function agent, the anionic Tc(V) complex with 2,3-bis(mercaptoacetamido)propanoate (map)

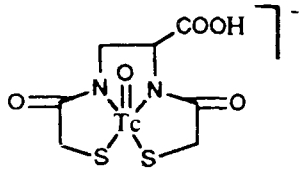

was prepared. The *syn* and *anti* epimers, configurationally based on the Tc=O and carboxylate group relationship, were isolated and structurally identified. *Syn*-[Ph_4As][TcO(map)] crystallizes in the monoclinic space group $P2_1/c$ with a=12.729(1), b=13.225(2), c=18.318(2) Å, β= 91.67(1)°, and Z=4, *anti*-[Ph_4As][TcO(map)] in the same space group with a=11.260(2), b=23.662(3), c=11.834(3) Å, β=94.53(2)°, and Z=4. Both epimeric complex salts are yellow and very stable at 25–100 °C over a pH range of 1–11. Tc(V) is coordinated in an approximately square pyramidal geometry. The average distance of Tc from the basal plane in *syn*-[TcO(map)] is 0.747 Å, the Tc=O bond distance is 1.656(7) Å. The carboxylic group exhibits no interaction with Tc. This epimer is excreted faster by the renal tubular system in humans than the *anti*-epimer [156]. In addition, oxotechnetium(V) complexes with 4,5-bis(mercaptoacetamido) pentanoic acid were prepared and the stereochemistry of the epimers assigned by NMR spectroscoy [157].

To vary the biological behavior of oxotechnetium(V)-diaminodithiol complexes the diamine portion of the ligand was expanded from ethanediamine to butanediamine, thus producing complexes containing a seven-membered ring in addition to the two five-membered rings. N,N′-bis(mercaptoacetyl)butane-1,4-diamine (H_4DBDS), in which the thiol functionalities were protected as benzoylesters, was dissolved in an alkaline aqueous solution of NH_4TcO_4. Reaction occurred by reduction with $S_2O_4^{2-}$. The anionic complex formed was precipitated with $[Ph_4P]^-$. The brown complex salt [Ph_4P][TcO(DBDS)] was spectroscopically identified. The Tc=O stretching vibration

appeared at 954 cm^{-1}. $[Ph_4P][TcO(DBDS)] \cdot 1/4\ CH_3OH$ crystallizes in the monoclinic space group $P2_1/n$ with a=9.398(4), b=13.942(3), c=23.749(8) Å, β=98.54(3)°, and Z=4. The structure of the complex anion exhibits again the coordination of Tc(V) by an approximately square pyramidal arrangement with the oxo oxygen at the apex. The Tc=O bond distance is 1.66 Å. Tc lies 0.67 Å out of the mean N_2S_2 basal plane. The chelate bite angles for S–Tc–N are 82° and 83°. The 7-membered butanediamine ring is in a distorted twisted boat conformation. The average Tc-S bond distance is 2.29(2) Å, the average Tc–N bond length 2.04(2) Å. The absence of hydrogen atoms on the nitrogens was established by ^1H NMR. $[TcO(DBDS)]^-$ is very stable in methanol or mixed methanol/water solutions. The kinetics of the isotope exchange (Sect. 6.3)

$$[TcO(DBDS)]^- + H_2{}^{17}O \leftrightarrow [Tc^{17}O(DBDS)] + H_2O$$

were studied in DMSO [158].

Neutral oxotechnetium(V) complexes with amide-thiol-thioether chelating ligands were synthesized to design potential radiopharmaceuticals of the general formula $[TcO(emaR)]^\circ$, where ema^4 stands for $(SCH_2CONHCH_2CH_2NHCOCH_2S)^{4-}$ and R for $-CH_3$, $-CH_2Ph$, $-(CH_2)_{10}COOH$ and $-CH_2CH_2NC_4H_8O$. R forms mono-S-alkylated derivatives giving the ligand $H_3(ema)R$. The complex $[TcO(ema)(CH_2CH_2NC_4H_8O)]$, where $-CH_2CH_2NC_4H_8O$ is ethylenemorpholine (morph), was synthesized by ligand exchange reaction of $[TcO(OCH_2CH_2O)_2]^-$ with the ligand $H_3(ema)(morph)$ in alkaline methanol. The red compound $[TcO(ema)(morph)]^\circ \cdot H_2O$ crystallizes in the monoclinic space group $P2_1/n$ with a=12.120(1), b=7.172(1), c=18.933(2) Å, β=94.29(1)°, and Z=4. The structure is a distorted square pyramidal $TcO(N_2S_2)$-core with the ethylenemorpholine side chain occupying the least sterically hindered position, *anti* with respect to the oxo ligand. The weaker Tc–S (thioether) bond distance of 2.387(1) Å is 0.13 Å longer than the Tc–S (thiolate) bond distance of 2.257(1) Å. The Tc=O bond length is 1.658(3) Å [159].

The neutral complex N,N′–1,2-ethylene-bis(L-cysteine)diethylester-oxotechnetate(V), $[TcO(L,L\text{-}ECD]^\circ$, which was found to be an excellent ^{99m}Tc marker of regional cerebral blood flow, is readily prepared by ligand exchange from the precursor $[TcO_2(py)_4]^+$ with N,N′–1,2-ethylene-bis(L-cysteine) [160]. This ligand was synthesized by reduction of L-thiazolidine-4-carboxylic acid with sodium in liquid ammonia [161]. $[TcO(L,L\text{-}ECD)]^\circ$ forms yellow-orange needles crystallizing in the orthorhombic space group $P2_12_12_1$ with the unit cell parameters a=7.121(1), b=9.670(1), c=24.530(3) Å, and Z=4. The structure (Fig. 12.24.A) of the complex core has again a distorted square pyramidal geometry with the basal plane made up of two nitrogen and two sulphur donor atoms. The Tc atom is located 0.73 Å above the plane. The Tc=O bond distance is 1.666 Å. The nitrogen donor N(2) is deprotonated, as evident from the 0.24 Å shorter Tc–N bond length compared to the Tc–N(1) bond distance of 2.168 Å [160].

Another neutral diaminodithiolate complex, which showed high pulmonary accumulation in rodents, was synthesized by reduction of TcO_4^- with $S_2O_4^{2-}$ in a basic medium in the presence of 4-N-ethyl-2,9-dimethyl-4,7-diaza-2,9-decanedithiol dihydrochloride. X-ray structure analysis of the pale-brown needle-shaped crystals confirm a distorted square pyramidal arrangement around Tc(V). The ethyl substituent

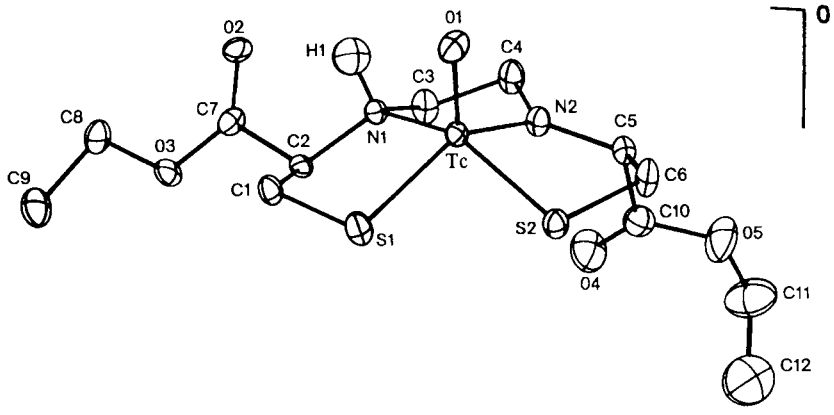

Fig. 12.24.A N,N'-1,2-ethylene-bis(L-cysteinediethylester)oxotechnetium(V), [TcO(L,L-ECD)]$^{+}$ [160].

adopts the *syn* configuration with respect to the oxo oxygen. The unsubstituted nitrogen N(1) is deprotonated resulting in a neutral molecule. The Tc–S(1) bond *trans* to the substituted quarternary nitrogen N(2) is shorter (2.265 Å) than the Tc-S(2) bond of 2.300 Å. The Tc–N(1) bond distance of 1.921(2) Å is 0.303 Å shorter than the Tc–N(2) distance of 2.224 Å. *Syn*-(4-N-ethyl-2,9-dimethyl-4,7-diaza-2,9-decanedithiolato) oxotechnetium(V), *syn*-[TcO(NEt-tmdadt)]$^{+}$ crystallizes in the monoclinic space group $P2_1/n$ with a=9.638(2), b=14.371(5), c=11.893(3) Å, β=100.79(2)°, and Z=4 [162]. For the analogous neutral complex containing the 4-N-methyl group instead of 4-N-ethyl, the *syn/anti* isomerism was conclusively established by X-ray structure analysis [163].

To develop new brain perfusion imaging agents racemic mixtures of bis(amino-ethanethiol) (BAT) derivates containing an N'-benzylpiperazinyl (BPA) side chain were reacted with TcO_4^- and $S_2O_4^{2-}$ to form the neutral *syn* and *anti* isomers of the Tc(V)oxo complexes. *Syn*-[TcO-BAT-BPA]$^{+}$

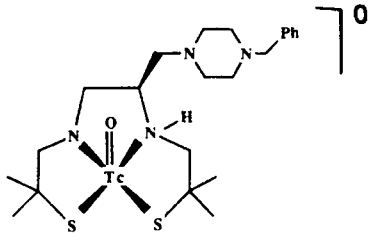

crystallizes in the monoclinic space group $P2_1/n$ with a=15.241(5), b=15.658(7), c=11.385(3) Å, β=109.91(2)°, and Z=4, the *anti* isomer in the same space group with a=12.243(7), b=11.022(2), c=19.180(5) Å, β=102.19(3)°, and Z=4. The Tc=O stretch for both isomers was observed at 900 cm^{-1}. The *syn* form revealed a higher *in vivo* brain uptake and a longer brain retention in rats than the *anti* form [164].

Contrary to [TcO-BAT-BPA]$^{+}$, the brain uptake of the *anti* isomer of [TcO-BTA-PPP]$^{+}$ containing a phenylpiperidine side chain (PPP) showed slightly higher cerebral

uptake than the *syn* isomer. The gold-brown *syn* and *anti* isomers of [TcO-BAT-PPP]° were prepared by the reduction of TcO_4^- with Sn^{2+} under basic conditions in the presence of the *racemic* BAT-PPP ligand. The neutral, lipophilic complexes were isolated by column chromatography. The molecules exhibit Tc=O stretching frequencies at 919 and 900 cm^{-1} for the *syn* and *anti* form, respectively. *Syn*-[TcO-BAT-PPP]° crystallizes in the monoclinic space group $P2_1/n$ with a=12.390(2), b=11.470(2), c=18.320(3) Å, β=103.09(1)°, and Z=4, *anti*-[TcO-BAT-PPP]° in the orthorhombic space group $Pna2_1$ with a=19.823(2), b=11.530(2), c=22.373(4) Å, and Z=8. The Tc=O bond distance in the *syn*-form was found to be 1.681(2) Å which is rather long and consistent with the low Tc=O stretching frequency [165].

A neutral oxotechnetium(V)-2-thiohydantoin complex was prepared by reduction of TcO_4^- with alkaline dithionite in the presence of excess 2-thiohydantoin. The deep orange compound is soluble in water and is reported to contain, in the *trans* position of the oxo oxygen of the $TcON_2S_2$ core, a hydroxyl group [166].

In context with the preparation of technetium-labeled steroids as agents for the diagnosis of breast cancer, the neutral complex

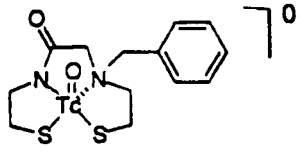

was synthesized by treating the corresponding ligand with $[n\text{-}Bu_4N][TcOCl_4]$ in basic methanol. The *syn* and *anti* products, defined by the position of the benzyl group relative to the Tc=O bond, could be separated by flash column chromatography. The two diastereomers were differentiated by ^1H NMR due to the upfield shifts of the methylene protons on the *anti* benzyl substituent. An unambiguous structural assignment was established by an X-ray analysis of the analogous rhenium compounds [167].

As a new approach toward the inhibition of ribonucleases, the water-stable ribonucleoside technetium-chelate

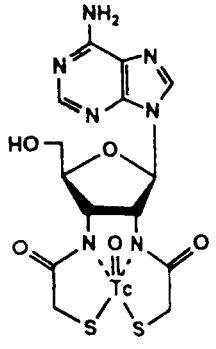

was reported to be synthesized starting from 2′,3′-diamino-2′,3′-dideoxy adenosine. The compound was purified by reverse-phase chromatography. Analysis of the complex by HPLC showed the product to be a 2.4:1 mixture of diastereomers [168].

Neutral, mixed ligand complexes of oxotechnetium(V) were prepared by reacting Tc(V)gluconate with a tridentate S,N,N, chelating ligand and a monodentate thiol. The reaction yielded for instance the compound 4-methylbenzenethiolato-N-(2-mercaptoethyl)(2-pyrrolidine-1-yl)ethylamine-oxotechnetium(V) in dark red crystals that adopt the monoclinic space group $P2_1/n$. The unit cell parameters are a=10.223(1), b=9.283(1), c=18.337(2) Å, β=97.262(2)°, and Z=4. The coordination sphere of Tc(V) is again formed by two sulphur atoms, two nitrogen atoms and the oxygen in the apical position of a distorted square pyramid. Tc(V) lies 0.68 Å out of the basal square plane (Fig. 12.25.A) toward the oxygen. The Tc=O bond length is 1.677(3) Å. The Tc–N(1) distance of 1.930(3) Å indicates a double bond character, while the Tc–N(2) distance of 2.202(3) Å is typical for a Tc–N(amine) single bond. Other structurally related compounds have been synthesized [169,170].

Reduction of TcO_4^- with stannous tartrate in aqueous solution in the presence of ethane-1,2-bis(N-1-amino-3-ethylbutyl-3-thiol) {H_3(BAT-TE)} yields the neutral complex [Tc^VO(BAT-TE)]° in brownish-gold crystals that crystallize in the monoclinic space group $P2_1/c$ with a=12.453(2), b=11.747(1), c=12.645(2) Å, β=99.66(0)°, and Z=4. Tc(V) resides in a distorted square pyramidal coordination geometry with the oxygen in the apical position. The remaining proton of the amine nitrogen is in *syn* position relative to the Tc=O oxygen. This structure appears to be maintained in solution, as shown by ^{1}H NMR measurements. The Tc=O bond distance is 1.694(2) Å. The S(1)–Tc–S(2) angle is 87.56(3)°, the N(1)–Tc–N(2) angle 79.83(8)°. A similar Tc(V) complex is formed with the ligand biphenyl-2,2′-bis(N-1-amino-2-methylpro-

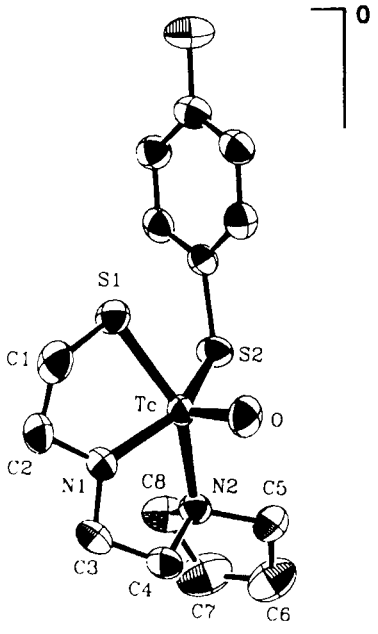

Fig. 12.25.A (4-Methylbenzenethiolato)-{N-(2-mercaptoethyl)(2-pyrrolidine-1-yl)ethylamine}oxotechnetium(V) [169].

pane-2-thiol {H_3(BP-BAT-TM)}. However, the proton of the amine nitrogen in the complex [$Tc^{V}O$(BP-BAT-TM)]^{e} is in *anti* position to the Tc=O oxygen. Presumably, steric requirements for the biphenyl group dictate this *anti* position [171].

Several *cationic* diaminodithiol complexes of oxotechnetium(V) have been identified. 3,6-dimethyl-3,6-diazaoctane-1,8-dithiolato-oxotechnetium(V)pertechnetate was synthesized by the direct reaction of the ligand with NH_4TcO_4 in sulphuric acid solution and isolated in red-brown, monoclinic needles of the space group $P2_1/c$. The complex cation, methylated at both nitrogens, exhibits lipophilic character and may find use as a ^{99m}Tc agent for imaging purposes. The donor atoms form a rough square pyramid. The Tc atom is located 0.770(3) Å above the N_2S_2 plane. The Tc=O bond length of 1.646(8) Å and the Tc–N distances of 2.137(7) and 2.186(8) Å are comparable to those in similar compounds, but the Tc–S bond distances of 2.266(3) and 2.238(3) Å are somewhat shorter [172]. In addition, the X-ray structure of the similar complex cation 2,2′-dimethyl-1,1-{(N,N′-$^{2}H_2$)-ethylenediamino}dipropane-2-thiolato-N,N′,S,S′-oxotechnetium(V) was determined [173].

Some oxotechnetium(V) complex cations containing N-(thiocarbamoyl)benzamidine ligands have been prepared. By simple substitutions in the molecular framework of the ligands the lipophilic properties of the complexes can be easily varied to optimize their biodistribution. N-(N,N-dialkylthiocarbamoyl)benzamidines (HR_2tcb) coordinate bidentately via the S and N donor atoms with single deprotonation of the NH_2 group. Bis{N-(N,N-diethylthiocarbamoyl)benzamidinato}oxo-technetium(V) chloride, [$TcO(Et_2tcb)_2$]Cl, was readily obtained by displacement of the chloride ions of $[TcOCl_4]^-$ with Et_2tcb^- ligands in methanol or acetone. The red-brown compound crystallizes in the triclinic space group $P\bar{1}$ with a=10.872(2), b=11.587(2), c=12.374(2) Å, α=91.94(2), β=106.04(2), γ=112.18(2)°, and Z=2. The Tc=O stretch was found at 978 cm^{-1}. The coordination of the Tc atom (Fig. 12.26.A) shows a *cis* arrangement of

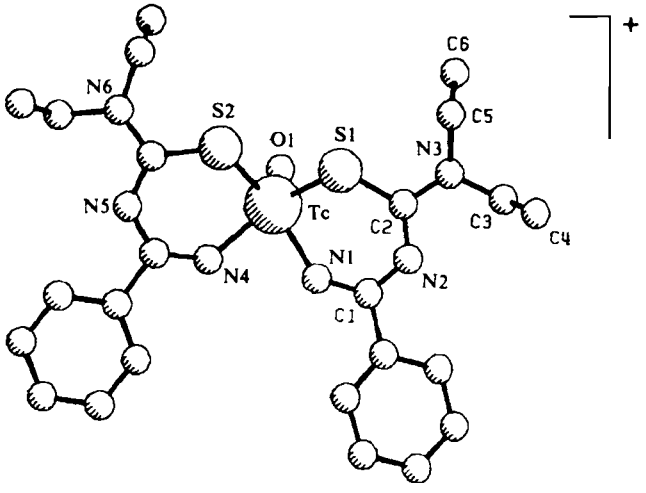

Fig. 12.26.A Bis-{N-(N,N-diethylthiocarbamoyl)benzamidinato}oxotechnetium(V), [$TcO(Et_2tcb)_2$]$^{+}$ [174].

the S and N donor atoms resulting in a distorted square pyramidal geometry. The Tc–S(1) and Tc–S(2) bond lengths are 2.315 and 2.321 Å, respectively, the Tc–N(1) and Tc–N(4) bond distances are 2.015 and 2.027 Å, respectively. The Tc=O distance is 1.651 Å. In addition, the complex salts bis[N-(N-morpholinylthiocarbonyl)-benzamidinato]- and bis[N-(N-piperidinylthiocarbonyl)benzamidinato]oxotechnetium(V) chloride have been prepared and identified [174].

Diaminedithiol ligands of the type $HSCR_2CH_2NR'CH_2CH_2NR'CH_2CR_2SH$, where R = Me or Et and R′ = Me, Et or H react with $[AsPh_4][TcOCl_4]$ in methanolic solution to form cationic complexes containing again the distorted square pyramidal $TcO(N_2S_2)$-core. The orange tetraphenylborate salt of the cation

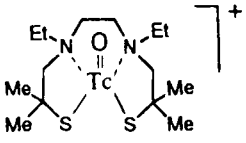

crystallizes in the orthorhombic space group $P2_12_12_1$ with a=14.293(2), b=14.936(6), c=17.202(4) Å, and Z=4. The Tc=O stretch was found at 960 cm^{-1}. The compound is air-stable and soluble in polar organic solvents. The ^1H NMR spectrum showed a *syn*-configuration. The chloride salt of the cation

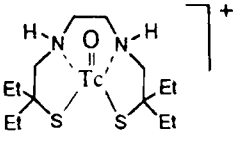

adopts the monoclinic space group $P2_1/c$ with a=12.153(1), b=12.917(3), c=12.410(2) Å, β=94.76(1)°, and Z=4. The Tc=O stretching frequency is 955 cm^{-1}. X-ray structure analysis showed also a *syn* configuration. The Tc atom is displaced from the mean N_2S_2 plane towards the oxygen atom by 0.773(3) Å. The Tc=O bond distance of 1.657(1) Å indicates strong multiple-bond character. The Tc-S bond distances are 2.2494(6) Å and 2.2731(6) Å, the Tc–N distances 2.121(1) Å and 2.107(1) Å [175].

Reaction of N,N′-ethylene-bis(acetylacetonethioimine) $\{(sacac)_2enH_2\}$ with $[n\text{-}Bu_4N][TcOCl_4]$ in ethanol produces the brown complex salt $[TcO(sacac)_2en(H_2O)]Cl$. The compound crystallizes in the orthorhombic space group *Pbcn* with a=24.609(1), b=12.4708(6), c=10.995(5) Å, and Z=8. The Tc=O stretch was found at 964 cm^{-1}. The Tc atom is reported to be hexacoordinate, because a water molecule occupies the *trans* axial position (Fig. 12.27.A). The Tc=O bond distance is 1.643(3) Å, the Tc–O(water) bond length 2.384(3) Å. O=Tc–O(water) form an angle of 172.3(1)°. The Tc–S(1) distance is 2.304(1) Å, the Tc–S(2) distance 2.311(1) Å. The Tc–N bond lengths are very similar, Tc–N(1) 2.092(3) Å, Tc–N(2) 2.089(2) Å. The ^1H NMR and UV/VIS spectra of the complex in solution are solvent dependent indicating the presence of different ligands at the *trans* axial position [176].

2-benzimidazole-2′-yl-ethanethiol (Hbls) reacts in methanol/water with TcO_4^- as both a reducing and a chelating agent to form the diamagnetic cation $[Tc^VO(bls)_2]^+$,

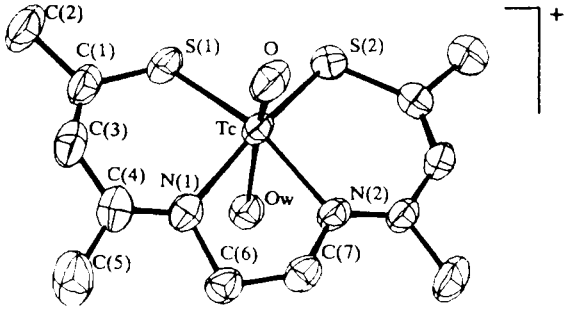

Fig. 12.27.A Aqua-N,N′-ethylene-bis-(acetylacetone-thioiminato)oxotechnetium(V), [TcO (sacac)$_2$en(H_2O)]$^+$ [176].

which precipitates as tetraphenylborate or as pertechnetate. The complex salts are stable in air and soluble in polar organic solvents. The Tc=O stretching vibration of $[TcO(bls)_2][BPh_4]$ appears at 966 cm^{-1}. The brown compound gives rise to green solutions. The simple procedure for synthesizing the complex could prove practical as a route to the preparation of a variety of ^{99m}Tc(V) radiopharmaceuticals [177]. The reaction of $[TcOCl_4]^-$ with the corresponding 2-benzimidazol-2′-yl-ethanol (Hblo) leads to the neutral six-coordinate complex $[TcOCl(blo)_2]^\circ$ [178].

Some $TcO(N_3S)$- and $TcO(NS_3)$-core complexes have been synthesized. The ligand exchange reaction of $[n\text{-}Bu_4N][TcOCl_4]$ in methanol with N-[2-{(2-((acetylamino)methyl)(thioacetyl)amino}ethyl]-2-pyridine-carboxamide, $H_2PIC(Acm)$, where Acm is the sulphur-protecting group (acetylamino)methyl, yielded the neutral complex N-[2-{(2-mercaptoacetyl)amino}ethyl]-2-pyridinecarboxamidooxotechnetium(V), $[TcO(PIC)]^\circ$. The protected ligand is deprotected upon coordination:

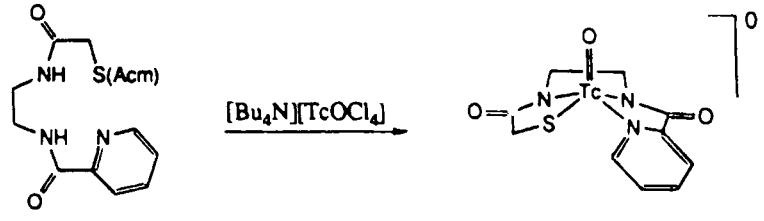

$H_2PIC(Acm)$ [TcO(PIC)]

The red complex crystallizes in the tetragonal space group $P4_32_12$ with a=8.010(2), c=36.845(7) Å, and Z=8. The crystal structure of $[TcO(PIC)]^\circ$ shows technetium to be five-coordinate in a square pyramidal geometry with an oxo ligand at the apical position and the N_3S chelate occupying the basal plane. The Tc–S and Tc=O bond distances are unexceptional, while the Tc–N(amido) bond lengths of 1.963(4) and 1.966(4) Å are slightly shorter than observed for similar complexes with a $TcO(N_2S_2)$ core [179].

Recently, the standard agent for renal function imaging, mercaptoacetylglycylglycylglycine oxotechnetate(V), $[^{99m}TcO(MAG)_3]^-$, was structurally characterized by using the long-lived ^{99}Tc. $[^{99}TcO(MAG)_3]^-$ was most successfully prepared by ligand

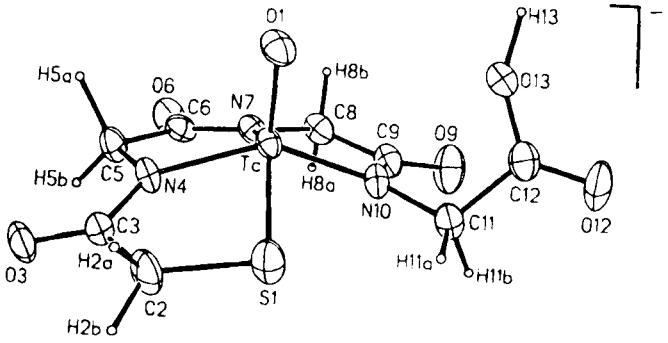

Fig. 12.28.A Mercaptoacetylglycylglycylglycine-oxotechnetate(V), $[TcO(MAG)_3]^-$ [180].

exchange reaction of $[TcOCl_4]^-$ with free MAG_3 in methanol and identified by UV/VIS spectroscopy, ^1H and ^{13}C NMR and FAB mass spectrometry. $[Ph_4As][TcO(MAG)_3]$ crystallizes in the monoclinic space group $P2_1/n$ with the lattice parameters a=12.252(6), b=10.169(6), c=24.579(7) Å, β=92.04(3)°, and Z=4. The Tc(V) coordination sphere is square pyramidal (Fig. 12.28.A) with the bond distances 1.647(3) Å for Tc=O, 2.279(2) Å for Tc–S, and 1.987(15) Å, on average, for Tc–N. The chelate bite angle is 82.8(1)° for S(1)–Tc–N(4) and 78.5(1)° for N(4)–Tc–N(7). The methyl ester derivative of MAG_3 also forms a stable complex anion $[TcO(MAG_3OMe)]^-$ that is a side product generated during the formation of $[TcO(MAG_3)]^-$. Two different conformations of the ligand in $[PPh_4][TcO(MAG_3OMe)]\cdot 2H_2O$ were established crystallographically [180]. The $[TcO(MAG)_3]^-$ derivative, mercaptoacetylalanylglycylglycinato-oxotechnetate(V), was prepared by reacting TcO_4^-, mercaptoacetyl-DL-alanylglycylglycine, and dithionite as the reducing agent in a phosphate buffer at pH 12. $[Ph_4As][TcO(C_9H_{11}N_3O_5S)]\cdot CHCl_3$ crystallizes from an MeOH/$CHCl_3$ solution in the monoclinic space group $P2_1/n$. The unit cell dimensions are a=9.484(5), b=10.949(7), c=35.74(2) Å, β= 93.87(4)°, and Z=4. The bond distances and bond angles are similar to those of $[TcO(MAG)_3]^-$. The methyl group of the complex adopts a *syn* configuration with respect to the Tc=O group [181].

Very recently the peptide dimethylglycyl-L-seryl-L-cysteinylglycinamide (RP294), a candidate for a bifunctional chelator for the labeling of small biologically important molecules, was reacted with TcO_4^- in aqueous solution containing sodium gluconate and $SnCl_2$. The red, neutral, mononuclear complex

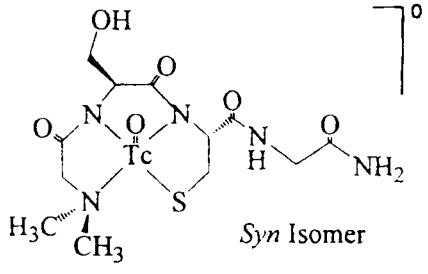

Syn Isomer

appears to exist in *syn* and *anti* conformations. The ν(Tc=O) stretch was observed at 977 cm $^{-1}$. The structure of the complex was identified by ^{1}H NMR and mass spectrometry [181a].

Reaction of $[TcOCl_4]^-$ with pyridine in methanol/water produces $[TcO_2(py)_4]^+$ in which *in situ* three pyridine molecules can be easily displaced by adding 2,4,6-triisopropylbenzenethiol (Htibt). The reaction strongly favors the formation of the neutral compound with one pyridine and three thiolate ligands. $[TcO(tibt)_3(py)]^\circ$ was obtained in red-orange crystals. The complex is diamagnetic. The Tc=O stretch is at 914 cm^{-1}. The coordination geometry of $[TcO(tibt)_3(py)]^\circ$, containing the $TcO(NS_3)$-core, is intermediate between a square pyramid and a trigonal bipyramid. The Tc=O bond distance is 1.665(3) Å. The Tc–S bond lengths range from 2.278(1) to 2.291(1) Å. The Tc–N bond distance is 2.205(4) Å. $[TcO(tibt)_3(py)]^\circ$ crystallizes in the monoclinic space group $P2_1/n$ with a=13.487(2), b=17.654(3), c=21.603(2) Å, β=96.676(9)°, and Z=4 [182].

In order to design neutral, lipid-soluble oxotechnetium(V) complexes as potential brain perfusion imaging agents, a series of tridentate ligands of aza-substituted 2,6-dimethyl-4-azaheptane-2,6-dithiols together with benzyl mercaptane as the coligand were used for complexation:

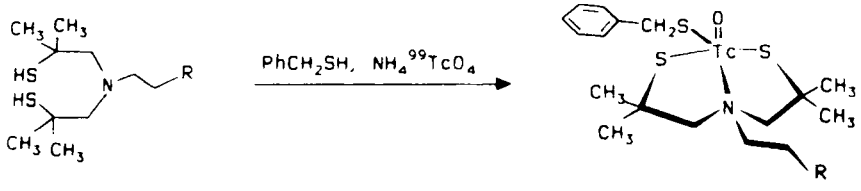

Here R stands for $N(C_2H_5)_2$, piperidine-1-yl, pyrrolidine-1-yl, or morpholine-4-yl. The green-brown complexes are air stable and soluble in most organic solvents. The X-ray structure of the complex containing the morpholine ring shows the coordination geometry of Tc to be trigonally distorted square pyramidal with the sulphur and nitrogen atoms in the basal plane and the doubly bonded oxygen atom occupying the apical position. The Tc=O bond length is 1.664(3) Å. The Tc–S bond lengths are in the range 2.2708(13) to 2.2877(12) Å, which are consistent with those for other technetium thiolato complexes, while the Tc–N bond distance of 2.256(3) Å is slightly longer than usual. The morpholine ring exists in the most stable chair form. The compound crystallizes in the monoclinic space group $P2_1/c$ with a=17.166(2), b=8.9282(7), c=17.738(2) Å, β=166.031(3)°, and Z=4 [183].

12.3.3.7 $TcO(N_3Cl_2)$-, $TcO(N_3Br_2)$-, $TcO(N_2Cl_3)$-, and $TcO(N_2Br_3)$-core complexes

In order to introduce lipophilic character into technetium complexes that might be potentially suitable as ^{99m}Tc radiopharmaceuticals, the hydro-tris(1-pyrazolyl)borate anion ($HBpz_3^-$) was used as a ligand. Dichloro{hydro-tris(1-pyrazolyl)borato}oxotech-

netium(V) with the $TcO(N_3Cl_2)$-core was synthesized by reduction of $^{99}TcO_4^-$ in aqueous 3 M HCl in the presence of $HBpz_3^-$ ion. The neutral, diamagnetic, light green complex $[TcO(HBpz_3)Cl_2]^\circ$ crystallizes in the triclinic space group $P\bar{1}$, with a=7.786(2), b=9.052(2), c=11.328(2) Å, α=103.20(2), β=92.07(3), γ=113.83(3)°, and Z=2. Tc(V) resides in a distorted octahedral coordination environment. The Tc=O distance of 1.656(3) Å is typical for doubly bonded oxo oxygen. The Tc–N bond *trans* to the oxo oxygen has a length of 2.259(4) Å, which is almost 0.2 Å longer than the other Tc–N bond distances. In addition, the Tc=O group causes the *cis* ligands to bend away from the oxo group towards the *trans* pyrazolyl ring. $[TcO(HBpz_3)Cl_2]^\circ$ is insoluble in water and soluble in most polar organic solvents [184]. The analogous complex $[TcO(HBpz_3)Br_2]^\circ$ was prepared by first generating $[TcOBr_4]^-$ in situ and subsequent reaction with $HBpz_3^-$. The yellow-brown product shows a Tc=O stretch at 970 cm^{-1} [87].

Another $TcO(N_3Cl_2)$-core complex was obtained by a ligand exchange reaction of $[TcOCl_4]^-$ in a twofold molar excess with 2,2′;6′,2″-terpyridine (terpy) in methanol. The cationic complex $[TcOCl_2(terpy\text{-}N,N',N'')]^+$ forms an orange precipitate with pertechnetate. The complex salt is moderately soluble in DMF, DMSO, and nitromethane. The Tc=O stretch was found at 979 cm^{-1}. The room temperature reaction of $[TcOCl_4]^-$ with an equimolar quantity of terpyridine in anhydrous dichloromethane led to the isolation of the neutral, orange-brown complex $[TcOCl_3(terpy\text{-}N,N')]^\circ$ in which terpy acts as a bidentate ligand. The Tc=O stretching vibration appeared at 974 cm^{-1} [185].

2,3-Bis(2-pyridyl)pyrazine (dpp) and 2,3-bis(2-pyridyl)quinoxaline (dpq) react with $[TcOCl_4]^-$ in ethanol to form the complexes $[TcOCl_3(dpp)]^\circ \cdot 2H_2O$ and $[TcOCl_3(dpq)]^\circ$. IR and ^{1}H NMR data suggest that the coordination of dpp to Tc(V) occurs in a bidentate manner through one pyrazine and one pyridine nitrogen. The bidentate coordination of dpq to technetium appears to take place only through the two pyridinic nitrogen atoms. Both neutral complexes are soluble in DMF and DMSO. The dark orange $[TcOCl_3(dpp)]^\circ \cdot 2H_2O$ displays a strong band at 982 cm^{-1} which is ascribed to the Tc=O stretching vibration, the green $[TcOCl_3\ (dpq)]^\circ$ complex absorbs at 963 cm^{-1} [186].

The $TcO(N_2Cl_3)$-core has also been found in the neutral complexes trichloro(2,2′-bipyridine)oxotechnetium(V), $[TcOCl_3(bpy)]^\circ$, and trichloro(1,10-phenanthroline) oxotechnetium(V) hydrate $[TcOCl_3(phen)]^\circ \cdot H_2O$. In addition, $[TcOBr_3(bpy)]$ has been prepared. Yellow-orange $[TcOCl_3(bpy)]^\circ$ and orange $[TcOBr_3(bpy)]^\circ$ were obtained by reaction of 2,2′-bipyridine in ethanol with $[TcOCl_4]^-$ or $[TcOBr_4]$ after addition of conc. HCl or HBr, while yellow-orange $[TcOCl_3\ (phen)]^\circ \cdot H_2O$ is accessible, when 1,10-phenanthroline is reacted in ethanol/water with TcO_4^- in the presence of conc. HCl. The Tc=O stretching vibrations of $[TcOCl_3(bpy)]^\circ$, $[TcOBr_3(bpy)]^\circ$, and $[TcOCl_3\ (phen)]^\circ \cdot H_2O$ are 980, 969, and 977 cm^{-1}, respectively [5].

12.3.3.8 $TcO(N_2O_2Cl)$-, $TcO(N_2O_2Br)$-, $TcO(N_2OCl_2)$-, $TcO(N_2OBr_2)$-, $TcO(NOCl_3)$-, $TcO(NOBr_3)$-, and $TcO(NO_2Cl)$-core complexes

The bidentate ligand N-phenylsalicylideneimine (Hphsal) reacts in ethanol with $[TcOCl_4]^-$ to yield chloro-bis(N-phenylsalicylideneiminato)oxotechnetium(V), $[TcOCl\ (phsal)_2]^\circ$. The neutral complex forms dark violet prisms that are soluble in CH_2Cl_2, acet-

onitrile or THF. The compound crystallizes in the monoclinic space group $P2_1/n$ with a=12.854(4), b=15.840(7), c=11.433(4) Å, β=93.43(2)°, and Z=4. The Tc(V) center is situated in a distorted octahedral environment (Fig. 12.29.A). The O(2), N(1), N(2), and Cl atoms define a plane with the Tc atom located 0.19 Å toward the oxo oxygen O(1). The angles Cl–Tc–N(1) and O(2)–Tc–N(2) are 171.0 and 168.7°, respectively. The O(1)–Tc–O(3) angle of 167.1° is also significantly non-linear, while the bond angles in the equatorial plane are rather close to 90°. The Tc=O(oxo) bond distance is 1.67 Å, the Tc-O(2) distance 1.99 Å. However, in spite of the expected *trans* weakening, the TcO(3) bond length *trans* to the oxo ligand is only 1.94 Å. The Tc=O stretch was found at 940 cm^{-1}. The complex is diamagnetic. Using milder conditions of preparation the anionic compound $[TcOCl_3(phsal)]$ was obtained and precipitated with $[AsPh_4]^-$ in the form of a yellow-brown powder [187].

The quadridentate Schiff-base ligand N,N′-propane-1,3-bis(salicylideneimine) (H_2salpd) leads to the light orange, neutral complex $[TcOCl(salpd)]^\circ$ by reaction with $[TcOCl_4]$ in ethanol. The compound crystallizes in the orthorhombic space group $Pn2_1a$ with a=12.010(4), b=11.702(4), c=11.625(6) Å, and Z=4. $[TcOCl(salpd)]^\circ$ exhibits a pseudo-octahedral coordination around the Tc(V). The Schiff-base ligand occupies the four equatorial positions, while the Cl and the oxo oxygen are *trans* to each other in axial positions. The angle between the two salicylideneimine groups is 138.6°, meaning that the groups are bent in an umbrella shape. The Tc=O(oxo) bond distance is 1.66 Å, the Tc–O distances 1.98 Å, the Tc–N and Tc–Cl distances are 2.12 and 2.44 Å, respectively. The Tc=O(oxo) stretching vibration appeared at the rather low frequency of 930 cm^{-1}. In addition, the complexes $[TcOCl_3(Hsalpd)]^-$, $[TcOCl(salbd)]^\circ$, and $[TcOCl_3(Hsalbd)]$ {H_2salbd = N,N′-butane-1,4-diyl-bis(salicylideneimine} have been isolated and characterized [188].

Pyridinemethanolate complexes of Tc^VO^{3+} were synthesized recently from the reaction of n-$Bu_4[TcOCl_4]$ or n-$Bu_4[TcOBr_4]$ with 2,6-di(hydroxymethyl)pyridine in methanol or ethanol. The isostructural brownish crystals of $[TcO(OCH_2py\text{-}CH_2OH)_2Cl]^\circ$ and $[TcO(OCH_2pyCH_2OH)_2Br]^\circ$ adopt the triclinic space group $P\bar{1}$. The former has the lattice constants a=7.479(2), b=8.043(2), c=14.940(4) Å,

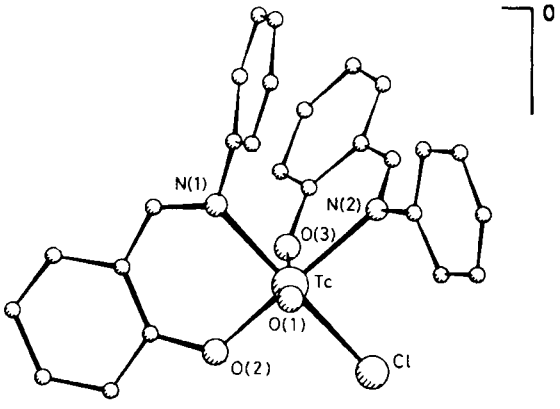

Fig. 12.29.A Chloro-bis(N-phenylsalicylideneiminato) oxotechnetium(V), $[TcOCl(phsal)_2]^\circ$ [187].

α=93.66(2), β=102.16(2), γ= 117.18(2)°, and Z=2. The coordination geometry is distorted octahedral with the oxo and halide ligands in *cis* position to each other. The pyridine ligands are bidentate. The Tc=O and Tc–Cl bond distances are 1.675(3) and 2.385(2) Å, respectively. The mean single bonded Tc–O length is 1.942 Å and the mean Tc–N bond length 2.202 Å. The chelate angles are 74.85 and 81.40°. One of the two hydroxymethyl groups of each pyridine ligand is not bonded to Tc(V) and oriented away from the Tc atom. In the IR, ν(Tc=O) appeared at 930 cm ^{1} [189].

Neutral oxotechnetium(V) complexes with 8-quino-linolates of the composition $[TcOL_2X]^{o}$ (L = 8-quinolinolate and its 5,7-dichloro, 5,7-dibromo, 5-nitro, and 2-methyl derivatives; X=Cl,Br) were synthesized by substitution of the 8-quinolinolate ligand onto $[TcOX_4]^-$ in methanol. *Cis*-chloro-bis(2-methyl-8-quinolinolate)oxotechnetium(V), obtained in deep red crystals, crystallizes in the triclinic space group $P\bar{1}$ with a=7.693(2), b=9.337(2), c=12.739(3) Å, α=86.52(2), β=85.99(2), γ=84.12(2)°, and Z=2. The two methylquinolinolato moieties each act as bidentate O,N donor ligands to the Tc atom that resides in an approximately octahedral coordination environment. The oxygen atom of one quinolinolate ligand is located *trans* to the technetium–oxo bond, while the remaining three donor atoms and the chloride occupy the four equatorial sites. The chloride ligand is *trans* to one nitrogen atom and *cis* to the oxo oxygen. The Tc=O distance is 1.649(3) Å. The bond length of Tc–O *trans* to oxo oxygen is 1.994(3) Å and the Tc–Cl distance 2.360(1) Å. In *cis*-$[TcO(8\text{-quinolinolate})_2X]^{o}$ the halide ligand is susceptible to solvolysis in methanol [190]. Also the base hydrolysis of this complex in alkaline solution was studied [191].

Another mixed ligand, neutral complex containing the $TcO(N_2O_2Cl)$-core is $[TcOCl(eg)(phen)]^{o}$ (eg=1,2-ethanediolate, phen=1,10-phenanthroline). The compound was obtained by reaction of $[TcOCl_4]$ with 1,2-ethanediol in methanol and subsequent addition of 1,10-phenanthroline to the reaction mixture. The green complex crystallizes in the monoclinic space group $P2_1/c$ with a=7.440(2), b=8.928(3), c= 21.355(4) Å, β=92.48(2)°, and Z=4. The Tc atom is six-coordinate, but is significantly distorted from octahedral geometry. The Tc=O(oxo) bond distance is 1.661(4) Å. The lengthening of the Tc–N bonds is due to the *trans* influence of the oxo oxygen and of the strongly bonded ethanediolato moiety, which may also cause the long Tc–Cl bond of 2.418(2) Å. The phen ligand is significantly non-planar, probably its fold accommodates the bonding to the Tc atom [192].

Oxotechnetium(V) complexes of naturally occurring binding moieties like oxazoline and thiazoline derivatives, found in siderophores, have been synthesized recently. Chloro-bis[2-(2′-oxyphenyl)-2-thiazolinato]oxotechnetium(V), $[TcOCl(thoz)_2]^{o} \cdot 0.5EtOH$, was obtained by reaction of $[TcOCl_4]^-$ with Hthoz in refluxing ethanol. The red, neutral complex is air-stable and crystallizes in the monoclinic space group $P2_1/n$ with a=16.506(1), b=7.664(1), c=16.3216(6) Å, β=111.154(4)°, and Z=4. The coordination geometry of Tc is a distorted octahedron. The Tc atom is located 0.19 Å above the equatorial plane formed by the two nitrogens, one oxygen, and one chloride atom. The Tc=O(oxo) bond distance is 1.661(3) Å. One phenolate oxygen is *trans* to the Tc=O bond; the Tc–O length of 1.978(3) Å is typical of a Tc–O bond *trans* to an oxo group. The Tc–N distances are normal, the Tc–Cl bond length is 2.362(1) Å. The axial O=Tc–O angle of 163.7(1)° is distinctly below the ideal of 180° for an octahedral complex. The O–Tc–N bite angle for the

equatorially coordinated ligand is 89.1(1)°, the bite angle for the axial ligand 82.2(1)°. In addition, the compounds chloro-bis{2-(2′-oxyphenyl)-2-oxazolinato} oxotechnetium(V), chloro-bis{2-(2′-oxy-3′-methylphenyl)-2-oxazolinato}oxotechnetium(V), and chloro-bis{2-(2′-oxyphenyl)benzoxalinato}oxotechnetium(V) has been isolated and identified by IR and mass spectra [193].

Red-purple crystals of chloro-bis{2-(2-oxyphenyl)benzothiazolato}oxotechnetium(V), $[TcO(hbt)_2Cl]^\circ$ were obtained by evaporation of a solution of $[TcO(sphsal)Cl]^\circ$ in dichloromethane/heptane. The Hhbt ligand is reported to be formed from H_2sphal by an oxidative intramolecular ring closure reaction:

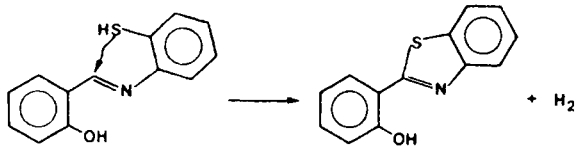

H_2Sphsal Hhbt

The Tc atom in $[TcO(hbt)_2Cl]^\circ$ resides in an approximately octahedral environment. The two hbt ligands coordinate through the phenolate oxygen atoms and the nitrogen atoms of the benzothiazole rings. One of the phenolate oxygens is *trans* to the Tc=O(oxo) linkage. The Tc=O(oxo) bond distance is 1.63(1) Å. The steric requirements of the oxo oxygen atom distort the geometry of the complex and result in non-orthogonal angles at Tc. The Tc–O bond *trans* to Tc=O(oxo) has a length of 1.97(1) Å [194].

The $TcO(N_2OCl_2)$-core was verified in the bis-(2-pyridyl)ketone complexes $[TcOCl_2\{(C_5H_4N)_2C(O)(OEt)\}]^\circ$ and $[TcOCl_2\{(C_5H_4N)_2C(O)(OH)\}]^\circ$ that were prepared by reacting $[TcOCl_4]^-$ and the dipyridylketone in refluxing ethanol and in benzene containing 0.02 % water, respectively. Dipyridylketone has the ability to undergo metal-promoted addition of various nucleophiles, including water and ethanol, at the carbon atom of the carbonyl group, to produce the uninegative ligand $\{(C_5H_4N)_2C(O)(OR)\}^-$ after initial coordination to the transition metal ion. The green neutral compounds are diamagnetic and slightly soluble in common polar organic solvents. According to the structure analysis of the analogous rhenium complex $[ReOCl_2\{(C_5H_4N)_2C(O)(OH)\}]^\circ$, the Tc central atom is expected to reside in a highly distorted octahedral environment in which the two *cis* chlorides, along with the nitrogen donors, occupy the equatorial sites and the oxo ligand is *trans* to the HO^- oxygen atom [195].

Dibromoethoxy-bis(4-nitropyridine)oxotechnetium(V), which contains the corresponding $TcO(N_2OBr_2)$-core, was obtained by dissolving 4-nitropyridine and $[TcOBr_4]$ in ethanol and collecting the green precipitate. The neutral compound $[TcOBr_2(4\text{-nitropyridine})_2(OEt)]^\circ$ crystallizes in the triclinic space group $P\bar{1}$ with the cell constants a=10.820(1), b=11.146(2), c=9.006(1) Å, α=102.82(1), β=108.11(1), γ=64.53(1)°, and Z=2. The coordination geometry of the technetium atom is approximately octahedral (Fig. 12.30.A). The Tc=O(oxo) bond distance is 1.684(6) Å, while the Tc–O(1) bond length of 1.855(6) Å reflects a lower bond order assignment to the ethoxy ligand. The O(1)–Tc=O(2) bond angle is 172.9(3)°. The bromine atoms are at

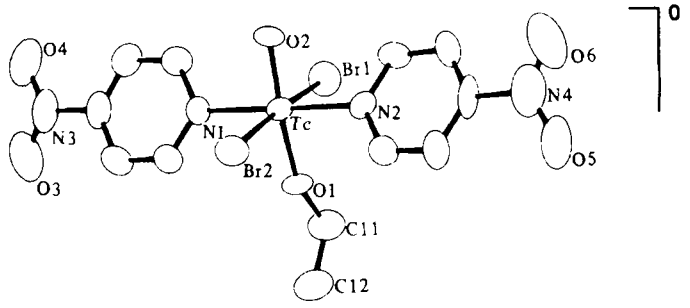

Fig. 12.30.A Dibromo-ethoxy-bis(4-nitropyridine)oxotechnetium(V), $[TcO(EtO)Br_2(4\text{-nitropyridine})_2]^\circ$ [196].

an average distance of 2.55(2) Å with a Br(1)–Tc–Br(2) bond angle of 174.3(1)°. The average Tc–N distance is 2.146 Å, the N(1)–Tc–N(2) bond angle 178.7(3)°. The pyridine rings are twisted, 59° for the N(1) ring and 49° for the N(2) ring, from a plane defined by the two nitrogens and the two bromines. The Tc=O(oxo) stretching vibration occurs at 938 cm^{-1}. All but the oxo ligands appear to be readily substituted in various solvents. In addition, other compounds of the type $[TcOX_2L_2(RO)]^\circ$ where X = Cl or Br, L = 4-cyanopyridine or 4-nitropyridine, and R = CH_3 or C_2H_5 have been synthesized [196].

Another $TcO(N_2OCl_2)$-core complex, 1-(8′-quinolyliminomethyl)-2-naphtholato-*trans*-dichloro-oxotechnetium(V), was prepared by ligand-exchange reaction of $[TcOCl_4]^-$ with 1-(8′-quinolyliminomethyl)-2-naphthol (quinim-naphH) in methanol. The green, neutral complex $[TcOCl_2(quinim\text{-}naph)]^\circ$ crystallizes in the monoclinic space group $P2_1/a$ with a=23.262(8), b=7.301(4), c=11.444(5) Å, β=98.98(5)°, and Z=4. The Tc environment is severely distorted octahedral, with the equatorial plane formed by the tridentate ligand with the N_2O donor atoms and the Tc=O(oxo) oxygen. The two chlorine atoms are *trans* to each other in axial positions. The N_2O ligand is coordinated in an unusual fashion, because the central imino nitrogen is located *trans* to the Tc=O group. The chelate ligand is very nearly planar. The small angle N–Tc–N of 75.5(2)° corresponds to the very large O=Tc–O angle of 113.4(3)°. Similar neutral oxotechnetium(V) dichloro complexes have been prepared using the chelating Schiff-base N_2O donor set ligands N-(8′-quinolyl)salicylideneiminate, 3-methoxy-N-(8′-quinolyl)salicylideneiminate and N-(2′-dimethylaminoethyl) salicylideneiminate. The compounds are air-stable and non-conducting in acetonitrile [197].

Reaction of $[AsPh_4][TcOX_4]$ (X = Cl,Br) with 2-(2-hydroxyphenyl)benzothiazole (Hhbt) in isopropyl alcohol under mild conditions yields a red-orange precipitate of the composition $[AsPh_4][TcOX_3(hbt)]$ containing the $TcO(NOX_3)$-core. The complex salts are soluble in CH_2Cl_2, $CHCl_3$, and acetone. $[AsPh_4][TcOCl_3(hbt)]$ crystallizes in the orthorhombic space group $P2_12_12_1$ with a=12.104(2), b=13.772(3), c=20.539(4) Å, and Z=4. The coordination geometry around the Tc atom is nearly octahedral (Fig. 12.31.A). The three chlorine atoms and the neutral nitrogen atom of the hbt ligand are located in the plane that is normal to the Tc=O(2) linkage and the anionic phenolato O(1) oxygen *trans* to the Tc=O linkage. The distortion from octahedral symmetry

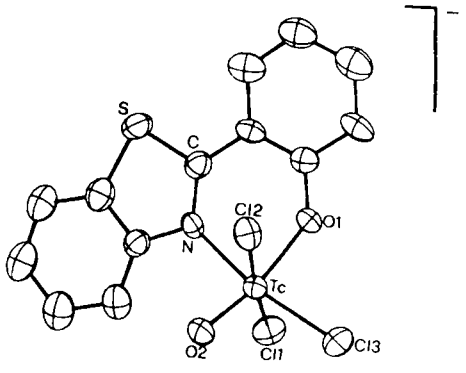

Fig. 12.31.A Trichloro[2-(2-hydroxyphenyl)benzothiazolato]oxotechnetate(V). $[TcOCl_3(hbt)]^-$ [198].

is mainly caused by repulsion between the sterically demanding Tc=O(2) group and the coordinate chloride ligands. The O(2)–Tc–Cl(2) and O(2)–Tc–Cl(3) angles are 98.5(2) and 99.7(2)°, respectively. The Tc=O(2) distance is 1.650(6) Å. The hbt ligand is remarkably planar. The complex anion is diamagnetic, consistent with the spin-paired d^2 configuration [198].

The tridentate Schiff-base ligand N-(2-hydroxyphenyl)salicylideneimine (H_2ophsal) reacts with $[TcOCl_4]^-$ in methanol to form the dark purple, neutral complex $[TcO(ophsal)Cl]^0$ with the $TcO(NO_2Cl)$-core by simple ligand exchange. By the same route the analogous complex $[TcO(sphsal)Cl]^0$ was obtained by using the ligand N-(2-mercaptophenyl)salicylideneimine (H_2sphsal). Both compounds are only slightly soluble in methanol, but more soluble in chloroform and dichloromethane. $[TcO(ophsal)Cl]^0$ crystallizes in the monoclinic space group $P2_1/a$ with a=13.423(6), b=12.570(5), c=7.769(3) Å, β=106.53(5)°, and Z=4. The complex has a distorted square pyramidal coordination geometry with the oxo ligand in the apical position. The steric requirement of the Tc=O group causes the Tc atom to be displaced 0.67 Å out of the mean equatorial plane of the four donor atoms. The Tc=O bond distance is 1.634(7) Å, the basal Tc–O lengths are 1.948 Å. The Tc–Cl distance of 2.302(3) Å is similar to that in $[TcOCl_4]^-$. The Tc=O stretching vibration appears at 980 cm^{-1} [199].

12.3.3.9 $TcO(N_2OS)$-, $TcO(N_2OS_2)$-, $TcO(NOS_2)$-, $TcO(NO_2S)$-, $TcO(N_2S_2Cl)$-,$TcO(NOSCl)$-, and $TcO(N_2SCl)$-core complexes

The tetradentate ligand N-(mercaptoacetyl)-N′-{4-(pentene-3-one-2)}-ethane-1,2-diamine (H_3mpd) reacts with $[TcOCl_4]^-$ in methanol to yield an orange crystalline precipitate. The neutral $TcO(N_2OS)$-core compound $[TcO(mpd)]^0$ crystallizes in the triclinic space group $P\bar{1}$ with a=7.7650(3), b=8.1969(6), c=10.4043(7) Å, α=92.944(6), β=110.805(5), γ=109.957(5)°, and Z=2. Tc(V) is five-coordinate with the O(1) oxo oxygen at the apex of a distorted square pyramid (Fig. 12.32.A). The Tc atom lies about 0.709(1) Å out of the plane, formed by the four donor atoms of the organic ligand, towards the O(1) oxygen. The Tc=O bond distance of 1.657(2) Å is in the normal range, as is the Tc–S distance of 2.2720(7) Å. The Tc–N(1) and Tc–N(2) distances of 1.959(2) and 2.041(2) Å, respectively, are remarkably different. The bite angles S–Tc–

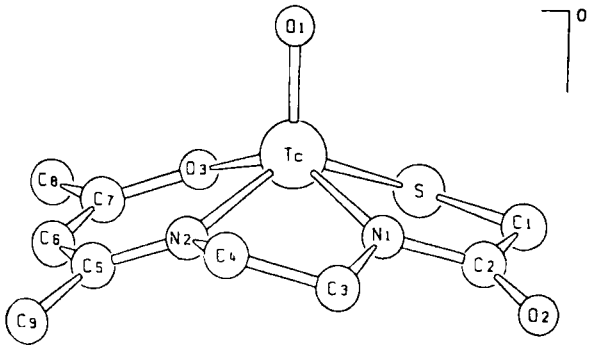

Fig. 12.32.A N-(2-mercaptoacetyl)-N′-[4-(pentene-3-one-2)]ethane-1,2-diaminato-oxotechnetium(V), [TcO(mpd)]° [200].

N(1) and O(3)–Tc–N(2) are 83.21(6) and 87.79(9)°, respectively. In the IR the intense absorption at 952 cm^{-1} is attributed to the Tc=O stretching vibration [200].

The anionic complex 2-mercaptoacetyl diglycinato-oxotechnetate(V) [TcO $(MAG_2)]^-$ (H_4MAG_2) represents another instance of the $TcO(N_2OS)$-core. Reaction of mercaptoacetyl diglycine with Tc(V) gluconate in alkaline aqueous solution forms $[TcO(MAG_2)]$, which can be precipitated as the tetraphenylarsonium salt. $[AsPh_4][TcO(MAG_2)] \cdot C_2H_5OH$ forms dark brown crystals of the monoclinic space group $P2_1/n$ with a=12.478(5), b=14.922(5), c=17.183(9) Å, β=103.13(4)°, and Z=4. The coordination geometry of Tc(V) is again a distorted square pyramid with the oxo oxygen at the apex. The Tc=O(oxo) bond distance is 1.644 Å. The Tc=O stretch was found at 960 cm^{-1}. Remarkably, the hydroxyl oxygen atom of the carboxylic group is bonded to Tc; carboxylate ligands in Tc complexes have scarcely been described. The corresponding Tc–O bond length is 2.016 Å. Both Tc–N bond distances are 1.968 Å. The Tc–S distance is 2.271 Å. The Tc atom is displaced by 0.756 Å towards the oxo ligand from the equatorial plane [201,202].

To characterize potential ^{99m}Tc radiopharmaceuticals such as ^{99m}Tc penicillamine complexes, the neutral $TcO(N_2OS_2)$-core complex D-penicillaminato-(N,S,O)-D-penicillaminato-(N,S)-oxotechnetium(V) was obtained by reaction of $[TcOCl_4]^-$ in hydrochloric acid with D(-)-penicillamine. After evaporation of the dark reddish brown solution, crystals were isolated, crystallizing in the orthorhombic space group $P2_12_12_1$ with a=21.878(5), b=11.711(2), c=5.924(1) Å, and Z=4. The structure comprises a distorted octahedron of donor atoms about the Tc(V). Technetium is bonded to the S,N, and O atoms of a D-penicillamine dianion deprotonated at S and O, and to the S and N atoms of another D-penicillamine anion deprotonated at S. The Tc=O(oxo) bond distance is 1.657(4) Å. The S and N atoms of the two D-penicillamine groups are *cis* arranged in the equatorial plane and are bent away from the oxo oxygen. Also this complex reveals a bonding to Tc via the ionized carboxylate group. The O atom is *trans* to the oxo oxygen. Its bond distance of 2.214(4) Å is comparable to the Tc–N distances. The Tc–S bond lengths of 2.296(2) and 2.283(2) Å are normal. The molecular structure of the technetium penicillamine complex was, in addition,

extensively elucidated by NMR and vibrational spectra [203]. The mixed complex [(D-penicillaminato)(L-penicillaminato)TcO]$^-$ is fluxional, racemizing by exchange of carboxylates at the site *trans* to the oxo ligand [204] (Sect. 6.3).

The neutral, mixed ter- and bidentate Schiff-base oxotechnetium(V) complex [TcO(haf)(pac)]$^\circ$ {H_2haf = S-methyl-β-N-(2-hydroxyphenylethylidene)dithiocarbazate, Hpac = S-methyl-β-N-(isopropylidene)dithiocarbazate}, with the $TcO(N_2OS_2)$-core, was synthesized by reaction of $[TcOCl_4]$ with H_2haf in methanol/acetone without adding Hpac. The isolated dark red crystals crystallize in the monoclinic space group $P2_1/c$ with a=14.799(5), b=7.470(2), c=19.272(5) Å, β=104.31(10)°, and Z=4. The formation of the ligand (pac)$^-$ from H_2haf is unexpected and surprising. As reported, this may be the result of ketone exchange between the solvent acetone and the 2-hydroxyacetophenone group of a H_2haf molecule, if the H_2haf used for complexation was not contaminated with Hpac. The six-coordinate Tc(V) complex [TcO(haf)(pac)]$^\circ$ is diamagnetic. The IR spectrum displays an intense band at 926 cm^{-1}, attributed to the Tc=O stretch. The coordination environment of Tc(V) is distorted octahedral (Fig. 12.33.A). The phenolic oxygen O(2) occupies the site *trans* to the oxo oxygen O(1). The S and N atoms of the two ligating ligands form a *cis* arrangement in the equatorial plane. Distortions from an octahedron are primarily due to the steric requirements of the O(1) oxo oxygen and to the bite angles N(2)–Tc–S(1) of 78.9(3)° and N(4)–Tc–S(2) of 81.0(3)°. The Tc=O(1) distance is 1.633(8) Å. The Tc atom is displaced by 0.20 Å from the mean equatorial plane toward O(1). The distortion also results in a non-linear O(1)=Tc–O(2) axis of 157.0(4)° [205,206].

A compound containing the $TcO(NOS_2)$-core was obtained by reaction of tris(2,4,6-triisopropyl-benzenethiolato)-pyridino-oxotechnetium(V) (Sect. 12.3.3.6) with (phenylazo)formic acid 2-phenyl-hydrazide in methanol. The neutral, purple-green complex $[TcO\{SC_6H_2(isopropyl)_3\}_2(PhNNCON_2HPh)]^\circ$ crystallizes in the triclinic space group $P\bar{1}$ with a=13.3613(8), b=14.0268(6), c=13.0857(6) Å, α=113.949(4), β=100.265(4), γ=76.019(4)°, and Z=2. The Tc atom is five-coordinate with the coordination geometry intermediate between square pyramidal and trigonal bipyramidal. The Tc=O(oxo) distance is 1.658(2) Å. The Tc–S bond distances are typical for

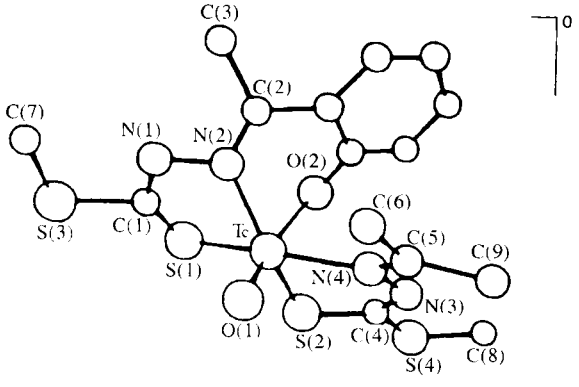

Fig. 12.33.A {S-methyl-β-N-(2-oxyphenylethylidene) dithiocarbazato}, {S-methyl-β-N-(isopropylidene) dithiocarbazato}oxotechnetium(V), $[TcO(haf)(pac)]^\circ$ [205].

Tc(V)-thiolate sulphur bonds. Two coordination sites are occupied by the α-nitrogen and the carbonyl oxygen atom of the five-membered chelate ring. In the IR spectrum the Tc=O(oxo) stretching vibration occurs at 950 cm ^{1} [207].

Another neutral, mixed ligand $TcO(NOS_2)$-core complex, benzenethiolato-{N-(2-sulphidophenyl)salicylideneiminato}-oxotechnetium(V) was synthesized by reaction of $[TcOCl_4]^-$, dissolved in chloroform, with an ethanolic solution of benzenethiol and 2-(salicylideneimino)benzenethiol. The red-brown compound crystallizes in the monoclinic space group $P2_1$ with a=7.901(1), b=10.147(1), c=11.370(2) Å, β=93.60(1)°, and Z=2. Tc(V) is surrounded by a distorted tetragonal pyramid (Fig. 12.34.A) of donor atoms. The basal plane is defined by the thiolate S(1) atom, the nitrogen N(1) and the phenolic oxygen O(2) of the tridentate, dianionic N-(2-sulphidophenyl)salicylidene-iminato ligand and the S(2) atom of the benzenethiolato group. The Tc atom lies 0.66 Å above the basal plane towards the O(1) oxo oxygen in the apical position. The Tc=O(1) bond distance is 1.661(7) Å. The angle between the Tc=O(1) axis and the normal of the basal plane is 177.2°. The mean plane of the benzenethiolato ligand and the basal plane form an angle of 102.4°. The Tc–S(1), Tc–S(2), Tc–N(1), and Tc–O(2) bond distances are 2.225(5), 2.265(5), 2.126(11), and 2.037(11) Å, respectively [208,209]. In addition, other $TcO(NOS_2)$-core complexes were synthesized by replacing benzenethiol by 4-$CH_3OOCC_6H_4SH$, n-$C_8H_{17}SH$ or $C_2H_5OOCCH_2SH$. Furthermore, 2-(salicylideneimino)benzenethiol was substituted by the Schiff-base ligand N-acetylacetone-2-aminothiophenol [209].

N-salicylidine-cysteine-oxotechnetium(V), a brown, neutral, diamagnetic complex, probably containing a $TcO(NO_2S)$-core, was prepared by reaction of an ethanolic solution of salicylaldehyde with an aqueous TcO_4^- solution, alkaline $S_2O_4^{2-}$ as a reductant and an alkaline solution of L-cysteine. The amino acid Schiff-base ligand is quadridentate and appears to coordinate through the carboxylate, phenolate, and thiolate group and the uncharged azomethine group:

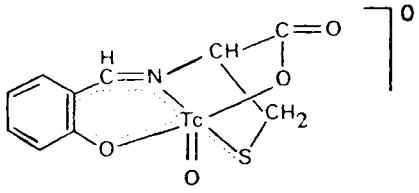

Similar Schiff-base ligand Tc(V) complexes were obtained with L-serine, L-histidine, L-threonine, L-glutamic acid, and L-tryptophane [210].

A series of oxotechnetium(V) complexes with bidentate, monoanionic Schiff-bases derived from S-methyldithiocarbazate have been synthesized. The neutral, six-coordinate, diamagnetic, red compounds are suggested to contain the $TcO(N_2S_2Cl)$-core. The complexes were prepared by ligand exchange reaction of $[TcOCl_4]^-$ with the corresponding Schiff-base ligands in ethanol or methanol. According to IR spectra the complexes show a definite correlation between the strength of the Tc=O bond and the degree of double bond character of the coordinating C=N bonds. The stronger the Tc=O bond, the weaker the nitrogen coordination and the more double bond character is in the coordinating C=N bond [211].

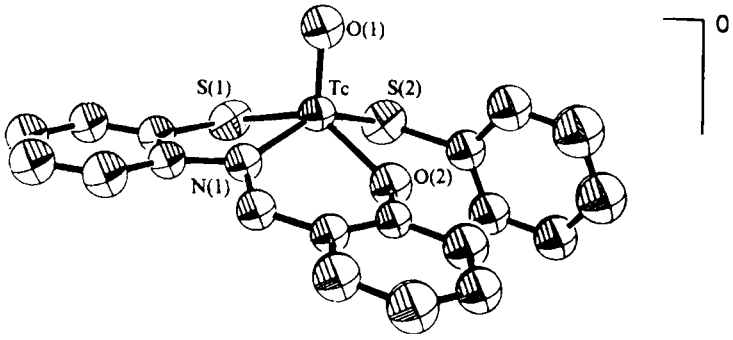

Fig. 12.34.A Benzenethiolato-{N-(2-mercaptophenyl)salicylideneiminato}oxotechnetium(V), [TcO(bt)(sphsal)]° [208].

Other $TcO(N_2S_2Cl)$-core complexes were obtained when $[TcOCl_4]$ was reacted with 2-amino-1-cyclo-pentene-1-dithiocarboxylic acid (Hacd) or its N- and S-alkyl derivatives in acetone. Orange-red crystals of $[TcOCl(acd)_2]^\circ$ and of the derivative complexes were isolated. The diamagnetic, neutral compounds are fairly soluble in acetonitrile and DMF. According to IR and ^1H NMR spectra, Tc(V) is coordinated through the thiolate and the amino group in the equatorial plane, while the chloro ligand resides in the *trans* position to the Tc=O(oxo) oxygen. The Tc=O stretching vibrations occur at 964 cm^{-1} [212].

The tetradentate Schiff-base ligand N,N'-ethylene-bis(acetylacetonethioimine) reacts with $[TcOCl_4]^-$ in acetonitrile in an inert atmosphere to give a green precipitate of the neutral complex $[TcOCl\{(sacac)_2en\}]^\circ$. The ligand coordinates in the equatorial plane orthogonal to the Tc=O linkage. The Tc=O stretch was found at 938 cm^{-1}. The complex is unstable in solution. When dissolved in CH_2Cl_2, $CHCl_3$ or acetonitrile the color of the green solution turns red-brown mainly due to the high lability of the chlorine ligand *trans* to the Tc=O group. Traces of moisture lead to the substitution of chlorine by H_2O [213].

The $TcO(NOSCl)$-core has also been found in some complexes. The reaction of the tridentate Schiff-base ligand N-(2-mercaptophenyl)salicylideneimine(H_2sphsal) with $[TcOCl_4]^-$ in methanol yields dark red crystals of the neutral complex $[TcOCl(sphsal)]^\circ$ that crystallizes in the monoclinic space group $P2_1/a$ with a=14.255(9), b=12.495(7), c=7.865(6) Å, β=105.22(5)°, and Z=4. The complex is soluble in dichloromethane, chloroform or DMF. The preparation of the compound requires that $[TcOCl_4]^-$ and the Schiff-base ligand be used in stoichiometric amounts. $[TcOCl(sphsal)]^\circ$ proved to be diamagnetic. The coordination geometry of Tc(V) is square pyramidal. The ligand occupies three of the four coordination sites of the basal plane. The Tc atom is displaced from the mean equatorial plane towards the oxo oxygen by about 0.7 Å. The Tc=O(oxo) bond distance is 1.62(1) Å, the Tc–Cl, Tc–S, Tc–N, and Tc–O distances are 2.31(1), 2.33(1), 2.15(2) and 1.92(2) Å, respectively [214].

The same core of donor atoms has been verified in the complex chloro{S-methyl-3-(2'-hydroxy-1-naphthylmethylene)dithiocarbazato}-oxotechnetium(V), which was

synthesized by treating $[TcOCl_4]^-$ with the corresponding tridentate, dianionic Schiff-base ligand (H_2tcbn) in ethanol. The red compound $[TcOCl(tcbn)]^\circ$ crystallizes in the orthorhombic space group $P2_12_12_1$ with a=7.102(3), b=14.697(5), c=14.732(4) Å, and Z=4. Tc(V) resides again in a distorted square pyramidal environment (Fig. 12.35.A). The tridentate O, N, S ligand and the chlorine atom *trans* to N(2) form the basal plane. The Tc atom is displaced by 0.693(1) Å from the plane defined by N(2), S(1), O(2) and Cl, pointing towards the O(1) oxo atom. The Tc=O(1) distance is 1.645(7) Å, indicating strong multiple bond character. The Tc=O stretch was found at 980 cm^{-1}. The complex is diamagnetic in solution [215].

Some years prior to the appearance of [215], it was shown that the very similar tridentate Schiff-base ligand S-methyl-β-N-(2-hydroxyphenyl-ethylidene)dithiocarbazate reacts with $[TcOCl_4]^-$ to form the corresponding neutral, red complex $[TcOCl(haf)]^\circ$ which, however, was reported to be paramagnetic with a magnetic moment of 2.45 B.M. This moment would roughly correspond to the presence of two unpaired electrons, in contrast with previously synthesized square pyramidal oxotechnetium(V) complexes found to be diamagnetic. One explanation would be to consider a trigonal bipyramidal geometry of the complex. However, this exception would be surprising, because other analogous oxotechnetium(V) complexes synthesized by the same route with derivative tridentate Schiff-base ligands were also found to be diamagnetic [216,217].

Very recently, $TcO(N_2SCl)$-core complexes were obtained by reaction of $[TcOCl_4]^-$ with derivatized amino acids in CH_2Cl_2/EtOH. The tridentate N_2S ligands (H_2L) were synthesized by conjugating N-protected amino acids with S-methyl-2-methyldithiocarbazate. The purple compounds $[Tc^VO(L)Cl]^\circ$ are stable and possess a square pyrami-

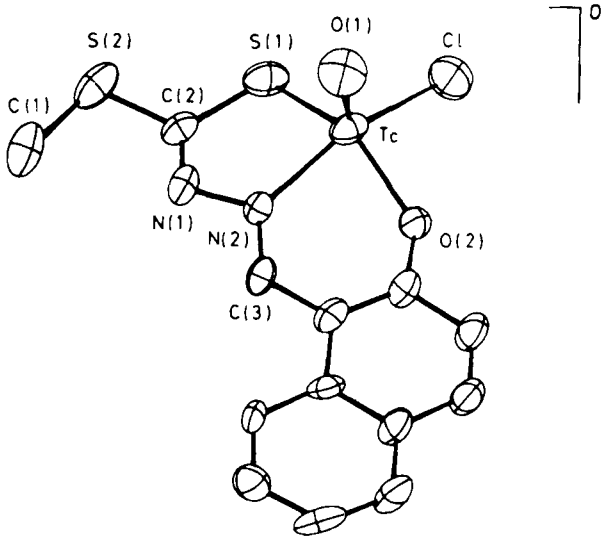

Fig. 12.35.A Chloro-{S-methyl-3-(2′-oxy-1-naphthylmethylene)dithiocarbazato}oxotechnetium(V), $[TcOCl(tcbn)]^\circ$ [215].

dal geometry. The ligands (L) and the chloride form the basal plane. Structurally analogous, yellow complexes $[Tc^{V}N(L)(PPh_3)]^{\circ}$ were prepared when $[TcNCl_2(PPh_3)_2]^{\circ}$ was reacted with H_2L [217a].

12.3.3.10 $TcO(N_2OP_2)$-, $TcO(P_2S_2Cl)$-, $TcO(P_2O_2Cl)$-, $TcO(P_2O_3)$-, and $TcO(NP_3Cl_2)$-core complexes

In this section we describe those oxotechnetium(V) complexes which contain, in addition to other donor atoms, coordinated phosphorus.

(2-Aminophenyl)diphenylphosphine, $(2\text{-}NH_2C_6H_4)PPh_2$ (Happ), reacts with $[NBu_4]TcO_4$ in methanol or ethanol at the controlled stoichiometric molar ratio of Tc:Happ=1:3 to produce the neutral $TcO(N_2OP_2)$-core complex $[TcO(app)_2(OR)]^{\circ}$ (R = Me or Et) in which the amino groups are deprotonated. Pertechnetate is reduced to oxotechnetium(V) by 1 mole of the Happ ligand. The dark purple compound is soluble in acetonitrile, dichloromethane, and chloroform. $[TcO(app)_2(OEt)]^{\circ}$ is quite stable in the solid state, more stable than $[TcO(app)_2(OMe)]^{\circ}$. However, both complexes slowly decompose in solution. $[TcO(app)_2(OMe)]$ crystallizes in the monoclinic space group $P2_1/c$ with a=12.156(3), b=26.005(6), c=10.953(2) Å, β=102.49(2)°, and Z=4. The coordination geometry about Tc is highly distorted octahedral (Fig. 12.36.A). The O(1)–Tc–O(2) angle is only 158.3°, the bite angles P(1)–Tc–N(1) and P(2)–Tc–N(2) are 79.8(3) and 79.6(3)°, respectively. Each pair of bidentate PN ligand donor atoms is nearly coplanar with their benzene ring, however, the rings are bent away from the oxo oxygen. The angles between the Tc=O(1) bond and the equatorial nitrogen donors O(1)–Tc–N(1) and O(1)–

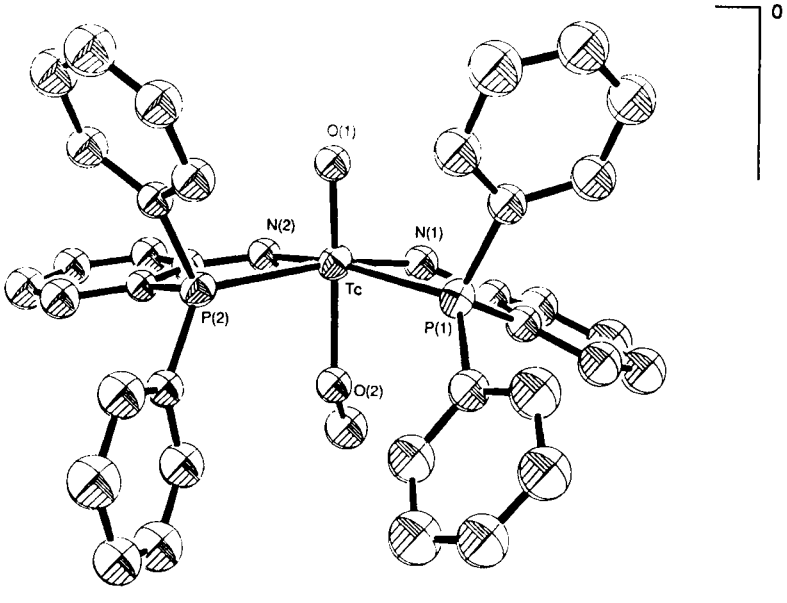

Fig. 12.36.A {Bis(2-aminophenyldiphenylphosphine)(methoxy)}oxotechnetium(V), $[TcO(app)_2(OMe)]^{\circ}$ [218].

Tc–N(2) are 105.8(4) and 103.6(4)°, respectively, while they are close to 90° with the phosphorus donors. The alcoholate O(2) oxygen is at a distance of 1.999(8) Å. The Tc=O(1) bond shows a remarkable weakening as demonstrated by the bond length of 1.700(8) Å accompanied by a very low value of the Tc=O(1) stretching vibration of 878 cm $^{-1}$ for the methoxo derivative and 857 cm $^{-1}$ for the ethoxo one. The unusually low frequency values much below the low-frequency end of the range thus far observed for monooxotechnetium(V) complexes and tailing into the region characteristic of *trans*-dioxo asymmetric stretching (750–850 cm^{-1}), is due to the presence of both the *trans*-oxo-alcoholate group and mainly the amido groups in the equatorial plane [218].

Reaction of the tetradentate, dianionic ligand N,N′-bis{2-(diphenylphosphino)phenyl}-propane-1,3-diamine (H_2dppd) with TcO_4^- in methanol yielded the neutral, stable, six-coordinate complex [TcO(dppd)(OMe)]°. The red-brown compound, which is soluble in chlorinated solvents, crystallizes in the monoclinic space group $P2_1/m$ with a=9.157(2), b=20.391(3), c=9.948(1) Å, β=114.76(1)°, and Z=2. The tetradentate P_2N_2 ligand occupies the four equatorial positions of a distorted octahedron around the metal atom. In the axial positions reside the oxo oxygen atom and the methoxo ligand. The angle O=Tc–O is only 155.2°. The Tc atom is displaced from the equatorial P_2N_2 plane by 0.31 Å towards the oxo oxygen. The Tc–P distance is 2.450(1) Å, the P–Tc–P angle 102.9(1)°, and the N–Tc–N angle 91.9(1)°. The P–Tc–N bite angle is 80.4(1)° [219].

The bidentate, monoanionic phosphino-thiol ligand 2-(diphenylphosphino)benzenethiol (Hpbt), treated with $[TcOCl_4]^-$ in the exact molar ratio of 2:1 in CH_2Cl_2 at –80 °C, produces the neutral complex $[TcOCl(pbt)_2]^\circ$. The purple complex contains the $TcO(P_2S_2Cl)$-core and shows a strong Tc=O stretch at 940 cm $^{-1}$ [220].

2-Hydroxyphenyldiphenylphosphine reacts in ethanol with $[TcOCl_4]^-$ to form the purple crystalline product $[TcOCl(OC_6H_4PPh_2)_2]^\circ$. The compound is soluble in chloroform and dichloromethane. The Tc=O stretching vibration occurs at 940 cm^{-1} [221]. The same compound was recently obtained by reduction-substitution reaction of TcO_4^- with (2-hydroxyphenyl)diphenylphosphine in ethanol/HCl. The dark violet rhomboids crystallize in the orthorhombic space group $P2_12_12_1$ with a=10.183(9), b=14.028(9), c=21.40(1) Å, and Z=4. The coordination geometry of the $TcO(P_2O_2Cl)$-core is distorted octahedral. The chelating, bidentate, uninegative ligands form with Tc(V) two five-membered rings with bite angles of 78.1 and 81.9°. Tc(V) is out of the mean P_2OCl equatorial plane by 0.29 Å towards the oxo atom. The Tc=O(oxo) distance is 1.665(7) Å and the Tc–Cl distance 2.389(4) Å. The Tc–O single bond distances are about 1.99 Å. The axial O–Tc=O angle is 164.5(3) Å [222].

$[TcOCl_4]^-$ was also treated in EtOH with bis(2-hydroxyphenyl)phenylphosphine [$Ph(OH)_2PPh$], a potentially tridentate, dianionic ligand. A brown powder of the neutral complex $[TcO(PhO_2)PPH(PhOOH)PPh]^\circ$, soluble in DMSO and DMF, was isolated and characterized by ^{1}H NMR, mass spectrometry, and IR spectroscopy. The Tc=O stretch was found at 965 cm^{-1}. The compound has a $TcO(P_2O_3)$-core [221].

A cationic oxotechnetium(V) complex containing the $TcO(NP_3Cl_2)$-core was prepared by treating TcO_4^- in ethanol with conc. HCl and with the tetradentate tripodal ligand 2-diphenylphosphino-N,N-bis(2-diphenylphosphinoethyl)ethanamine (NP_3). After addition of the tetraphenylborate anion, the orange crystalline product $[TcOCl_2(NP_3)][BPh_4]$ was obtained and identified [223].

The structural data of $(TcO)^{3+}$-core complexes discussed in Sects 12.3.3.1–12.3.3.10 are summarized in Table 12.6.A.

Table 12.6.A Some structural data of selected $(TcO)^{3+}$-core complexes described in Sects. 12.3.3.1 to 12.3.3.10.

Complex	Geometry	Tc=O [Å]	ν(Tc=O) IR [cm^{-1}]	Tc (displacement) [Å]	References
12.3.3.1					
$[TcOCl_4]^-$	sq.pyr.	1.593(8)	1025	0.67	[86]
$[TcOBr_4]$	sq.pyr.	1.613(9)	1010	–	[88,89]
$[TcOBr_4(H_2O)]$	octah.	1.618(9)	1000	0.37	[89]
$[TcOI_4]$	sq.pyr.	–	993	–	[90]
$[TcOCl_5]^{2-}$	octah.	–	956	–	[98]
$[TcOBr_5]^{2-}$	octah.	–	962	–	[98]
12.3.3.2					
$[TcO(CN)_5]^{2-}$	octah.	–	910	–	[99]
$[TcO(CN)_4(OMe)]^{2-}$	octah.	–	932	–	[99]
$[TcO(CN)_4(H_2O)]^-$	octah.	–	–	–	[100]
$[TcO(CN)_4(NCS)]^{2-}$	octah.	–	–	–	[100]
$[TcO(NCS)_5]^{2-}$	octah.	–	945		[101]
12.3.3.3					
$[TcO(eg)_2]^-$	sq.pyr.	–	970		[102,103]
$[TcO(cat)_2]$	sq.pyr.	1.648(5)	972	0.7014(4)	[102]
$[TcO(nitrocat)_2]$	sq.pyr.	1.634(4)	983	0.6947(5)	[104]
$[TcO(chlorocat)_2]$	sq.pyr.	1.945(4)	969	–	[70]
$[TcO(hmpo)_2Cl]^+$	octah.	–	965	–	[105]
$[TcO(dpp)_2Cl]^+$	octah.	–	950	–	[105]
$[TcO(hmpo)Cl_3]$	octah.	1.647(2)	965	0.2	[105]
$[TcO(ox)_2(Hox)]^{2-}$	octah.	1.640(6)	985	0.25(1)	[68]
12.3.3.4					
$[TcO\{S(CH_2)_2S\}_2]$	sq.pyr.	1.64(1)	940	0.761(2)	[106,107]
$[TcO\{S(CH_2)_3S\}_2]$	sq.pyr.	–	945	–	[106,107]
$[TcO(SCH_2CHCH_3S)_2]^-$	sq.pyr.	–	925	–	[106,107]
$[TcO(SCH_2COS)_2]$	sq.pyr.	1.672(8)	950	0.791	[108]
$[TcO(SCOCOS)_2]$	sq.pyr.	1.646(4)	972/980	0.759	[109,110]
$[TcO(mnt)_2]^-$	sq.pyr.	1.655(6)	947	0.742(3)	[109,112]
$[TcO(tdt)_2]$	sq.pyr.	–	930	–	[109]
$[TcO(bdt)_2]$	sq.pyr.	1.658(5)	–	0.732(1)	[111]

Table 12.6.A Continued.

Complex	Geometry	Tc=O [Å]	ν(Tc=O) IR [cm^{-1}]	Tc (displacement) [Å]	References
$[TcO\{(CH_3)_3C_6H_2S\}_4]^-$	sq.pyr.	1.659(11)	940	0.846	[113]
$[TcO\{(CH_3CHCH_3)_3C_6H_2S\}_4]^-$	sq.pyr.	–	940	–	[113]
$[TcO(Ph_2C_6H_3S)_4]$	sq.pyr.		960		[113]
$[TcO(tmbt)_4]^-$	sq.pyr.	–	933	–	[114]
$[TcO(tmtu)_4]^{3+}$	sq.pyr.	–	975	–	[115]
$[TcO(tmtu)_2(CH_3)_2NCSS]^{2+}$	sq.pyr.	1.661(6)	–	–	[116]
$[TcO(DMSE)_2]^-$	sq.pyr.	1.672(6)	950/940	0.78	[117,123]
$[TcO(NC-N=CS_2)_2]$	sq.pyr.	–	980	–	[117]
$[TcO(C_6H_3CH_3S_2)_2]$	sq.pyr.	–	935		[117]
$[TcO(MoS_4)_2]^-$		–	895	–	[126]
$[TcO(SCH_2CH_2O)_2]^-$	sq.pyr.	1.64(1)	948	0.720(1)	[127]
$[TcO\{Se_2C=C(CN)_2\}_2]$	sq.pyr.	1.67(2)	965	0.88	[130]
$[TcO\{SeSC-C(CN)_2\}_2]$	sq.pyr.		970	–	[131]
12.3.3.5					
$[TcO(HNC_6H_4NH)_2]$	sq.pyr.	1.668(7)	891	0.67	[25]
$[TcO(pnao)]^0$	sq.pyr.	1.679(3)	923	0.678(1)	[132–134]
$[TcO(oep)]^+$		–	918/962	–	[135]
$[TcO(ped)]^0$	sq.pyr.	1.666(3)	953	–	[137,138]
$[TcO(aps)]^0$	octah.	1.685(6)	888	0.30	[139]
$[TcO(apa)]^0$	octah.	1.678(2)	910/915	0.28	[140]
$[TcO(ophsal)(bpy)]^+$	octah.	–	965	–	[141]
$[TcO(ophsal)(phen)]^+$	octah.	–	957	–	[141]
$[TcO(ophsal)(dpk \cdot EtOH)]^-$	octah.	–	957		[141]
$[TcO(epa)]^-$	sq.pyr.	1.648(3)	925	0.65	[142]
$[TcO(bgO)_2]^+$	sq.pyr.	–	952	–	[144]
$[TcO(bgO)_2Cl]^0$	octah.		945	–	[144]
$[TcO\{(acac)_2en\}(H_2O)]^+$	octah.	1.648(2)	–	0.39	[145]
$[TcO\{(sal)_2en\}Cl]^0$	octah.	1.626(11)	–	0.25/0.28	[145]
$[TcO(ophsal)(quin)]^0$	octah.	1.659(7)	948	0.08	[148]
$[TcO(gluca)(sal)]^0$	octah.	1.656(8)	970	0.422	[150]
12.3.3.6					
$[TcO(NHC_6H_4S)_2]$	sq.pyr.	1.73(2)	906	0.72	[151]
$[TcO(ema)]$	sq.pyr.	1.679(5)	945	0.771(5)	[153,154]
$[TcO(map)]^-$	sq.pyr.	1.656(7)	945	0.747	[156]
$[TcO(DBDS)]^-$	sq.pyr.	1.66	954	0.67	[158]

Table 12.6.A Continued.

Complex	Geometry	Tc=O [Å]	ν(Tc=O) IR [cm^{-1}]	Tc (displacement) [Å]	References
[TcO(cma)(morph)]^{0}	sq.pyr.	1.658(3)	–	–	[159]
[TcO(L,L-ECD)]^{0}	sq.pyr.	1.666	940	0.73	[160]
[TcO(NEt-tmdadt)]^{0}	sq.pyr.	1.681	–	–	[162]
[TcO(NMe-tmdadt)]^{0}	sq.pyr.	1.678/1.671	916/924	–	[163]
[TcO(BAT-BPA)]^{0}	sq.pyr.	–	900	–	[164]
[TcO(BAT-PPP)]^{0}	sq.pyr.	1.681/1.691	900/919	0.74	[165]
[TcO(ddd)]$^{+}$	sq.pyr.	1.646(8)	–	0.770(3)	[172]
[TcO(dedt)]$^{+}$	sq.pyr.	1.646(4)	–	–	[173]
[TcO(Et_2tcb)$_2$]$^{-}$	sq.pyr.	1.651	978	–	[174]
[TcO(Et_4dadt)]$^{+}$	sq.pyr.	1.657(1)	955	0.773	[175]
[TcO(sacac)$_2$en(H_2O)]	octah.	1.643(3)	964	0.42	[176]
[TcO(bls)$_2$]$^{-}$	sq.pyr.	–	966/972	–	[177]
[TcO(pic)]^{0}	sq.pyr.	1.653(4)	965	–	[179]
[TcO(MAG_3)]	sq.pyr.	1.647(3)	–	0.74/0.76	[180]
[TcO(MAG_3OMe)]	sq.pyr.	1.654/1.658	–	0.74/0.76	[180]
[TcO(tibt)(py)]^{0}	sq.pyr./ trig.bipyr.	1.665(3)	914	–	[182]
[TcO(bzt)(dta-morph)]^{0}	sq.pyr.	1.664(3)	928	–	[183]
12.3.3.7					
[TcO(HBPz$_3$)Cl$_2$]^{0}	octah.	1.656(3)	970	–	[184]
[TcOCl$_2$(terpy)]$^{+}$	octah.	–	979	–	[185]
[TcOCl$_3$(terpy)]^{0}	octah.	–	974	–	[185]
[TcOCl$_3$(dpp)]^{0}	octah.	–	982	–	[186]
[TcOCl$_3$(dpq)]^{0}	octah.	–	966	–	[186]
[TcOCl$_3$(bpy)]^{0}	octah.	–	980	–	[5]
[TcOBr$_3$(bpy)]^{0}	octah.	–	969	–	[5]
[TcOCl$_3$(phen)]^{0}	octah.	–	977	–	[5]
12.3.3.8					
[TcOCl(phsal)$_2$]^{0}	octah.	1.67	940	0.19	[187]
[TcOCl$_3$(phsal)]$^{-}$	octah.	–	951	–	[187]
[TcOCl(salpd)]^{0}	octah.	1.66	930	–	[188]
[TcOCl$_3$(Hsalpd)]	–	–	943	–	[188]
[TcOCl(Mequin)$_2$]$^{-}$	octah.	1.649(3)	945	0.22	[190]
[TcOCl(quin)$_2$]^{0}	octah.	–	945	–	[190]
[TcOCl(eg)(phen)]^{0}	octah.	1.661(4)	952	–	[192]

Table 12.6.A Continued

Complex	Geometry	Tc=O [Å]	ν(Tc=O) IR [cm^{-1}]	Tc (displacement) [Å]	References
[TcOCl(thoz)$_2$]^n	octah.	1.661(3)	970	0.19	[193]
[TcO(OCH$_2$pyCH$_2$OH)$_2$Cl]^o	octah.	1.675(3)	930	-	[189]
[TcOCl(hbt)$_2$]$^-$	octah.	1.63(1)	-	0.20	[194]
[TcOCl$_2$(dpk)(OH)]^o	octah.	–	939	–	[195]
[TcOBr$_2$(NO$_2$py)(EtO)]^n	octah.	1.684(6)	938		[196]
[TcOCl$_2$(quinim-naph)]^o	octah.	1.648(5)	956	–	[197]
[TcOCl$_3$(hbt)]$^-$	octah.	1.650(6)	945	0.154	[198]
[TcOCl(ophsal)]^o	sq.pyr.	1.634(7)	980	0.67	[199]
12.3.3.9					
[TcO(mpd)]^o	sq.pyr.	1.657(2)	952	0.709(1)	[200]
[TcO(MAG$_2$)]$^-$	sq.pyr.	1.644	960	0.756	[201,202]
[TcO(penamin)]^o	octah.	1.657(4)	958	-	[203]
[TcO(haf)(pac)]^o	octah.	1.633(8)	926	0.20	[205,206]
[TcO(SC$_6$H$_2$Pr$^i_3$)$_2$(PhNN-CON$_2$HPh)]^o	sq.pyr./ trig.bipyr.	1.658(2)	950	–	[207]
[TcO(bt)(salabt)]^o	sq.pyr.	1.661(7)	950	0.66	[208,209]
[TcO(salcys)]^o	sq.pyr.	–	892	–	[210]
[TcOCl(acd)$_2$]^o	octah.	-	964	–	[212]
[TcOCl(sphsal)]^n	sq.pyr.	1.62(1)	979	0.7	[214]
[TcOCl(tcbn)]^n	sq.pyr.	1.645(7)	980	0.693(1)	[215]
[TcOCl(haf)]^o	trig.bipyr.	–	985	–	[216,217]
12.3.3.10					
[TcO(OMe)(NHPhPPh$_2$)$_2$]^o	octah.	1.700(8)	878	0.22	[218]
[TcO(OMe)(dppd)]^o	octah.	1.691(2)	882	0.31	[219]
[TcOCl(pbt)$_2$]^o	octah.	-	940	-	[220]
[TcOCl(OPhPPh$_2$)$_2$]^o	octah.	1.665	940	0.29	[221,222]
[TcOCl$_2$(NP$_3$)]$^+$	octah.	–	–	–	[223]

12.3.4 $(TcS)^{3+}$-core complexes

12.3.4.1 $TcS(S_4)$-and $TcS(N_3Cl_2)$-core complexes

From the reaction of $K_2[TcCl_6]$, suspended in methanol, with excess ethane-1,2-dithiol (H_2edt), the anionic technetium(V) sulphido complex $[TcS(edt)_2]^-$ was prepared in low yield. The mixture was heated at reflux temperature under an argon atmosphere.

After addition of tetraphenylarsonium chloride, $[AsPh_4][TcS(edt)_2]$ was isolated as a blood-red solid. The complex salt is diamagnetic in acetone solution and was characterized by IR, ^1H NMR and FAB mass spectra. The IR absorption at 520 cm^{-1} was assigned to the Tc=S stretching vibration. $[TcS(edt)_2]^-$ can be converted to the corresponding orange $[TcO(edt)_2]$ by refluxing in CH_2Cl_2 in the presence of air [224,225].

$[TcOCl_2\{HB(pz)_3\}]^\circ$ {$HB(pz_3)$ = hydro-tris(1-pyrazolyl)borato, see Sect. 12.3.3.7} reacts in dichloromethane with suspended B_2S_3 at 80 °C under argon to form dark green $[TcSCl_2\{HB(pz)_3\}]^\circ$. The neutral compound is unstable in solution and easily converted back to the corresponding oxo complex in the presence of air. Therefore the preparation requires the careful exclusion of oxygen and water. Also this complex proved to be diamagnetic. IR/UV/VIS spectroscopy, and FAB mass spectra identified the sulphidotechnetium(V) compound [224,225].

12.3.5 *Trans*-$(TcO_2)^+$-core complexes

12.3.5.1 $TcO_2(N_4)$-core complexes

Reaction of $TcOCl_4^-$ with ethylenediamine (en) in THF yielded *trans*-dioxo-$[TcO_2(en)_2]^+$ that could be obtained as the chloride salt in orange needles. The diamagnetic compound crystallizes in the monoclinic space group $P2_1/c$ with a=5.637(1), b=11.177(2), c=16.112(3) Å, β=101.11(1)°, and Z=4. The $[TcO_2(en)_2]^+$ cation exhibits a distorted octahedral geometry. The four nitrogen atoms are coplanar. The average Tc–N distance is 2.15 Å. The O=Tc=O moiety is nearly linear and perpendicular to the plane of the nitrogens. The Tc=O distances are 1.752(1) and 1.741(1) Å. The mutual lengthening of the Tc=O bonds is consistent with the *trans* effect exerted by the respective oxo ligand. The intense IR absorption at 833 cm^{-1}, which has been attributed to the O=Tc=O group, differs appreciably from the higher Tc=O stretching frequencies observed in the monooxotechnetium(V) complexes [226].

$[TcO_2(en)_2]^+$ has recently been prepared through an alternative route involving the reaction of excess ethylenediamine with $[TcCl_4(PPh_3)_2]^\circ$ in acetonitrile at room temperature. In similar procedures the analogous *trans*-dioxotechnetium(V) cations $[TcO_2(pn)_2]^+$ (pn = 1,3-propanediamine), $[TcO_2(tad)]^+$ (tad = 1,5,8,12-tetraaza-dodecane), $[TcO_2(cyclam)]^+$ (cyclam = 1,4,8,11-tetraaza-cyclotetradecane), $[TcO_2(monooxocyclam)]^+$ (monooxo-cyclam = 1,4,8,11-tetraazacyclotetradecane-5-one), and $[TcO_2(dioxocyclam)]^+$ (dioxocyclam = 1,4,8,11-tetraaza-cyclotetradecane-5,7-dione) have been synthesized and characterized. Adventitious water will be the source of oxygen atoms in these reactions. The complex ions proved to be diamagnetic [227]. $[TcO_2(en)_2]^+$ and $[TcO_2\ (pn)_2]^+$ are rather stable in aqueous solution and inert to substitution [228].

Very recently the structure of $[Tc^VO_2(pn)_2]^+$ was determined. The cation was synthesized by reduction of TcO_4^- with $S_2O_4^{2-}$ in aqueous solution in the presence of 1,3-propanediamine. To the pink solution obtained, a large excess of NaI was added resulting in a pink solid of $[Tc^VO_2(pn)_2]I \cdot H_2O$. The complex salt crystallizes in the orthorhombic space group $P2_12_12_1$ with a=14.873(2), b=16.994(2), c=5.5945(5) Å, and Z=4. The coordination geometry around Tc(V) is a tetragonally distorted octahedron.

The bond distances of O=Tc=O are 1.748(4) and 1.754(4) Å. The Tc–N distances range from 2.163(5) to 2.179(5) Å. The $(TcO_2)^+$-core is nearly linear and perpendicular to the plane defined by the four nitrogens [229].

$[TcO_2(cyclam)]ClO_4 \cdot H_2O$ crystallizes as yellow orange rectangular plates in the triclinic space group $P\bar{1}$ with a=9.964(3), b=9.473(2), c=11.815(3) Å, α=101.38(2)°, β=112.54(2)°, γ=113.50(2)°, and Z=2. The coordination geometry of $[TcO_2(cyclam)]^+$ is slightly distorted octahedral. The average Tc=O distance is 1.751(4) Å, and the average Tc–N distance 2.125(11) Å. The N–Tc–N angle and the N–Tc=O angle are 96.2(1) and 90.4(1)°, respectively. The asymmetric stretching vibration of the O=Tc=O group was observed at 790 cm^{-1} [189].

By reaction of $[TcOCl_4]^-$ with 1,4,8,11-tetraaza-undecane (2,3,2-tet) in THF the cation *trans*-dioxo-$[TcO_2(2,3,2\text{-tet})]^+$ was obtained and precipitated as hexafluorophosphate in yellow crystals. A strong IR absorption at 790 cm^{-1} was assigned to the *trans*-dioxotechnetium moiety [231].

Some amine oxime complexes contain the $(TcO_2)^+$-core. When 3,3,11,11-tetramethyl-4,10-diazatridecane-2,12-dionedioxime $[Hpent(ao)_2]$ is reacted in aqueous solution with TcO_4^- after its reduction with Sn(II) tartrate, an orange, crystalline, neutral compound *trans*-dioxo-$[TcO_2\{pent(ao)_2\}]^\circ$ is obtained, which crystallizes in the triclinic space group $P\bar{1}$ with a=11.418(2), b=13.940(7), c=18.992(10) Å, α=69.29(4), β=90.00, γ=83.69(3)°, and Z=4. $[TcO_2\{pent(ao)_2\}]^\circ$ has a slightly distorted octahedral geometry with the Tc atom lying in the plane of the four nitrogens. The O=Tc=O angle is 170.2(1)°. One oxime proton is lost upon coordination, resulting in a neutral complex with a strong hydrogen bond between the oxime oxygen atoms. The average Tc–N bond length of 2.22 Å is in the range observed for Tc–N single bonds and the average Tc–O bond distance of 1.74 Å is typical for *trans*-dioxo-technetium(V) complexes. Bands at 794 and 789 cm^{-1} are attributed to the asymmetric stretch of the O=Tc=O moiety [134].

Imidazole (im), 1-methyl-(1-Me-im), and 4-methyl-imidazole (4-Me-im) react with $[TcOCl_4]^-$ in ethanol to form the pink *trans* dioxo compounds $[TcO_2(im)_4]Cl$, $[TcO_2(1\text{-}Me\text{-}im)_4]Cl$, and $[TcO_2(4\text{-}Me\text{-}im)_4]Cl$. *Trans*-dioxo-$[TcO_2(im)_4]Cl \cdot 2H_2O$ crystallizes in the monoclinic space group *C2/c* with a=13.249(3), b=11.239(2), c=14.358(3) Å, β=115.56(2)°, and Z=4. The cation core is a tetragonally distorted octahedron (Fig. 12.37.A) with Tc=O bond distances of 1.71(2) Å and Tc–N distances of 2.15(2) Å. The dihedral angles between the imidazole rings and the Tc–N equatorial plane are 75° and 82°. The IR vibration frequency $\nu_{asym}(TcO_2)$ is 810 cm^{-1}. The imidazole complexes are diamagnetic due to the strong tetragonal distortion exerted by the oxo ligands. They are unstable in aqueous solution. The formation of dioxo instead of monooxo complexes is probably due to the attack of water during the reaction [232]. $[TcO_2(thiazole)_4]Cl \cdot 3H_2O$ was obtained in orange crystals by reaction of $[TcOCl_4]^-$ with thiazole in methanol. The complex is unstable in solution in the absence of excess thiazole [192].

The first report on a *trans*-dioxo-pyridine complex, $[TcO_2(py)_4]^+$, dates back to 1972. $[TcCl_6]^{2-}$ in hydrochloric acid solution reacts at pH 4–5 with pyridine to produce orange, highly hygroscopic crystals of $[TcO_2(py)_4]Cl \cdot 10H_2O$. The complex salt readily dissolves in water, methanol and ethanol. An intense band at 825 cm^{-1} was attributed to the O=Tc=O stretching vibration [233]. The same complex cation was also obtained

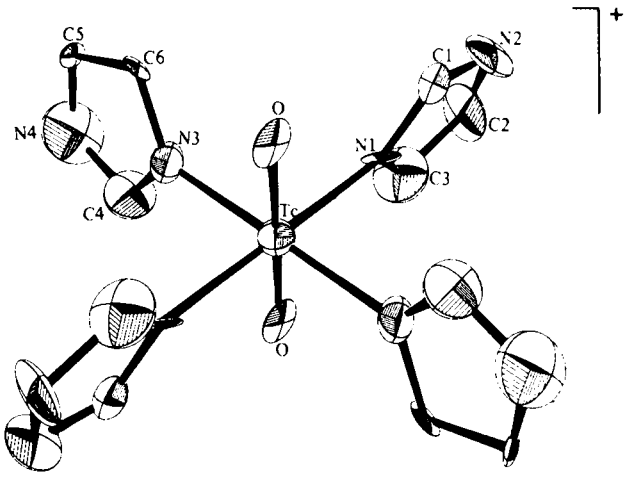

Fig. 12.37.A Tetrakis(imidazole)-*trans*-dioxotechnetium(V), $[TcO_2(im)_4]^+$ [232].

in later work, when $[Tc^{III}O(tmtu)_4]^+$ (tmtu = tetramethylthiourea) was reacted with pyridine in acetone. $[TcO_2(py)_4]PF_6$ forms yellow needles [115].

Trans-dioxo-$[TcO_2(tbpy)_4]^+$ (tbpy = 4-*tert*-butylpyridine) was prepared by reacting $[TcOCl_4]^-$ with tbpy in ethanol. By adding $[F_3CSO_3]^-$ the complex salt $[TcO_2(tbpy)_4][F_3CSO_3]$ was precipitated in yellow crystals belonging to the triclinic space group $P\bar{1}$. The cell constants are a=13.876(5), b=15.429(4), c=11.822(2) Å, α=111.83(2), β=108.77(2)°, γ=65.24(2)°, and Z=2. The coordination sphere of Tc is again tetragonally distorted octahedral. The average Tc=O bond distance is 1.743(5) Å, the average Tc–N distance 2.15(2) Å. The pyridine rings are twisted away from the O=Tc=O axis by varying degrees and form an average dihedral angle of 74° with a plane defined by the Tc atom and two adjacent nitrogen atoms. In similar preparation routes the analogous *trans*-dioxo cations $[TcO_2(pico)_4]^+$ (pico = 4-methylpyridine=picoline), $[TcO_2(lut)_4]^+$ (lut = 3,5-dimethylpyridine=lutidine), $[TcO_2(apy)]^+$ (apy = 4-aminopyridine), and $[TcO_2(dmapy)]^+$ {dmapy = 4-(dimethylamino)pyridine} were synthesized. IR absorptions, assigned to the asymmetric O=Tc=O stretch, were found between 818 and 828 cm^{-1}. All these compounds were shown to be diamagnetic [234].

The substitution kinetics of the *trans*-dioxo cations $[TcO_2(py)_4]^+$, $[TcO_2(pico)_4]^+$, and $[TcO_2(lut)_4]^+$ were studied with 4-aminopyridine, 4-(dimethylamino)pyridine, imidazole, ethylenediamine, cyanide, and cyclam as substituting ligands in methanol, ethanol and partially in DMF. In alcohols the reactions proceed by a solvent-mediated mechanism and are independent of the concentration of both the substituting and leaving ligands. In DMF the reactions were described by a dissociative mechanism. In methanol/DMF mixtures specific solvation effects can significantly alter the substitution rates [235].

$[TcO_2(bptz)_2]Cl$ {bptz = 3,6-bis(2′-pyridyl)-1,2,4,5-tetrazine} was synthesized by the reaction of $[TcOCl_4]^-$ with an excess of the ligand bptz in ethanolic solution. The indigo colored complex is only slightly soluble in organic solvents and unstable in solution. The asymmetric O=Tc=O stretching vibration appeared in the IR at 798 cm^{-1} [6].

12.3.5.2 $TcO_2(N_2S_2)$-, $TcO_2(NO_3)$-, $TcO_2(N_2O_2)$-, and $TcO_2(NO_2S)$-core complexes

The reaction of 1,4-dithia-8,11-diazacyclotetradecane (14ane-N_2S_2) with $[TcOBr_4]^-$ in THF and addition of $[PF_6]^-$ yielded yellow crystals of *trans*-dioxo-$[TcO_2$(14-ane-N_2S_2)$][PF_6]$, which crystallizes in the monoclinic space group $P2_1/n$ with a=9.726(3), b=9.668(2), c=19.262(3) Å, β=95.84(2)°, and Z=4. The coordination around Tc^V has the geometry of a distorted octahedron with the N_2S_2 donor atoms located in the equatorial plane. The Tc=O bond distances are 1.748(2) Å. The average Tc–N and Tc–S bond lengths are 2.150(4) and 2.395(1) Å, respectively. The O=Tc=O axis is almost linear with 176.6(1)°. The bite angles N–Tc–N and S–Tc–S are 82.9(2) and 84.1(1)°, respectively. The IR spectrum shows a strong absorption at 800 cm^{-1} assignable to the asymmetric O=Tc=O stretching vibration [236,237].

The *trans*-dioxo-$TcO_2(N_2S_2)$-core is also represented by the complex anion $[TcO_2(bem)_2]^-$ which contains the monoanionic, bidentate Schiff-base ligand benzylidine-2-thioaniline (Hbem). $[TcO_2(bem)_2]^-$ {ν_{as}(Tc=O) = 743 cm^{-1}} was obtained by reaction of the ligand with dithionite-reduced TcO_4^-. In a similar route $[TcO_2(atp)_2]$ (Hatp = 2-aminothiophenol) {ν_{as}(Tc=O) = 743 cm^{-1}} was synthesized. The anions $[TcO_2(hbh)(H_2O)]^-$ (H_2hbh = 2′-hydroxybenzylidine-2-hydroxyaniline) {ν_{as}(Tc=O) = 798 cm^{-1}}, $[TcO_2(hba)_2]^-$ (Hhba = 2′-hydroxybenzylidine-aniline) {ν_{as}(Tc=O) = 808 cm^{-1}}, $[TcO_2(hpa)(H_2O)]^-$ (H_2hpa) = 4′-hydroxypentyl-2′-idine-2-hydroxyaniline) {ν_{as}(Tc=O) = 781 cm^{-1}}, and $[TcO_2(ap)_2]^-$ (Hap = 2-aminophenol) {ν_{as}(Tc=O) = 798 cm^{-1}} contain the $TcO_2(NO_3)$- or the $TcO_2(N_2O_2)$-core. The $TcO_2(NO_2S)$-core has been verified in $[TcO_2(hbta)(H_2O)]^-$ (H_2hbta = 2′-hydroxybenzylidine-2-thioaniline) {ν_{as}(Tc=O) = 748 cm^{-1}} and $[TcO_2(hpt)(H_2O)]^-$ (H_2hpt = 4′-hydroxypentyl-2′-idine-2-thioaniline) {ν_{as}(Tc=O) = 747 cm^{-1}}. The Tc atom is six-coordinate in all these complexes, which are diamagnetic. The $[Bu_4N]^+$ salts are crystalline red solids [238].

12.3.5.3 $TcO_2(P_4)$-, $TcO_2(P_3)$-, and $TcO_2(P_2N_2)$-core complexes

Reduction of pertechnetate with excess bis(1,2-dimethylphosphino)ethane (dmpe) at ambient temperature under mild alkaline conditions and short reaction time yields yellow *trans*-dioxo-$[TcO_2(dmpe)_2]^+$ which was precipitated with $[F_3CSO_3]^-$. The IR stretching vibration of ν_{as}(Tc=O) appeared at 775 cm^{-1}. The protonated form of this complex cation was obtained by dissolving $[TcO_2(dmpe)_2][F_3CSO_3]$ in hot 2-propanol and adding several drops of conc. F_3CSO_3H. Addition of diethyl ether, followed by cooling to –4 °C, produced a dark orange precipitate of $[TcO(OH)(dmpe)_2]$ $[F_3CSO_3]_2$. At the ionic strength of 0.5 M and 25 °C the pK_a of the cation is 0.80. Reddish orange needles of this salt crystallize in the monoclinic space group $P2_1/c$ with a=8.052(2), b=11.527(2), c=16.070(3) Å, β=101.96(2)°, and Z=2. Tc(V) is approximately octahedrally coordinated with four equatorial P atoms at an average distance of 2.477(5) Å. The oxygen atoms occupy mutually *trans* positions in the (O=Tc–OH)$^{2+}$-core. The average Tc–O bond length is 1.795(3) Å. An EXAFS (extended X-ray absorption fine structure) study gives a Tc=O distance of 1.66 Å and a Tc–OH distance of 1.96 Å [239].

In addition, the myocardial perfusion imaging cationic agent $[TcO_2(tetrofosmin)_2]^+$ {tetrofosmin = 1,2-bis[bis(2-ethoxyethyl)phosphino]ethane} contains the *trans*-dioxo $TcO_2(P_4)$-core. The compound was prepared by mixing TcO_4^- and tetrofosmin in aqueous ethanol. A pink precipitate of $[TcO_2(tetrofosmin)_2][Cr(SCN)_4(NH_3)_2]$ was isolated by addition of $[Cr(SCN)_4(NH_3)_2]^-$. The structural formula shows the axial *trans*-dioxo core (Fig. 12.38.A) with the four P atoms of the two bidentate diphosphine ligands forming an exactly planar array. The coordination geometry of Tc is nearly octahedral. The Tc=O bond distance is 1.738(17) Å, the average Tc–P distance 2.473 Å. $[TcO_2(tetrofosmin)_2][Cr(SCN)_4(NH_3)_2]$ crystallizes in the triclinic space group $P\bar{1}$ with a=12.635(3), b=12.939(3), c=12.021(3) Å, α=106.95(3), β=113.11(3), γ=60.83(3)°, and Z=1 [240].

Very recently $TcO_2(P_3)$-core complexes have been found in the cations $[TcO_2(PEt_3)_3]^+$ and $[TcO_2(PPr_3)_3]^+$, which were synthesized by reacting TcO_4^- with the pertinent phosphine and precipitated as tetraphenylborate. $[TcO_2(PEt_3)_3][BPh_4]$ crystallizes in two crystallographic forms occurring in the monoclinic space groups $P2_1/n$ and $P2_1/c$. $[TcO_2(PPr_3)_3][BPh_4]$ belongs to the monoclinic space group $C2/c$. Dark brown $[TcO_2(PEt_3)_3][BPh_4]$ of the space group $P2_1/n$ has the unit cell dimensions a=14.354(3), b=11.731(2), c=26.478(6) Å, β=101.220(10)°, and Z=4. The cations show a distorted trigonal bipyramid structure, not yet known for cationic dioxo technetium(V) complexes. The two oxo ligands and the P(2) donor atom form the trigonal plane (Fig. 12.39.A). This *cis*-dioxo structure was also found for $[TcO_2(PPr_3)_3]^+$. The Tc=O bond distances of both cations range from 1.707(4) to 1.726(3) Å, the Tc–P bonds from 2.506(1) to 2.528(2) Å for the axial ligands and from 2.395(1) to 2.403(1) Å for the equatorial bond. The O=Tc=O angles vary between 141.5(2) and 143.4(2)°. The ν(Tc=O) stretching vibration was observed around 850 cm^{-1}. The compounds are paramagnetic. Reaction of the complexes with pyridine in methanol produced the $TcO_2(P_2N_2)$-*trans,cis,cis*-core cations $[TcO_2(PR_3)_2(py)_2]^+$ of distorted octahedral structure. Their tetraphenylborate salts are diamagnetic, indicating a significant distortion of the octahedral geometry [241].

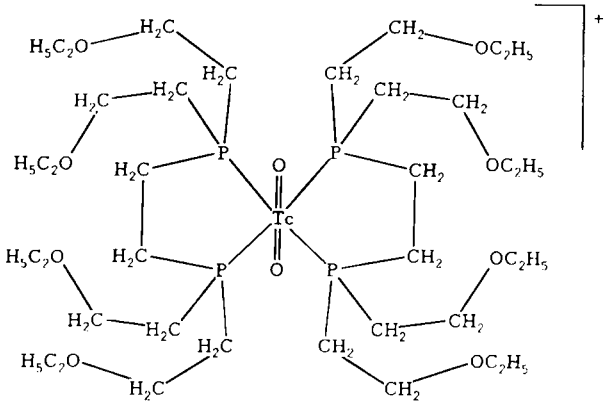

Fig. 12.38.A Bis(tetrofosmin)-*trans*-dioxotechnetium(V), $[TcO_2(tetrofosmin)_2]^+$ [240].

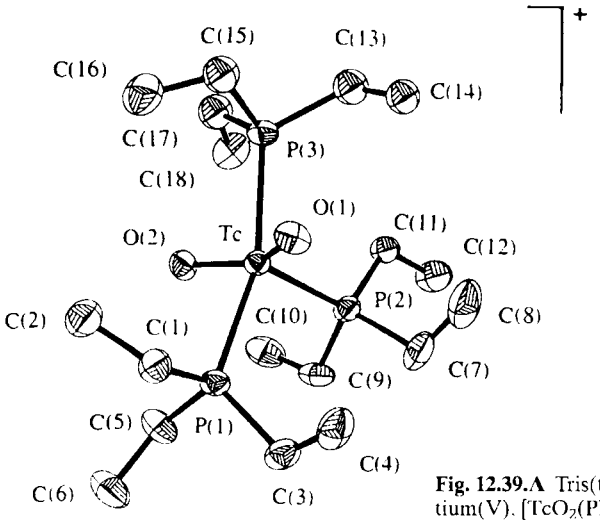

Fig. 12.39.A Tris(triethylphosphine)-*cis*-dioxotechnetium(V). $[TcO_2(PEt_3)_3]^+$ [241].

12.3.5.4 *Trans*-dioxotetracyanotechnetate(V), $[TcO_2(CN)_4]^{3-}$

Reaction of *trans*-dioxo $[TcO_2(py)_4]^+$ with a large excess of KCN in aqueous solution leads to the formation of $K_3[TcO_2(CN)_4]$ that can be recrystallized from methanol/water to yield lemon-yellow needles. The compound can also be obtained by repeated hydrolysis of either $K_4[Tc(CN)_7]\cdot 2H_2O$ or $K_2[TcO(CN)_5]\cdot 4H_2O$. The asymmetric O=Tc=O stretching vibration of $[TcO_2(CN)_4]^{3-}$ appears in the IR at 785 cm^{-1} [99]. The diamagnetic anion represents a highly deshielded ^{99}Tc environment as observed in ^{99}Tc NMR spectroscopy [3].

The structural data of dioxotechnetate(V) complexes are summarized in Table 12.7.A.

Table 12.7.A Some structural data for selected $(TcO_2)^+$-core complexes treated in Sect. 12.3.5

Complex	Geometry	Tc=O [Å]	ν_{as} (O=Tc=O) IR [cm^{-1}]	References
12.3.5.1				
$[TcO_2(en)_2]^+$	octah.	1.746(1)	833	[226]
$[TcO_2(pn)_2]^+$	octah.	..	830	[227]
$[TcO_2(tad)_2]^-$	octah.	–	810	[227]
$[TcO_2(cyclam)]^+$	octah.	1.751(4)	790	[227,230]
$[TcO_2(2,3,2\text{-tet})]^+$	octah.	–	790	[231]
$[TcO_2\{pent(ao)_2\}]^0$	octah.	1.743(3)	789/794	[134]
$[TcO_2(im)_4]^+$	octah.	1.71(2)	810	[232]
$[TcO_2(py)_4]^+$	octah.	–	825	[233]

Table 12.7.A Continued.

Complex	Geometry	Tc=O [Å]	ν_{as} (O=Tc=O) IR [cm^{-1}]	References
$[TcO_2(tbpy)_4]^+$	octah.	1.743(6)	821	[234]
$[TcO_2(bptz)_2]^+$	octah.	–	798	[6]
12.3.5.2				
$[TcO_2(14\text{-ane-}N_2S_2)]^+$	octah.	1.748(2)	800	[236,237]
$[TcO_2(bcm)_2]^-$	octah.		743	[238]
$[TcO_2(atp)_2]$	octah.	–	743	[238]
$[TcO_2(hbh)(H_2O)]$	octah.	–	798	[238]
$[TcO_2(hba)_2]^-$	octah.		808	[238]
$[TcO_2(hpa)(H_2O)]^-$	octah.	–	781	[238]
$[TcO_2(ap)_2]$	octah.	–	798	[238]
$[TcO_2(hbta)(H_2O)]^-$	octah.	–	748	[238]
$[TcO_2(hpt)(H_2O)]^-$	octah.	–	747	[238]
12.3.5.3				
$[TcO_2(dmpe)_2]^+$	octah.	1.795(3)	775	[239]
$[TcO_2(tetrofosmin)_2]^-$	octah.	1.738(17)	–	[240]
$[TcO_2(PEt_3)_3]^+$	trig.bipy.	1.712(3), 1.726(3)	850	[241]
$[TcO_2(PEt_3)_2(py)_2]^+$	octah.	1.728(7), 1.736(7)	805–810	[241]
12.3.5.4				
$[TcO_2(CN)_4]^{3-}$	octah.	–	785	[99]

12.3.6 Dinuclear oxo complexes

12.3.6.1 μ-Oxo compounds

The quadridentate Schiff base N,N′-propane-1,3-bis(salicylideneimine) (H_2salpd) reacts with $[TcOCl_4]^-$ in ethanol to produce an orange precipitate of $[\mu\text{-O}\{TcO(salpd)\}_2]$°. The red-violet crystals adopt the monoclinic space group $P2_1/c$ with a=15.041(2), b=12.630(3), c=16.522(4) Å, β=95.35(3)°, and Z=4. The structure of the dinuclear μ-oxo complex is characterized by the almost linear $[O=Tc\text{-}O\text{-}Tc=O]^{4+}$ group. The coordination geometry of both Tc atoms is nearly octahedral. Each central atom is displaced by 0.12 Å from the mean plane of the N_2O_2 donor atoms towards the terminal oxygens. The bridging Tc–O distance is 1.90(1) Å which is distinctly shorter than the average Tc–O distances of 2.01 Å in the equatorial plane. The mean Tc–N bond length is 2.12 Å, the mean Tc=O distance

1.69 Å. The O=Tc–O angle is 167.0(5)°. The IR absorption at 685 cm^{-1} is attributed to the Tc–O–Tc vibration. $[\mu$-O{TcO (salpd)}$_2]^\circ$ melts at 215 °C [188].

Reaction of the very similar Schiff base N,N′–2-hydroxypropane-1,3-bis(salicylideneimine) (H_3salhpd) with $[TcOCl_4]^-$ in methanol yielded a deep red crystalline solid which is soluble in DMF, DMSO, CH_2Cl_2, and $CHCl_3$. The neutral diamagnetic compound $[\mu$-O{TcO (Hsalhpd)}$_2]^\circ$ crystallizes in the same monoclinic space group $P2_1/c$ with a=9.423(6), b=19.666(9), c=22.785(11) Å, β=99.41(4), and Z=4. The structure involves two distorted octahedra of Tc(V) (Fig. 12.40.A) bridged by a single oxygen atom of the nearly linear $Tc_2O_3^{4+}$ group. The average μ–O–Tc bond distance is 1.91 Å and the average terminal Tc=O bond length is 1.71 Å. The Tc and Tc′ atoms are displaced by 0.14 and 0.10 Å, respectively, from the mean equatorial plane of the N_2O_2 donor atoms towards the terminal oxygens. The structure of $[\mu$-O{TcO (Hsalhpd)}$_2]^\circ$ is strongly related to the structure of the parent compound $[\mu$-O{TcO (salpd)}$_2]^\circ$ [188]. The IR bands at 625 cm^{-1} and 912 cm^{-1} are assigned to the asymmetric Tc–O–Tc and the terminal Tc=O vibration, respectively. The redox reaction of $[\mu$-O{TcO(Hsalhpd)}$_2]^\circ$, dissolved in DMF, reveals a one electron transfer for the $Tc_2O_3^{4+}/Tc_2O_3^{3+}$ and $Tc_2O_3^{4+}/Tc_2O_3^{5+}$ couples [242].

Amine phenol ligands like N,N′-bis(2-hydroxy-benzyl)-1,3-diaminopropane (H_2hbdp), and some derivatives, form highly lipophilic μ-oxo-bis(oxo) dinuclear complexes of Tc(V) by reduction of TcO_4^- with Sn(II)-tartrate in the presence of the ligand in aqueous alcoholic solution. The brown compound $[\mu$-O{TcO(hbdp)}$_2]^\circ$ crystallizes in the tetragonal space group $P42_1c$ with a=29.505(6), c=9.544(3) Å, and Z=8. The coordination geometry of the Tc atoms is distorted octahedral, similar to the μ-oxo complexes mentioned before. The O=Tc–O–Tc=O backbone shows significant deviation from linearity. The O=Tc–O(bridging) angle is 164.4°. The Tc=O(terminal) and Tc–O(bridging) bond distances are 1.677(1) and 1.917(27) Å, respectively. The Tc

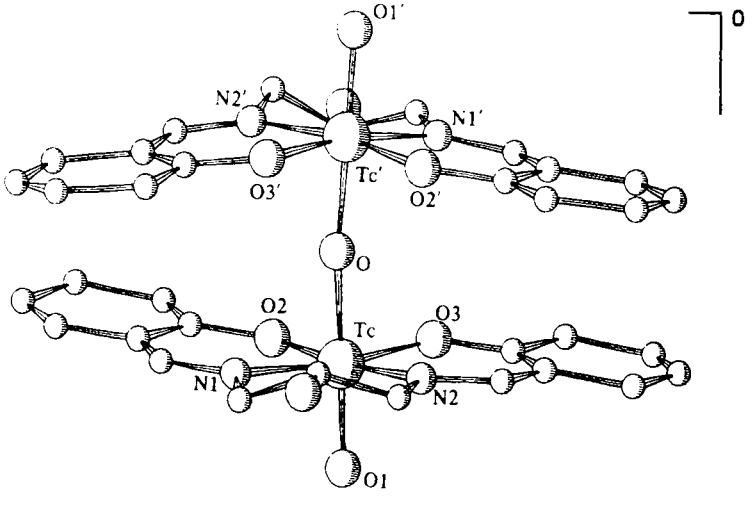

Fig. 12.40.A μ-Oxo-bis [oxo[N,N′-2-hydroxypropane-1,3-bis(salicylideneiminato)]]technetium(V), $[\mu$-O{TcO(Hsalhpd)}$_2]^\circ$ [242].

atoms are 0.1 Å out of the planes defined by the N_2O_2 donor atoms, toward the terminal oxygen atoms. The Tc–O(phenol) and Tc–N bond lengths are 1.99(1) and 2.17(3) Å, respectively. The IR vibration frequency of 674 cm ^{1} was attributed to the Tc–O–Tc group, the vibration at 920 cm^{-1} to the terminal Tc=O bond [243].

Another amine phenolate ligand containing a nitrobenzyl group for binding the Tc(V) complex to biomolecules, N,N′-bis(2-hydroxybenzyl)-1,3-diamino-2-(4-nitrobenzyl)propane (H_2hbdnp), reacts with $[TcO(eg)_2]$ to form the brown, neutral dinuclear complex $\{\mu\text{-O}\{TcO(hbdnp)\}_2\}^{c}$. The compound crystallizes in the monoclinic space group $P2_1/c$ with a=10.633(2), b= 13.705(1), c=16.364(3) Å, β=94.65(1)°, and Z=2. Two distorted octahedral $TcO(N_2O_2)$-cores are connected by a μ-oxo ligand. The structure is similar to those described before. The terminal Tc=O and the bridging Tc–O bond distances are 1.655(7) and 1.903(1) Å, respectively. The IR vibration frequency at 950 cm^{-1} was assigned to the Tc=O stretch. The Tc–O–Tc unit is linear and forms an angle of 163.4(4)° with the terminal oxo ligand. The Tc atoms reside 0.117 Å outside of the N_2O_2 plane towards the terminal oxygen [244].

A dinuclear μ-oxo complex containing an S_2Cl_2 plane was obtained by reaction of the bidentate thioether 5,8-dithiadodecane ($C_4H_9SCH_2CH_2SC_4H_9$) with $[TcOCl_4]^-$ in acetone/methanol solution. The yellow-green compound $[\mu\text{-O}\{TcO(dithiadod)Cl_2\}_2]^{c}$ crystallizes in the orthorhombic space group *Pbca* with a=16.474(7), b=17.044(6), c=23.756(9) Å, and Z=8. Each Tc atom is centered in a flattened octahedron with the equatorial plane formed by the S_2Cl_2 donor set. The S and Cl atoms of the octahedra are in the *anti* position with respect to the bridging oxygen. The Tc atoms reside 0.12 Å out of the S_2Cl_2 planes towards the terminal oxygens. The average terminal Tc=O bond distance is 1.670 Å. The IR vibration of the Tc=O group appeared at 920 cm^{-1}. The mean bridging Tc–O distance is 1.899 Å and the mean Tc–Cl and Tc–S bond lengths are 2.402 and 2.442 Å, respectively. Using 3,6-dithiaoctane ($C_2H_5SCH_2CH_2SC_2H_5$) as a bidentate thioether ligand, the reaction with $[TcOCl_4]$ yielded the analogous μ-oxo compound $[\mu\text{-O}\{TcO(dithiaoct)Cl_2\}_2]^{c}$ showing the Tc=O stretch in the IR also at 920 cm^{-1}. Both dinuclear complexes are stable in air and soluble in acetone and acetonitrile. With 1,8-dihydroxy-3,6-dithiaoctane the mononuclear complex $[TcO(8\text{-hydroxy-}3,6\text{-dithiaoctane-}1\text{-olato})Cl_2]^{c}$ was obtained and contains the $[O{=}Tc{-}O]^{2+}$ group [245].

The tetradentate Schiff-base ligand N,N′-ethylene-bis(thioacetylacetonylideneimine) $\{(sacac)_2en\ H_2\}$ reacts with $[TcOCl_4]^-$ in refluxing methanol to produce the red-brown, dinuclear complex $[\mu\text{-O}\{TcO(sacac)_2en\}_2]^{c}$ which is poorly soluble in common organic solvents. The frequencies at 910 and 680 cm^{-1} are attributed to the terminal Tc=O and Tc–O–Tc stretching vibrations, respectively [213].

The cationic dinuclear complex $[\mu\text{-O}\{TcOCl(terpy)\}_2]^{2+}$ was synthesized by reaction of excess terpyridine with $[TcOCl_4]^-$ in refluxing ethanol. The blue-violet chloride precipitate is soluble in DMF and DMSO. IR absorptions at 679 and 936 cm ^{1} are ascribed to ν(Tc–O–Tc) and ν(Tc=O), respectively [185].

12.3.6.2 Other ligand-bridged compounds

The remarkable sulphur-bridged dinuclear complex $[\mu\text{-S,S′}\{(TcO)_2(SCH_2CH_2S)_3\}]^{c}$ was obtained by reaction of $[TcOCl_4]^-$ with ethanedithiol in methanolic solution.

The orange compound crystallizes in the monoclinic space group $P2_1/c$ with a=8.833(2), b=15.034(3), c=11.350(2) Å, β=108.17(1)°, and Z=4. Each Tc atom sits in the center of a square pyramid, the base formed by four sulphur atoms, and the apex occupied by an oxo oxygen atom (Fig. 12.41.A). The Tc=O(1) and Tc=O(2) bond distances are 1.665(3) and 1.661(3) Å, respectively. Tc(1) is 0.7410(3) Å, Tc(2) 0.8025(4) Å above the sulphur atom planes. The bonds to the unique ethane-1,2-dithiolate group are quite short, with Tc(1)–S(1)=2.260(1) and Tc(1)–S(2)=2.256(2) Å, whereas the distance to the bridging sulphur atoms *trans* to the former are 0.15 Å longer. The two square pyramidal systems are arranged in the *syn* configuration. The Tc(1)–Tc(2) distance is 3.654(1) Å. The pyramids share an edge with an angle of 106.0(1) between the basal planes. Two Tc=O stretching vibrations are observed in the IR at 953 and 946 cm^{-1}. The compound is soluble in CH_2Cl_2, acetone and acetonitrile [246]. The reaction of 1,3-propanedithiol with $[TcOCl_4]^-$ gives the corresponding compound $[\mu\text{-S,S'}\{(TcO)_2(SCH_2CH_2CH_2S)_3\}]^c$ [128].

An uncommon dinuclear oxo-complex of "lantern" structure was produced by reaction of N,N'-ethylene-bis(2-mercaptoacetamide) (H_4ema) ($HSCH_2CONHCH_2CH_2NHCOCH_2SH$) with $[TcOCl_4]^-$ in methanolic sodium methoxide. The blue, microcrystalline complex salt $[AsPh_4]_2[Tc_2O_2(H_2ema)_4]\cdot 6H_2O$ was formed. It crystallizes in the monoclinic space group $P2_1/n$ with a=19.099(4), b=14.144(6), c=15.809(5) Å, β=109.17(2)°, and Z=2. The dianion is centrosymmetric and consists of two square-pyramidal $OTcS_4$-cores bridged by four $(H_2ema)^{2-}$ ligands. Each Tc atom is positioned 0.769 Å above the S_4 basal plane. The oxo ligand occupies the apical position of each square pyramid (Fig. 12.42.A). A most interesting feature of this anion is that the oxo ligands are found inside the cage created by the bridging ligands. The Tc=O bond distance is 1.64(1) Å. The Tc–S bond lengths are within the range 2.283–2.485 Å.

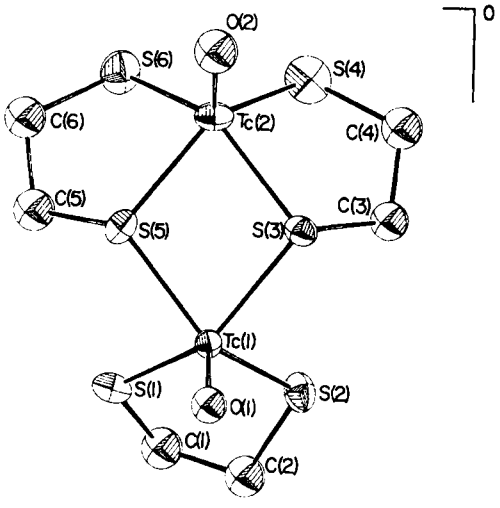

Fig. 12.41.A Bis(ethane-1,2-dithiolato-S,μ-S')oxo-technetium(V)-(ethane-1,2-dithiolato-S,S')oxotechnetium(V), $[\mu\text{-S,S'}\{(TcO)_2(SCH_2CH_2S)_3\}]^c$ [246].

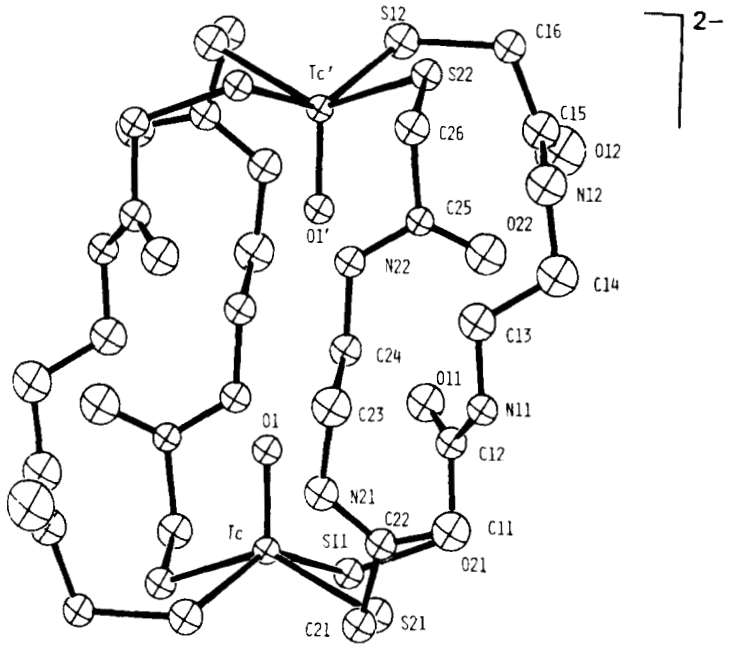

Fig. 12.42.A Lantern dimer, $[Tc^{V}_2O_2(SCH_2CONHCH_2CH_2NHCOCH_2S)_4]$ [247].

The intramolecular Tc–Tc′ distance is 7.175(4) Å, and the distance between the oxo ligands O(1)–O(1)′ 3.96(2) Å. The Tc=O stretch was observed at 962 cm^{-1}. $[AsPh_4]_2[Tc_2O_2(H_2ema)_4]$ decomposes immediately in aqueous basic solution to give two equivalents of $[AsPh_4][TcO(ema)]$ [247].

2,3,5,6-Tetrakis(2-pyridyl)pyrazine (tppz) reacts with $[TcOCl_4]^-$ in ethanol to give a dark green precipitate of $[\mu\text{-tppz}\{TcOCl_2(OEt)\}_2]^0$ which is soluble in CH_2Cl_2, acetonitrile, DMF, and nitromethane. As indicated by the presence of two distinct Tc=O stretching vibrations at 938 and 916 cm^{-1}, the two Tc(V) centers are reported to experience different coordination environments, one Tc atom is deduced to be seven-coordinate and the other six-coordinate [248].

The dinuclear complex $[(TcOCl_3)(\mu\text{-dpp})\{TcOCl_2(OEt)\}]^0$, with dpp = 2,3-bis(2-pyridyl)pyrazine, was synthesized by heating excess $[TcOCl_4]^-$ with dpp in ethanol under reflux. The orange-brown precipitate proved to be diamagnetic. Two strong IR absorptions at 986 and 936 cm^{-1} are observed, which are related to the Tc=O(oxo) bonds. The dpp coordination is bidentate through a pyrazine and a pyridine nitrogen atom [186].

Some structural data of dinuclear oxo complexes are reviewed in Table 12.8.A.

Table 12.8.A Structural data of selected dinuclear oxo complexes described in Sect. 12.3.6.

Complex	Geometry	Tc–L Distance [Å]	ν(Tc–L) IR [cm^{-1}]	Ref.
12.3.6.1				
[μ-O{TcO(salpd)}$_2$]^c	octah.	1.90(Tc–μO)	685(Tc O Tc)	[188]
[μ-O{TcO(IIsalhpd)}$_2$]^c	octah.	1.91(Tc–μO)	625(Tc–O–Tc)	[242]
[μ-O{TcO(hbdp)}$_2$]^c	octah.	1.917(Tc–μO)	674(Tc–O–Tc)	[243]
[μ-O{TcO(hbdnp)}$_2$]^c	octah.	1.903(Tc μO)	950(Tc–O)	[244]
[μ-O{TcO(dithiadod)Cl$_2$}$_2$]^c	octah.	1.899(Tc–μO)	920(Tc=O)	[245]
[μ-O{TcOCl(terpy)}$_2$]$^{2+}$	–	–	679(Tc–O–Tc)	[185]
12.3.6.2				
[μ-S,S′{(TcO)$_2$ (SCH$_2$CH$_2$S)$_3$}]^c	square pyr.	3.654(Tc–Tc)	953(Tc=O)	[246]
			946(Tc=O)	
[Tc$_2$O$_2$(H$_2$ema)$_2$]$^{2-}$	square pyr.	1.64(Tc=O)	962(Tc=O)	[247]
[μ-tppz{TcOCl$_2$(OEt)}$_2$]^c	–	–	916(Tc=O)	[248]
			938(Tc=O)	

12.3.7 $(TcN)^{2+}$-core complexes

12.3.7.1 Nitridohalogeno-, nitridothiocyanato-, and nitridocyanotechnetate

In contrast to the well characterized nitridohalogeno complexes $[TcNCl_4]^-$ and $[TcNBr_4]^-$ of Tc(VI), the existence of the corresponding complexes of Tc(V), $[TcNX_4]^{2-}$, could not yet be proved. Only spectroelectrochemical studies at –60 °C showed a reversible one-electron reduction of $[Tc^{VI}NX_4]^-$, but the reduced species have not been isolated [249].

The reaction of $[TcNCl_4]^-$ in acetonitrile with an excess of thiocyanate in aqueous solution results in the reduction of Tc(VI) to Tc(V) and the formation of $[TcN(NCS)_4(CH_3CN)]^{2-}$, which was precipitated as tetraethylammonium salt and recrystallized from acetonitrile to give red-brown crystals. Its composition is based on elemental analysis and IR absorption. A band at 1081 cm^{-1} was attributed to the $Tc^V{\equiv}N$ stretch [53]. In a similar preparation route $[AsPh_4]_2[TcN(NCS)_4]$ was obtained, which crystallizes in orange-red needles and dissolves in $CHCl_3$ or acetone [43,250]. Crystal structure determination revealed that the compound crystallized from acetonitrile/ethanol is the *trans*-aqua complex $[AsPh_4]_2[TcN(OH_2)(NCS)_4]\cdot$ EtOH [251]. In the distorted octahedral complex anion $[TcN(NCS)_4(CH_3CN)]^{2-}$, the Tc atom is disordered over two sites with the N atom of the acetonitrile ligand sharing equally the *trans*-axial coordination sites with the nitrido N atom [252].

The neutral nitrido-isothiocyanato complex $[TcN(NCS)_2(CH_3CN)(PPh_3)_2]^c\cdot 0.5CH_3CN$ was synthesized by substitution of the chloride atoms in $[TcNCl_2(PPh_3)_2]^c$ with NCS$^-$ in water/ethanol followed by the reaction of $[TcN(NCS)_2(PPh_3)_2]^c$ with

acetonitrile. The orange-red crystals are monoclinic, space group $P2_1/c$ with a=9.296(3), b=18.614(5), c=23.307(6) Å, β=109.63(2)°, and Z=4. The technetium coordination environment is distorted octahedral. The terminal Tc≡N bond distance is 1.629(4) Å, the Tc≡N stretching frequency in the IR 1088 cm $^{-1}$. The bonding of the thiocyanato groups is through the nitrogen atoms, the Tc–N single bond distances of which are 2.045(4) and 2.068(3) Å. Both NCS groups are linear with N–C–S angles of 177.6(5) and 179.3(3)°. The two *trans* PPh_3 ligands are bonded to technetium also in an approximately linear fashion with a P–Tc–P angle of 174.0(1). The Tc–P bond distances are 2.494(1) and 2.524(1) Å. The exceptionally long Tc–N bond distance of 2.491(4) Å for the acetonitrile group is a result of the *trans* influence of the nitrido ligand. Dissolution of $[TcN(NCS)_2(CH_3CN)(PPh_3)_2]^\circ$ in chloroform resulted in the complete loss of acetonitrile and the formation of $[TcN(NCS)_2(PPh_3)_2]^\circ$ [253].

The reaction of $[Tc^{VI}NCl_4]^-$ with CN^- in acetonitrile/water leads to the reduction of Tc(VI) to Tc(V) and the formation of $[TcN(CN)_4(OH_2)]^{2-}$, which was isolated as the tetraphenylarsonium salt in yellow, water-soluble crystals. $[AsPh_4]_2[TcN(CN)_4(OH_2)]\cdot 5H_2O$ crystallizes in the monoclinic space group $P2_1/n$ with a=17.107(5), b=19.965(7), c=15.473(5) Å, β=101.70(2)°, and Z=4. Tc(V) is coordinated in a distorted octahedron containing the terminal nitrogen. The cyano ligands occupy the equatorial positions (Fig. 12.43.A). The Tc≡N bond distance is only 1.596(10) Å. The long Tc–O bond length of 2.559(9) Å for the coordinated water molecule is again a consequence of the strong *trans* influence of the nitrido ligand. The N≡Tc–O angle of 177.9(5)° demonstrates an almost linear arrangement. The Tc atom is displaced by 0.35 Å above the plane of the four equatorial cyano ligands towards the terminal nitrogen. The Tc–C≡N angles of 171(1) to 179(1)° are also close to linearity. ESR results confirm that $[TcN(CN)_4(OH_2)]^{2-}$ is diamagnetic. The C≡N absorption in the IR occurred as a single sharp peak at 2112 cm^{-1}, indicating the equivalence of the cyano ligands. The Tc≡N stretch appeared at 1100 cm^{-1} [254].

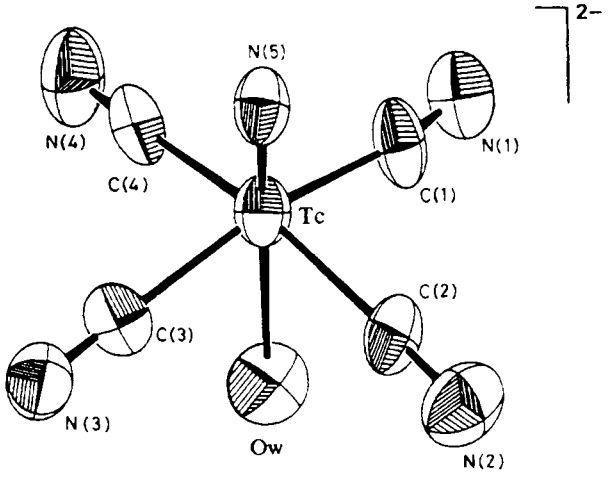

Fig. 12.43.A Trans-aqua-tetracyano-nitridotechnetate(V), $[TcN(CN)_4(OH_2)]^{2-}$ [254].

The structurally characterized *trans*-$[TcN(CN)_4(N_3)]^{3}$ is obtained by ligand exchange of $[TcN(CN)_4Cl]^{3}$ with a large excess of NaN_3. $[TcN(CN)_5]^{3-}$ was synthesized by reaction of $[TcN(tu)_4Cl]Cl$ with CN^- [249].

12.3.7.2 $TcN(O_4)$-, $TcN(O_2S_2)$-, $TcN(S_4)$-,$TcN(Se)_4$-, and $TcN(S_4Cl)$-core complexes

Technetium(V) nitrido β-diketonate complexes were readily prepared by ligand exchange reaction of $[TcNCl_2(PPh_3)_2]^{\circ}$ with the β-diketone ligands acetylacetone (Hacac), benzoylacetone (Hbza), dibenzoylmethane (Hdbm) and dipivaloylmethane (Hdpm) in CH_2Cl_2/ethanol solution containing potassium bicarbonate. The formulation of the neutral, red, $TcN(O_4)$-core complexes as $[TcN(acac)_2]^{\circ}$, $[TcN(bza)_2]^{\circ}$, $[TcN(dbm)_2]^{\circ}$, and $[TcN(dpm)_2]^{\circ}$ was supported by elemental analysis and IR spectra. The Tc≡N stretching vibrations were observed around 1045 cm^{-1}. The lipophilicity of the β-diketonato compounds increases in the given sequence [255]. Thiodibenzoylmethane reacts with $[Tc^{VI}NCl_4]$ in acetone to form the dark brown, crystalline $TcN(O_2S_2)$-core complex bis(thiodibenzoylmethanato)-nitridotechnetium(V), $[TcN\{S=C(C_6H_5)\text{-}CH=C(C_6H_5)O\}_2]^{\circ}$, which is soluble in acetone, benzene and chloroform [256].

Isotrithionedithiolate ($dmit^{2-}$) liberated from the benzoyl-protected compound through reaction with NaOH, was reacted with $[Tc^{VI}Cl_4]$ in CH_3CN. Addition of $[Bu_4N]Cl$ to the reddish reaction mixture finally yielded red needles of $[Bu_4N]_2[Tc^{V}N(dmit)_2]$. The $TcN(S_4)$-core compound crystallizes in the monoclinic space group *C2/c* with Tc(V) and the nitrido ligand located on a two-fold crystallographic axis. The unit cell dimensions are a=23.143(5), b=8.342(2), c=26.382(5) Å, β=95.12(3)°, and Z=4. Tc(V) is five-coordinate with the four sulphur atoms forming the basal plane of a square pyramid and the nitrido nitrogen at the apex (Fig. 12.44.A). The Tc atom is situated 0.620(2) Å above the basal plane, being displaced towards the nitrido ligand. The Tc≡N bond distance is 1.615(2) Å. The Tc–S(1) and Tc–S(2) bond lengths are 2.396(2) and 2.370(2) Å, respectively. The isotrithionedithiolato ligands are planar within 0.120(3) Å and form an angle of 168.5° to each other. The ν(Tc≡N) stretching vibration appeared in the IR at 1055 cm^{-1} [257].

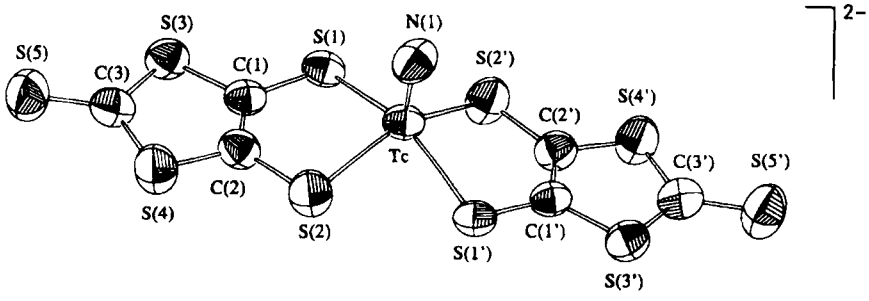

Fig. 12.44.A Bis(isotrithionedithiolato)nitridotechnetate(V), $[TcN(dmit)_2]^{-}$ [257].

Bis(diethyldithiocarbamato)nitridotechnetium(V), $[TcN(S_2CNEt)_2]^\circ$, the first compound containing the $Tc{\equiv}N^{2+}$ core, was synthesized by the reduction of TcO_4^- with hydrazine and the following reaction with diethyldithiocarbamate in aqueous solution. The nitrido nitrogen atom presumably originates from the deprotonation of hydrazine. The yellow crystals of the neutral complex are monoclinic, space group $P2_1/c$ with a=14.823(1), b=9.159(1), c=12.865(1) Å, β=107.98(1)°, and Z=4. The Tc atom is again in a distorted square pyramidal environment with the nitrido nitrogen in the apical position and four sulphur atoms forming the base. The Tc≡N bond has a length of 1.604(6) Å and the Tc–S distances range from 2.392(2) to 2.405(2) Å. The Tc atom is 0.745(1) Å above the plane of the four sulphur atoms. The angle between the two (S_2CNEt_2) planes is 59.4°. The S–Tc≡N bond angles are between 107.0(2) and 108.9(2)°. A strong IR absorption at 1070 cm^{-1} was assigned to the Tc≡N stretching frequency [258]. Later, $[TcN(S_2CNEt_2)_2]^\circ$ was prepared by reacting $[Tc^{VI}NCl_4]^-$ with diethyldithiocarbamate in acetonitrile, resulting in the reduction of Tc(VI) to Tc(V) [53].

A series of nitrido-bis(dialkyldithiocarbamato)-technetium(V) complexes were obtained by reaction of hyrazine-reduced pertechnetate with dialkyldithiocarbamate or by ligand exchange reaction starting from $[TcNCl_2(PPh_3)_2]^\circ$. The Tc=N stretching vibrations in the IR were found in the 1050–1100 cm^{-1} region. The compounds are diamagnetic and stable in solution [259].

Very recently, unusual, mixed Tc(V)nitridoferrocenedithiocarboxylate complexes have been synthesized. When $[Tc^{V}NCl_2(PPh_3)_2]^\circ$ is reacted with piperidinium ferrocenedithiocarboxylate in CH_2Cl_2, a deep-violet microcrystalline precipitate is obtained. The isolated product $[Tc^{V}N\{Fe^{II}(C_5H_4CS_2)(C_5H_5)\}_2]^\circ$ is insoluble in water and soluble in CH_2Cl_2. In the IR, ν(Tc≡N) was found at 1040 cm^{-1}. The probable geometry of the complex is square pyramidal with the nitrido nitrogen in the apical position and the basal plane formed by the four sulphur atoms. The compound is non-conducting in CH_3CN/CH_2Cl_2. Reaction of ferrocenedithiocarboxylate with $[Tc^{VI}NCl_4]^-$ yielded, among other compounds, an ink-blue product, the analytical and spectroscopic data of which correspond to the mixed-valence, monocationic complex $[Tc^{V}N\{Fe^{II}(C_5H_4CS_2)(C_5H_5)\}\{Fe^{III}(C_5H_4CS_2)(C_5H_5)\}]^+$. The presence of the mixed iron valency was supported by electrochemical measurements [260].

Tetraphenylarsonium-bis(1,2-dithiooxalato)nitridotechnetate(V), $[AsPh_4]_2[TcN(SCOCOS)_2]$, was prepared by reaction of dithiooxalate, dissolved in acetone/water, with $[AsPh_4][Tc^{VI}NCl_4]$ in acetonitrile. The pale purple $TcN(S_4)$-core compound crystallizes in the triclinic space group $P\bar{1}$ with a=14.225(5), b=17.778(2), c=10.993(3) Å, α=101.52(2), β=111.74(2), γ=100.68(2)°, and Z=2. The geometry about Tc(V) is again distorted square pyramidal. The distortion arises from the large *trans* influence of the nitrido ligand and is manifested by the displacement of the technetium atom from the basal plane by 0.647 Å. The Tc≡N bond length is 1.613(4) Å and the Tc–S bond distances are between 2.378(2) and 2.391(2) Å. In the corresponding compound $[AsPh_4][Tc^{V}O(SCOCOS)_2]$, the Tc=O bond distance of 1.646(4) Å proved to be significantly longer, indicative of a weaker π-interaction with the Tc atom. In the IR spectrum of the nitrido complex the Tc≡N stretching vibration appeared at 1071 cm^{-1} [110]. $[AsPh_4]_2[TcN(SCOCOS)_2]$ may also be synthesized from $[TcNCl_2(PPh_3)_2]^\circ$ by

ligand exchange and crystallizes in a second modification, space group $C2/c$, a=19.424(3), b=11.254(2), c=24.958(3) Å, β=107.68(1), and Z=4. This monoclinic modification is reported to be deep purple. The bond distances and angles show no significant deviation from those in the triclinic compound [261].

The mixed ligand complex compound $[AsPh_4][Tc^{V}N(S_2CNEt_2)(SCOCOS)]$ was obtained by reaction of $[Tc^{VI}NCl_2(S_2CNEt_2)]^{\circ}$ with $K_2(SCOCOS)$ in acetonitrile/water and addition of $[AsPh_4]Cl$. The red-brown crystals are monoclinic, space group $P2_1/n$, with a=20.670(10), b=15.740(6), c=10.162(5) Å, β=93.61(4)°, and Z=4. The Tc atom resides again in a distorted square pyramidal environment and is displaced by 0.66(1) Å above the S_4 basal plane. The Tc≡N length of 1.54(2) Å is noticeably shorter than is generally found for nitridotechnetium complexes. The Tc≡N stretching vibration in the IR was found at 1071 cm^{-1} [67].

$[TcNCl_2(PPh_3)_2]^{\circ}$ reacts with $K(S_2COEt)$ in a dichloromethane/benzene mixture to give pale yellow $[TcN(S_2COEt)_2]^{\circ}$ which, when treated with a water-ethanol mixture, forms by hydrolysis of the ester the crystalline potassium bis(dithiocarbonato)nitridotechnetate(V) complex salt $K_2[TcN(S_2CO)_2]$. Dithiocarbonate complexes generally cannot be obtained directly from the ligand because of its instability. The complex salt crystallizes in the monoclinic space group $P2_1/n$ with a=8.353(5), b=15.630(4), c=9.230(5) Å, β=90.94(3)°, and Z=4. Tc(V) has a distorted square pyramidal environment and is bonded to the two dithiocarbonato dianions and to the apical nitrogen. Tc is displaced by 0.71 Å from the base plane of the four sulphur atoms. All Tc–S–C angles are essentially 90°. The Tc–S bond distances are about 2.39 Å, the Tc≡N bond length is 1.621(6) Å. The IR spectrum shows the Tc≡N vibration frequency at 1060 cm^{-1} [262].

The reaction of $[TcNCl_2(PPh_3)_2]^{\circ}$ with the bis(diphenylthiophosphoryl)amide anion in a refluxing mixture of CH_2Cl_2/MeOH yields a yellow, air-stable solid of $[TcN\{N(SPPh_2)_2\}_2]^{\circ}$. The amide anion acts as a chelating ligand coordinated via the sulphur atoms. $[TcN\{N(SPPh_2)_2\}_2]^{\circ} \cdot CH_2Cl_2$ crystallizes in the monoclinic space group $P2_1/c$ with a=18.078(4), b=21.250(3), c=13.168(6) Å, β=103.16(4)°, and Z=4. The complex is five-coordinate with the nitrido nitrogen atom at the apex of a square pyramid. Tc(V) is displaced by about 0.60 Å from the basal plane. The Tc-nitrido nitrogen bond distance is 1.608(5) Å. The Tc–S distances range from 2.405(2) to 2.451(2) Å. The Tc≡N vibration was assigned to an absorption in the IR at 1081 cm^{-1}. The mixed ligand complex $[Tc^{V}N(Cl)(PPhMe_2)_2\{N(SPPh_2)_2\}]^{\circ}$ can be obtained when $[TcNCl_2(PPhMe_2)_3]^{\circ}$ is reacted in refluxing methanol with equimolar amounts of $Na[N(SPPh_2)_2]$. The yellow compound crystallizes with one molecule of methanol in the triclinic space group $P\bar{1}$. The lattice constants are a=10.453(3), b=11.790(5), c=18.919(6) Å, α=90.54(2), β=92.52(2), γ=110.43(2)°, and Z=2. Tc(V) resides in a distorted octahedral coordination geometry with the chloride bonded *trans* to the nitrido nitrogen. The exceptionally long Tc–Cl bond of 2.661(1) Å is due to the *trans* labilizing influence of the nitrido ligand [271].

Bis(1,2-dicyanoethenedithiolato)nitridotechnetate(V) $[TcN(mnt)_2]^{2-}$, (mnt = 1,2-dicyanoethenedithiolate) was prepared by reaction of $[AsPh_4][Tc^{VI}NCl_4]$ with Na_2mnt in acetonitrile/ethanol and concomitant reduction of Tc(VI) to Tc(V). The bright yellow crystals of $[AsPh_4]_2[TcN(mnt)_2]$ are monoclinic, space group Pn, with

a=11.369(2), b=15.530(2), c=14.421(3) Å, β=97.58(2)°, and Z=2. The Tc atom in $[TcN(mnt)_2]^2$ is five-coordinate. The four sulphur atoms form an almost exact plane with the disordered Tc atoms displaced in equal distances (0.6 Å) above and below the plane. Each $(N_2C_4S_2)^{2-}$ ligand deviates slightly from planarity. The Tc–S bond distances range from 2.367(4) to 2.419(4) Å. The Tc≡N bond length is 1.59(1) Å. The N≡Tc–S angles vary between 101.8(8) and 106.8(8)°. The Tc≡N stretch appeared at 1060 cm^{-1} [263].

$[TcN(mnt)_2]^{2-}$ was also obtained by ligand exchange reaction of $[TcNCl_2(PPh_3)_2]^0$ with $(mnt)^{2-}$ in acetonic or ethanolic solution. In analogous preparation routes, a series of new neutral, anionic or cationic nitrido complexes of Tc(V) were synthesized using similar ligands. The yellow to orange crystalline compounds are highly soluble in chloroform or methylene chloride and the solutions are air-stable for several days. The Tc≡N stretching vibrations in the IR range between 1071 and 1089 cm^{-1} [264.265]. In addition, $[Tc^{VI}NCl_4]^-$ or $[Tc^{VI}NBr_4]^-$ react by ligand exchange in acetone with dialkyldithiocarbamates, diisopropyldithiophosphate, 1,2-dicyanoethenedithiolate, thiocyanate, pyridine, and imidazole to give Tc(V)-nitrido complexes containing S_4 or N_4 donor sets [43]. A new synthesis of Tc(V)-nitrido complexes of the composition $[TcNCl_2L_3]$ (L = dimethyl- or diethylphenylphosphine) in very good yield by reaction of $Tc^{III}Cl_3L_3$ with NaN_3 in boiling ethanol was suggested [266].

The complex anion bis(1,2-dicyanoethenediselenolato)nitridotechnetate(V) $[TcN(mns)_2]^{2-}$ was obtained by reaction of $K_2[(CN)_2C{=}CSe_2]$ with $[NBu_4][Tc^{VI}NCl_4]$ in acetonitrile. The yellow compound $[NBu_4]_2[TcN(mns)_2]$ precipitated after addition of $[NBu_4]Br$. The complex salt crystallizes in the triclinic space group $P\bar{1}$ with a=9.620(1), b=10.567(1), c=26.774(1) Å, α=91.453(4), β=92.395(5), γ=112.546(5)°, and Z=2. The structure (Fig. 12.45.A) of the anion resembles that of $[TcN(mnt)_2]^{2-}$. The basal plane of the distorted square pyramid is formed by the four selenium atoms. The Tc atom resides 0.768(1) Å out of this plane towards the nitrido ligand. The Tc≡N distance is 1.61(1) Å, the mean Tc–Se bond length 2.52(1) Å. The compound is soluble in acetone and dichloromethane. The Tc≡N stretching vibration was found at 1072 cm^{-1} [267].

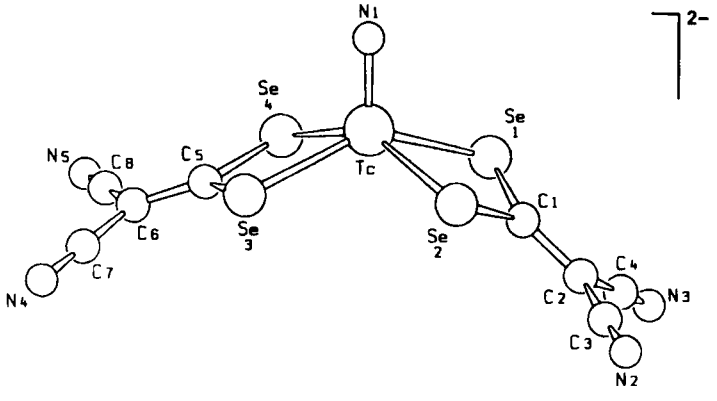

Fig. 12.45.A Bis(1,2-dicyanoethenediselenolato)nitridotechnetate(V), $[TcN\{(CN)_2C{=}CSe_2\}_2]^{2-}$ [267].

The reaction of excess thiourea (tu) with the $[Tc^{VI}NCl_4]$ anion in acetonitrile gives an orange crystalline product of $[Tc^{V}N(tu)_4Cl]Cl$ which is readily soluble in water to produce a strongly acid solution, indicating extensive hydrolysis. The presence of the Tc≡N group in $[TcN(tu)_4Cl]^+$ is confirmed by the IR absorption at 1042 cm^{-1}. This value is consistent with the presence of a ligand (Cl) *trans* to the nitrido group. Substitution reactions on $[TcN(tu)_4Cl]^+$ may be performed in aqueous solution leading to the preparation of new Tc(V) nitrido complexes in good yield [268].

Cationic nitridotechnetium(V) complexes with thiacrown ethers also contain a $TcN(S_4Cl)$-core. Ligand exchange reactions on $[NBu_4][Tc^{VI}NCl_4]$ with the thiacrown ethers 1,4,8,11-tetrathiacyclotetradecane (14S4), 1,5,9,13-tetrathiacyclohexadecane (16S4), 1,5,9,13-tetrathiacyclohexadecane-3,11-diol {16S4-$(OH)_2$} or 1,4,7,10,13,16-hexathiacyclooctadecane (18S6), proceeding in acetone/methanol solutions, result in the formation of cationic complexes containing always only four coordinated S-atoms. The X-ray structures of $[TcNCl(14S4)]^+$, $[TcNCl(18S6)]^+$, and $[TcNCl(16S4\text{-}(OH)_2]^+$ reveal Tc(V) to be in a distorted octahedral geometry with four sulphur atoms of the macrocyclic ligand in the equatorial plane and the nitrido and the chlorine atom in the axial positions. In $[TcNCl(14S4)]^+$ the Tc atom is displaced from the plane by 0.236 Å toward the nitrido nitrogen. The Tc≡N bond distance is 1.615 Å and the Tc–Cl distance is 2.178 Å, which is lengthened by the *trans* influence of the nitrido ligand. The mean Tc–S bond length is 2.410 Å and the N–Tc–Cl angle is 176.4(1)°. The structures of the cations $[TcNCl(18S6)]^+$ and $[TcNCl(16S4\text{-}(OH)_2]^+$ are similar to that of $[TcNCl(14S4)]^+$. Coordination of Tc(V) by four sulphur atoms in the equatorial plane was found to be the common feature, regardless of differences in ring size or the presence of two additional sulphur atoms in the ring of 18S6 or two hydroxyl groups in {16S4-$(OH)_2$} [269,270].

12.3.7.3 $TcN(N_4)$-, $TcN(N_4O)$-, $TcN(N_4Cl)$-, $TcN(N_4Br)$-, and $TcN(N_3Br_2)$-core complexes

So far only a few $TcN(N_4)$-core complexes are known. Phthalocyanine-nitrido-technetium(V) was obtained by melting NH_4TcO_4 and phthalodinitrile at 280 °C. The dark blue compound dissolves completely in conc. H_2SO_4 and sublimates in vacuum without decomposition. The formation of the compound presupposes the presence of NH_4^+. Phthalocyanine-nitrido-technetium(V) is diamagnetic and was characterized by elemental analysis, mass spectrometry and IR spectroscopy. The absorption at 1078 cm^{-1} was assigned to the Tc≡N stretching vibration [272]. $[TcN(py)_4]^{2+}$ and $[TcN(im)_4]^{2+}$ were prepared by reaction of $[Tc^{VI}NCl_4]^-$ with pyridine or imidazol in refluxing acetone. The red $[TcN(py)_4]Cl_2$ and the orange-brown $[TcN(im)_4]Cl_2$ show the Tc≡N stretching vibrations at 1072 and 1075 cm^{-1}, respectively [43].

The nitrido-technetium(V) complex containing the $TcN(N_4O)$-core with the tetradentate amine oxime ligand pnao (propyleneamineoxime), i.e. 3,3,9,9-tetramethyl-4,8-diazaundecane-2,10-dione dioxime, was synthesized recently. Ligand exchange reaction of $[TcNCl_2(PPh_3)_2]^0$ with pnao in CH_2Cl_2/ethanol yielded yellow $[TcN(pnao)(H_2O)]^+$ which was precipitated with $[BPh_4]^-$. The coordination around the Tc

atom is distorted octahedral (Fig. 12.46.A). The four N atoms of the pnao ligand are located in the equatorial plane, the nitrido and the O(3)(H_2O) ligand in the axial positions. The Tc atom resides at 0.399 Å from the plane, defined by the four basal N atoms, toward the nitrido nitrogen. The Tc≡N(1) bond distance is 1.610(5) Å. The N(1)≡Tc–O(3) arrangement is approximately linear with an angle of 176.0(2)°. The Tc–O(3) bond of 2.481(4) Å is lengthened by the *trans* effect of the nitrido ligand. The distance between the two oxime oxygen atoms O(1)···O(2) of 2.720(5) Å suggests the loss of an oxime proton and the formation of a hydrogen bond. The relatively long bond lengths of Tc-N(4) with 2.094(4) Å and Tc–N(5) with 2.113 Å can be explained by a weak interaction between Tc(V) and the proton bearing nitrogens. In the IR spectrum the absorption at 1061 cm^{-1} indicates the Tc≡N stretching vibration. [TcN(pnao)(H_2O)][BPh_4]·$2C_2H_5OH$ crystallizes in the triclinic space group $P\bar{1}$ with a=14.897(2), b=17.075(3), c=9.731(1) Å, α=104.50(1), β=104.39(1), γ=62.12(1)°, and Z=2 [273]. Very recently the corresponding structures of analogous nitridotechnetium(V) amine oxime complexes of longer carbon chains was communicated [273a].

The tetraazamacrocycle 1,4,8,11-tetraazacyclotetradecane-5,7-dione (H_2dioxocyclame) reacts with [$TcNCl_2(PPh_3)_2$]° in dichloromethane/ethanol to produce yellow crystals of the neutral complex [TcN(dioxocyclame)H_2O]°·$2H_2O$ which crystallizes in the monoclinic space group $P2_1/c$ with a=10.154(5), b=10.453(5), c=28.937(4) Å, β=92.69(3)°, and Z=8. The Tc atom is six-coordinate in a rather distorted octahedral geometry, being bonded to four N atoms of the macrocyclic ligand in the equatorial plane and the nitrido N atom and one H_2O molecule in axial positions. The Tc atom is displaced by 0.52 Å from the basal plane towards the nitrido nitrogen atom. The N≡Tc–O(H_2O) angle of 173.7(2)° is approximately linear. The Tc≡N bond length is 1.612(4) Å and the Tc–O(H_2O) distance is 2.688(4) Å. The mean N–Tc–N angles in the five- and six-membered cycles are 80.8 and 92.4°, respectively. The Tc≡N stretch was found in the IR at 1080 cm^{-1} [274]. Using the monooxocyclame ligand 1,4,8,11-tetraazacyclotetradecane-5-one for the reaction with [$TcNCl_2(PPh_3)_2$]°, the orange, monocationic complex [TcN(oxocyclame)(H_2O)]$^+$ was obtained through deprotonation of one amide group [275]. The structure closely resembles that of the before-mentioned neutral [TcN(dioxocyclame)(H_2O)]° complex [274].

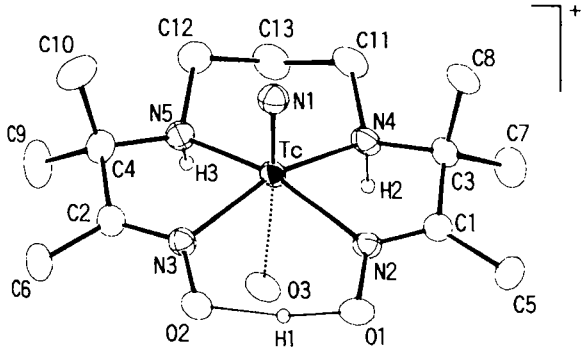

Fig. 12.46.A *Trans*-aqua-3,3,9,9-tetramethyl-4,8-diazaundecane-2,10-dione dioximato-nitridotechnetium(V), [TcN(pnao)(H_2O)]$^+$ [273].

Another complex cation, $[TcN(OH)(py)_4]^+$, containing the $TcN(N_4O)$-core, is formed by reduction of $[Tc^{VI}NCl_4]^-$ in the presence of pyridine in methanol solution. $[TcN(OH)(py)_4][BPh_4]$ precipitates in feathery orange crystals. The Tc≡N stretching vibration appeared at 1050 cm^{-1} in the IR. As in the oxo analogue $[TcO_2(py)_4]^+$ the pyridine ligands are labile and undergo exchange with free pyridine in solution [276].

The reaction of $[TcNCl_2(PPh_3)_2]^0$ with excess diethylenetriamine in a benzene/ethanol mixture and in the presence of air leads surprisingly to the formation of the dicationic complex $[TcN(en)_2(aec)]^{2+}$, where en = ethylenediamine and aec = N-(2-aminoethyl)carbamic acid. The compound $[TcN(en)_2(aec)][BPh_4]_2$ crystallizes in the monoclinic space group *Cc* with a=22.903(6), b=9.346(3), c=25.731(5) Å, β=91.76(2)°, and Z=4. The two ethylenediamine ligands are coordinated in the plane normal to the $Tc{\equiv}N^{2+}$ group, and a unique structural form of N-(2-aminoethyl)carbamic acid is coordinated in a *trans* position through one oxygen atom of the carboxylic group. The resulting coordination around the Tc atom is distorted octahedral, the Tc being displaced from the plane defined by the N atoms of the two ethylenediamine ligands by 0.3268 Å towards the nitrido group. The ligand aec is in the zwitterionic form $^-OOCNHCH_2CH_2NH_3^+$ stabilized in an intramolecular head-to-tail hydrogen bond. The species en and aec of this $TcN(N_4O)$-core complex may be generated as a consequence of the Tc-promoted degradation of diethylenetriamine during the reaction with $[TcNCl_2(PPh_3)]^0$ [277].

Substitution reactions of $[TcNCl_2(PPh_3)_2]^0$ with ethylenediamine (en), 1,3-propanediamine (pn), or 1,5,8,12-tetraazadodecane (tad) in CH_2Cl_2/EtOH solutions lead to the monocationic, light yellow complexes $[TcN(en)_2Cl]^+$, $[TcN(pn)_2Cl]^+$ and $[TcN(tad)Cl]^+$, containing the $TcN(N_4Cl)$-core, which were precipitated as $[BPh_4]^-$ salts. The compounds are diamagnetic. $[TcN(en)_2Cl][BPh_4]$ crystallizes in the monoclinic space group $P2_1/n$, with a=9.316(1), b=12.404(1), c=24.367(5) Å, β=93.76(1)°, and Z=4. The coordination around the Tc atom is approximately octahedral with two molecules of ethylenediamine in the basal plane and the Cl atom at the apical position *trans* to the nitrido group. The Tc atom is displaced from the basal plane by 0.3231(3) Å toward the nitrido nitrogen. The *trans* influence of the nitrido ligand causes an extreme lengthening of the Tc–Cl bond distance which is 2.7320(8) Å. The Tc≡N bond length is 1.603(3) Å and the Tc≡N stretching vibration appears in the IR at 1085 cm^{-1}. The average Tc–N(NH_2) bond distance is 2.156 Å. $[TcN(tad)Cl][BPh_4]$ crystallizes in the orthorhombic space group $Pna2_1$, with a=9.966(2), b=31.203(10), c=9.706(4) Å, and Z=4. The coordination geometry of $[TcN(tad)Cl]^+$ is likewise distorted octahedral. The Tc atom is displaced from the equatorial plane by 0.2163(6) Å toward the nitrido nitrogen. The Tc≡N and the Tc–Cl bond distances are 1.626 and 2.663 Å, respectively. The Tc≡N stretch was found again at 1085 cm^{-1}. The mean Tc-N(aza) bond length is 2.158 Å and the Cl–Tc≡N(nitrido) angle 176.6(2)° [278].

The 1,10-phenanthroline complex *cis*-$[TcN(phen)_2Cl]Cl \cdot H_2O$ was prepared by reaction of $[Tc^{VI}NCl_4]^-$ with phenanthroline in methanol. The reddish-yellow compound was precipitated upon addition of diethyl ether. It crystallizes in the triclinic space group $P\bar{1}$ with a=11.4148(8), b=12.332(1), c=8.5835(6) Å, α=101.244(3), β=107.363(1), γ=80.326(6)°, and Z=2. The coordination geometry of *cis*-$[Tc^{V}N$

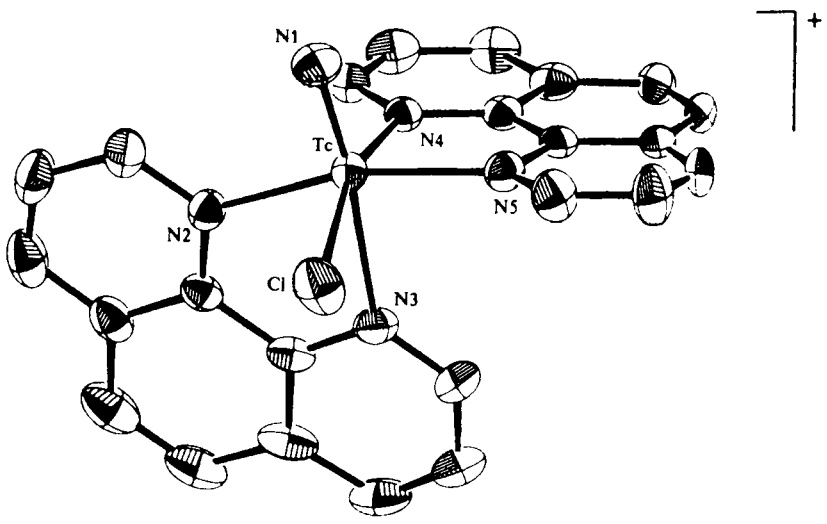

Fig. 12.47.A *Cis*-chloro-bis(1,10-phenanthroline)-nitridotechnetium(V), $[TcN(phen)_2Cl]^+$ [279].

$(phen)_2Cl]^+$ is essentially octahedral (Fig. 12.47.A) with an N(1)≡Tc–N(3) angle of 170.0°. The equatorial plane is formed by the nitrogen atoms N(2), N(4), N(5), and the chlorine atom Cl. The dihedral angle between the two phenanthroline molecules is 73.85°. The Tc≡N(nitrido) distance is 1.603(5) Å and the Tc–Cl distance 2.412(2) Å. The Tc–N(3) bond distance of 2.399(4) Å is, as expected, considerably longer than the average Tc–N distance of 2.127 Å for the phenanthroline nitrogens in the equatorial plane. Two Tc≡N stretching frequencies appeared in the IR at 1071 and 1054 cm^{-1}. The small value of the magnetic moment μ_{eff}=0.6 B.M. is probably due to temperature-independent paramagnetism [279]. The structure of $[TcN(phen)_2Cl]^+$ resembles closely that of $[TcO(phen)_2Cl]^{2+}$ [136].

Reaction of $[Tc^{VI}NBr_4]$ with an excess of 2,2′-bipyridyl (bpy) in methanol gives the orange cation $[Tc^{V}N(bpy)_2Br]^+$ isolated as the tetraphenylborate salt. However, when the reaction is carried out in absolute ethanol a deep red product is obtained showing the composition *cis*-$[Tc^{V}N(bpy)_2Br]_2[Tc^{II}Br_4]$ with the new tetrahedral $[Tc^{II}Br_4]^{2-}$ counter anion. This complex salt crystallizes in the monoclinic space group $P2_1/c$ with a=9.143(2), b=35.014(7), c=15.581(3) Å, β= 105.96(2)°, and Z=4. The $TcN(N_4Br)$-core cation $[TcN(bpy)_2Br]^+$ exhibits distorted octahedral coordination about the Tc(V) with the feature that the nitride and bromide ligands are in *cis* configuration. This may reflect both the small bite angle exerted by the bipyridyl ligand and the steric difficulties of accommodating two bipyridyl ligands in the equatorial plane. The Tc=N bond distance is 1.621(20) Å. The two bipyridyl ligands are folded towards one another with a mean dihedral angle between the plane of these ligands of 70.8°. The strong *trans* influence of the nitrido nitrogen is again reflected in the lengthening of the Tc–N bond, 2.415(19) Å, *trans* to the nitrido atom. The angle N≡Tc–N is 161.6(8)° showing a strong deviation from linearity. The Tc=N stretching vibration appeared in the IR at 1050 cm^{-1} [280–282].

$[TcN(PPh_3)_2Br_2]^0$ reacts with the tridentate ligand bis(2-pyridylmethyl)-2-benzylthio-2,2-dimethylethylamine (pybta) in acetonitrile under reflux to give an orange solid of $[Tc^VNBr_2\{(pyCH_2)_2NCH_2C(CH_3)_2SCH_2Ph\}]^0$. The neutral $TcN(N_3Br_2)$-core complex crystallizes in the triclinic space group $P\bar{1}$ with a=7.458(1), b=10.852(3), c=16.598(6) Å, α=84.07(2), β=86.24(2), γ=72.44(2)°, and Z=2. It is stable in air and soluble in most polar organic solvents. The IR spectrum showed the Tc≡N stretching vibration at 1072 cm^{-1}. The geometry about Tc(V) is distorted octahedral, the S atom is uncoordinated. The Tc≡N(nitrido) distance is 1.61(1) Å and the Tc–N bond length *trans* to the nitrido nitrogen 2.47(1) Å. The average of the Tc–Br bond lengths is 2.535 Å. ^{1}H NMR spectroscopy showed that in $CDCl_3$ solution of the complex there is an equilibrium between this structure and one in which a bromide ion is expelled and the thioether sulphur is ligated [283].

12.3.7.4 $TcN(N_2S_2)$-, $TcN(N_2P_2Cl)$-, TcN(N,S,O,P)-, $TcN(NSO_2)$-, TcN(N,S,Cl,P)-, and $TcN(NO_2P)$-core complexes

$[Tc^{VI}NCl_4]^-$ undergoes reduction upon reaction with 8-quinolinethiol in acetonitrile to yield neutral bis(8-quinolinethiolato)nitridotechnetium(V), $[Tc^VN(C_9H_6NS)_2]^0$. The orange compound crystallizes in the monoclinic space group *C2/c* with a=15.92(1), b=7.347(6), c=15.33(2) Å, β=110.89(8)°, and Z=4. The coordination environment of technetium is distorted square pyramidal with the nitrido nitrogen at the apical position. The 8-quinolinethiolato ligands are arranged with the like donor atoms diametrically opposed. The N_2S_2 donor atoms are markedly distorted from coplanarity. The Tc≡N(nitrido) bond distance is 1.623(4) Å, the Tc–N distance 2.135(2) Å, and the Tc–S distance 2.3559(7) Å. Each 8-quinolinethiolate ligand is almost planar. The N≡Tc–N angle and the N≡Tc–S angle are 98.98(6) and 112.19(2)°, respectively. The bite angle of the 8-quinolinethiolato ligand N–Tc–S is 82.16(6)°. The strong absorption in the IR at 1064 cm^{-1} may be attributed to the Tc≡N stretch [53].

The bidentate ligand S-methyl-3-isopropylidenedithiocarbazate reacts with $[Tc^{VI}NCl_4]^-$ in ethanol/methylene chloride or with $[Tc^VNCl_2(PPh_3)_2]^0$ in benzene to produce $[Tc^VN\{(CH_3)_2CNNCS(SCH_3)\}_2]^0$. The compound crystallizes in the monoclinic space group *C2/c* with a=16.707(3), b=8.838(1), c=12.514(2) Å, β=106.85(1)°, and Z=4. The Tc≡N stretching vibration appears in the IR at 1070 cm^{-1}. The coordination around the Tc atom is again distorted square pyramidal. The Tc atom resides 0.8443(3) Å above the mean N_2S_2 plane towards the nitrido nitrogen atom. The Tc≡N(nitrido) distance is 1.613(3) Å, the Tc–N and the Tc–S distances are 2.161(2) and 2.3442(6) Å, respectively. The bite angle S–Tc–N is 80.80(4)°. The basal ligands are bent away from the nitrido nitrogen [284].

The tetradentate, unsaturated Schiff-base ligand N,N′-ethylene-bis(thioacetylacetonylideneimine) $\{H_2(sacac)_2en\}$ reacts by a reduction-substitution route with $[Tc^{VI}NCl_4]^-$ in a mixture of CH_2Cl_2/EtOH to yield orange, neutral $[TcN\{(sacac)_2en\}]^0$. The compound crystallizes in the monoclinic space group $P2_1/n$ with a=14.654(7), b=12.62(5), c=7.819(4) Å, β=92.60(3)°, and Z=4. The coordination around Tc(V) is nearly square pyramidal with the nitrido nitrogen at the apex and the N_2S_2 atoms of the tetradentate ligand composing the basal plane (Fig. 12.48.A). The ligand around the $(TcN)^{2+}$ moiety is almost planar.

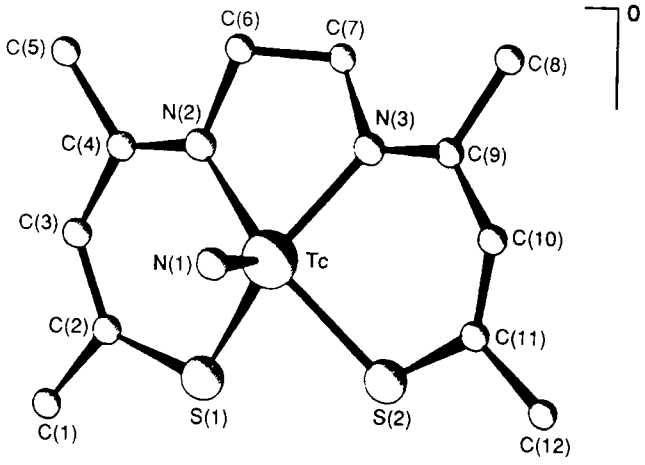

Fig. 12.48.A N,N′-ethylene-bis(thioacetylacetonylideneiminato)nitridotechnetium(V), $[TcN\{(sacac)_2en\}]^\circ$ [213].

The Tc≡N bond distance is 1.621(8) Å, the average Tc–N(2), Tc–N(3) distance is 2.112 Å, and the average Tc–S(1), Tc–S(2) distance is 2.351 Å. The displacement of Tc(V) from the base of the pyramid enlarges the N–Tc≡N angles to 102.8 and 107.5° and the S–Tc≡N angles to 106.3 and 105.0°. The Tc≡N stretching vibration was found in the IR at 1075 cm^{-1} [213].

Reaction of a similar diaminodithiol ligand, N,N′-ethylene-bis(methyl-2-aminocyclopentane-1-dithiocarboxylate) (H_2mact) with $[TcNCl_2(PPh_3)_2]^\circ$ in refluxing ethanol produced the brown complex $[TcN(mact)]^\circ$, which crystallizes in the monoclinic space group $P2_1/c$ with a=13.380(6), b=9.945(2), c=15.839(9) Å, β=113.91(3)°, and Z=4. The Tc atom resides in a slightly distorted square pyramid and is displaced by 0.59(6) Å from the mean basal N_2S_2 plane towards the nitrido nitrogen. The Tc≡N bond distance is 1.629(7) Å. Bond lengths and angles resemble those of the before-mentioned complex. The Tc≡N stretch appeared in the IR at 1060 cm^{-1} [285].

A series of tetradentate, symmetrical, methyl and ethyl derivatives of diaminodithiol (H_2L) was reacted with $[TcNCl_2(PPh_3)_2]^\circ$ in CH_2Cl_2/EtOH to form neutral, yellow nitridotechnetium(V) complexes of the general formula $[TcN(L)]^\circ$. All these complexes are air-stable, diamagnetic solids. Their IR spectra showed the absorptions of the Tc≡N group in the range 1060–1070 cm^{-1} [175].

N-(N′-morpholinylthiocarbonyl)benzamidine (Hmorphtcb) undergoes reaction with $[Tc^{VI}NCl_4]$ in acetone to yield the $TcN(N_2S_2)$-core complex $[Tc^{V}N(morphtcb)_2]^\circ$. The yellow, diamagnetic compound shows the Tc≡N stretching vibration in the IR at 1065 cm^{-1} and melts at 287–288 °C [286]. In addition, products obtained via substitution of one hydrogen of the amino group by phenyl derivatives were characterized [287].

Refluxing of $[TcNCl_2(Me_2PhP)_3]^\circ$ with N,N-diethylthiocarbamoylbenzamidine (HEt_2tcb) in methanol produces lemon-yellow crystals of $[TcN(Et_2tcb)_2]^\circ$ that adopt the triclinic space group $P\bar{1}$ with a=9.749(4), b=11.264(9), c=12.359(4) Å, α=75.34(2),

β=79.69(2), γ=87.55(2)°, and Z=2. The Tc(V)-core is a square pyramid, the basal plane of which is formed by the *cis* coordinated N_2S_2 ligands. Tc is located 0.607(2) Å above the basal plane toward the nitrido atom. The Tc≡N distance of 1.610(5) Å is comparatively short [288].

The nitridotechnetium(V) complex cation $[TcNCl(PPh_2C_6H_4NH_2)_2]^+$, containing the $TcN(N_2P_2Cl)$-core, was synthesized either by ligand exchange from $[TcNCl_2(PPh_3)_2]^0$ or by reduction-substitution from $[Tc^{VI}NCl_4]^-$ with 2-aminophenyldiphenylphosphine in acetonitrile. The pale yellow chloride is stable both in the solid state and in solution. The ionic nature was established by conductivity measurements. $[TcNCl(PPh_2C_6H_4NH_2)_2]Cl \cdot CH_3CN$ crystallizes in the triclinic space group $P\bar{1}$ with a=10.688(5), b=11.910(5), c=15.753(7) Å, α=70.18(3), β=81.59(4), γ=74.96(3)°, and Z=2. The Tc≡N stretch appeared in the IR at 1046 cm^{-1}. The coordination geometry of the Tc atom is highly distorted octahedral (compare Fig. 12.36.A). The two phosphorus atoms of the phophine ligands are in *cis* configuration and the neutral ligands are symmetrically coordinated in the equatorial plane. The Tc atom is displaced from the mean plane of the P_2N_2 donor set by 0.26 Å towards the nitrido nitrogen atom. The two PCCN rings are bent away from the nitrido nitrogen resulting in an umbrella arrangement of the complex. The Tc≡N, Tc–N(1), and Tc–N(2) bond distances are 1.627(3), 2.178(3), and 2.205(4) Å, respectively. The mean Tc–P distance is 2.433 Å. As a result of the *trans* influence of the nitrido nitrogen, the Tc–Cl distance is as long as 2.593(2) Å. The N≡Tc–Cl angle is almost linear with 179.5(1)° [289].

Reaction of the tridentate, dianionic dithiocarbazic acid derivative 2-C_6H_4OH-CH=N-NH-C(=S)SCH_3 (H_2dtcb) with $[Tc^{VI}NCl_4]^-$ and triphenylphosphine in a mixture of ethanol/methylene chloride gives yellow crystals of the neutral complex $[TcN(dtcb)(PPh_3)]^0$. The same compound can also be obtained by using $[TcNCl_2(PPh_3)_2]^0$ as starting material. $[TcN(dtcb)(PPh_3)]^0$ with the core TcN(N,S,O,P) crystallizes in the triclinic space group $P\bar{1}$ with a=8.309(1), b=12.294(1), c=13.308(3) Å, α=96.22(1), β=95.07(1), γ=101.34(1)°, and Z=2. The coordination around the Tc atom is distorted square pyramidal. The Tc atom is displaced by 0.569(1) Å towards the nitrido nitrogen from the plane defined by the atoms N,S,O,P. The Tc≡N bond length is 1.611(3) Å. The tridentate ligand occupies the three coordination sites of the base, the fourth position being occupied by the phosphorus atom of PPh_3 *trans* to the nitrogen in the base. The Tc–P and Tc–O distances are 2.4195(6) and 2.0215(14) Å, respectively. The complex is diamagnetic. The Tc≡N stretching vibration was found in the IR at 1060 cm^{-1} [284]. $[TcN(dtcb)(PPh_3)]^0$ may also be prepared directly by reaction of TcO_4^- with H_2dtcb in the presence of HCl and PPh_3. H_2dtcb and other derivatives of S-methyldithiocarbazate behave as sources of the nitrido nitrogen, giving rise to the formation of various technetium nitrido complexes [290].

The unusual cyclic nitrido-bridged tetrameric complex $[\{Tc^{V}N(tu)\}_4(edta)_2]^0 \cdot 6H_2O$ containing $TcN(NSO_2)$-cores was synthesized by reaction of $[Tc^{V}N(tu)_4Cl]Cl$ with Na_2H_2edta in aqueous solution. The deep brown, neutral compound, which is insoluble in water and organic solvents, crystallizes monoclinic in the space group $P2_1$ with a=16.374(2), b=12.525(1), c=12.205(1) Å, β=107.77(1)°, and Z=2. A medium peak at 984 cm^{-1} in the IR is assigned to ν(Tc≡N). The low value is consistent with a bridging nitrido

ligand in the presence of a *trans* ligand. The structure of the complex shows a cyclic tetrameric configuration for technetium with four asymmetrical Tc≡N–Tc bridges and with each diagonal pair of Tc atoms bridged by an $(edta)^{4-}$ ligand, one edta over and the other under the Tc_4N_4 core resulting in an open cage-like structure. The Tc=N(nitrido) distances range from 1.681(7) to 1.695(7) Å. The coordination geometry about each Tc atom is distorted octahedral with the nitrido nitrogen atom in an axial position [291].

Another mixed donor atom nitrido technetium(V) complex $[TcN(Cl)(PPh_3)\{PhN{=}C(OEt)S\}]^\circ$ with the TcN(N,S,Cl,P)-core was prepared by reaction of $[TcNCl_2(PPh_3)_2]^\circ$ with thiazetidine {PhN=C(OEt)SH} in toluene. The orange, neutral complex crystallizes in the triclinic space group $P\bar{1}$ with a=9.428(5), b=10.237(5), c=15.603(5) Å, α=89.29(3), β=102.74(3), γ=115.61(3)°, and Z=2. Tc(V) has a distorted square pyramidal coordination geometry (Fig. 12.49.A) with the nitrido nitrogen atom at the apex. The Tc≡N bond distance is 1.615(7) Å. The Tc atom is displaced by 0.78 Å toward the nitrido nitrogen N(1) from the mean plane defined by N(2), S, P, and Cl. The bidentate ligand PhN=C(OEt)S is approximately planar. The Tc–Cl, Tc–N(2), Tc–S, and Tc–P bond distances are 2.366(2), 2.135(7), 2.375(3), and 2.429(2) Å, respectively. The bite angle S–Tc–N(2) is 68.1(2)°. The absorption of the complex in the IR at 1100 cm^{-1} was attributed to ν(Tc≡N). When $[TcNCl_2(PPh_3)_2]^\circ$ was reacted in THF with the ligand salt PhN=C(OEt)SNa, generated *in situ* by treating PhN=C(OEt)SH with NaH, the orange complex $[TcN\{PhN{=}C(OEt)S\}_2]^\circ$ was obtained containing the $TcN(N_2S_2)$-core [292].

Synthesis and characterization of nitridotechnetium(V) complexes with L-cysteine-ethylester (HcysOEt), L-cysteine (Hcys) and cysteamine (Hsca) were reported recently. $[TcNCl_2(PPh_3)_2]^\circ$ was reacted in CH_2Cl_2/CH_3OH with the appropriate ligand. Yellow, air-stable crystals of $[TcNCl(cys\text{-}OEt)(PPh_3)]^\circ$, $[TcNCl(cys)(PPh_3)]^\circ$, and $[TcN(csa)_2]^\circ$ were obtained in high yield. Their IR spectra showed the Tc≡N absorption in the range 1060–1090 cm^{-1} and denote that the carboxylic group is not coordinated to the Tc atom. Magnetic susceptibility measurements established diamagnetism of the compounds. $[TcNCl(cys\text{-}OEt)(PPh_3)]^\circ$ has a distorted square pyramidal geometry around the Tc(V)

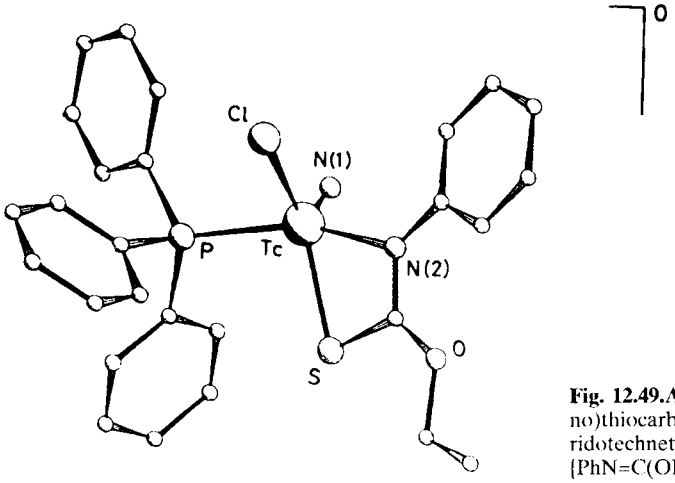

Fig. 12.49.A Chloro-{O-ethyl-(phenylimino)thiocarbonato}triphenylphosphine-nitridotechnetium(V), $[TcN(Cl)(PPh_3)\{PhN{=}C(OEt)S\}]^\circ$ [292].

which is displaced from the mean plane, defined by N, S, Cl, and P, towards the nitrido nitrogen atom by 0.594(1) Å. The Tc≡N bond distance of 1.605(3) Å is indicative of a strong triple bond. The bite angle N–Tc–S is 82.6(1)° [293].

Several complexes containing the core $TcN(NO_2P)$ were synthesized. The tridentate azomethine ligands N-{2-ethoxycarbonyl-3-oxobut(1)en(1)yl}aminoacetic acid and N-{2-acetyl-3-oxobut(1)en(1)yl}aminoacetic acid react with $[TcNCl_2(PPh_3)_2]^\circ$ in refluxing acetone/ methanol to yield orange crystals that are stable in air and easily soluble in chloroform and benzene [294]. Similar reactions proceed with the azomethine N-{2-ethoxycarbonyl-3-oxobut(1)en(1)yl}-2-aminophenol (H_2ecbap). The neutral complex $[TcN(ecbap)(PPh_3)]^\circ$ crystallizes in the monoclinic space group *C2/c* with a=27.480(5), b=11.4145(10), c=18.443(3) Å, β=103.22(2)°, and Z=8. The technetium atom is five-coordinate with the phosphorus atom of the triphenylphosphine group and the O,N,O donor atoms of the azomethine in the basal plane, and the nitrido ligand in the apical position, giving a distorted square pyramidal environment. Tc(V) is displaced by 0.66 Å towards the nitrido nitrogen from the plane. The Tc≡N bond length is 1.605(7) Å, the Tc–P distance 2.398(2) Å [295].

12.3.7.5 $TcN(PS_4)$-, $TcN(P_2S_2)$-, $TcN(P_2Cl_2)$-, TcN (P_2Br_2)-, $TcN(As_2Cl_2)$-, $TcN(As_2Br_2)$-, $TcN(P_3Cl_2)$-, $TcN(P_3Br_2)$-, $TcN(PCl_3)$-, $TcN(PBr_3)$-, and $TcN(P_4Cl)$-core complexes

A $TcN(PS_4)$-core complex, $[TcN(Me_2PhP)(Et_2dtc)_2]^\circ$, was obtained in orange-yellow crystals when $[TcNCl_2(Me_2PhP)_3]^\circ$ was refluxed in methanol with sodium diethyldithiocarbamate ($NaEt_2dtc$). The compound crystallizes in the monoclinic space group $P2_1/c$ with a=17.369(5), b=15.024(1), c=9.906(3) Å, β=76.47(1)°, and Z=4. The coordination geometry of Tc(V) is distorted octahedral (Fig. 12.50.A) with the chelate angles S(1)–Tc–S(2) of 72.54(3)° and S(3)–Tc–S(4) of 66.57(3)°. The Tc≡N distance is 1.624(3) Å. The Tc–S(4) distance of 2.826(1) Å is remarkably long by the *trans* effect of the nitrido ligand [288].

$[TcN(Me_2PhP)_2(mnt)]^\circ$ (mnt = 1,2-dicyanoethene-1,2-dithiolate) represents a $TcN(P_2S_2)$-core complex. The compound was recently prepared by reaction of $[TcNCl_2(Me_2PhP)_3]^\circ$ with Na_2mnt in refluxing methanol. The yellow, air-stable, diamagnetic crystals adopt the triclinic space group $P\bar{1}$ with a=10.000(5), b=14.182(6), c=17.77(1) Å, α=98.77(3), β=103.7(3), γ=104.55(3)°, and Z=4. The coordination geometry of Tc(V) is a distorted square pyramid with the P_2S_2 donor atoms as basal plane. The Tc atom lies out of this plane by 0.56 Å towards the nitrido ligand. The Tc≡N distance is 1.611(4) Å, the average Tc–S distance 2.374(2) Å. The Tc≡N stretching frequency was found at 1060 cm^{-1}. With a large excess of Na_2mnt the reaction with $[TcNCl_2(Me_2PhP)_3]^\circ$ yields $[TcN(mnt)_2]^{2-}$ [296].

Bis(2-diphenylphosphinobenzenethiolato)nitridotechnetium(V), $[TcN(dppbt)_2]^\circ$, was synthesized by reaction of $[TcNBr_2(PPh_3)_2]^\circ$ with Hdppbt in acetone. The bright yellow product showed the Tc≡N stretching vibration at 1070 cm^{-1} [220].

$[TcNCl_2(PPh_3)_2]^\circ$ containing the $TcN(P_2Cl_2)$-core was frequently used as starting compound for the synthesis of various nitridotechnetium(V) complexes. Its first preparation succeeded in reacting TcO_4^- with hydrazinedihydrochloride, triphenylphos-

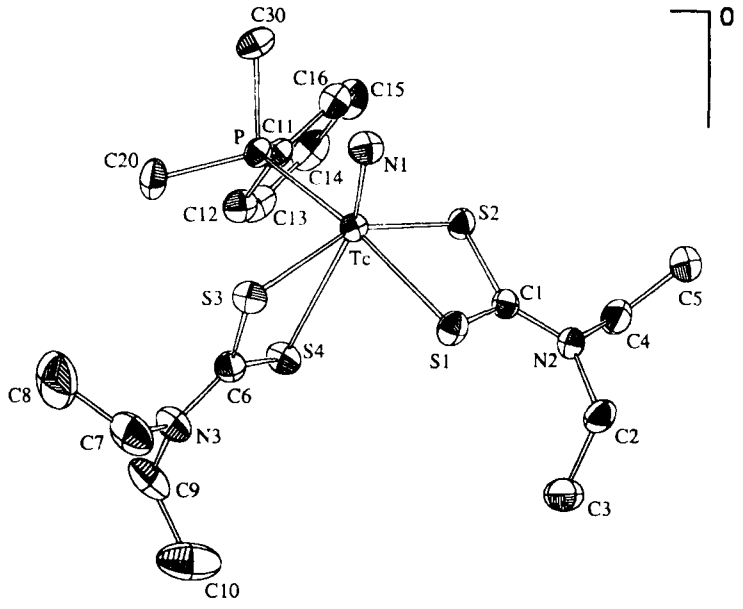

Fig. 12.50.A Bis(diethyldithiocarbamato)(dimethylphenylphosphine)nitridotechnetium(V), [TcN (Me_2PhP)(Et_2dtc)$_2$]° [288].

phine, and hydrochloric acid in ethanol/water and adding benzene. After removal of the ternary mixture of benzene/ethanol/water by distillation, the brick-red [$TcNCl_2(PPh_3)_2$]° was obtained [297]. [$Tc^{VI}NCl_4$]$^-$ undergoes reduction upon reaction with PPh_3 in acetonitrile to give [$TcNCl_2(PPh_3)_2$]°. Its melting point is 231–232 °C and the Tc≡N stretch appears in the IR at 1088 cm^{-1}. [$TcNCl_4$] obviously strongly favors substitution by soft rather than by hard ligands. Soft ligands are often reducing, resulting in the ready reduction of the [$Tc^{VI}N$]$^{3+}$-core to the more stable [$Tc^{V}N$]$^{2+}$-core [53]. Furthermore, the reaction of TcO_4^- with the S-methyl ester of dithiocarbazic acid, H_2N–NH–C(=S)SCH_3, in the presence of HCl and PPh_3, surprisingly leads to [$TcNCl_2(PPh_3)_2$]° [290].

When 1,1-diphenylhydrazine and [$TcCl_4(PPh_3)_2$]° are refluxed in dichloromethane for several hours, orange crystals of [$TcNCl_2(PPh_3)_2$]$\cdot 0.25CH_2Cl_2$ are obtained. [$TcNCl_2(PPh_3)_2$]$\cdot$ $0.25CH_2Cl_2$ crystallizes in the monoclinic space group *C2/c*, with *a*=24.081(9), *b*=9.539(4), *c*=15.650(6) Å, *β*=116.18(1)°, and *Z*=4. The coordination geometry about Tc is distorted square pyramidal with the nitrido nitrogen atom at the apical position and P_2Cl_2 defining the equatorial plane. The Tc atom resides 0.59 Å above this plane displaced towards the apical nitrogen. The Tc≡N bond distance is 1.602(8) Å. The mean Tc–P and Tc–Cl distances are 2.463 and 2.376 Å, respectively, and the P–Tc–P angle 162.0(1)°. The IR band at 1078 cm^{-1} is attributed to the Tc≡N stretching vibration and the absorption at 350 cm^{-1} to *ν*(Tc–Cl) [298].

The corresponding arsine complex $[TcNCl_2(AsPh_3)_2]^+$ crystallizes in the monoclinic space group *I2/a*, with a=15.823(4), b=9.638(2), c=22.490(7) Å, β= 101.91(2)°, and Z=4. Tc(V) resides in a distorted square pyramid. The Tc–As bond distance is 2.5440(4) Å, otherwise the molecular structure, including bond distances and bond angles, closely resembles that of $[TcNCl_2(PPh_3)_2]^+$. According to electron spin resonance studies the oxidation of $[Tc^{V}NCl_2(PPh_3)_2]^+$ and $[Tc^{V}NCl_2(AsPh_3)_2]^+$ with $SOCl_2$ at room temperature leads to $[Tc^{VI}NCl_4]^-$ via the intermediate species $[Tc^{VI}NCl_3(PPh_3)]^+$ and $[Tc^{VI}NCl_3(AsPh_3)]^+$, respectively. The oxidation of $[Tc^{V}NCl_2(AsPh_3)_2]^+$ is more rapid than that of $[Tc^{V}NCl_2(PPh_3)_2]$ [299].

The reactions of $[Tc^{VI}NCl_4]^-$ or $[Tc^{VI}NBr_4]^-$ with PPh_3, $AsPh_3$ or PMe_2Ph in refluxing acetone resulted in the formation of brick-red $[TcNCl_2(PPh_3)_2]^+$ {ν(Tc≡N) = 1095 cm^{-1}}, red-brown $[TcNBr_2(PPh_3)_2]^+$ {ν(Tc≡N) = 1090 cm^{-1}}, yellow-brown $[TcNCl_2(AsPh_3)_2]^+$ {ν(Tc≡N) = 1091 cm^{-1}}, red-brown $[TcNBr_2(AsPh_3)_2]^+$ {ν(Tc≡N) = 1091 cm^{-1}}, yellow $[TcNCl_2(PMe_2Ph)_3]^+$ {ν(Tc≡N) = 1048 cm^{-1}}, and orange $[TcNBr_2(PMe_2Ph)_3]^+$ {ν(Tc≡N) = 1028 cm^{-1}} [297,301].

$[TcNCl_2(PMe_2Ph)_3]^+$ was also synthesized by the reaction of *mer*-$[Tc^{III}Cl_3(PMe_2Ph)_3]$ with NaN_3 in refluxing ethanol. The nitrido complex crystallizes in the orthorhombic space group *Pbca*, with a=16.663(1), b=19.219(1), c= 16.769(1) Å,and Z=8. The coordination geometry of Tc(V) is distorted octahedral with the three dimethylphenylphosphine ligands in meridional positions (Fig. 12.51.A). The Tc≡N bond distance is 1.624(4) Å. Because of the strong *trans* influence of the nitrido nitrogen the Tc–Cl(2) bond length is 2.665(1) Å, while the Tc–Cl(1) bond distance is only 2.441(1) Å. The Tc–P(1), Tc–P(2) and Tc–P(3) bond distances are 2.444(1), 2.487(1),

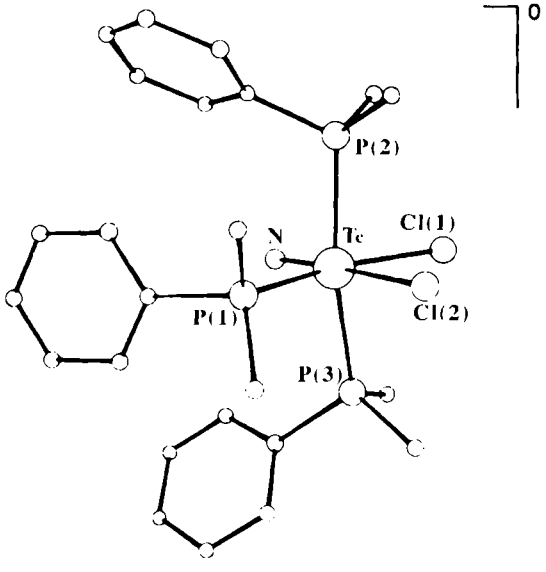

Fig. 12.51.A *Cis*-dichloro-*mer*-tris(dimethylphenylphosphine)nitridotechnetium(V). $[TcNCl_2(Me_2PPh)_3]^+$ [302].

and 2.486(1) Å, respectively. The P(2)–Tc–P(3) angle of 170.68(5)° shows some deviation from linearity. The N–Tc–P angles are almost rectangular. The Cl atoms are in *cis* configuration [302].

The chelating phosphines 1,8-bis(diphenylphosphino)-3,6-dioxaoctane (ppoo), bis(diphenylphosphinoethyl)propylamine (pppa), and 1,1,1-tris(diphenylphosphinomethyl)ethane (ppme), react with $[Tc^{VI}NCl_4]^-$ in a mixture of ethanol and dichloromethane to form the yellow complexes $[TcNCl_2(ppoo)]^\circ$, $[TcNCl_2(pppa)]^\circ$, and $[TcNCl_2(ppme)]^\circ$ containing the $TcN(P_2Cl_2)$-core. $[TcNCl_2(ppoo)]^\circ$ crystallizes in the orthorhombic space group *Fdd2* with a=28.714(7), b=23.915(5), c=8.779(2) Å, and Z=8. $[TcNCl_2(pppa)]^\circ$ in the orthorhombic space group $Pna2_1$ with a=11.650(3), b=23.570(2), c=13.003(2) Å, and Z=4. For $[TcNCl_2(ppoo)]^\circ$ the coordination around Tc(V) is trigonal bipyramidal with the two P atoms in apical positions and the terminal N,Cl,Cl′ atoms forming the basal plane. The trigonal bipyramidal coordination polyhedron for nitridotechnetium(V) complexes is unusual. The Tc≡N, Tc–P, and Tc–Cl bond distances are 1.601(4), 2.4730(8), and 2.385(1) Å, respectively. The P–Tc–P angle of 176.46 (4)° is almost linear and the Cl–Tc–P and P–Tc–N angles are about 90°. The structure of $[TcNCl_2(pppa)]^\circ$ shows square pyramidal coordination around Tc with the Tc atom displaced from the P_2Cl_2 plane toward the nitrido nitrogen atom by 0.410(2) Å. The Tc≡N bond distance is 1.60(1) Å, the mean Tc–P distance 2.410 Å. ν(Tc≡N) of $[TcNCl_2(pppa)]^\circ$ was found in the IR at 1057 cm^{-1}. The three nitrido technetium(V) complexes with the chelating phosphines are readily soluble in CH_2Cl_2 and react with a wide range of ligands [300].

Complex anions of the $TcN(PCl_3)$- and $TcN(PBr_3)$-core were obtained by reaction of $[Tc^{VI}NCl_4]$ and $[Tc^{VI}NBr_4]^-$ with tris(2-cyanoethyl)phosphine (cep) in refluxing acetone. Orange crystals of $[Bu_4N][Tc^{V}NCl_3(cep)]^\circ$ and red-brown crystals of $[Bu_4N][Tc^{V}NBr_3(cep)]^\circ$ were isolated. The Tc≡N stretch appeared at 1050 cm^{-1} in the IR [303].

The diphosphines 1,2-bis(dimethylphosphino)ethane (dmpe) and 1,2-bis(diphenylphosphino)ethane (dppe) react with $[Tc^{VI}NCl_4]^-$ in acetonitrile and ethanol, respectively, to give $[Tc^{V}NCl(dmpe)_2]^+$ and $[Tc^{V}NCl(dppe)_2]^+$. Both cationic complexes of the $TcN(P_4Cl)$-core were isolated as $[BPh_4]^-$ salts [281,282]. Reaction of $[Tc^{V}N(tu)_4Cl]Cl$ with dmpe in acetonitrile also yields the cation $[TcNCl(dmpe)_2]^+$, which was isolated as the yellow complex salt $[TcNCl(dmpe)_2]CF_3SO_3 \cdot 0.5tu$. The compound crystallizes in the orthorhombic space group $Cmc2_1$ with a=23.269(10), b=19.206(9), c=12.205(6) Å, and Z=8. The geometry around Tc(V) is distorted octahedral with the Cl ligand located *trans* to the nitrido nitrogen (Fig. 12.52.A). The angles around Tc(V) are close to 90 and 180°, but the chelate angles are only 81°. The Tc–Cl distance of 2.643(3) Å is very long, due to the strong *trans* influence of the nitrogen atom. The Tc–N distance is 1.613(9) Å. The Tc–P distances range between 2.450(3) and 2.459(3) Å. The reaction of $[TcN(tu)_4Cl]Cl$ with dppe in methanol produces yellow $[TcNCl(dppe)_2]Cl \cdot CH_3OH$ which adopts the monoclinic space group $P2_1/c$ with the lattice constants a=11.023(3), b=13.550(5), c=16.892(7) Å, β=95.22(3)°, and Z=2. The molecular structure of $[TcNCl(dppe)_2]^+$ is similar to that of $[TcNCl(dmpe)_2]^+$ [304].

Structural data of selected compounds discussed in Sect. 12.3.7 are reviewed in Table 12.9.A.

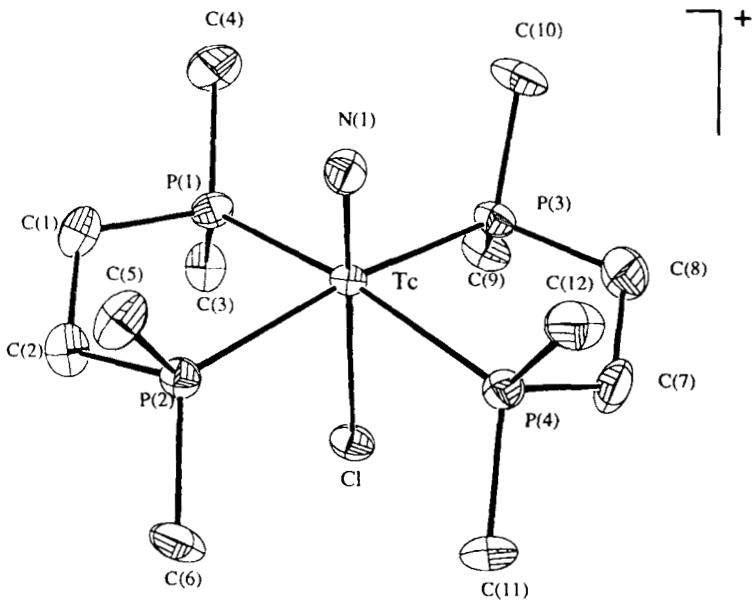

Fig. 12.52.A Bis[(dimethylphosphino)ethane]-*trans*-chloro-nitridotechnetium(V). $[TcN(dmpe)_2Cl]^+$ [304].

Table 12.9.A Some structural data for selected $(Tc{-}N)^{2+}$-core complexes

Complex	Geometry	Tc≡N [Å]	ν(Tc≡N) IR [cm^{-1}]	Tc (displacement) [Å]	Ref.
12.3.7.1					
$[TcN(OH_2)(NCS)_4]^{2-}$	octah.	1.59	–	–	[252]
$[TcN(NCS)_2(PPh_3)_2]^0$	octah.	1.629(4)	1088	–	[253]
$[TcN(OH_2)(CN)_4]^{2-}$	octah.	1.596(10)	1100	0.35	[254]
12.3.7.2					
$[TcN(S_2CNEt_2)_2]^+$	sq.pyr.	1.604(6)	1070	0.74	[258]
$[TcN(SCOCOS)_2]^{2-}$	sq.pyr.	1.613(4)	1071	0.647	[110,261]
$[TcN(S_2CNEt_2)(SCOCOS)]$	sq.pyr.	1.54(2)	1071	0.66(1)	[67]
$[TcN(S_2CO)_2]^{2-}$	sq.pyr.	1.621(6)	1060	0.71	[262]
$[TcN(mnt)_2]^{2-}$	sq.pyr.	1.59(1)	1060	0.6	[263]
$[TcN(mns)_2]^{2-}$	sq.pyr.	1.61(1)	1072	0.768(1)	[267]
$[TcN(tu)_4Cl]^+$	octah.	–	1042	–	[268]
$[TcNCl(14S4)]^+$	octah.	1.615	–	0.236	[269,270]
12.3.7.3					
$[TcN(py)_4]^{2+}$	sq.pyr.	–	1072	–	[43]

Table 12.9.A Continued.

Complex	Geometry	Tc≡N [Å]	ν(Tc≡N) IR [cm^{-1}]	Tc (displacement) [Å]	Ref.
$[TcN(pnao)(H_2O)]^+$	octah.	1.610(5)	1061	0.399	[273]
$[TcN(dioxocyclam)(H_2O)]^{\circ}$	octah.	1.612(4)	1080	0.52	[274]
$[TcN(OH)(py)_4]^{+}$	octah.	–	1050	–	[276]
$[TcN(en)_2(aec)]^{2+}$	octah.	1.607(9)	–	0.3268	[277]
$[TcN(en)_2Cl]^{+}$	octah.	1.603(3)	1085	0.3231(3)	[278]
$[TcN(phen)_2Cl]^+$	octah.	1.603(5)	1054/1071	–	[279]
$[TcN(bpy)_2Br]^{+}$	octah.	1.621(20)	1050	–	[282]
$[TcN(pybta)Br_2]^{\circ}$	octah.	1.61(1)	1072	–	[283]
12.3.7.4					
$[TcN(C_9H_6NS)_2]^{\circ}$	sq.pyr.	1.623(4)	1064	–	[53]
$[TcN(sacac)_2en]^{\circ}$	sq.pyr.	1.621(8)	1075	–	[213]
$[TcN(mact)]^{\circ}$	sq.pyr.	1.629(7)	1060	0.59(6)	[285]
$[TcN(Me_2PhP)(Et_2dtc)_2]^{\circ}$	octah.	1.624(3)	1069	–	[288]
$[TcN(Et_2tcb)_2]^{\circ}$	sq.pyr.	1.610(5)	1071	0.607(2)	[288]
$[TcNCl(PPh_2C_6H_4NH_2)_2]^+$	octah.	1.627(3)	1046	0.26	[289]
$[TcN\{(CH_3)_2CNNCS(SCH_3)\}_2]^{\circ}$	sq.pyr.	1.613(3)	1070	0.8443	[284]
$[\{TcN(tu)\}_4(edta)_2]^{\circ}$	octah.	1.681–1.695	984	–	[291]
$[TcNCl(PPh_3)\{PhN{=}C(OEt)S\}]^{\circ}$	sq.pyr.	1.615(7)	1100	0.78	[292]
$[TcNCl(cys\text{-}OEt)(PPh_3)]^{\circ}$	sq.pyr.	1.605(3)	–	0.594(1)	[293]
$[TcN(ecbap)(PPh_3)]^{\circ}$	sq.pyr.	1.605(7)	–	0.66	[295]
12.3.7.5					
$[TcN(Me_2PhP)_2(mnt)]^{\circ}$	sq.pyr.	1.611(4)	1060	0.56	[296]
$[TcNCl_2(PPh_3)_2]^{\circ}$	sq.pyr.	1.602(8)	1078	0.59	[298]
$[TcNCl_2(ppoo)]^{\circ}$	trig.bipyr.	1.601(4)	1057	–	[300]
$[TcNCl_2(PMe_2Ph)_3]^{\circ}$	octah.	1.624(4)	–	–	[302]
$[TcNCl(dmpe)_2]^{-}$	octah.	1.613(9)	–	–	[304]

12.3.8 Imido, hydrazido, diazenido, and diazene complexes

12.3.8.1 Imido complexes

The dianionic, terminal organoimido unit in its linear conformation is formally isoelectronic to the oxo group.

The technetium(V) phenylimido complex $[TcCl_3(NPh)(PPh_3)_2]^{\circ}$ was synthesized by reaction of TcO_4^- with N-acetyl-N′-phenylhydrazine ($PhNHNHCOCH_3$) and PPh_3 in methanol with a small amount of conc. hydrochloric acid. The phenylimido unit is

generated through the cleavage of the N–N bond in the organohydrazine. The yellow-green $[TcCl_3(NPh)(PPh_3)_2]^0$ crystallizes in the triclinic space group $P\bar{1}$ with a=10.8651(9), b=12.2236(9), c=16.687(2) Å, α=71.998(7), β=74.078(7), γ=80.336(7)°, and Z=2. The absorption at 1090 cm^{-1} was assigned to ν(Tc=N). The coordination geometry about the Tc(V) is slightly distorted octahedral. The steric bulk associated with the PPh_3 ligands results in their mutually *trans* coordination. The remaining coordination sites are occupied by the three chlorine atoms and the phenylimido unit. The mean Tc–P and Tc–Cl bond distances are 2.503 and 2.411 Å, respectively. The Tc=N bond length is 1.704(4) Å. The Tc–N–C bond angle of 171.8(4)° confirms the almost linear coordination mode of the phenylimido unit [305]. $[TcCl_3(NPh)(PPh_3)_2]^0$ reacts with pyridine (py) in refluxing methanol to give the mixed ligand, red-brown complex $[TcCl_3(NPh)(PPh_3)(py)]^0$ showing ν(Tc=N) unchanged at 1090 cm^{-1} [306]. The structures of the compounds $[TcCl_3(NPh)(PMePh_2)_2]^0$ and $[TcBr_3(NPh)(PMePh_2)_2]^0$ [307] resemble that of $[TcCl_3(NPh)(PPh_3)_2]^0$.

$[TcOCl_4]^-$ reacts in refluxing methanol with N-acetyl-N′-phenylhydrazine and 1,2-bis(diphenylphosphino)ethane (dppe) to yield the green technetium(V)phenylimido complex $[TcCl_3(NPh)(dppe)]^0$. In the IR the Tc=N stretching vibration appeared at 1110 cm^{-1}, which is characteristic of the linearly coordinated phenylimido unit. The Tc–N–C angle is 175.7°. The Tc=N bond distance is 1.687 Å. The afore-mentioned phenylimido complex containing PPh_3 instead of dppe can be synthesized analogously, starting with $[TcOCl_4]^-$ [306].

Reaction of $[TcCl_3(NPh)(PPh_3)_2]^0$ with 2,3,5,6-tetramethylbenzenethiol (Htmbt) gives $[Tc(NPh)(tmbt)_3(PPh_3)]^0$, an unstable product with the ν(Tc=N) IR absorption at 1100 cm^{-1}. Using 2,6-dimethylbenzenethiol (Hdmbt), the anionic phenylimido complex $[Tc(NPh)(dmbt)_4]^-$ is formed with ν(Tc=N) at 1093 cm^{-1}. Reaction of $[TcBr_3(NPh)(PPh_3)_2]^0$ with unsubstituted, sterically less hindered thiophenol (PhSH) yields the anionic oxotechnetium(V) complex $[TcO(PhS)_4]^-$ [308].

The cationic phenylimido complex $[TcCl_2(NPh)(PMe_2Ph)_3]^+$ was obtained by reaction of $[TcCl_3(NPh)(PPh_3)_2]^0$ with excess dimethylphenylphosphine in refluxing methanol and isolated as the tetraphenylborate salt. The orange-brown compound $[TcCl_2(NPh)(PMe_2Ph)_3][BPh_4]$ crystallizes in the triclinic space group $P\bar{1}$ with a=11.337(2), b=13.054(3), c=17.854(4) Å, α=72.36(3)°, β=88.51(3)°, γ=89.76(3)°, and Z=2. The coordination geometry of technetium is distorted octahedral displaying a meridional arrangement of the phosphine ligands with one chlorine atom *trans* to the phenylimido unit. The Tc=N bond distance is 1.711(2) Å. The average Tc–P bond length is 2.471 Å. The Tc–Cl bond lengths are 2.433(1) and 2.455(1) Å with the shorter bond to the chloride ligand *trans* to the phenylimido unit, which suggests that there is no *trans* influence. The almost linear Tc–N–C bond angle of 178.8(2)° reflects the *sp* hybridization of the phenylimido nitrogen atom. The three phenyl rings of the phosphine ligands are all directed to the phenylimido ligand forming a protective pocket around the nitrogen atom. The complex is diamagnetic. The IR spectrum displays an absorption at 1102 cm^{-1}, which is assigned to ν(Tc=N) [309].

$[TcOCl_4]^-$ reacts with aromatic amines ($arNH_2$) and triphenylphosphine in alcohol to produce neutral, diamagnetic, air-stable, green-brown solids of the composition $[TcCl_3(Nar)(PPh_3)_2]^0$. The derivative with 4-aminotoluene has been structurally char-

acterized. It is pseudo-octahedral with the two PPh_3 groups in *trans* position to each other. The tolylimido ligand is essentially linear with a Tc–N–C angle of 168° and a Tc=N distance of 1.7 Å [310].

Treatment of $[Tc^{VII}(NAr)_3I]^\circ$ (Ar=2,6-diisopropylphenyl) (Sect. 12.14) [35] with two equivalents of sodium causes the green solution to rapidly change to the orange-brown color of $[Tc^{V}(NAr)_3]^-$:

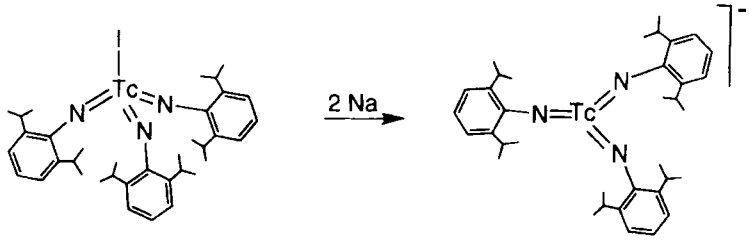

When the orange-brown solution of $[Tc(NAr)_3]^-$ is added to a solution of Ph_3PAuCl, an immediate reaction occurs, and the color of the mixture changes to green, yielding $[(ArN)_3TcAu(PPh_3)]^\circ$. The dark green compound crystallizes in the rhombohedral space group $R\bar{3}$, with a=14.943(3) and c=39.607(12) Å, Z=6. The geometry about the Tc(V) is best described as a distorted trigonal-based pyramid with gold occupying the apex. The imido ligands occupy the base with an Au–Tc–N angle of 97.2(1)° and a N–Tc–N angle of 118.5(1)°. The Tc–Au distance is 2.589(1) Å. The Tc=N and Au–P bond lengths are 1.758(5) and 2.278(2) Å, respectively. The Tc–Au–P angle is exactly linear with 180.0(1)°. This compound is the first example of a structurally characterized, terminal gold phosphine complex of technetium. Reaction of $[Tc^{V}(NAr)_3]^-$ with 0.5 equivalent of $HgBr_2$ yields $[(ArN)_3TcHgTc(ArN)_3]^\circ$. The red compound crystallizes in the cubic space group $Pa\bar{3}$, with a=19.560(3) Å and Z=8. The coordination geometry of technetium is again described as a distorted trigonal-based pyramid with mercury occupying the apex. The imido ligands are at the base with a Hg–Tc–N angle of 97.6(4)° and a N–Tc–N angle of 118.3(2)°. In fact, the $Tc(NAr)_3$ fragments in the structures of $[(ArN)_3TcAu(PPh_3)]^\circ$ and $[(ArN)_3TcHgTc(ArN)_3]^\circ$ are almost identical, suggesting that the nature of the metal cation has little effect on $Tc(NAr)_3^-$. The Tc–Hg and Tc=N bond distances are 2.615(1) and 1.718(10) Å, respectively. The Tc–Hg–Tc angle is 180.0(1)° [35].

The neutral imidotechnetium(V) complex $[Tc(NC_6H_4PPh_2)(NHC_6H_4PPh_2)Cl_2]^\circ$ is obtained by ligand exchange reaction of $[TcOCl_4]$ with 2-aminophenyl-diphenylphosphine in anhydrous benzene under nitrogen:

$$[TcOCl_4]^- + 2NH_2C_6H_4PPh_2 \rightarrow [Tc(NC_6H_4PPh_2)(NHC_6H_4PPh_2)Cl_2]^\circ + HCl + H_2O + Cl$$

The brown complex is soluble in acetone and dichloromethane. The ν(Tc=N) vibration is reported at 951 cm^{-1}. The structure of the analogous rhenium compound shows the ligands $(NC_6H_4PPh_2)^2$ and $(HNC_6H_4PPh_2)^-$ twisted to each other, with the imido group bonded *trans* to a chlorine atom, and the other chlorine atom coordinated equatorially [289].

12.3.8.2 Hydrazido, diazenido, and diazene complexes

Reaction of $[TcOCl_4]^-$ with hydralazine hydrochloride and PPh_3 in methanol at room temperature produces the Tc(V)-hydrazido(3–) complex $[Tc(C_8H_5N_4)Cl_2(PPh_3)_2]^\circ$. The green-violet dichroic crystals adopt the triclinic space group $P\bar{1}$ with a=11.592(3), b=12.205(3), c=17.884(4) Å, α=107.76(2), β=99.03(2), γ=106.11(2)°, and Z=2. However, if the reaction is carried out in refluxing CH_2Cl_2, N–N bond cleavage appears to be promoted and the nitrido species $[TcNCl_2(PPh_3)_2]^\circ$ [298] is the major product. The coordination geometry of $[Tc(C_8H_5N_4)Cl_2(PPh_3)_2]^\circ$ is distorted octahedral, with the phosphine donors adopting the *trans* axial configuration. The equatorial plane is defined by the two chlorine atoms and the nitrogen donors of the chelating hydralazino ligand (Fig. 12.53.A). The Tc–P and Tc–Cl average bond distances are 2.484(6) and 2.379(5) Å, respectively. The Tc–Cl(1) bond *trans* to the phthalazine N(3) donor is 0.026 Å longer than the Tc–Cl(2) bond *trans* to the hydrazido N(1) atom. The short Tc–N(1) distance of 1.77(1) Å is consistent with significant multiple bonding, in contrast to the Tc–N(3) distance of 2.151(9) Å. The N(1)–N(2) distance of 1.274(17) Å suggests a bond order approaching 2. The Tc–N(1)–N(2) angle is 138.6(7)°. IR absorption at 1542 and 1618 cm^{-1} are assigned to ν(N=N). The ^1H NMR spectrum indicates the triple deprotonation of the hydrazido moiety [311].

The technetium(V)phenyldiazenido complex $[Tc(NNPh)Br_2(PMe_2Ph)_3]^\circ$ was obtained by reaction of TcO_4^- with N-acetyl-N′-phenylhydrazine ($PhNHNHCOCH_3$),

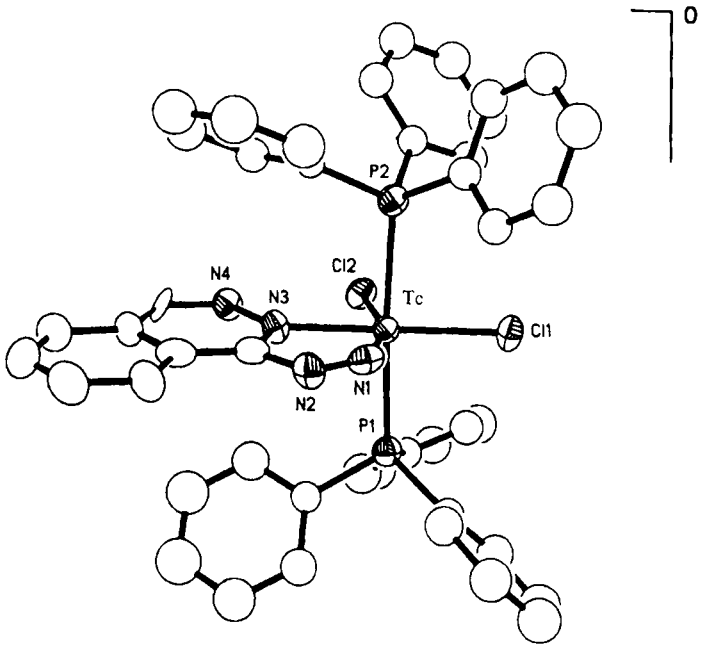

Fig. 12.53.A *Cis*-dichloro-hydralazino-*trans*-bis(triphenylphosphino)technetium(V), $[Tc(C_8H_5N_4)Cl_2(PPh_3)_2]^\circ$ [311].

dimethylphenylphosphine (PMe_2Ph) and HBr in methanol. The orange compound crystallizes in the orthorhombic space group $P2_12_12_1$, with a=8.475(4), b=12.633(4), c=31.171(14) Å, and Z=4. The formation of the diazenido complex is explained by the cleavage of the N–C bond of the hydrazine precursor. The coordination geometry of Tc(V) is distorted octahedral. The three PMe_2Ph ligands are in *mer* position with the two *trans* Tc–P distances of 2.458(5) Å (Fig. 12.54.A). The Tc–P(2) bond which is in *trans* position to Br(2) is shorter, with 2.409(5) Å. The Tc–Br(1) and Tc–Br(2) bond distances are 2.603(3) and 2.635(3) Å, respectively. The Tc–N(1) bond length is 1.753(13) Å. The Tc–N–N angle is almost linear at 172(1)°. The formal charge on the –NNPh ligand is –3. The N–N bond distance is 1.208(16) Å [307].

The bis(aryldiazenido)technetium complex $[TcCl(NNC_6H_4\text{-}4\text{-}Br)_2(PPh_3)_2]^\circ$ was synthesized by reacting $[TcCl_4(PPh_3)_2]^\circ$ with (4-bromophenyl)hydrazine hydrochloride and diisopropylethylamine in methanol. The bright orange compound crystallizes in the monoclinic space group $P2_1/n$, with a=12.174(2), b=19.008(3), c=20.162(3) Å, β=106.39(1)°, and Z=4. The bond angles of the bis(diazenido) complex show around the technetium little deviation from an ideal trigonal bipyramid. The P–Tc–P angle of 175.78(7)° is almost linear. The Tc atom, the chlorine atom, and the two (4-bromophenyl)diazenido ligands are essentially coplanar. The aryldiazenido units display nearly linear Tc–N–N linkages and the bond length Tc–N of 1.796(6) and 1.783(7) Å reflect multiple bonding throughout both units. The N=N stretching vibrations appear in the IR at 1518 and 1573 cm^{-1}. With dianionic aryldiazenido ligands the oxidation state of technetium is +5. Reaction of HCl with the complex dissolved in methanol yielded the six-coordinate dark red compound $[TcCl_2(NNC_6H_4Br)(NNHC_6H_4Br)(PPh_3)_2]^\circ$ [312]. TcO_4^- reacts with 2-hydrazinopyridine-dihydrochloride in methanol to give the purple-brown organodiazenido-organodiazene chelate $[TcCl_3(N{=}NC_5H_4NH)(H{-}N{=}NC_5H_4N)]^\circ$ [313].

A Tc(V) diazene complex is reported to be obtained by reaction of thiobenzoylhydrazine $\{H_2NNHC(S)C_6H_5\}$ with $[TcOCl_4]^-$ in methanol. The lustrous red crystals of $[Tc\{HNNC(S)C_6H_5\}_2(S_2CC_6H_5)]^\circ \cdot n\text{-}Bu_4NCl$ adopt the monoclinic space group $P2_1/c$

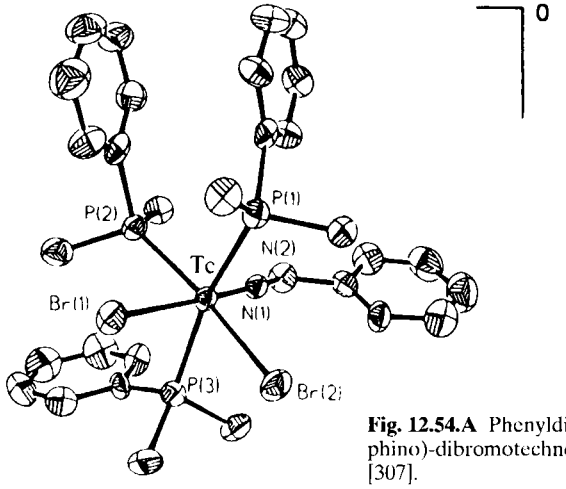

Fig. 12.54.A Phenyldiazenido-*mer*-tris(dimethylphenylphosphino)-dibromotechnetium(V), $[Tc(NNPh)(Me_2PPh)_3Br_2]^\circ$ [307].

with a=11.576(4), b=15.698(5), c=22.718(6) Å, β=94.93(2)°, and Z=4. The dithioacid $C_6H_5C(S)S^-$ ligand was a contaminant of thiobenzoylhydrazine. $[Tc\{HNNC(S)C_6H_5\}_2(S_2CC_6H_5)]^+$ exhibits distorted trigonal prismatic geometry through ligation to the S donors of the bidentate dithioacid group and the N_α and S donors of the chelating diazene ligands. The diazene form is suggested by the IR absorption at 3060 cm^{-1} which is attributed to ν(N–H) [314].

Table 12.10.A summarizes some structural data of complexes described in Sect. 12.3.8.

Table 12.10.A Some structural data of selected imido, hydrazido, diazenido, and diazene complexes.

Complex	Geometry	Tc=N [Å]	ν(Tc=N) IR [cm^{-1}]	Ref.
12.3.8.1				
$[TcCl_3(NPh)(PPh_3)_2]^0$	octah.	1.704(4)	1090	[305]
$[TcCl_3(NPh)(dppe)]^0$	octah.	1.687	1110	[306]
$[Tc(NPh)(tmbt)_3(PPh_3)]^0$	sq.pyr.	–	1100	[308]
$[TcCl_2(NPh)(PMe_2Ph)_3]^+$	octah.	1.711(2)	1102	[309]
$[TcCl_3(NCH_3C_6H_4)(PPh_3)_2]^0$	octah.	1.7	–	[310]
$[(ArN)_3TcAu(PPh_3)]^0$	trig. pyr.	1.758(5)	–	[35]
$[(ArN)_3TcHgTc(ArN)_3]^0$	trig. pyr.	1.718(10)	–	[35]
$[TcCl_2(NC_6H_4PPh_2)(NHC_6H_4PPh_2)]^0$	octah.	–	951	[289]
12.3.8.2				
$[TcCl_2(C_8H_5N_4)(PPh_3)_2]^0$	octah.	1.77(1)	–	[311]
$[TcBr_2(NNPh)(PMe_2Ph)_3]^0$	octah.	1.77(1)	–	[307]
$[TcCl(NNC_6H_4Br)_2(PPh_3)_2]^0$	trig. bipyr.	1.796(6)	–	[312]
$[Tc\{HNNC(S)C_6H_5\}_2$	trig.	1.969(7)	1610	[314]
$(S_2CC_6H_5)]^0$	prism	1.980(7)	(Tc–N–N)	

12.4 Technetium(IV)

Hexahalogeno and hexathiocyanato complex compounds of quadrivalent technetium were some of the earliest Tc species to be prepared and characterized. Frequently, halogeno complexes are used as starting compounds to synthesize mono- and dinuclear Tc(IV) complexes of various cores. The Tc(IV)-cores predominantly exhibit distorted octahedral coordination geometry. Due to the presence of three unpaired electrons, the magnetic moments of mononuclear complexes range between 3.5 and 4.1 B.M., whereas the dinuclear compounds are diamagnetic. In addition to halogen ligands, oxygen and sulphur containing ligands were mainly observed in complexes, but no terminal oxygen, sulphur or nitrogen atoms. Numerous halogeno complexes with phosphine ligands were prepared and identified.

12.4.1 Hexahalogeno and hexathiocyanato complexes, nonabromoditechnetate(IV)

$K_2[TcF_6]$ was prepared by fusion of $K_2[TcBr_6]$ with excess KHF_2. Recrystallization of potassium hexafluorotechnetate(IV) from water gave pale pink platelets. The resistance of $[TcF_6]^{2-}$ against hydrolysis is remarkable, only conc. alkaline solution decomposes the compound by precipitation of TcO_2-hydrate. The solubility of $K_2[TcF_6]$ is 1.5 g/100 g water at 25 °C. The complex salt adopts the trigonal $K_2[GeF_6]$ structure, space group $C\bar{3}m$, and is isostructural with $K_2[ReF_6]$ and a low-temperature version of $K_2[MnF_6]$. The hexagonal unit cell has the dimensions a=5.807(2) and c=4.645(2) Å [315,316]. The dimensions of the isostructural, less soluble $Rb_2[TcF_6]$ are a=5.986(2) and c=4.798(2) Å [317]. The magnetic moment of $K_2[TcF_6]$ is 3.95 B.M. with θ=–28K. This is similar to the "spin-only" value for three unpaired electrons [318]. The EPR hyperfine structure of $[^{99}TcF_6]^{2-}$ in mixed polycrystalline $K_2[TcF_6]/K_2[PtF_6]$ shows the expected 10 lines at 3 cm wavelength and 77 K. The parameters are $|g|$=3.884, $|A|=3.34 \cdot 10^{-2}$ cm^{-1}, and $|B|=1.76 \cdot 10^{-2}$ cm^{-1} [319]. The absorption spectrum of an aqueous solution of $K_2[TcF_6]$ was measured in the near IR, VIS, and UV between 8000 and 50000 cm^{-1}. The ligand field parameter A was determined as 28400 cm^{-1}, the Racah parameter B is 530 cm^{-1}, and the nephelauxetic ratio β_{35} is 0.75 [320]. The IR and Raman spectra of $K_2[TcF_6]$ and $Cs_2[TcF_6]$ were measured from 1000 to 45 cm^{-1} and the force constants were determined in the valence force field and in the standard Urey-Bradley field [321,322]. More recently $K_2[TcF_6]$ was obtained by reacting $K_2[TcBr_6]$ with 40 % HF and precipitation of Br^- with silver fluoride [323] according to the equation:

$$[TcBr_6]^{2-} + 6F^- + 6Ag^+ \rightarrow [TcF_6]^{2-} + 6AgBr$$

Hydraziniumhexafluorotechnetate(IV), $[N_2H_6][TcF_6]$, was prepared by reaction of TcF_6 in anhydrous hydrofluoric acid with $[N_2H_6]F_2$. The brown compound crystallizes in a body-centered cubic lattice with a=10.48 Å. The magnetic moment of $[N_2H_6][TcF_6]$ at 300 K is μ_{eff}=3.79 B.M. with a Weiss constant θ=52K. The IR spectrum shows a strong absorption at 545 cm^{-1}, which was tentatively assigned to ν_3 of $[TcF_6]^{2-}$ [324].

$K_2[TcCl_6]$ was obtained by reduction of $KTcO_4$ with KI in conc. hydrochloric acid. Recrystallization from hydrochloric acid yielded yellow crystals of $K_2[TcCl_6]$ [316,325,326]. The solubility of the complex salt at 25 °C in 3 M HCl is $1.16 \cdot 10^{-3}$ mole/l [327]. In aqueous solution $[TcCl_6]^{2-}$ is rapidly decomposed by precipitation of TcO_2-hydrate. $K_2[TcCl_6]$ crystallizes in the face-centered cubic lattice, space group $Fm\bar{3}m$, with a=9.825(2) Å [317]. Heat capacity measurements indicate no crystal structure change at low temperatures. The heat capacity of $K_2[TcCl_6]$ exhibits a lambda-type anomaly with a maximum at 7.0±0.1 K indicative of a cooperative-type transition. There is no doubt that this anomaly represents the transition from an ordered antiferromagnetic state below 7.0 K to a disordered paramagnetic state above this temperature. The Néel temperature of 7.0 K for $K_2[TcCl_6]$ is considerably lower than that of $K_2[ReCl_6]$ with 11.9 K [328]. The magnetic moment of $K_2[TcCl_6]$ was

found to be μ=4.05 B.M. with the Weiss constant θ=–68K [318]. The EPR hyperfine structure of ^{99}Tc(IV) in mixed single crystals of $K_2[TcCl_6]/K_2[PtCl_6]$ was measured at 3 cm wavelength at 1.7 K. Consistent with the nuclear spin of 9/2 of ^{99}Tc the spectrum (Fig. 12.55.A) reveals 10 strong lines [319,329,330]. The stepwise formation constant k_6 of $K_2[TcCl_6]$, dissolved in 3 M $HClO_4$, was determined potentiometrically at 15 °C to $k_6=4.6 \cdot 10^4$ mole $^{-1} \cdot$l which is almost 50 times smaller than that of $[ReCl_6]^{2-}$ [331]. The force constant of the Tc–Cl bond in $K_2[TcCl_6]$ was calculated in the valence force field from IR and Raman vibrations to be f_r=1.51 mdyne · Å $^{-1}$ [321]. The cubic ligand field paramter was derived from the polarized low temperature absorption spectrum in the VIS and UV at $\Delta=24.4 \cdot 10^3$ cm^{-1} [332]. Single crystal structure analysis of $K_2[TcCl_6]$ yielded 2.35 Å for the Tc–Cl bond distance in a regular octahedral structure. Assuming a value of 0.99 Å for the covalent radius of chloride, the octahedral covalent radius of 1.36 Å was obtained for Tc(IV) [333].

Some crystallographic and magnetic data of Tc(IV) hexahalogeno complex salts are collected in Table 12.11.A.

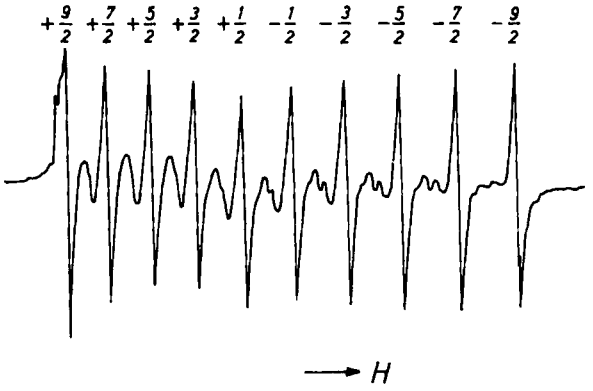

Fig. 12.55.A EPR hyperfine structure of a mixed single crystal of $K_2[TcCl_6]/K_2[PtCl_6]$ at 1.7 K and [111]-direction of the magnetic field [319].

Table 12.11.A Crystallographic and magnetic data of Tc(IV) hexahalogeno complex salts.

Complex salt	Structure	Lattice constants [Å]	Magnetic Moment [B.M.]	Weiss constant [θ]	Ref.
$K_2[TcF_6]$	$C\bar{3}m$	a=5.807	3.95	-28	[317,318]
		c=4.645			
$Rb_2[TcF_6]$	$C\bar{3}m$	a=5.986	–	–	[317]
		c=4.798			
$[N_2H_6][TcF_6]$	*bcc*	a=10.48	3.79	52	[324]
$K_2[TcCl_6]$	*Fm3m*	a=9.825	4.05	–68	[317,318]
$(NH_4)_2[TcCl_6]$	*Fm3m*	a=9.9072	–	-	[334]
$Rb_2[TcCl_6]$	*Fm3m*	a=9.965	-	-	[317]

Table 12.11.A Continued.

Complex salt	Structure	Lattice constants [Å]	Magnetic Moment [B.M.]	Weiss constant [Θ]	Ref.
$Cs_2[TcCl_6]$	*Fm3m*	a=10.237	–	–	[335]
$[AsPh_4]_2[TcCl_6]$	$P\bar{1}$	a=10.111, b=12.165 c=10.263 α=93.86° β=114.51° γ=99.08°		–	[337]
$K_2[TcBr_6]$	*Fm3m*	a=10.371	4.06	–75	[317]
$(NH_4)_2[TcBr_6]$	*Fm3m*	a=10.417		–	[335,336]
$Rb_2[TcBr_6]$	*Fm3m*	a=10.460	–	–	[317,318]
$Cs_2[TcBr_6]$	*Fm3m*	a=10.650	–	–	[338]
$K_2[TcI_6]$	$P2_1/c$	a=11.352 b=7.846 c=13.817 β=145.63°	4.20	–81	[318,339]
$(NH_4)_2[TcI_6]$	*ortho-rhombic*	a=11.24 b=8.02 c=7.92	–	–	[340]
$Rb_2[TcI_6]$	*Fm3m*	a=11.301	4.24	–126	[317,318]
$Cs_2[TcI_6]$	*Fm3m*	a=11.410	–	–	[340]

X-ray structure analysis of a single crystal of $(NH_4)_2[TcCl_6]$ established the Tc–Cl bond distance in the regular octahedral $[TcCl_6]^{2-}$ to be 2.3531(5) Å [334]. Structural studies of $[AsPh_4]_2[TcCl_6]$ showed this complex salt to crystallize in the triclinic space group $P\bar{1}$. The $[TcCl_6]^{2-}$ ion exhibits small but significant deviations from ideal octahedral geometry, with Tc–Cl bond distances 2.3441(7), 2.3635(7), 2.3649(7) Å, and Cl–Tc–Cl angles of 88.63(3), 89.95(3), and 90.26(3)°. The slight tetragonal distortion in the anion seems to be caused by crystal-packing forces arising from the presence of the bulky $[AsPh_4]^+$ ions [337].

Hexabromotechnetic(IV) acid, $(H_3O)_2[TcBr_6]$, forms red cubic crystals crystallizing in the space group *Fm3m* with a=10.410(4) Å and Z=4. The Tc–Br bond distance is 2.506(2) Å [341]. Salts of $[TcBr_6]^{2-}$ may be prepared by reduction of TcO_4^- with conc. HBr containing the appropriate cation. The solubility of $K_2[TcBr_6]$ at 25 °C in 3.5 M HBr is $8.96 \cdot 10^{-3}$ mole/l [327]. In aqueous solution $[TcBr_6]^{2-}$ is readily decomposed by precipitation of TcO_2-hydrate. The stepwise formation constant k_6 of $[TcBr_6]^{2-}$ in 3 M $HClO_4$ is $3.8 \cdot 10^3$ $mole^{-1} \cdot l$ at 15 °C, which is almost 50 times smaller than that of $[ReBr_6]^{2-}$, measured potentiometrically at the same conditions [331]. The force constant of the Tc–Br bond in $K_2[TcBr_6]$ was determined in the valence force field to be f_r=1.39 mdyne · Å^{-1} [321]. The cubic ligand field parameter of $[TcBr_6]^{2-}$ was derived as Δ=$18.7 \cdot 10^3$ cm^{-1} [332] and Δ=$21.6 \cdot 10^3$ cm^{-1} [342].

Purple black salts of $[TcI_6]^{2-}$ were obtained by reduction of TcO_4^- with moderately conc. HI in the presence of the required cation. $Rb_2[TcI_6]$ and $Cs_2[TcI_6]$ crystallizes in

the face-centered cubic lattice, $K_2[TcI_6]$ in the monoclinic space group $P2_1/c$ and $(NH_4)_2[TcI_6]$ in the orthorohombic system. The mean Tc–I bond distance is 2.725(1) Å [339]. $[TcI_6]^{2-}$ undergoes very rapid hydrolysis in water and is only stable in conc. HI. The absorption spectrum of $K_2[TcI_6]$ in 57 % HI was measured between 8000 and 35000 cm^{-1} along with the spectra of $K_2[TcF_6]$, $K_2[TcCl_6]$, and $K_2[TcBr_6]$ in aqueous or acidic solution (Fig. 12.56.A). Electron transfer bands indicate the optical electronegativity X_{opt}=2.25 for Tc(IV) and 2.05 for the less oxidizing Re(IV) [320]. The cubic ligand field parameter of $[TcI_6]^{2-}$ was reported as $\Delta=20.4 \cdot 10^3$ cm^{-1} [342].

When $KTcO_4$ in 11 M HCl is reduced with KI, the red precipitate $K_2[Tc(OH)Cl_5]$ is formed. The compound crystallizes in the space group $Fm3m$ with a=9.829 Å and is isostructural with $K_2[TcCl_6]$. The magnetic moment of $K_2[Tc(OH)Cl_5]$ is μ_{eff}=3.60 B.M. at 293 K with a Weiss constant of approximately 50 K. The most striking feature of the absorption spectrum is the distinct band around 18500 cm^{-1}, which is more intense than for $K_2[TcCl_6]$. This is presumably the reason for the red color of $K_2[Tc(OH)Cl_5]$. A weak absorption in the IR at 467 cm^{-1} was assigned to the ν(Tc–O) stretching mode. The OH stretch is observed as a very weak band at 3400 cm^{-1} [333].

$[TcCl_6]^{2-}$ and $[TcBr_6]^{2-}$ dissolved in hydrochloric acid and hydrobromic acid, respectively, were shown to be sensitive to visible and ultraviolet light. Changes of the spectra of the complexes in the VIS and UV were induced by irradiation of light. The aquation reactions

$$[TcX_6]^{2-} + H_2O \leftrightarrow [Tc(OH_2)X_5]^- + X^-(X=Cl,Br)$$

are reported to be responsible for the changes at least in the early stage of the photolysis. Kinetic parameters and equilibrium constants of the aquation reactions were determined and reaction species also for subsequent aquation stages were identified [343,349].

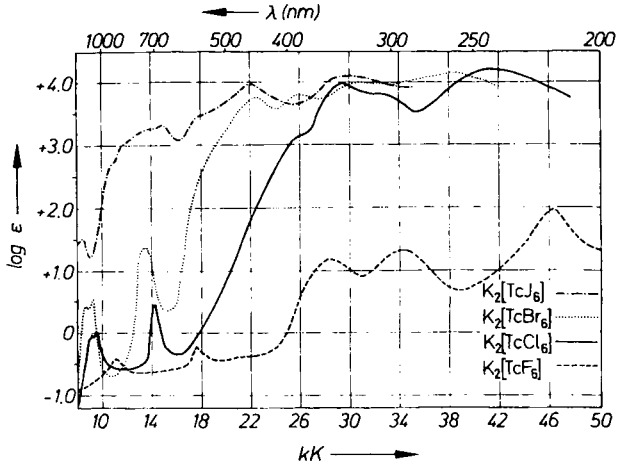

Fig. 12.56.A Absorption spectra of the hexahalogenotechnetate(IV) complexes in aqueous solution [320]; kK = 10^3 cm^{-1}.

The reaction of $TcCl_4$ with 1,4,7,10,13-pentaoxacyclopentadecane (15-Crown-5) in dichloromethane produced the yellow compound $[(15\text{-Crown-5})(H_3O)(15\text{-Crown-5})][TcCl_5(H_2O)]$, from which the X-ray structural parameters of the anion $[TcCl_5(H_2O)]$ were determined. Tc resides in a distorted octahedral environment with the average Tc-Cl bond distance of 2.34 Å and a Tc–O distance of 2.08 Å [350].

The mixed chloro-bromo-technetates(IV), $[TcCl_nBr_{6-n}]^{2-}$, n=1–5, were separated by ion exchange chromatography on diethylaminoethylcellulose. Due to the stronger *trans* effect of Br^- as compared to Cl^-, the ligand exchange reactions of $[TcBr_6]^{2-}$ with HCl and of $[TcCl_6]^{2-}$ with HBr proceeded stereospecifically to form either *cis/fac-* or *trans/mer* species for n=2,3,4, respectively. The IR and Raman spectra of the ten chloro-bromo-technetates(IV), including the pure geometrical isomers, were recorded at 80 K and completely assigned. The force constants were calculated in the valence force field [351].

The luminescence spectra $\Gamma_7(^2T_{2g}) \rightarrow \Gamma_8(^4A_{2g})$ of the mixed chloro-bromo-technetates(IV) $Cs_2[TcCl_nBr_{6-n}]$, n=1–5, in some host crystals such as $Cs_2[SnCl_6]$, $Cs_2[SnBr_6]$, and $Cs_2[TeCl_6]$, were measured at 10K between 12800 and 14000 cm^{-1}, including the pairs of pure geometrical isomers, with n=2,3,4. Due to the weak spin-orbit coupling of Tc(IV), only from the Γ_7 level does a phosphorescence transition arise. Because of the nephelauxetic effect the electronic origins of $[TcCl_nBr_{6-n}]^{2-}$ shift to higher wavenumbers with increasing n. While the splittings in *cis*-$[TcCl_4Br_2]^{2-}$ and *cis*-$[TcCl_2Br_4]^{2-}$ are the same but of opposite sign, the splittings of *trans* isomers are twice as large. The $\Gamma_7(^2T_{2g}) \rightarrow \Gamma_8(^4A_{2g})$ phosphorescence exhibits for all species a distinct vibronic structure [352,353].

Electrochemical studies on solutions of $[Bu_4N]_2[TcCl_6]$ and $[Bu_4N]_2[TcBr_6]$ in acetonitrile indicate the anodic irreversible oxidation reactions

$$[Tc^{IV}X_6]^{2-} \rightarrow [Tc^{V}X_6]^{-} + e^-$$

of $[TcCl_6]^{2-}$ and $[TcBr_6]^{2-}$ at $E_{1/2}$ of +1.88 and +1.70 V *vs* SCE, respectively, and the cathodic irreversible reduction reactions

$$[Tc^{IV}X_6]^{2-} + e^- \rightarrow [Tc^{III}X_6]^{3-}$$

at $E_{1/2}$ of –0.34 and –0.27 V *vs* SCE, respectively [354]. Spectroelectrochemical investigations on $[TcCl_6]^{2-}$ and $[TcBr_6]^{2-}$ in conc. HX/NaX aqueous media show that the complexes undergo a reversible one-electron reduction. The bromo system is 160 mV easier to reduce [355].

In addition to the aforementioned hexahalogeno complex salts, the orange-red $Ag_2[TcCl_6]$, the yellow 1,2-bis(diphenylphosphonium)ethane hexachlorotechnetate(IV), $[dppeH_2][TcCl_6]$, μ_{eff}=3.74 B.M. at 20 °C, and the orange $[dppeI_2][TcBr_6]$, μ_{eff}=4.02 B.M. at 20 °C, were prepared [356]. Also the green compounds $[pyH]_2[TcCl_6]$, $[bpyH]_2[TcCl_6]$, and $[quinH_2]_2[TcCl_6]$ were precipitated and characterized [233].

Thiocyanato complexes of technetium were used very early to determine technetium spectrophotometrically in solution [357–359]. Their isolation and identification was initiated several years later [360]. Reaction between $[TcCl_6]^{2-}$ and $(SCN)^-$ in

refluxing methanol yielded a deep red-violet solution with absorption bands in the visible region at 400 and 500 nm. Chromatography of the reaction mixture resulted in a purple and a yellow compound. The purple complex with the absorption at 500 nm was obtained as $(NH_4)_2[Tc^{IV}(NCS)_6]$ in a microcrystalline powder with a bright green reflex. A band in the IR at 320 cm^{-1} was assigned to the Tc–N stretching vibration. The magnetic moment μ_{eff} (298 K)=4.1 B.M. is consistent with a $^4A_{2g}$ ground state for an octahedral d^3 ion in the range observed for hexahalogenotechnetate(IV). $[Tc(NCS)_6]^{2-}$ shows a reversible one-electron reduction at $E_{1/2}$=0.18 V *vs* SCE in acetonitrile which produces $[Tc^{III}(NCS)_6]^{3-}$, the complex with the absorption maximum at 400 nm [361]. The redox system is illustrated (Fig. 12.57.A) by isosbestic points in the absorption spectrum of the technetium thiocyanate complexes [360,361]. $[AsPh_4]_2[Tc(NCS)_6]\cdot CH_2Cl_2$ crystallizes in the tetragonal space group *I4/m* with a=11.523(5), c=22.43(2) Å, and Z=2. The $[Tc(NCS)_6]^{2-}$ anion is octahedral and the thiocyanate groups are N-coordinated. Two Tc–NCS groups are constrained by crystal symmetry to perfect linearity, whereas the remaining four Tc–NCS groups situated on the mirror plane are almost linear with a Tc–N–C angle of 175.9(9)°. The Tc–N bond lengths are 2.00(1) and 2.01(1) Å with N–Tc–N angles of exactly 90° [362].

The nonabromoditechnetate(IV) complex $[Tc_2Br_9]^-$ was obtained when $[N(C_2H_5)_4]_2[TcBr_6]$ was heated with trifluoroacetic acid. During the heterogeneous reaction the red hexabromotechnetate is quantitatively converted to violet $[N(C_2H_5)_4][Tc_2Br_9]$. The compound is only stable by exclusion of light and is readily soluble in acetonitrile. The IR and Raman spectra of the face-sharing bioctahedral $[Tc_2Br_9]^-$ were assigned according to the point group D_{3h}. Due to the stronger bond-

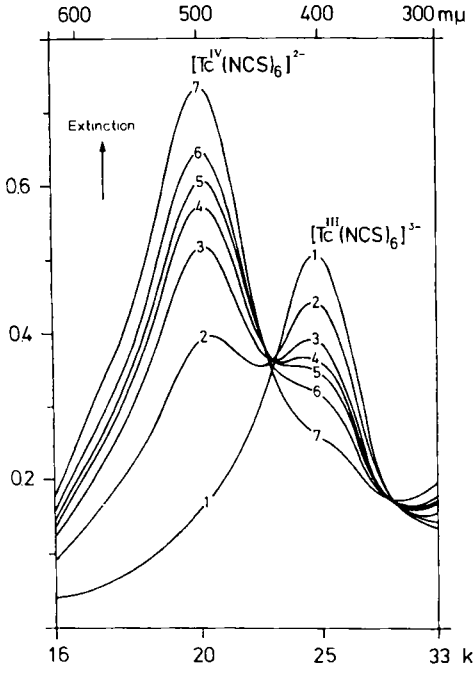

Fig. 12.57.A Isosbestic points in the absorption spectra of the isothiocyanatotechnetate redox system in acidic aqueous solution [360,361]; kK = 10^3 cm^{-1}

ing of the terminal (t) ligands as compared to the bridging (b) ligands, the valence force constant $f_r(Tc\text{-}Br_t)=1.045$ mdyne/Å is significantly higher than $f_r(Tc\text{-}Br_b)=0.80$ mdyne/Å [363].

12.4.2 $Tc(O)_6$-, $Tc(O_4Cl_2)$-, $Tc(O_4Br_2)$-, $Tc(O_2Cl_4)$-, $\{Tc(\mu\text{-}O)(O_2N_2)\}_2$-, $\{Tc(\mu\text{-}O)(O_3N)\}_2$-, and $\{Tc(\mu\text{-}O)O_4\}_2$-core complexes

Tris(acetylacetonato)technetium(III), $[Tc(acac)_3]^\circ$, reacts with ferricenium tetrafluoroborate in acetonitrile to yield the $Tc(O)_6$-core complex $[Tc^{IV}(acac)_3]BF_4$ as a brown crystalline compound showing a magnetic moment of $\mu_{eff}=3.5$ B.M. at 308 K. $[Tc(acac)_3]BF_4$ was also characterized by IR/VIS/UV, ^1H NMR, mass spectrometry, and conductivity measurements [364].

Reaction of $[TcCl_4(PPh_3)_2]^\circ$ and $[TcBr_4(PPh_3)_2]^\circ$ with pentane-2,4-dione (acac), by refluxing the mixtures in air, forms the brown $Tc(O_4Cl_2)$-core complex $[TcCl_2(acac)_2]^\circ$ and the green-brown $Tc(O_4Br_2)$-core complex $[TcBr_2(acac)_2]^\circ$, respectively [365]. Both compounds are resistant to the attack of water and acids. The halide (X) ions are much more labile against base hydrolysis than the bidentate acetylacetonate ligands. The hydrolysis rate equation is expressed by $R=k[OH^-][TcX_2(acac)_2]$ [366].

Salicylaldehyde reacts under reflux with $[PPh_4]_2[TcCl_6]$ to form the dark brown $[PPh_4][Tc(sal)Cl_4]$, $\{sal=C_6H_4(CHO)O^-\}$, a $Tc(O_2Cl_4)$-core compound that crystallizes in the monoclinic space group $P2_1/c$ with $a=14.20(1)$, $b=12.93(1)$, $c=16.91(1)$ Å, $\beta=105.5(1)^\circ$, and $Z=4$. The coordination geometry is slightly distorted octahedral. The equatorial region, defined by O(1) and O(2) of the salicylaldehyde group and the chlorine atoms Cl(2) and Cl(3), is virtually planar. Cl(1) and Cl(4) occupy the *trans* positions (Fig. 12.58.A). The Tc–O(1) and Tc–O(2) bond distances are 2.04(2) and 1.98(2) Å, respectively. The Tc–Cl bond lengths range between 2.31(1) and 2.36(1) Å. The angles Cl(4)–Tc–O(1), Cl(4)–Tc–O(2), and O(1)–Tc–O(2) are nearly rectangular. The magnetic moment of $[PPh_4][Tc(sal)Cl_4]$ is 3.8 B.M. [367].

The Tc(IV) alcoholato complexes $[Tc(OMe)_6]^{2-}$, $[Tc(eg)_3]^{2-}$, and $[Tc(butri)_2]^{2-}$ ($H_2eg = CH_2OHCH_2OH$, $H_3butri = CH_2OHCHOHCH_2CH_2OH$) have been reported to be synthesized. $K_2[Tc(OMe)_6]$ was obtained by reaction of $K_2[TcBr_6]$ with KOMe in methanol under nitrogen:

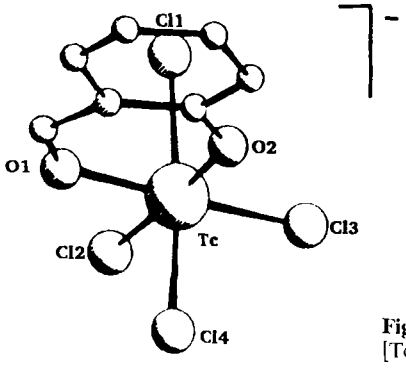

Fig. 12.58.A Tetrachloro-salicylaldehydatotechnetate(IV), $[TcCl_4(sal)]$ [367].

$$[TcBr_6]^{2-} + 6MeO^- \rightarrow [Tc(OMe)_6]^{2} + 6Br^-$$

The pale greenish salt $K_2[Tc(OMe)_6]$ is soluble in methanol or ethanol and decomposes rapidly in aqueous solution, if the pH is lower than 12. Substitution reactions of the compound with glycolate or 1,2,4-butanetriolate yielded the complex salts $K_2[Tc(eg)_3] \cdot 3C_2H_5OH$ and $K_2[Tc(butri)_2] \cdot CH_3OH$. IR absorptions between 450 and 460 cm^{-1} were assigned to the Tc–O stretching vibrations [368].

$K_2[TcBr_6]$ reacts with tris(hydroxymethyl)(trimethylammonium)methane iodide $(H_3thmt)I$ in methanol to form the white crystalline compound $[Tc(thmt)_2]^\circ \cdot 2(H_3thmt)I$ which crystallizes in the monoclinic space group *C2/c*, with a=28.334(5), b=10.199(2), c=15.196(2) Å, β=116.74(1)°, and Z=4. In the neutral complex $[Tc(thmt)_2]^\circ$ the six oxygen atoms of the two thmt ligands are bonded to the Tc atom in an octahedral geometry with D_{3d} symmetry. The three Tc–O bond lengths of 1.996 Å, on average, are equal within the standard deviations. The complex is zwitterionic with the two positive charges on the quaternary ammonium substituent and six negative charges delocalized over the technetium oxygen moiety, so that the resulting oxidation state for technetium is +4. The compound is readily soluble in water and is stable at pH > 4 for more than 24 h [369].

Reaction of $[TcBr_6]^{2-}$ with citric acid is reported to yield polymeric mono- and dicitrates and monomeric dicitrates of Tc(IV). Complex formation and hydrolysis of Tc(IV) were shown to be competitive reactions. Brown to violet solutions occurred, depending on the molar ratio of citrate/technetium and on the reaction time [370,371]. The complex formation of Tc(IV) with nitrilotriacetic acid (H_3nta), ethylenediaminetetraacetic acid (H_4edta), and cyclohexanediaminetetraacetic acid (H_4data) were studied in aqueous solution by means of ion exchange and electrophoresis [372] and the complex composition of solid di- and trinuclear compounds containing H_3nta were analyzed [373].

The dinuclear neutral complex $[(H_2edta)Tc(\mu\text{-}O)_2Tc(H_2edta)]^\circ \cdot 5H_2O$ was obtained by reduction of TcO_4^- with $NaHSO_3$ in the presence of Na_2H_2edta in aqueous solution. The red-brown compound crystallizes in the orthorhombic space group $Pna2_1$ with a=18.41(1), b=10.96(1), c=16.25(1) Å, and Z=4. The central $Tc(\mu\text{-}O)_2Tc$ unit completes its coordination by two H_2edta molecules. The axial positions of each Tc(IV) are occupied by the oxygen atoms of two carboxylate groups, the equatorial positions by amine nitrogens. Two acetate fragments of each edta are protonated and not involved in coordination. The TcO_2Tc ring is nearly planar. The Tc···Tc distance of 2.331 Å is very short in this bis(μ-O)bioctahedral complex. The average Tc–N bond distance is 2.207(16) Å. The complex is diamagnetic and shows a strong absorption band in the visible at 20200 cm^{-1} [374].

Reduction of TcO_4^- with SO_2 in aqueous solution in the presence of nitrilotriacetate (Na_2Hnta) yields the dianionic, dinuclear complex $[(CH_2COO)_3NTc(\mu\text{-}O)_2TcN(CH_2COO)_3]]^{2-}$. The blackish and hygroscopic sodium salt $Na_2[(CH_2COO)_3NTc(\mu\text{-}O)_2TcN(CH_2COO)_3] \cdot 6H_2O$ crystallizes in the triclinic space group $P\bar{1}$, with a=6.330(1), b=9.512(2), c=11.239(4)Å, α=64.97(2), β=83.00(2), γ=74.74(2)°, and Z=1. The complex anion has again a central TcO_2Tc ring. Each Tc atom is coordinated to the N atom and to three carboxylate oxygens of an nta^{3-} ligand. The anion exhibits approximate 2/*m* symmetry, the mirror plane coinciding with the TcO_2Tc ring. The

Tc···Tc distance is 2.363(2), the averaged Tc–N bond length 2.148(2) Å. The angle Tc–O–Tc is 76.0(1)°. Distances and angles at Tc are similar to the analogous values in the H_2edta complex mentioned before. Also the optical absorption spectrum with a band at 19950 cm^{-1} resembles that of $[(H_2edta)Tc(\mu\text{-}O)_2Tc(edtaH_2)]^0$. The nitrilotriacetato complex was shown to be diamagnetic [375].

The dissolution of $(NH_4)_2[TcBr_6]$ in aqueous oxalic acid and addition of $[AsPh_4]Cl$ resulted in the precipitation of tetraphenylarsonium-tris(oxalato)technetate(IV), $[AsPh_4]_2[Tc(C_2O_4)_3]$. The pale yellow compound crystallizes in the monoclinic space group *C2/c* with a=23.164(2), b=13.507(2), c=16.047(1) Å, β=104.90(5), and Z=4. In $[Tc(C_2O_4)_3]^{2-}$ the technetium atom is coordinated to six oxygen atoms in a distorted octahedral array. The angles O–Tc–O range, for adjacent oxygen atoms within the ligands, from 80.4(2) to 80.6(2)°, and are 90.3(2) to 97.8(2)° between the ligands, while for *trans* oxygens across Tc the angles are 167.9(2) and 177.2(2)°. The Tc–O bond distances range from 1.978(5) to 2.001(4) Å [376].

The oxygen-bridged dimeric oxalato complex salt $K_4[(C_2O_4)_2Tc(\mu\text{-}O)_2Tc(C_2O_4)_2] \cdot 3\ H_2O$ was obtained by reaction of $K_2[TcF_6]$ with oxalic acid in aqueous solution at 80 °C for three days. The dark red crystals adopt the triclinic space group $P\bar{1}$ with a=8.765(2), b=9.895(2), c=12.822(4) Å, α=87.47(1), β=88.41(1), γ=71.03(2)°, and Z=2. Each technetium atom in the central $Tc(\mu\text{-}O)_2Tc$ core is coordinated to two oxalato anions in a distorted octahedral arrangement (Fig. 12.59.A). The Tc(1)–Tc(2) distance is 2.361(1) Å. The angles of the bridging oxygens Tc(1)–O(9)–Tc(2) and Tc(1)–O(10)–Tc(2) are 76.21(5) and 75.2(3)°, respectively. The average Tc–O bond distances of 1.913 Å in the bridge are considerably shorter than the Tc–O bond

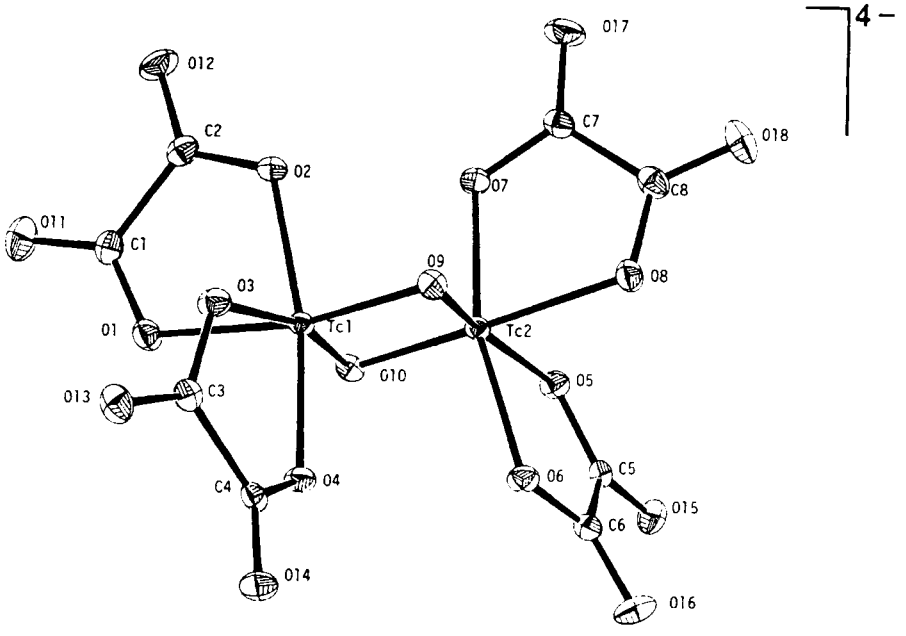

Fig. 12.59.A Bis-μ-oxo-bis[dioxalato-technetate (IV)], $[(C_2O_4)_2Tc(\mu\text{-}O)_2Tc(C_2O_4)_2]^{4-}$ [377].

lengths to the oxygens of the oxalato ligands, which range between 2.020(1) and 2.098(1) Å. The longer Tc–O(oxalato) bond lengths are due to the *trans* influence of the bridging oxygens. The $Tc(\mu\text{-}O)_2Tc$ ring core is approximately planar. Tc–O frequencies of the core were determined as ν_3=730 cm^{-1} and ν_4=401 cm^{-1} [377].

12.4.3 $\{Tc(S_4)\}_2$-, $Tc(S_6)$-, $Tc(S_8)$-, $Tc(SNCl_4)$-, $Tc(N_2Cl_4)$-, $Tc(N_2Br_4)$-, $Tc(N_4Cl_2)$-, and $Tc(N_3O_3)$-core complexes

NH_4TcO_4 reacts in aqueous ethanolic solution with benzene-1,2-dithiol (H_2bdt) to yield the binuclear, neutral $\{Tc(S_4)\}_2$-core complex $[Tc_2(bdt)_4]^\circ$. The wine-red compound crystallizes in the triclinic space group $P\bar{1}$ with a=8.534(1), b=8.842(2), c=11.192(3) Å, α=107.02(2), β=98.13(1), γ=100.60(2)°, and Z=1. Each technetium atom is coordinated to a trigonal-prismatic array of six sulphur atoms. These arrays are fused through a quadrilateral face defined by the four bridging sulphur atoms of two benzene-1,2-dithiolato ligands to result in a Tc_2S_8 core of D_{2h} pseudo-symmetry. This trigonal-prismatic geometry about the Tc(IV) atoms was not observed previously. A Tc–Tc bond passes through the center of the shared face of the trigonal prisms; thus the geometry around the Tc atoms can also be described in terms of capped trigonal prisms. The S_6 polyhedron is only slightly distorted from the idealized trigonal-prismatic geometry. The Tc–S bonds of the terminal ligands are significantly shorter, mean length 2.295(7) Å, than those of the bridging ligands with a mean length of 2.408(6) Å. The differences between bridging and terminal ligands are also reflected in the different bite angles. The terminal ligands have a bite angle of 83.9(2)°, whereas the bite angles of the bridging ligands have the much smaller value of 75.1(2)°. The Tc–Tc bond length is 2.591(3) Å [378,379].

Structurally similar to the complex mentioned above is the dimeric bis(μ-ethane-1,2-dithiolato)bis(ethene-1,2-dithiolato)technetium(IV), $[Tc_2(edt)_2(e{=}dt)_2]^\circ$. The dark green diamagnetic compound was obtained by reaction of ethane-1,2-dithiol with $[TcCl_6]^{2-}$ in methanol. The complex precipitated from the reaction mixture. The only source of e=dt can be H_2edt, which presumably undergoes a reductive process. $[Tc_2(edt)_2(e{=}dt)_2]^\circ$ crystallizes in the triclinic space group $P\bar{1}$ with a=8.624(4), b=8.064(4), c=8.303(5) Å, α=59.01(4), β=61.22(5), γ=65.07(3)°, and Z=1. X-ray structure analysis showed the Tc_2S_8-core containing each technetium atom coordinated in a trigonal prismatic array (Fig. 12.60.A). Two ethane-dithiolato groups provide four μ-sulphur atoms to yield a quadruply bridged Tc(IV) dimer. Each Tc atom is additionally coordinated to a terminal ethenedithiolato group. The complex possesses an exact C_i point symmetry. The average Tc–S(bridging) bond distance is 2.392(5) Å and the Tc–S(terminal) distance is 2.295(5) Å on average. As expected, the C(1)–C(2) and C(3)=C(4) bond lengths are different, being 1.49 and 1.39 Å, respectively. The Tc–Tc bond distance was found to be 2.610(3) Å [224].

The anionic, mononuclear $Tc(S_6)$-core complex tris(1,2-dicyanoethenedithiolato)-technetate(IV), $[Tc(mnt)_3]^{2-}$ was synthesized by reaction of $(NH_4)_2[TcBr_6]$ with $Na_2(mnt)$ in ethanol. Red-brown crystals of $[AsPh_4]_2[Tc(mnt)_3]$ were obtained after precipitation with $[AsPh_4]Cl$. The complex salt crystallizes in the orthorhombic space

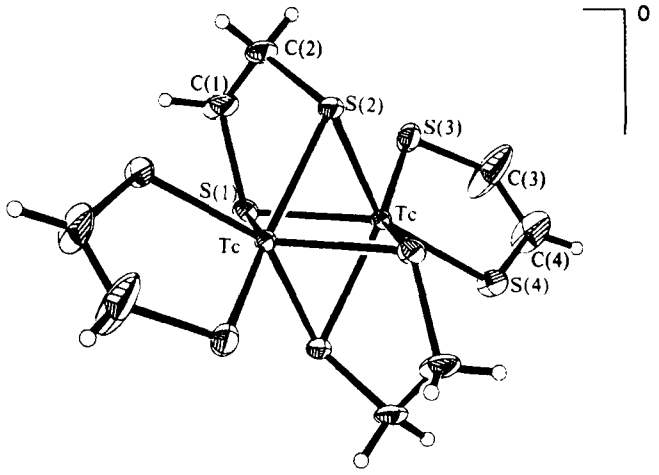

Fig. 12.60.A Bis(μ-ethane-1,2-dithiolato)bis[ethene-1,2-dithiolato-technetium(IV)], [(e=dt)Tc(μ-edt)$_2$ Tc(e=dt)]° [224].

group *Pbcn*, with a=20.256(1), b=15.513(1), c=18.274(1) Å, and Z=4. In $[Tc(mnt)_3]^{2-}$ six sulphur atoms are coordinated to Tc(IV) in a distorted octahedron. The *trans* S–Tc–S angle has an average of only 163°, while the mean bite angle of the ligands is 84.6°, and the adjacent interligand angles S–Tc–S are 100.8(1) and 109.8(1)°. The Tc–S bond distances range from 2.340(2) to 2.380(2) Å [380].

The facile cleavage of the Tc=O bond in $[Tc^{V}OCl_4]^-$ by morpholine-N-carbodithioate was reported to yield the eight-coordinate morpholine-N-carbodithioatetechnetium(IV) complex $[Tc(mdtc)_4]^\circ$. The neutral compound was prepared by reacting $[Bu_4N](TcOCl_4]$ in dried methanol with morpholinium morpholine-N-carbodithioate in dried acetone. A purple crystalline powder was obtained. The magnetic moment of this complex was found to be 3.73 B.M. [381].

Tetrachloro(pyrimidine-2-thiolato)technetate(IV) was prepared by reaction of $[TcOCl_4]$ in dry methanol with 2-mercaptopyrimidine. The red-brown $[Bu_4N][TcCl_4(SC_4N_2H_3)]$ crystallizes in the triclinic space group $P\bar{1}$ with a=11.182(6), b=11.505(4), c=12.235(4) Å, α=64.53(4), β=76.81(3), γ=84.10(5)°, and Z=2. The coordination about Tc(IV) is distorted octahedral. The N–Tc–S angle is 67.1(2)°, constituting the major angular distortion from an ideal octahedron. The Tc–N and Tc–S bond distances are 2.087(6) and 2.429(2) Å, respectively. The Tc-Cl bond lengths range between 2.346(2) and 2.396(2) Å. The pyrimidine ring is planar within the limits of experimental error [382].

The neutral $Tc(N_2Cl_4)$-core complex $[Tc(py)_2Cl_4]^\circ$ (py = pyridine) was prepared by solid-state reaction of pyridinium-hexachlorotechnetate(IV) at 300 °C in a stream of dry argon:

$$(pyH)_2[TcCl_6] \xrightarrow[Ar]{300^\circ C} [Tc(py)_2Cl_4]^\circ + 2HCl$$

The magnetic moment of $[Tc(py)_2Cl_4]^\circ$ was found to be 3.91 B.M. The far IR spectrum showed three Tc–Cl stretching vibrations in the range 300–360 cm^{-1} and two Tc–

N stretches between 220 and 265 cm $^{-1}$. The *cis* configuration of the complex appears to be probable. The compound is practically insoluble in organic or mineral acids, is reported to be not hydrolyzed in aqueous alkaline solutions and to be stable in oxidizing agents [383]. About 20 years earlier the $\alpha\alpha'$bipyridyl (bpy) complexes $[Tc(bpy)_2Cl_2]Cl_2$ and $[Tc(bpy)Cl_4]^\circ$ were isolated. The red-brown $[Tc(bpy)_2Cl_2]Cl_2$ precipitated out of the solution when $TcCl_4$ and bpy were heated under reflux in ethanol. Its magnetic moment at 20 °C was found to be μ_{eff}=3.7 B.M. The compound was soluble in dimethylformamide. Heating of $[Tc(bpy)_2Cl_2]Cl_2$ to 200 °C under vacuum yielded $[Tc(bpy)Cl_4]^\circ$, which is also red-brown and has a magnetic moment of μ_{eff}=3.48 B.M. at 20 °C [384].

$TcCl_4$ and $TcBr_4$ react slowly with acetonitrile or *tert*-butylisonitrile to form microcrystalline solids of yellow-green $[Tc(CH_3CN)_2Cl_4]^\circ$, red $[Tc(CH_3CN)_2Br_4]^\circ$, yellow $[Tc(tert\text{-}BuNC)Cl_4]^\circ$, and red $[Tc(tert\text{-}BuNC)_2Br_4]^\circ$. The IR spectra suggest *cis* coordination of the organic ligands [350].

Reaction of $(NH_4)_2[TcCl_6]$ in glacial acetic acid with the hexadentate Schiff-base ligand tris{2-(2'-hydroxybenzylideneethyl)}amine or its derivatives yielded monocationic technetium(IV) complexes that probably have a distorted octahedral arrangement of the N_3O_3 atoms about the Tc(IV). The complexes are paramagnetic [385].

12.4.4 Complexes containing phosphine ligands

Tetra- and pentachloro- and tetrabromo-complexes of Tc(IV) containing different phosphines were prepared by reaction of technetium tetrahalogenide with the pertinent phosphine [356] or by refluxing TcO_4^- with the phosphine in ethanol in the presence of hydrohalogenic acid [386]. Halogenophosphine complexes are summarized in Table 12.12.A.

Table 12.12.A Halogenophosphine complexes of Tc(IV).

Complex	Color	Geometry (Configuration)	Magnetic moment μ_{eff} [B.M.]	References
$[TcCl_4(PPh_3)_2]^\circ$	green	octah. (*trans*)	3.8	[387,388]
$[TcBr_4(PPh_3)_2]^\circ$	orange-red	octah.	3.97	[356]
$[TcCl_5(PPh_3)]^-$	yellow-orange	octah.	3.7	[388]
$[TcCl_4(PMe(Ph)_2)_2]^\circ$	green	octah. (*trans*)	4.1	[389]
$[TcCl_4\{P(C_2H_5)_3\}_2]^\circ$	green	octah. (*trans*)	–	[389]
$[TcCl_3\{P(C_2H_5)_3\}]$	yellow	octah. (*trans*)	–	[389]
$[TcCl_4(PMe_2Ph)_2]^\circ$	green	octah. (*trans*)	3.4	[386,387,390]
$[TcCl_4(PMe_2Ph)_2]^\circ \cdot 2SbCl_3$	green	pentag. bipyr.	–	[391]
$[TcBr_4(PMe_2Ph)_2]^\circ$	green	octah. (*trans*)	3.8	[386,387]
$[TcCl_4(PEt_2Ph)_2]^\circ$	green	octah. (*trans*)	3.7	[387]
$[TcBr_4(PEt_2Ph)_2]^\circ$	green	octah. (*trans*)	3.7	[387]

When $[TcCl_4(PPh_3)_2]^0$ is treated with hydrochloric acid, the anionic complex $[TcCl_5(PPh_3)]^-$ is formed, and is isolated as (1,1-dimethyl-3-oxobutyl)triphenylphosphonium salt $[PPh_3C(Me)_2CH_2COMe][TcCl_5(PPh_3)]$. The crystal structure of this compound was determined at −100 °C. The complex salt crystallizes in the monoclinic space group $P2_1/n$, with a=21.909(4), b=18.963(4), c=9.896(3) Å, β=103.05(5)°, and Z=4. The coordination geometry in $[TcCl_5(PPh_3)]^-$ is approximately octahedral with an average Tc–Cl bond distance of 2.34(1) Å, a Tc–P distance of 2.57(1) Å, and a mean Cl–Tc–Cl angle of 90.7(4)° [388].

$[TcCl_4\{P(CH_3)(Ph)_2\}_2]^0$ crystallizes in the triclinic space group $P\bar{1}$, with a=8.991(5), b=9.603(4), c=9.750(6) Å, α=66.67(4), β=88.65(4), γ=62.80(4)°, and Z=1. The Tc atom is located on the inversion center. The mean Tc–Cl bond distance is 2.322 Å, the Tc–P distance 2.556(1) Å. The angles around Tc are close to the expected octahedral values [389]. Crystals of $[TcCl_4\{P(C_2H_5)_3\}_2]^0$ are monoclinic, space group $P2_1/c$, with a=8.295(2), b=12.766(3), c=11.831(3) Å, β=123.35(2)°, Z=2. The molecular structure is very similar to that of $[TcCl_4\{P(CH_3)(Ph)_2\}_2]^0$. The Tc–P distance is 2.541(1) Å, the mean Tc–Cl distance 2.333 Å (Fig. 12.61.A) [389]. $[P(C_2H_5)_3H][TcCl_5\{P(C_2H_5)_3\}]$ crystallizes in the orthorhombic space group $Pca2_1$ with a=19.456(20), b=10.223(6), c=22.833(12) Å, and Z=8. There are two independent Tc atoms in the unit cell. The Tc–Cl bonds, located in *trans* position to the phosphine ligand, are 2.414(9) and 2.365(8) Å, while the *cis* bonds vary from 2.319(9) to 2.360(8) Å. The Tc–P bond distances are 2.493(8) and 2.499(8) Å. The angles around the Tc atoms are again close to the octahedral values [389].

$[TcCl_4(PMe_2Ph)_2]^0$ crystallizes in the monoclinic space group $P2_1/c$ with a=9.692(2), b=13.746(3), c=8.339(2) Å, β=106.56(2)°, and Z=2. The mean Tc–Cl distance is 2.324(2) Å and the Tc–P distance is 2.531(1) Å. The Cl–Tc–Cl and Cl–Tc–P angles are in good agreement with a slightly distorted octahedral environment of Tc(IV) [390].

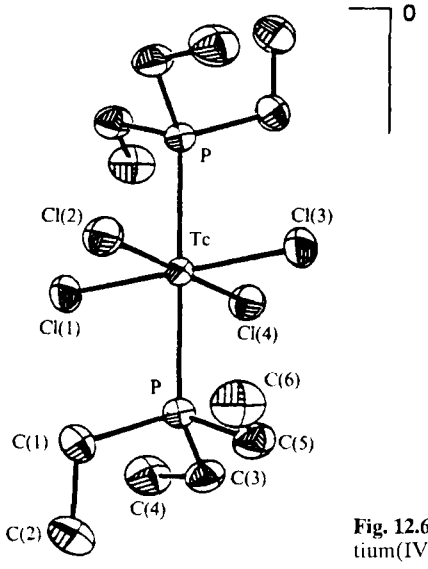

Fig. 12.61.A *Trans*-tetrachloro-bis(triethylphosphine)-technetium(IV), $[TcCl_4\{P(C_2H_5)_3\}_2]^0$ [389].

$[TcCl_4(PPh_3)_2]^\circ$ reacts with dimethyl sulphoxide or pyridine as coordinating solvents to yield pale yellow $[TcCl_4(DMSO)_2]^\circ$ or bright yellow $[TcCl_4(py)_2]^\circ$ by substitution of the phosphine ligands. The paramagnetic complexes were characterized by IR, ^1H NMR, and FAB mass spectrometry [392].

Reaction of $[TcCl_4(PPh_3)_2]^\circ$ with an excess of the bidentate Schiff bases N-methylsalicylideneimine (HMesal) or N-phenylsalicylideneimine (Hphsal) in refluxing toluene gives the red-violet microcrystalline solids $[TcCl_4(HMesal)_2]^\circ$ and $[TcCl_4(Hphsal)_2]^\circ$, which are slightly soluble in acetone. The Schiff-base ligands are coordinated to Tc through the aldimine nitrogen. Magnetic susceptibility measurements in solution gave μ_{eff}=3.7 B.M. as expected for a d^3 system in an octahedral environment. When the reaction of $[TcCl_4(PPh_3)_2]^\circ$ with HMesal or Hphsal was carried through in equimolar concentrations, the brown compounds $[TcCl_3(Mesal)(PPh_3)]^\circ$ and $[TcCl_3(phsal)(PPh_3)]^\circ$ were obtained. These solids are more readily soluble in organic solvents and showed the same magnetic moment of 3.7 B.M. [393].

The reaction of $[TcCl_4(PPh_3)_2]^\circ$ in acetone with an aqueous solution of $(NH_4)_2MoS_4$ was reported. By substitution the dark red neutral Tc(IV) complex $[Tc(PPh_3)_2(MoS_4)_2(H_2O)]^\circ$ was formed, which is indefinitely stable in DMF and nonconducting. Its magnetic moment was found to be 3.51 B.M. The compound was characterized, in addition, by IR spectroscopy. Reduction of $[Tc^VO(MoS_4)_2]$ in ethanol with PPh_3 yields the same complex:

$$[Tc^VO(MoS_4)_2]^- + 3PPh_3 \rightarrow [Tc^{IV}(PPh_3)_2(MoS_4)_2]^\circ + OPPh_3$$

where MoS_4^{2-} acts as a bidentate ligand [126].

Similar to triphenylphosphine, the tris(2-cyanoethyl)phosphine (cep) forms complexes with technetium in which cep is a monodentate ligand. Reaction of TcO_4^- in aqueous ethanolic solution containing hydrochloric acid yielded a blue, microcrystalline solid of $[TcCl_4(cep)_2]^\circ$ with a melting point of 175 °C [303].

Some structural data of Tc(IV) complexes are reviewed in Table 12.13.A.

Table 12.13.A Some structural data of selected Tc(IV) complexes.

Complex	Geometry	Tc–L [Å]	ν(Tc–L) IR [cm^{-1}]	μ_{eff} [B.M.]	References
$[AsPh_4]_2[Tc(NCS)_6]$	octah.	2.00 (Tc–N) 2.01 (Tc–N)	325	4.1	[361,362]
$[NEt_4][Tc_2Br_9]$	octah.	–	267 (ν_7) 245 (ν_{10})	–	[363]
$[Tc(acac)_3]BF_4$	octah.	–	–	3.5	[364]
$[TcCl_2(acac)_2]^\circ$	octah.	–	470ν_{sym}(Tc–O)	–	[365]
$[TcCl_4(sal)]$	octah.	2.01 (Tc–O)	–	3.8	[367]
$[Tc(OMe)_6]^{2-}$	octah.		450 (Tc–O)	–	[368]
$[Tc(thmt)_2]^\circ$	octah.	1.996	–	–	[369]
$[(H_2edta)Tc(\mu\text{-}O)_2Tc(H_2edta)]^\circ$	octah.	2.207 (Tc–N)	–	diamag.	[374]

Table 12.13.A Continued.

Complex	Geometry	Tc–L [Å]	ν(Tc–L) IR [cm^{-1}]	μ_{eff} [B.M.]	References
$[(CH_2COO)_3NTc(\mu\text{-}O)_2TcN(CH_2COO)_3]^{2-}$	octah.	2.148 (Tc–N)	–	diamag.	[375]
$[Tc(C_2O_4)_3]^{2}$	octah.	1.978–2.001	–	–	[376]
$[(C_2O_4)_2Tc(\mu\text{-}O)_2Tc(C_2O_4)_2]^{4-}$	octah.	2.098 2.020	–		[377]
$[Tc(bdt)_4]^{\circ}$	trig.prism	2.295	–	–	[378,379]
$[Tc_2(edt)_2(e\text{-}dt)_2]^{\circ}$	trig.prism	2.295	–	diamag.	[224]
$[Tc(mnt)_3]^{2-}$	octah.	2.340–2.380	–	–	[380]
$[TcCl_4(SC_4N_2H_3)]$	octah.	2.087 (Tc–N) 2.429 (Tc–S)	–		[382]
$[TcCl_4(py)_2]^{\circ}$	octah.	–	220–265 (Tc–N)	3.91	[383]
$[TcCl_2(bpy)_2]^{2-}$	octah.	–	–	3.7	[384]
$[TcCl_5(PPh_3)]$	octah.	2.57 (Tc–P)	–	3.7	[388]
$[TcCl_4(PMePh_2)_2]^{\circ}$	octah.	2.556 (Tc–P)	346 (Tc–Cl)	4.1	[389]
$[TcCl_4\{P(C_2H_5)_3\}_2]^{\circ}$	octah.	2.541 (Tc–P)	338 (Tc–Cl)	–	[389]
$[TcCl_5\{P(C_2H_5)_3\}]^{-}$	octah.	2.496 (Tc–P)	330 (Tc–Cl)	–	[389]
$[TcCl_4(PMe_2Ph)_2]^{\circ}$	octah.	2.531 (Tc–P)	–	–	[390]
$[TcCl_4(HMesal)_2]^{\circ}$	octah.	–	320 (Tc–Cl)	3.7	[393]
$[TcCl_3(Mesal)(PPh_3)]$	octah.	–	340 (Tc–Cl)	3.7	[393]

12.5 Technetium (III)

The complexes of Tc(III) represent the second most numerous class of compounds in coordination chemistry of technetium after the Tc(V) complexes. Again the distorted octahedral geometry is chiefly observed, but in addition, cores of coordination number 5 in trigonal bipyramidal and 7 in pentagonal bipyramidal or capped octahedral arrangements have been seen rather frequently. Dinuclear complexes with multiple Tc–Tc bonds display square pyramidal geometry for both Tc-cores. The low-spin magnetic moments ranging from 2.5 to 3.3 B.M. roughly correspond to two unpaired electrons in the octahedral ligand field. Trigonal bipyramidal compounds were found to be diamagnetic. Many of the Tc(III) complexes contain phosphine ligands, but also sulphur and nitrogen containing ligands are often reported. Some cyclopentadienyl complexes have been synthesized.

12.5.1 Cyano, nitrile, isonitrile, and isothiocyanato complexes

Potassium heptacyanotechnetate(III)-dihydrate, $K_4[Tc(CN)_7] \cdot 2H_2O$, was synthesized by reaction of $(NH_4)_2[TcI_6]$ with KCN in refluxing aqueous methanol under exclusion

of oxygen. The compound forms yellow-orange crystals that were shown to be diamagnetic, as expected from the strong-field ground state $^1A_1'$. The reduction of Tc(IV) to Tc(III) is accomplished by iodide ions of $[TcI_6]^{2-}$, and CN stabilizes the oxidation state +3. On the basis of IR and Raman spectra the pentagonal-bipyramidal structure of $[Tc(CN)_7]^{4-}$ is indicated both in solid and solution. In the presence of oxygen, solutions of the complex slowly decompose [99].

Some isonitrile complexes of tervalent technetium are known. $[Tc\{CNC(CH_3)_3\}_6]^{3+}$ was prepared by reaction of $[Tc(tu)_3]^{3+}$ with *tert*-butylisonitrile in methanol. The seven-coordinate *tert*-butylisonitrile-chloro and bromo complex salts, $[Tc^{III}\{CNC(CH_3)_3\}_6Cl][PF_6]_2$ and $[Tc^{III}\{CNC(CH_3)_3\}_6Br][PF_6]_2$, which can be obtained by addition of chlorine or bromine to $[Tc^{I}\{CNC(CH_3)_3\}_6][PF_6]$, readily dealkylate upon heating in the presence of 2,2′-bipyridine in acetonitrile to form the yellow penta-*tert*-butylisonitrile-cyano-halogeno complex salts $[Tc^{III}\{CNC(CH_3)_3\}_5(CN)X][PF_6]$ and concomitantly $[bpyH][PF_6]$. A neutral isonitrile ligand is converted in this dealkylation process into an anionic cyano ligand [394].

Hexakis(isothiocyanato)technetate(III), $[Tc(NCS)_6]^{3-}$, was synthesized by reaction of $(NH_4)_2[TcBr_6]$ with NH_4SCN in refluxed methanol and addition of $N_2H_4 \cdot H_2O$. Treating the solution with $[n\text{-}Bu_4N]ClO_4$ precipitated air-sensitive yellow crystals of $[n\text{-}Bu_4N]_3[Tc(NCS)_6]$. The observed magnetic moment of 3.0–3.3 B.M. at 298 K is in the range expected for a d^4 ion with two unpaired electrons. The compound crystallizes in the cubic space group $Pa3$ with a=24.444(6) Å and Z=8. The Tc atom is located on a crystallographic threefold rotation axis and $[Tc(NCS)_6]^{3-}$ has approximately octahedral symmetry. The mean Tc–N bond distance is 2.05(2) Å and the Tc–N–C and N–C–S angles are all within 10° of linearity. $[AsPh_4]_3[Tc(NCS)_6]$ exhibits a single, strong ν(NCS) absorption at 2070 cm^{-1} in the IR consistent with octahedral symmetry. $[Tc(NCS)_6]^{3-}$ shows in acetonitrile a reversible one-electron oxidation at 0.18 V vs SCE, indicating the oxidation to $[Tc^{IV}(NCS)_6]^{2-}$ [361].

Trans-$[TcCl_2(NCS)(Me_2PhP)_3]^0$ was obtained by replacement of one chloride ligand in *mer*-$[TcCl_3(Me_2PhP)_3]^0$ by NCS$^-$ in refluxing CH_2Cl_2/CH_3OH. No products with larger thiocyanate content could be isolated. The orange-red compound crystallizes in the monoclinic space group $P2_1/n$, with a=14.997(7), b=10.840(2), c=19.160(8) Å, β=113.04(2)°, and Z=4. The Tc atom in *trans*-$[TcCl_2(NCS)(Me_2PhP)_3]^0$ is coordinated in a distorted octahedral geometry. The phosphine ligands are in meridional positions. The linear NCS$^-$ ligand is coordinated in *trans* position to Me_2PhP. The relatively long Tc–N bond distance of 2.104(3) Å can be interpreted in terms of a structural *trans* influence of the phosphine ligand. The IR spectrum shows an intense band for the ν(NCS) vibration at 2076 cm^{-1}. The compound is readily soluble in CH_2Cl_2 or $CHCl_3$ and is indefinitely stable, even in solution [395].

When $[n\text{-}Bu_4N]_2[Tc_2Cl_8]$ was suspended in a mixture of CH_3CN and Et_2O and $HBF_4 \cdot Et_2O$ was syringed into the suspension, yellow crystals of $[TcCl_2(CH_3CN)_4][BF_4]$ were obtained after a week of heating, in addition to $[Tc_2(CH_3CN)_{10}][BF_4]_4$. The mononuclear compound crystallizes in the orthorhombic space group *Ibam* with a=6.250(1), b=12.189(2), c=20.880(5) Å, and Z=4. The solid, as well as solutions of $[TcCl_2(CH_3CN)_4][BF_4]$, are stable in air. The cation $[TcCl_2(CH_3CN)_4]^+$ shows a distorted octahedral coordination (Fig. 12.62.A) about the Tc(III) center; it has virtual

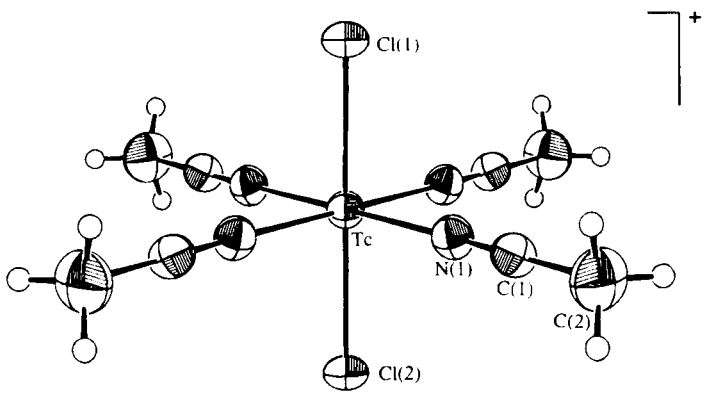

Fig. 12.62.A *Trans*-(dichloro)-tetrakis(acetonitrile) technetium(III). $[TcCl_2(CH_3CN)_4]^+$ [396].

D_{4h} symmetry. The chloride ligands are in *trans* disposition, the nitrile ligands reside in the equatorial plane. The angles around Tc are very close to 90 or 180°. The Tc–Cl and Tc–N distances are unexceptional. C≡N stretching frequencies occur at 2331 and 2301 cm^{-1} in the IR. The CH_3CN ligands are extremely labile. Cyclic voltammetry of the complex cation reveals a reversible one-electron reduction to give the neutral Tc(II) species $[TcCl_2(CH_3CN)_4]^0$ [396].

12.5.2 Halogeno-phosphine and -arsine complexes

Halogeno-phosphine and halogeno-arsine complexes of tervalent technetium are collected in Table 12.14.A.

Table 12.14.A Halogeno-phosphine and -arsine complexes of Tc(III).

Complex	Color	Geometry (Configuration)	Magnetic Moment μ_{eff} [B.M.]	References
$[TcCl_2(dmpe)_2]^+$	orange	octah.(*trans*)	–	[239,397,398]
$[TcBr_2(dmpe)_2]^+$	red	octah.(*trans*)		[239,397,398]
$[TcCl_2(dppe)_2]^+$	red-orange	octah.(*trans*)	2.74	[356,397,399–401]
$[TcBr_2(dppe)_2]^+$	dark pink	octah.(*trans*)	3.04	[356,397, 400, 401]
$[TcCl_3(dppe)_2]^0$	yellow-orange	–	–	[402]
$[TcCl_3(Me_2PhP)_3]^0$	yellow-orange	octah.(*mer*)	2.6 – 2.8	[386,387,403–405]
$[TcCl_3(Me_2P)_3]^0$	yellow-orange	octah.(*mer*)		[406]
$[TcBr_3(Me_2PhP)_3]^0$	red	octah.(*mer*)	2.8	[387]
$[TcCl_3(Et_2PhP)_3]^0$	orange	octah.(*mer*)	2.8	[387,407]
$[TcBr_3(Et_2PhP)_3]^0$	red	octah.(*mer*)	2.8	[387]
$[TcCl_2(depe)_2]^+$	orange	–	–	[397]

Table 12.14.A Continued.

Complex	Color	Geometry (Configuration)	Magnetic Moment μ_{eff} [B.M.]	References
$[TcBr_2(depe)_2]^+$	rose-red	–	–	[397]
$[TcCl_2(dppb)_2]^+$	red	–	–	[397]
$[TcCl_2(dppv)_2]^-$	orange-red	–	–	[397]
$[Tc(NCS)_2(dppe)_2]^+$	blue	–		[397]
$[TcCl_3(PPh_3)_3(DMF)]^o$	red	octah.(*mer*)	3.1	[408]
$[TcCl_3(PPh_3)_2CO]^o$	red	octah.(*mer*)	–	[409]
$[TcCl_3(PPh_3)_2(MeCN)]^o$	orange	–	–	[409,410]
$[TcCl_3\{P(C_6H_4Me\text{-}3)_3\}_2(MeCN)]^o$	red	octah.(*mer*)	–	[410]
$[TcCl_2\{C_6H_5P(OC_2H_5)_2\}_4]^+$	red	octah.(*trans*)	2.7	[411]
$[TcCl_2(diars)_2]^+$	orange-red	octah.(*trans*)	2.7	[412–414]
$[TcBr_2(diars)_2]^+$	red	–	3.2	[412, 415]
$[TcI_2(diars)_2]^+$	black	–	3.4	[412]

Trans-$[TcCl_2(dmpe)_2]^+$ was prepared by treating a slurry of $[TcCl_2(dmpe)_2]^o$ in toluene with Cl_2 gas. To prepare *trans*-$[TcBr_2(dmpe)_2]^+$ the corresponding Tc(II) compound was dissolved in toluene and, after addition of HBr, the complex was oxidized with air. Orange crystals of $[TcCl_2(dmpe)_2][F_3CSO_3]$ adopt the monoclinic space group $P2_1/c$, with a=8.076(2), b=24.401(4), c=13.435(4) Å, β=96.61(2)° and Z=4. The structure of the $[TcCl_2(dmpe)_2]^+$ cation shows the *trans* octahedral geometry. The P atoms of the two bidentate dmpe ligands occupy four equatorial coordination sites with the two *trans* Cl atoms completing the octahedral coordination. The mean Tc–Cl bond distance is 2.324 Å and the mean Tc–P distance 2.436(5) Å [239]. $[TcCl_2(dmpe)_2]^+$ and $[TcBr_2(dmpe)_2]^+$ exhibit characteristic, well defined, intense charge-transfer bands in the visible region at 21739 and 20121 cm^{-1} and show a reversible Tc(III)/Tc(II) redox couple in DMF at –232 mV and –99 mV *vs* Ag/AgCl, respectively [397].

Trans-$[TcCl_2(dppe)_2]^+$ was synthesized by dissolving NH_4TcO_4 in DMF, which was 0.1 M in NH_4Cl, and adding a great excess of dppe. TcO_4^- is reduced by the ligand. *Trans*-$[TcBr_2(dppe)_2]^+$ was obtained from $[TcBr_2(dppe)_2]^o$ by using the procedure for the preparation of $[TcBr_2(dmpe)_2]^+$. $[TcBr_2(dppe)_2][BF_4]$ crystallizes in the trigonal space group $P\bar{3}$ with a=20.926(5), c=11.178(2) Å, and Z=3. The Tc(III) center is six-coordinate with an approximately octahedral coordination geometry. The donor phosphorus atoms occupy the four equatorial coordination sites, while the two bromine atoms are located in the *trans* axial positions. The Tc–Br bond distance is 2.440(1) Å, the Tc–P distances are 2.488(1) and 2.513(1) Å. The P–Tc–P angle is 80.8(1)°. The charge-transfer absorptions for $[TcCl_2(dppe)_2]^+$ and $[TcBr_2(dppe)_2]^+$ appear in the VIS at 20833 and 19841 cm^{-1}, respectively. The reduction potentials for the Tc(III)/

Tc(II) redox couples in DMF are reported at –1 mV for $[TcCl_2(dppe)_2]^+$ and +103 mV for $[TcBr_2(dppe)_2]^-$ *vs* Ag/AgCl [397].

$[TcCl_3(Me_2PhP)_3]^\circ$ was synthesized by reacting NH_4TcO_4, Me_2PhP, and HCl in ethanol under reflux. The compound crystallizes in the monoclinic space group $P2_1/n$, with a=10.935(9), b=39.191(11), c=13.738(7) Å, β=107.33(7)°, and Z=8. The coordination around Tc is again distorted octahedral. The arrangement of the phosphine ligands is meridional. There is a noticeable *trans*-influence of the phosphine ligands on the Tc–Cl bonds [403]. Electroanalytical oxidation of $[TcCl_3(Me_2PhP)_3]^\circ$ in acetonitrile produces $[TcCl_4(Me_2PhP)_3]^\circ$ and $[TcCl_3(Me_2PhP)_3]^+$ [404] while the reduction yields species of Tc(II) and Tc(I) [405].

Reaction of $[TcOCl_4]^-$ with excess trimethylphosphine in refluxing acetonitrile yielded $[TcCl_3(Me_3P)_3]^\circ$ as a yellow-orange solid. Tc(III) is surrounded by a meridional arrangement of Me_3P and the three chlorines. The Tc–Cl distance of 2.440(1) Å for the chlorine *trans* to one phosphine is considerably lengthened compared to the other Tc–Cl bond distances. The coordination geometry of Tc(III) is distorted octahedral (406).

$[TcCl_3(PPh_3)_2(DMF)]^\circ \cdot 2PPh_3$ was synthesized by reacting NH_4TcO_4 with PPh_3 in DMF solution in the presence of HCl. The compound crystallizes in the monoclinic space group $P2_1/m$ with a=11.393(4), b=24.993(11), c=12.398(4) Å, β=106.98(3)°, and Z=2. The $[TcCl_3(PPh_3)_3]^\circ$ complex could not be prepared because the PPh_3 ligand is too bulky. The two PPh_3 ligands are located *trans* to each other and the three chlorine atoms are meridional. The mean Tc–P bond distance is 2.498 Å. DMF is coordinated through its oxygen atom with a Tc–O bond length of 2.115(12) Å [408].

$[TcCl_3(PPh_3)_2(CO)]^\circ$ was obtained by reaction of $[TcCl_3(PPh_3)_2(MeCN)]^\circ$ with carbon monoxide in toluene. CO cleanly replaces the acetonitrile. $[TcCl_3(PPh_3)_2(CO)]^\circ$ crystallizes in the monoclinic space group $C2/c$ with a=24.649(9), b=9.530(3), c=15.870(6) Å, β=116.40(3)°, and Z=4. The coordination geometry of the technetium atom is nearly octahedral. The structure of $[TcCl_3(PPh_3)_2(CO)]^\circ$ is similar to that of $[TcCl_3(PPh_3)_2(DMF)]^\circ$ mentioned before [408]. $[TcCl_3(PPh_3)_2(MeCN)]^\circ$ was synthesized by treating $[n\text{-}Bu_4N][TcOCl_4]$ with PPh_3 in acetonitrile [409] or by reduction of $[TcCl_4(PPh_3)_2]^\circ$ with finely divided zinc metal in acetonitrile [410].

When $[TcCl_4\{P(C_6H_4Me\text{-}3)_3\}_2]^\circ$ is reduced with zinc metal in acetonitrile, the complex $[TcCl_3\{P(C_6H_4Me\text{-}3)_3\}_2(MeCN)]^\circ$ is formed which crystallizes in the triclinic space group $P\bar{1}$ with a=10.157(2), b=10.320(2), c=22.073(2) Å, α=87.27(2), β=86.66(1), γ=66.87(1)°, and Z=2. The compound is pseudo-octahedral with the $P(C_6H_4Me\text{-}3)_3$ groups in *trans*-position and the chlorine atoms are disposed meridionally. The structure confirms the presence of a nitrogen-bonded acetonitrile ligand by a Tc–N bond distance of 2.058(3) Å and by the linearity of the Tc–N–C linkage. The acetonitrile moiety lies sandwiched between two *m*-tolyl groups in a relatively protected environment [410].

The phosphonite containing complex cation $[TcCl_2\{C_6H_5P(OC_2H_5)_2\}_4]^+$ was obtained by refluxing solutions of $(NH_4)_2[TcCl_6]$ with excess diethylphenylphosphonite in ethanol. The perchlorate salt forms red crystals with the magnetic moment μ_{eff} = 2.7 B.M. at 306 K [411]. In addition, the red-violet $[TcBr_2\{C_6H_5P(OC_2H_5)_2\}_4]ClO_4$ and the green $[TcI_2\{C_6H_5P(OC_2H_5\}_4]I$ were synthesized in analogous procedures and

showed the magnetic moments μ_{eff} of 2.5 and 2.3 B.M., respectively. The Tc–Cl, Tc–Br, and Tc–I stretching frequencies were found in the IR at 346, 275, and 237–222 cm^{-1}, respectively [416].

In early studies of technetium chemistry the halogeno-diarsine complex compounds of Tc(III) $[TcCl_2(diars)_2]Cl$, $[TcBr_2(diars)_2]Br$, and $[TcI_2(diars_2]I \cdot I_2$ were prepared according to the reactions:

$$K_2[TcCl_6] \xrightarrow[aq.alcoholic\ HCl]{excess\ arsine} [TcCl_2(diars)_2]\ Cl \xrightarrow[alcohol]{LiBr}$$

$$[TcBr_2(diars)_2]Br \xrightarrow[alcohol]{LiI \cdot I2} [TcI_2(diars)_2]I \cdot I_2$$

The complex salts were identified by magnetic moments, VIS/UV-spectra, and conductivity measurements [412]. *Trans*-$[TcCl_2(diars)_2]Cl$ crystallizes in the monoclinic space group $P2_1/c$ with a=9.354(5), b=9.662(2), c=15.341(4) Å, β=98.75(6)°, and Z=2. The *trans*-octahedral coordination geometry of $[TcCl_2(diars)_2]^+$ is typical for $[MX_2(diars)_2]^{n+}$ complexes. The mean Tc–As bond distance in $[TcCl_2(diars)_2]Cl$ is 2.509 Å, the Tc–Cl distance 2.329(1) Å. The As–Tc–Cl angles are nearly rectangular, while the As–Tc–As angle is only 82.4(1)° [413,414].

12.5.3 β-Diketonato- and carboxylato complexes

A pentane-2,4-dionato complex of Tc(III), containing triphenylphosphine and a chloride ligand, was obtained by refluxing pentane-2,4-dione with *trans*-$[TcCl_4(PPh_3)_2]^\circ$. The orange-red crystals of *trans*-$[TcCl(acac)_2(PPh_3)]^\circ$ adopt triclinic symmetry with the space group $P\bar{1}$. The unit cell parameters are a=13.152(8), b=15.042(10), c=15.532(13) Å, α=112.26(11), β=91.01(7), γ=104,70(9)°, and Z=4. The octahedral coordination geometry of Tc(III) is tetragonally elongated and approximates D_{4h} symmetry. The Tc–O bonds have an average length of 2.01(1) Å; the Tc–Cl and Tc–P bond distances are 2.42(1) and 2.46(1) Å, respectively. The array of the acac oxygen atoms is quasi-planar. The bond angles about Tc(III) differ slightly from 90°. The Cl–Tc–P angle is 174.4(1)°. The Tc atom is displaced from the basal TcO_4 ring by only 0.04 Å toward the phosphine ligand. There are two crystallographically independent *trans*-$[TcCl(acac)_2(PPh_3)]^\circ$ molecules which differ chiefly in the folding angles of the acac ligands [417,418].

In addition, several other pentane-2,4-dionato-technetium complexes have been prepared and characterized. $[TcCl_2(acac)(PPh_3)_2]^\circ$ was synthesized by reacting $[TcCl_4(PPh_3)_2]^\circ$ with pentane-2,4-dione under nitrogen. After refluxing for 1 hr, red crystals were separated. Red-violet $[TcBr_2(acac)(PPh_3)_2]^\circ$ was obtained under similar conditions, but shorter reaction time, starting with $[TcBr_4(PPh_3)_2]^\circ$. $[TcCl_2(acac)(PPh_3)_2]^\circ$ and the bromine analogue are air-stable and slightly soluble in benzene. The magnetic moments of μ_{eff} = 3.1–3.3 B.M. are somewhat higher than expected for two unpaired electrons. Orange crystals of $[TcBr(acac)_2(PPh_3)]^\circ$ were obtained by heating $[TcBr_2(acac)(PPh_3)_2]^\circ$ under reflux in anhydrous pentane-2,4-dione for 10 h. $[TcCl(acac)_2(PPh_3)]^\circ$ and $[TcBr(acac)_2(PPh_3)]^\circ$ are soluble in polar solvents. Their magnet-

ic moments are μ_{eff} = 2.7 and 2.8 B.M., respectively [365]. By increasing the time of the reaction between $[TcCl_4(PPh_3)_2]^\circ$ and anhydrous pentane-2,4-dione to 18 h, dark violet crystals of $[Tc(acac)_3]^\circ$ were produced, which are soluble in polar organic solvents. The magnetic moment μ_{eff} was found to be 2.7 B.M. VIS/UV and IR data are reported for the complexes described [365]. $[Tc(acac)_3]^\circ$ may also be synthesized by reacting pentane-2,4-dione in aqueous alcoholic solution with TcO_4^- which is reduced with dithionite [364]. $[Tc(acac)_3]^\circ$ crystallizes in the monoclinic space group $P2_1/c$ with a=14.050(3), b=7.497(2), c=16.509(3) Å, β=99.02(2)°, and Z=4. The coordination geometry of the oxygen atoms around Tc(III) is almost a regular octahedron (Fig. 12.63.A). The mean Tc–O bond distance is 2.025 Å and the O–Tc–O angles are close to 90 and 180°, respectively [419].

$[Tc(acac)_3]^\circ$ undergoes ligand exchange in acetylacetone (Hacac):

$$[Tc(acac^*)_3]^\circ + Hacac \leftrightarrow [Tc(acac)_3]^\circ + Hacac^*$$

The first-order exchange reaction was followed by the ^{14}C labeling method using $[Tc(acac\{2\text{-}^{14}C\})_3]^\circ$. The exchange rate R is expressed by

$$R = k[\text{complex}] \; (k = 2.1 \cdot 10^{-4}\ s^{-1} \text{ at } 141\ ^\circ C),$$

when the complex concentration varies between 3 and 7 mM and the concentration of acetylacetone is 9.7 M. The lability of $[Tc(acac)_3]^\circ$ was found to be very close to that of $[Cr(acac)_3]^\circ$ [420]. Furthermore, the base hydrolysis of $[Tc(acac)_3]^\circ$ was studied spectrophotometrically in 0.1–1 M NaOH at temperatures ranging from 25 to 53.5 °C [421].

In addition to tris(pentane-2,4-dionato)technetium(III), the analogous complexes with hexane-2,4-dione, heptane-2,4-dione, heptane-3,5-dione, and octane-3,5-dione were synthesized after reduction of TcO_4^- with dithionite, identified by FAB mass spectrometry, and characterized by VIS/UV and IR spectrophotometry. The hexane-

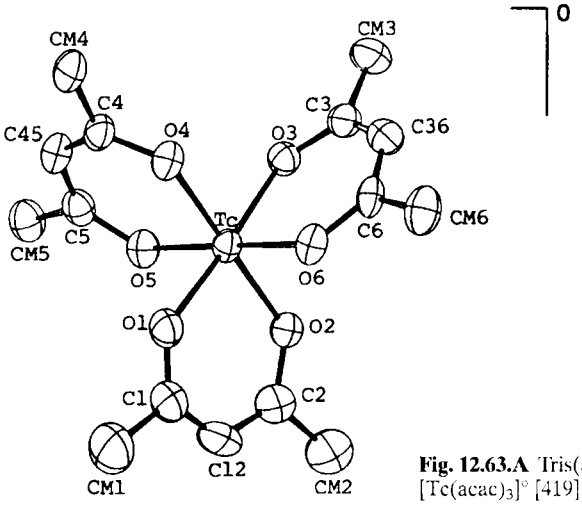

Fig. 12.63.A Tris(acetylacetonato)technetium(III), $[Tc(acac)_3]^\circ$ [419].

2,4-dionato complex crystallizes in the monoclinic space group $P2_1/c$, isostructurally with tris(pentane-2,4-dionato)technetium(III) [422].

Tris(dipivaloylmethanato)technetium(III) (dipivaloyl methane = 2,2,6,6-tetramethyl-3,5-heptanedione) was obtained by refluxing a mixture of dipivaloylmethane, $(NH_4)_2[TcCl_6]$, sodium methoxide and zinc powder in methanol. The red solid is readily oxidized at $E_{1/2}$ = + 0.12 V *vs* SCE to the cationic Tc(IV) complex. Tris(trifluoroacetylacetonato)technetium(III) (trifluoroacetylacetone: CF_3-CO-CH_2-CO-CH_3) and tris(hexafluoroacetylacetonato)technetium(III) (hexafluoroacetylacetone: CF_3-CO-CH_2-CO-CF_3) were prepared by reaction of the ligands with NH_4TcO_4 in refluxing ethanol and reduction with dithionite. These complexes are much more difficult to oxidize [423].

$[Tc(acac)_3]$ reacts with acetonitrile in the presence of $HClO_4$ to yield the cation $[Tc(acac)_2(MeCN)_2]^+$. $[Tc(acac)_2(MeCN)_2]ClO_4$ forms deep yellow crystals [424]. The acetonitrile ligands are easily substituted by benzoylacetone (Hbza), dipivaloylmethane (Hdpm) or dibenzoylmethane (Hdbm) leading to the neutral complexes $[Tc(acac)_2(bza)]^\circ$, $[Tc(acac)_2(dpm)]^\circ$, and $[Tc(acac)_2(dbm)]^\circ$, respectively. These substitution reactions offer convenient routes for the preparation of mixed ligand β-diketonatotechnetium(III) compounds [425].

Some monothio-β-diketonato complexes of Tc(III) have been synthesized. When monothiodibenzoylmethane (Htbm) is refluxed in methanol with hexakis(thioureato)-technetium(III) chloride, dark blue crystals of tris(monothiodibenzoylmethanato)-technetium(III), $[Tc(tbm)_3]^\circ$, are obtained [426]. The compound crystallizes in the monoclinic space group $P2_1/n$ with a=21.638(6), b=17.520(5), c=10.188(4) Å, β=100.24(5)°, and Z=4. The coordination geometry of Tc(III) is essentially octahedral with a slightly trigonal distortion. Within the six-membered $TcSOC_3$ rings the Tc–S distances, ranging between 2.32 and 2.34 Å, are almost equal, while the Tc–O bond distances vary between 2.01 and 2.08 Å. The O–Tc–O, S–Tc–S, and O–Tc–S angles show only small deviations from 90 or 180°. Hexakis(thioureato)technetium(III) also reacts with p-bromobenzoyl-thiobenzoylmethane, thiobenzoylacetone, thiothenoyltrifluoroacetone or 1-phenyl-3-methyl-4-benzoyl-5-thione to yield the corresponding monothio-β-diketonato complexes of Tc(III). The dark colored compounds are quite lipophilic and soluble in acetone or diethyl ether. They were identified by VIS/UV, IR, ^{1}H NMR, and mass spectrometry [427].

The mixed-ligand cationic complex Tc(III)-N,N′-ethylene-bis-(acetylacetonethioiminato)-bis-(triphenylphosphine) $[Tc(sacac)_2en(PPh_3)_2]Cl$ was prepared by reaction of $[Tc^VO(H_2O)(sacac)_2en]Cl$ with PPh_3 in methanol:

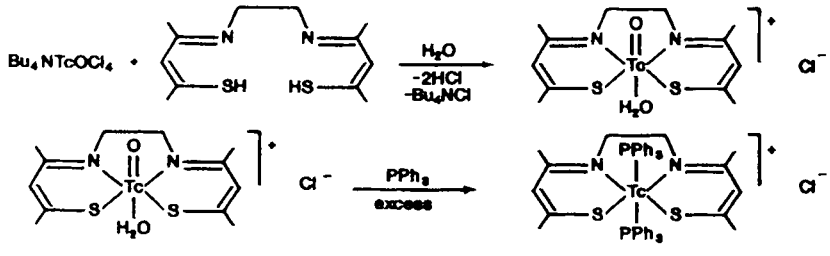

$[Tc(sacac)_2en(PPh_3)_2]^+$ was precipitated as the olive-green hexafluorophosphate and characterized spectroscopically [428].

Only a few carboxylato complexes of Tc(III) are known. H_4edta and H_3hedta {N-(2-hydroxymethyl)ethylenediamine-N,N′,N′-triacetic acid} complexes were synthesized by ligand substitution reactions of $[Tc(tu)_6]^{3+}$ with edta and hedta, however, none of the complexes were identified unambiguously [429,430].

NH_4TcO_4 reacts with 3-(diphenylphosphino)propionic acid in refluxing ethanol to form the yellow compound $[Tc(O_2CCH_2CH_2PPh_2)_3]^\circ \cdot 2DMSO$ after recrystallization from DMSO. It crystallizes in the monoclinic space group $P2_1/n$ with a=21.718(10), b=12.954(6), c=18.038(9) Å, β=106.59(4)°, and Z=4. The coordination environment about Tc(III) is a distorted octahedron. The three ligands are in meridional arrangement. There are two pairs of like-donor atoms *trans* to one another, leaving the remaining phosphorus atom *trans* to an oxygen atom. The bite angles around Tc are 85.4, 90.1, and 86.6°. The Tc–P bond distances range between 2.393(2) and 2.479(2) Å. In addition, phosphinocarboxylate complexes of Tc(III) were synthesized with 2-(diphenylphosphino)benzoic acid, (diphenylphosphino)acetic adic, and 3-(diethylphosphino)propionic acid. Cyclic voltammograms of the compounds are dominated by reversible Tc(III)/ Tc(II) couples [431].

12.5.4 Complexes containing nitrogen heterocycles, dioximes, Schiff bases, diazenido groups, and other nitrogen ligands

Red-orange trichlorotris(pyridine)technetium(III), $[TcCl_3(py)_3]^\circ$, and the corresponding complexes formed with 4-methylpyridine (4-picoline), $[TcCl_3(pico)_3]^\circ$ (yellow-orange) and 3,5-dimethylpyridine (3,5-lutidine), $[TcCl_3(lut)_3]^\circ$ (dark orange) were prepared by reacting $[TcCl_4(PPh_3)_2]^\circ$ in pyridine, 4-methylpyridine, or 3,5-dimethylpyridine with excess triphenylphosphine as the reducing agent. The meridional geometry of the pyridine complexes is revealed by ^{1}H NMR spectra that are contact-shifted by paramagnetism [392]. $[TcCl_3(py)_3]^\circ$ and $[TcCl_3(pico)_3]^\circ$ may also be synthesized by reducing $[n\text{-}Bu_4N][TcOCl_4]$ in pyridine or 4-picoline with PPh_3 under reflux. The magnetic moments μ_{eff} of $[TcCl_3(py)_3]^\circ$ and $[TcCl_3(pico)_3]^\circ$ are 2.65 and 2.81 B.M., respectively. $[TcCl_3(pico)_3]^\circ$ crystallizes in the monoclinic space group $P2_1/c$ with a=13.328(2), b=8.902(1), c=18.019(4) Å, β=103.25(1)°, and Z=4. The mean Tc–N bond distance is 2.140 Å. The Tc–Cl bond distance of 2.460(2) Å for the chlorine *trans* to the nitrogen is considerably longer then the mutually *trans* Tc–Cl bonds of 2.320(1) and 2.340(1) Å. The Cl–Tc–Cl, N–Tc–N, and Cl–Tc–N angles deviate only slightly from 180 or 90°. $[TcCl_3(pico)(Me_2PhP)_2]^\circ$ crystallizes in the triclinic space group $P\bar{1}$ with a=12.35(1), b=13.890(5), c=7.949(3) Å, α=97.29(3), β=101.56(6), γ=71.14(6)°, and Z=2. Its structure is similar to that of $[TcCl_3(pico)_3]^\circ$. The Tc(III)/Tc(II) reduction potentials for *mer*-$[TcCl_3(pico)_3]^\circ$ and *mer*-$[TcCl_3(py)_3]^\circ$ in 0.1 M $[Et_4N]ClO_4$ in DMF are 600 and 660 mV *vs* NHE, respectively [432].

$[TcCl_2(py)_3(PPh_3)][PF_6]$ was obtained by reaction of $[TcCl_3(PPh_3)_2(CH_3CN)]^\circ$ with pyridine, dissolved in 1,2-dimethoxyethane, and precipitation of the $[PF_6]^-$ salt. The yellow compound crystallizes in the triclinic space group $P\bar{1}$ with a=12.677(4),

b=13.064(4), c=13.103(5) Å, α=110.14(3), β=101.12(3), γ=96.61° and Z=2. The *trans*-$[TcCl_2(py)_3(PPh_3)]^+$ cation has a slightly distorted octahedral geometry around Tc(III). The two *trans*-pyridine ligands are bent away from the bulky triphenylphosphine ligand, their N(1)–Tc–N(2) angle is 175.6(2)°. The pyridine *trans* to the phosphine exhibits a longer Tc–N(3) bond length of 2.218(5) Å than those of Tc-N(1) (2.166 Å) and Tc–N(2) (2.165 Å). Typical Tc–Cl and Tc–P bond distances of 2.33 and 2.47 Å, respectively, are observed [433].

The complex salts $[TcCl_2(bpy)(PMe_2Ph)_2][BPh_4]$, $[TcCl_2(phen)(PMe_2Ph)_2][BPh_4]$, and $[TcCl_2(bpy)(PEtPh_2)_2][SO_3CF_3$ were synthesized by reaction of *mer*-$[TcCl_3(PMe_2Ph)_3]^\circ$ or *mer*-$[TcCl_3(PEtPh_2)_3]^\circ$ with bpy or phen in refluxing ethanol. Dark violet *cis*(Cl),*trans*(P)-$[TcCl_2(bpy)(PMe_2Ph)_2][BPh_4]$ crystallizes in the triclinic space group $P\bar{1}$ with a=10.700(2), b=14.231(2), c=16.018(2) Å, α=95.80(1), β=97.58(1), γ=108.34(1)°, and Z=2. Tc(III) resides in a slightly distorted octahedral environment with two *cis* chlorine atoms, which are both *trans* to the two nitrogen atoms of bpy, and the two *trans* PMe_2Ph ligands (Fig. 12.64.A). Dark purple *cis*(Cl), *trans*(P)-$[TcCl_2(phen)(PMe_2Ph)_2][BPh_4]$ crystallizes in the same triclinic space group $P\bar{1}$ with a=10.668(2), b=14.064(2), c=16.529(2) Å, α=95.50(1), β=97.61(1), γ=108.67(1)°, and Z=2, while dark red/purple *cis*(Cl),*trans*(P)-$[TcCl_2(bpy)(PEtPh_2)_2][SO_3CF_3]$ adopts the orthorhombic space group $P2_12_12_1$ with a=16.399(2), b=21.869(5), c=11.102(2) Å, and Z=4. The structures of the latter cations are very similar to that of $[TcCl_2(bpy)(PMe_2Ph)_2]^+$ [434].

$[TcCl_3(bpy)(PPh_3)]^\circ$ was obtained by refluxing $[TcCl_4(PPh_3)_2]^\circ$ with excess bipyridine in acetonitrile. The green/purple complex crystallizes in the monoclinic space group $P2_1/n$ with a=10.980(2), b=24.336(5), c=10.172(2) Å, β=106.89(1)°, and Z=4. The compound has a slightly distorted octahedral coordination geometry with a *facial*

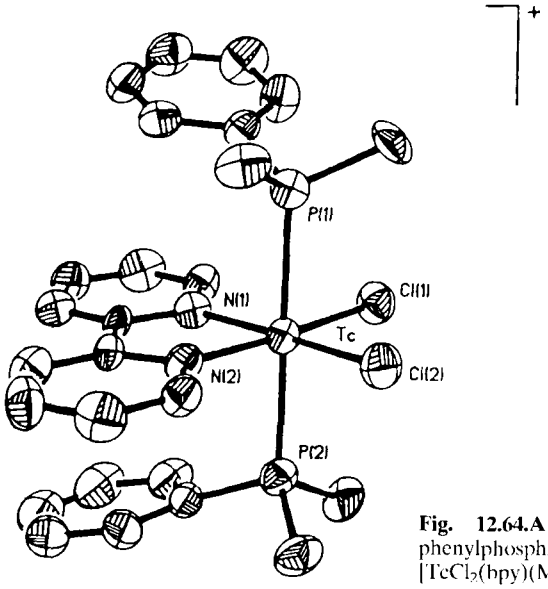

Fig. 12.64.A *Cis*-(dichloro)-bipyridyl-*trans*-bis(dimethylphenylphosphine)-technetium(III), $[TcCl_2(bpy)(Me_2PPh)_2]^+$ [434].

arrangement of the chloride ligands. Due to the *trans* influence of PPh_3, the Cl atom *trans* to the phosphorus atom has the longest Tc–Cl bond distance of 2.421(2) Å. The two Tc–N bond lengths are found to be unequal with 2.112(4) and 2.099(5) Å. The Tc–P distance is 2.465(2) Å, the axial Cl–Tc–P angle 174.51(6)°. In addition, the complexes $[TcCl_3(bpy)(PMe_2Ph)]^\circ$, $[TcCl_3(phen)(PMe_2Ph]^\circ$, $[TcCl_3(bpm)(PMe_2Ph)]^\circ$, and the cation $[TcCl_2(bpm)(PMe_2Ph)_2]^+$ were prepared and characterized [435].

The simple complex cation $[Tc(phen)_3]^{3+}$ was reported to be obtained by substitution reaction of $[Tc(tu)_6]^{3+}$ with 1,10-phenanthroline in aqueous solution at 60 °C and pH 3.2 under argon. $[Tc(phen)_3][PF_6]$ was precipitated as a dark red solid and purified by recrystallization in a water/methanol mixture. In neutral aqueous solution the compound shows a single strong absorption at 518 nm. Two broad ^1H NMR resonances at 7.3 and 8.3 ppm were observed. $[Tc(phen)_3]^{3+}$ appears to be stable in neutral aqueous solution [436].

An anionic, rose Tc(III)-adenosinediphosphate (ADP) complex was prepared by reduction of TcO_4^- with $S_2O_3^{2-}$ in the presence of excess ADP. According to the ^1H NMR spectrum the purine base of ADP is bonded to Tc(III). The complex showed good stability in aqueous solution in the pH range of 6–8 [437].

Some hydrotris(1-pyrazolyl)borato complexes of Tc(III) have been synthesized. $[TcCl_2\{HB(pyz)_3\}(PPh_3)]^\circ$ was obtained by reaction of $[TcOCl_2\{HB(pyz)_3\}]^\circ$ with triphenylphosphine in refluxing toluene. The dark yellow crystals revealed a magnetic moment μ_{eff} (308 K) = 2.9 B.M. In methylene chloride the reaction yielded the pale orange-yellow phosphineoxide compound $[TcCl_2\{HB(pyz)_3\}(Ph_3PO)]^\circ$ with μ_{eff} (308 K) = 3.0 B.M. This complex reacts in acetone with pyridine to from red-brown crystals of $[TcCl_2\{HB(pyz)_3\}(py)]$ with μ_{eff} (308 K) = 2.8 B.M. [438].

A unique series of seven-coordinate, monocapped boronic acid adducts of neutral technetium(III) tris(dioximato) compounds, so-called BATO complexes, has been described (Fig. 12.65.A). The complexes were prepared in ethanol by Sn^{2+} reduction of TcO_4^- or from $[TcOCl_4]^-$ or $[TcX_6]^{2-}$(X=Cl,Br) in the presence of vicinal dioximes and a boronic acid derivative. The color of the compounds is red to orange. $[TcBr(CDO)_3(BCH_3)]^\circ$ (CDO = cyclohexanedione dioximato) crystallizes in the trigonal space group $P3_1$ with a=11.056(6), c=17.321(9) Å, and Z=3, $[TcBr(DMG)_3(BC_4H_9]^\circ$ (DMG = dimethylglyoximato) in the monoclinic space group $P2_1/c$ with a=13.143(2), b=18.077(3), c=19.858(2) Å, β=100.76(1)°, and Z=8, and $[TcBr(CDO)_3(BC_4H_9)]$ in the monoclinic space group $C2/c$, with a=25.357(7), b=13.423(4), c=19.637(5) Å, β=124.97(2)°, and Z=8. In the structure of $[TcBr(DMG)_3(BC_4H_9)]^\circ$, which is representative of all of the BATO complexes, the heptacoordinate Tc(III) is surrounded by a hexadentate ligand and is also bonded to bromine, the seventh coordination site. The ligand consists of three bidentate dioximato groups joined through three covalent B–O bonds to a tetrahedral boron cap derived from butylboronic acid. The average Tc–N distance is 2.08 Å and the average bite angle for each dioximato group is 72°. The two dioximato groups flanking the bromine atom are spread away from the bromine by ~20° toward the third dioximato group. The three dioximato oxygens on the uncapped end of the molecule are intramolecularly hydrogen bonded to two bridging protons. The ^1H NMR resonances at 15 ppm are assigned to these bridging protons. The halogen can be readily exchanged for another halogen or for hydroxide [439–441].

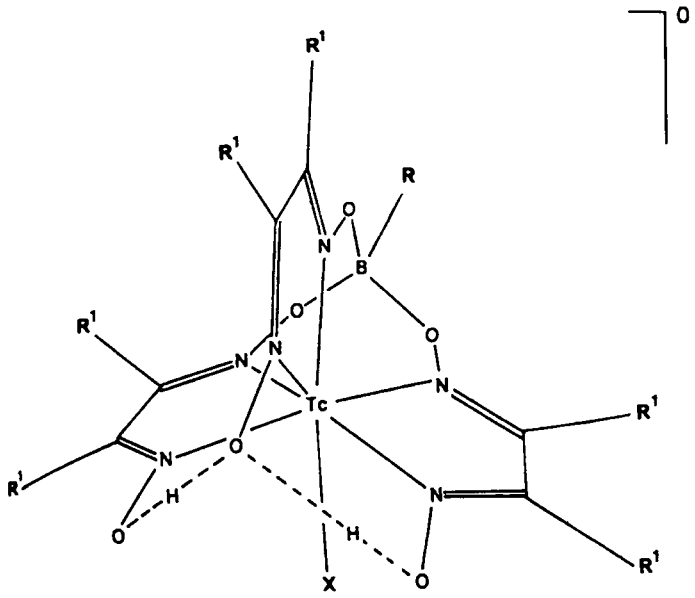

Fig. 12.65.A Halogeno-tris(dioximato)-alkylboratotechnetium(III), $[TcX(dioximato)_3BR]^\circ$, X=Cl or Br, R=$CH_3$ or n-C_4H_9, R^1=-CH_3-CH_2- or CH_3 [439,443].

The formation of the BATO complexes $[TcCl(dioximato)_3BR]^\circ$ according to the reaction:

$$TcO_4^- + 3\ \text{dioxime} + (OH)_2BR + 2\ SnCl_2 \xrightarrow[HCl]{EtOH} [TcCl(dioximato)_3BR]^\circ$$

proceeds through several intermediates, two of which are $[Tc(dioximato)_3(\mu\text{-}OH)SnCl_3]^\circ$ and $[TcCl(dioximato)_3]^\circ$. If the boronic acid is omitted, the major products isolated from the reaction mixture are seven-coordinate, tin-capped dioximato complexes $[Tc(dioximato)_3(\mu\text{-}OH)SnCl_3]^\circ$ [443]. The neutral compounds are stable to air and soluble in acetone and alcohol. The FAB mass spectra revealed peaks at a mass which indicates that the diamagnetic compounds contain Tc(III). These tin-capped complexes can be readily converted by treatment with HCl into a new class of uncapped Tc(III)dioxime compounds $[TcCl(dioximato)_3]^\circ$. The neutral, seven-coordinate $[TcCl(DMG)_3]^\circ$ crystallizes in the triclinic space group $P\bar{1}$ with a=9.617(1), b=12.135(3), c=9.244(2) Å, α=110.24(2), β=92.36(2), γ=88.92(2)°, and Z=2. The ligand geometry about Tc is similar to that in the BATO complexes. There are two equivalent dioxime ligands and one unique dioxime, which lie in a "paddle wheel" array about the Tc atom. The Tc–N bond distances for the two equivalent DMG ligands range from 2.120(4) to 2.131(3) Å. The Tc–N bond distances of the unique DMG are shorter, at 2.086(4) Å. The seventh position on Tc is occupied by the chlorine atom, which is *trans* to the unique dioxime. The Tc–Cl bond length is 2.415 Å. The dihedral angle between the planes of the two equivalent dioxime ligands is 129°, approaching the idealized trigonal prismatic value of 120° [443].

When $[TcCl_3(PPh_3)_2(CH_3CN)]^\circ$, dimethylglyoxime, and the boronic acid $(OH)_2BEt$ are refluxed in ethanol under N_2, the BATO complex $[TcCl(DMG)_3(BEt)]^\circ$ is formed together with the less lipophilic side product $[TcCl(DMG)_2(bdi)(BEt)]^\circ$ (bdi = butane-2,3-dione imine-oxime). The formation of the latter complex is increased if the reaction mixture is acidified with HCl, however, the mechanism of the formation of the imine-oxime ligand is not clear. The violet imine-oxime compound crystallizes in the monoclinic space group $P2_1/n$, with a=9.073(2), b=23.686(5), c=19.539(6) Å, β=93.77(2)°, and Z=8. The structure of the compound is very close to that of several BATO complexes. In the imine-oxime complex, one of the uncapped oximes of the BATOs is reduced to an imine and hydrogen bonding occurs only between the remaining pair of oximes, however, the coordination geometry appears to be relatively unaffected by the absence of one hydrogen bridge [444].

Various BATO complexes $[TcX(dioximato)_3BR]^\circ$(X = Cl^-, Br^-, OH ; R = OH, Me, Et, *n*-Bu, Bu^i, and Ph) and the uncapped tris-dioxime species $[TcCl(dioximato)_3]^\circ$ were studied by cyclic voltammetry, d.c. polarography, and controlled-potential coulometry in DMF. BATO complexes containing Cl or Br undergo an irreversible two-electron reduction at mercury, while for hydroxy BATOs two consecutive one-electron reductions are observed. The $[TcCl(dioximato)_3]^\circ$ complexes reveal similar reduction behavior. The two-electron peak potential for bromo-substituted BATOs is more positive than for chloro BATOs, while hydroxy-substituted BATOs are reduced ~1.0 V more negative. CDO complexes in general are reduced 60–90 mV more positive than the analogous DMG species. Changing the boronic acid cap has a relatively small effect on the reduction potential. The axial ligand (Cl, Br, OH) is lost upon reduction [445].

Several technetium(III) complexes containing both tetradentate Schiff-base and monodentate tertiary phosphine ligands have been synthesized. $[Tc\{(acac)_2en\}(PPh_3)_2]^+$ was obtained by reaction of $[TcOCl_4]$ with $H_2(acac)_2en$ and PPh_3 in methanol:

$$[TcOCl_4]^- + H_2(acac)_2en + 3PPh_3 \rightarrow [Tc\{(acac)_2en\}(PPh_3)_2]^- + OPPh_3 + 4Cl$$

The olive green hexafluorophosphate crystallizes in the triclinic space group $P\bar{1}$ with a=19.037(5), b=16.339(3), c=15.454(4) Å, α=95.37(2), β=96.47(2), γ=91.32(2)°, and Z=4. The coordination geometry around the technetium atom is approximately octahedral with the tetradentate Schiff-base ligand defining the equatorial plane and the two triphenylphosphine ligands occupying axial positions. The average Tc–P bond distance is 2.51(1) Å, and the mean Tc–N and Tc–O bond lengths are 2.06(2) and 2.02(1) Å, respectively. The P–Tc–P bond angle is 173.0°. In addition to $[Tc\{(acac)_2en\}(PPh_3)_2]^+$ the cationic complexes $[Tc\{(buac)_2en\}(PEt_2Ph)_2]^-$, $[Tc\{(bzac)_2en\}(PEtPh_2)_2]^+$, $[Tc\{(brac)_2en\}(PEtPh_2)_2]^+$, and $[Tc\{(sal)_2en\}(PEtPh_2)_2]^+$ have been prepared and identified, where $(buac)_2en$ = N,N′-ethylenebis(*tert*-butylacetoacetate iminato), $(bzac)_2en$ = N,N′-ethylenebis(benzoylacetone iminato), $(brac)_2en$ = N,N′-ethylenebis(3-bromoacetylacetone iminato), and $(sal)_2en$ = N,N′-ethylenebis (salicylidene iminato). The potentials of the Tc(III)/Tc(IV) and Tc(III)/Tc(II) redox

couples of these complexes are linearly related to the lowest energies of the Tc(III)-to-ligand charge-transfer bands [446,447].

Bidentate Schiff-base ligand neutral complexes containing a tertiary phosphine, $[TcCl(phsal)_2(PMe_2Ph]^\circ$ and $[TcCl(Mesal)_2)(PMe_2Ph)]^\circ$ (phsal = N-phenylsalicylidene iminato, Mesal = N-methylsalicylidene iminato) were obtained by reaction of $[TcOCl(phsal)_2]^\circ$ or $[TcOCl(Mesal)_2]^\circ$ with PMe_2Ph in boiling benzene. The oxotechnetium(V) compounds are reduced by PMe_2Ph. Both Tc(III) complexes are red, showing a magnetic moment of μ_{eff} = 2.5 B.M. $[TcCl(phsal)_2(PMe_2Ph)]^\circ$ crystallizes in the monoclinic space group $P2_1/c$ with a=9.500(4), b=10.596(4), c=31.000(9) Å, β=95.59(5)°, and Z=4. The coordination around Tc(III) is nearly octahedral. The two N-phenylsalicylidene iminato groups each act as bidentate O- and N-donor ligands. The chelate ligands are almost mutually orthogonal. The N atom of one ligand is located *trans* to the phosphorus atom. The P–Tc–N angle is 173.6(3)°. The bite angles O–Tc–N are 86.8 and 87.8° [393].

The three-dentate Schiff-base ligand N-(2-oxidophenyl)salicylidene iminato (ophsal), the bidentate quinoline-8-olato (quin), and the monodentate PEt_2Ph form the mixed ligand, neutral Tc(III) complex $[Tc(ophsal)(quin)(PEt_2Ph)]^\circ$ when the Tc(V) compound $[TcO(ophsal)(quin)]^\circ$ reacts in ethanol with PEt_2Ph. The dark red $[Tc(ophsal)(quin)(PEt_2Ph)]^\circ$ has a magnetic moment of μ_{eff}=2.6 B.M. and crystallizes in the triclinic space group $P\bar{1}$ with a=14.196(6), b=11.363(5), c=9.742(4) Å, α=68.04(3), β=101.09(3), γ=106.68(3)°, and Z=2. Tc(III) resides in an approximately octahedral coordination environment. The atoms O,N,O of the ophsal ligand occupy three equatorial sites, while the fourth equatorial site is occupied by the oxygen of the O,N bidentate quin ligand. The apical phosphine ligand is located *trans* to the quin nitrogen atom. The O–Tc–N bite angles are 76.3(9) and 78.9(6)° and the P–Tc–N(quin) angle is 174.1(5)°. The Tc–N(quin) distance of 2.15(2) Å is significantly longer than the average Tc–N distance of 2.07 Å. The complexes [Tc(sphsal)(quin)$(PPh_3)]^\circ$ and $[Tc(ophsal)(salen)(PMe_2Ph)]^\circ$ [sphsal = N-(2-sulphidophenyl)salicylidene iminato and salen = salicylidene iminato] were synthesized analogously to the above mentioned method [448].

Diazenido complexes have recently found much attention. $4\text{-}ClC_6H_4NHNH_2 \cdot HCl$ reacts with $[TcOCl_4]^-$ and PPh_3 in methanol to form a bright orange precipitate of $[TcCl(NNC_6H_4Cl\text{-}4)_2(PPh_3)_2]^\circ$. The oxidation state of Tc is +3, when the phenyldiazenido ligand is uninegatively charged [312]. The coordination sphere of Tc(III) contains mutually *trans* PPh_3 ligands in the axial positions of a trigonal bipyramid with the Cl atom and the *cis* aryldiazenido ligands occupying the equatorial positions. The Tc–N–N angles are essentially linear (Fig. 12.66.A). Refluxing $[TcOCl_4]^-$ with phenylhydrazine and dppe in methanol and adding $[PF_6]^-$ yields an orange precipitate of $[TcCl(NNPh)(dppe)_2][PF_6]$ that crystallizes in the monoclinic space group $C2/c$ with a=23.808(5), b=13.830(3), c=17.452(4) Å, β=92.53(2)°, and Z=4. The Tc atom in the complex cation $[TcCl(NNPh)(dppe)_2]^+$ has a slightly distorted octahedral geometry. The P–Tc–P bite angle is 81.5(1)°. The arrangement of the axial ligands Cl–Tc–N is nearly linear with 177.3(6)°. The Tc–N bond distance is 1.917(19) Å, the Tc–N–N angle 163(2)°. The diazenido ligand is thus singly bent. The angle compares reasonably with the two slightly different Tc–N–N bond angles of 166.1(6) and 172.1(7)° for

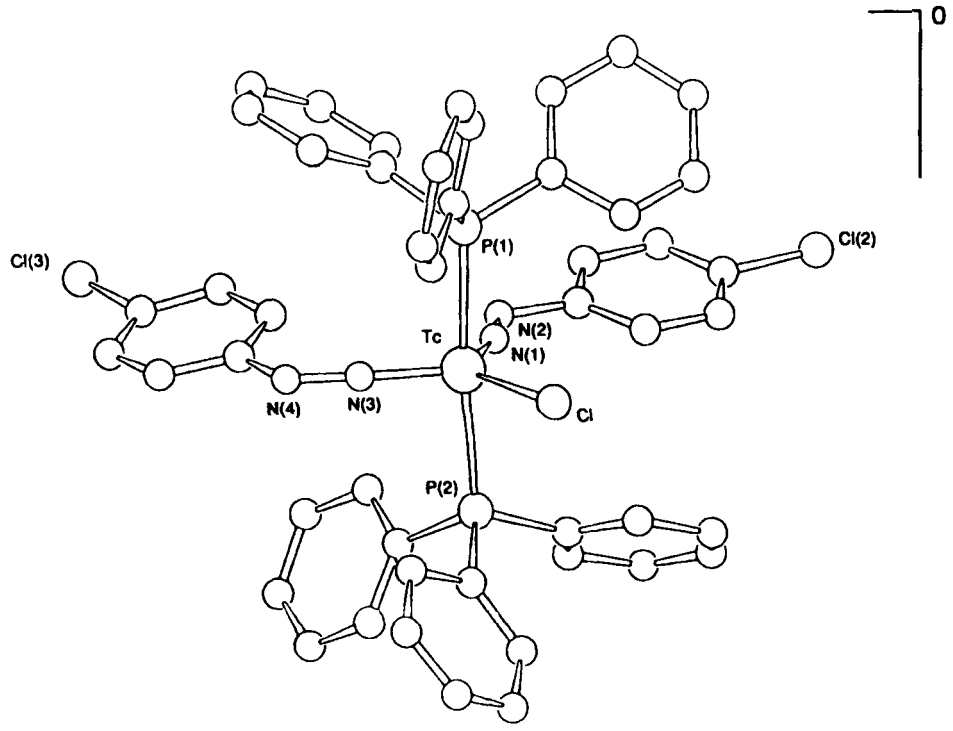

Fig. 12.66.A Chloro-bis(4-chlorophenyldiazenido)-*trans*-bis(triphenylphosphine)-technetium(III), $[TcCl(NNC_6H_4\text{-}4)_2(PPh_3)_2]^\circ$ [449].

the NNC_6H_4Cl-4 ligands in $[TcCl(NNC_6H_4Cl\text{-}4)_2(PPh_3)_2]^\circ$. Both diazenido complexes can also be synthesized by starting with NH_4TcO_4 + conc. HCl instead of $[NBu_4][TcOCl_4]$ [449, 450].

$[TcCl(NNC_6H_4Cl\text{-}4)_2(PPh_3)_2]^\circ$ reacts with dimethyldithiocarbamate in methanol with loss of Cl, one PPh_3 group and one diazenido ligand to yield $[Tc(NNC_6H_4Cl\text{-}4)\{(CH_3)_2NCS_2\}_2(PPh_3)]^\circ$.The dark orange compound crystallizes in the monoclinic space group *C2/c* with a=33.056(2), b=11.553(1), c=25.451(2) Å, β=131.065(5)°, and Z=8. Tc(III) resides in a distorted octahedral coordination sphere. One sulphur atom of one dithiocarbamate ligand and the phosphorus atom of the triphenylphosphine group occupy the axial positions with an angle S–Tc–P of 168.61(3)°. The equatorial sites are occupied by the $(NNC_6H_4Cl\text{-}4)$ ligand and three sulphur atoms of the dithiocarbamate groups. The Tc–N–N angle of the diazenido ligand is 178.6(4)° and the Tc–N bond distance is only 1.763(3) Å. As a result of the *trans* influence of the diazenido group one Tc–S bond distance of 2.537(1) Å is distinctly longer than the other Tc–S bond lengths ranging between 2.412(2) and 2.477(2) Å [451].

Another substitution reaction of $[TcCl(NNC_6H_4Cl\text{-}4)_2(PPh_3)_2]^\circ$ with dianionic, tetradentate N,N′-ethylene-bis(salicylideneimine) $\{H_2(sal)_2en\}$ in boiling methanol/toluene gives the neutral, dark green technetium(III) diazenido complex *cis*-$[Tc(NNC_6H_4Cl\text{-}4)\{(sal)_2en\}(PPh_3)]^\circ$. The compound crystallizes in the monoclinic space

group $P2_1/c$ with a=12.207(4), b=15.987(1), c=18.199(2) Å, β=100.16(4)°, and Z=4. The coordination geometry around Tc(III) is again distorted octahedral containing the diazenido ligand and PPh_3 in *cis* configuation. The diazenido ligand adopts the singly bent geometry with a Tc–N–N bond angle of 173.6(7)° and a Tc–N bond length of 1.764(8) Å. The Tc–P distance is 2.414(3) Å. The tetradentate $(sal)_2en$ ligand deviates significantly from planar geometry. In addition, some other diazenido complexes of Tc(III), such as $[TcCl(NNC_6H_4Cl\text{-}4)(hmpo)(PPh_3)_2]^\circ$ (Hhmpo = 3-hydroxy-2-methyl-4H-pyran-4-one) or $[TcCl(NNC_6H_4Cl\text{-}4)(bpy)_2]^+$ have been synthesized [452].

2-Hydrazinopyridine-hydrochloride reacts with $[Tc^{III}(MeCN)(PPh_3)_2Cl_3]^\circ$ in methanol under reflux to yield a pink precipitate of $[Tc^{III}(NNpy)(PPh_3)_2Cl_2]^\circ$. The chelating organohydrazide acts as a uninegative, unprotonated, bidentate ligand via the pyridine nitrogen. The additional binding of the pyridine nitrogen to Tc(III) to form the octahedral chelate complex may account for the diamagnetic behavior due to a formed π-system [453]. In a similar procedure $[Tc^{III}(MeCN)(PPh_3)_2Cl_3]^\circ$ reacts with 2-hydrazino-4-(trifluoromethyl)pyrimidine to form a peach-tan colored solid of $[Tc^{III}(NNC_4H_2N_2CF_3)(PPh_3)_2Cl_2]^\circ$ which crystallizes in the triclinic space group $P\bar{1}$ with a=11.9193(3), b=12.7026(3), c=14.1335(3) Å, α=109.9320(10), β=94.1250(10), γ=105.0490(10)°, and Z=2. The coordination geometry of Tc(III) is again a distorted octahedron with the chlorine atoms and the uninegative, bidentate diazenido ligand in the equatorial plane and the PPh_3 groups in axial *trans* position to each other. The mutiple bonding of the Tc–N(α) bond has a distance of only 1.810(8) Å while the bond length of Tc to the pyrimidine nitrogen is 2.181(7) Å. This compound is also diamagnetic [454].

The paramagnetic isodiazene complex $[Tc^{III}(N{=}NPh_2)(PPh_3)_2Cl_3]^\circ$ was synthesized by reaction of $[TcOCl_4]^-$ with excess Ph_2NNH_2 and PPh_3 in refluxing methanol. The isodiazene ligand $Ph_2N{=}N$ with an anionic metal bound α-nitrogen and a disubstituted, cationic β-nitrogen is formally neutral. In the reaction the organohydrazine precursor is oxidized by two electrons of Tc(V). The red crystals of $[Tc(N{=}NPh_2)(PPh_3)_2Cl_3]^\circ$ adopt the monoclinic space group $P2_1/n$ with a=10.1294(1), b=26.0792(3), c=18.8147(3) Å, β=98.814(1)°, and Z=4. The Tc–N absorption appeared in the IR in the 1100 cm^{-1} region. Tc(III) exhibits a distorted octahedral coordination geometry with the PPh_3 ligands in mutually *trans* sites. The remaining sites are occupied by the three chloride ligands and the linearly coordinated isodiazene ligand. The Tc–N bond length is 1.738(4) Å, and the N–N bond distance is 1.300(5) Å. Both bond distances indicate double bonds. The similar Tc–Cl bond lengths, ranging from 2.3985(12) to 2.4292(12) Å, suggest the absence of a *trans* effect exerted by the isodiazene ligand [455].

The tripodal tetradentate ligands 2-diphenyl-phosphino-N,N-bis(2-diphenylphosphinoethyl)ethaneamine(NP_3) and tris-2-diphenylphosphino-ethylphosphine (PP_3) react with $[TcCl_4(PPh_3)_2]^\circ$ in refluxing ethanol to form orange $[TcCl_2(NP_3)]^+$ and pale pink $[TcCl_2(PP_3)]^+$, respectively. The green cationic complex $[TcCl(NNC_6H_4Cl\text{-}4)(NP_3)]^+$ was obtained by reaction of TcO_4^-, $(H_2NNHC_6H_4Cl\text{-}4)\cdot HCl$, and NP_3 in refluxing methanol. The redox potentials of the complexes in DMF are reported [223].

Neutral and cationic Tc(III) complexes $[Tc(app)_3]^\circ$ and $[Tc(app)_2(Happ)]^+$ (Happ = 2-aminophenyldiphenylphosphine) were synthesized by reacting TcO_4^- with

$PPh_2(C_6H_4NH_2\text{-}2)$. When NH_4TcO_4 and Happ are refluxed in ethanol, a dark purple solid of tris-(2-amidophenyldiphenylphosphine)technetium(III) was formed, which is soluble in acetone and ether. Its magnetic moment at 293 K is μ_{eff} = 2.49 B.M. The reaction involves reduction to Tc(III) by the ligand which is oxidized to the phosphine oxide. In the presence of a non-coordinating acid, the blue cationic complex $[Tc(app)_2(Happ)]^+$ is produced showing a magnetic moment of μ_{eff} = 2.46 B.M. at 293 K. Between both complexes the equilibrium

$$[Tc(app)_3]^\circ + H^+ \leftrightarrow [Tc(app)_2(Happ)]^+$$

exists. {Bis(2-amidophenyl)diphenylphosphine}{(2-aminophenyl)diphenylphosphine} technetium(III) perchlorate, $[Tc(app)_2(Happ)]ClO_4$, crystallizes in the monoclinic space group $P2_1/n$ with a=11.009(2), b=19.361(3), c=24.473(3) Å, β=100.76(1)°, and Z=4. The coordination geometry about Tc(III) is distorted octahedral. The P atoms are arranged meridionally, two adopt the axial configuration, and one P atom together with the three N donor atoms represent the equatorial plane. The Tc–N(1) bond distance of 2.048(5) Å is significantly longer than the distances of Tc–N(2) (1.948 Å) and Tc–N(3) (1.979 Å) reflecting the weaker bonding to the completely protonated nitrogen N(1). The mean Tc–P bond length is 2.450 Å [456].

The unique cationic seven-coordinate complex $[Tc^{III}(H)NHC(NH_2)S(PMe_3)_4]^+$ containing, in addition to PMe_3, the unusual bidentate ligand $\{NHC(NH_2)S\}^-$ and a hydride ligand, was prepared by reaction of $[Tc(tu)_6][PF_6]_3$ and PMe_3 in methanol in a sealed tube heated to 75 °C for 12 h. The orange-yellow hexafluorophosphate crystallizes in the monoclinic space group Cc with a=9.305(2), b=16.726(2), c=19.951(3) Å, β=91.24(1)°, and Z=4. The mechanism of the complex formation is unknown. A band, characteristic of the Tc–H stretching mode, was observed in the IR at 1989 cm^{-1}. The hydride ion could be replaced by deuteride shifting the IR band to 1835 cm^{-1}. In the ^1H NMR spectrum the hydride resonance appeared at –8.9 ppm. IR and NMR measurements gave evidence for an anionic, asymmetrically bound thiourea ligand. The coordination geometry about the Tc center could not be fully described since the hydride ion was not located. If the hydride ligand is ignored then the geometry is a distorted octahedron. The structure does establish an unusual N,S bonding mode for the deprotonated thiourea ligand. The Tc–N bond distance of 2.190(13) Å is relatively long. An elongation is also found in the Tc–S bond length with 2.543(4) Å. The axial P–Tc–P angle is 166.3(2)° [406].

12.5.5 Thiolato, phosphinethiolato, dithiocarbamato, thioureato, xanthato, and other complexes with sulphur containing ligands

The methanethiolato complex cations $[Tc(SCH_3)_2(dmpe)_2]^-$ and $[Tc(SCH_3)_2(depe)_2]^+$ were prepared by reaction of the Tc(V) complexes $[TcO(OH)(dmpe)_2]^{2+}$ or $[TcO(OH)(depe)_2]^{2-}$ with excess $NaSCH_3$ in ethanol under exclusion of oxygen. Blue $[Tc(SCH_3)_2(dmpe)_2]CF_3SO_3$ crystallizes in the triclinic space group $P\bar{1}$ with a=7.9615(13), b=9.3019(7), c=18.5029(16) Å, α=88.093(7), β=89.686(11), γ=88.188(11)°,

and Z=2, blue $[Tc(SCH_3)_2(depe)_2][PF_6]$ in the monoclinic space group $P2_1/c$ with a=11.0724(13), b=11.2450(11), c=14.1331(14) Å, β=107.957(8)°, and Z=2. Both complex cations occur in *trans* geometry; the coordination geometry about Tc(III) is approximately octahedral. The most severe deviation from octahedral geometry arises from the bite angle of the bidentate phosphine ligand, which is 81.17(3)° for $[Tc(SCH_3)_2(depe)_2]^+$. In this complex S–Tc–S forms an angle of 84.9(3)° with the plane defined by the Tc and the phosphorus atoms. The average Tc–P length is 2.449 Å, the Tc–S bond distance 2.3025(5) Å. The reversible electrochemical reduction

$$[Tc^{III}(SCH_3)_2(depe)_2]^+ + e^- \leftrightarrow [Tc^{II}(SCH_3)_2(depe)_2]^0$$

studied by cyclic voltammetry, occurs in DMF at –0.554 V *vs* Ag/AgCl [457]. In addition, the complex cations *trans*-$[Tc(SR)_2(dmpe)_2]^+$ with R = C_2H_5, *n*-C_3H_7, $CH_2C_6H_5$, $CH_2C_6H_4$-4-OCH_3 were synthesized by routes analogous to that mentioned above. Their Tc(III)/Tc(II) couple varied from –0.513 V for R = benzyl to –0.622 V for R = *n*-propyl [458]. Similar mixed-ligand phosphine-thiol complex cations of Tc(III) were prepared by reaction of TcO_4^- with various ligands in acetic acid solutions [459,460].

The arenethiolato ligands SC_6H_4R-4, where R = H, Me, OMe, *tert*-Bu, or Cl, form the complex cations $[Tc(SC_6H_4R\text{-}4)_2(dmpe)_2]^+$, when *trans*-$[Tc^VO(OH)(dmpe)_2]^{2+}$ is both reduced and ligated by the action of excess arenethiol in ethanol under an argon atmosphere. *Cis*-$[Tc(SC_6H_5)_2(dmpe)_2][PF_6]$ crystallizes in the orthorhombic space group $P2_1nb$ with a=9.311(1), b=11.190(2), c=31.936(4) Å, and Z=4. Tc(III) resides again in a distorted octahedral environment. The most striking feature is the *cis* geometry for the arenethiolatotechnetium(III) complexes that is in contrast to the *trans* geometry observed for the alkyl- and benzyl-thiolato complexes. The *cis* S–Tc–S angle in $[Tc(SC_6H_5)_2(dmpe)_2]^+$ is 108.1(2)°, the average Tc–S distance is 2.29(2) Å. *Trans* to P the mean Tc–P bond length is 2.42(1) Å, *trans* to S the Tc–P distance is significantly larger with 2.49(3) Å. Cyclic voltammetry measurements in 0.5 M tetraethylammoniumperchlorate/DMF on this series of *cis* complexes reveal reversible Tc^{III}/Tc^{II} redox couples in the range of –0.19 to –0.38 V *vs* Ag/AgCl demonstrating that the S-arene complexes are easier to reduce than the S-alkyl complexes [461].

The mixed ligand cationic complex with dianionic 2-mercaptophenolate (meph) $[Tc^{III}(meph)(dmpe)_2]^+$ was obtained by reaction of $[Tc^{III}(dmpe)Cl_2]Cl$ with 2-mercaptophenol in ethanol. Addition of $Na[BPh_4]$ precipitated the red solid $[Tc^{III}(meph)(dmpe)_2][BPh_4]$, which crystallizes in the monoclinic space group $P2_1/c$ with a=12.525(1), b=9.961(1), c=33.789(6) Å, β=93.28(2)°, and Z=4. The coordination sphere of Tc(III) is a distorted octahedron (Fig. 12.67.A) with the atoms S,O,P(2),P(4) in the basal plane. The Tc–P distances, ranging between 2.356(3) and 2.403(2) Å, are shorter than in comparable Tc(III)dmpe complexes. The Tc–S and Tc–O distances are 2.352(3) and 2.095(4) Å, respectively [462].

Trans-$[Tc(SCH_3)_2(diars)_2][PF_6]$ was prepared by a method similar to that mentioned above using as starting material *trans*-$[Tc^VO(OH)(diars)_2][PF_6]_2$. The deep blue complex salt crystallizes in the monoclinic space group $C2/c$ with a=20.440(3), b=11.989(2), c=13.284(2) Å, β=98.24(1)°, and Z=4. The ligand arrangement around Tc(III) is roughly octahedral, with the primary distortion being the bite angle of

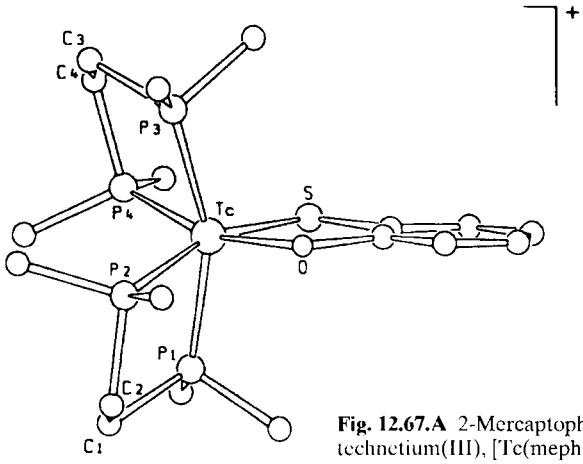

Fig. 12.67.A 2-Mercaptophenolato-bis(dimethylphosphineethane) technetium(III), $[Tc(meph)(dmpe)_2]^+$ [462].

82.39(2)° for As–Tc–As. The S–Tc–S axis is nearly orthogonal to the basal plane $TcAs_4$, making an angle of 87.5(4)° with it. The average Tc-As bond distance is 2.496 Å and the Tc–S distance 2.292(2) Å. The complex cations $[Tc(SCH_2C_6H_5)_2(diars)_2]^-$ and $[Tc(SC_6H_5)_2(diars)_2]^-$ have also been synthesized. When SR is an alkanethiolate or phenylmethanethiolate, the *trans* isomer is formed. Both *cis* and *trans* isomers are obtained for SR = benzenethiolate, although the *cis* isomer is more stable [463].

$[Tc^{V}O(OH)(dmpe)_2]^{2+}$ reacts in ethanol with toluene-3,4-dithiol (H_2tdt) to form $[Tc^{III}(tdt)(dmpe)_2]^+$, which was precipitated as the hexafluorophosphate salt. The dark orange $[Tc(tdt)(dmpe)_2][PF_6]$ crystallizes in the triclinic space group $P\bar{1}$ with a=9.1508, b=12.794(2), c=13.516(2) Å, α=93.94(1), β=95.24(1), γ=108.791(9)°, and Z=2. The ligand arrangement around the Tc atom is intermediate between octahedral and trigonal prismatic. 1,2-Dithiolate ligands are known for their ability to stabilize the relatively unusual trigonal-prismatic coordination geometry. The S–Tc–S bite angle of 84.49(4)° is larger than observed in most tris(1,2-dithiolato)metal complexes. The entire toluene-3,4-dithiolate ligand is almost planar and Tc is included in this plane. The average Tc–S bond length is 2.318(6) Å. The Tc–P bond distances average 2.396(3) Å *trans* to P and 2.407(1) Å *trans* to S. Spectropotentiostatic reduction of the complex in 0.5 M tetraethylammoniumperchlorate/DMF reveals the reversible Tc(III)/Tc(II) and Tc(II)/Tc(I) couples at –0.600 and –1.217 V, respectively, *vs* the Ag/AgCl electrode containing 3 moles NaCl/dm^3 [464].

The neutral, five-coordinate, diamagnetic complex $[Tc(tmbt)_3(MeCN)_2]°$, with Htmbt = 2,3,5,6-tetramethylbenzenethiol as a monodentate, sterically hindered ligand, was synthesized by reduction of $[TcCl_6]^{2-}$ with zinc dust in MeCN/MeOH in the presence of Htmbt. The blue compound crystallizes in the monoclinic space group $P2_1/n$ with a=11.227(1), b=15.784(1), c=20.411(1) Å, β=105.36(1)°, and Z=4. The donor set in the complex is a trigonal bipyramid with two inequivalent axial MeCN ligands (Fig. 12.68.A). Two of the bulky tetramethylbenzenethiolato groups are equivalent and on the same side of the equatorial plane containing the sulphur atoms. One tmbt ligand is below this plane. The N(1)–Tc–N(2) angle is almost linear and the

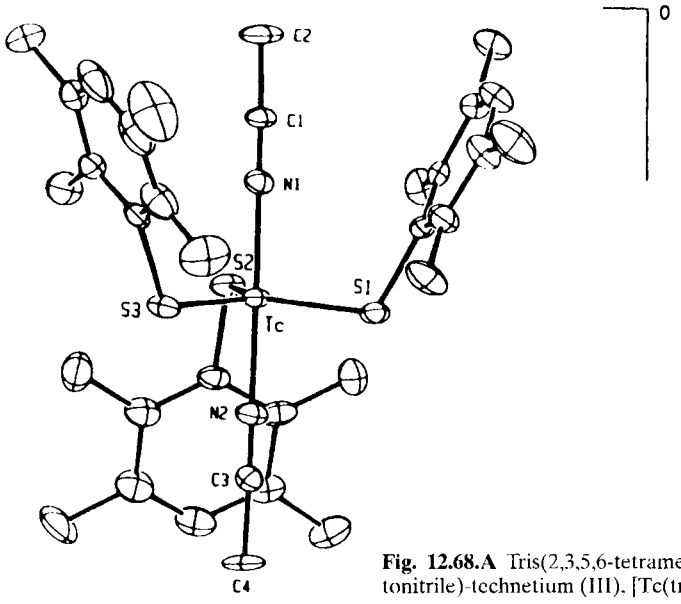

Fig. 12.68.A Tris(2,3,5,6-tetramethylbenzenethiolato)-bis(acetonitrile)-technetium (III), $[Tc(tmbt)_3(MeCN)_2]^\circ$ [114.465].

S–Tc–S angles are all close to 120°. The Tc–S(1), Tc–S(2), and Tc–S(3) bond distances are 2.255(3), 2.246(3), and 2.245(3) Å, respectively, while the Tc–N distances are identical with 2.04 Å [114, 465]. The acetonitrile ligands in $[Tc(tmbt)_3(MeCN)_2]^\circ$ or $[Tc(tibt)_3(MeCN)_2]^\circ$ (tibt = 2,4,6-triisopropyl-benzenethiolate) are readily displaced by carbon monoxide or isopropylnitrile (Pr^iNC) to yield $[Tc(SAr)_3(CO)_2]^\circ$ or $[Tc(SAr)_3(Pr^iNC)_2]^\circ$, respectively. One of the carbonyl ligands in $[Tc(SAr)_3(CO)_2]^\circ$ is labile, allowing the preparation of the complexes $[Tc(SAr)_3(CO)(MeCN)]^\circ$ and $[Tc(SAr)_3(CO)(py)]^\circ$. Orange $[Tc(tmbt)_3(CO)(MeCN)]^\circ$ crystallizes in the monclinic space group $P2_1/n$ with a=13.072(2), b=15.153(2), c=17.149(2) Å, β=98.46(1)°, and Z=4. The compound has essentially the same structure as $[Tc(tmbt)_3(MeCN)_2]^\circ$. Replacing MeCN in $[Tc(tmbt)_3(CO)(MeCN)]^\circ$ with pyridine results in $[Tc(tmbt)_3(CO)(py)]^\circ$, which crystallizes in the triclinic space group $P\bar{1}$. The cell parameters of the orange compound are a=10.773(1), b=18.018(1), c=9.034 Å, α=93.67(1)°, β=96.05(1)°, γ=87.08(1)°, and Z=2. Again, the compound has a slightly distorted trigonal bipyramidal geometry and shares the same disposition of the thiolate rings as the above mentioned two compounds. Pyridine sits on the side of the unique aryl ring and CO is found on the more sterically hindered side of the molecule. Trigonal bipyramidal compounds have a 3-fold rotation axis that causes the d orbitals to split as a, e', and e'', with e'' the lowest lying set of orbitals. Therefore, these $d^4(e'')^4$ systems are diamagnetic [465].

$[Tc(tmbt)_3(MeCN)_2]^\circ$ reacts with DMSO to yield the purple product $[Tc(tmbt)_3(MeCN)(DMSO)]^\circ$ which crystallizes in the monoclinic space group $P2_1/n$ with a=14.026(2), b=26.856(7), c=20.025(3) Å, β=104.20(1)°, and Z=8. The coordination geometry is again trigonal bipyramidal with the thiolate ligands bound in the equatorial plane and the acetonitrile and DMSO group sitting in the axial positions.

The arenethiolate rings show the familiar "two-up-one-down" orientation. $[Tc^{III}(tmbt)_3(MeCN)_2]^\circ$ readily reacts with pyridine N-oxide in refluxing ethanol to form an orange precipitate of $[Tc^{V}O(tmbt)_3(py)]^\circ$ by oxygen atom transfer. This complex can easily be reduced with triethylphosphine (PEt_3) in CH_2Cl_2 at ambient temperature by oxygen atom abstraction to restore the Tc(III)tris(thiolate) core in the form of the complex $[Tc(tmbt)_3(PEt_3)_2]^\circ$. The oxidative and reductive oxo-transfer reactions can be coupled to provide a catalytic cycle [182].

2,3,5,6-Tetramethylbenzenethiol (Htmbt) was reacted with $[n\text{-}Bu^t_4N][Tc^{II}(NO)Cl_4]$ in dichloromethane in the presence of the proton sponge 1,1,2,2,-tetramethylguanidine to yield the nitrosyl compound $[Tc(NO)(Cl)(tmbt)_3]^\circ$ containing Tc(III) and formally NO^+. Oxidation of Tc(II) to Tc(III) is facile with a limited amount of air. The robust, diamagnetic, red-orange compound crystallizes in the monoclinic space group *C2/c* with a=24.420(5), b=14.701(4), c=17.500(4) Å, β=93.50(2)°, and Z=8. The geometry about Tc(III) is trigonal bipyramidal with the chloride and nitrosyl group in the axial positions. The equatorial coordination sites are again occupied by the three thiolate sulphur atoms. The sterically hindered thiolate ligands adopt the less encumbered conformation showing the nitrosyl ligand directed toward the two thiolate aryl groups. This reflects the fact that the chloride ligand is larger than the nitrosyl ligand. The Tc–N–O bond angle is almost linear with 176.8(6)°. The Tc–N bond distance of 1.767(6) Å and the N–O bond distance of 1.150(7) Å reflect multiple bonding throughout the nitrosyl unit. The Tc–S and Tc–Cl bond lengths are typical of Tc(III) complexes [466].

The neutral complex tris(2-aminobenzenethio-lato(S,N)technetium(III), $[Tc(abt)_3]^\circ$ $(abt)^-$, was obtained in lime-green crystals by reduction of $[n\text{-}Bu_4N][Tc^{V}O(abt)_2]$ $(abt)^{2-}$ with excess 2-aminobenzenethiol in 0.2 M HCl. Cleavage of the Tc^{V}=O bond was achieved due to its apparent weakness, as demonstrated by the Tc^{V}=O bond distance of 1.73(2) Å that is substantially longer than the corresponding bond lengths typically found in square-pyramidal monooxotechnetium(V) complexes (Table 12.6.A). The Tc–S stretching frequency of $[Tc(abt)_3]^\circ$ was observed at 372 cm^{-1} and ν(Tc–N) occurred at 458 cm^{-1} [151].

Violet (3-oxapentane-1,5-dithiolato)(4-carbmethoxybenzenethiolato)(triphenylphosphine)technetium(III)

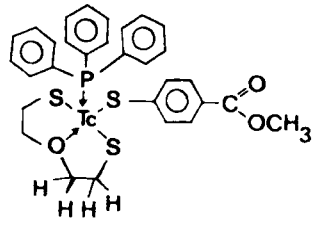

was synthesized by reduction of the corresponding oxotechnetium(V) complex with triphenylphosphine in a mixture of acetone and acetic acid. The abstraction of oxygen by PPh_3 was remarkably facile [467].

A cationic Tc(III) complex containing the tetradentatethioether 1,5,11,14-tetrathiaoctadecane (ttod) and two benzenethiolate ligands was prepared by reaction of

TcO_4^- with excess $SnCl_2$/HCl in a water/acetone mixture in the presence of ttod and benzenethiol. The purple complex was precipitated as $[PF_6]^-$ salt. $[Tc(ttod)(SC_6H_5)_2][PF_6]$, which is reported to be diamagnetic, crystallizes in the triclinic space group $P\bar{1}$ with a=8.913(6), b=13.685(3), c=15.260(6) Å, α=115.45(3), β=93.15(4), γ=91.58(4)°, and Z=2. Tc is coordinated by six sulphur atoms forming a distorted octahedron. The bond distances Tc–S(thioether) ranging from 2.418–2.465 Å are considerably longer than the Tc–S(thiolate) distances with 2.265 and 2.287 Å. The benzenethiolate ligands are in *cis*-orientation [468].

When TcO_4^- is reduced with triphenylphosphine in acidified ethanol/water in the presence of the tripodal, tetradentate ligand 2,2′,2″-nitrilotris(ethanethiol), $N(CH_2CH_2SH)_3$, a violet solid of $[Tc\{N(CH_2CH_2S)_3\}(PPh_3)]^\circ$ precipitates that crystallizes in the monoclinic space group $P2_1/c$ with a=8.906(2), b=25.804(6), c=11.061(4) Å, β=108.42(2)°, and Z=4. The coordination geometry of Tc(III) is trigonal bipyramidal (Fig. 12.69.A). The P–Tc–N angle of 178.7(2)° is almost linear and the S(1)–Tc–S(2), S(1)–Tc–S(3), and S(2)–Tc–S(3) angles are very near to 120°. The average Tc–S bond distance is 2.226 Å, the Tc–N distance 2.192(5) Å, and the Tc–P distance 2.325(2) Å [469,470].

A similar tetradentate "umbrella" ligand is tris(2-mercaptophenyl)phosphine. An alkaline solution of TcO_4^- in the presence of the ligand is reduced by dithionite to give a green intermediate that readily reacts with alkyl isocyanides. Using isopropyl isocyanide, the neutral, diamagnetic orange Tc(III) complex $[Tc\{P(2\text{-}C_6H_4S)_3\}(CNC_3H_7)]^\circ$ is obtained that crystallizes in the monoclinic space group $P2_1/c$ with a=10.3541(8), b=13.2274(6), c=16.437(1) Å, β=90.855(6)°, and Z=4. The coordination geometry of Tc(III) is again trigonal bipyramidal. The compound has virtually C_{3v} symmetry with the phenyl rings at right angles to the equatorial plane. The Tc atom lies only 0.172 Å out of the plane defined by the sulphur atoms. The P–Tc–S angles are close to 90°. The hemisphere opposite the phosphorus atom is occupied solely by the isonitrile ligand which is bound linearly. The P–Tc–C angle is almost linear with 176.1(3)°. The S–Tc–S angles are nearly 120°. $[Tc\{P(2\text{-}C_6H_4S)_3\}(CNC_3H_7)]^\circ$ reacts with excess isopropylisocyanide to yield $[Tc\{P(2\text{-}C_6H_4S)_3\}(CNC_3H_7)_2]^\circ$. The six-coordinate, blue, para-

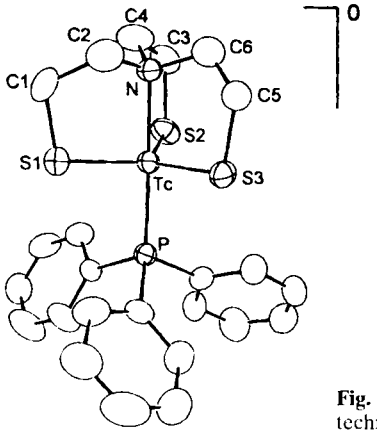

Fig. 12.69.A 2,2′,2″-Nitrilotris(ethanethiolato)-triphenylphosphine-technetium(III), $[Tc\{N(CH_2CH_2S)_3\}(PPh_3)]^\circ$ [393,394].

magnetic complex crystallizes in the orthohombic space group $Pna2_1$ with a=18.896(1), b=13.2815(8), c=10.3823(6) Å, and Z=4. Its structure is a very distorted octahedron. The angle between two sulphur atoms opens from 120 to 147.91(7)° to allow the coordination of a second isopropylisocyanide ligand [471]. Tris(2-mercaptophenylphosphine), $P(2\text{-}C_6H_4SH)_3$, reacts with $[Tc^{V}Cl_3(NPh)(PPh_3)_2]^{\circ}$ in methanol in the presence of a proton scavenger to give the neutral, reddish brown complex $[Tc^{III}\{P(2\text{-}C_6H_4S)_3\}(PPh_3)]^{\circ}$. The loss of the phenylimido unit is accompanied by a two-electron reduction [308].

$[Tc^{III}(2\text{-}Ph_2PC_6H_4S)_3]^{\circ}$ was obtained by reaction of 2-(diphenylphosphino)benzenethiol with $[TcCl_4(PPh_3)_2]$ in refluxing ethanol. The blue-green compound crystallizes in the monoclinic space group $P2_1/n$ with a=10.415(2), b=17.302(3), c=26.042(4) Å, β=100.91(1)°, and Z=4. Cyclic voltammetry in CH_2Cl_2 at a platinum electrode revealed a reversible reduction process for Tc(III)/Tc(II) at −0.581 V, and a reversible oxidation process for Tc(III)/Tc(IV) at +0.506 V *vs* the ferrocene/ferrocenium couple [220]. $[Tc^{III}(2\text{-}Ph_2PC_6H_4S)_3]^{\circ}$ may also be prepared by reduction of TcO_4^- with $2\text{-}Ph_2PC_6H_4SH$ and subsequent complexation. Magnetic susceptibility measurement yielded μ_{eff} = 3.0 B.M. X-ray crystal structure analysis shows Tc(III) residing in a severely distorted octahedral configuration. The Tc atom lies out of the mean equatorial plane by only 0.02 Å. The non-linearity of the axes P–Tc–S, P–Tc–P, and S–Tc–S is shown by the angles ranging from 158.8 to 166.8°. The structure of the analogous complex $[Tc^{III}(2\text{-}Ph_2PC_6H_4O)_3]^{\circ}$, containing the phenol instead of the thiophenol ligand, was shown to be very similar [472].

The neutral mixed ligand S,P-bidentate-thiolate complex $[Tc^{III}(SCH_2CH_2PPh_2)_2(SCH_2CH_2PPh_2O)]^{\circ}$ was synthesized by refluxing NH_4TcO_4 with liquid $HSCH_2CH_2PPh_2$ in ethanol under exclusion of oxygen. The phosphine-thiol function acts both as reducing and coordinating agent with the concomitant production of phosphine oxide. The five-coordinate, diamagnetic, red complex crystallizes in the triclinic space group $P\bar{1}$ with a=9.991(4), b=12.417(4), c=18.687(8) Å, α=73.37(3), β=76.88(3), γ=73.68(3)°, and Z=2. Tc(III) resides in a distorted trigonal bipyramid. The distortion is evidenced mainly by the axial P–Tc–P angle of 169.9°, while the equatorial plane given by the three S atoms is only slightly distorted: the maximum deviation of the S–Tc–S angles from 120° is 4.5°. In the coordinated bidentate ligands the two phenyl rings on the P atom are almost perpendicular to each other, while in the monodentate one the dihedral angle is 120.7°. The Tc–P distances are 2.379(3) and 2.392(3) Å, and the Tc–S distances range from 2.232(5) to 2.256(3) Å. In addition, the analogous lilac propanethiolato complex $[Tc(SCH_2CH_2CH_2PPh_2)_2(SCH_2CH_2CH_2PPh_2O)]^{\circ}$ was prepared. The five-coordinate complexes reveal a wide range of redox stability according to cyclic voltammetric measurements [473].

The complex cation $[Tc^{III}(SCP)_2(dmpe)_2]^{3+}$, where SCP is the novel zwitterionic ligand $^-SCH_2P^+(CH_3)_2(CH_2)_2P(S)(CH_3)_2$, is reported to be obtained by reaction of dithiocarbamates with excess dmpe in acid conditions in the presence of $[Tc^{V}O(OH)(dmpe)_2]^{2+}$. Dithiocarbamates are known to undergo an acid induced C–N cleavage to produce an amine and carbon disulphide. The carbon atom of CS_2 is susceptible to nucleophilic attack by a dmpe phosphorus lone pair yielding a positively charged phosphonium ion and a negatively charged thiol:

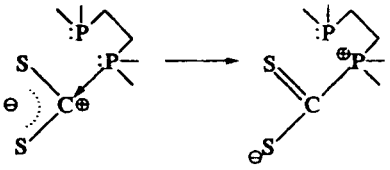

The final step in the formation of the SCP ligand is the transfer of the sulphido group to the terminal phosphorus atom and its oxidation to P(V). Tc(V) may be reduced to Tc(III) by excess dithiocarbamate or dmpe. The zwitterionic ligand SCP is formally neutral. The deep blue-black fluorophosphate complex salt $[Tc(SCP)_2(dmpe)_2][PF_6]_3$ precipitated from an ethanolic solution. Recrystallization from propylene carbonate ($C_4H_6O_3$) yielded $[Tc(SCP)_2(dmpe)_2][PF_6]_3 \cdot 2(C_4H_6O_3)$, which crystallizes in the monoclinic space group $P2_1/c$, with a=13.237(3), b=21.709(6), c=12.409(4) Å, β=112.77(2)°, and Z=2. The Tc atom is coordinated in a distorted *trans* octahedral geometry. The dmpe bite angle of 80.81(7)° is the largest distortion from an ideal octahedral surrounding. The Tc–S and average Tc–P bond lengths are 2.299(2) and 2.437(8) Å, respectively. $[Tc^{III}(SCP)_2(dmpe)_2]^{3+}$ is unusually easily reduced. The Tc(III)/Tc(II) reduction potential is –0.113 V *vs* Ag/AgCl (3 M NaCl) measured in 0.5 M $[NEt_4][ClO_4]$/DMF by cyclic voltammetry [474].

Several dithiocarbamato complexes of Tc(III) have been synthesized and identified. Reaction of $[TcCl_3(Me_2PhP)_3]^0$ with diethyldithiocarbamate (NaS_2CNEt_2) in refluxing acetone yielded dark brown crystals of $[Tc(S_2CNEt_2)_3(Me_2PhP)]^0$ which adopt the orthorhobic space group $P2_12_12_1$ with a=8.708(1), b=12.012(1), c=29.626(3) Å, and Z=4. Tc(III) exhibits a seven-coordinate environment in a distorted pentagonal bipyramid. Four S atoms of two dithiocarbamate ligands constitute the equatorial plane, while one S atom of the third dithiocarbamate ligand has an equatorial and the other S atom an axial position. The second axial position is represented by the P atom of the phosphine. The average Tc–S bond distance in the equatorial plane is 2.488 Å, while the axial Tc–S bond length of 2.520 Å is somewhat longer. The Tc–P bond distance of 2.330(3) Å is remarkably short. The axial angle P–Tc–S of 168.9(1)° demonstrates some deviation from linearity. The equatorial S–Tc–S bite angles are 67.8(1)° [475]. $[Tc(S_2CNEt_2)_3(Me_2PhP)]^0$ was found to be diamagnetic. It reacts with 1,2-dicyanoethylenedithiolate in acetone/EtOH in the presence of $[Ph_4P]^+$ to form the dark violet complex salt $[PPh_4][Tc^{III}\{S_2C_2(CN)_2\}_2(Me_2PhP)_2]$ [476].

Prior to the preparation of $[Tc(S_2CNEt_2)_3(Me_2PhP)]^0$ the carbonyl-dithiocarbamato)technetium(III) complex was synthesized and characterized. The structures of both compounds resemble each other closely. $[Tc(S_2CNEt_2)_3(CO)]^0$ was obtained by the reduction of NH_4TcO_4 with formamidinesulphinic acid in aqueous solution in the presence of $Na(S_2CNEt_2)$. Formamidinesulphinic acid, $NH_2(NH)CSO_2H$, was suggested to be a source of the carbonyl ligand after coordination of $NH_2(NH)CSO_2H$ to technetium. Orange-brown $[Tc(S_2CNEt_2)_3(CO)]^0$ crystallizes in the triclinic space group $P\bar{1}$ with a=9.510(1), b=9.976(1), c=14.637(3) Å, α=103.79(1), β=105.42(1), γ=72.52(1)°, and Z=2. Tc(III) resides again in a seven-coordinate, distorted pentagonal bipyramidal environment. Two of the S_2CNEt_2 ligands occupy equatorial positions, while the third spans an equatorial and an axial site. The remaining axial site is

occupied by the carbonyl group. The Tc–C–O angle is, at 178(1)°, almost linear. In the equatorial plane the Tc and four S atoms are nearly coplanar. The Tc=CO bond distance is 1.861(12) Å. The IR absorption at 1895 cm^{-1} was assigned to the carbonyl stretching frequency [477]. The analogous complexes $[Tc^{III}(S_2CNR_2)_3(CO)]^\circ$ where {R = Pr^i, *n*-Bu, Bu^i, R_2 = $-(CH_2)_5-$,$-(CH_2)_2-O-(CH_2)_2-$} were isolated and identified by UV, VIS, IR, and ^1H NMR spectroscopy [259].

Dibromo-bis(N,N-diethyldithiocarbamato)thionitrosyltechnetium(III), $[Tc(NS)(S_2CNEt_2)_2Br_2]^\circ$, was prepared by heating a mixture of $[Tc^VN(S_2CNEt_2)_2]^\circ$ and $SOBr_2$. The orange-brown complex crystallizes in the orthorhombic space group *Pnma* with *a*=14.864(7), *b*=15.857(7), *c*=8.938(4) Å, and *Z*=4. The coordination geometry about the Tc atom is distorted pentagonal bipyramidal (Fig. 12.70.A) with the thionitrosyl ligand and Br(1) in the axial positions. The equatorial atoms, comprising the four S atoms of the dithiocarbamato ligands and Br(2), are considerably distorted from planarity. The Tc atom is displaced by 0.061(1) Å from this mean plane towards the thionitrosyl ligand. The Tc–N≡S arrangement is essentially linear with 177.2(7)°. The Tc–N and N≡S distances of 1.754(9) and 1.504(9) Å, respectively, are similar to those observed in other thionitrosyl complexes. Also the Tc–S distances of 2.480(2) Å for Tc–S1 and 2.472(2) Å for Tc–S2 are within the range for Tc^{III}–S distances in seven-coordinate complexes. There is a small but significant difference in the Tc–Br bond lengths, with the Tc–Br(1) distance *trans* to the N≡S ligand of 2.595(1) Å and Tc–Br(2) *cis* to N≡S of 2.564(1) Å. The Br(1)–Tc–N(1) angle is linear, while Br(1)–Tc–Br(2), Br(1)–Tc–S(1), and Br(1)–Tc–S(2) are almost perpendicular as well as Br(2)–Tc–N(1) and S(1)–Tc–N(1). The IR spectrum showed an absorption at 1250 cm^{-1} assigned to ν(N≡S) [478]. The molecular structure of $[Tc^{III}(NS)(S_2CNEt_2)_2Cl_2]$ proved to be very similar, however, the crystal lattice was disordered and the structure of low accuracy [479].

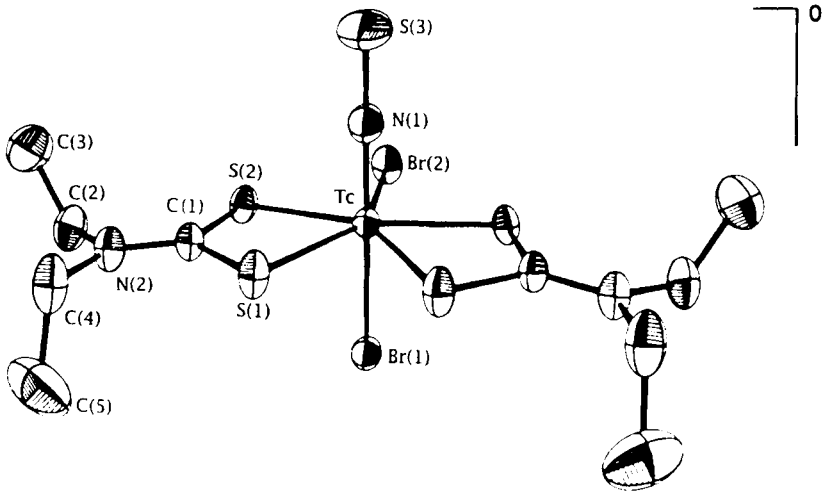

Fig. 12.70.A Dibromo-bis(N,N-diethyldithiocarbamato)-thionitrosyltechnetium(III), $[Tc(NS)(S_2CNEt_2)_2Br_2]^\circ$ [478].

Some complexes of Tc(III) with thiourea and its derivatives have been described. The hexakis(thiourea)technetium(III) cation $[Tc\{SC(NH_2)_2\}_6]^{3+}$ was obtained by reaction of thiourea with TcO_4^- in acid ethanol and isolated as the chloride or the tetrafluoroborate salt. The red-orange compounds are soluble in ethanol and methanol. Both complex salts have a magnetic moment of μ_{eff} = 2.7 B.M. at 308 K. $[Tc\{SC(NH_2)_2\}_6]Cl_3 \cdot 4H_2O$ crystallizes in the monoclinic space group *C2/c* with a=11.876(2), b=12.048(2), c=19.662(3) Å, β=95.32(1)°, and Z=4. The coordination geometry of Tc(III) is distorted octahedral. All S–Tc–S angles differ significantly from 90° in the range 4.2–9.2°. The Tc–S bond distances vary between 2.412 and 2.449 Å. The thiourea ligands are essentially planar. The structure is held together by an extensive hydrogen-bonding network. Because of the lability of the thiourea ligands, the complex is a very useful synthetic precursor in the lower valent technetium chemistry [480,481]. In addition to $[Tc\{SC(NH_2)_2\}_6]^{3+}$ the cation $[Tc\{SC(NH_2)_2\}_5Cl]^{2+}$ was obtained at increased HCl concentration [482].

N-methylthiourea (Metu) and N,N′-dimethylthiourea (Me_2tu) react in hydrochloric acid with TcO_4^- to form the cations $[Tc(Metu)_6]^{3+}$ and $[Tc(Me_2tu)_6]^{3+}$ that are precipitated as hexafluorophosphate salts. Red $[Tc(Metu)_6][PF_6]_3 \cdot H_2O$ crystallizes in the triclinic space group $P\bar{1}$ with a=6.754(3), b=11.737(8), c=13.217(7) Å, α=74.45(5), β=86.30(4), γ=86.39(5)°, and Z=1. The magnetic moment of the compound at 295 K is μ_{eff} = 2.9 B.M. The six methylthiourea ligands are S-bonded to Tc(III). The coordination in $[Tc(Metu)_6]^{3+}$ is distorted octahedral, similar to $[Tc(tu)_6]^{3+}$. The six Metu ligands display *cis* configuration, the methyl groups are oriented away from the Tc atom. The red $[Tc(Me_2tu)_6][PF_6]_3$ has the monoclinic space group $P2_1/c$ with a=13.306(13), b=20.943(15), c=17.082(13) Å, β=102.54(7)°, and Z=4 [483]. The magnetic moment at 308 K was reported to be μ_{eff} = 2.7 B.M. [115]. The coordination around the Tc(III) is again distorted octahedral with six S-bonded Me_2tu ligands. Important distortions are observed. The *cis* S–Tc–S angles vary from 80.9(1) to 99.6(1)°, while the *trans* angles are between 178.3(1) and 179.3(1)°. All six Me_2tu ligands display the *cis-trans* configuration with one methyl group oriented away from the Tc atom. This configuration corresponds to minimum repulsion [483].

Solvent extraction studies of $[Tc(tu)_6]^{3+}$, $[Tc(Metu)_6]^{3+}$, $[Tc(Me_2tu)_6]^{3+}$, and $[Tc(Et_2tu)_6]^{3+}$ with several pyrimidine derivatives indicate the occurrence of substitution reactions. $[Tc(Me_2tu)_6]^{3+}$ was shown to be the most sensitive complex for substitution with 4,6-dimethylpyrimidine-2-thione [484].

Neutral, seven-coordinate xanthate complexes of Tc(III) were synthesized by reaction of $[Bu_4N][TcOCl_4]$ with PPh_3 and ethyl-, isopropyl-, *n*-butyl-, or neopentylxanthate in ethanol or directly from the reaction of TcO_4^-, PPh_3, and xanthate. Red-brown technetium(III)-triphenylphosphine-tris(*n*-butyl-xanthate), $[Tc(PPh_3)(S_2COC_4H_9)_3]^0$, crystallizes in the rhombohedral space group *R3c(h)* (hexagonal axes), with a=15.437(4), c=53.49(1) Å, and Z=12. The coordination sphere about the Tc(III) consists of six sulphurs from three bidentate xanthate ligands and the phosphorus atom of the PPh_3 molecule. Tc is seven-coordinate with a capped octahedral geometry. Both technetium and phosphorus atoms sit on crystallographically defined three-fold axes. The Tc–S bond distances are identical, at 2.463(2) Å, and significantly longer than the Tc–S bonds in trigonal bipyramidal Tc(III)tris(thiolato) complexes.

The Tc–P bond distance is 2.381(2) Å. The ^{1}H NMR spectra show that the three-fold molecular symmetry is maintained in solution. The ν(C=S) vibration frequency appeared in the IR at 1235 cm^{-1} [485].

A pentagonal bipyramidal coordination geometry of Tc(III) was observed for the xanthate complex $[Tc(Me_2PhP)(S_2COEt)_3]^\circ$ that was prepared by refluxing $[TcCl_3(Me_2PhP)_3]^\circ$ with potassium ethylxanthate in THF. The dark red $[Tc(Me_2PhP)(S_2COEt)_3]^\circ$ crystallizes in the monoclinic space group $P2_1/c$ with a=18.44(5), b=9.2(1), c=15.36(6) Å, β=104.3(2)°, and Z=4. Fig. 12.71.A shows a plot of the structure. The axial angle P–Tc–S(1) is nearly linear with 174.5°. The equatorial S–Tc–S angles range between 68.6 and 76.3°. The atoms S(3), S(4), S(5), and S(6) are almost coplanar, while S(2) deviates from this plane by 0.946(1) Å because of the restricting bite angle of the xanthate ligand. The Tc–S bond distances vary between 2.44 and 2.49 Å. The Tc–P distance is 2.353(1) Å. The complex is diamagnetic. The C=S vibration was found at 1185 cm^{-1} in the IR [486].

$[TcCl_3(Me_2PhP)_3]^\circ$ reacts with ammonium dimethyldithiophosphate, $NH_4[SP(S)(OCH_3)_2]$, in refluxing acetone to yield the orange-red paramagnetic complex $[TcCl_2(Me_2PhP)_2\{SP(S)(OCH_3)_2\}]^\circ$ that crystallizes in the orthorhombic space group *Pbcn* with a=16.207(1), b=10.445(1), c=14.878(1), and Z=4. Tc(III) resides in a distorted octahedron with the axial chlorine ligands in *trans* position. The bond distances are in the expected range, Tc–S = 2.475(2), Tc–Cl = 2.347(1) and Tc–P = 2.416(1) Å. The angles Cl–Tc–Cl, S–Tc–S, and P–Tc–P are 173.04(4), 80.10(3), and 97.52(3)°, respectively. The P=S vibration was found at 770 cm^{-1} [486].

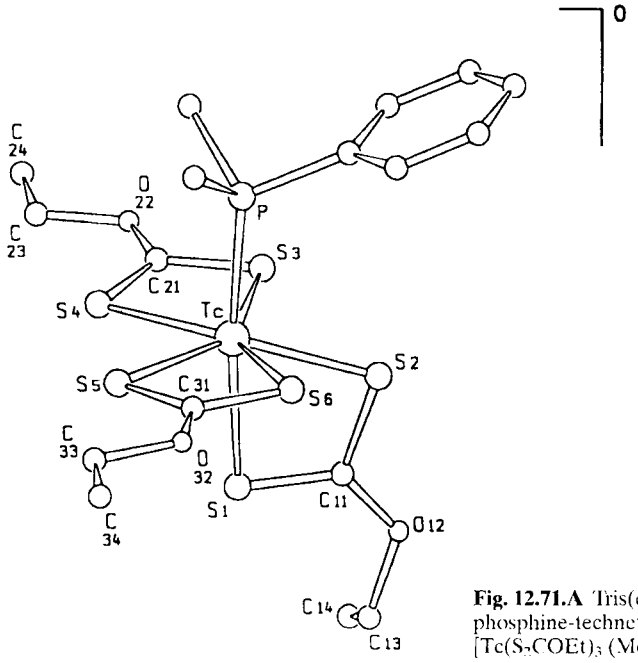

Fig. 12.71.A Tris(ethylxanthato)-dimethylphenylphosphine-technetium(III), $[Tc(S_2COEt)_3(Me_2PhP)]^\circ$ [486].

When $[TcOCl_4]^-$, PPh_3, and the monoanionic, bidentate ligand S-methyl-3-(2'-hydroxybenzylidene)dithiocarbazate (Hdtcb) are reacted in refluxing ethanol containing HCl, dark red crystals of the neutral Tc(III) complex $[TcCl_2(dtcb)(PPh_3)_2]^\circ$ are obtained that are recrystallized from dichloromethane. $[TcCl_2(dtcb)(PPh_3)_2] \cdot CH_2Cl_2$ crystallizes in the monoclinic space group $P2_1/n$ with a=14.504(6), b=16.281(8), c=19.752(11) Å, β=96.78(4)°, and Z=4. The complex is paramagnetic with μ_{eff} = 2.45 B.M. Tc(III) has a distorted octahedral coordination geometry formed by two Cl atoms, two P atoms, one N and the terminal S atom. The PPh_3 groups are in *trans* position to each other, the two Cl atoms in *cis* position. The phenolic oxygen remains protonated. The P–Tc–P angle is almost linear with 178.5(4)° [215].

12.5.6 Carbonyl and cyclopentadienyl complexes

The seven-coordinate, neutral complex carbonyltrichlorotris(dimethylphenylphosphine)technetium(III), $[TcCl_3(CO)(PMe_2Ph)_3]^\circ \cdot EtOH$, was synthesized by passing carbon monoxide through a boiling solution of *mer*-$[TcCl_3(PMe_2Ph)_3]^\circ$ in ethanol. The diamagnetic, pale yellow plates crystallize in the monoclinic space group $P2_1/c$ with a=11.732(9), b=11.807(9), c=23.588(12) Å, β=103.42(8)°, and Z=4. The molecular structure shows approximately C_{3v} symmetry. The coordination geometry of Tc(III) is a distorted capped octahedron. Tc is bonded to three phosphine ligands (capped face), three chlorine ligands, and to the CO group, which occupies the unique capping position (Fig. 12.72.A) The mean bond distances of Tc–CO, Tc–Cl, and Tc–P are 1.86(2), 2.48(1), and 2.44(1) Å, respectively. The average C–Tc–P, C–Tc–Cl, and P–Tc–P angles are 74.2, 126.6, and 112.9°, respectively, the axial angle Cl(3)–Tc–P(1) is

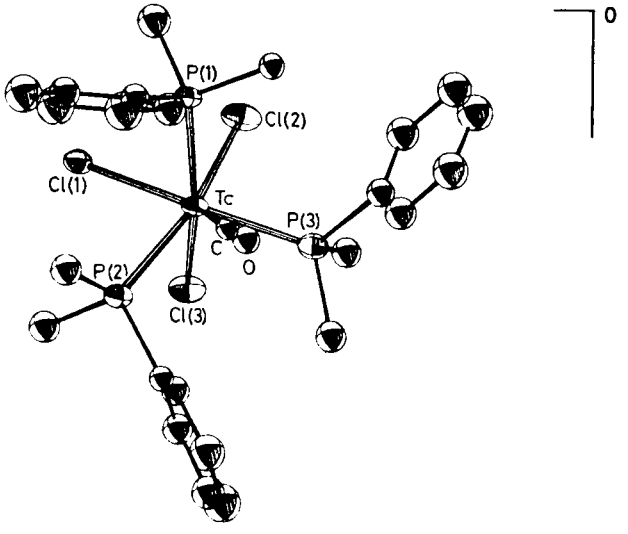

Fig. 12.72.A Carbonyltrichlorotris(dimethylphenylphosphine)technetium(III), $[Tc(CO)Cl_3(PMe_2Ph)_3]^\circ$ [487].

160.0(2)° and the Tc–C–O angle is 177.7(2)°. The compound is diamagnetic and has 18 valence electrons [487]. Another complex of Tc(III) containing a carbonyl group is $[Tc(S_2CNEt_2)_3(CO)]^+$ [477], which was already described in Sect. 12.5.5.

Some cyclopentadienyl compounds of Tc(III) have been synthesized. $TcCl_4$ was reacted with sodium cyclopentadienide and sodium borohydride at 50 °C in THF. By sublimation of the dry reaction mixture, extremely air sensitive, golden yellow crystals with a melting point of 155 °C were obtained. According to IR, ^1H NMR, tensimetric studies, and elemental analysis, the formation of the dimeric compound $[Tc(C_5H_5)_2]_2$° was reported already in 1961 [488]. Later it was shown that the compound, obtained under very similar reaction conditions, was the bis(cyclopentadienyl)-technetiumhydride $[Tc(C_5H_5)_2H]$° analogous to the known $[Re(C_5H_5)_2H]$°. $[Tc(C_5H_5)_2H]$° is readily soluble in benzene and toluene. The Tc–H stretching vibration was found in the IR at 1930 cm^{-1}. Aqueous hydrochloric acid extracts the hydrochloride $[Tc(C_5H_5)_2H_2]Cl$ from a solution in benzene. $[PF_6]^-$ precipitates white $[Tc(C_5H_5)_2H_2][PF_6]$ [489].

The reaction of $TcCl_4$ with potassium cyclopentadienide in boiling THF, without addition of $[BH_4]^-$, yields the diamagnetic, air-stable, red-brown compound $[Tc(C_5H_5)_2Cl]$°. The needle-shaped crystals adopt the orthorhombic space group *Ama2* with a=9.134(4), b=13.239(2), c=7.404(1) Å, and Z=4. The compound is readily soluble in aromatic hydrocarbons and polar solvents. Fig. 12.73.A shows the structure of $[Tc(C_5H_5)_2Cl]$°.The Tc–Cl bond distance is 2.450(3) Å, the average Cp–Tc distance 1.877(5) Å, and the average Cp–Tc–Cl angle 108.13°. The Cp rings form an angle of 143.76° with the Tc atom. The centers of the Cp rings, the Tc atom, and the chlorine atom are located in one plane. From the molecular structure the ionic radius of 0.61 Å was derived for Tc^{3+} [490]. $[Tc(C_5H_5)_2Cl]$° reacts in boiling THF with KCp in the molar ratio of 1:1 to form tris(cyclopentadienyl)technetium(III), $[Tc(C_5H_5)_3]$°. The orange-red, diamagnetic complex was found to be extremely sensitive to oxygen and water. It is soluble in organic solvents and crystallizes in the orthorhombic space group $Pna2_1$ with a=11.477(1), b=9.042(2), c=11.472(4) Å, and Z=4. Two Cp rings are π-bonded, while the third is σ-bonded. The centers of the two π-bonded Cp rings form an angle of 169.4° with Tc, the Cp–Tc bond distances are 1.883 and 1.781 Å. The Cp(σ)–Tc distance is considerably longer at 3.413 Å. The Cp(σ) ring is twisted [491].

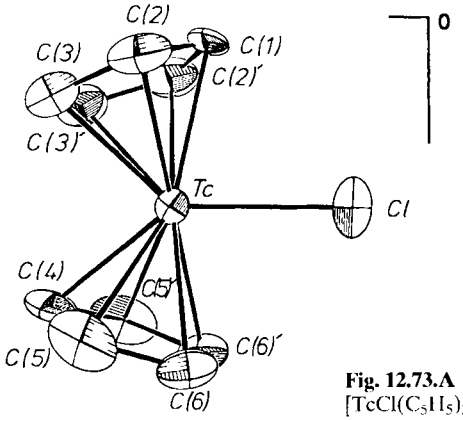

Fig. 12.73.A Chloro-bis(cyclopentadienyl)technetium (III), $[TcCl(C_5H_5)_2]$° [490].

12.5.7 Dinuclear μ-oxo-, μ-carboxylato-, μ-oxopyridinato-bridged complexes

When a solution of chloro{N-(2-oxidophenyl)salicylideneiminato}oxotechnetium(V), [TcO(ophsal)Cl]° [199] in ethanol is treated with an excess of PMe_2Ph, Tc(V) is reduced to Tc(III) and the red dinuclear complex μ-oxo-bis{(N-(2-oxidophenyl)salicylideneiminato-bis(dimethylphenylphosphine)} technetium(III), $[\mu\text{-O}\{Tc(ophsal)(PMe_2Ph)_2\}_2]^\circ$, is formed which is slightly soluble in acetonitrile, methanol, and ethanol. The compound crystallizes in the triclinic space group $P\bar{1}$ with a=16.709(7), b=15.255(6), c=11.702(4) Å, α=104.43(5), β=86.49(6), γ=106.91(6)°, and Z=2. Each Tc atom is bonded to the O_2N donor atoms of the ophsal ligand and to the two PMe_2Ph phosphorus donor atoms to form a distorted octahedron. The nitrogen atoms are *trans* to the bridging oxygen, and the equatorial plane of each Tc octahedron is defined by the O_2P_2 donor set. The Tc–O–Tc axis is almost linear with an angle of 176.1°; the Tc–O(bridging) bond lengths are 1.81(2) and 1.87(2) Å. The IR absorption at 625 cm^{-1} was tentatively attributed to the Tc–O–Tc stretching vibration. In addition, the μ-oxocomplexes $[\mu\text{-O}\{Tc(ophsal)(PPh_3)_2\}_2]^\circ$, $[\mu\text{-O}\{Tc(sphsal)(PMe_2Ph)_2\}_2]^\circ$, and $[\mu\text{-O}\{Tc(sphsal)(PPh_3)_2\}_2]^\circ$ were prepared and identified [492].

The dissymmetric compound $[Cl(pico)_4Tc\text{-}O\text{-}TcCl_4(pico)]^\circ \cdot H_2O$ can be readily synthesized from almost any common technetium starting material including NH_4TcO_4 + $NaBH_4$, $(NH_4)_2[TcCl_6]$, $[(n\text{-}Bu)_4N][TcOCl_4]$, or $[TcO_2(pico)_4]Cl$ by refluxing in neat picoline (pico). Precipitation of $[Cl(pico)_4Tc\text{-}O\text{-}TcCl_4(pico)]^\circ \cdot H_2O$ was achieved by addition of water. The complex is soluble and stable in common organic solvents, exhibits Tc–Cl stretching modes at 319 and 306 cm^{-1}, and a probable Tc–O–Tc stretch at 699 cm^{-1}. The magnetic moment is μ_{eff} = 1.1 B.M. Cyclic voltammetry shows the complex to be oxidized or reduced by a one-electron transfer. It crystallizes in the monoclinic space group $P2_1/c$ with a=11.709(4), b=20.243(8), c=33.41(2) Å, β=91.00(5)°, and Z=8. The two Tc atoms are in a pseudo-octahedral surrounding (Fig. 12.74.A). One Tc atom is in the plane of four equatorial nitrogens of the picoline ligands and has an axial chlorine atom opposite to the bridging oxygen. The other Tc atom has an axial picoline ligand and four equatorial chlorine atoms. The average Tc–O bond distance is 1.82(3) Å, the average Tc–O–Tc angle 176(2)°. The axial and equatorial Tc–N distances are 2.20(3) and 2.15(2) Å, respectively, while the axial and equatorial Tc–Cl distances are 2.39(1) and 2.37(1) Å, respectively. The arrangement of the chloride and picoline ligands is staggered. Formally, a 7+ charge must be distributed between the two Tc atoms, possibly in a Tc(III)–O–Tc(IV) or a Tc(II)–O–Tc(V) core [493].

The asymmetric compound $[(pico)Cl_3(pico)\text{-}Tc\text{-}O\text{-}TcCl(pico)_3Cl]^\circ$ is an isomer to the just described dissymmetric compound. The two types of complexes differ in their arrangement of equatorial ligands around each Tc atom. Both complexes were prepared in the same route. The asymmetric species was suggested to be the precursor of the dissymmetric complex. The dark reddish-brown $[(pico)Cl_3(pico)\text{-}Tc\text{-}O\text{-}TcCl(pico)_3Cl]^\circ$ crystallizes in the monoclinic space group $P2_1/n$ with a=12.421(1), b=15.471(1), c=18.764(1) Å, β=93.174(5)°, and Z=4. The geometry around each Tc atom is essentially octahedral. The Tc atoms are linked by a μ-oxo bridge with the

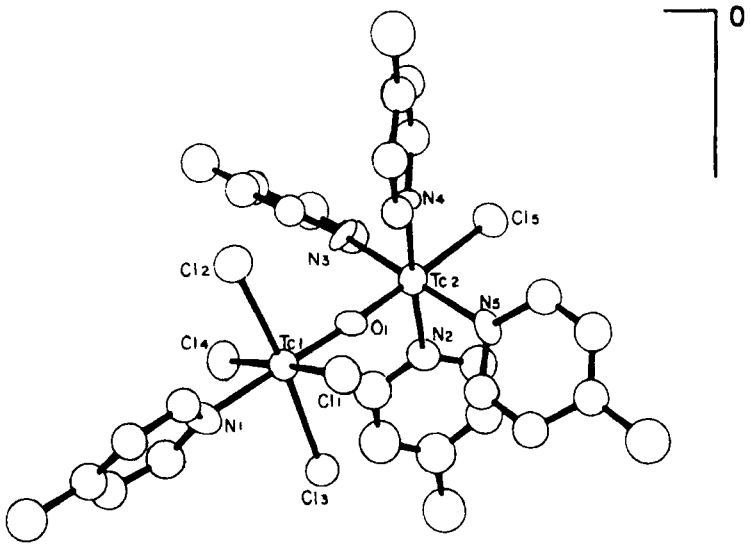

Fig. 12.74.A Chlorotetrakis(4-methylpyridine)-μ-oxo-tetrachloro-4-methylpyridine-ditechnetium, $[Cl(pico)_4Tc\text{-}O\text{-}TcCl_4(pico)]^c$ [493].

equatorial ligands on either Tc atom staggered relative to those on the other. The $Cl(pico)_3ClTc\text{–}O$ distance of 1.800(3) Å is clearly shorter than the $(pico)Cl_3(pico)$ Tc–O distance of 1.837(3) Å. The distance of 3.64 Å between the two Tc atoms precludes significant metal–metal bonding. Analogous compounds were prepared with pyridine, 3,5-lutidine, and bromine ligands [494]. The asymmetric and dissymmetric species spontaneously interconvert [495].

($Tc^{III}\text{-}O\text{-}Tc^{III}$) dimeric complexes containing halogen and 2,2′-bipyridine or 1,10-phenanthroline have been synthesized. $[(bpy)_2BrTc\text{-}O\text{-}TcBr(bpy)_2]Br_2 \cdot bpy$ was obtained by refluxing $[(n\text{-}Bu)_4N][TcOBr_4]$ with bpy in DMF. The purple crystals adopt the orthorhombic space group *Pbcn* with a=18.584(6), b=9.9602(8), c=26.131(2) Å, and Z=4. The ν(Tc–O–Tc) frequency was found in the IR at 730 cm^{-1}. The compound is diamagnetic. The coordination geometry is distorted octahedral around each Tc atom. Steric hindrance forces the bromide ligands to adopt a slightly staggered configuration and pushes the equatorial plane back from the Tc. The molecule is bent along the Tc–O–Tc axis by 173.0(3)°. The Tc–O bond length is 1.8278(6) Å, which precludes significant Tc–Tc bonding. The Tc–Br bond distance is 2.5665(7) Å, the average Tc–N bond length 2.123 Å, including the somewhat longer Tc–N length of 2.154(4) Å *trans* to the bridging oxygen. The structures of the complex cations $[(bpy)_2ClTc\text{-}O\text{-}TcCl(bpy)_2]^{2+}$ and $[(phen)_2ClTc\text{-}O\text{-}TcCl(phen)_2]^{2+}$ were found to be very similar to that of the described bipyridine bromo compound. The Tc^{III}–Tc^{III} oxidation state is stabilized by the π-acceptor ligands. The halide ligands are easily lost in aqueous media [496].

The bis(μ-oxo) mixed valence complex anion $[(tcta)Tc^{III}(\mu\text{-}O)_2Tc^{IV}(tcta)]^{3-}$ (where $tcta^{3-}$ = 1,4,7-triazacyclononane-N,N′,N″-triacetate) was obtained as a deep inky blue

aqueous solution, when the Tc(V) complex salt $Na_2[TcO(eg)(tcta)]$ (eg = ethylene glycolate) was reduced with $Na[BH_4]$ and, after the decomposition of $[BH_4]^-$, the solution was oxidized by air. The deep blue barium salt $Ba_2[(tcta)Tc^{III}(\mu\text{-}O)_2Tc^{IV}(tcta)][ClO_4]\cdot 9H_2O$ crystallizes in the monoclinic space group $P2_1/n$ with a=15.128(1), b=18.822(2), c=15.582(1) Å, β=105.43(7)°, and Z=4. The crystal structure analysis reveals a dimeric structure of the complex anion with pseudooctahedral geometry at each Tc atom. The two Tc atoms are linked by a planar four-membered $Tc(\mu\text{-}O)_2Tc$ ring. The other four coordination sites on each Tc are filled by a tcta ligand, bound by an N_3O donor set. One acetate group from each tcta ligand bridges the two Tc atoms. The remaining acetate groups are coordinated to the barium counterions. The short Tc–Tc distance of 2.402 Å indicates a metal-metal multiple bond. The four Tc–O bond lengths in the four-membered ring have an average distance of 1.936 Å. The average Tc–O–Tc angle is 76.7°. The planar TcO_2Tc core found in several complexes appears to be a relatively rigid entity. The $Tc^{III}(\mu\text{-}O)_2Tc^{IV}$ core complex undergoes a reversible one-electron oxidation with $K_2S_2O_8$ to form the $Tc^{IV}(\mu\text{-}O)_2Tc^{IV}$ core complex:

$$[(tcta)Tc^{III}(\mu\text{-}O)_2Tc^{IV}(tcta)]^{3-} \leftrightarrow [(tcta)Tc^{IV}(\mu\text{-}O)_2Tc^{IV}(tcta)]^{2-} + e^-$$

The optical spectrum of $[(tcta)Tc^{III}(\mu\text{-}O)_2Tc^{IV}(tcta)]^{3-}$ in water is dominated by an intense band at 592 nm [497].

The polymeric compound $[Tc_2O_3(C_5Me_5)]_n$ was reported to be synthesized by reaction of $[(\eta^5\text{-}C_5Me_5)Tc(CO)_3]^0$ with perhydrol. The needle-shaped, yellow compound crystallizes in the orthorhombic space group $Pmnm$ with a=5.946(5), b=8.697(4), c=10.630(7) Å, and Z=4. Two Tc atoms are bridged by three μ-oxo ligands. The C_5Me_5 rings are concomitantly a component of the neighboring units. The planes of the cyclopentadienyl rings and of the oxo-bridged ligands are parallel to one another. A striking feature is the unusually short distance of 1.867(4) Å between the two Tc atoms coupled by the three μ-oxo ligands. Formally, the two Tc centers have the oxidation state 3.5. The Tc–O stretching vibrations appear in the IR at 909 (symmetric) and 880 cm^{-1} (antisymmetric) [498]. However, the structure of $[Tc_2O_3(C_5Me_5)]_n$ was questioned mainly due to the Tc–O frequencies and the extremely short Tc–Tc distance [15].

Tetrapivalatodichloroditechnetate(III),$[Tc_2\{(CH_3)_3CCOO\}_4Cl_2]^0$, a dinuclear tetracarboxylato-bridged complex, was prepared by heating $(NH_4)_3[Tc_2Cl_8]$ with excess pivalic acid at about 150 °C for 36 h in a nitrogen atmosphere. The red compound crystallizes in the tetragonal space group $I4/m$ with a=11.515(2) Å, c=10.625(3) Å, and Z=2. Its structure is shown in Fig. 12.75.A. The Tc–Tc distance is 2.192(1) Å. The axial Tc–Cl bonds are remarkably strong with a distance of 2.408(4) Å. The relatively long Tc–Tc distance is attributed to the strong Tc–Cl bond. The average Tc–O bond length is 2.032(4) Å. The Tc–Tc–Cl angle is exactly linear and the average Tc–Tc–O angle nearly perpendicular [499].

The analogous tetraacetato complex $[Tc_2(CH_3COO)_4Cl_2]^0$ was obtained by reaction of $KTcO_4$ with HCl and CH_3COOH in an atmosphere of hydrogen. The cherry-red crystals are insoluble in hydrochloric and acetic acids, alcohol, acetone, and ether and are

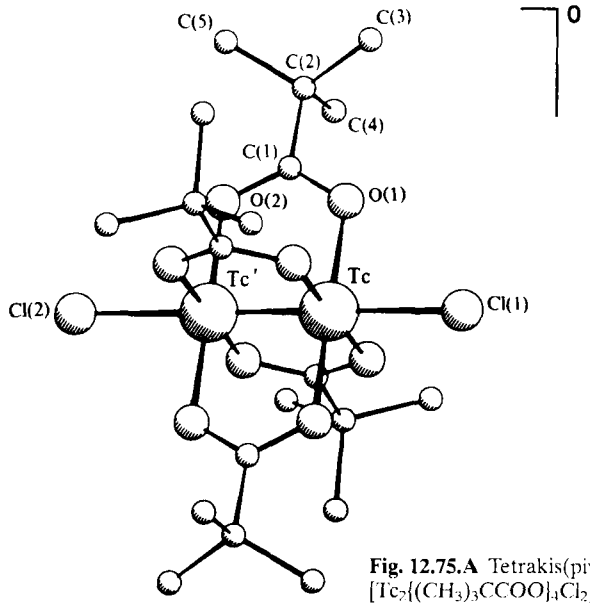

Fig. 12.75.A Tetrakis(pivalato)-dichloro-ditechnetium(III), $[Tc_2\{(CH_3)_3CCOO\}_4Cl_2]^\circ$ [499].

hydrolyzed in water. The compound [500] is diamagnetic and isostructural with $[Re_2(CH_3COO)_4Cl_2]^\circ$. The corresponding orange-red $[Tc_2(CH_3COO)_4Br_2]^\circ$ was synthesized by reacting $[Tc_2Br_8]^{2-}$ in a boiling mixture of glacial acetic acid and acetic anhydride. The vibrational spectra of $[Tc_2(CH_3COO)_4Cl_2]^\circ$ and $[Tc_2(CH_3COO)_4Br_2]^\circ$ were assigned according to the point group D_{4h}. The quadruply bridged Tc–Tc bond is stabilized by the bridging acetato and destabilized by the axial halogeno ligands. The valence force constants f_d(Tc–Tc) of both complexes are around 4.0 mdyne/Å [501].

Tetra(μ-acetato)ditechnetium(III)dipertechnetate $[Tc_2(CH_3COO)_4](TcO_4)_2$ was obtained as an admixture of single crystals in a host phase of $[Tc_2(CH_3COO)_4Cl_2]^\circ$. The red crystals adopt the monoclinic space group $P2_1/n$ with a=8.324(1), b=7.826(1), c=14.644(4) Å, β=101.81(2)°, and Z=2. $[Tc_2(CH_3COO)_4](TcO_4)_2$ constists of the binuclear cation and two pertechnetate anions which are axially coordinated to the Tc atoms by bridging oxygen atoms. $[Tc_2(CH_3COO)_4]^{2+}$ contains four bridging acetato ligands with the Tc–Tc bond distance of 2.149(1) Å. The Tc–O(acetate) distance varies from 2.00 to 2.03 Å. The Tc–O distances in the TcO_4 anions are 1.68 Å for terminal oxygen atoms and 1.73 Å for the bridging one [502,503].

$K[Tc_2(CH_3COO)_4Cl_2]$ was reported to be formed by reaction of $K_3[Tc_2Cl_8]$ with glacial acetic acid in an autoclave at 120 °C. The magnetic moment at 300 K was determined as μ_{eff} = 2.22 B.M. The formal oxidation state of each Tc atom in the tetraacetato complex is +2.5 [504]. The dark brown asterisks of $K[Tc_2(CH_3COO)_4Cl_2]$ crystallize in the tetragonal space group $P4_2/n$ with a=11.9885(3), c=11.2243(2) Å, and Z=4. The structure is similar to that of $[Tc_2\{(CH_3)_3CCOO\}_4Cl_2]^\circ$. The Tc–Tc bond distance is 2.1260(5) Å, the average Tc–O distance 2.074 Å, and the Tc–Cl distance 2.589(1) Å. The Tc–Tc–Cl angle is almost linear at 175.90(5)°, and the Tc–Tc–O angles are nearly 90° [505].

Another acetatochloroditechnetate(III) complex is the neutral compound $[Tc_2(CH_3COO)_2Cl_4(H_2O)_2]^0$, which was obtained by reaction of $[Tc_2Cl_8]^{2-}$ with acetic anhydride and $H[BF_4]$ at –30 °C as a dark green crystalline solid. Treating a solution of $[Tc_2(CH_3COO)_2Cl_4(H_2O)_2]^0$ in acetone with N,N-dimethylacetamide (DMAC) yields green crystals of *cis*-$[Tc_2(CH_3COO)_2Cl_4(DMAC)_2]$, which adopt the monoclinic space group *C2/c* with a=29.604(4), b=10.895(2), c=14.404(2) Å, β=97.87(2)°, and Z=8. The bridging acetato groups are found in *cis* position, the four chlorine atoms are *trans* to the acetato oxygen atoms. The DMAC oxygens are located in the axial positions. The Tc–Tc bond length is 2.1835(7) Å, the average Tc–O(acetate) distance 2.063 Å, while the axial Tc–O(DMAC) distances are 2.298(3) and 2.341(4) Å. The angles Tc–Tc–O(DMAC) deviate significantly from linearity. The Tc–Tc–O(acetate) angles are almost 90°. Both Tc atoms reside in a distorted octahedral geometry. From IR and Raman frequencies the stretching interaction constant f_d(Tc–Tc) was determined to be 3.38 mdyne/Å. With increasing donor strength of the axial ligands the intense Raman vibration ν(Tc–Tc) decreases, which indicates the weakening of the Tc–Tc bond [506,507].

$(NH_4)_3[Tc_2Cl_8]$ reacts with molten 2-hydroxypyridine at 150 °C in a nitrogen atmosphere to make dark green $[Tc_2(OC_5H_4N)_4Cl]^0$. The structure consists of infinite chains of $[Tc_2(OC_5H_4N)_4]^+$ units symmetrically linked by bridging Cl^- ions, while in each unit the Tc atoms are bridged by four 2-oxypyridinato ligands. The unit cell dimensions are a=11.793(3), c=7.454(1) Å, and Z=2. The tetragonal space group is *I4/m*. The Tc–Tc distance of 2.095(1) Å is exceptionally short. The Tc–Cl bond length is 2.679(1) Å and the Tc–Tc–Cl angle is 180° as required by symmetry. The Raman spectrum has a very strong line at 383 cm^{-1} which may be assigned to the totally symmetric Tc–Tc stretching mode. The compound was found to be paramagnetic [508]. When $K_3[Tc_2Cl_8] \cdot 2H_2O$ was heated in 8 M H_2SO_4 for 1 h at ~100 °C after addition of K_2SO_4, the green complex salt $K_2[Tc_2(SO_4)_4] \cdot 2H_2O$ was obtained [509].

12.5.8 Dinuclear complexes with multiple Tc–Tc bonds

The preparation of the first dinuclear complex salts, black $(NH_4)_3[Tc_2Cl_8] \cdot 2H_2O$ and $Y[Tc_2Cl_8] \cdot 9H_2O$, was described as early as 1963. $[Tc_2Cl_8]^{3-}$ was obtained by reduction of a $[TcCl_6]^{2-}$ solution with zinc pellets in conc. hydrochloric acid. The composition of the compounds was confirmed by elemental analysis and the oxidation state of 2.5 for Tc by oxidation with ceric sulphate. The density of $(NH_4)_3[Tc_2Cl_8] \cdot 2H_2O$ was found to be 2.4 $g \cdot cm^{-3}$. In dilute HCl or water the compounds decompose rapidly by oxidation and hydrolysis [510]. At 280 °C anhydrous $(NH_4)_3[Tc_2Cl_8]$ starts to decompose [511] according to the equation:

$$(NH_4)_3[Tc_2Cl_8] \xrightarrow{280\ ^\circ C} \xrightarrow{340\ ^\circ C} Tc + (NH_4)_2[TcCl_6] + NH_4Cl + \tfrac{1}{2}\,Cl_2$$

$(NH_4)_3[Tc_2Cl_8] \cdot 2H_2O$ crystallizes in the trigonal space group $P3_121$ with the hexagonal unit cell dimensions a=13.04, c=8.40 Å, and Z=3. Four chlorine atoms and one Tc atom compose the square pyramidal coordination sphere of $[Tc_2Cl_8]^{3-}$. The two $TcCl_4$ groups are joined by a very short Tc–Tc bond of 2.13(1) Å to give an eclipsed

rotational configuration (Fig. 12.76.A). The virtual symmetry is D_{4h}, but crystallographically the complex ion has only a single C_2 axis bisecting the Tc–Tc bond. The average Tc–Cl bond distance is 2.36 Å. The Cl–Tc–Cl angles vary between 84.4 and 87.8°, the Tc–Tc–Cl angles between 103.8 and 106.6° [512–514]. The charge of 3- on the anion $[Tc_2Cl_8]^{3-}$ appears surprising, however, the magnetic moment μ_{eff} = 1.78 B.M. in the temperature range 80–300 K and ESR spectra with hyperfine coupling to two equivalent ^{99}Tc atoms, are consistent with the presence of one unpaired electron [521]. The main absorption in the visible, which accounts for the turquoise blue color of the solution in conc. HCl, has a maximum at 638 nm. In $[Tc_2Cl_8]^{3-}$ there are nine electrons beyond those which are involved in the Tc–Cl bonds or belong to the non-bonding electrons on Cl atoms. Eight of these occupy one σ, two π, and one δ orbital constituting a Tc–Tc quadruple bond. The remaining electron resides in one of the more or less non-bonding δ orbitals [512, 514, 517]. The major components of the Tc–Tc bond are the π bonds in the $\sigma^2\pi^4\delta^2\delta^{*}$ configuration [515]. Spectroscopic studies of $[Tc_2Cl_8]^{3-}$ reveal a band in the near IR between 6000 and 8000 cm^{-1} showing vibronic structure. This band was assigned to the $\delta \rightarrow \delta^{*}$ transition [516]. The vibronic structure of the $\delta \rightarrow \delta^{*}$ transition was also reported for $[Tc_2Br_8]^{3-}$, which was prepared by reduction of $[Tc_2Br_8]^{2-}$ with $[BH_4]^-$ in acetone [518].

Grey-black $K_3[Tc_2Cl_8]\cdot nH_2O$ crystallizes in the trigonal space group $P3_121$ or $P3_221$ with a=12.838(3), c=8.187(2) Å, and Z=3. The Tc–Tc bond distance is 2.117(2) Å, the average Tc–Cl distance again 2.36 Å [519]. $Y[Tc_2Cl_8]\cdot 9H_2O$ crystallizes in the tetragonal space group $P42_12$ with a=11.712(2), c=7.661(2) Å, and Z=4. The Tc–Tc bond distance is 2.105(1) Å which is slightly shorter than that in $K_3[Tc_2Cl_8]\cdot nH_2O$. The average Tc–Cl distance in $Y[Tc_2Cl_8]\cdot 9H_2O$ is 2.364(2) Å, and the average Tc–Tc–Cl angle is 104.34(6)° [520].

Rotating disk electrode polarography and cyclic voltammetry at platinum electrodes of $[Tc_2Cl_8]^{3-}$ solutions in hydrochloric acid/ethanol mixtures suggested a quasi-reversible oxidation at $E_{1/2}$ = 0.140 V *vs* SCE involving one electron:

$$[Tc_2Cl_8]^{3-} \leftarrow [Tc_2Cl_8]^{2-} + e$$

The life-time of the oxidized product was concluded to be considerably longer than 300 s, however, attempts to isolate crystalline salts of $[Tc_2Cl_8]^{2-}$ failed at that time [521].

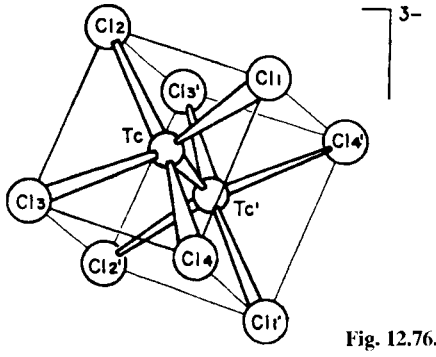

Fig. 12.76.A Octachloroditechnetate(II/III), $[Tc_2Cl_8]^{3-}$ [514].

Grey-blue $[n\text{-}(C_4H_9)_4N]_3[Tc_2Cl_8]$ was prepared by reduction of $[TcCl_6]^{2-}$ with Zn in conc. HCl, dissolving the purified product in dilute HCl, adding $[n\text{-}(C_4H_9)_4N]Cl$, extracting the solution with CH_2Cl_2, and precipitating the complex salt in acetone. Its vibrational spectrum was assigned according to D_{4h} symmetry. The Tc–Tc vibration (A_{1g}) was observed at 307 cm^{-1} [522]. The disproportionation and oxidation of $[Tc_2Cl_8]^{3-}$ in hydrochloric acid solutions was studied spectrophotometrically [523].

Soon after the conclusion that the life-time of $[Tc_2Cl_8]^{2-}$ will be longer than 300 s [521], the compound $[n\text{-}(C_4H_9)_4N]_2[Tc_2Cl_8]$ was synthesized and identified. When TcO_4^- in HCl was reduced with H_3PO_2, a dark green solution containing $[Tc_2Cl_8]^{2-}$ and $[TcCl_6]^{2-}$ was obtained. Upon adding $[n\text{-}(C_4H_9)_4N]Cl$, the green $[n\text{-}(C_4H_9)_4N]_2[Tc_2Cl_8]$ precipitated. However, the strong paramagnetic tetrabutylammonium salt of $[TcCl_6]^{2-}$ was precipitated concomitantly to some extent. After washing with ethanol the precipitate was recrystallized several times from acetone, until a pure olive green product was obtained. Magnetic susceptibility measurements in the range from room temperature down to liquid helium temperature proved the complex salt to be diamagnetic, indicating an even number of electrons at the central atoms. $[n\text{-}(C_4H_9)_4N]_2[Tc_2Cl_8]$ crystallizes in the monoclinic space group $P2_1/c$ with a=10.922, b=15.384, c=16.439 Å, β=122.37°, and Z=2. The compound was shown to be isostructural with $[n\text{-}(C_4H_9)_4N]_2[Re_2Cl_8]$. In the far IR spectrum of $[Tc_2Cl_8]^{2-}$ a doublet of the Tc–Cl stretching mode E_u was observed at 350 and 356 cm^{-1}. The doublet splitting can be explained by the distortion of the D_{4h} symmetry. Also, a single band at 337 cm^{-1} was assigned to the A_{2u} stretching mode and another single band at 173 cm^{-1} to the A_{2u} bending mode. The diffuse reflectance spectrum revealed a strong band in the visible at about 700 nm, which may be attributed to the orbitally allowed transition from the Tc–Tc bonding orbital δ to the antibonding orbital δ^*. In accordance with this assigment, the 700 nm band showed no decrease in intensity with decreasing temperature [524].

X-ray structure analysis of $[n\text{-}(C_4H_9)_4N]_2[Tc_2Cl_8]$ yielded a Tc–Tc bond distance of 2.147(4) Å, which is longer than would have been anticipated given the Tc–Tc distance of 2.117(2) Å in $[Tc_2Cl_8]^{3-}$, because the removal of the δ^* electron might be expected to shorten the bond. The mean Tc–Cl distance is 2.320(4) Å and the mean Tc–Tc–Cl angle is 103.8(4)° [525]. In the Raman spectrum of $[n\text{-}(C_4H_9)_4N]_2[Tc_2Cl_8]$ the intense Tc–Tc vibration (A_{1g}) was observed at 307 cm^{-1}. $[n\text{-}(C_4H_9)_4N]_2[Tc_2Br_8]$ was obtained in carmine red crystals when the analogous chloro complex dissolved in acetone was treated with conc. hydrobromic acid. The Tc–Tc vibration (A_{1g}) in $[Tc_2Br_8]^{2-}$ was found at 323 cm^{-1} [522].

12.5.9 Ternary chalcogenide clusters

The sulphides $K_4Tc_6S_{12}$, $Rb_4Tc_6S_{13}$, and $Cs_4Tc_6S_{13}$ were synthesized by heating alkali carbonates, powdered technetium metal, and sulphur under an argon atmosphere at 800 °C for about 8 h. The synthesis of the selenides $K_4Tc_6Se_{12}$, $Rb_4Tc_6Se_{12}$, and $Cs_4Tc_6Se_{13}$ was achieved analogously under a hydrogen atmosphere. All six chalcogenides were isolated in pure phases and form black, shiny crystals adopting the

monoclinic space group $C2/c$. Compounds of analogous composition are isostructural. The lattice constants are listed in Table 12.15.A.

Table 12.15.A Dimensions of the monoclinic unit cells for the ternary technetium chalcogenides [526].

Compound	*a*	*b*	*c*	*β*
$K_4Tc_6S_{12}$	16.463(4)	9.667(3)	11.841(2)	91.40(2)
$K_4Tc_6Se_{12}$	17.165(2)	10.019(2)	12.301(2)	91.42(1)
$Rb_4Tc_6S_{13}$	9.745(2)	16.595(4)	13.913(3)	99.83(2)
$Rb_4Tc_6Se_{12}$	17.640(4)	10.092(1)	12.464(1)	91.30(1)
$Cs_4Tc_6S_{13}$	9.983(1)	17.120(4)	13.643(3)	100.68(1)
$Cs_4Tc_6Se_{13}$	10.275(2)	17.826(3)	14.161(4)	100.89(2)

The structural units in the six compounds are $[Tc_6X_8]$ (X = S,Se) clusters. The six technetium atoms in the oxidation state +3 form nearly regular octahedra. The eight chalcogen atoms reside over the octahedral faces. The resulting cube is nearly regular (Fig. 12.77.A). The average Tc–Tc bond distances in the different compounds range from 2.60 to 2.65 Å. The Tc_6 octahedron of each Tc_6X_8 unit is linked in three directions to neighboring octahedra through additional X atoms or X_2 groups. The alkali ions are inserted in interstices of the anionic framework. The +3 oxidation state indicates that there are 24 valence electrons per Tc_6 unit to give a stable configuration. The compounds show a weak temperature-independent paramagnetism that is often observed for clusters [526]. Reaction of metallic technetium with Rb_2CO_3 and Cs_2CO_3 at 800 °C in a hydrogen stream charged with sulphur yielded, after 10–16 h, black, shiny crystals of the composition $Rb_{10}[Tc_6S_{14}]$ and $Cs_{10}[Tc_6S_{14}]$, respectively. The compounds crystallize in the space group $Fm\bar{3}m$ with the lattice constants a=15.006(2) Å for $Rb_{10}[Tc_6S_{14}]$ and a=15.619(2) Å for $Cs_{10}[Tc_6S_{14}]$. In the $[Tc_6S_{14}]$ cluster units, the regular Tc_6 octahedra are coordinated by sulphur atoms over their eight faces and six vertices. These units are not linked to each other. The Tc–Tc bond distance is 2.63 Å. The compounds are diamagnetic. The oxidation state of Tc is again +3. $Rb_{10}[Tc_6S_{14}]$ and $Cs_{10}[Tc_6S_{14}]$ are extremely sensitive to air and water [527].

Structural data of Tc(III) complexes are reviewed in Table 12.16.A.

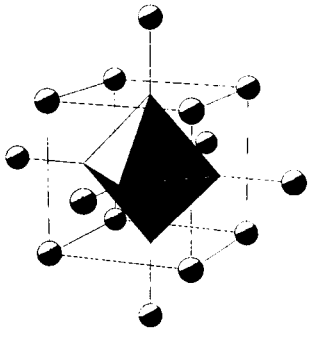

Fig. 12.77.A Structural unit of $[T_6S_8]$ and $[T_6Se_8]$ clusters with bridging chalcogen atoms [526].

Table 12.16.A Some structural data ot selected Tc(III) complexes.

Complex	Geometry	Tc–L [Å]	ν(Tc–L) IR/Ra [cm^{-1}]	μ_{eff} [B.M.]	References
12.5.1					
$K_4[Tc(CN)_7]$	pent.bipyr.	–		–	[99]
$[Tc(NCS)_6]^{3-}$	octah.	2.05	2070	3.0–3.3	[361]
trans-$[TcCl_2(NCS)(Me_2PhP)_3]^0$	octnh.	2.104 (Tc–N)	2076 (Tc–N)		[395]
trans-$[TcCl_2(CH_3CN)_4]^+$	octah	2.070 (Tc–N)		–	[396]
12.5.2					
trans-$[TcCl_2(dmpe)_2]^+$	octnh.	2.324 (Tc–P) 2.436 (Tc–P)	–		[239]
trans-$[TcCl_2(dppe)_2]^+$	octah.		–	2.74	[397]
trans-$[TcBr_2(dppe)_2]^+$	octah.	2.440 (Tc–Br) 2.500 (Tc–P)		3.04	[397]
mer-$[TcCl_3(Me_2PhP)_3]^0$	octnh.	–	–	2.6–2.8	[405]
mer-$[TcCl_3(Me_3P)_3]^0$	octnh.	2.440 (Tc–Cl)		–	[406]
mer-$[TcCl_3(PPh_3)_2(DMF)]^0$	octah.	2.371 (Tc–Cl) 2.498 (Tc–P)	330 (Tc–Cl)	3.1	[408]
mer-$[TcCl_3(PPh_3)_2(CO)]^0$	octah.	2.322 (Tc–Cl) 1.985 (Tc–C)		–	[409]
mer-$[TcCl_3\{P(C_6H_4Me\text{-}3)_3\}_2(MeCN)]^0$	octah.	2.058 (Tc–N)	–	–	[410]
trans-$[TcCl_2(diars)_2]^+$	octnh.	2.509 (Tc–As) 2.320 (Tc–Cl)	–	2.7	[413,414]
12.5.3					
trans-$[TcCl(acac)_2(PPh_3)]^0$	octnh.	2.01 (Tc–O) 2.42 (Tc–Cl) 2.46 (Tc–P)		–	[417,418]
trans-$[TcBr(acac)_2(PPh_3)]^0$	octah.	–	455 (Tc–O)$_{sym}$	2.7	[365]
$[Tc(acac)_3]^0$	octah.	2.025 (Tc–O)	440 (Tc–O)$_{sym}$	2.7	[365]
$[Tc(hexane\text{-}2,4\text{-}dionato)_3]^0$	octah.		438 (Tc–O)$_{sym}$		[422]
$[Tc(tbm)_3]^{3+}$	octah.	2.33 (Tc–S) 2.05 (Tc–O)	–	–	[427]
mer-$[Tc(O_2CCH_2CH_2PPh_2)_3]^0$	octah.	2.450 (Tc–P)	–		[431]
12.5.4					
mer-$[TcCl_3(pico)_3]^0$	octnh.	2.140 (Tc–N)	–	2.81	[432]
mer-$[TcCl_3(pico)(Me_2PhP)_2]^0$	octah.	2.198 (Tc–S)		2.58	[432]
trans-$[TcCl_2(py)_3(PPh_3)]^+$	octah	2.183 (Tc–N)	–		[433]
cis(Cl),-trans(P)-$[TcCl_2(bpy)(PMe_2Ph_2)_2]^+$	octah.	2.059 (Tc–N)		–	[434]
fac-$[TcCl_3(bpy)(PPh_3)]^0$	octah.	2.105 (Tc–N)	–		[435]
$[TcCl_2\{HB(pyz)_3\}(py)]^0$	–	–	–	2.8	[438]
$[TcBr(DMG)_3(BC_4H_9)]^0$	monocapped trigonal prism	2.01: (Tc–N)	–	–	[439]
trans-$[Tc\{(acac)_2en\}(PPh_3)_2]^+$	octah.	2.06 (Tc–N) 2.02 (Tc–O)	–	–	[446]
$[TcCl(phsal)_2(PMe_2Ph)]^0$	octah.	1.984 (Tc–O) 2.128 (Tc–N)		2.5	[393]
$[Tc(ophsal)(quin)(PEt_2Ph)]^0$	octah.	2.04 (Tc–N_{sal})	–	2.6	[448]
trans-$[TcCl(NNC_6H_4Cl\text{-}4)_2(PPh_3)_2]^0$	trig.bipyr		–	–	[449]
$[TcCl(NNPh)(dppe)_2]^+$	octah.	1.917 (Tc–N)			[449]
$[Tc(NNC_6H_4Cl\text{-}4)\{(CH_3)_2NCS_2\}_2(PPh_3)]^0$	octah.	1.763 (Tc–N_{diaz}) 2.475 (Tc–S)	–	–	[451]
cis-$[Tc(NNC_6H_4Cl\text{-}4)\{(sal)_2en\}(PPh_3)]^0$	octah.	1.764 (Tc–N_{diaz})			[452]
mer-$[Tc\{HNPhP(Ph)_2\}_2\{H_2NPhP(Ph)_2\}]^+$	octah.	1.964 (Tc–N_{amido}) 2.450 (Tc–P)	–	2.46	[456]
$[Tc(H)NHC(NH_2)S(PMe_3)_4]^+$	octah.	2.190 (Tc–N) 2.543 (Tc–S)	1989 (Tc–H)	–	[406]

Table 12.16.A Continued.

Complex	Geometry	Tc–L [Å]	ν(Tc–L) IR/Ra [cm^{-1}]	μ_{eff} [B.M.]	References
12.5.5					
trans-[Tc(SCH$_3$)$_2$(depe)$_2$]$^+$	octah.	2.449 (Tc–P) 2.303 (Tc–S)			[457]
cis-[Tc(SPh)$_2$(dmpe)$_2$]$^+$	octah.	2.29 (Tc–S) 2.46 (Tc–P)			[461]
[Tc(meph)(dmpe)$_2$]$^+$	octah.	2.352 (Tc–S)	–	–	[462]
trans-[Tc(SCH$_3$)$_2$(diars)$_2$]$^+$	octah.	2.292 (Tc–S) 2.496 (Tc–As)	–		[463]
[Tc(tdt)(dmpe)$_2$]$^+$	octah.-trig. prism.	2.318 (Tc–S) 2.402 (Tc–P)	–	–	[464]
[Tc(tmbt)$_3$(MeCN)$_2$]$^+$	trig.bipyr.	2.249 (Tc–S) 2.04 (Tc–N)	–	diamag.	[114,465]
[Tc(tmbt)$_3$(CO)(MeCN)]$^+$	trig.bipyr.	2.16 (Tc–N)	–	diamag.	[465]
[Tc(tmbt)$_3$(MeCN)(DMSO)]$^+$	trig.bipyr.	2.64 (Tc–S) 2.08 (Tc–N)		diamag.	[182]
[Tc(NO)(Cl)(tmbt)$_3$]$^+$	trig.bipyr.	1.767 (Tc–NO)	–	diamag.	[466]
cis-[Tc(ttod)(SC$_6$H$_5$)$_2$]$^-$	octah.	2.27 (Tc–S) 2.44 (Tc–S$_{ether}$)		diamag.	[468]
[Tc{(SCH$_2$CH$_2$)$_3$N}(PPh$_3$)]$^+$	trig.bipyr.	2.226 (Tc–S) 2.192 (Tc–N)	–	diamag.	[469,470]
[Tc{P(2-C$_6$H$_4$S)$_3$}(CN-Pr^i)]$^+$	trig.bipyr.	2.236 (Tc–S) 2.273 (Tc–P)	–	diamag.	[471]
[Tc(2-Ph$_2$PC$_6$H$_4$S)$_3$]$^+$	octah.	2.26–2.49 (Tc–S) 2.41–2.48 (Tc–P)		3.0	[472]
[Tc(SCH$_2$CH$_2$PPh$_2$)$_2$ (SCH$_2$CH$_2$PPh$_2$O)]$^+$	trig.bipyr.	2.23–2.49 (Tc–S) 2.27–2.51 (Tc–P)	–	diamag.	[473]
trans-[Tc(SCP)$_2$(dmpe)$_2$]$^{3+}$	octah.	2.30 (Tc–S) 2.44 (Tc–P)	–		[474]
[Tc(S$_2$CNEt$_2$)$_3$(Me$_2$PhP)]$^+$	pent.bipyr.	2.49–2.52 (Tc–S) 2.330 (Tc–P)	–	–	[475]
[Tc(S$_2$CNEt$_2$)$_3$(CO)]$^+$	pent.bipyr.	2.48–2.52 (Tc–S) 1.861 (Tc–CO)	–	–	[477]
[Tc(NS)(S$_2$CNEt$_2$)$_2$Br$_2$]$^+$	pent.bipyr.	1.754 (Tc–NS) 2.476 (Tc–S) 2.56–2.59 (Tc–Br)		–	[478]
[Tc(tu)$_6$]$^{3+}$	octah.	2.43 (Tc–S)		2.7	[480,481]
[Tc(Me$_2$tu)$_6$]$^{3+}$	octah.	2.440 (Tc–S)	–	2.7	[115,483]
[Tc(PPh$_3$)(S$_2$CO-*n*-C$_4$H$_9$)$_3$]$^+$	capped octah.	2.463 (Tc–S)	–	–	[485]
[Tc(Me$_2$PhP)(S$_2$COEt)$_3$]$^+$	pent.bipyr.	2.44–2.49 (Tc–S)		diamag.	[486]
trans-[TcCl$_2$(Me$_2$PhP)$_2${SP(S)(OCH$_3$)$_2$}]$^+$	octah.	2.475 (Tc–S)	–		[486]
trans-[TcCl$_2$(dtcb)(PPh$_3$)$_2$]$^+$	octah.	–		2.45	[215]
12.5.6					
[TcCl$_3$(CO)(PMe$_2$Ph)$_3$]$^+$	capped octah.	2.44 (Tc–P) 1.86 (Tc–CO) 2.48 (Tc–Cl)	–	diamag.	[487]
[Tc(C$_5$H$_5$)$_2$H]$^+$	–		1930 (Tc–H)	diamag.	[489]
[Tc(C$_5$H$_5$)$_2$Cl]$^+$	C_{2v}	2.450 (Tc–Cl) 1.877 (Tc–Cp)	425 (Tc–Cl)	diamag.	[490]
[Tc(C$_5$H$_5$)$_3$]$^+$	–	1.78–1.88 (Tc–Cp$_\pi$) 3.413 (Tc–Cp$_\sigma$)	–	diamag.	[491]
12.5.7					
[μ-O{Tc(ophsal)(PMe$_2$Ph)$_2$}$_2$]$^+$	octah.	1.81–1.87 (Tc–μO)	–		[492]
[Cl(pico)$_4$Tc^{III}-O-Tc^{IV}Cl$_4$(pico)]$^+$	octah.	1.82 (Tc–μO) 2.15–2.20 (Tc–N) 2.37–2.39 (Tc–Cl)	699 (Tc–O–Tc) 319,306 (Tc–Cl)	1.1	[493]

Table 12.16.A Continued.

Complex	Geometry	Tc–L [Å]	ν(Tc–L) IR/Ra [cm^{-1}]	μ_{eff} [B.M.]	References
$[\mu\text{-O}\{Tc(bpy)_2Br\}_2]^{2+}$	octah.	1.828 (Tc–μO) 2.567 (Tc–Br) 2.123 (Tc–N)	730 (Tc–O–Tc)	diamag.	[496]
$[(tcta)Tc^{III}(\mu\text{-O})_2Tc^{IV}(tcta)]^{3-}$	octah.	2.402 (Tc–Tc) 1.936 (Tc–μO)	-	-	[497]
$[Tc_2(O_2CCMe_3)_4Cl_2]$	octah.	2.192 (Tc–Tc) 2.408 (Tc–Cl) 2.032 (Tc–O)	–	–	[499]
$[Tc_2(CH_3COO)_4Cl_2]^0$	octah.	–	–	diamag.	[500]
$[Tc_2(CH_3COO)_4]^{2+}$	octah.	2.149 (Tc–Tc) 2.00–2.03 (Tc–O)	–	–	[502,503]
cis-$[Tc_2(CH_3COO)_2Cl_4(DMAC)_2]^0$	octah.	2.184 (Tc–Tc) 2.063 (Tc–O_{acet})	290 (Tc–Tc) 384 (Tc–O_{acet})	–	[506,507]
$[Tc^{III}Cl(OC_5H_4N)_2(OC_5H_4N)_2Tc^{II}]^0$	octah.	2.095 (Tc–Tc) 2.679 (Tc–Cl)		paramag.	[508]
12.5.8					
$[Cl_4Tc^{II}\text{-}Tc^{III}Cl_4]^{4-}$	square pyr.	2.105–2.13 (Tc–Tc) 2.36 (Tc–Cl)	307 (Tc–Tc)	1.78	[512–514, 519–522]
$[Br_4Tc^{II}\text{-}Tc^{III}Br_4]^{3-}$	square pyr.		-	–	[518]
$[Tc_2^{III}Cl_8]^{2-}$	square pyr.	2.147 (Tc–Tc) 2.320 (Tc–Cl)	307 (Tc–Tc) 337–356 (Tc–Cl)	diamag.	[522,524,525]
$[Tc_2^{III}Br_8]^{2-}$	square pyr.	–	323 (Tc–Tc)		[522]
12.5.9					
$[Tc_6^{III}S_8]^{2+}$	Tc_6(octah.) S_8(cube)	2.60–2.61 (Tc–Tc)	–	paramag.	[526]
$[Tc_6^{III}Se_8]^{2-}$	Tc_6(octah.) Se_8(cube)	2.64–2.65 (Tc–Tc)		paramag.	[526]
$[Tc_6^{III}S_{14}]^{10-}$	Tc_6(octah.) S_8(cube) S_6(vertices)	2.63 (Tc–Tc)	–	diamag.	[527]

12.6 Technetium(II)

Mononuclear, strong ligand field Tc(II) complexes are expected to be paramagnetic in different coordination spheres due to the low-spin magnetic moment of one unpaired electron. Effective magnetic moments ranging from 1.4 to 2.3 B.M were measured. Because of their paramagnetism the complex compounds of Tc(II) were often studied by EPR. Again, predominantly mixed ligand complexes, frequently containing phosphines, were synthesized and characterized. Mainly, compounds with sulphur, halogen, and nitrogen donor atoms are reported. Various nitrosyl and thionitrosyl complexes are known. In general, the coordination core geometry is distorted octahedral. Square pyramidal geometry is represented by dinuclear complexes with multiply bonded Tc atoms. This chapter also describes polynuclear halogeno compounds with low valent Tc_6 and Tc_8 cores.

12.6.1 Halogeno and isothiocyanato complexes with phosphine, phosphonite or arsine ligands

The tetrabromotechnetate(II) anion, $[TcBr_4]^{2-}$, was reported to be obtained by reaction of $[TcNBr_4]^-$ with 2,2′-dipyridyl in ethanol yielding *cis*-$[Tc^{V}NBr(bpy)_2]_2[TcBr_4]$. Tc(II) is tetrahedrally coordinated by Br^-. The Br–Tc–Br angles vary between 106.1 and 112.1°. The mean Tc–Br bond length is 2.401(4) Å [280,281].

$[TcCl_2(dppe)_2]^\circ$ and $[TcBr_2(dppe)_2]^\circ$ were prepared by reduction of the corresponding tervalent complexes with $Na[BH_4]$ in an ethanol/water mixture. The yellow-green chloro complex and the yellow bromo complex have a magnetic moment μ_{eff} at 20 °C of 2.05 and 2.28 B.M., respectively. Both compounds are soluble in benzene [356]. $[TcCl_2(dppe)_2]^\circ$ crystallizes in the monoclinic space group $P2_1/a$ with a=17.821(4), b=11.187(2), c=23.572(4) Å, β=103.55(1)°, and Z=4. Tc(II) resides in an approximately octahedral coordination environment. The phosphorus atoms occupy the four equatorial coordination sites while the two chloride ligands are mutually in *trans* position. The average Tc–P bond distance is 2.428 Å and the average Tc–Cl distance is 2.424 Å. Oxidation of *trans*-$[Tc^{II}Cl_2(dppe)_2]^\circ$ to *trans*-$[Tc^{III}Cl_2(dppe)_2]^+$ causes a shortening of the Tc–Cl bond by 0.105(2) Å and a lengthening of the Tc–P bond by 0.072(2) Å. $[TcCl_2(dppe)_2]^\circ$ and $[TcBr_2(dppe)_2]^\circ$ are facile reductants in non-aqueous media [399].

A structurally analogous compound is the isothiocyanato complex *trans*-$[Tc^{II}(NCS)_2(dppe)_2]^\circ$, which was synthesized by the action of excess LiSCN on $[Tc^{III}X_2(dppe)_2]^+$ (X = Cl,Br) in DMF or ethanol at 80–100 °C [397]. The rose-colored complex crystallizes in the triclinic space group $P\bar{1}$ with a=21.384(6), b=12.878(5), c=9.549(4) Å, =71.51(3), β=81.94(4), γ=83.38(4)°, and Z=2. The coordination geometry of Tc(II) is nearly octahedral. The phosphorus atoms again occupy the four equatorial sites, the NCS^- groups are in *trans*-axial positions, *N*-bonded to the Tc atom at an angle of 81° to the TcP_4 equatorial plane. The average Tc–P distance is 2.44(1) Å and the average Tc–N distance is 2.04(2) Å. Spectroelectrochemical measurements indicate the reversible oxidation and reduction processes [528]:

$$[Tc^{II}(NCS)_2(dppe)_2]^\circ \leftrightarrow [Tc^{III}(NCS)_2(dppe)_2]^+ + e$$

and

$$[Tc^{II}(NCS)_2(dppe)_2]^\circ + e^- \leftrightarrow [Tc^{I}(NCS)_2(dppe)_2]$$

Similarly, chloro-dimethylphenylphosphine complexes of Tc(II) and Tc(I) were obtained when $[TcCl_3(PMe_2Ph)_3]^\circ$ was reduced electrochemically in acetonitrile at platinum electrodes [405].

$[TcCl_2(PMe_2Ph)_2(dmpe)]^\circ$ with mixed phosphine ligands was prepared by reaction of $[Tc^{III}Cl_3(PMe_2Ph)_3]^\circ$ with excess dmpe in ethanol. The yellow compound crystallizes in the monoclinic space group $P2_1/c$ with a=12.899(6), b=13.142(8), c=19.088(9) Å, β=121.13(3)°, and Z=4. Tc(II) is located in a distorted octahedral surrounding, with the two Cl ligands located in *trans* position to each other and the two monodentate phosphines in *cis* position to each other (Fig. 12.78.A). The angles

around the Tc atom are close to 90 and 180°, however, the chelate angle P(1)–Tc–P(2) is only 80.1(1)°. Both Tc–Cl bond distances are 2.431(5) Å, and the average Tc–P distance for the bidentate dmpe ligand is 2.399(4) Å, while the average bond length between Tc and P in PMe_2Ph is 2.435(4) Å [529].

The phosphonite complex $[TcCl_2\{C_6H_5P(OC_2H_5)_2\}_4]^\circ$ was prepared by reduction of $(NH_4)_2[TcCl_6]$ with $NaBH_4$ in ethanol in the presence of diethylphenylphosphonite. The yellow compound crystallizes in the monoclinic space group $P2_1/c$ with a=21.740(19), b=11.750(10), c=18.312(12) Å, β=92.92(9)°, and Z=4. The magnetic moment of the complex in benzene solution at 306 K is μ_{eff}=1.4 B.M. The coordination geometry of Tc(II) is distorted octahedral with four phosphorus atoms in the equatorial plane and two chlorine atoms in the axial positions. The octahedron is tetrahedrally distorted as a result of the packing requirements of the bulky ligands. The four Tc–P distances are almost identical at 2.41(1) Å. The average Tc–Cl bond distance is also 2.41 Å. The Cl–Tc–Cl angle is 178.8(1)°. The P–Tc–P(*cis*) angles are nearly rectangular while the angles P–Tc–P(*trans*) are 164° [411].

The neutral diarsine complexes $[Tc^{II}(diars)_2X_2]^\circ$ (X=Cl,Br,I) are long known and are obtained by reducing the Tc(III) compounds $[Tc(diars)_2X_2]X$ with H_3PO_2. The yellow to brown non-electrolytes are slightly soluble in nitrobenzene and nitromethane. The magnetic moment of the complexes range from 1.9 to 2.1 M.B. at 20 °C. They are isostructural with the analogous complexes of Re(II) [79.412].

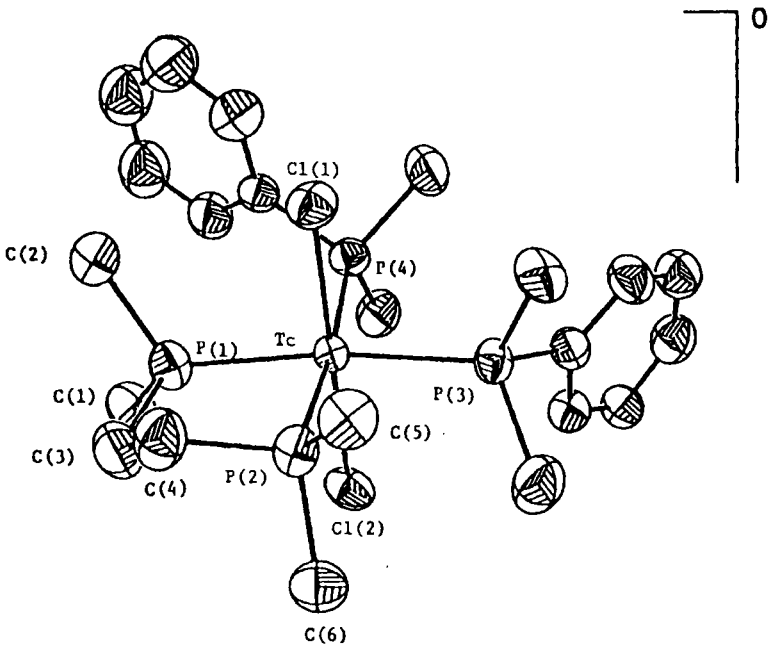

Fig. 12.78.A *Trans*-dichloro-*cis*-bis(dimethylphenylphosphine)-bis(1,2-dimethylphosphino) ethane-technetium(II), $[TcCl_2(Me_2PhP)_2(dmpe)]^\circ$ [529].

12.6.2 Oxalato, thiolato, thiocarbamato, and thioether complexes

The neutral complex $[Tc(ox)(dppe)_2]^0$ (ox = oxalato) was synthesized by reacting TcO_4^- in ethanol under nitrogen with dppe and oxalic acid. Orange-red crystals of $[Tc(ox)(dppe)_2]^0 \cdot K[PF_6] \cdot 1.5\ H_2O$ crystallize in the triclinic space group $P\bar{1}$ with a=16.991(13), b=18.301(8), c=19.114(12) Å, α=91.06(4), β=113.07(7), γ=91.25(4)°, and Z=4. The compound is paramagnetic. The Tc atom is hexacoordinated by four P atoms of the two dppe ligands and two O atoms of the bidentate oxalic acid. The average Tc–P bond distance is 2.42 Å and the average Tc–O distance is 2.13 Å [530].

$[Tc^{II}(SC_6H_4\text{-}4\text{-}Cl)_2(dmpe)_2]^0$ was obtained as both *cis* and *trans* isomer when *trans*-$[Tc^{V}O(OH)(dmpe)_2][PF_6]_2$ was reacted in ethanol with 4-chlorobenzenethiol in the presence of a small amount of NaOH. The Tc(V) cation is both reduced and ligated by excess thiol. Red-black *cis*-$[Tc(SC_6H_4\text{-}4\text{-}Cl)_2(dmpe)_2]^0$ crystallizes in the orthorhombic space group *Iba2* with a=10.4840(14), b=16.505(2), c=17.783(4) Å, and Z=4. The Tc atom resides in a roughly octahedral coordination. The thiolate ligands are mutually *cis*, which is an unusual configuration for $[TcX_2D_2]^{+/0}$ complexes when X is a halide or a pseudohalide ligand and D a chelating diphosphine or diarsine ligand. The Tc–S bond distance is 2.424(3) Å, the Tc–P (*trans* to P) distance is 2.385(2) Å, while the Tc–P (*trans* to S) distance of 2.439(3) Å is lengthened. Red *trans*-$[Tc(SC_6H_4\text{-}4\text{-}Cl)_2(dmpe)_2]^0$ crystallizes in the monoclinic space group $P2_1/c$ with a=9.882(2), b=15.311(3), c=10.285(2) Å, β=96.226(12)°, and Z=2. The ligand arrangement is *trans* octahedral. The bite angle of dmpe induces some distortion. The Tc–S and Tc–P distances are 2.424(2) and 2.397(2) Å, respectively. The isolation of the *trans* isomer is difficult because of its rapid isomerization to the more stable *cis* form. The half-life of this *trans-cis* isomerization in CH_2Cl_2 is about 74 min at room temperature. Cyclic voltammetry reveals a reversible Tc(II)/Tc(III) redox couple for *cis*-$[Tc(SC_6H_4\text{-}4\text{-}Cl)_2(dmpe)_2]^0$ at –0.182 V *vs* the Ag/AgCl electrode [531].

The phenylthiolate-diarsine complex *trans*-$[Tc^{II}(SC_6H_5)_2(diars)_2]^0$ was prepared by reaction of *trans*-$[Tc^{V}O(OH)(diars)_2][PF_6]_2$ with excess HSC_6H_5 in ethanol, similarly to the preparation of $[Tc(SC_6H_4\text{-}4\text{-}Cl)_2(dmpe)_2]^0$. The blue-purple *trans*-$[Tc(SC_6H_5)_2(diars)_2]^0$ crystallizes also in the monoclinic space group $P2_1/c$ with a=12.406(2), b=14.924(3), c=9.848(2) Å, β=108.62(2), and Z=2. The arrangement of the donor atoms is approximately octahedral. The bite angle of the diars ligand is 83.02(2)°. The Tc–S bond forms an angle of 83.3(9)° with the basal coordination plane defined by the four As atoms. The Tc–As bond lengths average 2.471(2) Å. The Tc–S bond distance is 2.410(2) Å. Concomitantly with the preparation of *trans*-$[Tc(SC_6H_5)_2(diars)_2]^0$, dark green *cis*-$[Tc(SC_6H_5)_2(diars)_2]^0$ is reported to be formed, but was not isolated from solution due to its high solubility. No interconversion of the *trans* to the *cis* isomer was observed [463].

The red-brown complex salt $[Tc^{II}\{(CH_3)_2NCSS\}(depe)_2][PF_6]$, containing dimethyldithiocarbamate, was obtained by reacting *trans*-$[Tc^{V}O(OH)(depe)_2][PF_6]_2$ with sodium dimethyldithiocarbamate and form-amidine sulphinic acid as a reductant in an alkaline ethanol/water mixture. Similarly, the analogous diethyldithiocarbamate and pentamethylenedithiocarbamate complexes were synthesized. $[Tc^{II}\{(CH_3)_2NCSS\}(depe)_2][PF_6]$ crystallizes in the orthorhombic space group $Pca2_1$ with a=19.626(5), b=10.854(1), c= 16.725(2) Å, and Z=4. Within the constraints of the chelate bite

angles, the Tc atom resides in an octahedral arrangement (Fig. 12.79.A). The $(CH_3)_2NCSS^-$ bite angle is 71.5(1)°, the depe bite angles are almost identical, at 81.8(1)° and 81.9(1)°. The Tc–S bond distances average 2.449(6) Å, the Tc–P distances 2.43(2) Å when the *trans* ligand is a phosphine, and 2.38(2) Å when the *trans* ligand is the dithiocarbamate. Cyclic voltammograms for the dithiocarbamate (dtc) complexes reveal two reversible redox couples,

$$[Tc^{II}(dtc)(depe)_2]^+ + e^- \langle \underline{0.52 \text{ to } 0.54 V} \rangle [Tc^{I}(dtc)(depe)_2]^0$$

and

$$[Tc^{II}(dtc)(depe)_2]^+ \langle \underline{-0.30 \text{ to } -0.31 V} \rangle [Tc^{III}(dtc)(depe)_2]^{2+} + e^-$$

in 0.5 M $[(C_2H_5)_4N][ClO_4]$/DMF at a platinum disk electrode *vs* Ag/AgCl [532].

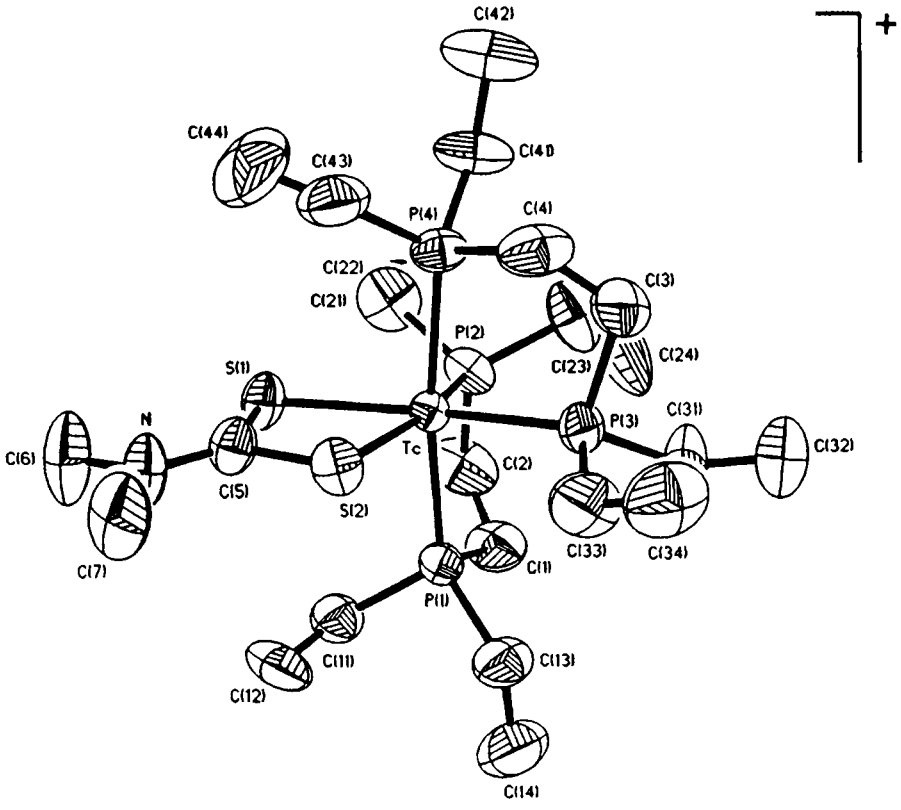

Fig. 12.79.A Dimethyldithiocarbamato-bis[1,2-bis(diethylphosphino)ethane]-technetium(II), $[Tc\{(CH_3)_2NCSS\}(depe)_2]^+$ [532].

When $[Tc^{V}O(tmtu)_4][PF_6]_3$ (tmtu = tetramethylthiourea) was reacted with dppe in DMF, brown crystals of $[Tc^{II}\{(CH_3)_2NCSS\}(dppe)_2][PF_6]$ were obtained, containing the dithiocarbamate ligand, which is reported to be produced from the bonded tetramethylthiourea in the reaction medium. $[Tc^{II}\{(CH_3)_2NCSS\}(dppe)_2][PF_6]$ crystallizes in the monoclinic space group $P2_1$ with a=11.693(8), b=19.282(7), c=12.148(6) Å, β=104.78(5)°, and Z=2. The coordination geometry of Tc(II) is a distorted octahedron. The Tc–P distances range from 2.413(6) to 2.473(6) Å. The chelate P–Tc–P angles are 81.0(2) and 81.8(2)° [116], very similar to those of $[Tc\{(CH_3)_2NCSS\}(depe)_2]^+$ described before.

A homoleptic thioether complex of Tc(II) was synthesized by reaction of $[Bu_4N]TcO_4$ with 1,4,7-trithiacyclononane (9S3) in refluxing acetone in the presence of $SnCl_2$ and $H[BF_4]$. A dark brown precipitate of $[Tc(9S3)_2][BF_4]_2 \cdot 2MeCN$ was obtained and identified. The compound crystallizes in the monoclinic space group $P2_1/c$ with a=10.961(4), b=15.284(3), c=8.554(1) Å, β=104.70(2), and Z=2. Structural characterization by X-ray diffraction established the existence of a TcS_6 core arising from two 9S3 ligands coordinated facially (Fig.12.80.A) in a tridentate fashion. The Tc–S bond lengths average 2.38 Å. Torsional angles of 9S3 itself indicate minimal deviation from those found in the free ligand. The magnetic moment μ_{eff} = 1.8 B.M. at 310 K is consistent with that expected for a low-spin d^5 system with minimal orbital contribution. Controlled-potential electrolyses afforded the analogous pale yellow Tc(III) complex and the cherry-red air-stable Tc(I) complex [533].

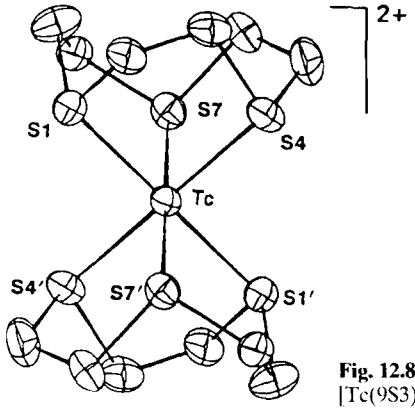

Fig. 12.80.A Bis-(1,4,7-trithiacyclononane)-technetium(II), $[Tc(9S3)_2]^{2+}$ [533].

12.6.3 Complexes containing nitrogen heterocycles

The pyridine complex $[TcCl_2(py)_4]^{\circ}$ was obtained by reduction of $[TcCl_4(py)_2]^{\circ}$, suspended in pyridine, with Zn powder. The purple compound crystallizes in the tetragonal space group $I4_1/acd$ with a=15.641(4), c=16.845(6) Å, and Z=8. The Tc atom is surrounded by a nearly perfect octahedral arrangement of donor atoms (Fig. 12.81.A). The Tc–N bond distance is 2.104(2) Å and the Tc–Cl distance 2.407(1) Å. The Cl–Tc–N angles of 90.5(1)° are almost right angles and the Cl–Tc–Cl (180.0°) and N–Tc–N

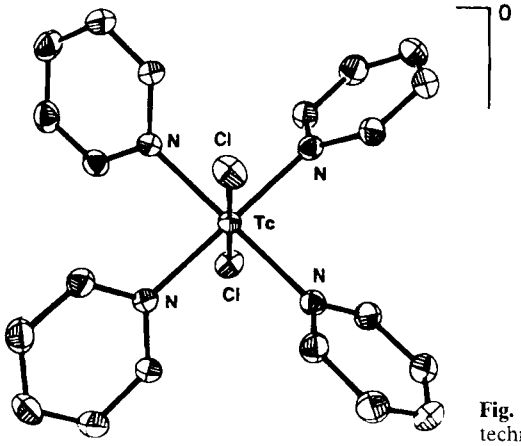

Fig. 12.81.A *Trans*-dichloro-tetrakis(pyridine)-technetium(II), $[TcCl_2(py)_4]^\circ$ [433].

(178.9°) angles are linear or nearly linear. $[TcCl_2(py)_4]^\circ$ exhibits in N,N′-dimethylacetamide (DMAC) reversible redox potentials for the Tc(II)/ Tc(III) and Tc(II)/Tc(I) couples of –0.38 and –1.33 V *vs* NHE, respectively [433].

The homoleptic 2,2′-bipyridine complex cation $[Tc(bpy)_3]^{2+}$ was prepared by reaction of the frequently used precursor $[TcCl_3(PPh_3)_2(MeCN)]^\circ$ with an excess of bpy in dry refluxing methanol. The deep blue compound $[Tc(bpy)_3][PF_6]_2$ crystallizes in the trigonal space group $P\bar{3}c1$ with a=10.847(2), c=16.299(3) Å, and Z=2. $[Tc(bpy)_3]^{2+}$ reveals exact D_3 symmetry. The Tc–N bonds are equivalent by symmetry with a distance of 2.077(10) Å. The main distortions from regular octahedral coordination are a result of the N–Tc–N bite angle of 76.2(4)° in the chelate ring. The cyclic voltammogram indicated three diffusion-controlled reversible one-electron reduction processes for $[Tc(bpy)_3]^{2+}$ in 0.2 M $[NBu_4][BF_4]$ in MeCN at $E_{1/2}$ of –0.34, –1.36, and –1.70 V *vs* SCE leading formally from Tc(II) to Tc(-I) [281,410]. The EPR spectrum of $[Tc(bpy)_3][PF_6]_2$ was measured in acetone at 130 K. In the trigonally distorted octahedral ligand field the unpaired electron occupies the d_{xy} orbital. From the ^{99}Tc hyperfine spectrum a considerable covalent Tc–bpy interaction is expected [534].

The mixed-ligand 2.2′-bipyridine complex *cis*(Cl),*trans*(P)-$[TcCl_2(PMe_2Ph)_2(bpy)]^\circ$ was obtained as a green precipitate, when *mer*-$[TcCl_3(PMe_2Ph)_3]^\circ$ was reacted with excess bpy in refluxing ethanol and aqueous NaOH was added. Similarly, blue-purple *cis*(Cl),*trans*(P)-$[TcCl_2(PMe_2Ph)_2(phen)]^\circ$ was synthesized, using 1,10-phenanthroline instead of 2,2′-bipyridine. The phenanthroline containing complex crystallizes in the tetragonal space group $P4_12_12$ with a=10.666(2), c=24.610(4) Å, and Z=4. Tc(II) resides in a distorted octahedral environment and lies on a crystallographic two-fold axis that bisects the Cl–Tc–Cl angle. Both chlorine atoms are *trans* to the nitrogen atoms of the phen ligand. The Tc–P distance of 2.391(2) Å is significantly shorter than the Tc(III)–P distance of 2.461(1) Å in *cis*(Cl),*trans*(P)-$[TcCl_2(PMe_2Ph)_2$ (phen)]$^+$ as a result of the greater π-back-bonding interactions in the lower oxidation state. The same applies to the shorter Tc(II)–N bond distance of 2.086(7) Å. But the Tc(II)–Cl distance of 2.435(3) Å is longer than the Tc(III)–Cl distance because the linkage is

dominated by electrostatic interactions. The P–Tc–P angle is 173.9(1)°, the N–Tc–N angle 78.2(4)°, and the Cl–Tc–Cl angle 95.8(1)° [535].

The 2,2′:6′,2″-terpyridine (terpy) containing compound *trans*(P)-[$TcBr(PMe_2Ph)_2$(terpy)]SO_3CF_3 was prepared by reaction of $[TcBr_3(PMe_2Ph)_3]^\circ$ with excess terpy in ethanol and addition of $NaSO_3CF_3$. The analogous complexes *trans*(P)-$[TcCl(PMe_2Ph)_2(terpy)][SO_3CF_3]$ and *trans*(P)-$[TcCl(PEtPh)_2(terpy)][PF_6]$ were synthesized similarly. The green *trans*(P)-$[TcBr(PMe_2Ph_2)_2(terpy)][SO_3CF_3]$ crystallizes in the orthorhombic space group $P2_12_12_1$ with a=18.975(3). b=19.336(4), c=9.615(1) Å, and Z=4. The coordination geometry of Tc(II) is again distorted octahedral. The equatorial positions are occupied by the three nitrogen atoms of terpy and one bromine atom. The Tc–Br distance is 2.558(8) Å, and the average Tc–P distance 2.399 Å. The shortest Tc–N bond length is 2.004(8) Å [535]. $[TcCl(PMe_2Ph)_3(bpy)]^+$ was synthesized by reacting $[TcCl_2(PMe_2Ph)_2(bpy)][PF_6]$ with excess PMe_2Ph in refluxing methanol and was isolated as the $[PF_6]^-$ salt in dark needles. In addition the neutral, 2,2′-bipyrimidine (bpm) containing complex $[TcCl_2(PMe_2Ph)_2(bpm)]^\circ$ was obtained as a dark microcrystalline solid, when $[TcCl_3(PMe_2Ph)_3]^\circ$ was reacted with bpm in refluxing methanol (435).

The formal redox potentials $E_{1/2}$ of some Tc(II) complexes determined by cyclic voltammetry are given in Table 12.17.A. The $E_{1/2}$ values were calculated from the average of the anodic and cathodic peak potentials, $E_{1/2} = (E_{p,a}+E_{p,c})/2$. The potentials were measured with a platinum disk electrode *vs* SCE in acetonitrile containing 0.1 M $[(C_2H_5)_4N][ClO_4]$.

Table 12.17.A. Formal redox potentials of Tc(II) complexes [536].

Complex	Tc(IV)/Tc(III) $E_{1/2}$ [V]	Tc(III)/Tc(II) $E_{1/2}$ [V]	Tc(II)/Tc(I) $E_{1/2}$ [V]
$[TcBr_2(PMe_2Ph)_2(bpy)]^\circ$	1.044	–0.049	–
$[TcCl_2(PEtPh_2)_2(bpy)]^\circ$	1.080	–0.077	–
$[TcCl_2(PMe_2Ph)_2(bpy)]^\circ$	1.033	–0.128	–
$[TcCl_2(PMe_2Ph)_2(phen)]^\circ$	1.039	–0.130	–
$[TcCl_2(PMe_2Ph)_2(Me_2bpy)]^\circ$	0.965	–0.189	–
$[TcCl(PEtPh_2)_2(terpy)]^+$		0.491	–1.072
$[TcBr(PMe_2Ph)_2(terpy)]^+$	–	0.467	–1.067
$[TcCl(PMe_2Ph)_2(terpy)]^+$	–	0.440	–1.123

As a rule, analogous complexes containing bromide instead of chloride are easier to reduce and harder to oxidize, because bromide is a better π-acceptor ligand than chloride and is thus better able to stabilize lower oxidation states. Furthermore, analogous complexes containing $PEtPh_2$ instead of PMe_2Ph are again easier to reduce and more difficult to oxidize, because the more phenyl-substituted phosphines are better π-acids that stabilize lower oxidation states [536].

The 1,10-phenanthroline cation $[Tc^{II}(phen)_3]^{2+}$ was incidentally reported to have been obtained by reaction of $[TcCl_3(MeCN)(PPh_3)_2]^\circ$ with excess phen in refluxing

methanol [537,538]. $[Tc(phen)_3]Cl_2$ was synthesized by reduction of NH_4TcO_4 with $NaBH_4$ in isopropanol/water in the presence of excess phen and NaCl. The violet compound was identified by a FAB mass spectrum. The magnetic moment μ_{eff}=1.89 B.M. at 295 K is in good agreement with the spin-only moment for one unpaired electron. The VIS spectrum displays well defined bands of decreasing intensity at 615, 560(sh), 495, and 403 nm [539].

When the heptadentate Schiff-base ligand tris{4-(2-pyridyl)-3-aza-3-butenyl}amine (tren-py_3), which is formed by condensation reaction between tris(2-aminoethyl)amine and 2-pyridinecarboxaldehyde, was refluxed in methanol with $[TcCl_3(PPh_3)(CH_3CN)]^\circ$, a purple fraction was obtained. Addition of $Na[PF_6]$ gave purple crystals of $[Tc(tren\text{-}py_3)][PF_6]_2$ which crystallize in the monoclinic space group $P2_1/c$ with a=15.082(1), b=10.7455(8), c=19.777(1) Å, β=110.29(1)°, and Z=4. Methanol may serve as a reducing agent. The complex cation shows a pseudo seven-coordinate capped octahedral geometry. The mean imine N–Tc distance is 2.071 Å, the mean pyridine N–Tc distance 2.109 Å, while the *tertiary* N–Tc distance is 2.933(7) Å. The N(imine)–Tc–N(imine) angles average 103°. Cyclic voltammetry shows a reversible Tc(II)/Tc(I) couple at –0.45 V *vs* Ag/AgCl in CH_2Cl_2 with 0.1 M $[Bu_4N][ClO_4]$ [540].

12.6.4 Complexes containing nitrosyl or thionitrosyl groups

The green compound *trans*-$[Tc^{II}(NH_3)_4(NO)(H_2O)]Cl_3$, the first identified nitrosyl complex of Tc(II), was prepared by oxidation of the pink complex salt *trans*-$[Tc^{I}(NH_3)_4(NO)(H_2O)]Cl_2$ [541] with Ce(IV) in 2M $HClO_4$. The magnetic moment of the Tc(II) complex was found to be μ_{eff}=1.7 B.M. at room temperature. The composition of the Tc(II) complex was confirmed by elemental analysis. The band in the IR at 1830 cm^{-1} was assigned to the N–O stretching vibration. The complex cation is stable in water only at low pH. In 3 M trifluoromethanesulphonic acid the redox potential of the Tc(II)/Tc(I) couple was measured to be –0.80 V *vs* NHE [542]. The EPR spectrum of *trans*-$[Tc^{II}(NH_3)_4(NO)(H_2O)]^{3+}$ at 77 K indicates that the Tc atom is in an octahedral environment with a tetragonal distortion [543].

The reaction of TcO_2-hydrate with NO gas at 75 °C in 4 M hydrobromic acid gave a blood-red solution from which, after addition of [*n*-Bu_4N]Br, red crystals of [*n*-Bu_4N][$Tc(NO)Br_4$] were isolated. $[Tc(NO)Cl_4]^-$ was prepared by bromide substitution. $[Tc(NO)Br_4]^-$ reacts with excess NH_4NCS in methanol to give $[Tc(NO)(NCS)_5]^{2-}$, which was isolated in ink-blue crystals of the tetrabutylammonium salt. The compounds were characterized by elemental analysis, conductivity measurements and the IR spectra, which showed the N–O stretch at 1795 cm^{-1} for nitrosyltetrabromotechnetate(II), and at 1785 cm^{-1} for the nitrosylpentaisothiocyanatotechnetate(II). A reversible one-electron couple at $E_{1/2}$=+0.14 V *vs* SCE exists in acetonitrile [544,545]:

$$[Tc^{II}(NO)(NCS)_5]^{2-} + e^- \leftrightarrow [Tc^{I}(NO)(NCS)_5]^{3-}$$

Green leaflets of [*n*-But_4N][$Tc(NO)I_4$] were obtained by reaction of the analogous bromo compound with HI in refluxing acetone [546]. The EPR hyperfine spectra of

$[n\text{-But}_4N]_2[Tc(NO)Cl_5]$, $[n\text{-But}_4N][Tc(NO)Br_4]$, $[n\text{-But}_4N][Tc(NO)I_4]$, and $[Ph_4As]_2[Tc(NO)(NCS)_5]$ in organic solvents were measured and evaluated and the formation of mixed-ligand complexes by ligand exchange reactions was studied [546,547]. The frozen acetone spectrum of $[n\text{-But}_4N][Tc(NO)I_4]$ at 130 K is characteristic for an axially symmetric, randomly oriented $S=1/2$ system. The degree of covalency of the equatorial Tc–I bonds is, as expected, higher than that in the corresponding bonds of $[Tc(NO)Cl_4]^-$ and $[Tc(NO)Br_4]^-$ [548]. $[AsPh_4]_2[Tc(NO)(NCS)_5]$, dissolved in a mixture of $CHCl_3$ and CH_2Cl_2, was studied by EPR in the liquid phase and at 120 K in the frozen glass phase. Tc(II) was again found to be in an axially symmetric environment with $g_{\parallel}=1.928$, $g_{\perp}=2.045$, $A_{\parallel}=0.0236$, and $A_{\perp}=0.0095$ cm^{-1}. The results are explained by a considerable tetragonal distortion of the complex from octahedral symmetry [549].

$[n\text{-Bu}_4N][Tc(NO)Cl_4]$ was also prepared by reaction of $[TcCl_6]^{2-}$ or $[TcOCl_4]^-$ with NH_2OH in methanol. The green crystals displayed IR absorptions at 1805 cm^{-1} for the N–O stretch and at 326 cm^{-1} for the Tc–Cl stretch [550]. Bright green crystals of $[n\text{-Bu}_4N][Tc(NO)Cl_4(CH_3OH)]$ grown from methanol/diethylether crystallize in the monoclinic space group $P2_1/n$ with $a=11.350(10)$, $b=11.450(5)$, $c=22.154(10)$ Å, $\beta=91.5(2)°$, and $Z=4$. $[Tc(NO)Cl_4(CH_3OH)]^-$ has a distorted octahedral geometry (Fig.12.82.A) with the nitrosyl and the coordinated methanol mutually *trans* and the four Cl atoms in an equatorial plane. The Tc atom resides 0.15 Å above this plane towards the nitrosyl group. The bond angles Cl(1)–Tc–Cl(2) and Cl(3)–Tc–Cl(4) are 172.5(1) and 172.8(2)°, respectively. The Tc–N–O bond angle is 175.5(10)° and the Tc–N bond distance 1.689(11) Å. The Tc–O(2) bond distance of 2.128(7) Å is probably elongated owing to the *trans* effect of the nitrosyl group [551].

When $[Tc(NO)Cl_4]^-$ in aqueous solution is heated with acetylacetone, the mixed ligand anion $[Tc(NO)(acac)Cl_3]^-$ is formed, which gives a red precipitate with $[As(Ph)_4]Cl$. $[AsPh_4][Tc(NO)(acac)Cl_3]$ crystallizes in the triclinic space group $P\bar{1}$

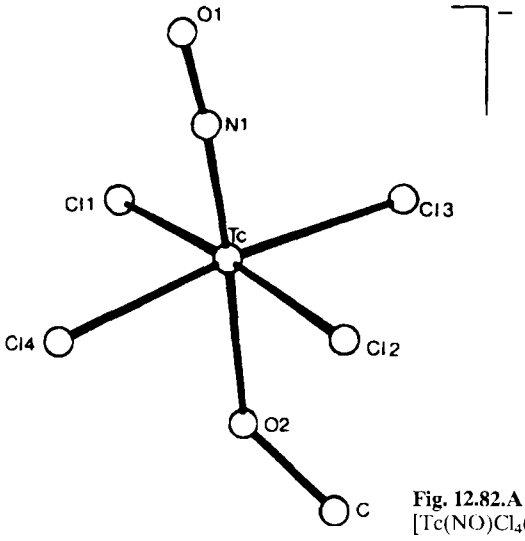

Fig. 12.82.A Tetrachloro-methanol-nitrosyl-technetate(II). $[Tc(NO)Cl_4(CH_3OH)]^-$ [551].

with a=19.261(4), b=11.261(10), c=13.686(10) Å, α=101.7(5), β=91.9(5), γ=97.3(5)°, and Z=2. The N–O stretching vibration appears at 1770 cm^{-1}. Tc(II) resides in a distorted octahedral surrounding with two Cl atoms mutually in *trans* position, the third Cl atom and the nitrosyl group are *trans* to the oxygens of the pentane-2,4-dionate ligand. The Tc–N–O bond angle is 158.6(33)°, the Tc–NO bond distance 1.74(3) Å [552,553].

$[Tc(NO)Cl_3(PMe_2Ph)_2]^\circ$ was obtained by reaction of $[TcCl_3(PMe_2Ph)_3]^\circ$ with NO in refluxing benzene. The black-green crystals melt at 175–177 °C and show N–O stretching vibrations at 1770 and 1795 cm^{-1}. The EPR spectrum of the compound in $CHCl_3$ at 27.2 K is characteristic of an axially symmetric, randomly oriented S=1/2 system with parallel and perpendicular sets of ^{99}Tc hyperfine lines. The hyperfine lines are split into well resolved triplets arising from interaction of the unpaired electron with two equivalent ^{31}P nuclei of the phosphine ligands. The hyperfine splitting shows remarkable covalent interactions [554]. $[Tc(NO)Cl_3(PPh_3)_2]^\circ$ was synthesized when nitric oxide was bubbled through a suspension of $[TcCl_3(PPh_3)_2(MeCN)]^\circ$. The dark, microcrystalline solid of $[Tc(NO)Cl_3(PPh_3)_2]^\circ$ showed an N–O stretching mode in the IR at 1805 cm^{-1} [409]. $[Tc(NO)Br_3(Me_2PhP)_2]^\circ$ was obtained by refluxing $[Tc(NO)Cl_3(Me_2PhP)_2]^\circ$ in acetone with hydrobromic acid. The green crystals of the bromo complex melt at 184–186 °C. The N–O stretch was observed in the IR at 1779 and 1794 cm^{-1}. $[Tc(NO)Br_3(Me_2PhP)_2]^\circ$ is easily soluble in organic solvents. Its EPR spectrum displays a larger extent of covalency than the corresponding chloro complex, as is expected [555].

$[Tc^{V}NCl_2(Me_2PhP)_3]^\circ$ reacts with excess S_2Cl_2 in refluxing dichloromethane to form the red thionitrosyl mixed phosphine/phosphine oxide complex $[(Tc(NS)Cl_3(Me_2PhP)(Me_2PhPO)]^\circ$, which crystallizes in the orthorhombic space group $P2_12_12_1$ with a=10.513(1), b=14.274(2), c=15.187(2) Å, and Z=4. The coordination geometry of Tc(II) is slightly distorted octahedral. The three Cl atoms are coordinated meridionally *cis* to the thionitrosyl group, the phosphine oxide ligand is arranged in *trans* position to the NS group. The Tc–N–S bond is perfectly linear. The Tc–N bond length is 1.746(5) Å. The phosphine oxide ligand is coordinated via oxygen with a Tc–O bond length of 2.097(4) Å. The Tc–P distance to the phosphine ligand is 2.464(2) Å [556].

Very recently it was reported that the compound $[Tc^{V}N(Cl)(PPhMe_2)_2\{N(SPPh_2)_2\}]^\circ$, containing the bis (diphenylthiophosphoryl)amide anion, reacts with S_2Cl_2 in CH_2Cl_2 to give *trans*-$[Tc^{II}(NS)Cl_3(PPhMe_2)_2]^\circ$. The green solid crystallizes in the triclinic space group $P\bar{1}$ with a=8.682(2), b=8.896(2), c=15.096(3) Å, α=97.78(1), β=93.04(1), γ=106.41(1)°, and Z=2. Tc(II) has again a slightly distorted octahedral environment with the phosphine ligands *trans* to each other. The Tc–NS bond distance is 1.761(4) Å. The Tc–N–S group is nearly linear with a bond angle of 176.2(3)° (Fig. 12.83.A) [271].

The thionitrosyl tetrahalogeno complex anions $[Tc(NS)Cl_4]^-$ and $[Tc(NS)Br_4]^-$ were synthesized by reaction of $[TcCl_6]^{2-}$ and $[TcBr_6]^{2-}$, respectively, with trithiazyl chloride, $(NSCl)_3$. Yellow $[Ph_4As][Tc(NS)Cl_4]$ was obtained when $[Ph_4As]_2[TcCl_6]$ was reacted with $(NSCl)_3$ in dichloromethane. The N–S stretch of the complex appeared at 1219 cm^{-1} in the IR. Red-brown $[Ph_4As][Tc(NS)Br_4]$ was obtained by

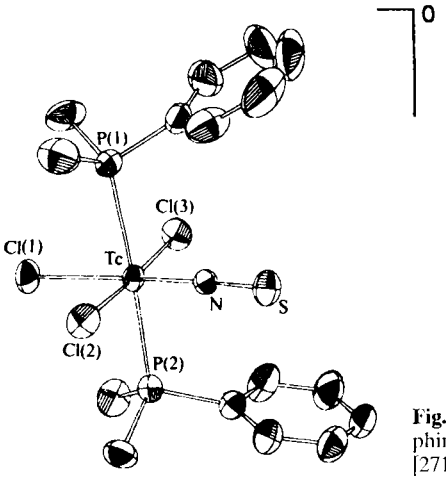

Fig. 12.83.A Trichloro-*trans*-bis(dimethylphenylphosphine)-thionitrosyltechnetium(II), $[Tc(NS)Cl_3(Me_2PhP)_2]^\circ$ [271].

reacting $[Ph_4As]_2[TcBr_6]$ with $(NSCl)_3$ in CH_2Cl_2, however, after refluxing the residue, dissolved in acetonitrile, with 40 % HBr, in order to avoid the formation of mixed chlorobromo compounds. The N–S stretching vibration was found at 1214 cm^{-1}. Reaction of $[Ph_4As][Tc(NS)Br_4]$ with NH_4SCN in acetonitrile/water yielded purple $[Ph_4As][Tc(NS)(NCS)_4]$ showing the N–S stretch at 1232 cm ^{1}. The complex salts are readily soluble in polar organic solvents, but they undergo considerable decomposition by cleavage of the N–S bond and formation of the corresponding nitrido technetium(VI) complexes $[TcNX_4]^-$. The thionitrosyl complexes were characterized by their EPR parameters [557]. Structural relationships derived from EPR spectra of nitrosyl and thionitrosyl Tc(II) complexes have been reported [558]. EPR investigations on paramagnetic technetium complexes in general were reviewed in [559].

12.6.5 Dinuclear and polynuclear complexes

The dinuclear complex of Tc(II) with the formal composition $K_2[Tc_2Cl_6]$ was obtained when $KTcO_4$ in hydrochloric acid was reduced by molecular hydrogen at about 30 atm and 140 °C in an autoclave. The dark brown crystals adopt the monoclinic space group *Cc* with a=8.287(2), b=13.956(3), c=8.664(2) Å, β=93.99(5)°, and Z=4. The polymeric $[Tc_2Cl_6]_n^{2-}$ anions consist of binuclear fragments of Tc_2Cl_8 linked by bridging chlorine atoms to infinite zigzag chains. The formula can be more informatively written as $[Tc_2Cl_4Cl_{4/2}]^2$. The rotational conformation is staggered. The structure is strongly distorted from ideal D_{4d} symmetry. Each Tc atom is surrounded by four chlorine atoms. The Tc–Tc distance [560] of 2.044(1) Å is considerably shorter than those in $[Tc_2Cl_8]^{3-}$ and $[Tc_2Cl_8]^2$. For the Tc_2^{4+} core a triple bond based on a $\sigma^2\pi^4\delta^2\delta^{*2}$ electron configuration is anticipated. When changes of δ bond order are accompanied by changes in the metal oxidation state, the Tc–Tc distance can be influenced as much or even more by the latter than the former, because δ bonding is weak.

The change in oxidation state Tc_2^{6+} to Tc_2^{4+} so enhances the σ and π bonding that a substantial contraction in the Tc–Tc distance occurs. Furthermore, the staggered rotational orientation of the chlorine atoms may allow an additional small reduction in the Tc–Tc bond distance [561].

Some ditechnetium(II) chloro phosphine complexes were synthesized by reduction of the corresponding $TcCl_4$ phosphine compounds in benzene or THF with finely divided metallic Zn:

$$2[TcCl_4(PR_3)_2]^0 \xrightarrow[6h\ sonication]{Zn/THF(benzene)} [Tc_2Cl_4(PR_3)_4]^0 + 2\,ZnCl_2$$

(PR_3 = PEt_3, PPr_3, $PMePh_2$, PMe_2Ph)

The purple, diamagnetic solids are readily soluble in aromatic solvents and dichloromethane. $[Tc_2Cl_4(PEt_3)_4]^\circ$ crystallizes in a body-centered cubic lattice of the space group $I\bar{4}3m$ with a=12.3261(1) Å and Z=2. $[Tc_2Cl_4(PMe_2Ph)_4]^\circ$ in the monoclinic space group $C2/c$ with a=17.613(5), b=9.957(5), c=23.861(6) Å, β=117.19(2)°, and Z=4, and $[Tc_2Cl_4(PMePh_2)_4]^\circ \cdot C_6H_6$ in the monoclinic space group $P2_1/c$ with a=22.910(2), b=12.286(2), c=21.550(2) Å, β=115.867(6)°, and Z=4. Each complex adopts an eclipsed Tc_2L_8 conformation with approximate D_{2d} symmetry. The Tc–Tc bond distances are 2.133(3), 2.127(1), and 2.1384(5) Å for $[Tc_2Cl_4(PEt_3)_4]^\circ$, $[Tc_2Cl_4(PMe_2Ph)_4]^\circ$, and $[Tc_2Cl_4(PMePh_2)_4]^\circ$, respectively. In the structure of $[Tc_2Cl_4(PMePh_2)_4]^\circ$ the chlorine atoms reside in clefts described by the two phenyl rings of one *cis*-phosphine and by a phenyl ring and one of the methyl groups of the other *cis*-phosphine. The average Tc–Cl bond distance is 2.372 Å, and the average Tc–P distance 2.484 Å. The Tc–Tc–Cl angles range between 109.72(3) and 113.20(3)°, and the Tc–Tc–P angles between 101.61(3) and 103.33(3)°. The complexes contain a Tc–Tc triple bond with a $\sigma^2\pi^4\delta^2\delta^{*2}$ ground-state configuration. The cyclic voltammograms of each complex indicate two reversible one-electron oxidation processes [562].

$[Tc_2Cl_4(PMe_2Ph)_4]^\circ$ readily undergoes a one-electron oxidation in acetonitrile using ferrocenium hexafluorophosphate, $[Cp_2Fe][PF_6]$, as an oxidant. A green crystalline product of the mixed-valent $[Tc_2Cl_4(PMe_2Ph)_4][PF_6]$ was isolated in three different structural forms. The monoclinic form crystallizes in the space group $P2_1/n$ with a=12.799(4), b=18.254(2), c=17.945(5) Å, β=96.39(1)°, and Z=4. The dinuclear cation adopts an eclipsed geometry (Fig. 12.84.A). The two *trans*-($TcCl_2P_2$) core fragments are rotated by 90° from each other, resulting in D_{2d} symmetry for the inner ($Tc_2Cl_4P_4$) core. The average Tc–Tc bond length of the three structural forms is 2.1074(9) Å. The mean distance is 0.02 Å shorter than that determined for $[Tc_2Cl_4(PMe_2Ph)_4]^\circ$, consistent with an increase in the bond order from 3 to 3.5. The average Tc–Cl bond length decreases by 0.06 Å from 2.394(2) to 2.333(2) Å upon oxidation, while the average Tc–P bond undergoes a slight increase in distance from 2.45(1) to 2.485(2) Å. The phenyl rings are directed away from the Tc_2 unit and lie parallel to the Tc–Tc bond. The paramagnetism of the complex was confirmed by EPR spectroscopy. The electronic spectrum of $[Tc_2Cl_4(PMe_2Ph)_4]^\circ[PF_6]$ in acetonitrile reveals a broad absorption in the near-IR at 1418 nm that is characteristic of a Tc_2^{5+} core possessing a $\sigma^2\pi^4\delta^2\delta^*$ ground state electronic configuration. This band is readily assigned to an allowed

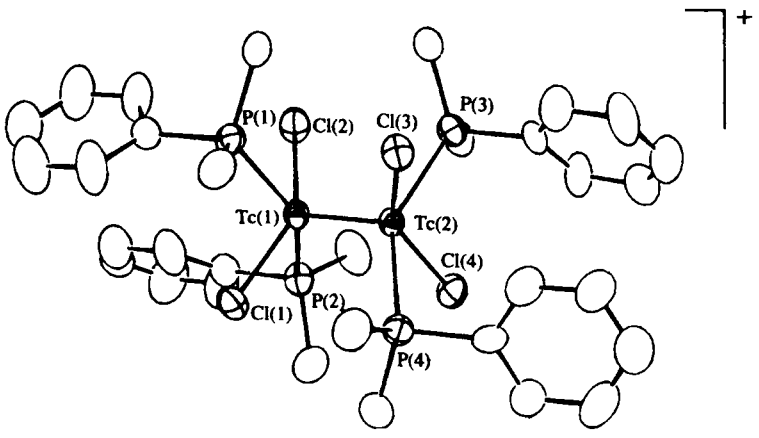

Fig. 12.84.A Tetrachlorotetrakis(dimethylphenylphosphine)-ditechnetium(II/III), $[Tc_2Cl_4(Me_2PhP)_4]^+$ [563].

$\delta \rightarrow \delta^*$ transition. One-electron oxidation of $[Tc_2Cl_4(PMe_2Ph)_4]^0$ with $[Cp_2Fe]^+$ in the presence of bis(triphenylphosphine)iminium chloride yielded the neutral, orange compound $[Tc_2Cl_5(PMe_2Ph)_3]^0$, which is also paramagnetic. It adopts the monoclinic space group $P2_1/c$ with the unit cell parameters a=11.134(1), b=14.406(1), c=19.501(5) Å, β=98.144(6)°, and Z=4. The complex is structurally similar to $[Tc_2Cl_4(PMe_2Ph)_4]^+$ and consists also of two eclipsed TcL_4 fragments. The Tc–Tc bond length is 2.1092(4) Å [563].

$[Tc_2Cl_4(PMePh_2)_4]^0$ reacts at 150–160 °C with molten diphenylformamidine (Hdpf) to produce a red solid of $[Tc_2(dpf)_4Cl]^0$. The displacement of three chlorides and the phosphine ligands is accompanied by the oxidation of the dimetal core from Tc_2^{II} to $Tc^{II}Tc^{III}$. $[Tc_2(dpf)_4Cl]^0 \cdot C_7H_8$ crystallizes in the tetragonal space group $P4/ncc$ with a=15.245(2) Å, c=21.832(3) Å, and Z=4. The structure of $[Tc_2(dpf)_4Cl]^0$ consists of four bridging formamidinate ligands. The molecule resides on a crystallographic four-fold axis that is colinear with the Tc–Tc bond. The chloride occupies an axial position at a rather short distance of 2.450(4) Å from Tc. The Tc–Tc distance of 2.119(2) Å does not vary significantly from those reported for other $Tc^{II}Tc^{III}$ compounds. Despite the presence of a partial δ bond, the two TcN_4 fragments are twisted from an eclipsed conformation by 12.8(2)°. The coordination geometry around one Tc approximates that of a square pyramid. The other Tc atom bound in addition to chloride lies at the center of a distorted octahedron. Red-purple $[Tc_2(dtf)_3Cl_2]^0$ (where Hdtf = N,N′-di-4-tolylformamidine) was obtained in a similar procedure as used for the preparation of $[Tc_2(dpf)_4Cl]^0$. The compound adopts the monoclinic space group $P2_1/n$ with a=16.185(2), b=15.637(2), c=17.812(1) Å, β=110.142(5)°, and Z=4. The fourth bridging formamidinate ligand is replaced by an equatorial chloride. The molecule maintains an essentially eclipsed conformation with the equatorial chlorides bound in a *syn* disposition. The Tc–Tc bond length of 2.0937 Å is among the shortest observed for Tc–Tc metal bonds. The six Tc–Tc–N angles are very close to 90°. The results of molecular orbital calculations support the presence of a $\sigma^2\pi^4\delta^2\delta^*$ ground

state configuration giving rise to a formal bond order of 3.5. Both compounds undergo reversible one-electron oxidation and reduction, presumably producing the respective Tc_2^{6+} and Tc_2^{4+} species [564].

When the ditechnetium(II) phosphine chloro complexes $[Tc_2Cl_4(PR_3)_4]^0$ are acidified with the strong acid $HBF_4{\cdot}Et_2O$ in a mixture of CH_3CN and CH_2Cl_2 the blue complex salt $[Tc_2(CH_3CN)_{10}][BF_4]_4$ is formed:

$$[Tc_2Cl_4(PR_3)_4]^0 \xrightarrow[CH_3CN/CH_2Cl_2]{HBF_4{\cdot}Et_2O} [Tc_2(CH_3CN)_{10}][BF_4]_4$$

This reaction takes advantage of the strong acidity of $HBF_4{\cdot}Et_2O$ to protonate the phosphine ligands forming the phosphonium salt and to convert the chloride to HCl that is removed from the reaction solution. $[Tc_2(CH_3CN)_{10}][BF_4]_4$ is readily soluble in acetonitrile and nitromethane. Its IR spectrum exhibits CN stretching vibrations at 2330 and 2302 cm^{-1}. The compound appears to be diamagnetic. It reveals in acetonitrile a reversible one-electron reduction process at $E_{1/2}$=–0.82 V *vs* Cp_2Fe/Cp_2Fe^+. $[Tc_2(CH_3CN)_8]^{4+}$ was obtained as the mixed ligand complex salt $[Tc_2(CH_3CN)_8(CF_3SO_3)_2][BF_4]_2{\cdot}CH_3CN$, which adopts the tetragonal space group $P4_12_12$ with a=12.181(2), c=27.385(3) Å, and Z=4. The structure of $[Tc_2(CH_3CN)_8]^{4+}$ consists of two $Tc(CH_3CN)_4$ fragments bound by a short Tc–Tc bond. The fragments are staggered with respect to each other resulting in a torsion angle of 43.5(1)°. The Tc–Tc bond distance is 2.122(1) Å. The axial positions of the dinuclear unit are occupied by triflate anions that are weakly bonded at a Tc–O distance of 2.414(6) Å. The mean Tc–N distance is 2.079 Å, the mean N–Tc–Tc angle 98.2° [396].

Acetonitrile solutions of $[Tc_2(CH_3CN)_{10}][BF_4]_4$, when exposed to a 1000 W Hg vapor lamp, lose their intense blue color by photodissociation of the Tc≡Tc triple bond. Irradiation into the absorption band at 616 nm appears to be responsible for the photolysis. The isolated dissociation product $[Tc(CH_3CN)_6][BF_4]_2$ of salmon color crystallizes in the monoclinic space group $P2_1/c$ with a=8.1750(9), b=8.3775(7), c=16.256(2) Å, β=92.058(5)°, and Z=2. The Tc atom is ligated by six acetonitrile ligands in an octahedral arrangement. The Tc–N bond distance is 2.062(4) Å and the N–Tc–N angles are in the range of 88.8 to 92.1°. The C≡N vibrational modes appear in the IR at 2280 and 2319 cm^{-1}. The magnetic moment of $[Tc(CH_3CN)_6][BF_4]_2$ in solution is γ_{eff}=2.1 B.M. Cyclic voltammograms in acetonitrile exhibit a reversible reduction at –0.81 V *vs* Cp_2Fe corresponding to the Tc(II)/Tc(I) redox couple [565].

More recently the reduction of $[Tc_2(CH_3CN)_{10}][BF_4]_4$ in acetonitrile by cobaltocene (Cp_2Co) yielded the Tc(I)–Tc(II) mixed valence compound $[Tc_2(\mu,\eta^1,\eta^2\text{-}CH_3CN)(CH_3CN)_{10}][BF_4]_3$ as a red-brown solid. The two Tc centers are reported to be linked together via a μ,η^1,η^2-acetonitrile ligand. $[Tc_2(\mu,\eta^1,\eta^2\text{-}CH_3CN)(CH_3CN)_{10}][BF_4]_3$ is readily soluble in acetonitrile and is air sensitive in both solution and the solid state. There are two crystallographically distinct Tc_2^{3+} cations in which the two Tc atoms are bridged by an acetonitrile molecule that is bonded to one Tc center via the lone pair on the nitrogen atom and to the second atom in an η^2 fashion using the filled π-orbitals of the C–N triple bond. Both Tc atoms reside in quasi-octahedral environments. The Tc–Tc distances of 4.047(2) and 4.028(1) Å preclude any metal–metal bonding interactions. The two $Tc(CH_3CN)_5$ fragments are in staggered conformation with an estimated torsion angle of

54.3(3)°. $[Tc_2(\mu,\eta^1,\eta^2\text{-}CH_3CN)(CH_3CN)_{10}][BF_4]_3 \cdot 0.83\,CH_3CN$ crystallizes in the triclinic space group $P\bar{1}$ with a=12.658(4), b=16.513(4), c=19.495(6) Å, α=90.21(2), β=99.33(3), γ=90.18(3)°, and Z=4. The IR absorption at 1822 cm^{-1} was assigned to the CN stretching vibration of the μ,η^1,η^2-nitrile ligand [566].

Polynuclear complexes of low valent technetium have been extensively studied by Russian researchers. Halogeno complexes are selectively compiled in Table 12.18.A. The compounds were prepared by reduction of $HTcO_4$ in conc. hydrogen halide solutions with molecular hydrogen under a pressure of 3–5 MPa at 140–220 °C [567].

Structural data of Tc(II) complexes are reviewed in Table 12.19.A.

Table 12.18.A. Selected polynuclear halogeno complexes of low valent technetium [567,568].

Complex	Tc cluster geometry	Tc–Tc multiple bond distance [Å]	References
$[Tc_6(\mu\text{-}Cl)_6Cl_6]^{-}$	trig. prism.	2.16	[569–571]
$[Tc_6(\mu\text{-}Cl)_6Cl_6]^{2-}$	trig. prism.	2.22	[570,571]
$[Tc_6(\mu\text{-}Br)_6Br_6]^{0}$	trig. prism.	2.19	[572]
$[Tc_6(\mu\text{-}Br)_6Br_6]$	trig. prism.	2.15	[572]
$[Tc_6(\mu\text{-}I)_6I_6]$	trig. prism.	2.17	[573]
$[Tc_8(\mu\text{-}Br)_8Br_4]^{0}$	tetrag. prism.	2.15	[574,575]
$[Tc_8(\mu\text{-}Br)_8Br_4]^{-}$	tetrag. prism.	2.15	[574–576]
$[Tc_8(\mu\text{-}Br)_4(\text{-}I)_4Br_2I_2]^{0}$	tetrag. prism.	2.16	[577]
$[Tc_6(\mu_3\text{-}Br)_5Br_6]^{2-}$	octah.	–	[574,575,578]

Table 12.19.A. Some structural data of selected Tc(II) complexes.

Complex	Geometry	Tc–L [Å]	μ_{eff} [B.M.]	References
12.6.1				
$[TcBr_4]^{2-}$	tetrah.	2.401	–	[280,281]
trans-$[TcCl_2(dppe)_2]^{0}$	octah.	2.428 (Tc–P) 2.424 (Tc–Cl)	2.05	[399]
trans-$[Tc(NCS)_2(dppe)_2]^{0}$	octah.	2.44 (Tc–P) 2.04 (Tc–N)	–	[397,528]
trans-$[TcCl_2(PMe_2Ph)_2(dmpe)]^{0}$	octah.	2.399 (Tc–P)(dmpe) 2.435 (Tc–P)(PMe_2Ph) 2.431 (Tc–Cl)	–	[529]
trans-$[TcCl_2\{C_6H_5P(OC_2H_5)_2\}_4]^{0}$	octah.	2.41 (Tc–P) 2.41 (Tc–Cl)	1.4	[411]
trans-$[TcX_2(diars)_2]^{0}$ (X=Cl,Br,I)	octah.	–	1.9–2.1	[79,412]
12.6.2				
$[Tc(ox)(dppe)_2]^{0}$	octah.	2.42 (Tc–P) 2.13 (Tc–O)	paramag.	[530]

Table 12.19.A. Continued.

Complex	Geometry	Tc-L [Å]	μ_{eff} [B.M.]	References
cis-[Tc(SC_6H_4-4-Cl)$_2$(dmpe)$_2$]$^{\circ}$	octah.	2.424 (Tc–S)	–	[531]
trans-[Tc(SC_6H_4-4-Cl)$_2$(dmpe)$_2$]$^{\circ}$	octah.	2.424 (Tc–S) 2.397 (Tc–P)	–	[531]
trans-[Tc(SC_6H_5)$_2$(diars)$_2$]$^{\circ}$	octah.	2.410 (Tc–S) 2.471 (Tc–P)	–	[463]
[Tc{$(CH_3)_2$NCSS}(depe)$_2$]$^{+}$	octah.	2.449 (Tc–S)	–	[532]
[Tc{$(CH_3)_2$NCSS}(dppe)$_2$]$^{+}$	octah.	2.439–2.448 (Tc–S) 2.413–2.473 (Tc–P)	–	[116]
[Tc(9S3)$_2$]$^{2+}$	trig.bipyr.	2.38 (Tc–S)	1.8	[533]
12.6.3				
trans-[$TcCl_2(py)_4$]$^{\circ}$	octah.	2.104 (Tc–N) 2.407 (Tc–Cl)	–	[433]
[Tc(bpy)$_3$]$^{2+}$	octah.	2.077 (Tc–N)	paramag.	[410]
[$TcCl_2(PMe_2Ph)_2$(phen)]$^{\circ}$ *cis*(Cl), *trans*(P)	octah.	2.391 (Tc–P) 2.086 (Tc–N) 2.435 (Tc–Cl)	–	[535]
trans(P)-[$TcBr(PMe_2Ph)_2$(terpy)]$^{+}$	octah.	2.399 (Tc–P) 2.558 (Tc–Br)	–	[535]
[Tc(phen)$_3$]$^{2+}$	octah.	–	1.89	[539]
[Tc(tren-py$_3$)]$^{2+}$	octah.	2.071 (Tc–N_{imine}) 2.109 (Tc–N_{py})	–	[540]
12.6.4				
[Tc(NO)$(NH_3)_4(H_2O)]^{3+}$	octah.	–	1.7	[543]
trans(NO)-[Tc(NO)$Cl_4(CH_3OH)]^{-}$	octah.	1.689 (Tc–N) 2.128 (Tc–O)	–	[551]
trans(NO)-[Tc(NO)(acac)$Cl_3]^{-}$	octah.	1.74 (Tc–N)	–	[552,553]
trans(NS)-[Tc(NS)$Cl_3(Me_2PhP)$ $(Me_2PhPO)]^{\circ}$	octah.	1.746 (Tc–N) 2.097 (Tc–O) 2.464 (Tc–P)	–	[556]
12.6.5				
$[Tc_2Cl_6]_n^{2-}$	polym. chain, staggered, D_{4d}	2.044 (Tc–Tc)	–	[560,561]
$[Tc_2Cl_4(PMePh_2)_4]^{\circ}$	D_{2d}, eclipsed	2.1384 (Tc–Tc) 2.372 (Tc–Cl) 2.484 (Tc–P)	–	[562]
$[Tc_2Cl_4(PMe_2Ph)_4]^{+}$	D_{2d}, eclipsed	2.1074 (Tc–Tc) 2.333 (Tc–Cl) 2.485 (Tc–P)	paramag.	[563]
$[Tc_2Cl_5(PMe_2Ph)_3]^{\circ}$	eclipsed	2.109 (Tc–Tc) 2.33–2.35 (Tc–Cl) 2.46–2.48 (Tc–P)	paramag.	[563]

Table 12.19.A. Continued.

Complex	Geometry	Tc-L [Å]	μ_{eff} [B.M.]	References
$[Tc_2(dpf)_4Cl]^+$	eclipsed	2.119 (Tc–Tc) 2.450 (Tc–Cl) 2.111 (Tc–N)	–	[564]
$[Tc_2(CH_3CN)_8(O_3SCF_3)_2]^{2+}$	D_{4d}, staggered	2.122 (Tc–Tc) 2.079 (Tc–N)	diamag.	[396]
$[Tc(CH_3CN)_6]^{2+}$	octah.	2.062 (Tc–N)	2.1	[565]
$[Tc_2(\mu.\eta^1,\eta^2\text{-}CH_3CN)(CH_3CN)_{10}]^{3+}$	octah. staggered	4.028–4.047 (Tc–Tc)	–	[566]

12.7 Technetium(I)

In spite of the expected sensitivity of Tc(I) complexes to oxidation, a surprisingly great number of compounds has been synthesized and identified. In particular the numerous carbonyl containing complexes are remarkable. Most of the known technetium carbonyl compounds appear in the oxidation state +1. In addition many isonitrile and nitrosyl complexes have been prepared and characterized. The prevailing coordination geometry is the distorted octahedron resulting in diamagnetism of the low-spin d^6 compounds. The striking stability of many hexa-coordinate Tc(I) compounds may be understandable when one considers the 18-electron rule that also explains the stability of the interesting diarene complexes. In cyclopentadienyltricarbonyl and related Tc(I) compounds the characteristic "piano stool" structure is observed.

12.7.1 Cyano and isonitrile complexes

Potassium hexacyanotechnetate(I), $K_5[Tc(CN)_6]$, was obtained by reducing an aqueous solution of TcO_2-hydrate in conc. KCN with potassium amalgam under rigorous exclusion of oxygen. The bright olive-green precipitate crystallizes in a cubic face-centered lattice with the lattice constant of 12.106 Å. The compound is isostructural with $K_5[Mn(CN)_6]$ and $K_5[Re(CN)_6]$. The lattice constant of $K_5[Re(CN)_6]$ is only 12.033 Å. The C≡N stretching vibration of $K_5[Tc(CN)_6]$ was found in the IR at 1950 cm^{-1}. In aqueous solution the complex shows an absorption in the visible at 810 nm, which disappeared rapidly by oxidation of the solution in air [579,580]. The Raman and IR spectra of $K_5[Tc(CN)_6]$ were recorded in the range 4000 to 40 cm^{-1}. The calculation of the force constants was based on the generalized valence force field. The low C≡N valence force constants indicate the relatively strong π-bonding character of the technetium–carbon bond. The Tc–C valence force constant was found to be 1.864 mdyne/Å [581].

Hexakis(alkylisonitrile) and hexakis(arylisonitrile) complexes of Tc(I), $[Tc(CNR)_6]^+$, were prepared by reduction of TcO_4^- in aqueous solution with $Na_2S_2O_4$ in the presence of the isonitrile ligands. White, crystalline hexakis(*tert*-butylisonitrile)technetium(I) hexafluorophosphate was obtained by refluxing a mixture of water and ethanol of pH 12 con-

taining NH_4TcO_4, *tert*-butylisonitrile and $Na_2S_2O_4$ and precipitating the complex salt with $NH_4[PF_6]$. $[Tc\{CNC(CH_3)_3\}_6][PF_6]$ is air- and water-stable and soluble in polar organic solvents [582]. The compound crystallizes in the tetragonal space group *I4/m* with a=15.841(2), c=16.899(2) A, and Z=4. The complex is almost octahedral with Tc lying on a *2/m* site symmetry. The Tc–C bond distances are 2.029(5) A. The angles around Tc(I) are nearly rectangular or linear [583]. In addition to $[Tc\{CNC(CH_3)_3\}_6][PF_6]$, the hexafluorophosphates of hexakis(methylisonitrile), hexakis(phenylisonitrile), and hexakis (cyclohexylisonitrile) were synthesized under similar conditions. The C≡N stretching modes of the complexes appear in the IR as intense absorptions between 2130 and 2040 cm^{-1}. Voltammetric studies in acetonitrile reveal a reversible one-electron oxidation at 0.82–0.88 V *vs* SCE. $[Tc(CNPh)_6][PF_6]$ is somewhat harder to oxidize, exhibiting a reversible oxidation at 1.18 V *vs* SCE [582].

Synthesis and characterization of a technetium(I) hexakis(isonitrile) complex containing a terminal methyl ester group, $[Tc\{CNC(CH_3)_2COOCH_3\}_6]^+$, was reported in work to develop new myocardial perfusion imaging agents. The cornpound was obtained in the same way as described above using excess 2-(carbomethoxy)-2-methylethylisonitrile. The octahedrally coordinated. diamagnetic complex shows a strong C≡N stretching mode at 2093 cm ^{1}. Addition of 6.5 equivalents of NaOH in methanol/H_2O produced the hydrolysis product $[Tc\{CNC(CH_3)_2COOH\}_6]^+$. Nine intermediate carboxylic acid containing species were separated and identified [584].

Hexakis(alkylisonitrile) complexes of Tc(I) are an important class of potential radiopharmaceuticals. Some ^{99}Tc NMR chemical shifts of selected $[Tc(CNR)_6]^+$ compounds are compiled in Table 12.20.A.

Table 12.20.A ^{99}Tc NMR chemical shifts of $[Tc(CNR)_6]^+$ cations in ppm *vs* the shift of $^{99}TcO_4^-$ as the reference at 0 ppm,(D_2O) [585].

Compound	Chemical shift [ppm]	Solvent
$[Tc(CNCH_3)_6]^+$	- 1916.5	CD_3OD
$[Tc(CNCH_2CH_3)_6]^+$	- 1916.4	CD_3Cl_3
$[Tc(CNCH_2CH_2CH_3)_6]^+$	- 1028.7	$CDCl_3$
$[Tc\{CNCH(CH_3)_2\}_6]^+$	- 1915.5	$CDCl_3$
$[Tc\{CNCH_2(CH)(CH_3)_2\}_6]^+$	1938.8	$CDCl_3$
$[Tc\{CNC(CH_3)_3\}_6]^+$	- 1914.0	$CDCl_3$
$[Tc\{CN(CH_2)_4CH_3\}_6]^+$	- 1930.3	$CDCl_3$
$[Tc(CNC_6H_{11})_6]^+$	- 1938.8	$CDCl_3$
$[Tc(CNC_6H_5)_6]^+$	- 1889.3	$CDCl_3$
$[Tc\{CNC_6H_3(CH_3)_2\}_6]^+$	- 1893.6	$CDCl_3$
$[Tc\{CNC(CH_3)_2COOCH_3\}_6]^+$	- 1936.6	50 % EtOH/D_2O with $CDCl_3$
$[Tc(CNCH_2COOCH_2CH_3)_6]^+$	- 1935.9	50 % EtOH/D_2O with $CDCl_3$
$[Tc(CNCH_2COOCH_3)_6]^+$	- 1936.3	50 % EtOH/D_2O with $CDCl_3$
$[Tc\{CNC(CH_3)_2COOH\}_6]^+$	1936.6	50 % EtOH/D_2O with $CDCl_3$
$[Tc\{CNCH_2C(CH_3)_2OCH_3\}_6]^+$	- 1950.3	$CDCl_3$

As would be anticipated for a quadrupolar nucleus, the more symmetric molecules produce very sharp lines [585]. In addition, the mixed ligand isonitrile complex cations $[Tc\{CNC(CH_3)_3\}_k\{CNC_6H_{11}\}_{6-k}]^+$ and $[Tc\{CNC(CH_3)_3\}_k\{CNCH_2COOC_2H_5\}_{6-k}]^+$ were obtained by refluxing $[Tc(tu)_6]Cl_3$ in methanol with mixtures of the corresponding isonitriles. Excess of thioureatechnetate(III) acts as the reducing agent. The molar ratio of the isonitrile ligands in the mixed ligand complexes was determined by the ^{99}Tc NMR spectra [586].

Several mixed ligand isonitrile complexes containing phosphines have been synthesized. *Trans*-$[Tc\{CNC(CH_3)_3\}_2(dppe)_2][PF_6]$ and *trans*-$[Tc(CNC_6H_{11})_2(dppe)_2][PF_6]$ were obtained when $[Tc^I(N_2)H(dppe)_2]^\circ$ and the corresponding isonitrile ligand were refluxed in methanol and $K[PF_6]$ dissolved in methanol was added. Colorless, diamagnetic crystals precipitated. *Trans*-$[Tc\{CNC(CH_3)_3\}_2(dppe)_2][PF_6]$ melts at 285–286 °C and exhibits C≡N stretching vibrations in the IR at 2049 and 2079 cm^{-1}, *trans*-$[Tc(CNC_6H_{11})_2(dppe)_2][PF_6]$ melts at 313–314 °C and the C≡N stretches appear at 2058 and 2115 cm^{-1} [587]. *Trans*-$[Tc\{CNC(CH_3)_3\}_2(dppe)_2][PF_6]$ can also be prepared by reaction of $[Tc(tu)_6]^{3+}$ with a mixture of $CNC(CH_3)_3$ and dppe in refluxing ethanol and precipitation with $[PF_6]^-$. The complex salt crystallizes in the triclinic space group $P\bar{1}$ with one molecule of ethanol. The lattice parameters are a=9.999(5), b=12.059(5), c=13.776(7) Å, α=113.55(2), β=92.18(3), γ=101.50(3)°, and Z=1. The coordination geometry of Tc(I) is distorted octahedral with the isonitrile ligands *trans* to each other. The Tc–C bond distance of 2.034 Å agrees well with that in $[Tc\{CNC(CH_3)_3\}_6]^+$ [583]. The Tc–C–N–C group has an almost linear arrangement. The mean Tc–P distance is 2.426 Å. *Trans*-$[Tc\{CNC(CH_3)_3\}_2(dppe)_2][PF_6]$ undergoes, in 0.2 M $[Bu_4N][BF_4]$/THF, at the Pt electrode a reversible one-electron oxidation at $E_{1/2}$ = 0.91 V *vs* SCE [588].

Reaction of NH_4TcO_4 with triphenylphosphine and *tert*-butylisonitrile in refluxing ethanol yielded $[Tc\{CNC(CH_3)_3\}_5(PPh_3)]^+$ and $[Tc\{CNC(CH_3)_3\}_4(PPh_3)_2]^+$ as a function of the molar ligand ratio. Both complexes were precipitated as hexafluorophosphate salts. The presence of a single ^1H NMR resonance in the alkyl region for $[Tc\{CNC(CH_3)_3\}_4(PPh_3)_2]^+$ points to the *trans* configuration. The IR spectra suggest that the isonitrile ligands in both compounds are linear. The reversible one-electron oxidation of $[Tc\{CNC(CH_3)_3\}_5(PPh_3)][PF_6]$ and $[Tc\{CNC(CH_3)_3\}_4(PPh_3)_2][PF_6]$ in CH_3CN/ $[Bu_4N][ClO_4]$ was observed at 0.81 and 0.79 V *vs* SCE, respectively [589].

When *mer*-$[Tc(PMe_2Ph)_3Cl_3]^\circ$ in refluxing ethanol solution was reacted with *tert*-butylisonitrile, the complexes *trans*-$[Tc\{CNC(CH_3)_3\}_4(PMe_2Ph)_2]^+$ and $[Tc\{CNC(CH_3)_3\}_5(PMe_2Ph)]^+$ were obtained and again isolated as $[PF_6]^-$ salts. The first complex salt gives only one ^1H NMR resonance at 1.297 ppm, while the second showed two peaks at 1.390 and 1.479 ppm. Once the complexes are formed, there are no ligand exchange reactions. *Trans*-$[Tc\{CNC(CH_3)_3\}_4(PMe_2Ph)_2][PF_6]$ crystallizes in the monoclinic space group *C2/c* with a=17.933(9), b=9.878(6), c=25.675(19) Å, β=105.29(5)°, and Z=4. The geometry around the Tc atom is distorted octahedral (Fig. 12.85.A). The Tc atom is located on an inversion center. The angles around the Tc atom are close to 90 and 180°. The Tc–C distances range from 2.036(15) to 2.045(13) Å. The Tc–P bonds of 2.389(3) Å are quite short caused by the presence of multiple bonding. The isonitrile ligands are linear, the average Tc–C≡N angle is 175(1)°. $Tc\{CNC(CH_3)_3\}_5(PMe_2Ph)][PF_6]$ crystallizes in the tetragonal space group *P4/n* with a=29.561(11), c=10.614(5) Å, and Z=8. The coordination

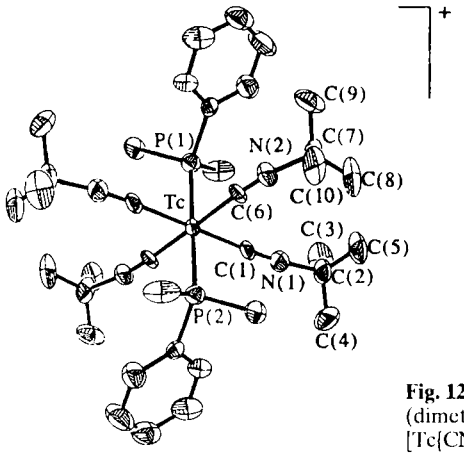

Fig. 12.85.A Tetrakis-(*tert*-butylisonitrile)-*trans*-bis (dimethylphenylphosphine-technetium (I). $[Tc\{CNC(CH_3)_3\}_4(Me_2PhP)_2]^+$ [590].

geometry of Tc is again distorted octahedral. The *trans* C–Tc–C angles are 175.6(8) and 176.3(6)°. The Tc–P bond distance is 2.403(6) Å and the Tc–C distances vary between 1.966(19) and 2.064(18) Å [590].

$[Tc\{CNC(CH_3)_3\}_4(bpy)][PF_6]$ was prepared by reaction of NH_4TcO_4, 2,2′-bipyridine, *tert*-butylisonitrile, and $Na_2S_2O_4$ in a refluxing alkaline aqueous-ethanolic solution and precipitation of the formed complex with $[PF_6]^-$. The red-orange complex salt is reported to be obtained also by irradiating a mixture of $[Tc\{CNC(CH_3)_3\}_6][PF_6]$ and 2,2′-bipyridine in acetone with ultraviolet light for some days. $[Tc\{CNC(CH_3)_3\}_4(bpy)][PF_6]$ crystallizes in the orthorhombic space group *Pbca* with a=25.060(8), b=18.717(3), c=15.769(8) Å, and Z=8. The coordination sphere is again a distorted octahedron. The most prominent feature of the structure is that one of the isonitrile ligands, which is *trans* to the bipyridine, is significantly bent at the nitrogen atom, resulting in a C–N–C angle of 148°. The remaining C–N–C angles vary between 165° and 168°. The C–Tc–C angles are close to 90 and 180°, respectively. The Tc–C bond distances range from 1.90(2) to 2.04(2) Å, while the average Tc–N_{bpy} distance is 2.16 Å. CN stretching vibrations appear at 1917, 2052, and 2137 cm^{-1}. The addional stretch can be accounted for by a lowering of symmetry due to the varying degrees of C–N–C bending. A series of other isonitrile complexes with bidentate aromatic amine ligands like $[Tc(CN\textit{tert}\text{-}Bu)_4Me_4phen][PF_6]$, $[Tc(CN\textit{tert}\text{-}Bu)_4(Me_2bpy)][PF_6]$, $[Tc(CN\textit{tert}\text{-}But)_4(phen)][PF_6]$, $[Tc(CN\textit{tert}\text{-}Bu)_4(NO_2phen)][PF_6]$, $[Tc(CN\textit{tert}\text{-}Bu)_4$ (Me-phen)$][PF_6]$, $[Tc(CNMe)_4(bpy)][PF_6]$, and $[Tc(CNmxyl)_4(bpy)][PF_6]$ (where CNmxyl = 2,6-dimethylphenyl isonitrile) were synthesized and characterized. Most of the compounds exhibit one-electron reversible oxidation waves of similar $E_{1/2}$ values at around 0.4 V *vs* SCE [591].

$[Tc(CN\textit{tert}\text{-}Bu)_3(CO)_3]NO_3$ was obtained when $[NEt_4]_2[TcCl_3(CO)_3]$ was reacted in methanol with CN*tert*-Bu and the complex cation precipitated with $[NEt_4]NO_3$. The colorless crystals of $[Tc(CN\textit{tert}\text{-}Bu)_3(CO)_3]NO_3$ adopt the orthorhombic space group *Ima2* with a=16.070(2), b=12.028(1), c=12.344(1) Å, and Z=4. Tc(I) is coordinated through a *facial* arrangement of three carbonyl and three isonitrile ligands in an almost octahedral geometry. The average Tc–CN bond distances of 2.088(3) Å are sig-

nificantly longer than in $[Tc(CN\textit{tert}\text{-}Bu)_6]^+$ of 2.029(5) Å. This finding can be explained by the stronger π-back-bonding of the CO ligands. The Tc–CO bond lengths average 1.969(3) Å. The bond angles N–C–Tc are close to 180° [592].

The hexacoordinate complexes $[Tc^I(CNR)_6][PF_6]$ readily undergo oxidative addition with X_2 (X = Cl, Br) to provide the seven-coordinate, light-yellow complex salts $[Tc^{III}(CNR)_6X][PF_6]_2$ [394].

12.7.2 Phosphine, phosphite, phosphonite, and phosphinite complexes

Excess 1,2-bis(dimethylphosphino)ethane (dmpe) reacts with TcO_4^- in alkaline ethanolic solution under rigorous conditions at 150 °C to form $[Tc(dmpe)_3]^+$ in high yield. The cation was precipitated with $[PF_6^-]$, ClO_4^-, $F_3CSO_3^-$, or F^-. The ^{99}Tc NMR spectrum with the seven-line splitting pattern is consistent with one Tc atom being bonded to six equivalent phosphorus atoms. $[Tc(dmpe)_3]^+$ is colorless, as expected for a low-spin, diamagnetic d^6 complex of π-back-bonding ligands. EXAFS (extended X-ray absorption fine structure) gives a Tc–P bond distance of 2.40 Å and a coordination number of 6 [239]. $[Tc(dmpe)_3]^+$ is reversibly oxidized to Tc(II) in non-aqueous media:

$$[Tc^I(dmpe)_3]^+ \leftrightarrow [Tc^{II}(dmpe)_3]^{2+} + e^-$$

Cyclic voltammetry on a platinum disk electrode, using 0.5 M $[NEt_4]Cl$ as a supporting electrolyte, reveals in propylene carbonate a redox potential of $E_{1/2}$ = 0.329 V *vs* Ag/AgCl. For $[Tc^I(depe)_3]^+$ the potential was found to be only 0.166 V, indicating that $[Tc(depe)_3]^+$ is considerably more easily oxidized [593]. The above electron-transfer reaction has been thoroughly studied kinetically [594–596]. Electrochemical reduction of $[Tc^{III}Cl_3(PMe_2Ph)_3]^\circ$ in acetonitrile was reported to produce $[Tc^ICl(PMe_2Ph)_3(MeCN)_2]^\circ$ [405].

$[Tc^ICl(dppe)_2]^\circ$ was prepared by reduction of $[TcCl_4(PPh_3)_2]^\circ$, suspended in benzene, with zinc powder in the presence of dppe. Dark green, air-sensitive $[TcCl(dppe)_2]^\circ \cdot C_7H_8$ crystallizes in the triclinic space group $P\bar{1}$ with a=12.920(3), b=13.115(3), c=16.091(5) Å, α=101.09(3), β=95.96(3), γ=111.85(3)°, and Z=2. The coordination geometry is a distorted trigonal bipyramid. The Tc–Cl bond distance is 2.432(2) Å. The Tc–P distances range from 2.240(2) to 2.376(2) Å. Treatment of $[TcCl(dppe)_2]^\circ$ in THF with H_2 gas results in the formation of the η^2-dihydrogen complex *trans*-$[Tc(H_2)Cl(dppe)_2]^\circ$. This reaction is completely reversible:

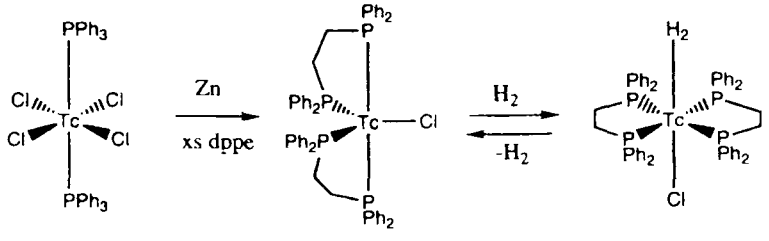

$cCl(dppe)_2]^+$ by simply heating in toluene [597].

ovides a rich chemistry and undergoes facile reactions with small

ienylacetylene is added to a solution of $[TcCl(dppe)_2]^+$ in THF, ution changed from green to orange and the neutral vinylidene $[Ph(Cl)(dppe)_2]^+$ is formed. $[Tc{=}C{=}CHPh(Cl)dppe)_2]^+ \cdot 1.5\ C_6H_6$: plates and adopts the triclinic space group $P\bar{1}$ with a=10.175(3), 35(9) Å, α=96.09(3), β=92.17(3), γ=107.80(2)°, and Z=2. The coor- of Tc is a distorted octahedron. The Tc=C bond length of ent with the assignment of a double bond. The Tc=C=C angle is 3.0(8)°. The mean Tc–P distance is 2.40 Å and the Tc–Cl distance nt of a THF solution of $[Tc{=}C{=}CHPh(Cl)(dppe)_2]^+$ with HBF_4 loss of color and the formation of the cationic carbyne complex $lppe)_2]^+$:

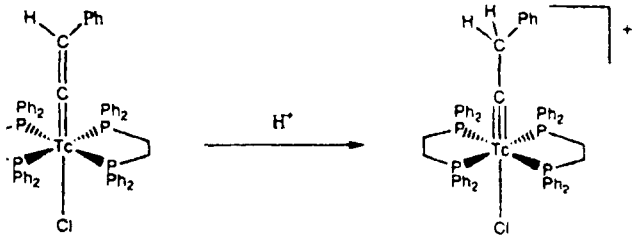

ne) distance is 1.72 Å. The carbyne complex salt $[Tc{\equiv}C\text{-}CH_2tert\text{-}_4]$ crystallizes in colorless cubes. The structure of the cation is dis- 98].

phosphine-phosphite complex $[Tc(dppe)(tmp)_4]^+$ containing tri- np). $P(OCH_3)_3$, was obtained by reaction of $[Tc(N_2)H(dppe)_2]^+$ np in refluxing methanol. Addition of $[PF_6^-]$ precipitated the col- $c(dppe)(tmp)_4][PF_6]$, which melts at 182–186 °C. The diamagnetic e in air and soluble in polar organic solvents. The ^{99}Tc NMR spec- let signal at –1664 ppm relative to TcO_4^- in D_2O [599]. The homo- thylphosphite)technetium(I) cation, $[Tc(tmp)_6]^+$, was synthesized ion of TcO_4^- with $P(OCH_3)_3$ in methanolic solution in a pressure The complex cation was precipitated as the white $[Tc(tmp)_6]$ proved to be stable in air [600]. $[Tc(tmp)_6]^+$ was also obtained as reacted in refluxing methanol with $P(OCH_3)_3$. $[Tc(tmp)_6][PF_6]$

is soluble in polar organic solvents [480]. The ^{99}Tc NMR spectrum of $[Tc(tmp)_6]^+$ in deuterated chloroform consists of a septet centered at –422 ppm *vs* TcO_4^- implying that the cation contains six equivalent P atoms coupled to Tc. The P–O bond vibrations were found in the IR at 1048 and 762 cm^{-1} [600,601].

The hexakis(dimethylphenylphosphonite)technetium(I) cation, $[Tc\{(MeO)_2PPh\}_6]^+$, was prepared by reaction of $[Tc(tu)_6]Cl_3$ with excess diisopropylphenylphosphonite in refluxing methanol. $Na[B(C_6H_5)_4]$ precipitated colorless $[Tc\{(MeO)_2PPh\}_6][B(C_6H_5)_4]$, which is air-stable and soluble in chloroform and acetone. The diamagnetic compound melts at 129–132 °C. Diisopropylphenylphosphonite is reported to be converted to dimethylphenylphosphonite during the reaction [602]. Hexakis(dimethylmethylphosphonite-technetium(I)-tetraphenylborate, $[Tc\{(MeO)_2PCH_3\}_6][B(C_6H_5)_4]$, was obtained similarly to $[Tc(tmp)_6][B(C_6H_5)_4]$ by direct reduction of TcO_4^- with excess ligand and phenylborate precipitation. The ^{99}Tc NMR chemical shift is –248 ppm *vs* TcO_4^-. In addition, the methyldiethylphophinite-technetium(I)-tetraphenylborate, $[Tc\{(MeO)PEt_2\}_6][B(C_6H_5)_4]$, was synthesized in an identical manner [601].

12.7.3 Complexes containing nitrogen ligands

When $[TcCl_3(tpy)]^\circ$ (tpy = terpyridine) suspended in dme (1,2-dimethoxyethane) was reduced with Zn dust in the presence of pyridine, *trans*-$[TcCl(tpy)(py)_2]^\circ$ was obtained. The dark violet crystals are orthorhombic, space group $C222_1$, with a=9.359(3), b=16.088(6), c=18.367(4) Å, and Z=4. The coordination geometry about Tc(I) is distorted octahedral (Fig. 12.86.A). The bite angle of terpyridine N(1)–Tc–(N(3) is only 158.2(2)°, the Tc–N(1) and Tc–N(2) bond distances are 2.075(6) and 1.915(7) Å, respectively. The Tc–Cl distance is 2.518(2) Å. The bond angles Cl–Tc–N(2) and Cl–Tc–N(4) are linear and rectangular, respectively. Cyclic voltammetry measurements in DMAC show a Tc(I)/Tc(II) redox potential of –0.82 V *vs* NHE [433].

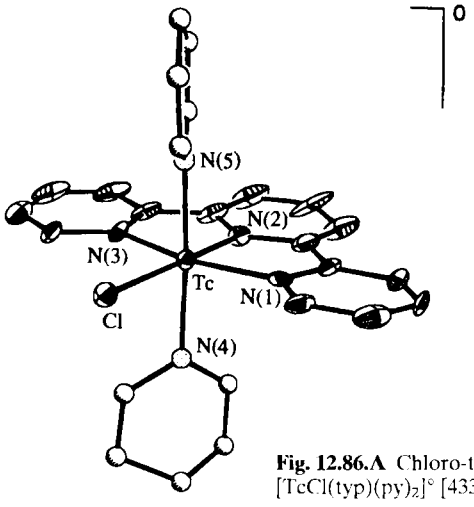

Fig. 12.86.A Chloro-terpyridine-*trans*-bis(pyridine)-technetium(I), $[TcCl(typ)(py)_2]^\circ$ [433].

Dark blue $[Tc^{I}(phen)_3]Cl$ was synthesized by controlled potential reduction of a $2 \cdot 10^{-3}$ M solution of $[Tc^{II}(phen)_3]Cl_2$ in 0.15 M NaCl under argon at a platinum cathode at −1.2 V *vs* the saturated Ag/AgCl electrode. The compound was identified by its FAB mass spectrum. The turquoise solution of $[Tc^{I}(phen)_3]^{+}$ in CH_2Cl_2 has an absorption maximum at 630 nm and is readily oxidized in air to $[Tc^{II}(phen)_3]^{2+}$ [603]:

$$[Tc(phen)_3]^{+} \leftrightarrow [Tc(phen)_3]^{2+} + e^{-}$$

Reaction of NH_4TcO_4 with excess hydralazine in dry ethanol gives the cationic tris-diazene complex $[Tc^{I}(C_8H_5N_2N{=}NH)_3]^{+}$:

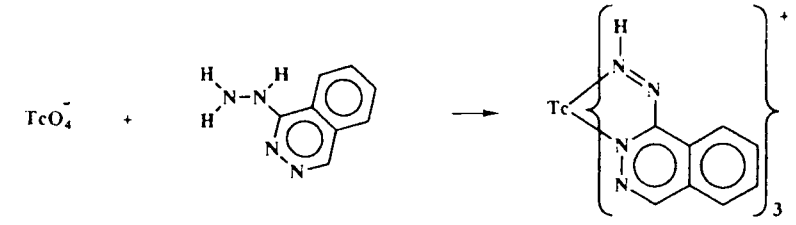

Hydralazine serves concomitantly as the reducing agent. The dark green tetraphenylborate salt is air-stable, freely soluble in ethanol, but stable in solution only in the presence of excess ligand. This property prevented recrystallization for X-ray structure analysis. The compound was characterized by FAB-MS, IR, ^{99}Tc NMR, and cyclic voltammetry [604].

The unusual, dinitrogen and hydrido hydrogen containing diphosphine complex of Tc(I), hydrido-bis-[1,2-bis(diphenylphosphinoethane)]-dinitrogen-technetium(I), $[HTc(N_2)(dppe)_2]^{\circ}$, was obtained by reduction of $[TcCl_4(PPh_3)_2]^{\circ}$ in benzene with sodium amalgam in an N_2 atmosphere and in the presence of excess dppe. The yellow, crystalline compound is air-stable for some hours and readily soluble in benzene and toluene. The strong absorption in the IR at 2046 cm^{-1} can be assigned to the N–N stretching vibration of the dinitrogen group [605]. $[HTc(N_2)(dppe)_2]^{\circ}$ crystallizes in the monoclinic space group $P2_1/n$ with a=11.090(3), b=24.550(5), c=16.379(4) Å, β=96.02(2)°, and Z=4. The Tc atom has a distorted octahedral coordination geometry (Fig. 12.87.A) with the hydrido hydrogen *trans* to the dinitrogen group. The N(1)–Tc–H(Tc) angle is 169(3)°, the Tc–N(1) distance 2.05(1) Å, the Tc–H distance 1.7(1) Å. The hydrido hydrogen atom was confirmed by ^{1}H NMR showing a shift of δ= −10.08 ppm. The four P atoms of the dppe molecules are coplanar; the average Tc–P bond distance is 2.359(7) Å [606]. $[HTc(N_2)(dppe)_2]^{\circ}$ was shown to be a starting material for synthesizing mixed ligand complexes of Tc(I), because the N_2 ligand is most labile and can be exchanged under mild conditions. The reactions proceed under nitrogen in dried solvents. $[HTc(CO)(dppe)_2]^{\circ}$ was obtained by stirring a solution of $[HTc(N_2)(dppe)_2]^{\circ}$ in benzene at room temperature under carbon monoxide. Analogous procedures produced $[HTc(C_6H_{11}CN)(dppe)_2]^{\circ}$, $HTc(tert\text{-}BuNC)(dppe)_2]^{\circ}$, and $[HTc\{(CH_3O)_3P\}(dppe)_2]^{\circ}$. Reaction of $[HTc(CO)(dppe)_2]^{\circ}$ with acetonitrile yields by substitution of the hydrido ligand the cation $[Tc(CO)(CH_3CN)(dppe)_2]^{+}$, which was precipitated as the $[PF_6]^{-}$ salt. $[HTc(tert\text{-}BuNC)(dppe)_2]^{\circ}$ reacts similarly in acet-

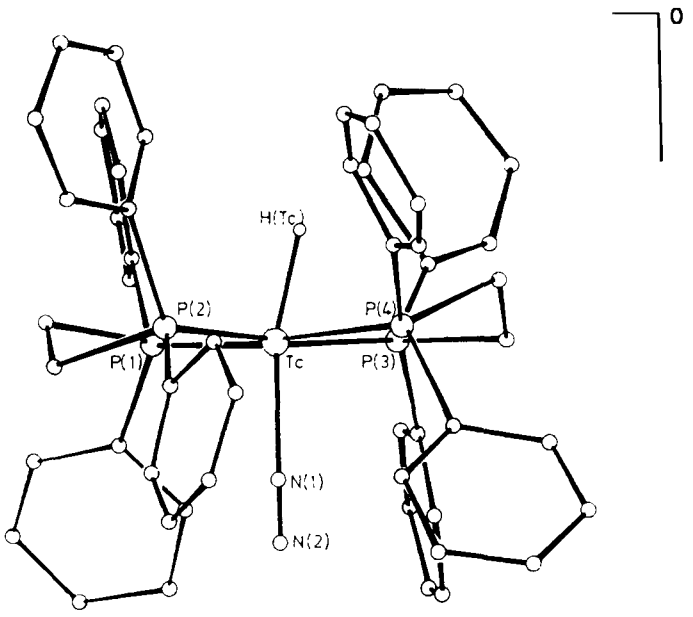

Fig. 12.87.A Hydrido-bis[1,2-bis(diphenylphosphino-ethane)]-dinitrogen-technetium(I), $[HTc(N_2)(dppe)_2]^\circ$ [606].

onitrile to form $[Tc(tert\text{-}BuNC)(CH_3CN)(dppe)_2]^+$, isolated as hexafluorophosphate. All the complexes are diamagnetic [607].

12.7.4 Complexes containing nitrosyl or thionitrosyl ligands

When $(NH_4)_2[TcCl_6]$ was reacted with 2M $NH_2OH{\cdot}HCl$, an immediate color change was observed indicating reduction of Tc(IV). To the water solution ammonia was added until the pH was 7.0. Finally, a pink microcrystalline precipitate was obtained, the formula of which was reported to be $[Tc(NH_2OH)_2(NH_3)_3(H_2O)]Cl_2$ [510]. Later on, the chemical formulation of the pink complex salt was shown to be $[Tc(NO)(NH_3)_4(H_2O)]Cl_2$ with Tc in the oxidation state +1 and with a positively charged nitrosyl group. The compound crystallizes in the monoclinic space group $P2_1/m$ with a=6.858(2), b=10.579(3), c=6.646(2) Å, β=94.01(2)°, and Z=2. The coordination geometry of Tc(I) is distorted octahedral. The Tc–N–O angle is almost linear at 178.7(2)°. The dominating role of π-bonding in the TcNO linkage is displayed in the combination of the short Tc–NO distance of 1.716(4) Å with the relatively long N–O distance of 1.203(6) Å. The Tc atom is displaced by 0.165 Å from the mean plane of the four NH_3 ligands. The four ON–Tc–NH_3 angles average 94.4°. The Tc–OH_2 bond length of 2.168(4) Å is nearly as long as the average Tc–NH_3 distance of 2.164 Å [541]. The nitrosyl group shows a stretch at 1680 cm $^{-1}$ in the IR, the low frequency indicating great stabilization by Tc→(NO) back-bonding. The compound is

diamagnetic. $[Tc(NO)(NH_3)_4(H_2O)]^{2+}$ is reversibly oxidized to $[Tc(NO)(NH_3)_4(H_2O)]^{3+}$ in trifluoromethane sulfonic acid at $E_{1/2} = -0.80$ V *vs* NHE [542].

Reduction of $[n\text{-}Bu_4N]_2[Tc^{II}(NO)(NCS)_5]$ with hydrazine or its electrochemical reduction at $E_{1/2} = 0.14$ V *vs* SCE yielded rust-colored crystals of $[n\text{-}Bu_4N]_3[Tc^{I}(NO)(NCS)_5]$, the N–O stretching vibration of which appeared in the IR at 1690 cm^{-1} [544].

$[Tc^{I}(NO)(CNCMe_3)_5][PF_6]_2$ was obtained by reaction of $[Tc^{I}(CNCMe_3)_6]NO_3$ in glacial acetic acid with conc. nitric acid and addition of $Na[PF_6]$, or by reaction with $NO[PF_6]$ in acetonitrile. The yellow needles exhibit a very strong N–O stretching vibration at 1865 cm^{-1} and two isonitrile (C≡N) stretches at 2200 and 2240 cm^{-1} in the IR. The complex is air- and water-stable and soluble in polar organic solvents. Refluxing of $[Bu_4N][Tc^{II}(NO)Br_4]$ and *tert*-butylisonitrile in methanol yielded purple $[Tc^{I}(NO)Br_2(CNCMe_3)_3]^{\circ}$, which is thermally unstable. Two C≡N stretches appear in the IR at 2230 and 2160 cm^{-1}, the N–O stretch at 1755 cm^{-1}. $[Tc(NO)Br_2(CNCMe_3)_3]^{\circ}$ crystallizes in the orthorhombic space group $P2_1cn$ with a=10.985(2), b=14.250(2), c=14.677(2) Å, and Z=4. The Tc(I) coordination is slightly distorted from octahedral geometry as the four ligands *cis* to the nitrosyl (Fig. 12.88.A) bend out of the equatorial plane away from the nitrosyl. The Tc–N–O bond angle of 175.9(1.6)° is almost linear, the Tc–NO bond length 1.726(1.5) Å. The three isonitrile ligands are coordinated meridionally. The Tc–isonitrile distance of 2.137(22) Å *trans* to the nitrosyl is considerably longer than the average Tc–C(11) and Tc–C(21) bond distances of 2.081 Å. The Tc–Br bond distances of 2.852(3) Å for Tc–Br(1) and 2.543(3) Å for Tc–Br(2)

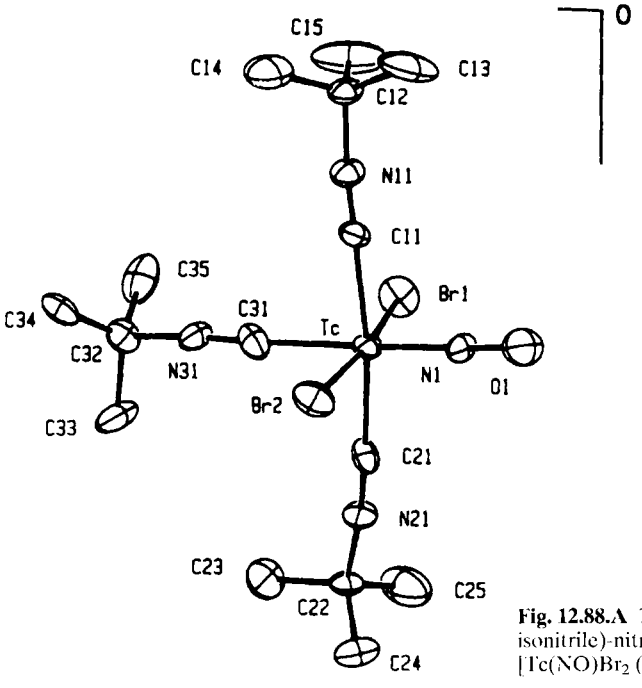

Fig. 12.88.A *Trans*-dibromo-tris(*tert*-butylisonitrile)-nitrosyl-technetium(I), $[Tc(NO)Br_2(CNCMe_3)_3]^{\circ}$ [608].

are unexceptional [608]. $[Tc(NO)Cl_2(CNCMe_3)_3]^o$ was prepared analogously to $[Tc(NO)Br_2(CNCMe_3)_3]^o$ [609].

The mixed ligand nitrosyl complex $[Tc^I(NO)Cl_2(PPh_3)_2(CH_3CN)]^o$ was synthesized by reaction of $[n\text{-}Bu_4N][Tc^{II}(NO)Cl_4]$ with excess triphenylphosphine in acetonitrile. PPh_3 acts as a reducing agent. The neutral, air-stable, yellow-orange compound is diamagnetic and only sparingly soluble in benzene or methanol. The presence of the nitrosyl moiety is confirmed by a strong absorption in the IR at 1721 cm^{-1}. ^1H NMR reveals equivalent *trans*-triphenylphosphine ligands and shows the lability of the CH_3CN ligand. Refluxing a solution of $[Tc(NO)Cl_2(PPh_3)_2(CH_3CN)]^o$ in pyridine yields $[Tc(NO)Cl_2(py)_3]^o$ with ν(NO) at 1688 cm^{-1} in the IR. Red needles of $[Tc(NO)Cl_2(py)_3]\cdot 2CH_3CN$ crystallize in the monoclinic space group *C2/c* with a=19.182(1), b=10.8725(8), c=11.9371(8) Å, β=116.580(7)°, and Z=4. The coordination of Tc(I) is in nearly octahedral geometry. The structure confirms the meridional pyridine ligand arrangement and the linearity of the NO group. The Tc–N(NO) distance is 1.781(5) Å and the average Tc–N(py) distance 2.129 A. Each pyridine is tilted 35–45° from the vertical, relative to the Tc–NO bond. Substitution reactions yielded, in addition, the compounds $[Tc(NO)Cl_2(PPh_3)_2(CH_3OH)]^o$, $[Tc(NO)Cl_2(PPh_3)_2(py)]^o$, $[Tc(NO)Cl_2(PPh_3)_2(lut)]^o$, $[Tc(NO)Cl_2(PPh_3)_2(py)_2]^o$, $[Tc(NO)Cl_2(PPh_3)(lut)_2]^o$, $[Tc(NO)Cl_2(PPh_3)(bpy)]^o$, $[Tc(NO)Cl_2(PPh_3)(phen)]^o$, $[Tc(NO)Cl_2(lut)_3]^o$, and $[Tc(NO)Cl_2(terpy)]^o$ [610]. With neutral bidentate 2-hydrazinopyridine the complex $[Tc(NO)Cl_2(HN{=}NC_5H_4N)(PPh_3)]^o$ was obtained and with anionic, bidentate 2-hydrazino-4-trifluoromethylpyrimidine the complex $[Tc(NO)Cl(N{=}NC_4H_2N_2CF_3)(PPh_3)_2]^o$ [610a].

Very recently the bis-pyridyldiphenylphosphine complex $[TcCl_2(NO)(pyPPh_2\text{-}P,N)(pyPPh_2\text{-}P)]^o$ was obtained when excess 2-pyridyldiphenylphosphine was reacted with $[Bu_4N][Tc^{II}(NO)Cl_4]$ in refluxing methanol. The yellow-brown, neutral compound crystallizes in the triclinic space group $P\bar{1}$ with a=9.8440(3), b=13.4854(5), c=14.2401(5) Å, α=106.406(1), β=96.013(1), γ=92.792(1)°, and Z=2. The coordination geometry of Tc(I) is a very distorted octahedron. The P–Tc–N bite angle is only 66.1(1)°. Unexpectedly, the phosphine ligands are in *cis*-configuration with one phosphine bonded in a monodentate manner (P) and the other bidentate (P,N). The Tc–NO bond length is 1.743(5) Å and the Tc–N–O bond angle 177.2(5)° [611].

Using the versatile starting material $[Tc(NO)Cl_2(PPh_3)_2(CH_3CN)]^o$, nitrosyl complexes of Tc(I) with sulphur-containing cores were synthesized. Isobutylxanthate reacts with the nitrosyl complex in refluxing CH_2Cl_2 to form the bright yellow $[Tc(NO)Cl(PPh_3)_2(S_2COBu^i)]^o$ or the red-orange $[Tc(NO)(PPh_3)(S_2COBu^i)_2]^o$. In analogous reactions with methylxanthate or neopentylxanthate the red-orange compounds $[Tc(NO)(PPh_3)(S_2COMe)_2]^o$ and $[Tc(NO)(PPh_3)(S_2COnPe)_2]^o$ were obtained. Reaction of $[Tc(NO)Cl_2(PPh_3)_2(CH_3CN)]^o$ with 2-mercaptopyridine (Spy) in refluxing dichloromethane and in the presence of 1,1,3,3-tetramethylguanidine as a proton sponge yielded a purple precipitate of $[Tc(NO)Cl(PPh_3)_2(Spy)]^o$ [612].

The nitrosyl-hydrido complex $[Tc(NO)(PPh_3)_3(H)_2]^o$ was synthesized by refluxing a mixture of $[Tc^{II}(NO)(PPh)_3Cl_3]^o$, PPh_3 and $Na[BH_4]$ in absolute ethanol. The diamagnetic, bright yellow precipitate was characterized spectroscopically. In the IR (NO) appeared at 1636 cm^{-1}, ν(Tc–H) at 1733 cm^{-1} and 1185 cm^{-1}. The ^1H NMR in

$C_6D_5CD_3$ showed hydride resonances at δ= –1.5 ppm and δ= –3.45 ppm. The hydride ligands are labile [613].

The 1,10-phenanthroline containing complex salt $[Tc(NO)(NH_3)(phen)_2][PF_6]_2$ was obtained by boiling NH_4TcO_4 in water containing $NH_2OH{\cdot}HCl$ and phenanthroline and adding $NH_4[PF_6]$. Brown crystals of *cis*-$[Tc(NO)(NH_3)(phen)_2][PF_6]_2{\cdot}Me_2CO$ adopt the triclinic space group $P\bar{1}$ with a=11.12(1), b=14.25(6), c=10.79(2) Å, α=90.4(2), β=107.9(1), γ=86.0(2)°, and Z=2. The coordination geometry of Tc is distorted octahedral. The Tc–NO bond distance is 1.739(9) Å, and the Tc–N–O-angle 171.9(8)°. The Tc–N(phen) distance is 2.11 Å on average, which is 0.075 Å shorter than the Tc–NH_3 bond length. The NO stretching vibration was found in the IR at 1630 cm^{-1} [614].

The thionitrosyl complex salt *cis*-$[Tc^{I}(NS)Cl(phen)_2][PF_6]$ was synthesized by refluxing $[Tc^{V}N(Cl)(phen)_2]Cl{\cdot}H_2O$ with S_2Cl_2 in chloroform and precipitation of the cation with $[PF_6]^-$. The dark brown compound crystallizes also in the triclinic space group $P\bar{1}$ with a=9.850(3), b=16.293(3), c=8.349(2) Å, α=100.06(2), β=93.84(3), γ=106.96(3)°, and Z=2. Owing to the similar sizes of the Cl^- and NH_3 ligands in $[Tc(NS)Cl(phen)_2]^+$ and $[Tc(NO)(NH_3)(phen)_2]^{2+}$, the degree of distortion from octahedral geometry around Tc(I) is quite similar. The Tc–NS and the Tc–Cl distances in $[Tc(NS)Cl(phen)_2]^+$ are 1.782(6) and 2.387(2) Å, respectively. The NS stretch appeared in the IR at 1173 cm $^{-1}$. The thionitrosyl group in Tc(I) complexes binds less strongly than the nitrosyl group [614].

$[Tc(NS)Cl_2(pico)_3]^{\circ}$ was prepared by refluxing $[Bu_4N][Tc^{VI}NCl_4]$ with $Na_2S_2O_4$ in 4-picoline. The green crystals of *mer*-$[Tc(NS)Cl_2(pico)_3]^{\circ}{\cdot}CHCl_3$ adopt the orthorhombic space group $Pna2_1$ with a=19.628(1), b=11.848(3), c=11.332(4) Å, and Z=4. The NS stretching vibration was found in the IR again at 1173 cm $^{-1}$. The core atom arrangement about Tc(I) is essentially octahedral (Fig. 12.89.A). The Tc atom is displaced by 0.096 Å toward the thionitrosyl group out of the basal plane defined by Cl(2), N(2), N(3), and N(4). The Tc–NS angle of 176(1)° is almost linear. The Tc–NS distance of 1.73(1) is 0.41 Å shorter than the Tc–N(pico) length average at 2.14(1) Å. The N–S bond distance is 1.54(1) Å. The axial Tc–Cl(1) bond distance of 2.443(1) Å is only 0.013 Å longer than the equatorial Tc–Cl(2) distance, in spite of the expected

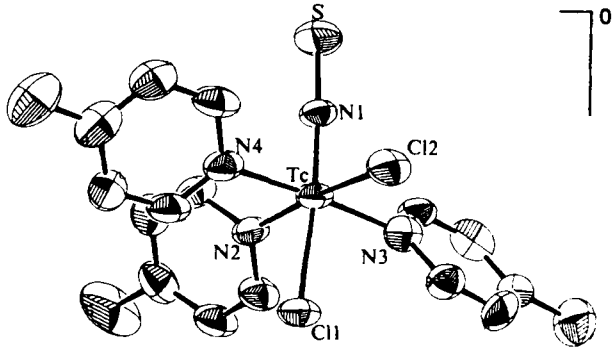

Fig. 12.89.A Dichloro-*mer*-tris(4-methylpyridine)-thionitrosyl-technetium(I), $[Tc(NS)Cl_2(pico)_3]^{\circ}$ [615].

trans effect of the thionitrosyl ligand. The compounds *mer*-$[Tc(NS)Cl_2(py)_3]^\circ$ and *mer*-$[Tc(NS)Cl_2(lut)_3]^\circ$ were similarly synthesized and characterized spectroscopically [615].

Mer-$[Tc(NS)Cl_2(Me_2PhP)_3]^\circ$ is accessible by reaction of $[Tc^{V}NCl_2(Me_2PhP)_3]^\circ$ with equimolar amounts of S_2Cl_2 in dichloromethane [556]. The red crystalline compound melts at 141–143 °C and crystallizes in the monoclinic space group $P2_1/c$ with a=9.4730(6), b=18.6904(9), c=16.1676(6) Å, β=93.467(4)°, and Z=4. The coordination geometry of Tc(I) is slightly distorted octahedral. The three phosphine ligands are coordinated meridionally *cis* to the thionitrosyl group and are bent out of the equatorial plane away from the thionitrosyl. The Tc–N–S angle is 178.8(2)°, the N–S bond length 1.548(4) Å, the Tc–N bond length 1.747(3) Å. The NS ligand again shows a negligible *trans*-effect as mentioned before for the structurally similar complex *mer*-$[Tc(NS)Cl_2(pico)_3]^\circ$. The diamagnetic $[Tc(NS)Cl_2(Me_2PhP)_3]^\circ$ reveals a ^{99}Tc NMR resonance at +645 ppm *vs* TcO_4^- and a (NS) vibration in the IR at 1177 cm^{-1} [556,616].

12.7.5 Arene complexes

The bis(benzene)technetium(I) cation $[Tc(C_6H_6)_2]^+$ was synthesized by heating $TcCl_4$, aluminum powder, $AlCl_3$, and benzene in a sealed tube at 135 °C for two days:

$$TcCl_4 + Al + 2C_6H_6 \rightarrow [Tc(C_6H_6)_2][AlCl_4]$$

After hydrolysis of the anion of $[Tc(C_6H_6)_2][AlCl_4]$, the cation was precipitated as hexafluorophosphate. The yellow-green, diamagnetic complex salt is stable in air, acids and bases [617]. Prior to the preparation of ponderable amounts, the cation was produced by irradiating *bis*(benzene)molybdenum with thermal neutrons:

$$[^{98}Mo(C_6H_6)_2]^\circ \xrightarrow{n,\gamma} [^{99}Mo(C_6H_6)_2]^\circ \xrightarrow{\beta} [^{99}Tc(C_6H_6)_2]^-$$

Taking into account the benzene π electrons, $[Tc(C_6H_6)_2]^-$ attains the electron configuration of xenon. The cation is decomposed in melting Na_2O_2 [618, 619].

Reduction of $[Tc(C_6H_6)_2][PF_6]$ in 1,2-dimethoxy-ethane with $LiAlH_4$ yields benzene-cyclohexadienyl-technetium(I), $[(C_6H_6)Tc^{I}(C_6H_7)]^\circ$. The yellow diamagnetic compound is easily soluble in hydrocarbons, the solid is air-stable only for a short time. Fig. 12.90.A shows the proposed structure that was confirmed by ^1H NMR and IR spectroscopy. The low energy frequency at 2752 cm^{-1} was assigned to the C–H(β) stretching vibration. Reaction of hexamethylbenzene-technetium(I) with $LiAlH_4$ produced the analogous, more air-stable complex $[\{C_6(CH_3)_6\}Tc^{I}\{C_6(CH_3)_6H\}]^\circ$. Its reduction with liquid lithium is reported to result in the formation of the dinuclear, neutral complex of Tc(I) $[Tc\{C_6(CH_3)_6\}_2]_2$ [620]. The cations bis(1,3,5-trimethyl-benzene)technetium(I), $[Tc\{C_6(CH_3)_3H_3\}_2]^+$, and bis(1,2,3,5-tetramethylbenzene)technetium(I), $[Tc\{C_6(CH_3)_4H_2\}_2]^+$, were obtained by reacting $NaTcO_4$ instead of $TcCl_4$ with aluminum powder, $AlCl_3$, and the corresponding methylbenzene at 135 °C. The

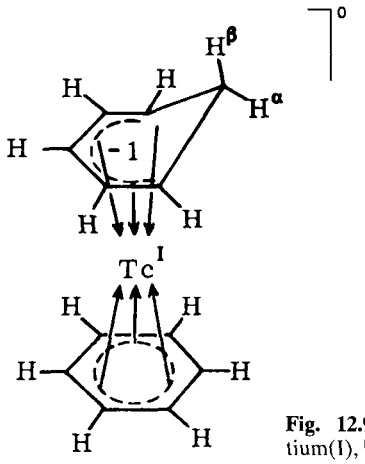

Fig. 12.90.A Proposed structure of benzene-cyclohexadienyl-technetium(I), $[(C_6H_6)Tc(C_6H_7)]^{\circ}$ [620].

complex cations were precipitated as hexafluorophosphate salts and identified by FAB-MS [621].

12.7.6 Compounds containing carbonyl ligands

The pentacarbonyl halides, $[Tc(CO)_5X]^{\circ}$, (X = Cl, Br, I) were prepared by the action of the halogens on $[Tc_2(CO)_{10}]^{\circ}$ [622] or by reaction of $K_2[TcX_6]$ with CO under a pressure of 250–270 atm at 230–250 °C in the presence of copper powder to bind the halogens [623]. To synthesize $[Tc(CO)_5Cl]^{\circ}$, $[Tc_2(CO)_{10}]$ was dissolved in CCl_4, previously saturated with Cl_2 gas at 25 °C. A mixture of $[Tc(CO)_5Cl]^{\circ}$ and $[Tc(CO)_4Cl]_2^{\circ}$ precipitated, which was entirely converted to colorless crystals of $[Tc(CO)_5Cl]^{\circ}$ by treating the mixture with carbon monoxide at a pressure of 1000 psi at 100 °C. $[Tc(CO)_5Cl]^{\circ}$ exhibits CO stretching frequencies in the IR at 1991, 2028, 2057, and 2153 cm $^{-1}$. The spectrum is in agreement with a C_{4v} structure [622]. $[Tc(CO)_5Cl]^{\circ}$ crystallizes in the orthorhombic space group *Pnma* with the lattice parameters a=11.17, b=10.98, c=5.78 Å, and Z=4 [624].

$[Tc(CO)_5Br]^{\circ}$ was prepared by replacing Cl_2 by Br_2 dissolved in CCl_4. The practically pure, colorless $[Tc(CO)_5Br]^{\circ}$ was obtained without carbon monoxide pressurization. The CO stretching bands were found in the IR at 1995, 2027, 2056, and 2150 cm^{-1} which again point to the C_{4v} molecular structure [622]. $[Tc(CO)_5Br]^{\circ}$ is isostructural with $[Tc(CO)_5Cl]^{\circ}$. The lattice constants are a=11.76, b=11.56, and c=6.10 Å [624].

The reaction of $[Tc_2(CO)_{10}]^{\circ}$ in CCl_4 solution with I_2 is extremely slow. Direct action of I_2 on $[Tc_2(CO)_{10}]^{\circ}$ at 100 °C in sealed ampules yielded the dimer $[Tc_2(CO)_4I]_2^{\circ}$ which was converted to $[Tc(CO)_5I]^{\circ}$ by high-pressure carbonylation. The diamagnetic, colorless compound absorbs in the IR at 2000, 2024, 2055, and 2146 cm^{-1}, again in agreement with C_{4v} symmetry [622]. The temperature dependence of the $[Tc(CO)_5I]^{\circ}$ vapor pressure was determined [627].

Heating the pentacarbonyl halides to 100 °C in air resulted in complete conversion to the tetracarbonyl dimers within 24 h. The monomers also were observed to lose

CO slowly when standing in solution at room temperature [622]. The conversion of $[Tc(CO)_5X]^\circ$ does not stop at $[Tc(CO)_4X]_2^\circ$, but after prolonged boiling in chlorobenzene it is said to be completely converted into $[Tc(CO)_3X]_4^\circ$:

$$[Tc(CO)_5X]^\circ \cdots [Tc(CO)_4X]^\circ \rightarrow [Tc(CO)_3X]_4$$

The tetrameric tricarbonyl halides are greenish-yellow, finely crystalline compounds adopting a cubane structure with triply bridging halides [625,626]. $[Tc(CO)_3Cl]_4^\circ$ crystallizes in the cubic space group $I\bar{4}3m$ with a=10.322(3) Å and Z=2. The structure of the Tc_4Cl_4 core can be described as a distorted cube. The shortest Tc···Tc distance is 3.84(1) Å with no direct Tc–Tc bond. The mean Tc–Cl, Tc–C, and C–O distances are 2.559(1), 1.903(3), and 1.128(4) Å, respectively. The average Tc–C–O, C–Tc–C, and Tc–Cl–Tc angles are 88.4(1), 178.6(3), and 97.23(2)°, respectively [573]. The dependence of the $[Tc(CO)_3Cl]_4^\circ$ vapor pressure on the temperature was measured [627]. Gaseous $[Tc(CO)_3Cl]_4^\circ$ absorbs at 210 °C in the IR at 2065 and 1984 cm^{-1}, $[Tc(CO)_3Br]_4$ at 250 °C at 2063 and 1982 cm^{-1} [628].

The carbonyl stretching frequencies obtained from high resolution IR spectra of the tetracarbonyl halide dimers of technetium are given in Table 12.21.A together with their assignments. The IR spectra greatly support the D_{2h} halogen-bridged structure, which was confirmed by X-ray structure analysis of $[Mn(CO)_4Br]_2^\circ$.

Table 12.21.A Carbonyl stretching frequencies [cm^{-1}] of the tetracarbonyl halide dimers of technetium, and their assignments [629,630].

Compound	$B_{3u}(a)$	B_{1u}	$B_{3u}(b)$	B_{2u}
$[Tc(CO)_4Cl]_2^\circ$	2119 (w)	2048 (s)	2011 (m)	1972 (m)
$[Tc(CO)_4Br]_2^\circ$	2116 (w)	2046 (s)	2012 (m)	1973 (m)
$[Tc(CO)_4I]_2^\circ$	2108 (w)	2042 (s)	2012 (m)	1975 (m)

A technetium tricarbonyl hydroxide $[Tc(CO)_3(OH)]_n^\circ$ was reported to be synthesized by heating $KTcO_4$ with an excess of formic acid in an autoclave at 170–180 °C for 3–4 h. The colorless compound was characterized by elemental analysis, the IR spectrum, and the X-ray powder diffraction pattern [632]. A rhenium compound of the composition $[Re(CO)_3(OH)]_4^\circ$ exhibits a similar IR spectrum and has a tetrameric structure in which the corners of a cube are formed by alternating $Re(CO)_3$ and OH groups [633].

A unique cubane-type cluster of Tc(I) is the compound $Na[Tc_3(CO)_9(OCH_3)_4]$ that was shown to be an intermediate product formed by the incomplete carbonylation of $NaTcO_4$ conducted in CH_3OH:

$$NaTcO_4 \xrightarrow[CH_3OH]{CO} Na[Tc_3(CO)_9(OCH_3)_4]$$

The reaction proceeds at a CO pressure of 90 atm and a temperature of 150 °C during 4 days. The colorless crystals are soluble in acetone, acetonitrile, and methanol. $Na[Tc_3(CO)_9(OCH_3)_4]\cdot 2CH_3CN$ crystallizes in the monoclinic space group $P2_1/n$ with

a=8.526(4), b=17.61(1), c=18.437(9) Å, β=93.93(4)°, and Z=4. The Na atom is integrated into the cubane structure. Each Tc atom is surrounded by 3 carbonyl groups and 3 oxygens of the methoxy group in a strongly distorted octahedron (Fig. 12.91.A). The relatively short Na–OCH_3 bond distances, averaging 2.39 Å, infer a strong Na–O coordination. The compound is not dissociated in methanol or acetonitrile into Na^+ and $[Tc_3(CO)_9(OCH_3)_4]^-$. The mean bond distances of Tc–O(123)(μ_3) of 2.19 Å are significantly longer than the other Tc–O bond lengths of 2.14–2.16 Å. The carbonyl C–O distance is about 1.16 Å, the Tc–CO distance 1.90 Å [634].

The reduction of $[TcOCl_4]$ or TcO_4^- with a 1 M BH_3 solution in THF and concomitant carbonylation at 1 atm of CO in diglyme/$[n\text{-}Bu_4N]Cl$ resulted in a high yield production of the dianion $[TcCl_3(CO)_3]^{2-}$ which was precipitated as colorless $[NEt_4]_2[TcCl_3(CO)_3]$. This procedure provides a novel route to synthesize a variety of Tc(I) carbonyl complexes without high CO pressure reaction conditions. The halide ligands of $[NEt_4]_2[fac\text{-}TcX_3(CO)_3]$ are readily subsituted by other ligands at ambient temperature in various solvents. Reaction of $[NEt_4]_2[TcCl_3(CO)_3]$ in THF with *tert*-butyl-isonitrile yielded yellow $[TcCl(tert\text{-}BuCN)_2(CO)_3]$°. Substitution of the third halide is apparently more difficult. $[TcCl(tert\text{-}BuCN)_2(CO)_3]$° crystallizes in the orthorhombic space group $P2_12_12_1$ with a=6.1348(4), b=9.9930(7), c=29.083(3) Å, and Z=4. The coordination geometry of Tc(I) is distorted octahedral with angles close to 180 and 90°. Chloride and *tert*-BuCN are *trans* to CO. The mean Tc–CO distance is 1.93 Å, the mean Tc–CN distance 2.10 Å, and the Tc–Cl distance 2.496(2) Å. The sulphur macrocycle 1,4,7-trithiacyclononane substitutes all three chlorides of $[TcCl_3$

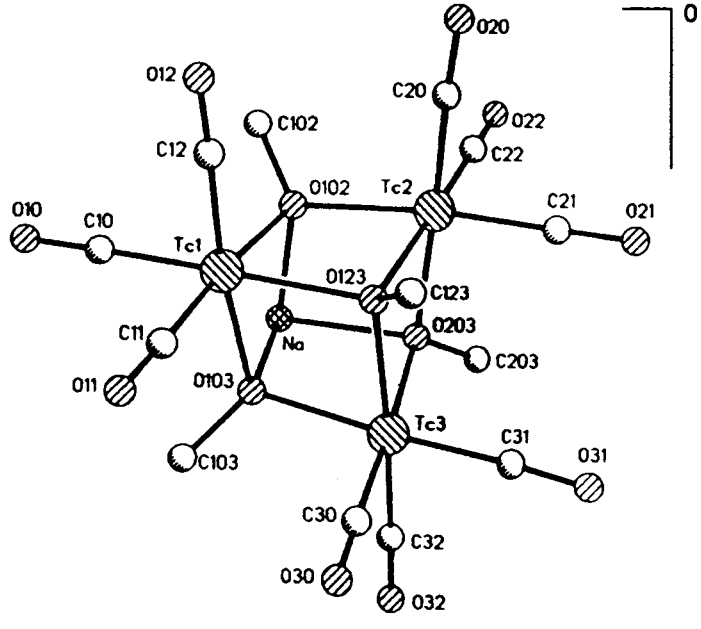

Fig. 12.91.A Natrium{enneacarbonyl-tetrakis(μ_3-methoxy)-tritechnetate(I)}, $Na[Tc_3(CO)_9(OCH_3)_4]$ [634].

$(CO)_3]^{-2}$ at room temperature in diglyme solution [635]. Dinuclear carbonyl complexes of Tc(I) containing macrocyclic thioethers of larger ring sizes were synthesized and structurally characterized [635a].

Recently, the cation $[Tc(tert\text{-}BuCN)_3(CO)_3]^+$ was prepared by reaction of $[NEt_4]_2[TcCl_3(CO)_3]$ with Ag^+ in aqueous solution, precipitation of AgCl and addition of *tert*-BuCN in ethanol to the technetium solution. $[Tc^I(tert\text{-}BuCN)_3(CO)_3]NO_3$ was obtained in colorless crystals which adopt the orthorhombic noncentrosymmetric space group *Ima2* with a=16.070(2), b=12.028(1), c=12.344(1) Å, and Z=4. The Tc(I) center is coordinated by a *facial* arrangement of three carbonyl and three isocyanide ligands in an almost octahedral geometry (Fig. 12.92.A). The average bond distance of Tc(I) to the isocyanide ligands of 2.088(3) Å is significantly longer than in $[Tc(tert\text{-}BuCN)_6]^+$ of 2.029(5) Å. The mean Tc–CO bond length is 1.969(3) Å, the mean Tc–C–O angle 177.5°. $[NEt_4]_2[TcCl_3(CO)_3]$ reacts with 2-mercaptoethanol in H_2O/methanol or THF to form the dinuclear compound $[NEt_4][Tc_2^I(\mu\text{-}SCH_2CH_2OH)_3(CO)_6]\cdot 0.5THF$ in pale yellow crystals that crystallize in the orthorhombic space group *Pbnc* with a=16.427(3), b=18.525(4), c=20.779(2) Å, and Z=8. The dimeric anion consists of two *fac*-$Tc(CO)_3$ units that are bridged by the sulphur atoms of the three mercaptoethanolato ligands. The six CO groups are in a completely ecliptic conformation. The Tc–Tc distance is 3.35 Å, which is too long for a single bond. The most significant deviation from octahedral geometry is demonstrated in the three S–Tc–S angles that are only

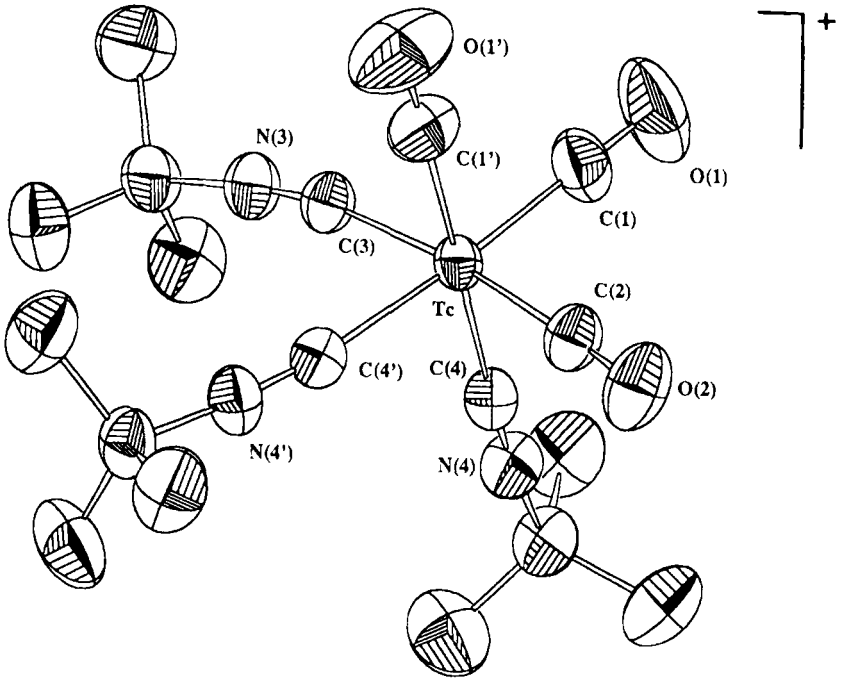

Fig. 12.92.A Tris-(*tert*-butylisonitrile)-tricarbonyl-technetium(I), $[Tc\{CNC(CH_3)_3\}_3(CO)_3]^+$ [636].

around 80°. The Tc–S–Tc angles are 83°. The average bond lengths for Tc–C and Tc–S are 1.902(6) and 2.513(3) Å, respectively [636]. Not too long ago, $[NEt_4]_2[TcCl_3(CO)_3]$ was reacted with sodium bis(diphenylthiophosphoryl)amide in acetonitrile to form $[Tc(CO)_3\{(Ph_2PS)_2N\}(CH_3CN)]$. Tc(I) has a distorted octahedral coordination geometry with facially arranged carbonyls [636a].

Already in 1965 a series of $[Tc(CO)_3L_2X]^\circ$ compounds (X=Cl,Br,I) was obtained by reaction of technetium pentacarbonylhalides with various ligands L. Independent of the reaction conditions always two carbonyls were substituted by L:

$$[Tc(CO)_5X]^\circ + 2L \xrightarrow[\text{ethanol or benzene}]{50\text{–}70^\circ C} [Tc(CO)_3L_2X]^\circ + 2CO$$

Reactions with isonitriles require benzene instead of ethanol. The following compounds were prepared and identified by elemental analysis (Table 12.22.A).

Table 12.22.A. Carbonyl substitution compounds $[Tc^I(CO)_3L_2X]^\circ$ [623].

Compound	Color
$[Tc(CO)_3\{P(C_6H_5)_3\}_2Cl]^\circ$	colorless
$[Tc(CO)_3\{P(OC_6H_5)_3\}_2Cl]^\circ$	colorless
$[Tc(CO)_3\{As(C_6H_5)_3\}_2Cl]^\circ$	colorless
$[Tc(CO)_3\{Sb(C_6H_5)_3\}_2Cl]^\circ$	colorless
$[Tc(CO)_3(4\text{-}C_8H_7N)_2Cl]^{\circ a}$	colorless
$[Tc(CO)_3(4\text{-}C_8H_7ON)_2Cl]^{\circ b}$	colorless
$[Tc(CO)_3(C_5H_5N)_2Cl]^{\circ c}$	colorless
$[Tc(CO)_3(C_{12}H_8N_2)Cl]^{\circ d}$	yellow-brown
$[Tc(CO)_3\{P(C_6H_5)_3\}_2Br]^\circ$	colorless
$[Tc(CO)_3(C_{12}H_8N_2)Br]^{\circ d}$	light brown
$[Tc(CO)_3\{P(C_6H_5)_3\}_2I]^\circ$	yellowish
$[Tc(CO)_3(C_{12}H_8N_2)I]^{\circ d}$	brown

[a]4-tolylisonitrile, [b]4-anisylisonitrile, [c]pyridine, [d]1,10-phenanthroline

The undissociated neutral compounds are readily soluble in benzene, diethylether, and hexane [623].

Technetium pentacarbonylchloride also reacts with thiols by replacing one carbonyl group and the chlorine to form sulphur-bridged dinuclear compounds:

$$2[Tc(CO)_5Cl]^\circ + 2RSH \xrightarrow[\text{methanol}]{50^\circ C} [Tc(CO)_4SR]_2^\circ + 2CO + 2HCl$$

The yellowish complexes are non-electrolytes and easily soluble in benzene and chloroform. Mononuclear, brown N,N-dialkyldithiocarbamides of technetium were obtained by reacting $[Tc(CO)_5Cl]^\circ$ with sodium N,N-dialkyldithiocarbamides:

$$[Tc(CO)_5Cl]^\circ - NaS_2CNR_2 \xrightarrow[\text{acetone}]{50^\circ C} [Tc(CO)_4S_2CNR_2]^\circ$$

The compounds prepared by the given reactions and identified by elemental analysis are summarized in Table 12.23.A.

Table 12.23.A. S-bridged dinuclear complexes $[Tc^{I}(CO)_4SR]_2^{\circ}$ and mononuclear N,N-dialkyldithiocarbamides $[Tc^{I}(CO)_4(S_2CNR_2)]^{\circ}$ [623].

Compound	Color
$[Tc(CO)_4SC_6H_5]_2^{\circ}$	light yellowish
$[Tc(CO)_4SC_7H_5]_2^{\circ}$	light yellowish
$[Tc(CO)_4SCH_3]_2^{\circ}$	yellowish
$[Tc(CO)_4S_2CN(CH_3)_2]^{\circ}$	yellow-brown
$[Tc(CO)_4S_2CN(C_2H_5)_2]^{\circ}$	yellow-brown

$[Tc(CO)_5Cl]^{\circ}$ and $[Tc(CO)_3\{P(C_6H_5)_3\}_2Cl]^{\circ}$ react with CO under a pressure of 300–400 atm in the presence of $AlCl_3$ to produce the cationic complexes:

$$[Tc(CO)_5Cl]^{\circ} + AlCl_3 + CO \xrightarrow[90\,^{\circ}C]{300\ atm} [Tc(CO)_6][AlCl_4]$$

$$[Tc(CO)_3\{P(C_6H_5)_3\}_2Cl]^{\circ} + AlCl_3 + CO \xrightarrow{400\ atm} [Tc(CO)_4\{P(C_6H_5)_3\}_2][AlCl_4]$$

Both compounds are electrolytes and readily soluble in polar organic solvents. The carbalkoxo-bis(triphenylphosphine)tricarbonyl technetium complexes were readily formed by reaction of $[Tc(CO)_4\{P(C_6H_5)_3\}_2][AlCl_4]$ with alcoholates:

$$[Tc(CO)_4\{P(C_6H_5)_3\}_2][AlCl_4] + 5RO \xrightarrow{alcohol} [Tc(CO)_3\{P(C_6H_5)_3\}_2CO_2R]^{\circ} + [Al(OR)_4]^{-} + 4Cl$$

These neutral and air-stable complexes are recrystallized from a mixture of benzene and petroleum ether. Synthesized compounds are given in Table 12.24.A.

Table 12.24.A Cationic carbonyl complexes and carbalkoxo carbonyls of technetium(I) [623].

Compound	Color
$[Tc(CO)_6][AlCl_4]$	colorless
$[Tc(CO)_4\{P(C_6H_5)_3\}_2][AlCl_4]$	reddish
$[Tc(CO)_3\{P(C_6H_5)_3\}_2COOCH_3]^{\circ}$	ivory
$[Tc(CO)_3\{P(C_6H_5)_3\}_2COOC_2H_5]^{\circ}$	light yellow
$[Tc(CO)_3\{P(C_6H_5)_3\}_2COOCH_2C_6H_5]^{\circ}$	yellow

Halogen-carbonyl-phosphine complexes of Tc(I) were also obtained when CO at 1 atm was passed through a refluxing solution of *mer*-$[Tc^{III}X_3(PMe_2Ph)_3]^{\circ}$ in ethyleneglycol methyl ether. The colorless compounds *trans*-$[TcX(CO)_3(PMe_2Ph)_2]^{\circ}$ and *cis*-$[TcX(CO)_2(PMe_2Ph)_3]^{\circ}$ (X = Cl, Br) were isolated. When $[Tc^{IV}X_4L_2]^{\circ}$ (X = Cl, Br, and L = PPh_3, PMe_2Ph) reacts with CO under the same conditions, the

exclusively formed products are $[TcX(CO)_3L_2]^\circ$. The diamagnetic complexes, identified by elemental analysis, IR, and ^1H NMR spectroscopy, are summarized in Table 12.25.A.

Table 12.25.A Halogen-carbonyl-phosphine complexes of Tc(I) [637].

Compound	Melting point [°C]	ν(Tc–X) [cm^{-1}]
trans-$[TcCl(CO)_3(PPh_3)_2]^\circ$	174 (dec.)	278
trans-$[TcBr(CO)_3(PPh_3)_2]^\circ$	172 (dec.)	192
trans-$[TcCl(CO)_3(PMe_2Ph)_2]^\circ$	100	275
trans-$[TcBr(CO)_3(PMe_2Ph)_2]^\circ$	122	175
cis-$[TcCl(CO)_2(PMe_2Ph)_3]^\circ$	142 (dec.)	272
cis-$[TcBr(CO)_2(PMe_2Ph)_3]^\circ$	144	170

Coulometric oxidation of $[TcCl(CO)_2(PMe_2Ph)_3]^\circ$ and $[TcCl(CO)_3(PMe_2Ph)_2]^\circ$ in acetonitrile revealed the formation of Tc(III) species. The complex salt $[Tc^{III}Cl(CO)(MeCN)_2(PMe_2Ph)_3][ClO_4]_2$ was isolated and identified [638].

The dicarbonyl-phosphonite-technetium(I) cation $[Tc(CO)_2\{P(OEt)_2Ph\}_4]^+$ was synthesized by reacting $[Tc^{III}Cl_2\{P(OEt)_2Ph\}_4][ClO_4]$ with CO at 50 °C in an ethanolic solution containing diethylphenylphosphonite. The chloride atoms are replaced by CO. Colorless crystals of *trans*-$[Tc(CO)_2\{P(OEt)_2Ph\}_4][ClO_4]$ precipitated. Concomitantly the analogous *cis*-complex was formed and isolated. *Cis*-$[Tc(CO)_2\{P(OEt)_2Ph\}_4][ClO_4]$ adopts the triclinic space group $P\bar{1}$ with a=17.708(15), b=13.977(12), c=10.185(10) Å, α=93.22(8), β=90.48(9), γ=96.13(11)°, and Z=2. The coordination geometry of Tc(I) is distorted octahedral. The angles around Tc are rather close to 90 or 180°. Both Tc–CO distances are 1.90(2) Å, and the mean Tc–P distance is 2.42(1) Å. The *cis*- and the *trans*-complex are diamagnetic, air-stable, and soluble in polar organic solvents [416].

Refluxing of $[Tc(CO)_5Br]^\circ$ in CH_3CN and addition of $Ag[PF_6]$ yielded the complex salt $[Tc(CO)_3(CH_3CN)_3][PF_6]$, which proved to be a starting material to obtain carbonyl complexes of Tc(I) by replacing the labile nitrile groups. The colorless crystals melt at 138–140 °C. Reaction of $[Tc(CO)_3(CH_3CN)_3][PF_6]$ with several phenylphosphines in CH_2Cl_2 or $CHCl_3$ gave the compounds *fac*-$[Tc(CO)_3(3\text{-}NaO_3SC_6H_4PPh_2)_3][PF_6]$. $[Tc(CO)_3(CH_3CN)(PPh_3)_2][PF_6]$. $[Tc(CO)_3(CH_3CN)(dppe)][PF_6]$, and $[Tc(CO)_3Cl(Me_2PhP)_2]$, which were structurally characterized by IR spectroscopy [639]. ^{99}Tc NMR spectra of a series of neutral and cationic Tc(I) carbonyl complexes were measured and evaluated [640]. Also the following compounds (Table 12.26.A) were obtained by reaction of $[Tc(CO)_5Br]^\circ$ with π-acceptor ligands L in ethanol. The structure of the compounds was derived from IR and ^1H NMR measurements [641].

Table 12.26.A $[Tc(CO)_3BrL_2]^0$ complexes [641].

Compounds	Melting point [°C]	Color	Symmetry
fac- $[Tc(CO)_3Br(PPh_3)_2]^0$	160 (dec.)	colorless	C_s
fac- $[Tc(CO)_3Br(PMe_2Ph)_2]^0$	130 (dec.)	colorless	C_s
fac- $[Tc(CO)_3Br(dppe)]^0$	180 (dec.)	colorless	C_s
$[Tc(CO)_3Br(PEtPh_2)_2]^0$	135–140 (dec.)	colorless	C_s
mer-$[Tc(CO)_3Br(Ph_2PC_6H_4SO_3Na\text{-}3)_2]^0$	225 (dec.)	colorless	C_{2v}
$[Tc(CO)_3Br(py)_2]^0$	190–240	-	C_s ?
fac- $[Tc(CO)_3Br(bpy)]^0$	275 (dec.)	orange	C_s
fac- $[Tc(CO)_3Br(py\text{-}aldoxime)_2]^0$	192 (dec.)	yellow	C_s
fac- $[Tc(CO)_3Br(py\text{-}amidoxime)_2]^0$	178	yellow	C_s
fac- $[Tc(CO)_3Br(Ph\text{-}py\text{-}ketoneoxime)_2]^0$	187 (dec.)	yellow	C_s
fac- $[Tc(CO)_3Br(Me\text{-}py\text{-}ketoneoxime)]^0$	>300	yellow	C_s
fac- $[Tc(CO)_3Br(tert\text{-}BuNC)_2]^0$	131	colorless	C_s
fac- $[Tc(CO)_3Br(cyclohexyl\text{-}NC)_2]^0$	93	colorless	C_s

$[TcCl(CO)_3(PPh_3)_2]^0$ may also be synthesized by reaction of $[n\text{-}Bu_4N][Tc^VOCl_4]$ under a stream of CO in a mixture of toluene and acetonitrile containing triphenylphosphine. The air-stable, colorless complex crystallizes in the triclinic space group $P\bar{1}$ with a=10.245(1), b=12.744(1), c=14.423(1) Å, α=69.42, β=74.89(1), γ=81.51(1)°, and Z=2. Tc(I) exhibits an almost undistorted octahedral coordination geometry (Fig. 12.93.A) with a meridional arrangement of the carbonyl ligands. The Tc–P bond distances of 2.44 Å differ only slightly. The carbonyl group located *trans* to chlorine shows a shorter Tc–C distance of 1.887(2) Å and a longer C–O distance of 1.145(2) Å than the other carbonyl groups with a mean Tc–C distance of 1.981 Å and mean C–O distance of 1.124 Å. The bond angles around Tc(I) are close to 90 and 180° [642].

$[TcCl(CO)_3(PPh_3)_2]^0$ was shown to also be a useful starting compound for substitution reactions. Chloride, one CO, and one PPh_3 are readily displaced in THF by the N,N,N-amines, 1,4,7-triazacyclononane (9N3), and hydridotris(pyrazolyl)borate, $\{HB(pyz)_3\}$, resulting in the complexes $[Tc(CO)_2\{(9N3)(PPh_3)\}]^+$, and $[Tc(CO)_2\{HB(pyz)_3\}(PPh_3)]^0$. $[Tc(CO)_2(9N3)(PPh_3)]Cl \cdot CH_3OH$ forms colorless needles crystallizing in the monoclinic space group $P2_1/c$ with a=12.997(5), b=8.680(1), c=25.189(5) Å, β=101.13(4)°, and Z=4, while $[Tc(CO)_2\{HB(pyz)_3\}(PPh_3)]^0$ crystallizes in yellowish blocks adopting the monoclinic space group C_2/c with a=31.191(8), b=9.7252(6), c=18.818(5) Å, β=93.36(1)°, and Z=8. Both compounds have an octahedral core geometry with the three nitrogen atoms in *facial* positions [642].

When a solution of *n*-butyl-lithium in hexane is added to a benzene solution of $4\text{-}CH_3C_6H_4NH\text{-}N{=}NC_6H_4CH_3\text{-}4$(Hdtt), the lithium salt of the bidentate triazenido ligand is generated, which reacts *in situ* with *mer*-$[TcCl(CO)_2(PMe_2Ph)_3]^0$ to produce the neutral compound $[Tc(CO)_2(PMe_2Ph)_2(dtt)]^0$. The orange complex crystallizes in the orthorhombic space group *Pbca* with a=11.036(2), b=14.657(4), c=38.92(1) Å, and Z=8. The coordination geometry of Tc(I) is roughly octahedral, with the two PMe_2Ph

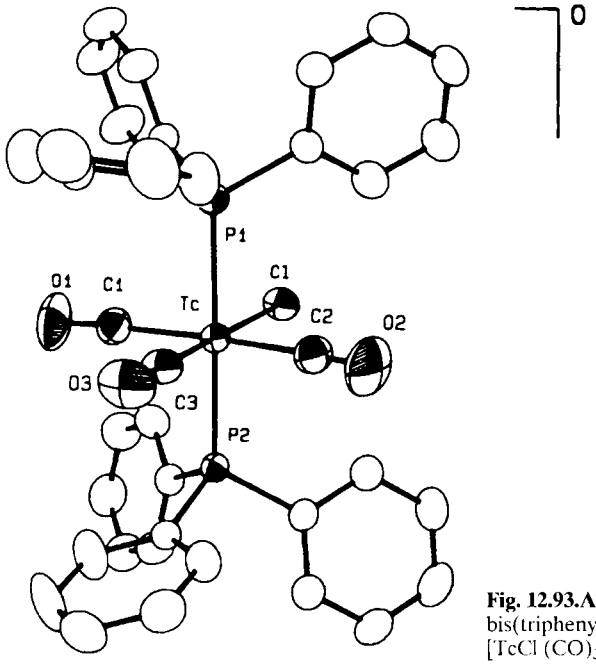

Fig. 12.93.A Chloro-*mer*-tricarbonyl-*trans*-bis(triphenylphosphine)-technetium(I). $[TcCl(CO)_3(PPh_3)_2]^\circ$ [642].

ligands in *trans* position forming a P–Tc–P angle of 173.80(4)°. The maximum deviation from octahedral symmetry is observed in the equatorial plane as a consequence of the small bite angle N–Tc–N of the bidentate ligand of 57.2(1)°. The mean Tc–N distance is 2.184 Å. The two CO groups are in *cis*-position to each other. In a similar procedure, the complex $[Tc(CO)_2(PMe_2Ph)_2(dpa)]^\circ$ {where $(dpa)^-$ = $[C_6H_5N(CMe)NC_6H_5]$ } was prepared. The pale yellow compound again crystallizes in the orthorhombic space group *Pbca* and has the lattice parameters a=8.954(3), b=16.727(2), c=41.435(5) Å, and Z=8. Its structure resembles that of $[Tc(CO)_2(PMe_2Ph)_2(dtt)]^\circ$. Other compounds synthesized are orange-yellow $[Tc(CO)_2(PMe_2Ph)_2(dct)]^\circ$ {where (dct) = $(4\text{-}ClC_6H_4N(N)NC_6H_4Cl\text{-}4)^-$}, yellow $[Tc(CO)_2(PMe_2Ph)_2(dtf)]^\circ$ {where (dtf) = $(4\text{-}MeC_6H_4N(CH)NC_6H_4Me\text{-}4)^-$}, and orange $[Tc(CO)_2(PPh_3)_2(dtt)]^\circ$ [643].

Using again *n*-butyl-lithium in hexane, adding a benzene solution of amido, carboxylato or thiazolato derivatives and reacting their lithium salts with $[TcCl(CO)_3(PPh_3)_2]^\circ$ yielded the compounds given in Table 12.27.A.

The compounds are air-stable and soluble in Me_2CO, CH_2Cl_2, and $CHCl_3$. The two ν(C=O) stretching vibrations for each compound suggest a *cis* arrangement of the carbonyl groups [644].

$[Tc(CO)_2(PPh_3)_2(4\text{-}MeC_6H_4NCHO)]^\circ$ reacts with excess PhNCS in wet benzene at reflux to yield $[Tc^I(CO)_2(PPh_3)_2\{SC(NHPh)S\}]^\circ$ containing a bidentate, monoanionic dithiocarbamate derivative. The compound crystallizes in the triclinic space group $P\bar{1}$ with a=13.864(5), b=12.842(5), c=12.610(5) Å, α=103.53(3), β=112.90(3), γ=94.52(3)°, and Z=2. The Tc core has a distorted octahedral geometry with *trans* PPh_3 groups and *cis* CO groups. Selected bond distances are Tc–P 2.443(2) and 2.428(2) Å, Tc–S

Table 12.27.A Amido, carboxylato, and thiazolato carbonylphosphine technetium(I) complexes [644].

Compound	Color	ν(C=O)[cm^{-1}]	
$[Tc(CO)_2(PPh_3)_2(4\text{-}MeC_6H_4NCHO)]^\circ$	white	1920,	1840
$[Tc(CO)_2(PPh_3)_2(4\text{-}MeOC_6H_4NCHO)]^\circ$	white	1920,	1840
$[Tc(CO)_2(PPh_3)_2(amt_1)]^\circ$	yellow	1920,	1840
$[Tc(CO)_2(PPh_3)_2(amt_2)]^\circ$	pale yellow	1927,	1850
$[Tc(CO)_2(PPh_3)_2(Ph_2CHCO_2)]^\circ$	white	1935,	1854
$[Tc(CO)_2(PPh_3)_2(PhCH_2CO_2)]^\circ$	white	1935,	1860
$[Tc(CO)_2(PPh_3)_2(CCl_3CO_2)]^\circ$	pale yellow	1940,	1860

$Hamt_1$ = 2-(methylamino)thiazole
$Hamt_2$ = 2-(4-methoxyphenylamino)thiazole

2.530(2) and 2.482(2) Å, and Tc–CO 1.88(1) Å. In addition, the complexes $[Tc(CO)_2(PPh_3)_2\{OC(NHPh)S\}]^\circ$, $[Tc(CO)_2(PPh_3)_2\{SC(OEt)S\}]^\circ$, and $[Tc(CO)_2(PPh_3)_2\{C_6H_5NC(OEt)O\}]^\circ$ were synthesized and characterized [645].

The neutral complex $[Tc(CO)_2(PPh_3)_2\{PhN{=}C(OEt)S\}]^\circ$ with the bidentate, monoanionic thiazetidine ligand was obtained by refluxing $[Tc(CO)_3Cl(PPh_3)_2]^\circ$ in THF with PhNC(OEt)SNa. The white crystals of the complex adopt the monoclinic space group $P2_1$ with a=12.825(5), b=16.713(5), c=9.480(5) Å, β=94.29(3)°, and Z=2. The Tc(I) environment is distorted octahedral. Again the PPh_3 groups are in *trans* position and the CO groups in *cis* position. The thiazetidine ligand has a bite angle of only 64.7(1)°. The Tc–N and Tc–S distances are 2.228(5) and 2.529(1) Å, respectively [292].

Another structurally similar complex $[Tc(CO)_2(PPh_3)_2\{(C_3H_2NS)N{=}CHC_6H_4O\}]^\circ$, containing the Schiff-base chelating monoanionic, bidentate ligand (LH) N-2-hydroxybenzylidene-2-thiazolylimine, was synthesized by adding $[Tc(CO)_3Cl(PPh_3)_2]^\circ$ to a boiling THF solution of the lithium salt of the ligand generated *in situ* by treating LH with *n*-BuLi. Red-violet $[Tc(CO)_2(PPh_3)_2\{(C_3H_2NS)N{=}CHC_6H_4O\}]^\circ$ crystallizes in the monoclinic space group $P2_1/n$ with a=17.905(5), b=24.895(4), c=9.285(6) Å, β=102.63(3)°, and Z=4. The coordination geometry is distorted octahedral with *trans* PPh_3 and *cis* CO. The O–Tc–N bite angle of the chelate is 83.6(2)°. The chelate anion forms with Tc(I) a hexa-atomic planar ring. The Tc–O and Tc–N distances are 2.164(5) and 2.210(7) Å, respectively [646].

Reaction of $[Tc(CO)_3Cl(PPh_3)_2]^\circ$ with dithio ligands in acetone or THF under reflux yielded colorless or yellowish crystals of N,N-diethyldithiocarbamato-$[Tc(CO)_2(PPh_3)_2S_2CN(C_2H_5)_2]^\circ$, ethylxanthogenato-$[Tc(CO)_2(PPh_3)_2S_2COC_2H_5]^\circ$, and dimethyldithiophosphato-$[Tc(CO)_2(PPh_3)_2S_2P(OCH_3)_2]$-dicarbonylbis(triphenylphosphine)technetium(I) compounds which were characterized by ^{99}Tc NMR and IR spectroscopy [647].

Very recently technetium carbonyl triphenylphosphine complexes containing 1,4-benzodiazepine derivatives were synthesized by reaction of $[Tc(CO)_3Cl(PPh_3)_2]^\circ$ in refluxing CH_2Cl_2/EtOH with 7-chloro-5-(2-chlorophenyl)-1,3-dihydro-2H-1,4-benzodiazepine-2-one-4-oxide (LH) and other derivative ligands. Pale yellow crystals of the

complex $[Tc^{I}(CO)_2(PPh_3)_2\ (L)]\cdot C_2H_5OH$ adopt the monoclinic space group $P2_1/n$ with a=12.022(3), b=24.377(4), c=17.763(6) Å, β=106.45(3)°, and Z=4. The coordination geometry around the Tc atom is roughly octahedral with the two PPh_3 ligands in *trans* position and the two carbonyl groups *cis* to each other:

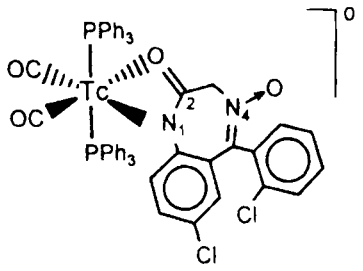

The maximum deviation from octahedral symmetry is observed in the equatorial plane as a consequence of the small bite angle N–Tc–O of only 59.2(1)°. The Tc–N bond length is 2.214(3) Å, the Tc–O distance 2.238(3) Å [648].

Technetium-pentacarbonyl-trifluoroacetate, $[Tc^{I}(CO)_5CF_3CO_2]^{\circ}$, was obtained by grinding a mixture of $[Tc(CO)_5Cl]^{\circ}$ with CF_3COOAg under a layer of $CHCl_3$. The compound sublimes upon heating in vacuum at 60–75 °C and condenses as colorless crystals. It is stable in CCl_4 solution. Upon reaction of $[Tc(CO)_5CF_3CO_2]^{\circ}$ with ethylenediamine (en) in ethanol two CO groups are replaced and $[Tc(CO)_3CF_3CO_2(en)]^{\circ}$ is formed. Reaction of $[Tc(CO)_5Cl]^{\circ}$ with CH_3COONa in ethanol is reported to yield $[Tc(CO)_3CH_3CO_2]^{\circ}$ which was transferred into $[Tc(CO)_3CH_3CO_2(en)]^{\circ}$ upon reaction with ethylenediamine. The compounds were characterized by IR spectroscopy [649].

Grinding of $[Tc(CO)_5Cl]^{\circ}$ with the potassium salts of several β-diketonates (KL) under a layer of CCl_4 induces the exchange reaction:

$$[Tc(CO)_5Cl]^{\circ} + KL \rightarrow [Tc(CO)_4L]^{\circ} + KCl + CO$$

The used β-diketones are acetylacetone (Hacac), trifluoroacetylacetone (Htfa), pivaloyltrifluoroacetone (Hptfa), and hexafluoroacetylacetone (Hhfa). However, the complexes $[Tc(CO)_4L]^{\circ}$ are unstable in CCl_4 and gradually convert to the hydrated tricarbonyl β-diketonates $[Tc(CO)_3L]^{\circ}$. The coordinatively unsaturated compounds seem to exist in the dimeric form. In addition, adducts of tricarbonyl β-diketonates with amines were obtained [650]:

$$[Tc(CO)_5Cl]^{\circ} + 2Et_2NH + HL \rightarrow [Tc(CO)_3L\cdot Et_2NH]^{\circ} + Et_2NH\cdot HCl + 2CO$$

Reaction of $[Tc(CO)_3Br]_4^{\circ}$ with an excess of THF produced the crystalline, probably dimeric compound $[Tc(CO)_3Br\cdot THF]_2^{\circ}$. In acetonitrile the analogous complex $[Tc(CO)_3Br\cdot CH_3CN]_2^{\circ}$ was reported to be formed [651]. The mass spectra of technetium carbonyl compounds were studied extensively [652].

$[Tc(CO)_3Br(en)]^\circ$ was structurally characterized, however, no information about its preparation seems to be accessible. The neutral complex crystallizes in the monoclinic space group $P2_1/n$ with a=7.013(1), b=13.177(8), c=10.736(5) Å, β=101.73(3)°, and Z=4. The coordination geometry of Tc(I) is a distorted octahedron with Br in *trans*-position to one of the carbonyl carbons. The angles OC–Tc–CO and Br–Tc–CO are close to 90 or 180°, while the bite angle N–Tc–N is only 77.2(2)°. The Tc–CO distances are almost identical, with the mean value of 1.886 Å demonstrating the absence of a *trans* influence. The Tc–Br and the mean Tc–N distances are 2.640(1) and 2.217 Å, respectively [573].

In *trans*-$[Tc^I(CO)_4(PPh_3)_2][BF_4]$, synthesized from the monohydride complex $[HTc(CO)_3(PPh_3)_2]^\circ$, the carbonyl ligands are susceptible to attack by a variety of nucleophiles. The pale yellow formyl compound $[Tc(CO)_3\{C(O)H\}(PPh_3)_2]^\circ$ was obtained by treating $[Tc(CO)_4(PPh_3)_2][BF_4]$ with $LiBEt_3H$ in toluene. Addition of $CH_3SO_3CF_3$ to a toluene solution of the formyl compound yielded the carbene $[Tc(CO)_3\{C(OMe)H\}(PPh_3)_2][SO_3CF_3]$ containing a Tc=C bond. Reaction of $[Tc(CO)_4(PPh_3)_2][BF_4]$ with NaOH in MeCN led to the precipitation of the white hydroxycarbonyl complex $[Tc(CO)_3\{C(O)OH\}(PPh_3)_2]^\circ$, while the reaction with NaOH in methanol or ethanol gave the corresponding white ester complexes $[Tc(CO)_3(COOR)(PPh_3)_2]^\circ$. The analogous beige colored aryloxycarbonyl complex $[Tc(CO)_3(COOC_6H_4CH_3)(PPh_3)_2]^\circ$ was obtained with the nucleophile $KOC_6H_4CH_3$ in THF. Reacting the starting material in MeOH with NaN_3 yielded the cream colored isocyanate compound $[Tc(CO)_3(NCO)(PPh_3)_2]^\circ$ [653].

The hydrido-tris(1-pyrazolyl)borato-tricarbonyltechnetium(I) complexes $[HB(C_3H_3N_2)_3Tc(CO)_3]^\circ$ and $[HB(3,5\text{-}Me_2C_3HN_2)_3Tc(CO)_3]^\circ$ were synthesized by refluxing $[TcBr(CO)_5]^\circ$ in THF with $KHB(C_3H_3N_2)_3$ and $KHB(3,5\text{-}Me_2C_3HN_2)_3$, respectively. $[HB(C_3H_3N_2)_3Tc(CO)_3]^\circ$ crystallizes in the trigonal space group P_3 with a=11.464(4), c=8.091(3) Å, and Z=2. The colorless compound Tc(I) reveals a distorted octahedral coordination geometry and is surrounded by three nitrogen atoms and three carbonyl groups in *facial* arrangement. The symmetry of the molecule is C_{3v}. The Tc–CO distances of 1.82(3) Å are almost identical, as well as the Tc–N distances of 2.12(1) Å. $[HB(3,5\text{-}Me_2C_3HN_2)_3Tc(CO)_3]^\circ$ adopts the monoclinic space group $P2_1/c$ with a=8.026(3), b=14.081(4), c=18.995(6) Å, β=97.51(2)°, and Z=4. The compound has the same molecular structure as $[HB(C_3H_3N_2)_3Tc(CO)_3]^\circ$. Both complexes were, in addition characterized spectroscopically and by the determination of the charge distribution within the molecules [654].

When $[HB(C_3H_3N_2)_3Tc(CO)_3]^\circ$ in THF solution is irradiated with UV-radiation at an intensity maximum of 254 nm, a photolytic CO substitution reaction with added PPh_3 as a substituent is catalyzed leading to the compound $[HB(C_3H_3N_2)_3Tc(CO)_2PPh_3]^\circ$ that was obtained as yellow crystals. In a similar procedure $[HB(3,5\text{-}Me_2C_3HN_2)_3Tc(CO)_3]^\circ$ was reacted with trimethylphosphite, $P(OMe)_3$, yielding $[HB(3,5\text{-}Me_2C_3HN_2)Tc(CO)_2\{P(OMe)_3\}]^\circ$. The colorless crystals adopt the monoclinic space group $P2_1/c$ with a=19.960(4), b=8.180(3), c=33.759(5) Å, β=107.51(2)°, and Z=2×4. The unit cell contains two crystallographically independent molecules of somewhat different bond distances and bond angles. Tc(I) is distorted octahedrally, surrounded by three boropyrazolyl nitrogen atoms, two carbonyl carbon atoms, and

the phosphorus atom of the trimethylphosphite group. The Tc–P distance is only 2.299(5) Å and the Tc–CO distance 1.84(2) Å [655].

After UV irradiation of $[HB(3,5\text{-}Me_2C_3HN_2)_3Tc(CO)_3]^\circ$ in THF, the intermediary compound $[HB(3,5\text{-}Me_2C_3HN_2)_3Tc(CO)_2(THF)]^\circ$ reacts with elemental N_2 to yield the air-stable N_2-bridged binuclear complex $[\{HB(3,5\text{-}Me_2C_3HN_2)_3Tc(CO)_2\}_2(\mu\text{-}N_2)]^\circ$. The dark brown complex crystallizes in the monoclinic space group $C2/c$ with a=20.322(6), b=14.547(4), c=14.270(5) Å, β=103.95(2)°, and Z=4, and is readily soluble in polar and aromatic solvents. Each Tc core has a distorted octahedral environment. The Tc–N–N–Tc group is almost linear with a Tc–N–N angle of 174.0(10)°. The hydro-tris(pyrazolyl)borato ligands are in a skew conformation to each other. The N–N(μ-N_2) bond distance is 1.160(3) Å, which is 0.06 Å longer than in elemental N_2. The Tc–N(μ-N_2) distance is 1.94(2) Å. This remarkable compound was additionally characterized by IR, ^{1}H NMR, UV, and MS spectroscopy [656].

Reaction of technetium pentacarbonylchloride with diphenylsulphide or diphenylselenide in refluxing ethanol results in the formation of the dinuclear Cl-bridged complexes:

$$2[Tc(CO)_5Cl]^\circ + 2(C_6H_5)_2S(Se) \rightarrow [Tc(CO)_3(C_6H_5)_2S(Se)Cl]_2^\circ + 4\ CO$$

which easily react with excess tetrahydrothiophene to the dimeric substitution product $[Tc(CO)_3(SC_4H_8)Cl]_2^\circ$; however, with excess pyrrolidine by opening of the chlorine bridge to the monomeric complex $[Tc(CO)_3(HNC_4H_8)_2Cl]^\circ$ because of its more basic character. Tc(I) is octahedrally coordinated in these colorless to light yellow, diamagnetic compounds [657].

An unusual dinuclear complex of Tc(I) containing carbonyl groups is μ-[*meso*-tetraphenylporphinato-bis(tricarbonyl)technetium(I), $[TPP\{Tc(CO)_3\}_2]^\circ$, which was prepared by refluxing $[Tc_2(CO)_{10}]^\circ$ with *meso*-tetra-phenylporphine in decalin under argon. Reddish brown crystals, m.p. 323–325 °C, were obtained, which crystallize in the monoclinic space group $P2_1/c$ with the lattice constants a=11.934(1), b=16.295(1), c= 11.596(1) Å, β=117.02(1)°, and Z=2. The structure of the complex is centrosymmetric (Fig. 12.94.A). The two Tc atoms are bonded to tetraphenylporphyrin, one above and one below the plane of the macrocycle. The Tc atoms are located 1.42 Å from the plane and set to one side such that each Tc is bonded to three nitrogens. The Tc–N(1) distance is 2.16 Å, while the Tc–N(2) bonds are much longer, averaging 2.39 Å. The Tc–Tc distance is 3.10 Å. The porphyrin macrocycle is distorted. The coordination geometry of each Tc is octahedral; each Tc is in addition bonded to three carbonyls. Other technetium-porphyrin complexes were synthesized by replacing *meso*-tetraphenylporphin by *meso*-porphyrin IX dimethylester (H_2MP). Using a similar preparation procedure the reaction with $[Tc_2(CO)_{10}]^\circ$ yielded the greenish brown solid $[(H\text{-}MP)Tc(CO)_3]^\circ$ and, by changing the ratio of reactants, the dark reddish-brown solid $[(MP)\{Tc(CO)_3\}_2]^\circ$ was obtained. When $[(H\text{-}MP)Re(CO)_3]^\circ$ was mixed with $[Tc_2(CO)_{10}]^\circ$ and the mixture refluxed in decalin under argon, the unusual heterodinuclear metalporphyrin complex $[(OC)_3Tc(MP)Re(CO)_3]^\circ$ was isolated as a dark red solid. The compounds were characterized by UV, IR, ^{1}H NMR, and mass spectroscopy [658–661].

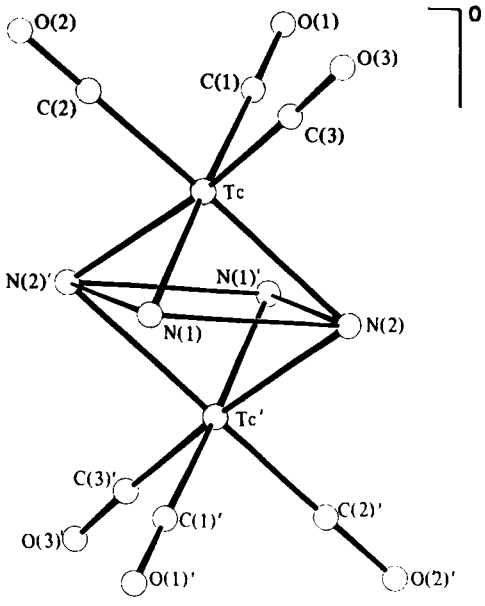

Fig. 12.94.A μ-(*meso*-tetraphenylporphinato)-bis{tricarbonyl-technetium(I)}, [TPP[Tc $(CO)_3]_2]^\circ$. The lines between the nitrogen signify the macrocycle plane [658].

With the goal of labeling bioactive molecules with ^{99m}Tc, the tricarbonyl-dithioether-^{99}Tc(I) complex bearing the steroid ligand 3,17β-estradiol was synthesized and identified recently [661a].

Cyclopentadienyl-tricarbonyl-technetium(I) was prepared by reacting $TcCl_4$ in the presence of copper powder with CO under a pressure of 325 atm to yield technetium carbonylchloride which was then heated in ethyleneglycoldimethylether with sodium cyclopentadienyl. The sublimable, colorless, and diamagnetic $[(C_5H_5)Tc(CO)_3]^\circ$ melts at 87.5 °C [662]. Irradiation of the dimeric compound $[(C_5H_5)Mo(CO)_3]_2^\circ$ with thermal neutrons produced $[(C_5H_5)^{99m}Tc(CO)_3]^\circ$ by nuclear transformation of molybdenum to technetium [663]:

$$[(C_5H_5(Mo(CO)_3]_2^\circ + n_{therm} \rightarrow [(C_5H_5^{99}Mo(CO)_3]_2^\circ \rightarrow [(C_5H_5)^{99m}Tc(CO)_3]^\circ + \beta$$

$[(C_5H_5)Tc(CO)_3]^\circ$ undergoes a Friedel-Crafts reaction in CS_2 with a mixture of aluminum chloride and benzoyl chloride under reflux yielding $[(C_6H_5COC_5H_4)Tc(CO)_3]^\circ$ by acylation of C_5H_5. The colorless, crystalline compound melts at 87.5 °C and was characterized by IR spectroscopy [664]. Pentamethylcyclopentadienyl-tricarbonyl-technetium(I), $[(\eta^5\text{-}C_5Me_5)Tc(CO)_3]^\circ$ is accessible in a simple route by reaction of $Na[Tc_3(CO)_9(OCH_3)_4]$ with pentamethylcyclopentadiene, $C_5(CH_3)_5H$. The complex is readily soluble in organic solvents. $Na[Tc_3(CO)_9(OCH_3)_4]$ reacts with benzene/HCl to form the yellow complex salt $[(\eta^6\text{-}C_6H_6)Tc(CO)_3]Cl$ [634].

Reaction of $[Tc(CO)_5I]^\circ$ with lithium cyclopentadienides (LiCp) in THF at room temperature led readily to the formation of cyclopentadienyltricarbonyl-technetium(I) and some derivatives:

$$[Tc(CO)_5I]^{\circ} - LiCp \xrightarrow{THF} CpTc(CO)_3^{\circ} + LiI + 2CO$$

where Cp = η^5-C_5H_5, η^5-C_5Me_5, η^5-$C_5Me_4(CH_2)_3NMe_2$. The amino group in $[\{Me_2N(CH_2)_3C_5Me_4\}Tc(CO)_3]^{\circ}$ was quaternized by treating the complex with excess MeI to yield the complex salt $[\{Me_3N^+(CH_2)_3C_5Me_4\}Tc(CO)_3]I$, which crystallizes in the monoclinic space group $P2_1/c$ with a=14.081(2), b=9.089(1), c=17.207(3) Å, β=91.13(1)°, and Z=4. The geometry around Tc may be described as a piano stool composed of three carbonyl groups and the η^5-coordinated cyclopentadienyl ligand with a side chain bearing the ammonium group. The Tc–C bond distances to the cyclopentadienyl ring carbon atoms range between 2.275(9) and 2.30(1) Å. The mean Tc–CO distance is 1.90(1) Å. The OC–Tc–CO angles are close to 90°. $[(C_5Me_5)Tc(CO)_3]^{\circ}$ reacts easily with $NO[PF_6]$ in acetonitrile to give the cationic nitrosyl complex $[(C_5Me_5)Tc(CO)_2(NO)]^+$ with the hexafluorophosphate anion [665].

The complexes $[(\eta^5\text{-}C_5Me_5)Tc(CO)_3]^{\circ}$, $[(\eta^5\text{-}C_5Me_4Et)Tc(CO)_3]^{\circ}$, and $[(\eta^5\text{-}C_9H_7)Tc(CO)_3]^{\circ}$ were prepared by reaction of $[Tc_2(CO)_{10}]^{\circ}$ with excess pentamethylcyclopentadiene, tetramethylethylcyclopentadiene or indene at 200 °C. Colorless $[(\eta^5\text{-}C_5Me_5)Tc(CO)_3]^{\circ}$, m.p. 119–120 °C, crystallizes in the triclinic space group $P\bar{1}$ with a=6.980(1), b=7.854(2), c=12.936(4) Å, α=85.46(2), β=87.57(2), γ=75.32(2)°, and Z=2. Fig. 12.95.A shows the piano stool structure of the complex. The Tc–C bond distances to the carbon atoms of the cyclopentadienyl ring vary from 2.276(5) to 2.356(5) Å. The OC–Tc–CO angles are again close to 90° and the Tc–C–O angles are almost linear. $[(\eta^5\text{-}C_5Me_4Et)Tc(CO)_3]^{\circ}$ is also colorless and melts at 55 °C. It adopts the monoclinic $P2_1/m$ space group with the lattice parameters a=7.050(6), b=11.300(11),

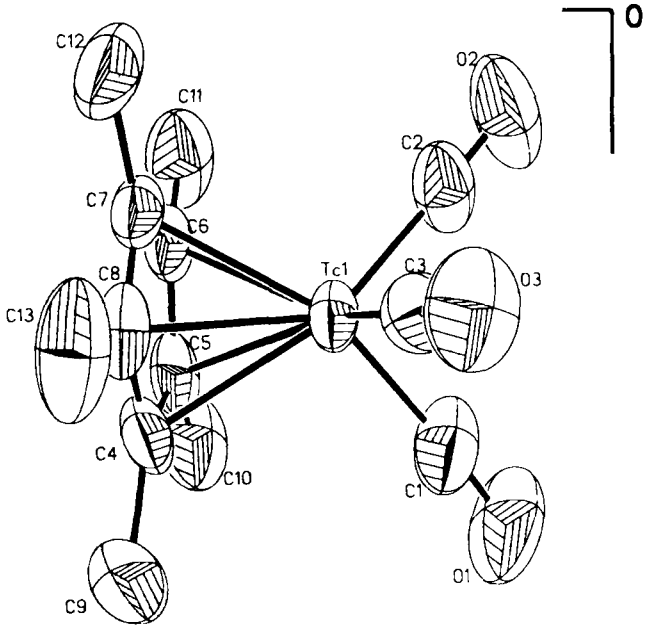

Fig. 12.95.A Pentamethyl-cyclopentadienyltricarbonyl-technetium(I), $[(\eta^5\text{-}C_5Me_5)Tc(CO)_3]^{\circ}$ [666].

c=9.358(8) Å, β=94.86(7)°, and Z=2. The light yellow indenyl complex $[(\eta^5\text{-}C_9H_7)Tc(CO)_3]^\circ$ melts at 57–58 °C and crystallizes in the triclinic space group $P\bar{1}$ with a=6.737(5), b=7.317(6), c=12.281(9) Å, α=97.52(6), β=94.68(6), γ=109.38(6)°, and Z=2. The core geometries of both compounds are very similar to that of $[(\eta^5\text{-}C_5Me_5)Tc(CO)_3]^\circ$. All three compounds are air-stable. They were characterized in addition by IR, ^{1}H NMR, ^{13}C NMR, and UV spectroscopy [666].

The heterocyclic compound η^5-tetramethylpyrrolyl-technetiumtricarbonyl $[(Me_4C_4N)Tc(CO)_3]^\circ$ was synthesized by reacting $[TcBr(CO)_5]^\circ$ with excess tetramethylpyrrolyl potassium $(Me_4C_4N)K$ in refluxing THF under exclusion of air and water. The compound $[(\eta^5\text{-}Me_4C_4N)Tc(CO)_3]]^\circ \cdot HNC_4Me_4$, containing one molecule of tetramethylpyrrol, crystallizes in colorless needles in the orthorhombic space group $Pna2_1$. The lattice constants are a=20.967(5), b=11.556(2), c=8.741(3) Å, and Z=4. $[(\eta^5\text{-}Me_4C_4N)Tc(CO)_3]]^\circ$ also shows a piano stool structure. The distance Tc–ring center is 1.957(1) Å, very similar to the corresponding distance of 1.944(6) Å in $[(\eta^5\text{-}C_5Me_5)Tc(CO)_3]]^\circ$. The Tc–N bond distance of 2.167(9) Å is significantly shorter than the average Tc–C bonds to the ring carbon atoms at 2.32 Å. As a consequence of the nitrogen *trans* effect, one Tc–CO distance is only 1.84(1) Å. The three carbonyl atoms are located in a plane parallel to the ring plane. The compound is very unstable in air. It was also characterized spectroscopically [667].

Irradiation of a solution of $[(C_5H_5)Tc(CO)_3]^\circ$ and PPh_3 in cyclohexane with UV radiation leads to the formation of the complex $[(C_5H_5)Tc(CO)_2(PPh_3)]^\circ$. The light yellow-brown crystals adopt the triclinic space group $P\bar{1}$ with a=9.453(5), b=10.699(5), c=11.679(5) Å, α=75.87(4), β=76.50(4), γ=77.20(4)°, and Z=2. The bond distance of Tc(I) from the ring center is 1.96(1) Å. The distances of Tc to the ring carbon atoms range between 2.272(6) and 2.307(6) Å. The Tc–P distance is only 2.341(1) Å. The OC–Tc–P angles are close to 90°. In a similar preparation procedure the complex $[(C_5Me_5)Tc(CO)_2(PPh_3)]^\circ$ was obtained in brown prisms, which crystallize in the monoclinic space group $P2_1/c$ with a=9.470(7), b=15.49(1), c=18.71(2) Å, β=101.96(6)°, and Z=4. Its structure strongly resembles that of $[(C_5H_5)Tc(CO)_2(PPh_3)]^\circ$. IR, ^{1}H NMR, and UV spectroscopic data have been communicated [655].

When $[(C_5Me_5)Tc(CO)_3]^\circ$ is irradiated in cyclohexane with UV light under exclusion of oxygen and water, the remarkable dinuclear complexes $[(C_5Me_5)_2Tc_2(CO)_3]^\circ$and $[(C_5Me_5)_2Tc_2(CO)_5]^\circ$ are produced. The red $[(C_5Me_5)_2Tc_2(CO)_3]^\circ$ crystallizes in the triclinic space group $P\bar{1}$ with a=8.823(11), b=10.172(12), c=13.590(15) Å, α=71.28(9), β=85.91(9), γ=77.97(9)°, and Z=2. It is stable in air and in solution. The Tc–Tc core is triply bonded and additionally bridged by three CO groups (Fig. 12.96.A). The Tc–Tc distance is 2.413(3) Å. Both cyclopentadienyl rings are parallel to each other and to the plane of the carbonyl carbon atoms. The distance between the cyclopentadienyl ring centers is 6.22(2) Å. The rings are in ecliptic arrangement, with the CH_3 groups bending away from the Tc centers. The average Tc–ring center distance is 2.25(1) Å and the Tc–CO distance 2.09(1) Å. The Tc–CO–Tc angle was found to be 70.7(4)°. From spectroscopic data of $[(C_5Me_5)_2Tc_2(CO)_5]^\circ$, it is believed that the compound may have the same structure as the analogous Re complex, that is, the two Tc centers are connected by a Tc–Tc single bond and a bridging CO group. The coordination of each Tc atom is completed by a C_5Me_5 ring and two terminal CO groups [668].

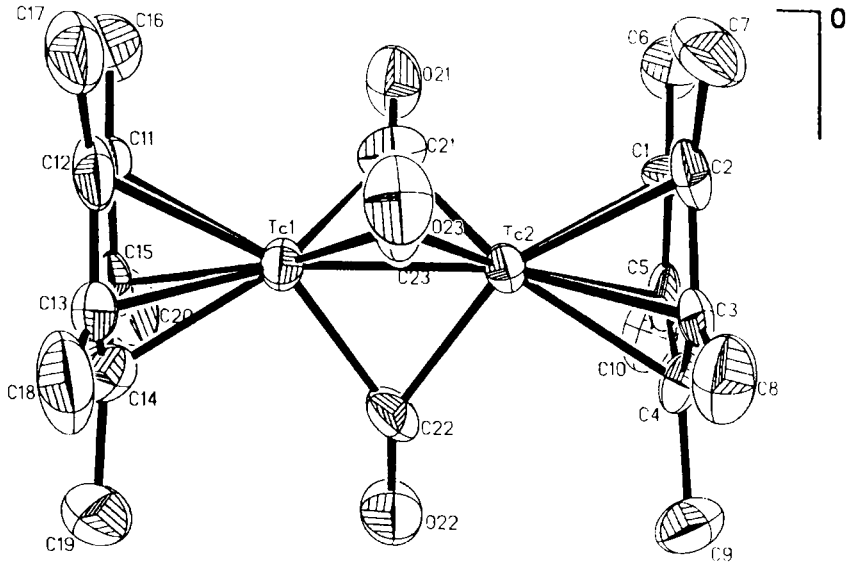

Fig. 12.96.A Tris(μ-carbonyl)-bis-(pentamethyl-cyclopentadienyl)ditechnetium(I), $[(\eta^5\text{-}C_5Me_5)_2Tc_2(CO)_3]^\circ$ [668].

Reaction of $[(\eta^5\text{-}C_5Me_5)Tc(CO)_3]^\circ$ in diethylether with a suspension of LiPh in benzene/ether results in the formation of the acyl complex $Li[(C_5Me_5)Tc(CO)_2C(O)Ph]$:

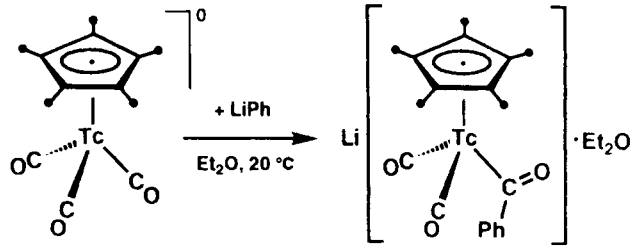

X-ray structure analysis of the orange-red crystals demonstrated its dimeric composition [669]. The diamagnetic compound is sensitive to air and water. It is converted at 20 °C into the carbene complex $[(C_5Me_5)(CO)_2Tc{=}C(OEt)Ph]^\circ$ by addition of $[Et_3O][BF_4]$ to the melting CH_2Cl_2 solution of the acyl complex:

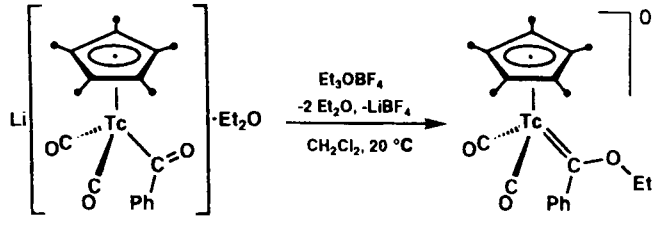

The yellow, air-stable, diamagnetic carbene complex crystallizes in the monoclinic space group $P2_1/n$ with the unit cell constants a=8.468(2), b=22.648(7), c=10.412(2) Å, β=95.72(3)°, and Z=4. The structure reveals the nearly perpendicular orientation of the carbene ligand relative to the C_5Me_5 ring. The distance Tc–(C_5Me_5)(center) is 1.966(1) Å. The Tc–C–O(carbonyl) angles of 171(2) and 175(2)° deviate significantly from linearity. The Tc=C(carbene) bond distance of 1.97(2) Å is considerably shorter than the Tc–C(C_5Me_5) ring distances, with a mean value of 2.31 Å. The carbene compound reacts with BCl_3 in pentane at –20 °C to form the cationic carbyne complex $[(C_5Me_5)(CO)_2Tc{\equiv}CPh]BCl_4$ in high yield:

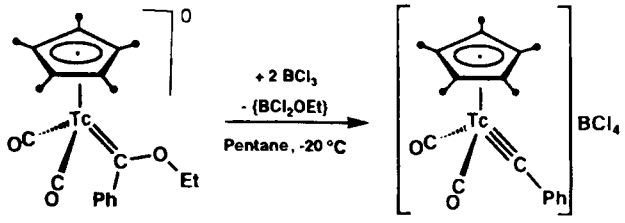

The yellow, diamagnetic compound is thermally rather stable. Reaction of the carbyne complex in Et_2O with NaOCy (Cy = cyclohexyl) gives the carbene complex $[(C_5Me_5)(CO)_2Tc{=}C(OCy)Ph]$°:

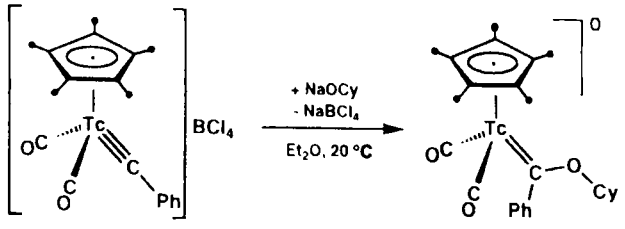

Addition of $P(OMe)_3$ to $[(C_5Me_5)(CO)_2Tc{\equiv}CPh]Cl$ in dichloromethane induces a carbyne-carbonyl coupling reaction yielding the green, diamagnetic ketenyl complex $[(C_5Me_5)(CO)P(OMe_3)TcC(CO)Ph]Cl$:

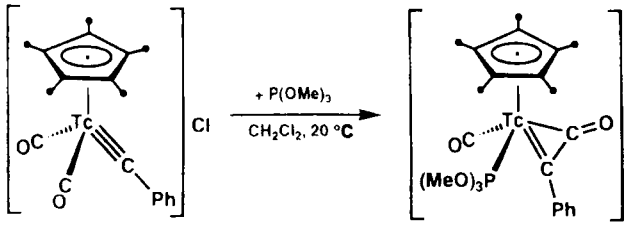

The compounds were identified by IR, ^1H NMR, and UV spectroscopy [670].

Structural data of Tc(I) complexes are reviewed in Table 12.28.A.

Table 12.28.A Some structural data of selected Tc(I) complexes.

Complex	Geometry	Tc–L distance [Å]	Magnetic property	References
12.7.1				
$[Tc(CN)_6]^{5-}$	octah.	–	diamag.	[579–581]
$[Tc\{CNC(CH_3)_3\}_6]^+$	octah.	2.029(5) (Tc–C)	–	[582,583]
$[Tc\{CNC(CH_3)_2COOCH_3\}_6]^+$	octah.	–	diamag.	[584]
trans-$[Tc\{CNC(CH_3)_3\}_2(dppe)_2]^+$	octah.	2.034(Tc–C) 2.43 (Tc–P)		[588]
trans-$[Tc\{CNC(CH_3)_3\}_4(PMe_2Ph)_2]^+$	octah.	2.04 (Tc–C) 2.389(Tc–P)	–	[590]
$[Tc\{CNC(CH_3)_3\}_5(PMe_2Ph)]^+$	octah.	1.97–2.06(Tc–C) 2.403 (Tc–P)		[590]
$[Tc\{CNC(CH_3)_3\}_4bpy]^+$	octah.	1.90–2.04(Tc–C) 2.16 (Tc–N)	–	[591]
fac-$[Tc\{CNC(CH_3)_3\}_3(CO)_3]^+$	octah.	2.088 (Tc–CN) 1.969 (Tc–CO)	–	[592]
12.7.2				
$[Tc(dmpe)_3]^+$	octah.	2.40 (Tc–P)	diamag.	[239]
$[TcCl(dppe)_2]^+$	trig.bipyr.	2.432 (Tc–Cl) 2.24–2.38(Tc–P)	–	[597]
$[Tc{=}C{=}CHPh(Cl)(dppe)_2]^0$	octah.	1.861 (Tc=C)	–	[598]
trans-$[Tc(H_2)Cl(dppe)_2]^0$	octah.	2.629 (Tc–Cl) 2.38 (Tc–P)	–	[597]
$[Tc\{P(OCH_3)_3\}_6]^+$	octah.	–	–	[600,601]
12.7.3				
trans-$[TcCl(tpy)(py)_2]^0$	octah.	2.518 (Tc–Cl)	–	[433]
$[Tc(phen)_3]^+$	octah.	–	–	[603]
$[HTc(N_2)(dppe)_2]^0$	octah.	2.05 (Tc–N 1.7 (Tc–H) 1.359 (Tc–P)	diamag.	[606,607]
12.7.4				
$[Tc(NO)(NH_3)_4(OH_2)]^{2+}$	octah.	1.726 (Tc–NO) 2.168 (Tc–OH_2) 2.164 (Tc–NH_3)	diamag.	[541,542]
$[Tc(NO)Br_2\{(CNC(CH_3)_3)\}_3]^+$	octah.	1.726 (Tc–NO) 2.543–2.582(Tc–Br)	–	[608]
mer-$[Tc(NO)Cl_2(py)_3]^0$	octah.	2.129 (Tc–N_{py}) 1.781 (Tc–NO) 2.37–2.43 (Tc–Cl)	–	[610]
$[Tc(NO)(PPh_3)_3(H_2)]^+$	octah.	–	diamag.	[613]

Table 12.28.A Continued.

Complex	Geometry	Tc-L distance [Å]	Magnetic property	References
cis-[Tc(NO)(NH_3)(phen)$_2$]$^{2+}$	octah.	1.739 (Tc–NO) 2.11 (Tc–N_{phen}) 2.175 (Tc–NH_3)	–	[614]
cis-[Tc(NS)Cl(phen)$_2$]$^+$	octah.	1.782 (Tc–NS) 2.387 (Tc–Cl)		[614]
mer-[Tc(NS)Cl_2(pico)$_3$]^0	octah.	1.73 (Tc–NS) 2.14 (Tc–N_{pic})	–	[615]
mer-[Tc(NS)Cl_2(Me_2PhP)$_3$]^0	octah.	1.747 (Tc–NS) 2.448 (Tc–P)	diamag.	[616]
12.7.5				
[Tc(C_6H_6)$_2$]$^+$			diamag.	[617–619]
[{C_6(CH_3)$_6$}Tc{C_6(CH_3)$_6$H}]^0	–	–	diamag.	[620]
[{C_6(CH_3)$_3H_3$}Tc{C_6(CH_3)$_3H_3$}]$^+$	–	–	diamag.	[621]
12.7.6				
[Tc(CO)$_5$X]^0	–	–	diamag.	[622–624]
[Tc(CO)$_4$X]$_2^0$	D_{2h} symmetry	–	diamag.	[622,629]
[Tc(CO)$_3$Cl]$_4^0$	Tc_4Cl_4 cube	2.559 (Tc–Cl) 1.903 (Tc–CO)	–	[573,627,628]
Na[Tc_3(CO)$_9$(OCH_3)$_4$]	octah.	2.39 (Na–OCH_3) 2.14–2.19 (Tc–OCH_3) 1.90 (Tc–CO)	–	[634]
[TcCl{CNC(CH_3)$_3$}$_2$(CO)$_3$]]^0	octah.	1.93 (Tc–CO) 2.10 (Tc–CN) 2.496 (Tc–Cl)		[635]
trans-[TcCl(CO)$_3$(PPh_3)$_2$]^0	octah.	2.44 (Tc–P) 1.89–1.98 (Tc–CO)	diamag.	[637,642]
cis-[Tc(CO)$_2${P(OEt)$_2$Ph}$_4$]$^+$	octah.	1.90 (Tc–CO) 2.42 (Tc–P)	diamag.	[416]
fac-[Tc(CO)$_3$Br(PPh_3)$_2$]^0	C_s symmetry	–	diamag.	[641]
[Tc(CO)$_2$(9N3)(PPh_3)]$^+$	octah.	1.86 (Tc–CO) 2.388 (Tc–P)		[642]
[Tc(CO)$_2$(PMe_2Ph)$_2$(dtt)]^0	octah.	2.39–2.43 (Tc–P) 2.184 (Tc–N)	–	[643]
[Tc(CO)$_2$(PPh_3)$_2$[SC(NHPh)S]]^0	octah.	2.48–2.53 (Tc–S) 1.88 (Tc–CO)	–	[645]
[Tc(CO)$_2$(PPh_3)$_2$[PhN–C(OEt)S]]^0	octah.	2.529 (Tc–S) 2.228 (Tc–N)	–	[292]
[Tc(CO)$_2$(PPh_3)$_2$[(C_3N_2NS)N=CHC_6H_4O]]^0	octah.	2.164 (Tc–O) 2.210 (Tc–N)		[646]

Table 12.28.A Continued.

Complex	Geometry	Tc-L distance [Å]	Magnetic property	References
$[Tc(CO)_3Br(en)]^0$	octah.	1.886 (Tc–CO) 2.217 (Tc–N) 2.640 (Tc–Br)	–	[573]
$[HB(C_3H_3N_2)_3Tc(CO)_3]^0$	octah.	1.82 (Tc–CO) 2.12 (Tc–N)	–	[654]
$[HB(3,5\text{-}Me_2C_3HN_2)Tc(CO)_2\{P(OMe)_3\}]^0$	octah.	2.299 (Tc–P) 1.84 (Tc–CO)	–	[655]
$[(\mu\text{-}N_2)\{HB(3,5\text{-}Me_2C_3HN_2)_3Tc(CO)_2\}_2]^0$	octah.	1.160 (N–N)(μ-N_2) 1.94 (Tc–N)	–	[656]
$[Tc(CO)_3(C_6H_5)_2SCl]_2^0$	octah.	–	diamag.	[657]
$[TPP\{Tc(CO)_3\}_2]^0$	octah.	2.16–2.39 (Tc–N) 3.101 (Tc–Tc)	–	[658–661]
$[CpTc(CO)_3]^0$	–		diamag.	[662,663]
$[Me_3N(CH_2)_3C_5Me_4Tc(CO)_3]^+$	piano stool	2.27–2.30 (Tc–C_{cp}) 1.90 (Tc–CO)	–	[665]
$[(\eta^5\text{-}C_5Me_5)Tc(CO)_2(NO)]^+$	–	–	–	[665]
$[(\eta^5\text{-}C_5Me_5)Tc(CO)_3]^0$	piano stool	2.28–2.36 (Tc–C_{Cp^*})	–	[666]
$[(\eta^5\text{-}C_9H_7)Tc(CO)_3]^0$	piano stool	2.28–2.36 (Tc–C_{Ind})	–	[666]
$[(\eta^5\text{-}C_4Me_4N)Tc(CO)_3]^0$	piano stool	1.957 (Tc–Pyr*) 2.167 (Tc–N)	–	[667]
$[CpTc(CO)_2(PPh_3)]^0$	piano stool	1.96 (Tc–Cp) 2.27–2.31 (Tc–C_{cp}) 2.341 (Tc–P)	–	[655]
$[(\eta^5\text{-}C_5Me_5)_2Tc_2(CO)_3]^0$	piano stool ecliptic	2.413 (Tc–Tc) 2.25 (Tc–Cp*) 2.09 (Tc–CO)	–	[668]
$[(\eta^5\text{-}C_5Me_5)(CO)_2Tc{=}C(OEt)Ph]^0$	piano stool	1.966 (Tc–Cp*) 1.97 (Tc–C) 2.26–2.35 (Tc–C_{cp^*})	diamag.	[670]
$[(\eta^5\text{-}C_5Me_5)(CO)_2Tc{\equiv}CPh]^+$	–	–	diamag.	[670]
$[(\eta^5\text{-}C_5Me_5)(CO)P(OMe)_3TcC(CO)Ph]^+$	–	–	diamag.	[670]

12.8 Technetium(O)

Only a few complexes of technetium in the zero oxidation state are known, and are exclusively formal derivatives of ditechnetium decacarbonyl. Heteronuclear decacarbonyls have been synthesized in which one Tc nucleus is substituted by Co, Mn, or Re. The carbonyl groups in $[Tc_2CO_{10}]^0$ were partially or completely replaced by PF_3 or one CO group could be substituted by a carbene ligand. Also, the butadiene-

bridged ditechnetium octacarbonyl has been synthesized and characterized. The coordination geometry of the Tc(O) compounds is distorted octahedral.

Ditechnetium decacarbonyl, $[Tc_2(CO)_{10}]^0$, was first prepared in 1961 by reaction of Tc_2O_7 with CO in a copper-plated autoclave at 220 °C for 20 h under a pressure rising from 3000 psig (25 °C) to 5100 psig [671], or at 275 °C for 12 h under 250 atm as measured at 20 °C [672]. More recently, $[Tc_2(CO)_{10}]^0$ was obtained with a yield of more than 70 % when NH_4TcO_4 in THF was reacted with sodium amalgam in an autoclave at 120 °C for 72 h under a CO pressure of 100 atm [665]. Starting with NH_4TcO_4 in toluene and simply reacting with CO at 200 °C for 4 h under a pressure of 90 atm gives a yield of even 96 % [673]. The colorless diamagnetic crystals of $[Tc_2(CO)_{10}]^0$ melt at 159–160 °C [671]. They adopt the monoclinic space group *I2/a* with a=14.65, b=7.18, c=14.93 Å, β=105.6°, and Z=4 [674]. The measured density is 2.11 g/cm³ [675]. The dimeric molecule has approximately D_{4d} symmetry with octahedral coordination about each Tc atom, such that the two sets of four equatorial carbonyls are in a staggered configuration (Fig. 12.97.A). The Tc–Tc bond distance is 3.036 Å. The apical Tc–C distance of 1.90 Å is shorter than the equatorial Tc–C distance of 2.00 Å, while the apical C–O distance is 1.20 Å and the equatorial C–O distance 1.12 Å. The equatorial carbonyls are bent away from the apical carbonyl by an average value of 3.8°. The Tc atom is displaced by 0.13 Å from the mean plane of the four equatorial carbon atoms in the direction of the apical carbonyl ligand. The Tc–C–O angles are almost 180° and the adjacent C–Tc–C angles are close to 90°. The axial C–Tc–Tc angle is 177.3° [674]. The calculation of the electronic structure of $[Tc_2(CO)_{10}]^0$ was undertaken using the extended Hückel molecular orbital method. The Tc–Tc bond energy was computed to be 3.14 kcal·mol^{-1} [676]. The IR spectrum was measured in the region 3000–290 cm^{-1} and the absorptions were assigned [677]. From IR and Raman

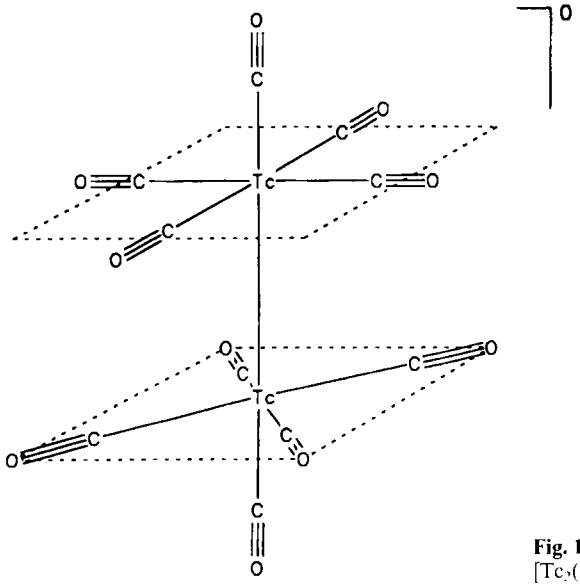

Fig. 12.97.A Ditechnetiumdecacarbonyl, $[Tc_2(CO)_{10}]^0$ [674].

data the equatorial and the axial C–O force constants of 16.642 and 16.316 mdyne·Å $^{-1}$, respectively, were calculated in a C–O factored force field [678]. The ^{99}Tc NMR spectrum of $[Tc_2(CO)_{10}]^\circ$ in C_6D_6 reveals a single line at $\delta = -2477$ ppm *vs* TcO_4^-, demonstrating the two Tc atoms to be also magnetically equivalent [679].

The heteronuclear decacarbonyls $[TcMn(CO)_{10}]^\circ$ and $[TcRe(CO)_{10}]^\circ$ were synthesized by reaction of a pentacarbonyl anion with the respective pentacarbonyl bromide:

$$[Mn(CO)_5]^- + [Tc(CO)_5Br]^\circ \rightarrow [TcMn(CO)_{10}]^\circ + Br^-$$
$$[Mn(CO)_5]^- + [Re(CO)_5Br]^\circ \rightarrow [TcRe(CO)_{10}]^\circ + Br^-$$

A solution of $[Mn_2(CO)_{10}]^\circ$ or $[Tc_2(CO)_{10}]^\circ$ in THF was reduced with excess sodium amalgam to produce the pentacarbonyl anions to which the corresponding pentacarbonyl bromide in THF was added slowly. $[TcMn(CO)_{10}]^\circ$ and $[TcRe(CO)_{10}]^\circ$ were readily separated on nonpolar columns by gas chromatography from by-products and were identified by IR spectroscopy and mass spectrometry. The carbonyl stretching frequencies for the metal and mixed metal decacarbonyls of Mn, Tc, and Re are compiled in Table 12.29.A.

Table 12.29.A IR carbonyl stretching frequencies [cm^{-1}] of homo- and hetero-nuclear decacarbonyls of the subgroup VII elements [680].

Compound	ν (C–O) [cm^{-1}]		
$[Mn_2(CO)_{10}]^\circ$	2044	2013	1983
$[Tc_2(CO)_{10}]^\circ$	2065	2017	1984
$[TcMn(CO)_{10}]^\circ$	2051	2024	1979,1975
$[Re_2(CO)_{10}]^\circ$	2070	2014	1976
$[MnRe(CO)_{10}]^\circ$	2054	2017	1978
$[TcRe(CO)_{10}]^\circ$	2067	2017	1979

The technetium-cobalt carbonyl $[TcCo(CO)_9]^\circ$ was prepared in a similar procedure by reacting $[Tc(CO)_5Br]$ with the tetracarbonyl cobaltate anion $[Co(CO)_4]^-$ in THF:

$$[Tc(CO)_5Br]^\circ + [Co(CO)_4]^- \rightarrow [(CO)_5Tc - Co(CO)_4]^\circ + Br^-$$

$[Co(CO)_4]^-$ was obtained by reduction of $[Co_2(CO)_8]^\circ$ with a liquid sodium-potassium alloy. $[TcCo(CO)_9]^\circ$ forms yellow crystals which are soluble in common organic solvents. It was identified by its IR spectrum which was compared with the spectra of the analogous compounds $[MnCo(CO)_9]^\circ$ and $[ReCo(CO)_9]^\circ$. The IR absorptions of $[MCo(CO)_9]^\circ$ (M = Mn,Tc,Re) were assigned and the stretching force and interaction constants calculated [681,682].

Substitution reactions of $[Tc_2(CO)_{10}]^\circ$ with PF_3 were observed under thermal conditions at 110 °C and under photolytic conditions at room temperature using a 450 W medium-pressure mercury lamp. Thermal reactions produced compounds with up to six of the carbonyls replaced by trifluorophosphine, photolytic reactions yielded prod-

ucts in which up to eight of the CO groups were substituted by PF_3. Disubstituted axial and equatorial products are readily formed [683]. Technetium metal vapor, obtained by cathodic sputtering of the metal, reacts in a krypton atmosphere with a matrix of PF_3 cooled to 77 K. The white compound isolated by sublimation was identified by elemental analysis, IR and mass spectrometry to be $[Tc_2(PF_3)_{10}]^\circ$. It is stable at room temperature, decomposes in basic solution and hydrolyzes slowly in air. The vapor pressure of $[Tc_2(PF_3)_{10}]^\circ$ at 293 K is $7{\cdot}10^{-2}$ Pa [684].

$[Tc_2(CO)_{10}]^\circ$ in diethylether reacts with organolithium compounds LiR (R = C_6H_5,CH_3) according to

$$[Tc_2(CO)_{10}]^\circ + LiR \rightarrow [(OC)_9Tc_2C(OLi)R]^\circ$$

Subsequent methylation in water with $[Me_3O][BF_4]$ affords the carbene complexes $[(OC)_9Tc_2C(OCH_3)C_6H_5]^\circ$ and $[(OC)_9Tc_2C(OCH_3)CH_3]^\circ$. Both compounds were extracted with ether and isolated as diamagnetic, volatile, crystalline solids which are air-stable, but readily oxidizable in solution. The yellow-orange phenyl methoxycarbene complex melts at 88 °C and the yellow methylmethoxycarbene complex at 103 °C. Both compounds were characterized by ^1H NMR and IR spectroscopy. The CO stretching frequencies indicate the equatorial position of the phenylmethoxy and methylmethoxycarbene ligands in the technetium-carbonyl structure [685].

UV photolysis of $[Tc_2(CO)_{10}]^\circ$ in pentane at –20 °C in the presence of butadiene yields the complex $[(\mu\text{-}C_4H_6)Tc_2(CO)_8]^\circ$. The yellow-green crystals adopt the monoclinic space group $P2_1/n$ with a=7.469(4), b=13.070(7), c=15.65(1) Å, β=92.63(6)°, and Z=4. The compound is isostructural with the corresponding butadiene-bridged complexes of manganese and rhenium. Two $Tc(CO)_4$ units are combined by a Tc–Tc bond and the butadiene molecule in the *s-trans*-configuration (Fig.12.98.A). As a conse-

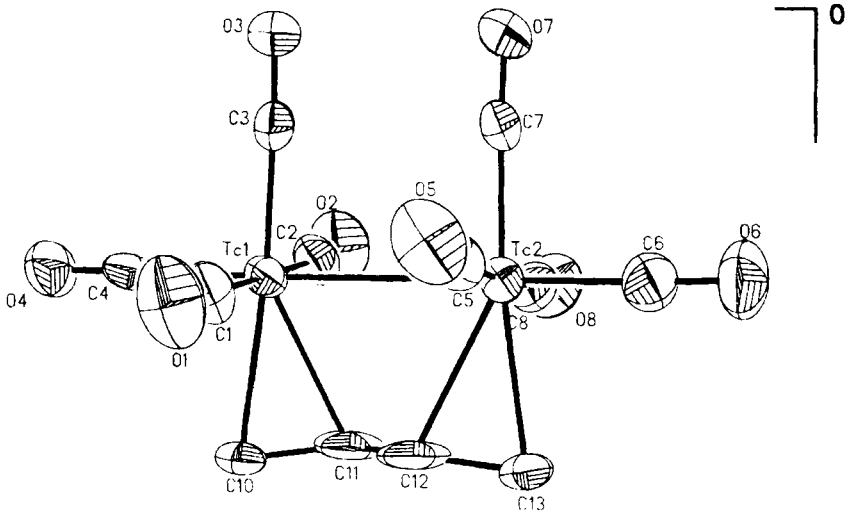

Fig. 12.98.A *μ-trans*-butadien-ditechnetiumoctacarbonyl, $[(\mu\text{-}C_4H_6)Tc_2(CO)_8]^\circ$ [686].

quence of the butadiene bridging, the Tc–Tc bond distance is lengthened to 3.117(1) Å compared to 3.036 Å in $[Tc_2(CO)_{10}]^0$. Also the equatorial CO groups are no longer in a staggered configuration with a twisting angle of 45°, but are twisted by only 12.1°. The mean axial Tc–CO distances are 1.896(8) Å, while the average equatorial Tc–CO distances of 1.982(9) Å are significantly longer. The mean Tc–C(butadiene) distance is 2.390(8) Å. The axial Tc–Tc–C angles are close to 180° [686].

Tc(O) complexes are reviewed in Table 12.30.A.

Table 12.30.A Some structural data of selected Tc(O) complexes.

Complex	Geometry	Tc-L distance [Å]	Magnetic property	References
12.8				
$[Tc_2(CO)_{10}]^0$	octah.	3.036 (Tc–Tc) 1.90 ($Tc–C_{ax}$) 2.00 ($Tc–C_{eq}$)	diamag.	[671–679]
$[TcMn(CO)_{10}]^0$	octah.	-	–	[680]
$[TcRe(CO)_{10}]^0$	octah.	-	–	[680]
$[TcCo(CO)_9]^0$	octah.	–	-	[681,682]
$[Tc_2(PF_3)_{10}]^0$	octah.	–	–	[683,684]
$[(OC)_9Tc_2C(OCH_3)C_6H_5]^0$	octah.	–	diamag.	[685]
$[(\mu\text{-}C_4H_6)Tc_2(CO)_8]^0$	octah.	3.117 (Tc–Tc 1.896 ($Tc–C_{ax}$) 1.982 ($Tc–C_{eq}$)	–	[686]

12.9 Technetium(-I)

Evidence for Tc(-I) in complex compounds appears in the synthesis of the carbonyl anion $[Tc(CO)_5]^-$, the carbonyl hydride $[HTc(CO)_5]^0$, and the heteronuclear carbonyl anion $[TcFe_2(CO)_{12}]^-$. Their existence was suggested by a comparison of their IR absorption bands with those of the corresponding compounds of manganese and rhenium, however, no structural determinations or magnetic measurements were reported.

When freshly sublimed $[Tc_2(CO)_{10}]^0$ in dry THF was reduced with 1 % Na-amalgam at 0 °C, a reddish coloration of THF with evolution of CO was observed. The IR spectra of THF solutions showed two strong bands at 1865 and 1911 cm^{-1}. A comparison of these bands with those from solutions of $[Mn(CO)_5]^-$ indicated the presence of $[Tc(CO)_5]^-$. The action of Na-amalgam on $[Re_2(CO)_{10}]^0$ also led to $[Re(CO)_5]^-$, with strong IR absorptions in THF at 1864 and 1910 cm^{-1} [622].

After removal of THF from $[Tc(CO)_5]^-$ solution and addition of cyclohexane, the heterogeneous mixture was treated at 0 °C with an excess of thoroughly degassed H_3PO_4. During this acidification, H_2 was evolved indicating formation of $[Tc_2(CO)_{10}]^0$. In a distillate two principal carbonyl absorptions at 2015 and 2021 cm^{-1} and one strong band at 685 cm^{-1} were observed in cyclohexane. These bands were assigned to $[HTc(CO)_5]^0$ in analogy to IR absorptions of $[HRe(CO)_5]^0$ at 2006, 2015

and 683 cm $^{-1}$. The bands at 685, respectively 683 cm $^{-1}$, are reported to be most likely the metal–hydrogen deformation frequencies [622,631]. When diethyl ether is used in place of cyclohexane during the acidification step, the yield of $[HTc(CO)_5]^\circ$ was found to be much higher [687].

The anion $[TcFe_2(CO)_{12}]^-$ was synthesized by irradiation of a solution of $[Tc_2(CO)_{10}]^\circ$ and $[Fe(CO)_5]^\circ$ in THF under a dry nitrogen atmosphere with a high-pressure mercury arc lamp. The solution went from almost colorless to very deep red-violet after extended irradiation. Addition of $[(C_2H_5)_4N]Br$ in ethanol to the solution gave the salt $[(C_2H_5)_4N][TcFe_2(CO)_{12}]$. The IR spectrum of the salt in THF was remarkably similar to the spectra of the analogous manganese and rhenium compounds in the carbonyl stretch region. The formation of the triangular anion $[TcFe_2(CO)_{12}]^-$ is favored in polar solvents like THF or diethyl ether. The anion is proposed to exhibit an $[Fe_3(CO)_{12}]$-like structure, in which one $[Fe(CO)_4]$ moiety is replaced by a $[Tc(CO)_4]$ group [688].

Data of Tc(I-) complexes are given in Table 12.31.A.

Table 12.31.A Complexes of Tc(I-).

Complex	Structure	Tc–L distance [Å]	Magnetic property	References
$[Tc(CO)_5]^-$	–	–	–	[622]
$[HTc(CO)_5]^\circ$	–	–	–	[622,631]
$[TcFe_2(CO)_{12}]$	triangular	–	–	[688]

12.10 References

[1] A.P. Ginsberg, Inorg. Chem. *3*, 567–569 (1964)
[2] S.C. Abrahams, A.P. Ginsberg, and K. Knox, Inorg. Chem *3*, 558–567 (1964)
[3] K.J. Franklin, C.J.L. Lock, B.G. Sayer, and G.J. Schrobilgen, J. Am. Chem. Soc. *104*, 5303–5306 (1982)
[4] H. Basch and A.P. Ginsberg, J. Phys. Chem. *73*, 854–857 (1969)
[5] A. Davison, A.G. Jones, and M.J. Abrams, Inorg. Chem. *20*, 4300–4302 (1981)
[6] J.G.H. DuPreez, T.J.A. Gerber, and M.L. Gibson, J. Coord. Chem. *22*, 33–42 (1990)
[7] R.M. Pearlstein and A. Davison, Polyhedron *7*, 1981–1989 (1988)
[8] R.M. Pearlstein, Ph.D. Thesis, Massachusetts Institute of Technology (1988)
[9] J.E. Joachim, C. Apostolidis, B. Kanellakopulos, R. Maier, and M.L. Ziegler, Z. Naturforschg. *48b*, 227–229 (1993)
[10] J.A. Thomas and A. Davison, Inorg. Chim. Acta *190*, 231–235 (1991)
[11] I.A. Degnan, W.A. Herrmann, and E. Herdtweck, Chem. Ber. *123*, 1347–1349 (1990)
[12] I.A. Degnan, J. Behm, M.R. Cook, and W.A. Herrmann, Inorg. Chem. *30*, 2165–2170 (1991)
[13] H.J. Banbery, W. Hussain, I.G. Evans, T.A. Hamor, C.J. Jones, J.A. McCleverty, H.-J. Schulte, B. Engels, and W. Kläui, Polyhedron *9*, 2549–2551 (1990)
[14] J.A. Thomas and A. Davison, Inorg. Chem. *31*, 1976–1978 (1992)
[15] W.A. Herrmann, R. Alberto, P. Kiprof, and F. Baumgärtner, Angew. Chem. *102*, 208–210 (1990)
[16] R. Alberto, W.A. Herrmann, J.C. Bryan, P.A. Schubiger, F. Baumgärtner, and D. Mihalios, Radiochem. Acta *63*, 153–161 (1993)
[17] I.R. Beattie and P.J. Jones, Inorg. Chem. *18*, 2318–2319 (1979)
[18] B. Kanellakopulos, K. Raptis, B. Nuber, and M.L. Ziegler, Z. Naturforschg. *46b*, 15–18 (1991)

[19] E. Herdtweck, P. Kiprof, W.A. Herrmann, J.G. Kuchler, and I. Degnan, Z. Naturforschg. *45b*, 937–942 (1990)
[20] K. Dehnicke and J. Strähle, Angew. Chem. Int. Ed. Engl. *20*, 413–426 (1981)
[21] J. Baldas, S.F. Colmanet, and M.F. Mackay, J. Chem. Soc. Chem. Commun. 1890–1891 (1989)
[22] J. Baldas and S.F. Colmanet, Inorg. Chim. Acta *176*, 1–3 (1990)
[23] J. Baldas, S.F. Colmanet, and G.A. Williams, J. Chem. Soc. Dalton Trans. 1631–1633 (1991)
[24] M.J. Abrams, Q. Chen, S.N. Shaikh, and J. Zubieta, Inorg. Chim. Acta *176*, 11–13 (1990)
[25] T.J.A. Gerber, H.J. Kemp, J.G.H. duPreez, G. Bandoli, and A. Dolmella, Inorg. Chim. Acta *202*, 191–196 (1992)
[26] W.A. Nugent, Inorg. Chem. *22*, 965–969 (1983)
[27] J.C. Bryan, A.K. Burrell, M.M. Miller, W.H. Smith, C.J. Burns, and A.P. Sattelberger, Polyhedron *12*, 1769–1777 (1993)
[28] M.T. Benson, J.C. Bryan, A.K. Burrell, and T.R. Cundari, Inorg. Chem. *34*, 2348–2355 (1995)
[29] A.K. Burrell and J.C. Bryan, Organometallics *11*, 3501–3503 (1992)
[30] K. Schwochau, L. Astheimer, J. Hauck, and H.J. Schenk, Angew. Chem. Internat. Edit. *13*, 346 (1974)
[31] K. Schwochau and U. Pleger, Radiochim. Acta *63*, 103–110 (1993)
[32] J.H. Holloway and H. Selig, J. Inorg. Nucl. Chem. *30*, 473–478 (1968)
[33] R. Kirmse, J. Stach, and U. Abram, Inorg. Chem. *24*, 2196–2198 (1985)
[34] R. Colton and I.B. Tomkins, Aust. J. Chem. *21*, 1981–1985 (1968)
[35] A.K. Burrell, D.L. Clark, P.L. Gordon, A.P. Sattelberger, and J.C. Bryan, J. Am. Chem. Soc. *116*, 3813–3821 (1994)
[36] A.K. Burrell and J.C. Bryan, Angew. Chem. *105*, 85–86 (1993)
[37] A.K. Burrell and J.C. Bryan, Organometallics *12*, 2426–2428 (1993)
[38] J. Baldas, J.F. Boas, J. Bonnyman, and G.A. Williams, J. Chem. Soc. Dalton Trans. 2395–2400 (1984)
[39] J. Baldas, J. Bonnyman, and G.A. Williams, Aust. J. Chem. *38*, 215–219 (1985)
[40] U. Abram and R. Wollert, Radiochim. Acta *63*, 149–151 (1993)
[41] R. Kirmse, J. Stach, and U. Abram, Inorg. Chim. Acta *117*, 117–121 (1986)
[42] K. Köhler, R. Kirmse, and U. Abram, Z. Anorg. Allg. Chem. *600*, 83–87 (1991)
[43] U. Abram, S. Abram, H. Spies, R. Kirmse, J. Stach, and K. Köhler, Z. Anorg. Allg. Chem. *544*, 167–180 (1987)
[44] U. Abram, K. Köhler, R. Kirmse, N.B. Kalinichenko, and I.N. Marov, Inorg. Chim. Acta *176*, 139–142 (1990)
[45] K. Köhler, R. Kirmse, and U. Abram, Z. Chem. *26*, 339–340 (1986)
[46] R. Kirmse, K. Köhler, U. Abram, R. Böttcher, L. Golic, and E. de Boer, Chem. Phys. *143*, 75–82 (1990)
[47] K. Köhler, R. Kirmse, R. Böttcher, U. Abram, M.C.M. Gribnau, C.P. Keijzers, and E. de Boer, Chem. Phys. *143*, 83–95 (1990)
[48] B.N. Figgis, P.A. Reynolds, and J.W. Cable, J. Chem. Phys. *98*, 7743–7745 (1993)
[49] K. Köhler, R. Kirmse, R. Böttcher, and U. Abram, Chem. Phys. *160*, 281–287 (1991)
[50] R. Kirmse and U. Abram, Isotopenpraxis *26*, 151–159 (1990)
[51] J.B. Raynor, T.J. Kemp, and A.M. Thyer, Inorg. Chim. Acta *193*, 191–196 (1992)
[52] J. Baldas, S.F. Colmanet, and G.A. Williams, Inorg. Chim. Acta *179*, 189–194 (1991)
[53] J. Baldas, J. Bonnyman, and G.A. Williams, Inorg. Chem. *25*, 150–153 (1986)
[54] J. Baldas, J.F. Boas, and J. Bonnyman, J. Chem. Soc. Dalton Trans. 1721–1725 (1987)
[55] R. Kirmse, J. Stach, and U. Abram, Polyhedron 4, 1403–1406 (1985)
[56] J. Baldas and J.F. Boas, J. Chem. Soc. Dalton Trans. 2585–2589 (1988)
[57] J. Baldas, J.F. Boas, and J. Bonnyman, Aust. J. Chem. *42*, 639–648 (1989)
[58] J. Baldas, S.F. Colmanet, and G.A. Williams, J. Chem. Soc., Chem. Commun., 954–956 (1991)
[59] J. Baldas, J.F. Boas, S.F. Colmanet, A.D. Rae, and G.A. Williams, Proc. R. Soc. Lond. *A442*, 437–461 (1993)
[60] H.-J. Pietzsch, U. Abram, R. Kirmse, and K. Köhler, Z. Chem. *27*, 265–266 (1987)
[61] T. Takayama, T. Sekine, and K. Yoshihara, J. Radioanal. Nucl. Chem., Letters *176*, 325–331 (1993)
[62] T. Takayama, Y. Kani, T. Sekine, H. Kudo, and K. Yoshihara, J. Radioanal. Nucl. Chem. Letters *199*, 217–227 (1995)
[63] J. Baldas, J.F. Boas, Z. Ivanov, and B.D. James, Inorg. Chim. Acta *204*, 199–212 (1993)
[64] J. Baldas, J.F. Boas, S.F. Colmanet, Z.Ivanov, and G.A. Williams, Radiochim. Acta *63*, 111–115 (1993)

[65] J. Baldas, J.F. Boas, J. Bonnyman, S.F. Colmanet, and G.A. Williams, J. Chem. Soc., Chem. Commun., *1990*, 1163–1165
[66] J. Baldas, J.F. Boas, J. Bonnyman, S.F. Colmanet, and G.A. Williams, Inorg. Chim. Acta *179*, 151–154 (1991)
[67] J. Baldas, J.F. Boas, S.F. Colmanet, and G.A. Williams, J. Chem. Soc. Dalton Trans. *1992*, 2845–2853
[68] J. Baldas, S.F. Colmanet, and M.F. Mackay, J. Chem. Soc. Dalton Trans. *1988*, 1725–1731
[69] L.A. deLaeric, R.C. Haltiwanger, and C.G. Pierpont, J. Am. Chem. Soc. *111*, 4324–4328 (1989)
[70] M.J. Abrams, S.K. Larsen, and J. Zubieta, Inorg. Chem. *30*, 2031–2035 (1991)
[71] R. Kirmse, J. Stach, and H. Spies, Inorg. Chim. Acta *45*, L251–L253 (1980)
[72] J. Baldas, J. Boas, J. Bonnyman, M.F. Mackay, and G.A. Williams, Aust. J. Chem. *35*, 2413–2422 (1982)
[73] J. Baldas, J.F. Boas, J. Bonnyman, J.R. Pilbrow, and G.A. Williams, J. Am. Chem. Soc. *107*, 1886–1891 (1985)
[74] K. Yamanouchi and J.H. Enemark, Inorg. Chem. *17*, 2911–2917 (1978)
[75] A.J. Edwards, D. Hugill, and R.D. Peacock, Nature *200*, 672 (1963)
[76] D. Hugill and R.D. Peacock, J. Chem. Soc. (A), 1339–1341 (1966)
[77] R.D. Peacock, Technetium in: The Chemistry of Manganese, Technetium and Rhenium, Pergamon Texts in Inorganic Chemistry, Vol. 22, (R.D.W. Kemmitt and R.D. Peacock, eds.), Pergamon Press, Oxford (1973)
[78] B. Frlec, H. Selig, and H.H. Hyman, Inorg. Chem. *6*, 1775–1783 (1967)
[79] J.E. Fergusson and R.S. Nyholm, Chem. Ind. (London) 347–348 (1960)
[80] K.A. Glavan, R. Whittle, J.F. Johnson, R.C. Elder, and E. Deutsch, J. Am. Chem. Soc. *102*, 2103–2104 (1980)
[81] J. Cook, W.M. Davis, A. Davison, and A.G. Jones, Inorg. Chem. *30*, 1773–1776 (1991)
[82] R.A. Bell, J.F. Britten, A. Guest, C.J.L. Lock, and J.F. Valliant, Chem. Commun. 585–586 (1997)
[83] F.A. Cotton, A. Davison, V.W. Day, L.D. Gage, and H.S. Trop, Inorg. Chem. *18*, 3024–3029 (1979)
[84] W. Preetz and G. Peters, Z. Naturforschg. *35b*, 1355–1358 (1980)
[85] A. Davison, H.S. Trop, B.V. Depamphilis, and A.G. Jones, Inorg. Synth. *21*, 160–162 (1982)
[86] J. Baldas and S.F. Colmanet, Aust. J. Chem. *42*, 1155–1159 (1989)
[87] R.W. Thomas, A. Davison, H.S. Trop, and E. Deutsch, Inorg. Chem. *19*, 2840–2842 (1980)
[88] R. Hübener and U. Abram, Z. Anorg. Allg. Chem. *617*, 96–98 (1992)
[89] D. Mantegazzi, F. Janoz, P. Lerch, and K. Tatsumi, Inorg. Chim. Acta *167*, 195–198 (1990)
[90] G. Peters and W. Preetz, Z. Naturforschg. *36b*, 138–140 (1981)
[91] A. Davison and A.G. Jones, Int. J. Appl Radiat. Isot. *33*, 875–881 (1982)
[92] E.J. Baran and C.I. Cabello, Z. Naturforschg. *38a*, 563–565 (1983)
[93] R.W. Thomas, M.J. Heeg, R.C. Elder, and E. Deutsch, Inorg. Chem. *24*, 1472–1477 (1985)
[94] J.E. Fergusson, A.M. Greenaway, and B.R. Penfold, Inorg. Chim. Acta *71*, 29–34 (1983)
[95] B. Jezowska-Trzebiatowska and M. Baluka, Bull. Acad. Polon. Sci., Ser. Sci. Chim. *13*, 1–4 (1965)
[96] B. Jezowska-Trzebiatowska and L. Natkanei, J. Struct. Chem. *8*, 460–462 (1967)
[97] M. Baluka, J. Hanuza, and B. Jezowska-Trzebiatowska, Bull. Acad. Polon. Sci., Ser. Sci. Chim. *20*, 271–278 (1972)
[98] J. Hanuza, M. Baluka, W. Machner, and B. Jezowska-Trzebiatowska, Acta Phys. Polon. *A71*, 91–110 (1987)
[99] H.S. Trop, A.G. Jones, and A. Davison, Inorg. Chem. *19*, 1993–1997 (1980)
[100] A. Roodt, J.G. Leipoldt, E.A. Deutsch, and J.C. Sullivan, Inorg. Chem. *31*, 1080–1085 (1992)
[101] A Davison, A.G. Jones, L. Müller, R. Tatz, and H.S. Trop, Inorg. Chem. *20*, 1160–1163 (1981)
[102] A. Davison, B.V. De Pamphilis, A.G. Jones, K.J. Franklin, and C.J.K. Lock, Inorg. Chim. Acta *128*, 161–167 (1987)
[103] G. Huber, G. Anderegg, and K. May, Polyhedron *6*, 1707–1708 (1987)
[104] F.D. Rochon, R. Melanson, and P.-C. Kong, Acta Cryst. *C48*, 785–788 (1992)
[105] H. Luo, S.J. Rettig, and C. Orvig, Inorg. Chem. *32*, 4491–4497 (1993)
[106] J.E. Smith, E.F. Byrne, F.A. Cotton, and J.C. Sekutowski, J. Am. Chem. Soc. *100*, 5571–5572 (1978)
[107] E.F. Byrne and J.E. Smith, Inorg. Chem. *18*, 1832–1835 (1979)
[108] B.V. De Pamphilis, A.G. Jones, M.A. Davis, and A. Davison, J. Am. Chem. Soc. *100*, 5570–5571 (1978)

[109] A. Davison, C. Orvig, H.S. Trop, M. Sohn, B.V. De Pamphilis, and A.G. Jones, Inorg. Chem. *19*, 1988–1992 (1980)
[110] S.F. Colmanet and M.F. Mackay, Inorg. Chim. Acta *147*, 173–178 (1988)
[111] S.F. Colmanet and M.F. Mackay, Aust. J. Chem. *40*, 1301–1307 (1987)
[112] S.F. Colmanet and M.F. Mackay, Aust. J. Chem. *41*, 151–155 (1988)
[113] T.A. Hamor, W. Hussain, C.J. Jones, I.A. McCleverty, and A.S. Rothin, Inorg. Chim. Acta *146*, 181–185 (1988)
[114] A. Davison, N. De Vries, and J. Dewan, Inorg. Chim. Acta *120*, L15–L16 (1986)
[115] M.J. Abrams, D. Brenner, A. Davison, and A.G. Jones, Inorg. Chim. Acta *77*, L127–L128 (1983)
[116] F.D. Rochon, R. Melanson, and P.-C. Kong, Inorg. Chim. Acta *194*, 43–50 (1992)
[117] H. Spies and B. Johannsen, Inorg. Chim. Acta *48*, 255–258 (1981)
[118] H. Spies and B. Johannsen, Inorg. Chim. Acta *33*, L113 (1979)
[119] H. Spies, B. Johannsen, and R. Münze, Z. Chem. *20*, 222–223 (1980)
[120] H. Spies and D. Scheller, Inorg. Chim. Acta *116*, 1–4 (1986)
[121] H. Spies and B. Johannsen, React. Kinet. Catal. Lett. *10*, 153–155 (1979)
[122] H. Spies, React. Kinet. Catal. Lett. *10*, 131–133 (1979)
[123] G. Bandoli, M. Nicolini, U. Mazzi, H. Spies, and R. Münze, Transition Met. Chem. *9*, 127–129 (1984)
[124] H.-J. Pietzsch, H. Spies, and S. Hoffmann, Inorg. Chim. Acta *161*, 15–16 (1989)
[125] H.-J. Pietzsch, H. Spies, and S. Hoffmann, Inorg. Chim. Acta *165*, 163–166 (1989)
[126] J.G.H. du Preez and T.I.A. Gerber, Inorg. Chim. Acta *110*, 59–62 (1985)
[127] A.G. Jones, B.V. DePamphilis, and A. Davison, Inorg. Chem. *20*, 1617–1618 (1981)
[128] D.V. DePamphilis, A.G. Jones, and A. Davison, Inorg. Chem. *22*, 2292–2297 (1983)
[129] M.M. Morelock, T.A. Cormier, and G.L. Tolman, Inorg. Chem. *27*, 3137–3140 (1988)
[130] G. Bandoli, U. Mazzi, U. Abram, H. Spies, and R. Münze, Polyhedron *6*, 1547–1550 (1987)
[131] U. Abram and H. Spies, Z. Chem. *24*, 74–75 (1984)
[132] C.K. Fair, D.E. Troutner, E.O. Schlemper, R.K. Murmann, and M.L. Hoppe, Acta Cryst. *C40*, 1544–1546 (1984)
[133] S. Jurisson, E.O. Schlemper, D.E. Troutner, L.R. Canning, D.P. Nowotnik, and R.D. Neirinckx, Inorg. Chem. *25*, 543–549 (1986)
[134] S. Jurisson, K. Aston, C.K. Fair, E.O. Schlemper, P.R. Sharp, and D.E. Troutner, Inorg. Chem. *26*, 3576–3582 (1987)
[135] A.J. Lawrence and J.R. Thornback, Inorg. Chim. Acta *141*, 165–166 (1988)
[136] K. Schwochau, K.H. Linse, P. Pleger, U. Pleger, C. Kremer, and A.A. de Graaf, J. Labelled Compd. Radiopharm. *38*, 1031–1038 (1996)
[137] G.F. Morgan, M. Deblaton, W. Hussein, J.R. Thornback, G. Evrard, F. Durant, J. Stach, U. Abram, and S. Abram, Inorg. Chim. Acta *190*, 257–264 (1991)
[138] G.F. Morgan, U. Abram, G. Evrard, F. Durant, M. Deblaton, P. Clemens, P. Van den Broeck and J.R. Thornback, J. Chem. Soc., Chem. Commun. *1990*, 1772–1773
[139] F. Refosco, F. Tisato, U. Mazzi, G. Bandoli, and M. Nicolini, J. Chem. Soc. Dalton Trans. 611–615 (1988)
[140] S. Liu, S.J. Rettig, and C. Orvic, Inorg. Chem. *30*, 4915–4919 (1991)
[141] J.G.H. Du Preez, T.I.A. Gerber, and H.J. Kemp, J. Coord. Chem. *26*, 177–186 (1992)
[142] M.J. Abrams, S.N. Shaikh, and J. Zubieta, Inorg. Chim. Acta *186*, 87–90 (1991)
[143] H. Luo, S. Liu, S.J. Rettig, and C. Orvig, Can. J. Chem. *73*, 2272–2281 (1995)
[144] J.G.H. Du Preez, T.I.A. Gerber, and M.L. Gibson, J. Coord. Chem. *22*, 159–163 (1990)
[145] S. Jurisson, L.F. Lindoy, K.P. Dancey, M. McPartlin, P.A. Tasker, D.K. Uppal, and E. Deutsch, Inorg. Chem. *23*, 227–231 (1984)
[146] R.M. Mahfouz, A.S. El-Shatawy, S.A. El-Shatoury, and R.M. Hassan, Spectroscopy Letters *28*, 127–135 (1995)
[147] A.S. El-Shahawy, R.M. Mahfouz, A.A.M. Aly, and M. El-Zohry, J. Chem. Tech. Biotechnol. *56*, 227–231 (1993)
[148] U. Mazzi, F. Refosco, F. Tisato, G. Bandoli, and M. Nicolini, J. Chem. Soc. Dalton Trans. 1623–1628 (1986)
[149] F. Refosco, U. Mazzi, E. Deutsch, J.R. Kirchhoff, W.R. Heinemann, and R. Seeber, Inorg. Chem. *27*, 4121, 4127 (1988)
[150] A. Duatti, A. Marchi, L. Magon, E. Deutsch, V. Bertolasi, and G. Gilli, Inorg. Chem. *26*, 2182–2186 (1987)

[151] G. Bandoli and T.I.A. Gerber, Inorg. Chim. Acta *126*, 205–208 (1987)
[152] H. Spies, H.-J. Pietzsch, and I. Hoffmann, Inorg. Chim. Acta *161*, 17–19 (1989)
[153] A. Davison, A.G. Jones, C. Orvig, and M. Sohn, Inorg. Chem. *20*, 1629–1632 (1981)
[154] A.G. Jones, A. Davison, M.R. LaTegola, J.W. Brodack, C. Orvic, M. Sohn, A.K. Toothaker, C.J.L. Lock, K.J. Franklin, C.E. Costello, S.A. Carr, K. Biemann, and M.L. Kaplan, J. Nucl. Med. *23*, 801–809 (1982)
[155] D. Brenner, A. Davison, J. Lister-James, and A.G. Jones, Inorg. Chem. *23*, 3793–3797 (1984)
[156] T.N. Rao, D. Adhikesavalu, A. Camerman, and A.R. Fritzberg, J. Am. Chem. Soc. *112*, 5798–5804 (1990)
[157] T.N. Rao, D.I. Brixner, A. Srinivasan, S. Kasina, J.-L. Vanderheyden, D.W. Wester, and A.R. Fritzberg, Appl. Radiat. Isot. *42*, 525–530 (1991)
[158] B. Chen, M.J. Heeg, and E. Deutsch, Inorg. Chem. *31*, 4683–4690 (1992)
[159] N. Bryson, J.C. Dewan, J. Lister-James, A.G. Jones, and A. Davison, Inorg. Chem. *27*, 2154–2161 (1988)
[160] D.S. Edwards, E.H. Cheesman, M.W. Watson, L.J. Maheu, S.A. Nguyen, L. Dimitre, T. Nason, A.D. Watson, and R. Walovitch in: Technetium in Chemistry and Nuclear Medicine 3, (M. Nicolini, G. Bandoli, U. Mazzi, eds.), Cortina International, Verona, Raven Press, New York, (1990) pp. 433–444
[161] P. Blondeau, C. Berse, and D. Gravel, Can. J. Chem. *45*, 49–52 (1967)
[162] A. Mahmood, W.A. Halpin, K.E. Baidoo, D.A. Sweigart, and S.Z. Lever, Acta Cryst. *C47*, 254–257 (1991)
[163] S.Z. Lever, K.E. Baidoo, and A. Mahmood, Inorg. Chim. Acta *176*, 183–184 (1990)
[164] H.F. Kung, Y.-Z. Guo, C.-C. Yu, J. Billings, V. Subramanyam, and J.C. Calabrese, J. Med. Chem. *32*, 433–437 (1989)
[165] L.C. Francesconi, G. Graczyk, S. Wehrli, S.N. Shaikh, D. McClinton, L. Liu, J. Zubieta, and H.F. Kung, Inorg. Chem. *32*, 3114–3124 (1993)
[166] R.M. Mahfouz, A.S. El Shahawy, and A.A. Hassan, Trans. Met. Chem. *19*, 385–386 (1994)
[167] J.P. O'Neil, S.R. Wilson, and A. Katzenellenbogen, Inorg. Chem. *33*, 319–323 (1994)
[168] Y.-C.J. Chen and K.D. Janda, J. Am. Chem. Soc. *114*, 1488–1489 (1992)
[169] M.S. Papadopoulos, M. Pelecanou, I.C. Pirmettis, D.M. Spyriounis, C.P. Raptopoulou, A. Terzis, C.I. Stassinopoulou, and E. Chiotellis, Inorg. Chem. *35*, 4478–4483 (1996)
[170] I.C. Pirmettis, M.S. Papadopoulos, S.G. Mastrostamatis, C.P. Raptopoulou, A. Terzis, and E. Chiotellis, Inorg. Chem. *35*, 1685–1691 (1996)
[171] C.S. John, L.C. Francesconi, and H.F. Kung, Polyhedron *11*, 1145–1155 (1992)
[172] R. Faggiani, C.J.L. Lock, L.A. Epps, A.V. Kramer, and D. Brune, Acta Cryst. *C44*, 777–779 (1988)
[173] R. Faggiani, C.J.L. Lock, L.A. Epps, A.V. Kramer, and H.D. Brune, Acta Cryst. *C46*, 2324–2327 (1990)
[174] U. Abram, R. Muenze, J. Hartung, L. Beyer, R. Kirmse, K. Koehler, J. Stach, H. Behm, and P.T. Beurskens, Inorg. Chem. *28*, 834–839 (1989)
[175] A. Marchi, L. Marvelli, R. Rossi, L. Magon, V. Bertolasi, V. Ferretti, and P. Gilli, Chem. Dalton Trans. 1485–1490 (1992)
[176] C.I. Stassinopoulou, S. Mastrostamatis, M. Papadopoulos, H. Vavouraki, A. Tercis, A. Hountas, and E. Chiotellis, Inorg. Chim. Acta *189*, 219–224 (1991)
[177] J.G.H. Du Preez, T.I.A. Gerber, and M.L. Gibson, J. Coord. Chem. *22*, 321–325 (1991)
[178] J.G.H. Du Preez, T.I.A. Gerber, M. Gibson, and H.J. Kemp, J. Coord. Chem. *25*, 53–61 (1992)
[179] N.Bryson, J. Lister-James, A.G. Jones, W.M. Davis, and A. Davison, Inorg. Chem. *29*, 2948–2951 (1990)
[180] G. Grummon, R. Rajagopalan, G.J. Palenik, A.E. Koziol, and D.L. Nosco, Inorg. Chem. *34*, 1764–1772 (1995)
[181] N.M. Blaton, G. Bormans, O.M. Peeters, and A. Verbruggen, Acta Cryst. *C53*, 449–451 (1997)
[181a] E. Wong, T. Fauconnier, S. Bennet, J. Valliant, T. Nguyen, F. Lau, L.F.L. Lu, A. Pollak, R.A. Bell, and J.R. Thornback, Inorg. Chem. *36*, 5799–5808 (1997)
[182] N. de Vries, A.G. Jones, and A. Davison, Inorg. Chem. *28*, 3728–3734 (1989)
[183] D.M. Spyriounis, M. Pelecanou, C.I. Stassinopoulou, C.P. Raptopoulou, A. Terzis, and E. Chiotellis, Inorg. Chem. *34*, 1077–1082 (1995)
[184] R.W. Thomas, G.W. Estes, R.C. Elder, and E. Deutsch, J. Am. Chem. Soc. *101*, 4581–4585 (1979)
[185] J.G.H. Du Preez, T.I.A. Gerber, and R. Jacobs, J. Coord. Chem. *26*, 259–268 (1992)

[186] J.G.H. Du Preez, T.I.A. Gerber, and R. Jacobs, J. Coord. Chem. *33*, 147–160 (1994)
[187] G. Bandoli, U. Mazzi, D.A. Clemente, and E. Roncari, J. Chem. Soc. Dalton Trans., 2455–2459 (1982)
[188] G. Bandoli, M. Nicolini, U. Mazzi, and F. Refosco, J. Chem. Soc. Dalton Trans. 2505–2511 (1984)
[189] F.D. Rochon, R. Melanson, and P.-C. Kong, Inorg. Chim. Acta *254*, 303–307 (1997)
[190] B.E. Wilcox, M.J. Heeg, and E. Deutsch, Inorg. Chem. *23*, 2962–2967 (1984)
[191] T. Omori, Y. Yamada, S. Iino, and K. Yoshihara, J. Radioanal. Nucl. Chem., Letters *119*, 223–233 (1987)
[192] R.M. Pearlstein, C.J.L. Lock, R. Faggiani, C.F. Costello, C.-H. Zeng, A.G. Jones, and A. Davison, Inorg. Chem. *27*, 2409–2413 (1988)
[193] E. Shuter, H.R. Hoveyda, V. Karunaratne, S.J. Rettig, and C. Orvig, Inorg. Chem. *35*, 368–372 (1996)
[194] B.E. Wilcox, J.N. Cooper, R.C. Elder, and E. Deutsch, Inorg. Chim. Acta *142*, 55–58 (1988)
[195] T.I.A. Gerber, H.J. Kemp, J.G.H. Du Preez, and G. Bandoli, J. Coord. Chem. *28*, 329–336 (1993)
[196] P.H. Fackler, M.E. Kastner, and M.J. Clarke, Inorg. Chem. *23*, 3968–3972 (1984)
[197] F. Tisato, F. Refosco, A. Moresco, G. Bandoli, U. Mazzi, and M. Nicolini, J. Chem. Soc. Dalton Trans. 2225–2232 (1990)
[198] A. Duatti, A. Marchi, R. Rossi, L. Magon, E. Deutsch, V. Bertolasi, and F. Bellucci, Inorg. Chem. *27*, 4208–4213 (1988)
[199] G. Bandoli, U. Mazzi, B.E. Wilcox, S. Jurisson, and E. Deutsch, Inorg. Chim. Acta *95*, 217–223 (1984)
[200] U. Abram, S. Abram, W. Hiller, G.F. Morgan, J.R. Thornback, M. Deblaton, and J. Stach, Z. Naturforsch. *46b*, 453–458 (1991)
[201] B. Johannsen, B. Noll, P. Leibnitz, G. Reck, S. Noll, and H. Spies, Radiochim. Acta *210*, 209–214 (1993)
[202] B. Johannsen, B. Noll, P. Leibnitz, G. Reck, S. Noll, and H. Spies, Radiochim. Acta *63*, 133–137 (1993)
[203] K.J. Franklin, H.E. Howard-Lock, and C.J.L. Lock, Inorg. Chem. *21*, 1941–1946 (1982)
[204] D.L. Johnson, A.R. Fritzberg, B.L. Hawkins, S. Kasina, and D. Eshima, Inorg. Chem. *23*, 4204–4207 (1984)
[205] T.I.A. Gerber, J.G.H. Du Preez, R. Jacobs, and B.J.A.M. van Brecht, J. Coord. Chem. *31*, 31–38 (1994)
[206] T. Gerber, H. Kemp, J. du Preez, and G. Bandoli, Radiochim. Acta *63*, 129–132 (1993)
[207] T. Nicholson, A. Davison, and A.G. Jones, Inorg. Chim. Acta *168*, 227–231 (1990)
[208] G. Bandoli, U. Mazzi, H.-J. Pietzsch, and H. Spies, Acta Cryst. *C48*, 1422–1425 (1992)
[209] H.-J. Pietzsch, H. Spies, S. Hoffmann, and D. Scheller, Appl. Radiat. Isot. *41*, 185–188 (1990)
[210] J.G.H. du Preez, T.I.A. Gerber, P.J. Fourie, and A.J. van Wyk, J. Coord. Chem. *13*, 173–178 (1984)
[211] G.H. du Preez, T.I.A. Gerber, and O. Knoesen, Inorg. Chim. Acta *132*, 241–245 (1987)
[212] T.I.A. Gerber, J.G.H. du Preez, and H.J. Kemp, J. Coord. Chem. *33*, 245–255 (1994)
[213] F. Tisato, U. Mazzi, G. Bandoli, G. Cros, M.-H. Darbieu, Y. Coulais, and R. Guiraud, J. Chem. Soc. Dalton Trans. 1301–1307 (1991)
[214] F. Tisato, F. Refosco, U. Mazzi, G. Bandoli, and M. Nicolini, J. Chem. Soc. Dalton Trans. 1693–1699 (1987)
[215] A. Marchi, R. Rossi, L. Magon, A. Duatti, R. Pasqualini, V. Ferretti, and V. Bertolasi, J. Chem. Soc. Dalton Trans. 1411–1416 (1990)
[216] J.G.H. du Preez, T.I.A. Gerber, and O. Knoesen, J. Coord. Chem. *16*, 285–291 (1987)
[217] J.G.H. du Preez, T.I.A. Gerber, and O. Knoesen, Inorg. Chim. Acta *130*, 9–10 (1987)
[217a] M. Cattabriga, A. Marchi, L. Marvelli, R. Rossi, G. Vertuani, R. Pecoraro, A. Scatturin, V. Bertolasi, and V. Ferretti, J. Chem. Soc., Dalton Trans. 1453–1459 (1998)
[218] F. Refosco, F. Tisato, G. Bandoli, C. Bolzati, A. Dolmella, A. Moresco, and M. Nicolini, J. Chem. Soc. Dalton Trans. 605–618 (1993)
[219] F. Tisato, F. Refosco, A. Moresco, G. Bandoli, A. Dolmella, and C. Bolzati, Inorg. Chem. *34*, 1779–1787 (1995)
[220] J.R. Dilworth, A.J. Hutson, S. Morton, M. Harman, M.B. Hursthouse, J. Zubieta, C.M. Archer, and J.D. Kelly, Polyhedron *11*, 2151–2155 (1992)
[221] H. Luo, I. Setyawati, S.J. Rettig, and C. Orvig, Inorg. Chem. *34*, 2287–2299 (1995)
[222] C. Bolzati, F. Tisato, F. Refosco, and G. Bandoli, Inorg. Chim. Acta *247*, 125–127 (1996)

[223] J.R. Dilworth, D.V. Griffiths, J.M. Hughes, S. Morton, C.M. Archer, and J.D. Kelly, Inorg. Chim. Acta *195*, 145–149 (1992)
[224] F. Tisato, C. Bolzati, A. Duatti, G. Bandoli, and F. Refosco, Inorg. Chem. *32*, 2042–2048 (1993)
[225] A. Duatti, F. Tisato, F. Refosco, U. Mazzi, and M. Nicolini, Inorg. Chem. *28*, 4564–4565 (1989)
[226] M.E. Kastner, M.J. Lindsay, and M.J. Clarke, Inorg. Chem. *21*, 2037–2040 (1982)
[227] F. Riché, M. Vidal, C. Bolzati, L. Uccelli, A. Marchi, and A. Duatti, Inorg. Chim. Acta *231*, 147–151 (1995)
[228] C. Kremer, A. León, and E. Kremer, J. Radioanal. Nucl. Chem. Letters *176*, 143–152 (1993)
[229] C. Kremer, J. Gancheff, E. Kremer, A.W. Mombru, O. González, R. Mariezcurrena, L. Suescun, M.L. Cubas, and O.N. Ventura, Polyhedron *16*, 3311–3316 (1997)
[230] A. Zuckman, G.M. Freeman, D.E. Troutner, W.A. Volkert, R.A. Holmes, G. van Derveer, and E.K. Barefield, Inorg. Chem. *20*, 2386–2389 (1981)
[231] P. Bläuenstein, G. Pfeiffer, P.A. Schubiger, G. Anderegg, K. Zollinger, K. May, Z. Proso, E. Ianovici, and P. Lerch, Int. J. Appl. Radiat. Isot. *36*, 315–317 (1985)
[232] P.H. Fackler, M.J. Lindsay, M.J. Clarke, and M.E. Kastner, Inorg. Chim. Acta *109*, 39–49 (1985)
[233] A.F. Kuzina, A.A. Oblova, and V.I. Spitsyn, Russ. J. Inorg. Chem. *17*, 1377–1379 (1972)
[234] M.E. Kastner, P.H. Fackler, M.J. Clarke, and E. Deutsch, Inorg. Chem. 23, 4683–4688 (1984)
[235] J. Lu and M.J. Clarke, Inorg. Chem. *28*, 2315–2319 (1989)
[236] E. Ianoz, D. Mantegazzi, P. Lerch, F. Nicolò, and G. Chapuis, Inorg. Chim. Acta *156*, 235–239 (1989)
[237] S. Truffer, E. Ianoz, P. Lerch, and M. Kosinski, Inorg. Chim. Acta *149*, 217–222 (1988)
[238] J.G.H. Du Preez, T.I.A. Gerber, P.J. Fourie, and A.J. Van Wyk, Inorg. Chim. Acta *82*, 201–205 (1984)
[239] J.-L. Vanderheyden, A.R. Ketring, K. Libson, M.J. Heeg, L. Roecker, P. Motz, R. Whittle, R.C. Elder, and E. Deutsch, Inorg. Chem. *23*, 3184–3191 (1984)
[240] J.D. Kelly, A.M. Forster, B. Highley, C.M. Archer, F.S. Booker, L.R. Canning, K.W. Chiu, B. Edwards, H.K. Gill, M. McPartlin, K.R. Nagle, I.A. Latham, R.D. Pickett, A.E. Storey, and P.M. Webbon, J. Nucl. Med. *34*, 222–227 (1993)
[241] F.D. Rochon, R. Melanson, and P.-C. Kong, Inorg. Chem. *37*, 87–92 (1998)
[242] F. Tisato, F. Refosco, U. Mazzi, G. Bandoli, and A. Dolmella, Inorg. Chim. Acta *164*, 127–135 (1989)
[243] M.R.A. Pillai, C.S. John, J.M. Lo, E.O. Schlemper, and D.E. Troutner, Inorg. Chem. *29*, 1850–1856 (1990)
[244] U. Abram, S. Abram, H.R. Mäcke, and P. Koch, Z. Anorg. Allg. Chem. *621*, 854–860 (1995)
[245] H.-J. Pietzsch, H. Spies, P. Leibnitz, G. Reck, J. Beger, and R. Jacobi, Polyhedron *12*, 187–193 (1993)
[246] A. Davison, B.V. DePamphilis, R. Faggiani, A.G. Jones, C.J.L. Lock, and C. Orvig, Can. J. Chem. *63*, 319–323 (1985)
[247] N.J. Bryson, D. Brenner, J. Lister-James, A.G. Jones, J.C. Dewan, and A. Davison, Inorg. Chem. *28*, 3825–3828 (1989)
[248] J.G.H. Du Preez, T.I.A. Gerber, M.L. Gibson, and R. Geyser, J. Coord. Chem. *22*, 249–254 (1990)
[249] J. Baldas, G.N. Heath, R.G. Raptis, and G.A. Williams (unpublished) in: J. Baldas, The Chemistry of Technetium Nitrido Complexes, Topics in Current Chemistry *176*, 40 (1996)
[250] U. Abram, H. Spies, S. Abram, R. Kirmse, and J. Stach, Z. Chem. *26*, 140–141 (1986)
[251] J. Baldas, S.F. Colmanet, and G.A. Williams (unpublished) In J. Baldas "The Chemistry of Technetium Nitrido Complexes", Topics in Current Chemistry *176*, 41 (1996)
[252] G.A. Williams and J. Baldas, J. Nucl. Med. Allied Sciences *33*, 327 (1989)
[253] J. Baldas, J. Bonnyman, and G.A. Williams, J. Chem. Soc. Dalton Trans. 833–837 (1984)
[254] J. Baldas, J.F. Boas, S.F. Colmanet, and M.F. Mackay, Inorg. Chim. Acta *170*, 233–239 (1990)
[255] A. Mutalib, T. Sekine, T. Omori, and K. Yoshihara, Radiochim. Acta *63*, 123–127 (1993)
[256] E. Uhlemann, H. Spies, H.-J. Pietzsch, and R. Herzschuh, Z. Naturforsch *47b*, 1441–1443 (1992)
[257] J.R. Dilworth, R. Hübener, and U. Abram, Z. Anorg. Allg. Chem. *623*, 880–882 (1997)
[258] J. Baldas, J. Bonnyman, P.M. Pojer, G.A. Williams, and M.F. Mackay, J. Chem. Soc. Dalton Trans. 1798–1801 (1981)
[259] U. Abram and H. Spies, Inorg. Chim. Acta *94*, L3-L16 (1984)
[260] C. Bolzati, L. Uccelli, A. Duatti, M. Venturini, C. Morin, S. Cheradame, F. Refosco, F. Ossala, and F. Tisato, Inorg. Chem. *36*, 3582–3585 (1997)

[261] U. Abram, R. Münze, R. Kirmse, K. Köhler, W. Dietzsch, and L. Golic, Inorg. Chim. Acta *169*, 49–53 (1990)
[262] R. Rossi, A. Marchi, L. Magon, U. Casellato, and R. Graziani, J. Chem. Soc. Dalton Trans. 2923–2925 (1990)
[263] G.A. Williams and J. Baldas, Aust. J. Chem. *42*, 875–884 (1989)
[264] U. Abram, H. Spies, W. Görner, R. Kirmse, and J. Stach, Inorg. Chim. Acta 109, L9-L11 (1985)
[265] J. Stach, W. Dietzsch, and U. Abram, Z. Chem. *29*, 295 (1989)
[266] B. Lorenz, K. Schmidt, L. Kaden, and M. Wahren, Isotopenpraxis *22*, 444–446 (1986)
[267] U. Abram, S. Abram, J. Stach, W. Dietzsch, and W. Hiller, Z. Naturforschg. *46b*, 1183–1187 (1991)
[268] J. Baldas and J. Bonnyman, Inorg. Chim. Acta *141*, 153–154 (1988)
[269] H.-J. Pietzsch, H. Spies, P. Leibnitz, and G. Reck, Polyhedron *12*, 2995–3002 (1993)
[270] H.-J. Pietzsch, H. Spies, P. Leibnitz, G. Reck, and B. Johannsen, Radiochim Acta *63*, 163–166 (1993)
[271] U. Abram, E. Schulz-Lang, S. Abram, J. Wegmann, J.R. Dilworth, R. Kirmse, and D. Woolins, J. Chem. Soc. Dalton Trans. 623–630 (1997)
[272] S. Rummel, M. Hermann, and K. Schmidt, Z. Chem. *25*, 152–153 (1985)
[273] Y. Kani, T. Takayama, S. Inomata, T. Sekine, and H. Kudo, Chem. Letters 1059–1060 (1995)
[273a] Y. Kani, T. Takayama, T. Sekine, and H. Kudo, J. Chem. Soc., Dalton Trans. 209–214 (1999)
[274] A. Marchi, R. Rossi, L. Magon, A. Duatti, U. Casellato, R. Graziani, M. Vidal, and F. Riche, J. Chem. Soc. Dalton Trans. 1935–1940 (1990)
[275] V. Bertolasi, V. Ferretti, P. Gilli, A. Marchi, and L. Marvelli, Acta Cryst. *C47*, 2535–2539 (1991)
[276] N. de Vries, C.E. Costello, A.G. Jones, and A. Davison, Inorg. Chem. *29*, 1348–1352 (1990)
[277] A. Duatti, A. Marchi, V. Bertolasi, and V. Ferretti, J. Am. Chem. Soc. *113*, 9680–9682 (1991)
[278] A. Marchi, P. Garuti, A. Duatti, L. Magon, R. Rossi, V. Ferretti, and V. Bertolasi, Inorg. Chem. *29*, 2091–2096 (1990)
[279] M.J. Clarke and J. Lu, Inorg. Chem. *31*, 2476–2480 (1992)
[280] C.M. Archer, J.R. Dilworth, J.D. Kelly, and M. McPartlin, J. Chem. Soc., Chem. Commun. 375–376 (1989)
[281] C.M. Archer, J.R. Dilworth, J.D. Kelly, and M. McPartlin, Polyhedron *8*, 1879–1881 (1989)
[282] C.M. Archer, J.R. Dilworth, D.V. Griffiths, M. McPartlin, and J.D. Kelly, J. Chem. Soc. Dalton Trans. 183–189 (1992)
[283] J.R. Dilworth, D.V. Griffiths, J.M. Hughes, S. Morton, W. Hiller, C.M. Archer, J.D. Kelly, and G. Walton, Inorg. Chim. Acta *192*, 59 (1992)
[284] A. Marchi, A. Duatti, R. Rossi, L. Magon, R. Pasqualini, V. Bertolasi, V. Ferretti, and G. Gilli, J. Chem. Soc. Dalton Trans. 1743–1749 (1988)
[285] G. Cros, H.B. Tahar, D. de Montauzon, A. Gleizes, Y. Coulais, R. Guiraud, E. Bellande, and R. Pasqualini, Inorg. Chim. Acta *227*, 25–31 (1994)
[286] U. Abram, J. Hartung, L. Beyer, R. Kirmse, and K. Köhler, Z. Chem. *27*, 101–102 (1987)
[287] U. Abram, J. Hartung, L. Beyer, J. Stach, and R. Kirmse, Z. Chem. *30*, 180–181 (1990)
[288] U. Abram, S. Abram, and J.R. Dilworth, Z. Anorg. Allg. Chem. *622*, 1257–1262 (1996)
[289] F. Refosco, F. Tisato, A. Moresco, and G. Bandoli, J. Chem. Soc. Dalton Trans. 3475–3482 (1995)
[290] A. Duatti, A. Marchi, and R. Pasqualini, J. Chem. Soc. Dalton Trans. 3729–3733 (1990)
[291] J. Baldas, S.F. Colmanet, Z. Ivanov, and G.A. Williams, J. Chem. Soc., Chem. Commun. 2153–2154 (1994)
[292] R. Rossi, A. Marchi, S. Aggio, L. Magon, A. Duatti, U. Casellato, and R. Graziani, J. Chem. Soc. Dalton Trans. 477–481 (1990)
[293] A. Marchi, R. Rossi, L. Marvelli, and V. Bertolasi, Inorg. Chem. *32*, 4673–4674 (1993)
[294] U. Abram, R. Münze, E.-G. Jäger, J. Stach, and R. Kirmse, Inorg. Chim. Acta *162*, 171–173 (1989)
[295] U. Abram, S. Abram, R. Münze, E.-G. Jäger, J. Stach, R. Kirmse, G. Admiraal, and P.T. Beurskens, Inorg. Chim. Acta *182*, 233–238 (1991)
[296] S. Ritter, U. Abram, and J.R. Dilworth, Z. Anorg. Allg. Chem. *622*, 1975–1978 (1996)
[297] L. Kaden, B. Lorenz, K. Schmidt, H. Prinz, and M. Wahren, Isotopenpraxis *17*, 174–175 (1981)
[298] M.J. Abrams, S.K. Larsen, S.N. Shaikh, and J. Zubieta, Inorg. Chim. Acta *185*, 7–15 (1991)
[299] J. Baldas, J.F. Boas, S.F. Colmanet, and G.A. Williams, J. Chem. Soc. Dalton Trans. 2441–2447 (1991)

[300] A. Marchi, L. Marvelli, R. Rossi, L. Magon, L. Uccelli, V. Bertolasi, V. Ferretti, and F. Zanobini, J. Chem. Soc. Dalton Trans. 1281–1286 (1993)
[301] U. Abram, B. Lorenz, L. Kaden, and D. Scheller, Polyhedron *7*, 285–289 (1988)
[302] A.S. Batsanov, Y.T. Struchkov, B. Lorenz, and B. Olk, Z. Anorg. Allg. Chem. *564*, 129–134 (1988)
[303] U. Abram, P. Mäding, R. Kirmse, and K. Köhler, Z. Chem. *29*, 183–184 (1989)
[304] F.D. Rochon, R. Melanson, and P.-C. Kong, Polyhedron *15*, 2641–2646 (1996)
[305] T. Nicholson, A. Davison, and A.G. Jones, Inorg. Chim. Acta *187*, 51–57 (1991)
[306] T. Nicholson, S.L. Storm, W.M. Davis, A. Davison, and A.G. Jones, Inorg. Chim. Acta *196*, 27–34 (1992)
[307] F.D. Rochon, R. Melanson, and P.-C. Kong, Inorg. Chem. *34*, 2273–2277 (1995)
[308] T. Nicholson, J. Cook, A. Davison, and A.G. Jones, Inorg. Chim. Acta *218*, 97–101 (1994)
[309] T. Nicholson, A. Davison, J.A. Zubieta, Q. Chen, and A.G. Jones, Inorg. Chim. Acta *230*, 205–208 (1995)
[310] C.M. Archer, J.R. Dilworth, P. Jobanputra, R.M. Thompson, M. McPartlin, D.C. Povey, G.W. Smith, and J.D. Kelly, Polyhedron *9*, 1497–1502 (1990)
[311] M.J. Abrams, S.K. Larson, and J. Zubieta, Inorg. Chim. Acta *173*, 133–135 (1990)
[312] T. Nicholson, N. de Vries, A. Davison, and A.G. Jones, Inorg. Chem. *28*, 3813–3819 (1989)
[313] T. Nicholson, J. Cook, A. Davison, D.J. Rose, K.P. Maresca, J.A. Zubieta, and A.G. Jones, Inorg. Chim. Acta *252*, 421–426 (1996)
[314] M.J. Abrams, S.N. Shaikh, and J. Zubieta, Inorg. Chim. Acta *171*, 133–134 (1990)
[315] K. Schwochau and W. Herr, Angew. Chem. *75*, 95–96 (1963)
[316] K. Schwochau in: Handbuch der Präparativen Anorganischen Chemie, Vol. 3, Technetium, (G. Brauer, ed.), Enke, Stuttgart (1981) pp. 1597–1606
[317] K. Schwochau, Z. Naturforschg. *19a*, 1237–1238 (1964)
[318] K. Schwochau, A. Knappwost, E. Burkard, and T.S.B. Narasa Raju, Z. Naturforschg. *19a*, 1128 (1964)
[319] G. Römelt and K. Schwochau, Z. Naturforschg. *22a*, 519–522 (1967)
[320] C.K. Jørgensen and K. Schwochau, Z. Naturforschg. *20a*, 65–75 (1965)
[321] K. Schwochau and W. Krasser, Z. Naturforschg. *24a*, 403–407 (1969)
[322] W. Krasser and K. Schwochau, Z. Naturforschg. *25a*, 206–210 (1970)
[323] R. Alberto and G. Anderegg, Polyhedron *4*, 1067 (1985)
[324] B. Frlec, H. Selig, and H.H. Hyman, Inorg. Chem. *6*, 1775–1783 (1967)
[325] C.M. Nelson, G.E. Boyd, and W.T. Smith, Jr., J. Am. Chem. Soc. *76*, 348–352 (1954)
[326] J. Dalziel, N.S. Gill, R.S. Nyholm, and R.D. Peacock, J. Chem. Soc. 4012–4016(1958)
[327] I.V. Vinogradov, L.L. Zaitseva, M.I. Konarev, and S.V. Shepel'kov, Russ. J. Inorg. Chem. *19*, 1488–1490 (1974)
[328] R.H. Busey, R.B. Bevan, Jr., and R.A. Gilbert, Oak Ridge National Laboratory ORNL-4581, (1970) pp. 121–122
[329] W. Low and P.M. Llewellyn, Phys. Rev. *110*, 842–843 (1958)
[330] S. Maniv, J. Bronstein, and W. Low, Phys. Rev. *187*, 403–406 (1969)
[331] K. Schwochau, Z. Naturforschg. *20a*, 1286–1289 (1965)
[332] H.J. Schenk and K. Schwochau, Z. Naturforschg. *28a*, 89–97 (1973)
[333] M. Elder, J.E. Fergusson, G.J. Gainsford, J.H. Hickford, and B.R. Penfold, J. Chem. Soc. A 423–1425 (1967)
[334] R.C. Elder, G.W. Estes, and E. Deutsch, Acta Cryst. *B35*, 136–137 (1979)
[335] L.L. Zaitseva, M.I. Konarev, P.B. Kozhevnikov, I.V. Vinogradov, A.A. Kruglov, and N.T. Chebotarev, Russ. J. Inorg. Chem. *17*, 1258–1260 (1972)
[336] S.V. Shepel'kov, M.I. Konarev, N.T. Chebotarev, L.L. Zaitseva, and I.V. Vinogradov, Russ. J. Inorg. Chem. *20*, 1828–1830 (1975)
[337] J. Baldas, J. Bonnyman, D.L. Samuels, and G.A. Williams, Acta Cryst. *C40*, 1343–1346 (1984)
[338] L.L. Zaitseva, M.I. Konarev, V.S. Il'yashenko, I.V. Vinogradov, S.V. Shepel'kov, A.A. Kruglov, and N.T. Chebotarev, Russ. J. Inorg. Chem. *18*, 1276–1278 (1973)
[339] S.V. Kryuchkov, M.S. Grigor'ev, A.F. Kuzina, and V.I. Spitsyn, Russ. J. Inorg. Chem. *32*, 1708–1711 (1987)
[340] L.L. Zaitseva, M.I. Konarev, I.V. Vinogradov, E.G. Kozhinov, A.A. Kruglov, and N.T. Chebotarev, Russ. J. Inorg. Chem. *19*, 531–532 (1974)
[341] S.V. Kryuchkov, M.S. Grigor'ev, A.F. Kuzina, and V.I. Spitsyn, Russ. J. Inorg. Chem. *32*, 1714–1716 (1987)

[342] E. Verdonck and L.G. Vanquickenborne, Inorg. Chim. Acta *23*, 67–76 (1977)
[343] T. Fujinaga, M. Koyama, and Y. Kanchiku, Bull. Chem. Soc. Japan *40*, 2970–2971 (1967)
[344] M. Koyama, Y. Kanchiku, and T. Fujinaga, Coord. Chem. Rev. *3*, 285–291 (1968)
[345] Y. Kanchiku, Bull. Chem. Soc. Japan *42*, 2831–2835 (1969)
[346] M. Kawashima, M. Koyama, and T. Fujinaga, J. inorg. nucl. Chem. *38*, 819–822 (1976)
[347] E. Janovici, M. Kosinski, P. Lerch, and A.G. Maddock, J. Radioanal. Chem. *64*, 315–326 (1981)
[348] M. Colin, E. Ianovici, P. Lerch, and A.G. Maddock, J. Radioanal. Nucl. Chem., Articles, *92*, 283–292 (1985)
[349] M. Colin, E. Ianovici, and P. Lerch, J. Radioanal. Nucl. Chem., Articles, *120*, 175–183 (1988)
[350] U. Abram, R. Wollert, and W. Hiller, Radiochim. Acta *63*, 145–147 (1993)
[351] W. Preetz and A. Wendt, Z. Naturforsch. *46b*, 1496–1502 (1991)
[352] A. Wendt and W. Preetz, Z. Naturforschg. *47a*, 882–886 (1992)
[353] C.D. Flint and P.F. Lang, J. Chem. Soc. Dalton Trans. 921–923 (1986)
[354] H.S. Trop, A. Davison, G.H. Carey, B.V. DePamphilis, A.G. Jones, and M.A. Davis, J. Inorg. Nucl. Chem. *41*, 271–272 (1979)
[355] E.W. Huber, W.R. Heineman, and E. Deutsch, Inorg. Chem. *26*, 3718–3722 (1987)
[356] J.E. Fergusson and J.H. Hickford, Aust. J. Chem. *23*, 453–461 (1970)
[357] C.E. Crouthamel, Anal. Chem. *29*, 1756–1760 (1957)
[358] O.H. Howard and C.W. Weber, Anal. Chem. *34*, 530–533 (1962)
[359] R.E. Foster, W.J. Maeck, and J.E. Rein, Anal. Chem. *39*, 563–566 (1967)
[360] K. Schwochau, L. Astheimer, and H.J. Schenk, J. Inorg. Nucl. Chem. *35*, 2249–2257 (1973)
[361] H.S. Trop, A. Davison, A.G. Jones, M.A. Davis, D.J. Szalda, and S.J. Lippard, Inorg. Chem. *19*, 1105–1110 (1980)
[362] G.A. Williams, J. Bonnyman, and J. Baldas, Aust. J. Chem. *40*, 27–33 (1987)
[363] A. Wendt and W. Preetz, Z. Anorg. Allg. Chem. *619*, 1669–1671 (1993)
[364] M.J. Abrams, A. Davison, A.G. Jones, and C.E. Costello, Inorg. Chim. Acta *77*, L235-L236 (1983)
[365] U. Mazzi, E. Roncari, G. Bandoli, and L. Magon, Trans. Met. Chem. *4*, 151–155 (1979)
[366] T. Omori, Y. Yamada, and K. Yoshihara, Inorg. Chim. Acta *130*, 99–104 (1987)
[367] U. Mazzi, E. Roncari, G. Bandoli, and D.A. Clemente, Trans. Met. Chem. *7*, 163–166 (1982)
[368] R. Alberto, G. Anderegg, and K. May, Polyhedron *5*, 2107–2108 (1986)
[369] R. Alberto, A. Albinati, G. Anderegg, and G. Huber, Inorg. Chem. *30*, 3568–3570 (1991)
[370] R. Münze and B. Grossmann, Radiochem. Radioanal. Letters *31*, 95–104 (1977)
[371] R. Münze, Radiochem. Radioanal. Letters *48*, 281–288 (1981)
[372] B. Gorski and H. Koch, J. Inorg. Nucl. Chem. *32*, 3831–3836 (1970)
[373] B. Noll, S. Seifert, and R. Münze, Radiochem. Radioanal. Letters *43*, 215–218 (1980)
[374] H.-B. Bürgi, G. Anderegg, and P. Bläuenstein, Inorg. Chem. *20*, 3829–3834 (1981)
[375] G. Anderegg, E. Müller, K. Zollinger, and H.-B. Bürgi, Helv. Chim. Acta *66*, 1593–1598 (1983)
[376] S.F. Colmanet, G.A. Williams, M.F. Mackay, J. Chem. Soc. Dalton Trans. 2305–2310 (1987)
[377] R. Alberto, G. Anderegg, and A. Albinati, Inorg. Chim. Acta *178*, 125–130 (1990)
[378] S.F. Colmanet and M.F. Mackay, J. Chem. Soc., Chem. Commun. 705–706 (1987)
[379] S.F. Colmanet and M.F. Mackay, Aust. J. Chem. *41*, 269–277 (1988)
[380] S.F. Colmanet and M.F. Mackay, Aust. J. Chem. *41*, 1127–1131 (1988)
[381] J.G.H. du Preez, T.I.A. Gerber, and O. Knoesen, Inorg. Chim. Acta *109*, L17–L18 (1985)
[382] C.D. Bush, T.A. Hamor, W. Hussain, C.J. Jones, J.A. McCleverty, and A.S. Rothin, Acta Cryst. *C43*, 2088–2091 (1987)
[383] O.Y. Levanda, A.A. Oblova, A.F. Kuzina, L.I. Belyaeva, and V.I. Spitsyn, Russ. J. Inorg. Chem. *30*, 522–525 (1985)
[384] J.E. Fergusson and J.H. Hickford, J. Inorg. Nucl. Chem. *28*, 2293–2296 (1966)
[385] G. Hunter and N. Kilcullen, J. Chem. Soc. Dalton Trans. 2115–2119 (1989)
[386] U. Mazzi, G. De Paoli, G. Rizzardi, and L. Magon, Inorg. Chim. Acta *10*, L2 (1974)
[387] U. Mazzi, G. De Paoli, P. Di Bernardo, and L. Magon, J. Inorg. Nucl. Chem. *38*, 721–725 (1976)
[388] G. Bandoli, D.A. Clemente, U. Mazzi, and E. Roncari, J. Chem. Soc. Dalton Trans. 1381–1384 (1982)
[389] F.D. Rochon, R. Melanson, and P.-C. Kong, Acta Cryst. *C47*, 732–737 (1991)
[390] F.A. Cotton, C.S. Day, M.P. Diebold, and W.J. Roth, Acta Cryst. *C46*, 1623–1624 (1990)
[391] F.A. Cotton, S.C. Haefner, and A.P. Sattelberger, Inorg. Chim. Acta *271*, 187–199 (1999)
[392] A.I. Breikss, A. Davison, and A.G. Jones, Inorg. Chim. Acta *170*, 75–79 (1990)

[393] A. Duatti, A. Marchi, S.A. Luna, G. Bandoli, U. Mazzi, and F. Tisato, J. Chem. Soc. Dalton Trans. 867–871 (1987)
[394] J.P. Farr, M.J. Abrams, C.E. Costello, A. Davison, and S.J. Lippart, Organometallics *4*, 139–142 (1985)
[395] U. Abram, S. Abram, and J.R. Dilworth, Acta Cryst. *C52*, 605–607 (1996)
[396] J.C. Bryan, F.A. Cotton, L.M. Daniels, S.C. Haefner, and A.P. Sattelberger, Inorg. Chem. *34*, 1875–1883 (1995)
[397] K. Libson, B.L. Barnett, and E. Deutsch, Inorg. Chem. *22*, 1695–1704 (1983)
[398] A. Roodt, J.C. Sullivan, D. Meisel, and E. Deutsch, Inorg. Chem. *30*, 4545–4549 (1991)
[399] K. Libson, M.N. Doyle, R.W. Thomas, T. Nelesnik, M. Woods, J.C. Sullivan, R.C. Elder, and E. Deutsch, Inorg. Chem. *27*, 3614–3619 (1988)
[400] R.W. Hurst, W.R. Heineman, and E. Deutsch, Inorg. Chem. *20*, 3298–3303 (1981)
[401] E. Unger, Anal. Chem. *56*, 363–368 (1984)
[402] R. Münze, S. Seifert, D. Kloetzer, P. Maeding, and W. Goerner, Int. J. Appl. Radiat. Isot. *35*, 831–835 (1984)
[403] G. Bandoli, D.A. Clemente, and U. Mazzi, J. Chem. Soc. Dalton Trans. 125–130 (1976)
[404] G.A. Mazzocchin, R. Seeber, U. Mazzi, and E. Roncari, Inorg. Chim. Acta *29*, 1–4 (1978)
[405] G.A. Mazzocchin, R. Seeber, U. Mazzi, and E. Roncari, Inorg. Chim. Acta *29*, 5–9 (1978)
[406] P.L. Watson, J.A. Albanese, J.C. Calabrese, D.W. Ovenall, and R.G. Smith, Inorg. Chem. *30*, 4638–4643 (1991)
[407] J.E. Fergusson and P.F. Heveldt, J. Inorg. Nucl. Chem. *38*, 2231–2237 (1976)
[408] F.D. Rochon, R. Melanson, and P.-C. Kong, Can. J. Chem. *69*, 397–403 (1991)
[409] R.M. Pearlstein, W.M. Davis, A.G. Jones, and A. Davison, Inorg. Chem. *28*, 3332–3334 (1989)
[410] C.M. Archer, J.R. Dilworth, R.M. Thompson, M. McPartlin, D.C. Povey, and J.D. Kelly, J. Chem. Soc. Dalton Trans. 461–466 (1993)
[411] U. Mazzi, D.A. Clemente, G. Bandoli, L. Magon, and A.A. Orio, Inorg. Chem. *16*, 1042–1048 (1977)
[412] J.E. Fergusson and R.S. Nyholm, Nature *183*, 1039–1040 (1959)
[413] K.A. Glavan, R. Whittle, J.F. Johnson, R.C. Elder, and E. Deutsch, J. Am. Chem. Soc. *102*, 2103–2104 (1980)
[414] R.C. Elder, R. Whittle, K.A. Glavan, J.F. Johnson, and E. Deutsch, Acta Cryst. *B36*, 1662–1665 (1980)
[415] M. Thompson, A.D. Nunn, and E.N. Treher, Anal. Chem. *58*, 3100–3103 (1986)
[416] M.B. Cingi, D.A. Clemente, L. Magon, and U. Mazzi, Inorg. Chim. Acta *13*, 47–59 (1975)
[417] G. Bandoli, D.A. Clemente, and U. Mazzi, J. Chem. Soc. Dalton Trans. 1837–1844 (1977)
[418] G. Bandoli, D.A. Clemente, U. Mazzi, and E. Roncari, Acta Cryst. *B34*, 3359–3361 (1978)
[419] K. Hashimoto, C. Kabuto, T. Omori, and K. Yoshihara, Chem. Lett. 1379–1380 (1988)
[420] H. Kido and Y. Hatakeyama, Inorg. Chem. *27*, 3623–3625 (1988)
[421] A. Mutalib, T. Omori, and K. Yoshihara, J. Radioanal. Nucl. Chem., Articles, *170*, 67–77 (1993)
[422] K. Leesmeister and K. Schwochau, Nucl. Med. Biol. *19*, 73–78 (1992)
[423] G.S. Patterson, A. Davison, A.G. Jones, C.F. Costello, and S.D. Maleknia, Inorg. Chim. Acta *114*, 141–144 (1986)
[424] A. Mutalib, T. Omori, and K. Yoshihara, J. Radioanal. Nucl. Chem., Letters, *165*, 19–25 (1992)
[425] A. Mutalib, T. Sekine, T. Omori, and K. Yoshihara, J. Radioanal. Nucl. Chem., Articles, *178*, 311–318 (1994)
[426] H. Spies, U. Abram, E. Uhlemann, and E. Ludwig, Inorg. Chim. Acta *109*, L3-L14 (1985)
[427] G. Bandoli, U. Mazzi, H. Spies, R. Münze, E. Ludwig, E. Uhlemann, and D. Scheller, Inorg. Chim. Acta *132*, 177–185 (1987)
[428] H. Vavouraki, M. Papadopoulos, S. Mastrostamatis, A.D. Varvarigou, M. Psilla, and E. Chiotellis, J. Labelled Compd. Radiopharm. *33*, 249–257 (1993)
[429] M. Hashimoto, H. Wada, T. Omori, and K. Yoshihara, J. Radioanal. Nucl. Chem., Letters, *153*, 283–291 (1991)
[430] M. Hashimoto, H. Wada, T. Omori, and K. Yoshihara, Radiochim. Acta *63*, 173–177 (1993)
[431] F. Refosco, F. Tisato, G. Bandoli, and E. Deutsch, J. Chem. Soc. Dalton Trans. 2901–2908 (1993)
[432] J. Lu, A. Yamano, and M.J. Clarke, Inorg. Chem. *29*, 3483–3487 (1990)
[433] J. Barrera, A.K. Burrel, and J.C. Bryan, Inorg. Chem. *35*, 335–341 (1996)
[434] B.E. Wilcox, D.M. Ho, and E. Deutsch, Inorg. Chem. *28*, 1743–1751 (1989)
[435] A.I. Breikss, T. Nicholson, A.G. Jones, and A. Davison, Inorg. Chem. *29*, 640–645 (1990)

[436] C. Kremer and E. Kremer, J. Radioanal. Nucl. Chem., Letters, *175*, 445–453 (1993)
[437] J. Torres, C. Kremer, and E. Kremer, J. Radioanal. Nucl. Chem., Letters, *201*, 1–12 (1995)
[438] M.J. Abrams, A. Davison, and A.G. Jones, Inorg. Chim. Acta *82*, 125–128 (1984)
[439] E.N. Treher, L.C. Francesconi, J.Z. Gougoutas, M.F. Malley, and A.D. Nunn, Inorg. Chem. *28*, 3411–3416 (1989)
[440] E.N. Treher, J. Gougoutas, M. Malley, A.D. Nunn, and S.E. Unger, J. Labelled Compd. Radiopharm. *23*, 1118–1120 (1986)
[441] S.E. Unger, T.J. McCormick, E.N. Treher, and A.D. Nunn, Anal. Chem. *59*, 1145–1149 (1987)
[442] E. Deutsch, R.C. Elder, B.A. Lange, M.J. Vaal, and D.G. Lay, Proc. Natl. Acad. Sci. U.S.A. *73*, 4287–4289 (1976)
[443] K.E. Linder, M.F. Malley, J.Z. Gougoutas, S.E. Unger, and A.D. Nunn, Inorg. Chem. *29*, 2428–2434 (1990)
[444] K.E. Linder, D.P. Nowotnik, M.F. Malley, J.Z. Gougoutas, and A.D. Nunn, Inorg. Chim. Acta *190*, 249–255 (1991)
[445] J.E. Cyr, K.E. Linder, and D.P. Nowotnik, Inorg. Chim. Acta *206*, 97–104 (1993)
[446] S.S. Jurisson, K. Dancey, M. McPartlin, P.A. Tasker, and E. Deutsch, Inorg. Chem. *23*, 4743–4749 (1984)
[447] A. Ichimura, W.R. Heineman, and E. Deutsch, Inorg. Chem. *24*, 2134–2139 (1985)
[448] U. Mazzi, F. Refosco, F. Tisato, G. Bandoli, and M. Nicolini, J. Chem. Soc. Dalton Trans. 847–850 (1988)
[449] C.M. Archer, J.R. Dilworth, P. Jobanputra, R.M. Thompson, M. McPartlin, and W. Hiller, J. Chem. Soc. Dalton Trans. 897–904 (1993)
[450] C.M. Archer, J.R. Dilworth, P. Jobanputra, R.M. Thompson, M. McPartlin, D.C. Povey, G.W. Smith, and J.D. Kelly, Polyhedron *9*, 1497–1502 (1990)
[451] J.R. Dilworth, P. Jobanputra, R.M. Thompson, C.M. Archer, J.D. Kelly, and W. Hiller, Z. Naturforschg. *46b*, 449–452 (1991)
[452] J.R. Dilworth, P. Jobanputra, R.M. Thompson, D.C. Povey, C.M. Archer, and J.D. Kelly, J. Chem. Soc. Dalton Trans. 1251–1256 (1994)
[453] M. Hirsch-Kuchma, T. Nicholson, A. Davison, W.M. Davis, and A.G. Jones, Inorg. Chem. *36*, 3237–3241 (1997)
[454] M. Hirsch-Kuchma, T. Nicholson, A. Davison, W.M. Davis, and A.G. Jones, J. Chem. Soc. Dalton Trans. 3185–3188 (1997)
[455] T. Nicholson, M. Hirsch-Kuchma, A. Davison, and A.G. Jones, Inorg. Chim. Acta *271*, 191–194 (1998)
[456] F. Refosco, C. Bolzati, A. Moresco, G. Bandoli, A. Dolmella, U. Mazzi, and M. Nicolini, J. Chem. Soc. Dalton Trans. 3043–3048 (1991)
[457] T. Konno, M.J. Heeg, and E. Deutsch, Inorg. Chem. *27*, 4113–4121 (1988)
[458] T. Konno, J.R. Kirchhoff, W.R. Heineman, and E. Deutsch, Inorg. Chem. *28*, 1174–1179 (1989)
[459] U. Abram, R. Beyer, P. Mäding, I. Hoffmann, R. Münze, and J. Stach, Z. Anorg. Alig. Chem. *578*, 229–239 (1989)
[460] J. Stach, U. Abram, and R. Münze, Z. Chem. *29*, 249–250 (1989)
[461] T. Konno, R. Seeber, J.R. Kirchhoff, W.R. Heineman, and E. Deutsch, Trans. Met. Chem. *18*, 209–217 (1993)
[462] R. Münze, U. Abram, J. Stach, and W. Hiller, Inorg. Chim. Acta *186*, 151–154 (1991)
[463] T. Konno, M.J. Heeg, J.A. Stuckey, J.R. Kirchhoff, W.R. Heineman, and E. Deutsch, Inorg. Chem. *31*, 1173–1181 (1992)
[464] T. Konno, J.R. Kirchhoff, M.J. Heeg, W.R. Heineman, and E. Deutsch, J. Chem. Soc. Dalton Trans. 3069–3075 (1992)
[465] N. de Vries, J.C. Dewan, A.G. Jones, and A. Davison, Inorg. Chem. *27*, 1574–1580 (1988)
[466] N. de Vries, J. Cook, A. Davison, T. Nicholson, and A.G. Jones, Inorg. Chem. *29*, 1062–1064 (1990)
[467] H.-J. Pietzsch, H. Spies, and S. Hoffmann, Inorg. Chim. Acta *168*, 7–9 (1990)
[468] H.-J. Pietzsch, H. Spies, P. Leibnitz, G. Reck, J. Beger, and R. Jacobi, Polyhedron *13*, 1623–1628 (1992)
[469] H. Spies, M. Glaser, H.-J. Pietzsch, F.E. Hahn, O. Kintzel, and T. Lügger, Angew. Chem *106*, 1416–1419 (1994)
[470] H. Spies, M. Glaser, H.-J. Pietzsch, F.E. Hahn, and T. Lügger, Inorg. Chim. Acta *240*, 465–478 (1995)

[471] N. de Vries, J. Cook, A.G. Jones, and A. Davison, Inorg. Chem. *30*, 2662–2665 (1991)
[472] C. Bolzati, F. Refosco, F. Tisato, G. Bandoli, and A. Dolmella, Inorg. Chim. Acta *201*, 7–10 (1992)
[473] F. Tisato, F. Refosco, G. Bandoli, C. Bolzati, and A. Moresco, J. Chem. Soc. Dalton Trans. 1453–1461 (1994)
[474] K.-I. Okamoto, J.R. Kirchhoff, W.R. Heineman, and E. Deutsch, Polyhedron *12*, 749–757 (1993)
[475] A.S. Batsanov, Y.T. Struchkov, B. Lorenz, and M. Wahren, Z. Anorg. Allg. Chem. *510*, 117–122 (1984)
[476] B. Lorenz and K. Schmidt, Z. Chem. *23*, 423 (1983)
[477] J. Baldas, J. Bonnyman, P.M. Pojer, G.A. Williams and M.F. Mackay, J. Chem. Soc. Dalton Trans. 451–455 (1982)
[478] J. Baldas, S.F. Colmanet, and G.A. Williams, Aust. J. Chem. *44*, 1125–1132 (1991)
[479] J. Baldas, J. Bonnyman, M.F. Mackay, and G.A. Williams, Aust. J. Chem. *37*, 751–759 (1984)
[480] M.J. Abrams, A. Davison, R. Faggiani, A.G. Jones, and C.J.L. Lock, Inorg. Chem. *23*, 3284–3288 (1984)
[481] M.J. Abrams, A. Davison, J.W. Brodack, A.G. Jones, R. Faggiani, and C.J. Lock, J. Labelled Compd. Radiopharm. *14*, 1596–1597 (1982)
[482] R. Münze, I. Dreyer, B. Grossmann, and R. Dreyer, J. Radioanal. Nucl. Chem., Letters, *86*, 79–88 (1984)
[483] F.D. Rochon, R. Melanson, and P.C. Kong, Acta Cryst. *C46*, 571–576 (1990)
[484] K. Hashimoto, H. Kudo, T. Omori, and K. Yoshihara, Radiochim. Acta *63*, 167–171 (1993)
[485] T. Nicholson, J. Thornback, L. O'Connell, G. Morgan, A. Davison, and A.G. Jones, Inorg. Chem. *29*, 89–92 (1990)
[486] B. Lorenz, K. Schmidt, W. Hiller, U. Abram, and R. Hübener, Inorg. Chim. Acta *208*, 195–199 (1993)
[487] G. Bandoli, D.A. Clemente, and U. Mazzi, J. Chem. Soc. Dalton Trans. 373–380 (1978)
[488] D.K. Huggins and H.D. Kaesz, J. Am. Chem. Soc. *83*, 4474–4475 (1961)
[489] E.O. Fischer and M.W. Schmidt, Angew. Chem. *79*, 99–100 (1967)
[490] C. Apostolidis, B. Kanellakopulos, R. Maier, J. Rebizant, and M.L. Ziegler, J. Organomet. Chem. *396*, 315–326 (1990)
[491] C. Apostolidis, B. Kanellakopulos, R. Maier, J. Rebizant, and M.L. Ziegler, J. Organomet. Chem. *411*, 171–179 (1991)
[492] F. Tisato, F. Refosco, U. Mazzi, G. Bandoli, and M. Nicolini, Inorg. Chim. Acta *157*, 227–232 (1989)
[493] M.E. Kastner, P.H. Fackler, L. Podbielski, J. Charkoudian, and M.J. Clarke, Inorg. Chim. Acta *114*, L11–L15 (1986)
[494] M.J. Clarke, M.E. Kastner, L.A. Podbielski, P.H. Fackler, J. Schreifels, G. Meinken, and S.C. Srivastava, J. Am. Chem. Soc. *110*, 1818–1827 (1988)
[495] J. Lu and M.J. Clarke, Inorg. Chem. *27*, 4761–4766 (1988)
[496] J. Lu, C.D. Hiller, and M.J. Clarke, Inorg. Chem. *32*, 1417–1423 (1993)
[497] K.E. Linder, J.C. Dewan, and A. Davison, Inorg. Chem. *28*, 3820–3825 (1989)
[498] B. Kanellakopulos, B. Nuber, K. Raptis, and M.L. Ziegler, Angew. Chem. Int. Ed. Engl. *28*, 1955 (1989)
[499] F.A. Cotton and L.D. Gage, Nouv. J. Chim. *1*, 441–442 (1977)
[500] L.L. Zaitseva, A.S. Kotel'nikova, and A.A. Rezvov, Russ. J. Inorg. Chem. *25*, 1449–1451 (1980)
[501] J. Skowronek and W. Preetz, Z. Naturforschg. *47b*, 482–490 (1992)
[502] N.A. Baturin, K.E. German, M.S. Grigoriev, and S.V. Kryuchkov, Koord. Khim. *17*, 1375–1383 (1991)
[503] M.S. Grigoriev and S.V. Kryutschkov, Radiochim. Acta *63*, 187–193 (1993)
[504] V.I. Spitsyn, B. Baierl, S.V. Kryuchkov, A.F. Kuzina, and M. Varen, Dokl. Akad. Nauk SSSR *256*, 608–612 (1981)
[505] P.A. Koz'min, T.B. Larina, and M.D. Surazhskaya, Koord. Khim. *8*, 851–854 (1982)
[506] J. Skowronek, W. Preetz, and S.M. Jessen, Z. Naturforschg. *46b*, 1305–1314 (1991)
[507] J. Skowronek and W. Preetz, Z. Anorg. All. Chem. *615*, 73–76 (1992)
[508] F.A. Cotton, P.E. Fanwick, and L.D. Gage, J. Am. Chem. Soc. *102*, 1570–1577 (1980)
[509] S.V. Kryuchkov and A.F. Simonov, Koord. Khim. *16*, 339–343 (1990)
[510] J.D. Eakins, D.G. Humphreys, and C.E. Mellish, J. Chem. Soc. 6012–6016 (1963)

[511] V.I. Spitsyn, A.F. Kuzina, S.V. Kryuchkov, and A.E. Simonov, Russ. J. Inorg. Chem. *32*, 1278–1280 (1987)
[512] F.A. Cotton and W.K. Bratton, J. Am. Chem. Soc. *87*, 921 (1965)
[513] P.A. Koz'min and G.N. Novitskaya, Russ. J. Inorg. Chem. *17*, 1652–1653 (1972)
[514] W.K. Bratton and F.A. Cotton, Inorg. Chem. *9*, 789–793 (1970)
[515] M.B. Cingi and E. Tondello, Inorg. Chim. Acta *11*, L3–L4 (1974)
[516] F.A. Cotton, P.E. Fanwick, L.D. Gage, B. Kalbacher, and D.S. Martin, J. Am. Chem. Soc. *99*, 5642–5645 (1977)
[517] F.A. Cotton and B.J. Kalbacher, Inorg. Chem. *16*, 2386–2396 (1977)
[518] G. Peters, J. Skowronek, and W. Preetz, Z. Naturforschg. *47a*, 591–594 (1992)
[519] F.A. Cotton and L.W. Shive, Inorg. Chem. *14*, 2032–2035 (1975)
[520] F.A. Cotton, A. Davison, V.W. Day, M.F. Fredrich, C. Orvig, and R. Swanson, Inorg. Chem. *21*, 1211–1214 (1982)
[521] F.A. Cotton and E. Pedersen, Inorg. Chem. *14*, 383–387 (1975)
[522] W. Preetz and G. Peters, Z. Naturforschg. *35b*, 797–801 (1980)
[523] S.V. Kryuchkov, A.F. Kuzina, and V.I. Spitsyn, Russ. J. Inorg. Chem. *28*, 1124–1129 (1983)
[524] K. Schwochau, K. Hedwig, H.J. Schenk, and O. Greis, Inorg. Nucl. Chem. Letters *13*, 77–80 (1977)
[525] F.A. Cotton, L. Daniels, A. Davison, and C. Orvig, Inorg. Chem. *20*, 3051–3055 (1981)
[526] W. Bronger, M. Kanert, M. Loevenich, D. Schmitz, and K. Schwochau, Angew. Chem. Int. Ed. Engl. *32*, 576–578 (1993)
[527] W. Bronger, M. Kanert, M. Loevenich, and D. Schmitz, Z. Anorg. Allg. Chem. *619*, 2015–2020 (1993)
[528] G. Bandoli, U. Mazzi, A. Ichimura, K. Libson, W.R. Heineman, and E. Deutsch, Inorg. Chem. *23*, 2898–2901 (1984)
[529] F.D. Rochon, R. Melanson, and P.-C. Kong, Can. J. Chem. *72*, 2183–2187 (1994)
[530] S. Seifert, R. Muenze, P. Leibnitz, G. Reck, and J. Stach, Inorg. Chim. Acta *193*, 167–172 (1992)
[531] T. Konno, M.J. Heeg, and E. Deutsch, Inorg. Chem. *28*, 1694–1700 (1989)
[532] K.-I. Okamoto, B. Chen, J.R. Kirchhoff, D.M. Ho, R.C. Elder, W.R. Heineman, and E. Deutsch, Polyhedron *12*, 1559–1568 (1993)
[533] D.J. White, H.-J. Küppers, A.J. Edwards, D.J. Watkin, and S.R. Cooper, Inorg. Chem. *31*, 5351–5352 (1992)
[534] R. Kirmse and U. Abram, Z. Anorg. Allg. Chem. *608*, 184–187 (1992)
[535] B.E. Wilcox, D.M. Ho, and E. Deutsch, Inorg. Chem. *28*, 3917–3923 (1989)
[536] B.E. Wilcox and E. Deutsch, Inorg. Chem. *30*, 688–693 (1991)
[537] C.M. Archer and J.R. Dilworth, J. Nucl. Med. *30*, 939 (1989)
[538] C.M. Archer, J.R. Dilworth, R.M. Thompson, M. McPartlin, D.C. Povey, and J.D. Kelly in: Technetium and Rhenium in Chemistry and Nuclear Medicine 3, (M. Nicolini, G. Bandoli, and U. Mazzi, eds.), Cortina International, Verona, Raven Press, New York (1990) pp. 201–206
[539] K. Schwochau, K.H. Linse, and Z.F. Su, Appl. Radiat. Isot. *43*, 1079–1082 (1992)
[540] J.A. Thomas, A. Davison, and A.G. Jones, Inorg. Chim. Acta *184*, 99–105 (1991)
[541] L.J. Radonovich and J.L. Hoard, J. Phys. Chem. *88*, 6711–6716 (1984)
[542] R.A. Armstrong and H. Taube, Inorg. Chem. *15*, 1904–1909 (1976)
[543] G.C. Yang, M.W. Heitzmann, L.A. Ford, and W.R. Benson, Inorg. Chem. *21*, 3242–3243 (1982)
[544] C. Orvig, A. Davison, and A.G. Jones, J. Labelled Compd. Radiopharm. *18*, 148 (1981)
[545] A.G. Jones and A. Davison, Int. J. Appl. Radiat. Isot. *33*, 867–874 (1982)
[546] R. Kirmse, J. Stach, U. Abram, and I.N. Marov, Z. Anorg. Allg. Chem. *518* 210–226 (1984)
[547] R. Kirmse and U. Abram, Z. Anorg. Allg. Chem. *573*, 63–74 (1989)
[548] R. Kirmse, J. Stach, and U. Abram, Polyhedron *4*, 1275–1277 (1985)
[549] J. Baldas, J.F. Boas, J. Bonnyman, and G.A. Williams, J. Chem. Soc. Dalton Trans. 827–831 (1984)
[550] C.T. Cheah, J.L. Newman, D.P. Nowotnik, and J.R. Thornback, Nucl. Med. Biol. *14*, 573–577 (1987)
[551] D.S. Brown, J.L. Newman, J.R. Thornback, and A. Davison, Acta Cryst. *C43*, 1692–1694 (1987)
[552] D.S. Brown, J.L. Newman, J.R. Thornback, R.M. Pearlstein, A. Davison, and A. Lawson, Inorg. Chim. Acta *150*, 193–196 (1988)
[553] D.S. Brown, J.L. Newman, and J.R. Thornback, Acta Cryst. *C44*, 973–975 (1988)
[554] R. Kirmse, B. Lorenz, and K. Schmidt, Polyhedron *2*, 935–939 (1983)
[555] U. Abram, R. Kirmse, K. Köhler, B. Lorenz, and L. Kaden, Inorg. Chim. Acta *129*, 15–20 (1987)

[556] L. Kaden, B. Lorenz, R. Kirmse, J. Stach, H. Behm, P.T. Beurskens, and U. Abram, Inorg. Chim. Acta *169*, 43–48 (1990)
[557] U. Abram, R. Hübener, R. Wollert, R. Kirmse, and W. Hiller, Inorg. Chim. Acta *206*, 9–14 (1993)
[558] J.B. Raynor, T.J. Kemp, and A.M. Thyer, Inorg. Chim. Acta *193*, 191–196 (1992)
[559] R. Kirmse and U. Abram, Isotopenpraxis *26*, 151–159 (1990)
[560] S.V. Kryuchkov, M.S. Grigor'ev, A.F. Kuzina, B.F. Gulev, and V.I. Spitsyn, Dokl. Akad. Nauk. SSSR, *228*, 389–393 (1986)
[561] F.A. Cotton, L.M. Daniels, L.R. Falvello, M.S. Grigoriev, and S.V. Kryuchkov, Inorg. Chim. Acta *189*, 53–54 (1991)
[562] C.J. Burns, A.K. Burrell, F.A. Cotton, S.C. Haefner, and A.P. Sattelberger, Inorg. Chem. *33*, 2257–2264 (1994)
[563] F.A. Cotton, S.C. Haefner, and A.P. Sattelberger, Inorg. Chem. *35*, 1831–1838 (1996)
[564] F.A. Cotton, S.C. Haefner, and A.P. Sattelberger, Inorg. Chem. *35*, 7350–7357 (1996)
[565] F.A. Cotton, S.C. Haefner, and A.P. Sattelberger, J. Am. Chem. Soc. *118*, 5486–5487 (1996)
[566] F.A. Cotton, S.C. Haefner, and A.P. Sattelberger, Inorg. Chim. Acta *266*, 55–63 (1997)
[567] S.V. Kryutchkov, Chemistry of Technetium Cluster Compounds. Topics in Current Chemistry *176*, 189–252 (1996). In: Technetium and Rhenium. Their Chemistry and ist Applications. (K. Yoshihara and T. Omori, eds.), Springer Verlag, Tokyo (1996)
[568] V.I. Spitsyn, A.F. Kuzina, A.A. Oblova, and S.V. Kryuchkov, Russ. Chem. Rev. *54*, 373–393 (1985)
[569] P.A. Koz'min, T.B. Larina, and M.D. Surazhskaya, Dokl. Akad. Nauk SSSR *271*, 1157–1159 (1983)
[570] P.A. Koz'min, M.D. Surazhskaya, and T.B. Larina, Koord. Khimiya *11*, 1559–1567 (1985)
[571] K.E. German, S.V. Kryuchkov, A.F. Kuzina, and V.I. Spitsyn, Dokl. Akad. Nauk SSSR *288*, 381–384 (1986)
[572] S.V. Kryuchkov, M.S. Grigor'ev, A.I. Yanovskii, Y.T. Struchkov, and V.I. Spitsyn, Dokl. Akad. Nauk SSSR *297*, 867–871 (1987)
[573] M.S. Grigoriev and S.V. Kryuchkov, Radiochim. Acta *63*, 187–193 (1993)
[574] V.I. Spitzin, S.V. Kryutchkov, M.S. Grigoriev, and A.F. Kuzina, Z. Anorg. Allg. Chem. *563*, 136–152 (1988)
[575] S.V. Kryutchkov, A.F. Kuzina, and V.I. Spitzin, Z. Anorg. Allg. Chem. *563*, 153–166 (1988)
[576] S.V. Kryuchkov, M.S. Grigor'ev, A.F. Kuzina, B.F. Gulev, and V.I. Spitsyn, Dokl. Akad. Nauk SSSR *288*, 893–897 (1986)
[577] S.V. Kryuchkov, M.S. Grigor'ev, A.I. Yanovskii, Y.T. Struchkov, and V.I. Spitsyn, Dokl. Akad. Nauk SSSR *301*, 618–622 (1988)
[578] S.V. Kryuchkov, M.S. Grior'ev, A.F. Kuzina, B.F. Gulev, and V.I. Spitsyn, Dokl. Akad. Nauk SSSR *290*, 866–869 (1986)
[579] K. Schwochau and W. Herr, Z. Anorg. Allg. Chem. *319*, 147–158 (1962)
[580] W. Herr and K. Schwochau, Angew. Chem. *73*, 492–493 (1961)
[581] W. Krasser, E.W. Bohres, and K. Schwochau, Z. Naturforschg. *27a*, 1193–1196 (1972)
[582] M.J. Abrams, A. Davison, A.G. Jones, C.E. Costello, and H. Pang, Inorg. Chem. *22*, 2798–2800 (1983)
[583] T.H. Tulip, J. Calabrese, J.F. Kronauge, A. Davison, and A.G. Jones, Technetium in: Chemistry and Nuclear Medicine 2. (M. Nicolini, G. Bandolini, and U. Mazzi, eds.), Cortina International (Verona), Raven Press, New York (1986) pp. 119–122
[584] J.F. Kronauge, A. Davison, A.M. Roseberry, C.E. Costello, S. Maliknia, and A.G. Jones, Inorg. Chem. *30*, 4265–4271 (1991)
[585] L.A. O'Connell, R.M. Pearlstein, A. Davison, J.R. Thornback, J.F. Kronauge, and A.G. Jones, Inorg. Chim. Acta *161*, 39–43 (1989)
[586] U. Abram, R. Beyer, R. Münze, M. Findeisen, and B. Lorenz, Inorg. Chim. Acta *160*, 139–142 (1989)
[587] U. Abram, S.Abram, R. Beyer, R. Münze, L. Kaden, B. Lorenz, and M. Findeisen, Inorg. Chim. Acta *148*, 141–142 (1988)
[588] L. Kaden, A.J.L. Pombeiro, Y. Wang, and U. Abram, Inorg. Chim. Acta *230*, 189–192 (1995)
[589] L.A. O'Connell and A. Davison, Inorg. Chim. Acta *176*, 7–9 (1990)
[590] F.D. Rochon, R. Melanson, and P.-C. Kong, Inorg. Chim. Acta *245*, 251–256 (1996)
[591] L.A. O'Connell, J. Dewan, A.G. Jones, and A. Davison, Inorg. Chem. *29*, 3539–3547 (1990)

[592] R. Alberto, R. Schibli, P.A. Schubiger, U. Abram, and T.A. Kaden, Polyhedron *15*, 1079–1089 (1996)
[593] A. Ichimura, W.R. Heineman, J.-L. Vanderheyden, and E. Deutsch, Inorg. Chem. *23*, 1272–1278 (1984)
[594] M.N. Doyle, K. Libson, M. Woods, J.C. Sullivan, and E. Deutsch, Inorg. Chem. *25*, 3367–3371 (1986)
[595] K. Libson, M. Woods, J.C. Sullivan, J.W. Watkins II, R.C. Elder, and E. Deutsch, Inorg. Chem. *27*, 999–1003 (1988)
[596] A. Roodt, J.C. Sullivan, D. Meisel, and E. Deutsch, Inorg. Chem. *30*, 4545–4549 (1991)
[597] A.K. Burrell, J.C. Bryan, and G.J. Kubas, J. Am. Chem. Soc. *116*, 1575–1576 (1994)
[598] A.K. Burrell, J.C. Bryan, and G.J. Kubas, Organometallics *13*, 1067–1069 (1994)
[599] U. Abram, R. Beyer, R. Münze, J. Stach, L. Kaden, B. Lorenz, and M. Findeisen, Polyhedron *8*, 1201–1204 (1989)
[600] D.W. Wester, D.H. White, F.W. Miller, and R.T. Dean, Inorg. Chem. *23*, 1501–1502 (1984)
[601] D.W. Wester, D.H. White, F.W. Miller, R.T. Dean, J.A. Schreifels, and J.F. Hunt, Inorg. Chim. Acta *131*, 163–169 (1987)
[602] U. Abram and S. Abram, Z. Chem. *26*, 181 (1986)
[603] K. Schwochau, K.H. Linse, M.F. Cerdá, and C. Kremer in: Technetium and Rhenium in Chemistry and Nuclear Medicine *4*, (M. Nicolini, G. Bandoli, and U. Mazzi, eds.). SGE Ditoriali, Padova (1995), p. 247–250
[604] T. Nicholson, A. Mahmood, G. Morgan, A.G. Jones, and A. Davison, Inorg. Chim. Acta *179*, 53–57 (1991)
[605] L. Kaden, B. Lorenz, K. Schmidt, H. Sprinz, and M. Wahren, Z. Chem. *19*, 305–306 (1979)
[606] Y.T. Struchkov, A.S. Bazanov, L. Kaden, B. Lorenz, M. Wahren, and H. Meyer, Z. Anorg. Allg. Chem. *494*, 91–97 (1982)
[607] L. Kaden, M. Findeisen, B. Lorenz, K. Schmidt, and M. Wahren, Inorg. Chim. Acta *193*, 213–215 (1992)
[608] K.E. Linder, A. Davison, J.C. Dewan, C.E. Costello, and S. Maleknia, Inorg. Chem. *25*, 2085–2089 (1986)
[609] J.L. Newman, J.R. Thornback, and D.P. Nowotnik, J. Labelled Compd. Radiopharm. *26*, 24–26 (1989)
[610] S.S. Blanchard, T. Nicholson, A. Davison, W. Davis, and A.G. Jones, Inorg. Chim. Acta *244*, 121–130 (1996)
[610a]T. Nicholson, M. Hirsch-Kuchma, E. Freiberg, A. Davison, and A.G. Jones, Inorg. Chim. Acta *279*, 206–209 (1998)
[611] T. Nicholson, M. Hirsch-Kuchma, A. Shellenbarger-Jones, A. Davison, and A.G. Jones, Inorg. Chim. Acta *267*, 319–322 (1998)
[612] S.S. Blanchard, T. Nicholson, A. Davison, and A.G. Jones, Inorg. Chim. Acta *241*, 95–100 (1996)
[613] A.M. Roseberry, A. Davison, and A.G. Jones, Inorg. Chim. Acta *176*, 179–181 (1990)
[614] J. Lu and M.J. Clarke, J. Chem. Soc. Dalton Trans. 1243–1248 (1992)
[615] J. Lu and M.J. Clarke, Inorg. Chem. *29*, 4123–4125 (1990)
[616] W. Hiller, R. Hübener, B. Lorenz, L. Kaden, M. Findeisen, J. Stach, and U. Abram, Inorg. Chim. Acta *181*, 161–165 (1991)
[617] C. Palm, E.O. Fischer, and E. Baumgärtner, Tetrahedron Lett. 253–254 (1962)
[618] E. Baumgärtner, E.O. Fischer, and U. Zahn, Naturwissenschaften *48*, 478 (1961)
[619] E. Baumgärtner, E.O. Fischer, and U. Zahn, Chem. Ber. *94*, 2198–2203 (1961)
[620] E.O. Fischer and M.W. Schmidt, Chem. Ber. *102*, 1954–1960 (1969)
[621] D.W. Wester, J.R. Coveney, D.L. Noscon, M.S. Robbins, and R.T. Dean, J. Med. Chem. *34*, 3284–3290 (1991)
[622] J.C. Hileman, D.K. Huggins, and H.D. Kaesz, Inorg. Chem. *1*, 933–938 (1962)
[623] W. Hieber, F. Lux, and C. Herget, Z. Naturforsch. *20b*, 1159–1165 (1965)
[624] A.A. Kruglov, L.L. Zaitseva, and A.S. Kotel'nikova, Russ. J. Inorg. Chem. 26, 518–519 (1981)
[625] A.E. Miroslavov, G.V. Sidorenko, I.V. Borisova, E.K. Legin, A.A. Lychev, D.N. Suglobov, and M.V. Adamov, Radiokhimiya *32*, No. 4, 6–14 (1990)
[626] A.E. Miroslavov, G.V. Sidorenko, I.V. Borisova, E.K. Legin, A.A. Lychev, and D.N. Suglobov, Radiokhimiya *32*, No. 6, 14–21 (1990)
[627] I.V. Borisova, A.E. Miroslavov, G.V. Siderenko, and D.N. Suglobov, Radiokhimiya *33*, No. 6, 9–13 (1991)

[628] A.E. Miroslavov, I.V. Borisova, G.V. Sidorenko, and D.N. Suglobov, Radiokhimiya *33*, No. 6, 20–26 (1991)
[629] M.A. El-Sayed and H.D. Kaesz, Inorg. Chem. *2*, 158–162 (1963)
[630] L.E. Orgel, Inorg. Chem. *3*, 303, (1964)
[631] D.K. Huggins and H.D. Kaesz, J. Am. Chem. Soc. *86*, 2734–2736 (1964)
[632] A.E. Miroslavov, G.V. Sidorenko, I.V. Borisova, E.A. Legin, A.A. Lychev, and D.N. Suglobov, Ra-diokhimiya 31, No. *6*, 33–35 (1989)
[633] M. Herberhold, G. Süss, J. Ellermann, and H. Gäbelein, Chem. Ber. *111*, 2931–2941 (1978)
[634] W.A. Herrmann, R. Alberto, J.C. Bryan, and A.P. Sattelberger, Chem. Ber. *124*, 1107–1111 (1991)
[635] R. Alberto, R. Schibli, A. Egli, P.A. Schubiger, W.A. Herrmann, G. Artus, U. Abram, and T.A. Kaden, J. Organomet. Chem. *493*, 119–127 (1995)
[635a] R. Schibli, R. Alberto, U. Abram, S. Abram, A. Egli, P.A. Schubiger, and T.A. Kaden, Inorg. Chem. *37*, 3509–3516 (1998)
[636] R. Alberto, R. Schibli, P.A. Schubiger, U. Abram, and T.A. Kaden, Polyhedron *15*, 1079–1089 (1996)
[636a] U. Abram, S. Abram, R. Schibli, R. Alberto, and J.R. Dilworth, Polyhedron *17*, 1303–1309 (1998)
[637] U. Mazzi, A. Bismondo, N. Kotsev, and D.A. Clemente, J. Organomet. Chem. *135*, 177–182 (1977)
[638] U. Mazzi, F. Roncari, R. Seeber, and G.A. Mazzocchin, Inorg. Chim. Acta *41*, 95–98 (1980)
[639] L. Kaden, B. Lorenz, S. Rummel, K. Schmidt, and M. Wahren, Inorg. Chim. Acta *142*, 1–2 (1988)
[640] M. Findeisen, L. Kaden, B. Lorenz, and M. Wahren, Inorg. Chim. Acta *142*, 3–4 (1988)
[641] B. Lorenz, M. Findeisen, B. Olk, and K. Schmidt, Z. Anorg. Allg. Chem. *566*, 160–168 (1988)
[642] R. Alberto, W.A. Herrmann, P. Kiprof, and F. Baumgärtner, Inorg. Chem. *31*, 895–899 (1992)
[643] A. Marchi, R. Rossi, A. Duatti, V. Bertolasi, V. Ferretti, and G. Gilli, Inorg. Chem. *24*, 4744–4748 (1985)
[644] A. Marchi, R. Rossi, A. Duatti, G.L. Zucchini, and L. Magon, Trans. Met. Chem. *11*, 164–166 (1986)
[645] R. Rossi, A. Marchi, L. Magon, U. Casellato, and R. Graziani, J. Chem. Research (S) 78–79 (1990)
[646] R. Rossi, A. Marchi, L. Magon, A. Duatti, U. Casellato, and R. Graziani, Inorg. Chim. Acta *160*, 23–28 (1989)
[647] B. Lorenz, M. Findeisen, and K. Schmidt, Isotopenpraxis *27*, 266–267 (1991)
[648] A. Marchi, L. Marvelli, R. Rossi, V. Bertolasi, and V. Ferretti, Inorg. Chim. Acta *272*, 267–273 (1998)
[649] I.V. Borisova, A.E. Miroslavov, G.V. Sidorenko, and D.N. Suglobov, Radiokhimiya *33*, No. 6, 1–8 (1991)
[650] I.V. Borisova, A.E. Miroslavov, G.V. Sidorenko, D.N. Suglobov, and L.L. Shcherbakova, Radiokhimiya *33*, No. 4, 27–38 (1991)
[651] I.V. Borisova, A.E. Miroslavov, G.V. Sidorenko, and D.N. Suglobov, Radiokhimiya *33*, No. 3, 1–8 (1991)
[652] V.M. Adamov, B.N. Belyaev, I.V. Borisova, A.E. Miroslavov, G.V. Sidorenko, and D.N. Suglobov, Radiokhimiya *33*, No. 4, 38–53 (1991)
[653] J. Cook and A. Davison, J. Organomet. Chem. *507*, 47–51 (1996)
[654] J.E. Joachim, C. Apostolidis, B. Kanellakopulos, R. Maier, N. Marques, D. Meyer, J. Müller, A.P. de Matos, B. Nuber, J. Rebizant, and L. Ziegler, J. Organomet. Chem. *448*, 119–129 (1993)
[655] J.E. Joachim, C. Apostolidis, B. Kanellakopulos, D. Meyer, B. Nuber, K. Raptis, J. Rebizant, and M.L. Ziegler, J. Organomet. Chem. *492*, 199–210 (1995)
[656] J.E. Joachim, C. Apostolidis, B. Kanellakopulos, R. Maier, D. Meyer,J. Rebizant, and M.L. Ziegler, J. Organomet. Chem. *455*, 137–141 (1993)
[657] W. Hieber, W. Opavsky, and W. Rohm, Chem. Ber. *101*, 2244–2255 (1968)
[658] M. Tsutsui, C.P. Hrung, D. Ostfeld, T.S. Srivastava, D.L. Cullen, and E.F. Meyer, Jr., J. Am. Chem. Soc. *97*, 3952–3965 (1975)
[659] M. Tsutsui and C.P. Hrung, J. Am. Chem. Soc. *96*, 2638–2640 (1974)
[660] M. Tsutsui and C.P. Hrung, J. Am. Chem. Soc. *95*, 5777–5758 (1973)
[661] M. Tsutsui and C.P. Hrung, Chem Lett. 941–942 (1973)
[661a] M. Reisgys, F. Wüst, R. Alberto, R. Schibli, P.A. Schubiger, H.-J. Pietzsch, H. Spies, and B. Johannsen, Bioorg. Med. Chem. Lett. *7*, 2243–2246 (1997)

[662] C. Palm, E.O. Fischer, and F. Baumgärtner, Naturwissenschaften *49*, 279 (1962)
[663] F. Baumgärtner, F.O. Fischer, and U. Zahn, Naturwissenschaften *49*, 156 (1962)
[664] E.O. Fischer and W. Fellmann, J. Organomet. Chem. *1*, 191–199 (1963)
[665] H.H. Knight Castro, A. Meetsma, J.H. Teuben, W. Vaalburg, K. Panek, and G. Ensing, J. Organomet. Chem. *410*, 63–71 (1991)
[666] K. Raptis, F. Dornberger, B. Kanellakopulos, B. Nuber, and M.L. Ziegler, J. Organomet. Chem. *408*, 61–75 (1991)
[667] J.F. Joachim, C. Apostolidis, B. Kanellakopulos, D. Meyer, K. Raptis, J. Rebizant, and M.L. Ziegler, J. Organomet. Chem. *476*, 77–84 (1994)
[668] K. Raptis, B. Kanellakopulos, B. Nuber, and M.L. Ziegler, J. Organomet. Chem. *405*, 323–331 (1991)
[669] J. Rebizant, unpublished results (1994)
[670] E.O. Fischer, C. Apostolidis, F. Dornberger, A.C. Filippou, B. Kanellakopulos, B. Lungwitz, J. Müller, B. Powietzka, J. Rebizant, and W. Roth, Z. Naturforschg. *50b*, 1382–1395 (1995)
[671] J.C. Hileman, D.K. Huggins, and H.D. Kaesz, J. Am. Chem. Soc. *83*, 2953–2954 (1961)
[672] W. Hieber and C. Herget, Angew. Chem. *73*, 579–580 (1961)
[673] F. Calderazzo, U. Mazzi, G. Pampaloni, R. Poli, F. Tisato, and P.F. Zanazzi, Gazz. Chim. Ital. *119*, 241–247 (1989)
[674] M.F. Bailey and L.F. Dahl, Inorg. Chem. *4*, 1140–1145 (1965)
[675] D. Wallach, Acta Cryst. *15*, 1058 (1962)
[676] K. Missner and D.V. Korol'kov, J. Struc. Chem. [USSR] *13*, 639–647 (1972)
[677] N. Flitcroft, D.K. Huggins, and H.D. Kaesz, Inorg. Chem. *3*, 1123–1130 (1964)
[678] G. Bor and G. Sbrignadello, J. Chem. Soc. Dalton Trans. 440–448 (1974)
[679] M. Findeisen, L. Kaden, B. Lorenz, S. Rummel, and M. Wahren, Inorg. Chim. Acta *128*, L15-L16 (1987)
[680] G.D. Michels and H.J. Svec, Inorg. Chem. *20*, 3445–3447 (1981)
[681] G. Sbrignadello, G. Tomat, L. Magon, and G. Bor, Inorg.nucl. Chem. Letters *9*, 1073–1077 (1973)
[682] G. Sbrignadello, Inorg. Chim. Acta *48*, 237–242 (1981)
[683] C.C. Grimm and R.J. Clark, Organometallics *9*, 1123–1127 (1990)
[684] V.D. Klimov, A.V. Mamchenko, and A.P. Babichev, Radiokhimiya *33*, No. 5, 33–40 (1991)
[685] E.O. Fischer, E. Offhaus, J. Müller, and D. Nöthe, Chem. Ber. *105*, 3027–3035 (1972)
[686] B. Kanellakopulos, B. Nuber, K. Raptis, and M.L. Ziegler, Z. Naturforschg. *46b*, 55–59 (1991)
[687] H.D. Kaesz and D.K. Huggins, Can. J. Chem. *41*, 1250–1254 (1963)
[688] M.W. Lindauer, G.O. Evans, and R.K. Sheline, Inorg. Chem. *7*, 1249–1250 (1968)

B. ^{99m}Tc Radiopharmaceutical Applications

This Page Intentionally Left Blank

1 Introduction

For more than three decades ^{99m}Tc radiopharmaceuticals have been used for diagnostic purposes in nuclear medicine via imaging of internal organs by single photon emission computed tomography (SPECT) or planar scintigraphy. The aim of the diagnostic application is the detailed description of the morphologic structure of organs and above all the testing of their physiological function through the accumulation of ^{99m}Tc, which is predominantly a stoichiometric component in complexes with organic ligands or sometimes in inorganic compounds. Also macromolecular biomolecules, which are not stoichiometrically labeled with ^{99m}Tc, have been used as radiopharmaceuticals. Like other radiodiagnostic species, ^{99m}Tc radiopharmaceuticals are applied in minimal concentrations, in the range of 10^{-6} to 10^{-8} M, with no intension of any pharmacological effect [1].

On average, over 80 % of radiopharmaceuticals applied world-wide in clinics are labeled with ^{99m}Tc. Because of the almost optimal nuclear properties of ^{99m}Tc, as well as its convenient and low cost production by means of commercial generator columns, ^{99m}Tc radiopharmaceuticals are generally preferentially applied. The half-life of ^{99m}Tc of only 6 h and the almost negligible tissue damaging radiation [2] allow the injection of activities of more than 30 mCi (1110 MBq) with low radiation exposure of the patient [3]. The half-life is, however, long enough to perform the labeling syntheses and the scintigraphic measurements without significant losses in activity. First of all, the energy of the emitted photons of 140 keV is sufficient to study even organs that lie deep in the body. Second, photons of this energy can be collimated using lead collimators with relatively low wall thickness and can be detected effectively with NaI(Tl) scintillation counters [4]. ^{99}Tc, the decay product of ^{99m}Tc, is a pure β^- emitter with a half-life of $2.1 \cdot 10^5$ a and does not contribute noticeably to the radiation exposure.

The versatile chemistry of the transition element technetium, as apparent from the multitude of compounds in a large number of oxidation states, is an advantage for the synthesis of appropriate ^{99m}Tc radiopharmaceuticals. However, in general, the labeling requires the complexing of ^{99m}Tc with ligands containing suitable functional groups. Metabolizable biomolecules must be functionalized as complexing ligands, and as a result suffer a change in their biochemical properties, particularly through coordination to the central technetium atom. Consequently, the use of ^{99m}Tc complexes with ligands without biomolecular character has been more successful to date. Nevertheless, the labeling of biomolecules with ^{99m}Tc to prepare macromolecular tracers is of great significance, for instance for the labeling of blood cells, monoclonal antibodies or receptor-binding molecules.

The development of ^{99m}Tc radiopharmaceuticals is generally focused on complexes whose ligands are chosen under consideration of the expected lipophilicity, charge, kinetic inertness, and structure of the compound. Thermodynamically stable complexes may be reactive when administered in the blood of patients and the complexing ligands could be substituted by various enzymes, proteins or metabolites. Therefore, kinetic inertness is an important requirement. For specific syntheses, knowledge of the relationship between molecular structure and organ distribution is necessary. Mo-

lecular structures are, however, only analyzable on weighable compounds that are obtained by synthesis of a model radiopharmaceutical with the long-lived nuclide ^{99}Tc. Its structure will be determined with standard methods used in complex chemistry. After adapting the synthesis procedure for the ^{99}Tc compound in a modified form to the analogous ^{99m}Tc compound, the same structure of the radiopharmaceutical can be confirmed by radiochromatographic techniques (HPLC, TLC) and electrophoresis. However, the structure of several ^{99m}Tc radiopharmaceuticals, which have been successfully applied for some decades, have still not been characterized [1]. A number of reviews and books dealing with ^{99m}Tc radiopharmaceuticals has appeared in the last ten years [1,4–14].

2 Generation of ^{99m}Tc

^{99m}Tc is available through the β^--decay of ^{99}Mo (Fig. 2.1.B), which can be obtained by irradiation of natural molybdenum or enriched ^{98}Mo with thermal neutrons in a nuclear reactor. The cross section of the reaction $^{98}Mo(n_{th},\gamma)^{99}Mo$ is 0.13 barn [15]. Molybdenum trioxide, ammonium molybdate or molybdenum metal are used as targets. This so-called (n,γ)-molybdenum-99 is obtained in high nuclidic purity. However, its specific activity amounts to only a few Ci per gram. In contrast, ^{99}Mo with a specific activity of more than 10^4 Ci ($3.7 \cdot 10^8$ MBq) per gram is obtainable by fission of ^{235}U with thermal neutrons in a fission yield of 6.1 atom % [16]. Natural or ^{235}U-enriched uranium, in the form of metal, uranium-aluminum alloys or uranium dioxide, is used for the fission. The isolation of ^{99}Mo requires many separation steps, particularly for the separation of other fission products and transuranium elements that are also produced.

The nuclide ^{99}Mo decays with a probability of 87 % to ^{99m}Tc, which decays almost quantitatively by isomeric transition with a half-life of 6 h under emission of 140 keV photons to the ground state ^{99g}Tc. The loss of photons due to internal conversion is reported to be about 10 % [16]. Only $4 \cdot 10^{-3}$ % of the decays of ^{99m}Tc leads under β^--emission directly to stable ^{99}Ru.

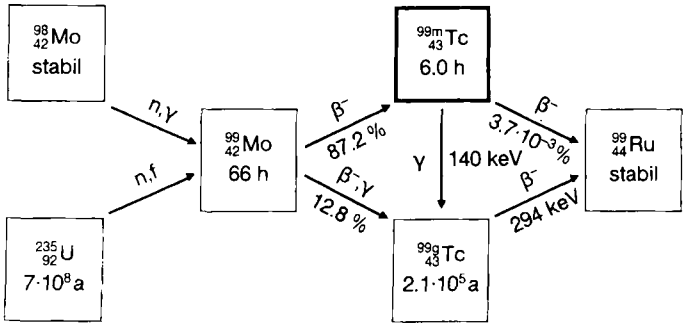

Fig. 2.1.B Generation and decay of ^{99m}Tc and ^{99g}Tc [2]

^{99m}Tc is separated from ^{99}Mo mainly by column chromatography, and only for special cases by sublimation processes or solvent extraction. The development of the first chromatographically functioning ^{99m}Tc generator succeeded as early as the late 1950's at Brookhaven National Laboratory, U.S.A. [17]. A historical perspective on ^{99m}Tc is presented in [18]. Currently, acidic aluminum oxide with anion exchange properties is used as the column packing material. ^{99}Mo is bound as $^{99}MoO_4^{2-}$ at the top end of the column, while ^{99m}Tc can simply be eluted as mononegatively charged $^{99m}TcO_4^-$ with a physiological (0.15 M) sodium chloride solution. $^{99m}TcO_4^-$ is regenerated on the generator column by ^{99}Mo decay.

The ^{99m}Tc activity A_T formed after the time t as a percentage of the activity A_M of the parent nuclide ^{99}Mo can be calculated according to the equation

$$\frac{A_T}{A_M} = \delta \frac{\lambda_T}{\lambda_T - \lambda_M}\left(1 - \varepsilon^{-(\lambda_T - \lambda_M)t}\right),$$

where $\delta = 87.2\ \%$ is the branching ratio, that is the probability of the decay of ^{99}Mo into ^{99m}Tc, $\lambda_T = 0.1155\ h^{-1}$ is the radioactive decay constant of the daughter nuclide ^{99m}Tc, and $\lambda_M = 0.0105\ h^{-1}$ that of the mother nuclide ^{99}Mo. As an example, 24 h after elution of the generator column, the activity of ^{99m}Tc is already 88.2 % of that of ^{99}Mo (Fig. 2.2.B). For imaging and functional testing of organs in human bodies about 0.5 to 30 mCi (18.5 to 1110 MBq) ^{99m}Tc are needed, which corresponds to a maximum of 6 ng.

The generator eluates have to be sterile and pyrogen free, and their nuclidic purity must conform to the demands of the European Pharmacopoeia. Under the assumption that ^{99m}Tc is applied within 12 h of the elution, the upper limits per mCi ^{99m}Tc obtained from ^{99}Mo by fission of ^{235}U are given in Table 2.1.B.

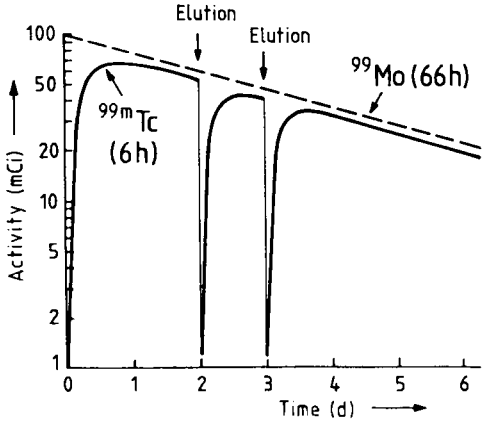

Fig. 2.2.B Production of the ^{99m}Tc activity in the system ^{99}Mo/^{99m}Tc after elution from the generator column [1]

Table 2.1.B Upper limits of nuclidic impurities per mCi ^{99m}Tc [19].

Nuclide	Activity	Half-life
^{99}Mo	1 μCi ($3.7 \cdot 10^4$ Bq)	66.02 h
^{103}Ru	50 nCi ($1.85 \cdot 10^3$ Bq)	39.35 d
^{131}I	50 nCi ($1.85 \cdot 10^3$ Bq)	8.04 d
all other γ-emitters together	100 nCi ($3.70 \cdot 10^3$ Bq)	
^{89}Sr	0.6 nCi (22.2 Bq)	50.55 d
^{90}Sr	0.06 nCi (2.22 Bq)	28.5 d
each α-emitter	1 pCi ($3.7 \cdot 10^{-2}$ Bq)	

3 Imaging of organs

^{99m}Tc, injected into the body, depending on its chemical form and its molecular structure, should accumulate in the organ to be investigated, and emits 140 keV γ quanta that permit the imaging of the organ using planar scintigraphic or emission tomographic processes. The imaging of the spatial distribution of ^{99m}Tc in the organ proceeds through the focusing of the gamma camera on sections or planes. The camera head moves circularly or elliptically around the patient, while the rotation axis coincides with the longitudinal axis of the body. Within the reconstructed layers, the obtainable resolution, under favorable measurement conditions, amounts to about 7 mm. The resolution is particularly dependent on the collimator and the distance between collimator and object [20].

The lead collimator has many holes that are parallel in most cases. The collimator shields the detector from background radiation. The image resolution of the collimator improves with decreasing hole diameter and increasing length (>5 cm) of the bore. Collimators in gamma cameras for the detection of the 140 keV γ quanta of ^{99m}Tc have up to 40 000 bores, hole diameters from 1 to 2 mm, and lead septa with a wall thickness of 0.25 mm [21,22].

The detector is a Tl-activated NaI single crystal of about 0.6 cm thickness and over 25 cm in diameter. Thicker crystals have, on the one hand, the disadvantage that multiple interactions can occur, which reduce the image resolution. On the other hand, the detector sensitivity increases with growing thickness of the crystal.

The development of high-resolution SPECT cameras for brain imaging has proceeded to multiheaded units, which provide multiplane, total body imaging, and to dedicated brain units, which usually provide one-to-three-slice non-continguous imaging in a transverse plane. 3D-SPECT systems with three heads, which can be used to image all body organs, may obtain a 360° view with only a 120° rotation. Such systems reduce the total acquisition time to 10–15 min. They potentially improve cortex resolution to 5 mm and brain center resolution to 7–8 mm. Much more common than the multiheaded rotating camera systems are the multidetector one-to-three-slice dedicated brain systems. Further development of high-resolution

fan-beam or slant-hole collimators and more sophisticated software has increased image contrast [23].

4 Synthesis aspects and requirements

The development of ^{99m}Tc radiopharmaceuticals of known composition and structure requires the synthesis and characterization of conceptional compounds with long-lived ^{99}Tc. Milligram or even microgram quantities of ^{99m}Tc could hardly be handled experimentally due to the short half-life of 6 h and the enormous radioactivity. Only 0.1 mg $Na^{99m}TcO_4$ has an activity of 270 Ci (10^7 MBq). In contrast, 50 mg $Na^{99g}TcO_4$ with an activity of 0.45 mCi (160 MBq) can be handled readily in a well-ventilated fume cupboard without any special radiation protection except for following generally accepted practices of radiation protection. The weak β^- radiation (E_{max} = 0.29 MeV) is largely shielded by the glass walls of standard laboratory vessels [24].

The starting material for the synthesis of ^{99m}Tc radiopharmaceuticals is $Na^{99m}TcO_4$, which is available after elution of the generator column with physiological saline, that is, 0.15 M aqueous NaCl solution. The concentration of $^{99m}TcO_4^-$ in the eluate is about 50 to 500 mCi ($1.85 \cdot 10^3$ to $1.85 \cdot 10^4$ MBq) per 5 ml, corresponding to $2 \cdot 10^{-8}$ to $2 \cdot 10^{-7}$ M. Saline $^{99m}TcO_4^-$ can be applied as such for thyroid and brain imaging, however, for brain imaging only then, when the blood-brain barrier (BBB) is not intact [25]. The synthesis of the other ^{99m}Tc radiopharmaceuticals requires the reduction of TcO_4^- in the presence of appropriate complexing ligands.

A variety of reducing agents can be used for the reduction of $^{99m}TcO_4^-$. Transition metal ions such as Ti^{3+}, Cr^{2+}, Cu^+, and Fe^{2+}, which tend to form complexes, should be avoided, since they could compete with ^{99m}Tc for ligands. Equally unsuitable are oxalate, formate, hyroxylamine or hydazine which may form undesired complexes with ^{99m}Tc. Even when using the common reductant Sn(II), technetium was shown to form the heteronuclear Tc-Sn-dimethylglyoxime complex $[Tc(DMG)_3(\mu\text{-}OH)SnCl_3]^\circ$ upon reduction of TcO_4^- with $SnCl_2$ in the presence of dimethylglyoxime [26, 27]. As reported recently, stannous ions can be effectively and conveniently used for the reduction of $^{99m}TcO_4^-$ in the preparation of ^{99m}Tc radiopharmaceuticals, when Sn(II) is chelated by a resin containing functional aminophosphonic acid groups. The ^{99m}Tc imaging agents were shown to be almost free of Sn(II) and the reducing capability of the resin was quite stable despite long-term storage [28]. The potentials *vs* the standard hydrogen electrode of several suitable redox systems for the reduction of $^{99m}TcO_4^-$ are given in Table 4.1.B. Numerous complexing ligands can simultaneously act as reducing agents.

Table 4.1.B Standard electrode potentials *E*h of redox systems [29] for the reduction of $^{99m}TcO_4^-$

Medium	Redox System				Eh [V]
	$S_2O_3^{2-}$	$+3H_2O \leftrightarrow 2H_2SO_3$	$+2H^+$	$+4e$	0.40
	Sn^{2+}	$\leftrightarrow Sn^{4+}$		$+2e$	0.15
acidic	$S_2O_6^{2-}$	$+2H_2O \leftrightarrow 2SO_4^{2-}$	$+4H^+$	$+2e^-$	−0.22
	H_3PO_3	$+H_2O \leftrightarrow H_3PO_4$	$+2H^+$	$+2e^-$	−0.276
	H_3PO_2	$+H_2O \leftrightarrow H_3PO_3$	$+2H^+$	$+2e$	−0.50
	$[Sn(OH)_3]^-$	$+3OH^- \leftrightarrow [Sn[OH)_6]^{2-}$		$+2e$	−0.90
	SO_3^{2-}	$+2OH \leftrightarrow SO_4^{2-}$	$-H_2O$	$+2e$	−0.936
basic	HPO_3^{2-}	$+3OH^- \leftrightarrow PO_4^{3-}$	$+2H_2O$	$+2e^-$	−1.12
	$S_2O_4^{2-}$	$+4OH^- \leftrightarrow 2SO_3^{2-}$	$+2H_2O$	$+2e$	−1.12
	BH_4^-	$+8OH^- \leftrightarrow H_2BO_3^-$	$+5H_2O$	$+8e$	−1.24
	$H_2PO_2^-$	$+3OH^- \leftrightarrow HPO_3^{2-}$	$+2H_2O$	$+2e^-$	−1.570

The controlled-potential electrolytic reduction of $^{99m}TcO_4^-$ at chemically inert electrodes, for example at Hg or Pt cathodes, is also applicable. It often permits the reduction to defined oxidation states in 5 to 10 min and avoids the addition of reducing agents which cause impurities in the radiopharmaceutical solution [30]. Electrolytic reduction has found little application in chemical practice, since it requires more equipment.

The synthesis of the radiopharmaceutical should proceed in one step directly after elution of $^{99m}TcO_4^-$ from the generator column and must be performed in a solvent which is appropriate for intravenous injections, such as physiological sodium chloride solution. The reagents used should be non-toxic and the injected solutions must be sterile and pyrogen free. ^{99m}Tc should occur quite predominantly in the expected chemical form and molecular structure, that is, the so-called radiochemical purity should exceed 90 % to ensure the highest possible organ specifity. Usually, the concentrations of the reagents (ligand, reductant) are much greater than the concentration of $^{99m}TcO_4^-$. Then a pseudo first-order reaction for the formation of the radiopharmaceutical is to be expected:

$$\frac{d[\text{product}]}{dt} = -\frac{d[^{99m}TcO_4^-]}{dt} = k[^{99m}TcO_4^-].$$

k is the specific rate constant. The time t necessary for completing 99 % of the reaction

$$t = \frac{4.6}{k}$$

is a function only of the pseudo first-order rate constant k and not of the $^{99m}TcO_4^-$ concentration [3].

In addition to the physical half-life $t_{1/2} = t_{phys}$ of ^{99m}Tc, the biological half-life t_{bio} is of importance. The latter indicates the time, regardless of radioactive decay, at which the activity of the radiopharmaceutical in the body has decreased to one-half by biolo-

gical elimination. Naturally, t_{bio} depends on the specific radiopharmaceutical. The so-called effective half-life t_{eff} follows from t_{phys} and t_{bio} according to the equation

$$t_{eff} = \frac{t_{phys} \cdot t_{bio}}{t_{phys} + t_{bio}}.$$

Considering the exposure of the patient to radiation, t_{eff} should not be any longer than it takes to carry out the required diagnostic investigations [14]. The value of t_{eff} is always less than the shorter of the two half-lives t_{phys} and t_{bio}. For ^{99m}Tc radiopharmaceuticals $t_{bio} < t_{phys}$ is valid throughout, and the biological half-life is frequently smaller than desirable for the measurements.

A high organ specificity is one of the particular aims of the development of radiopharmaceuticals. The injected radioactivity should preferably accumulate in the organ to be investigated, that is, a high activity ratio of the target organ to non-target areas of the body is desired. High activity in adjacent organs and particularly in the blood can severely obscure the target organ image, the reproduction of structural details, and the organ function testing. In addition, a high organ specifity permits the reduction of the injected activity dose and consequently the exposure of the patient to radiation.

A radiopharmaceutical should not change chemically *in vivo* during its transport to the target organ, i.e. it should be kinetically inert. However, the metabolization of the labeled complex in the target organ can be of advantage, in particular, if the functioning of the organ should be tested. The *in vivo* stability prior to the accumulation in the organ is a necessary precondition, if information concerning the relationships between molecular structure and organ distribution is to be gained [1].

5 Kits

Kits are sterile and pyrogen-free, non-radioactive reagent mixtures which are dried by lyophilization and stored under nitrogen in sealed glass vials. These kits contain the substance to be labeled, which is mostly the complexing ligand, and in addition, generally a reductant and some other preservative components which ensure the reliability of the final ^{99m}Tc radiopharmaceutical formed by reaction with $^{99m}TcO_4^-$ of the generator eluate. The kits are commercially available and can be stored for long periods of time. Stannous salts are the preferred reductants for kit formulations, because of their water solubility, chemical stability under dry conditions, low toxicity, and effectiveness at room temperature. Currently available kits contain a stannous salt as reductant. Without the complexing ligand, the reduction of pertechnetate yields predominantly the thermodynamically stable TcO_2-hydrate. Even in the presence of a ligand, the production of TcO_2-hydrate may compete with the ^{99m}Tc complex formation. Therefore TcO_2-hydrate may be present as an impurity in ^{99m}Tc radiopharmaceuticals [31].

Additional kit components are antioxidants, buffers and other additives such as so-called catalysts, accelerators, solubilizing agents and fillers. Antioxidants, for instance

ascorbic acid, gentisic acid, and 4-amino-benzoic acid, have been used to protect ^{99m}Tc radiopharmaceuticals against oxygen or oxidants in addition to stannous salts. Frequently, the radiochemical purity of pharmaceuticals is highly pH dependent and the ^{99m}Tc product may vary with the pH of the solution; thus buffers can be important components in kit formulations. However, sometimes the ligand itself act as a buffer. Yields of desired complexes may be improved by adding another ligand (catalyst), such as gluconate, dtpa or citrate, which form weak technetium complexes and provide for ligand exchange reactions. This approach was adopted for ^{99m}Tc isonitrile radiopharmaceuticals. Accelerators with vicinal hydroxyl groups appear to increase the rate of complex formation and to improve the radiochemical yield. Solubilizing agents are surfactants which help to dissolve lipophilic ^{99m}Tc radiopharmaceuticals, and the ready dissolution of the solids within the vial is of high significance for the formation of the expected radiopharmaceutical. Rapid solubilization is also achieved through the control of the particle size during the lyophilization process. The particle size is controlled, if necessary, by the presence of inert fillers, such as NaCl or mannitol [5,31].

6 Synthesis, structure and development

Numerous clinically approved ^{99m}Tc radiopharmaceuticals are currently used in nuclear medicine for studying the morphological structure of organs and testing their physiological function. Several aspects of these radiopharmaceuticals and some future prospects will be presented below, mainly with regard to human organs.

6.1 Brain perfusion imaging agents

Brain radiopharmaceuticals should be capable of penetrating the intact blood-brain barrier (BBB). The barrier arises from epithelial-like tight junctions that virtually cement adjoining capillary endothelium together in the brain microvasculature. There are no pores in brain capillaries [32,33]. Lipid-soluble, uncharged molecules can pass through the BBB by passive diffusion, as long as a concentration difference exists on both sides of the capillary wall. The lipophilicity of complexes is often quantified by the logarithm of the octanol/water coefficient. Compounds with values of log P between 0.9 and 2.5 appear to penetrate the BBB rather easily (Fig. 6.1.B), while more strongly lipophilic substances are increasingly bound to blood components. Percentage brain extraction rises almost linearly in the range of log P values from –1 to +1, remains constant over the range of log P 1.0–3.0, and then declines linearly as lipophilicity increases further. However, such relationships, as expected, are dependent on the structure of the respective compounds [35,36]. The permeability of the BBB, naturally, also increases with decreasing molar mass. For compounds with molar masses up to 400 daltons, good agreement between lipophilicity and permeability was observed, but above 400 daltons, the permeability was reduced independent of the

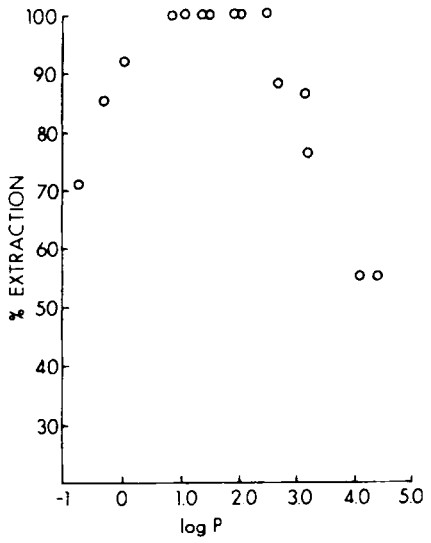

Fig. 6.1.B Calculated brain extraction of ^{11}C-labeled compounds plotted against log *P* values at cerebral blood flow of 100 ml·min^{-1}·100 g^{-1} studied in adult baboons [34]

lipophilicity [37]. In addition, the BBB permeability may be inversely related to the intermolecular hydrogen bond strength of a lipid-soluble compound [38].

^{99m}Tc brain radiopharmaceuticals developed to date appear to penetrate the BBB by simple diffusion. However, non-lipid-soluble substances, such as glucose, as the most important energy source of the brain cells, and also essential amino acids, which cannot be synthesized by the brain, must be able to pass through the membrane of the endothelial cells. At least ten amino acids penetrate the membranes of the endothelial cells by the same transport system [33]. The binding of an uncharged ^{99m}Tc complex to a large neutral amino acid could, by using this transport system of the endothelial cells, accelerate the passage of ^{99m}Tc into the brain [39].

In addition to the diffusion of radiopharmaceuticals through the BBB into the brain, their retention in the brain is of great importance for scintigraphic measurements. In particular, the rediffusion of radiopharmaceutical agents from the brain should be limited, either by binding to intracellular components of the brain cells or through metabolic trapping. Thus, the development of new ^{99m}Tc brain radiopharmaceuticals is focused on those compounds which not only can penetrate the BBB in the direction of the brain, but also lose their neutral and/or lipophilic character by metabolization in the brain, so that the diffusion out of the brain is hindered [25,38]. Furthermore, the distribution of the agent within the cerebral tissues should be in proportion to regional blood flow, with no redistribution of the radioactivity with time.

6.1.1 [$^{99m}Tc^{V}O$-*d,l*-HM-PAO]°

The title neutral complex is prepared by reduction of $^{99m}TcO_4^-$ in saline with Sn(II) in the presence of the ligand *d,l*-HM-PAO (hexamethyl propylene amine oxime) or, more precisely, 3,6,6,9-tetramethyl-4,8-diazaundecane-2,10-dione dioxime [40]. According to structural investigations of [$^{99g}Tc^{V}O$-*d,l*-HM-PAO]° the molecular struc-

ture of the *d,l*-diasteroisomeric complex core is a square pyramid with the oxygen atom at the apex (Fig. 6.2.B). Technetium in the oxidation state +5 is located 0.68 Å above the basal plane defined by the four nitrogen atoms. The oxime oxygen atoms form a strong intramolecular hydrogen bond. The +3 charge of the TcO core is neutralized by the two secondary amines and the ionization of one of the oxime OH groups. The Tc=O distance is 1.682(5) Å. The $Tc-N_{amide}$ distances of 1.91 Å are considerably shorter than the $Tc-N_{amine}$ distances of 2.07 Å. The yellow complex crystallizes in the orthorhombic space group $P2_12_12_1$ with a=6.948(2), b=12.460(3), c=19.299(4) Å and Z=4. The Tc=O stretching vibration was found in the IR at 911 cm^{-1}. The compound is quite lipophilic, as indicated by the ready extraction into diethyl ether [40]. It has a log P of ≈ 2 and readily penetrates the intact BBB [41].

The human brain accumulates, for instance, 3.4 to 5.7 % of the injected activity up to at least 8 h after the injection [42]. The retention mechanism appears to be a chemical reaction in the brain which may be associated with intracellular glutathione [8]. Obviously, [$^{99m}Tc^{V}O$-*d,l*-HM-PAO]^{0} is unstable [43] and converts rapidly from the lipophilic to a hydrophilic compound that is unable to rediffuse through the BBB and is trapped in the brain. The rate-limiting step for this conversion is probably dependent on the reductant gluthathione [44–46]. More recently *in vitro* data have supported that intracellular retention of [$^{99m}Tc^{V}O$-*d,l*-HM-PAO]^{0} is generally dependent on the redox status of the tissue [47]. The *in vitro* stability of this agent is limited. Once the complex is prepared by dissolution of the lyophilized kit in the saline solution of $^{99m}TcO_4^-$, it must be injected within 30 min. The major products of the [$^{99m}Tc^{V}O$-*d,l*-HM-PAO]^{0} decomposition are $^{99m}TcO_4^-$ and other hydrophilic ^{99m}Tc species [48]. Gentisic acid (2,5-dihydroxybenzoic acid), an antioxidant, was employed to stabilize the kit, but its effect is highly pH dependent with optimum utility occurring near neutral pH. The stabilization would allow the kit to be used for up to six hours after reconstitution [49]. Very recently it was reported that [$^{99m}Tc^{V}O$-*d,l*-HM-PAO]^{0} is stable in basic solution, however, in an acid solution it is attacked by the hydrogen ions forming hydrophilic complexes [50]. Preparation of [^{99m}TcO-*d,l*-HM-PAO]^{0} in 85 % ethanol was found to increase its *in vitro* stability. Diluting the ethanolic solution by 1 to 10 with physiological saline provided a very stable preparation [51]. Further, it was shown that the ^{99m}Tc complex in aqueous solutions in the reconstitution vials is sensitive to self-radiolysis near neutral pH producing $^{99m}TcO_4^-$ as the primary hydrophilic species [52].

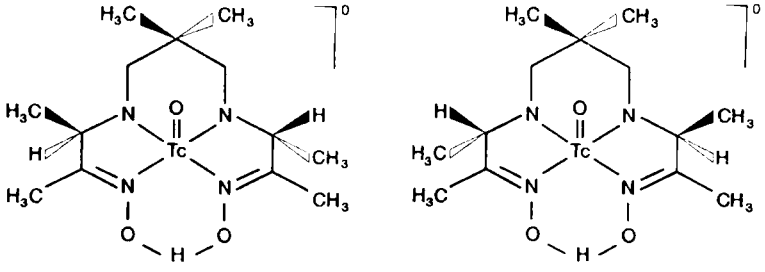

Fig. 6.2.B [$Tc^{V}O$-*d,l*-HM-PAO]^{0} [41]

[$^{99m}Tc^{V}O$-*d,l*-HM-PAO]° was the first approved cerebral perfusion imaging agent for human applications [53] that distributes in the brain in proportion to regional blood flow [54]. The time-activity curve demonstrates the rapid uptake of the agent into the brain. The maximal count rate is obtained 30–40 s after the injection. By 2 min after injection the brain activity decreases to about 90 % of the peak value and then remains constant throughout the period of observation. SPECT images demonstrated selective uptake of the complex in areas corresponding anatomically to cortical gray matter. Activity was visualized along the convexity of frontal, temporal, parietal, and occipital lobes and along the interhemispheric fissure. The basal ganglia were also clearly delineated. The region between the basal ganglia and the convexity had less activity and corresponded to cortical white matter and to the ventricular system. The cerebellar hemispheres could be seen at the base of the brain. The gray-to-white matter activity ratio was 1.77 at 1 h. The total brain activity was found to decrease slowly from the first hour up to 5–6 h by 8.6 %. Stroke patients showed perfusion defects involving the frontal, temporal, and parietal lobes with variable extension into the occipital lobe and the basal ganglia. In patients with cerebrovascular disorders, the low flow areas were well detected. [^{99m}TcO-*d,l*-HM-PAO]° presents considerable promise for cerebral blood flow tomographic imaging using commercial single-head rotating gamma cameras [54]. Fig. 6.3.B shows an emission tomogram of the brain of a patient with focal blood hypoperfusion.

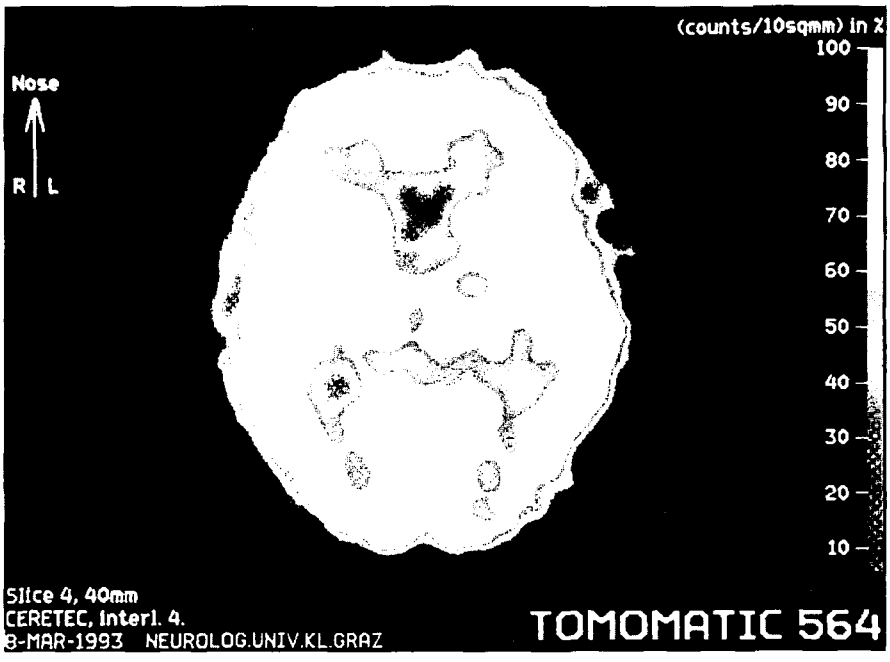

Fig. 6.3.B Emission tomogram of the brain of a patient suffering from focal blood hypoperfusion, taken after injection of [^{99m}TcO-*d,l*-HM-PAO]°. The scale on the right-hand edge of the picture gives the count rate per 10 mm^2 in % [1]

The agent was subjected to various clinical trials. One of the potential clinical uses is the investigation of dementia, in particular to differentiate between dementia of the Alzheimer type and multi-infarct dementia. Perfusion deficits were much more common in Alzheimer type dementia [55]. Reductions in uptake of the agent revealed posterior hemisphere abnormalities in the majority of patients suffering from Alzheimer's disease [56]. The predictive value of bilateral temporoparietal defects for Alzheimer's disease was found to be high [57]. [^{99m}TcO-*d,l*-HM-PAO]° allows monitoring of rapid changes of regional cerebral blood flow due to decreased neuronal activity in epileptic patients [58]. For detecting abnormalities in patients with a remote history of traumatic brain injury, the [^{99m}TcO-*d,l*-HM-PAO]° SPECT was shown to be more sensitive than X-ray computed tomography (CT) [59]. The agent was also applied to detect, by cerebral blood flow (CBF)-SPECT, a subdural hematoma [60] or to pursue the effect of radiotherapy on brain tumors [61]. Brain death was determined by demonstrating no uptake of the agent in either the cerebrum or the cerebellum, while uptake was present in all patients who were not clinically brain dead. Cerebral perfusion imaging with [^{99m}TcO-*d,l*-HM-PAO]° appears to be a simple and reliable test to confirm brain death [62,63].

6.1.2 [^{99m}Tc^{V}O-L,L-ECD]°

The title complex can be synthesized by reduction of $^{99m}TcO_4^-$ in saline with Sn^{2+} in the presence of N,N'–1,2-ethanediyl-bis(L-cysteine-diethylester) dihydrochloride [64]. The analogous compound with long-lived technetium [^{99g}Tc^{V}O-L,L-ECD]° is obtained by ligand exchange from $[TcOCl_4]^-$ or $[TcO_2(py)_4]^+$. The lipophilic product precipitates from the aqueous reaction mixture as an orange solid. The X-ray structure determination revealed a distorted square pyramidal geometry of the donor atoms with the oxygen atom at the apical position. The structure (Fig. 12.24.A) of the core is similar to that of [TcO-*d,l*-HM-PAO]°. The Tc atom is approximately 0.73 Å above the N_2S_2 plane. One nitrogen atom is protonated displaying a Tc–N bond distance of 2.168 Å, while the Tc–N distance to the deprotonated nitrogen of 1.924 Å is shorter by 0.24 Å. The neutral compound crystallizes in the orthorhombic space group $P2_12_12_1$ with a=7.121(1), b=9.670(1), c=24.530(3) Å, and Z=4 [65].

The [^{99m}TcO-L,L-ECD]° uptake in human brain is 5 to 6 % of the injected activity dose within a few minutes [64,69,70]. After one hour the activity decreases to 4 % [64]. The agent exhibits a rapid clearance from the blood to less than 10 % after 5 min [69,70] and from the surrounding anatomical regions of the brain. The high target-to-non-target ratio renders it more attractive for SPECT than [^{99m}TcO-*d,l*-HM-PAO]°. In monkey brain tissue [^{99m}TcO-L,L-ECD]° was shown to be metabolized enzymatically, while [^{99m}TcO-D,D-ECD]° did not react. It was postulated that the metabolite of [^{99m}TcO-L,L-ECD]° is the more polar monocarboxylate, monoester complex, resulting from hydrolysis of one of the ethylester groups [65,66]. *In vitro* evidence supports the hypothesis that esterase activity is the major determinant of the overall retention of [^{99m}TcO-L,L-ECD]° [67]. Only in primates and man does the agent show the long retention in the brain. Animal models tested, which included mice, rats, guinea pigs, cats, dogs, swine, and ferrets, showed a rapid washout over the

first few minutes or at most one hour [8]. The half-life of the agent in a monkey brain was found to be greater than 24 h [68].

In normal human subjects the agent allowed an excellent delineation of the cortical gray matter, the basal ganglia, the thalamus and cerebellar hemispheres as regions of relatively increased tracer uptake. White matter displayed substantially less uptake than gray matter. The primary route of excretion of the tracer is through the kidneys. [^{99m}TcO-L,L-ECD]° SPECT shows particular promise for the evaluation of patients with stroke [70].

6.1.3 [^{99m}Tc^{III}Cl(DMG)2MP]°

The boronic acid adduct of technetium dimethylglyoxime [^{99m}Tc^{III}Cl(dimethylglyoxime-(2-methyl-1-propyl)boron]° is also capable of penetrating the intact blood-brain barrier due to its neutral and lipophilic character. The complex forms by reduction of $^{99m}TcO_4^-$ with Sn^{2+} in the presence of dimethylglyoxime and 2-methylpropylboric acid. In [^{99g}Tc^{III}Cl(DMG)2MP]° technetium has the relatively rare coordination number of 7 and is surrounded by the nitrogen atoms of three dioxime ligands and a covalently bonded chlorine atom (Fig. 6.4.B). The boron atom resides in a tetrahedral environment, bound to three dioxime oxygen atoms and the 2-methylpropyl group. The remaining three oxygen atoms of the dioxime ligands are bound to each other through two strong hydrogen bonds [71].

The activity of the agent in monkey brain 5 min post-injection was 2.8 % of the injected dose. The activity cleared with a half-life of 86 min [72]. The slow cerebral clearance in human subjects may be caused by the high lipophilicity of log $P = 3.8$ of the agent [73]. The testing of this complex for clinical applications in brain imaging appears to be completed now. Unfortunately, the studies in human subjects were disappointing [8].

6.1.4 [^{99m}Tc^{V}O(MRP-20)]°

The ligand N-{2(1-H-pyrrolylmethyl)}N′-(4-pentene-3-one-2)ethane-1,2-diamine, called MRP-20, forms a neutral and lipophilic complex with the $Tc^{V}O^{3+}$ core by the loss of three protons. The compound (Fig. 6.5.B) is under investigation as a potential

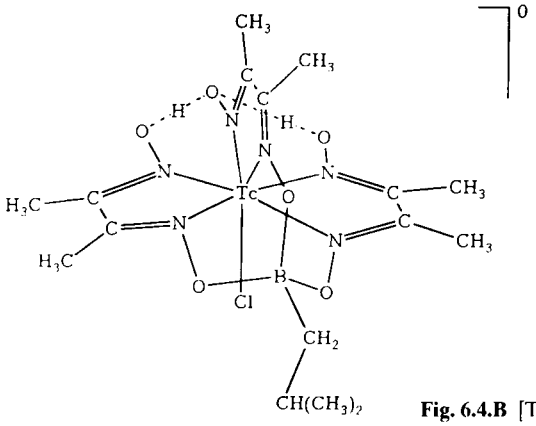

Fig. 6.4.B [Tc^{III}(DMG)$_3$2MP]° [71]

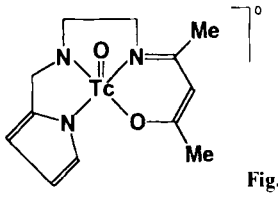

Fig. 6.5.B $[Tc^{V}O(MRP\text{-}20)]^{\circ}$ [74]

brain perfusion imaging agent. It is obtained by reaction of MRP-20 in ethanol with $^{99m}TcO_4^-$ in saline and $SnCl_2$ as reductant. $[^{99g}Tc^{V}O(MRP\text{-}20)]^{\circ}$ was prepared by ligand substitution of $[TcO(ethyleneglycolate)_2]^-$ with MRP-20. The lipophilicity of the complex is quantified by log P = 1.93. The radiochemical purity of $[^{99m}TcO(MRP\text{-}20)]^{\circ}$ was higher than 93 %.

The initial uptake of the agent in human subjects is shown in Fig. 6.6.B. Activity in the brain reached a maximum of almost 6 % of the injected dose within 1 min post-injection. The uptake level remained almost constant at 4.4 % over 24 h. The blood clearance was slow with $t_{1/2} > 4$ h. High quality brain SPECT images were obtained until 7 h post-injection. There was a good differentiation between gray and white matter. The trapping mechanism is presumed to be related to the *in vitro* tendency of the complex to hydrolyze generating a cationic species. The regional cerebral distribution is similar to that of $[^{99m}TcO\text{-}d,l\text{-}HM\text{-}PAO]^{\circ}$. The tracer is excreted by both urinary and hepatobiliary excretion. $[^{99m}TcO(MRP)\text{-}20)]^{\circ}$ appears to be still undergoing clinical trials [74–76].

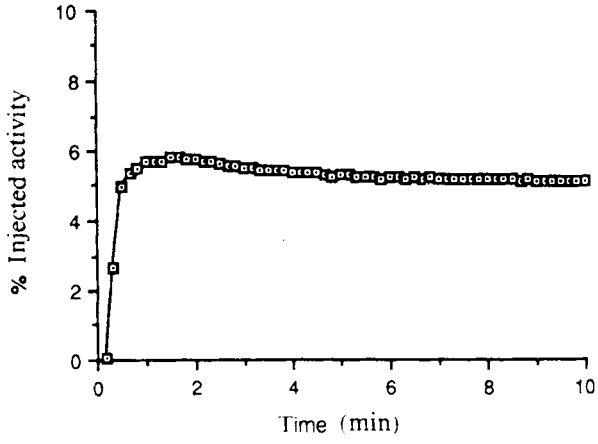

Fig. 6.6.B Dynamic planar brain time-activity curve of $[^{99m}Tc^{V}O(MRP\text{-}20)]^{\circ}$ for normal human subjects [75]

6.1.5 $[^{99m}Tc^{V}O(NEP\text{-}DADT)]^{\circ}$

Another diaminodithiol complex with N-ethyl piperidinyl hexamethyl diaminodithiol (NEP-DADT) as the complexing ligand is $[^{99m}Tc^{V}O(NEP\text{-}DADT)]^{\circ}$. The agent was synthesized by reduction of $Na^{99m}TcO_4$ in saline with $SnCl_2 \cdot 2H_2O$ in the presence of

the ligand and addition of a phosphate buffer [77]. Two stereoisomeric compounds are formed, the *syn* and the *anti* isomer. The *syn* isomer (Fig. 6.7.B), which has the N-piperidinylethyl side chain located *syn* to the technetium oxo core, allowed obtaining images of the brain in humans that are qualitatively related to regional brain blood flow [78]. Studies in patients have shown that [^{99m}Tc^{V}O(NEP-DADT)]$^{+}$ enters rapidly into the brain, but also clears rapidly with $t_{1/2}$ = 17 min [79].

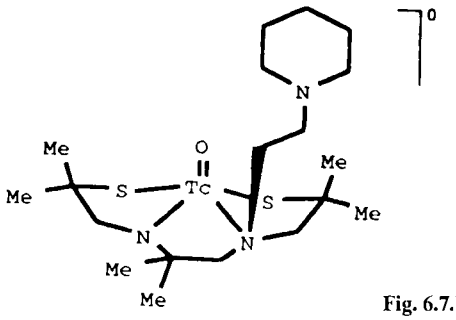

Fig. 6.7.B Syn-[Tc^{V}(NEP-DADT)]$^{+}$ [78]

6.1.6 [^{99m}Tc(DTPA)]$^{2-}$, [^{99m}Tc^{V}O(glucoheptonate)$_2$]$^{-}$, and Na^{99m}TcO$_4$

The title agents can not cross the intact blood-brain barrier, but can be applied for brain imaging when the BBB is damaged, for example by tumors.

[^{99m}Tc(DTPA)]$^{2-}$ is prepared by reduction of ^{99m}TcO$_4^-$ with Sn(II) and treatment of the solution with calcium-sodium-diethylene-triaminepentaacetate. The stable and radiochemically pure complex is reported to have a net charge of –2 [80], the composition [^{99g}Tc(DTPA)]$^{2-}$, and an absorption maximum at 490 nm [81]. The oxidation state of technetium is believed to be +4, however, no structural characterization of the complex was performed [82,83]. [^{99m}Tc(DTPA)]$^{2-}$ diffuses rapidly into the brain, and its uptake in the choroid plexus is negligible, thus obviating the need for the administration of perchlorate to block the choroid plexus. Images are obtained 1 h after injection of 10–20 mCi (370–740 MBq). The agent is readily filtered by the kidneys, thus necessitating the injection of a larger amount of radioactivity [84].

[^{99m}Tc^{V}O(glucoheptonate)$_2$]$^{-}$ is obtained by reaction of a mixture of calcium glucoheptonate and $SnCl_2$ with ^{99m}TcO$_4^-$. The molecular structure of the complex follows from NMR and IR spectra and shows a Tc^{V}O^{3+} core and two five-membered glucoheptonate rings that are bidentately bound through oxygen atoms (Fig. 6.8.B) to the Tc center. The net charge of the agent is –1 in aqueous solution. A 10^{-2} M solution of [^{99g}TcO(glucoheptonate)$_2$] in saline was chemically stable for more than 200 days at room temperature. The VIS/UV spectrum shows absorption bands at 502 and 270–280 nm. The presence of a Tc=O core is indicated by vibration frequencies observed in the IR at 930 and 970 cm^{-1} and in the Raman spectrum at 975 cm^{-1} [85]. As in the case of [^{99m}Tc(DTPA)]$^{2-}$, the blood flow in the carotid and cerebral arteries can be immediately visualized and then followed by a pool study. Epileptic seizures often cause increased blood flow in the region of discharge, which may appear as an area of increased radioactivity. In cases of head trauma, the dynamic phase of the scintigraphy

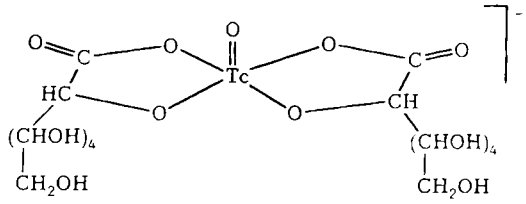

Fig. 6.8.B [$Tc^{V}O$(glucoheptonate)$_2$] [85]

may help distinguish between subdural and epidural hematomas [4]. [^{99m}TcO(glucoheptonate)$_2$]$^-$ was claimed to be a superior agent for detecting primary and metastatic lesions in the brain. It is also used for the detection of infarct or ischemic lesions. Usually 10–20 mCi (370–740 MBq) of the agent is administered and imaging is performed 1–3 h after injection [84].

$Na^{99m}TcO_4$ may also be applied to brain imaging. Again 10–20 mCi (370–740 MBq) of $Na^{99m}TcO_4$ in physiological saline is injected. Images are taken 30–180 min post-injection. The brain flow study in patients reveals the symmetry of blood flow in the two cerebral hemispheres. Increased perfusion would indicate vascularity in the lesion, as in some tumors, whereas decreased perfusion may indicate an infarct. The choroid plexus accumulates $^{99m}TcO_4^-$ and appears as a hot spot on the brain image. Its uptake is blocked with 200–300 mg of $KClO_4$, which is administered orally and saturates the binding sites [84].

6.2 Myocardial perfusion imaging agents

A strategy for the development of ^{99m}Tc myocardial perfusion imaging agents is based on the assumption that unipositive cationic complexes tend to accumulate in the myocardium [86]. This assumption is supported by the known concentration of alkali metal ions, such as K^+, Rb^+, and Cs^+ and particularly Tl^+, which is still used as $^{201}Tl^+$ in competition with ^{99m}Tc radiopharmaceuticals for heart perfusion imaging. However, the nuclear properties of ^{201}Tl (decay by electron capture with $t_{1/2}$ = 73.5 h, maximum γ energy 167 keV, but only 8.8 % decay probability) and the necessity of using accelerators for its production are disadvantageous when compared to ^{99m}Tc. It is also known that NH_4^+ derivatives accumulate in the heart muscle [87]. Whether, in addition to K^+ and Tl^+, also other cations concentrate in the heart muscle cells via Na^+/K^+-adenosinetriphosphatase (Na^+/K^+-ATPase pump) has yet to be proven [88]. However, it must be emphasized that the cationic character of the ^{99m}Tc myocardial perfusion imaging agents is obviously not an absolute precondition as demonstrated below.

The lipophilicity of the diagnostic agent is also of importance for its uptake in the myocardium. Agent-dependent parabola-like functions between the accumulation in the myocardium and log P were observed [88]. A reason for the decrease in the accumulation at high lipophilicity values of log $P > 5$ should again be the binding of the agent to blood protein. The heart muscle distribution of the desired radiopharmaceutical should be directly related to the regional myocardial blood flow, which requires a high extraction and a slow washout rate of the agent [9,88].

In addition, a rapid clearance from the background activity in the blood, lungs, and liver is needed.

6.2.1 $[^{99m}Tc^{I}(MIBI)_6]^+$

The cation $[^{99m}Tc^{I}$(methoxyisobutylisonitrile)$_6]^+$ or more precisely hexakis(2-methoxy-2-methylpropyl-1-isonitrile-technetium(I), has received worldwide approval as a myocardial perfusion agent and is the most widely used [5]. The complex is synthesized by reduction of $^{99m}TcO_4$ with $Na_2S_2O_4$ in the presence of the isonitrile ligand [89] or in a kit by reaction of tetrakis(2-methoxy-2-methylpropyl-1-isonitrile)-copper(I) tetrafluoroborate with $SnCl_2 \cdot 2H_2O$ and $^{99m}TcO_4^-$ [90]. The structure of the precursor of $[^{99m}Tc^{I}(MIBI)_6]^+$, the hexakis(*tert*-butyl-isonitrile) technetium(I) cation, was determined by single crystal X-ray structure analysis. The coordination geometry of ^{99}Tc in the complex cation is slightly distorted octahedral [91].

The uptake of $[^{99m}Tc^{I}(MIBI)_6]^+$ (Fig. 6.9.B) in the human heart is about 1.5 % of the injected activity, and decreases to 1 % after 4 h. The background activity in the blood, lungs, liver, and spleen is sufficiently low [92]. The presence of the methoxy groups on the periphery of the cation provides for optimal lipophilicity and allows for *in vivo* hydrolysis of the ethers to the respective alcohols which may increase the clearance rates from blood and liver [5]. The complex cation seems not to be taken up in the myocardium by the Na^+/K-ATPase pump but is retained in cellular membranes including mitochondrial membranes [93,94]. As for ^{201}Tl, the distribution of $[^{99m}Tc^{I}(MIBI)_6]^+$ reflects the myocardial blood flow, but unlike ^{201}Tl there is no evidence of

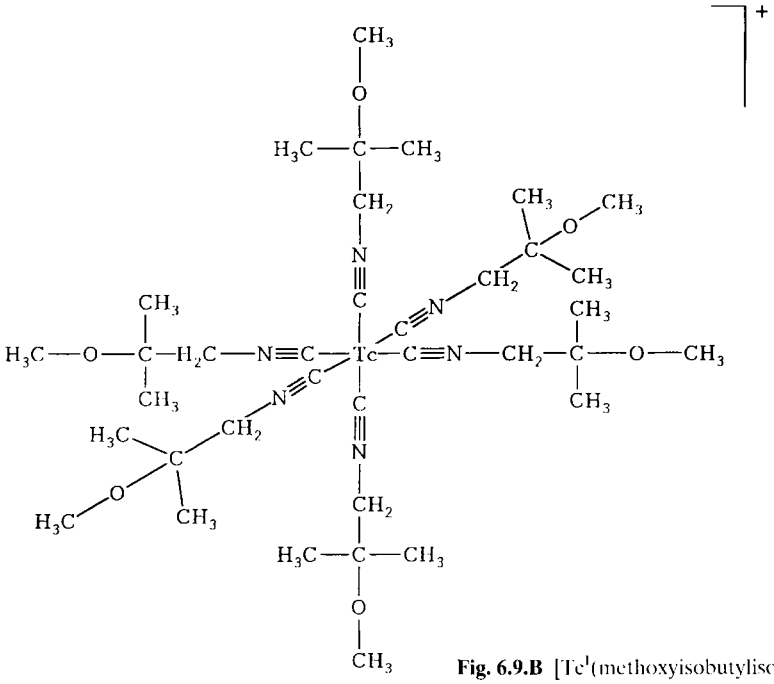

Fig. 6.9.B $[Tc^{I}$(methoxyisobutylisonitrile)$]^+$ [1]

significant myocardial redistribution following injection. Since it does not redistribute, two separate injections are needed in order to differentiate transient ischemic defects from fixed myocardial defects [95].

6.2.2 $[^{99m}Tc^{III}$(teboroxime)]°

The neutral and lipophilic compound is a seven-coordinate complex of Tc(III) with tris-(cyclohexane-dione-dioxime)-methylboron (CDO-MeB) and a chloride as ligands. It is prepared by template synthesis, reacting $^{99m}TcO_4^-$ with 3 equivalents of 1,2-cyclohexane-dione dioxime, methylboronic acid, and $SnCl_2$ in hydrochloric acid solution [96]. The complex contains three vicinal cyclohexanedionedioxime ligands bonded to the Tc(III) center in a nearly trigonal arrangement by six nitrogen atoms, the boronic acid derivative that caps the complex by attachment to three oxime oxygens and the chloride. The angle between two of the dioximes is opened by the chloride to greater than 120°. The chloride prevents the formation of a bis-capped complex. The three dioxime oxygens on the uncapped end are intramolecularly hydrogen bonded to two bridging protons [97] (Fig. 6.10.B). The chloride ligand is labile under physiological conditions and undergoes chloro/hydroxy exchange [98] with a half-life of 13 min. This exchange does not influence the efficacy of [^{99m}Tc-(teboroxime)]° as a myocardial perfusion imaging agent [6].

The complex displays a high myocardial uptake in man of 4–6 % five minutes after a resting injection, compared to 4.2 % for $^{201}Tl^+$ and 1–3 % for $[^{99m}Tc(MIBI)_6]^+$ [99]. The blood clearance is fast, more than 90 % of the injected dose cleared within three minutes [73]. However, the activity is washed out from the myocardium considerably more rapidly than that of $[^{99m}Tc(MIBI)_6]^+$. The washout from the myocardium is biphasic with a fast component with a 2 min half-life with ca. 65 % of activity, and a slow component with a 78 min half-life. The hepatic accumulation may interfere with the visualization of some myocardial segments [100]. The agent is also taken up by the skeletal muscles. [^{99m}Tc(teboroxime)]° has provided good planar and SPECT images in humans, but requires rapid SPECT techniques. After extensive clinical trials the agent was approved for myocardial perfusion imaging [73].

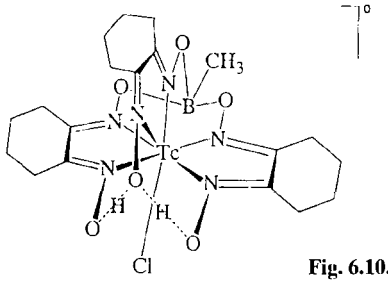

Fig. 6.10.B [Tc^{III}-teboroxime]° [8]

6.2.3 $[^{99m}Tc^{V}O_2$(tetrofosmin)$_2]^+$

This cationic myocardial perfusion imaging agent was developed more recently. Tetrofosmin is the ether functionalized diphosphine ligand 1,2-bis{bis(2-ethoxyethyl)phosphino}

ethane. The lipophilic complex was synthesized by reduction of $^{99m}TcO_4^-$ with $SnCl_2$ in the presence of tetrofosmin. The structure of the analogous ^{99g}Tc compound was determined by X-ray structure analysis. The *trans*-Tc^VO_2 core is linear, as expected. The four phosphorus atoms of the two bidentate diphosphine ligands form a planar array perpendicular to the *trans*-oxo core resulting in a distorted octahedral geometry (Fig. 12.38.A) of the complex. The main deviation from octahedral geometry arises from the steric requirements of the five-membered rings. The P–Tc–P angles are 81.4(2)°. The Tc–P bond distances are 2.47 Å and the Tc=0 distance 1.74 Å [101].

$[^{99m}Tc^VO_2(tetrofosmin)_2]^+$ exhibits a good heart uptake in humans of 1.2 % of the injected activity which only decreases to 1 % 2 h after injection. The clearance was shown to be excellent from blood with <5 % after 10 min and from liver with <4.5 % after 60 min. At rest there was only moderate uptake by the lungs from 0.7–3.0 % initially that rapidly cleared to almost undetectable levels within 4 h. The cationic agent is the first example of a $^{99m}Tc^VO_2^+$ entity to have shown substantial myocardial uptake and retention in combination with fast non-target clearance. The eight ethoxyethyl groups of the ligands apparently contribute to reduce the non-target background activity. There is no evidence for *in vivo* reduction of ^{99m}Tc(V) to lower oxidation states [101–103]. $[^{99m}TcO_2(tetrofosmin)_2]^+$ was evaluated in clinical trials. SPECT imaging was performed 45–60 min post-injection demonstrating the agent to be highly sensitive and specific for the detection of coronary artery disease [104].

6.2.4 $[^{99m}Tc^{III}(furifosmin)]^+$

After a systematic development of cationic Tc(III) complexes [105,106] which accumulate in the human myocardium without *in vivo* reduction to neutral, washed out Tc(II) species, the complex cation $[^{99m}Tc^{III}$furifosmin$]^+$ was attained. It contains the tetradentate Schiff-base ligand 1,2-bis-{dihydro-2,2,5,5-tetramethyl-3(2H)-furanato-4-methyleneamino}ethane in the equatorial plane and the two monodentate, tertiary phosphine ligands tris(3-methoxy-1-propyl)phosphine in the two axial positions (Fig. 6.11.B). $[^{99m}$Tc(furifosmin)$]^+$ is prepared by addition of $^{99m}TcO_4^-$ to a lyophilized kit consisting of the ligands, sodium ascorbate, sodium carbonate, and γ-cyclodextrin. The phosphine acts both as a ligand and as a reducing agent. Cyclodextrin stabilizes the lyophilized formulation [107]. The radiochemical purity of the agent was higher than 95 %. It clears rapidly from the blood and shows a fast heart uptake of 2 % of the injected dose at rest and 2.6 % at stress in human volunteers. There was no significant myocardial washout over 5 h. The bulk of the agent is rapidly cleared through the hepatobiliary system, 30 % through the renal system. $[^{99m}$Tc(furifosmin)$]^+$ is reported to be a myocardial perfusion tracer with optimal imaging properties. It seems to be still evaluated in cardiac patients [108].

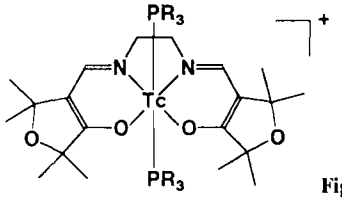

Fig. 6.11.B $[Tc^{III}(furifosmin)]^+$, R=3-methoxy-1-propyl [5,105,106]

6.2.5 [^{99m}Tc-pyrophosphate]

This agent is clinically used to some extent for imaging myocardial infarcts. It is prepared by reaction of $Na_4P_2O_7$ with $^{99m}TcO_4^-$ in the presence of $SnCl_2$. The composition of the compound appears to be unknown. The agent accumulates in infarcted heart muscle, probably by binding to calcium deposits. 12 to 24 h after the onset of infarction is needed for infarcts to accumulate a significant activity of [^{99m}Tc-(pyrophosphate)]. The uptake of the myocardium is inversely proportional to the regional blood flow [6,113].

6.3 Thyroid imaging with $Na^{99m}TcO_4$

$Na^{99m}TcO_4$ is used predominantly for thyroid imaging. Similarly to iodide, perhaps due to similar ion size and charge, $^{99m}TcO_4^-$ is taken up by the thyroid, but unlike iodine it is not incorporated by thyroglobulin. $^{99m}TcO_4^-$ can be replaced and washed out from the thyroid by ClO_4^-. The accumulation of $^{99m}TcO_4^-$ in the thyroid of man amounts to about 3–4 % of the injected radioactivity 10–20 min post-injection and decreases to 1–2 % after 6 h [109]. The agent is primarily used for studying the morphologic structure of the thyroid. Flow studies indicate the vascularity of lesions [14].

6.4 Lung imaging with ^{99m}Tc-MAA and $[^{99m}Tc(DTPA)]^{2-}$

^{99m}Tc-labeled macroaggregated human serum albumin (^{99m}Tc-MAA) for lung imaging and evaluation of pulmonary perfusion is prepared by reduction of $^{99m}TcO_4^-$ with $SnCl_2$ in the presence of a human serum albumin solution. The labeling proceeds at pH 5.5, the isoelectric point of the albumin, in a yield of over 95 %. It does not yet appear to be known in which oxidation state and how ^{99m}Tc is bound. Presumably, the binding of technetium in a lower oxidation state occurs through reduced disulphide groups of the albumin [6]. The accumulation of ^{99m}Tc-MAA in the lung takes place because particles with a size exceeding 10 μm are trapped in the capillaries of the lungs. The particle size, rather than the molecular structure, defines here the efficacy of the agent. About 10^6 ^{99m}Tc-MAA particles are administered per injection, but the number of lung capillaries occluded by this procedure is negligible relative to the total number of lung capillaries of $2.8 \cdot 10^{11}$. The effective half-life of ^{99m}Tc-MAA particles in the lung is 2–3 h. For lung ventilation examinations an aerosol of $[^{99m}Tc(DTPA)]^{2-}$ is recommended. Its biological half-life is about 45 min [14].

6.5 Hepatobiliary imaging agents

Hepatobiliary ^{99m}Tc radiopharmaceuticals are expected to demonstrate a highly specific liver uptake and biliary excretion. Other organs such as the kidneys should not interfere with the imaging of the liver and the biliary tract. The agents should show a rapid hepatocyte transit, clearing the radioactivity in the hepatocytes quickly into the

biliary system and should be competitive against endogenous compounds such as bilirubin. They are used for assessing diseases that affect hepatocyte function, the patency of intrahepatic ducts, the functional status of the cystic duct and gall bladder, and the patencies of downstream portions of the biliary tract [110].

6.5.1 $[^{99m}Tc^{III}(HIDA)_2]^-$

Anionic complexes of ^{99m}Tc(III) with iminodiacetic acid derivatives $[^{99m}Tc^{III}(HIDA)_2]$ (Hepatobiliary IDA) are obtained by reduction of $^{99m}TcO_4^-$ with $SnCl_2$ in the presence of excess iminodiacetic acid. The coordination of the Tc(III) center (Fig. 6.12.B) is achieved by two tridentate ligands chelating technetium through the carboxyl-oxygen atoms and the imino-nitrogen atoms in an octahedral arrangement. The proposed negative charge is in agreement with electrophoretic data [111]. The molecular structure was confirmed by FAB mass spectrometry [112]. Among the numerous $[^{99m}Tc^{III}(HIDA)_2]^-$ complexes synthesized with different iminodiacetic acid derivatives, $[^{99m}Tc(mebrofenin)_2]^-$ and $[^{99m}Tc(disofenin)_2]$ appear to be the best agents for hepatobiliary imaging. They provide superior images when the bilirubin level is lower than 20–30 mg/100 ml [113]. The formulas of the chelating mebrofenin and disofenin ligands are shown in Fig. 6.13.B. Both agents display high hepatic specificity, low renal extraction, rapid hepatocellular transit and are resistent to competition for hepatobili-

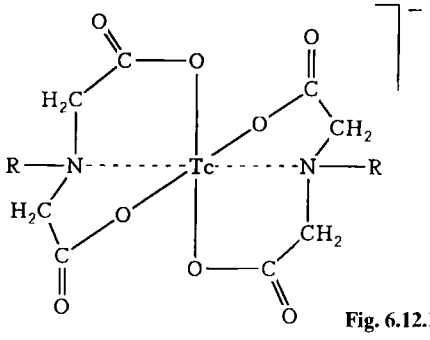

Fig. 6.12.B $[Tc^{III}(HIDA)_2]^-$ [11]

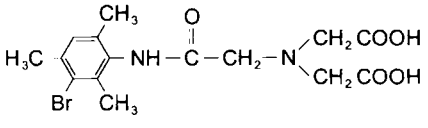

H_2mebrofenin

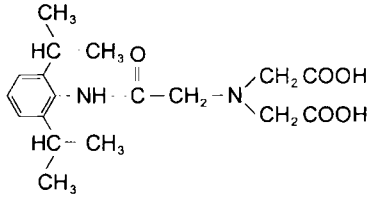

H_2disofenin

Fig. 6.13.B The chelating iminodiacetic acids H_2mebrofenin and H_2disofenin [113]

ary excretion from bilirubin. The lipophilic properties of the agents provide increased plasma protein binding and decreased renal clearance [113,114].

6.5.2 [^{99m}Tc-PMT]

^{99m}Tc-N-pyridoxyl-5-methyltryptophan, [^{99m}Tc-PMT], was prepared by reacting $^{99m}TcO_4^-$ saline solution with Sn(II) and N-pyridoxyl-5-methyltryptophan [115] (Fig. 6.14.B). The composition of the [^{99m}Tc-PMT] complex is not completely established, but there is some evidence that the ligand/Tc ratio is 2/1 and the net charge is zero. Dianionic ligands would then require the oxidation state of +4 for Tc in a neutral complex [116]. In rats the agent showed rapid blood clearance, fast hepatobiliary transit, low urinary excretion, and no intestinal reabsorption. Over 90 % of the radioactivity arrived in the intestine through the liver at 30 min post-injection, while only 2 % of the dose escaped through the kidneys. In rabbits the gall bladder was clearly visualized within 5 min post-injection [115]. A comparative evaluation of [^{99m}Tc(mebrofenin)$_2$]$^-$ and [^{99m}Tc–PMT] in rats revealed that [^{99m}Tc–PMT] was kinetically superior, with higher clearance and lower hepatocyte transit time, but slightly inferior in specificity [117]. The agent was approved for application in patients and also used for studying hepatic tumors by delayed imaging [118].

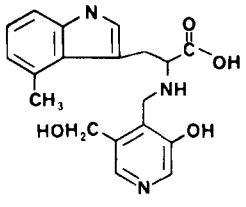

Fig. 6.14.B N-Pyridoxyl-5-methyltryptophan (PMT) [115]

6.5.3 ^{99m}Tc-sulphur colloid and ^{99m}Tc-albumin colloid

Both particulates accumulate in the reticuloendothelial system of the liver in a particle size of about 100 nm. The same particle size is used for spleen imaging, while smaller particles (<20 nm) are taken up by the bone marrow. ^{99m}Tc-sulphur colloid is prepared by reaction of $^{99m}TcO_4^-$ with $S_2O_3^{2-}$ in acidic solution that is heated to nearly 100 °C for 5–10 min. The pH of the mixture is adjusted to 6–7. $^{99m}TcO_4^-$ is almost completely converted. The reaction product is probably a sulphur colloid tagged with $^{99m}Tc_2S_7$ [6,119]. 80–85 % of the colloid is accumulated in the liver, 5–10 % in the spleen, and the rest in the bone marrow. The effective half-life of ^{99m}Tc sulphur colloid is almost equal to the physical half-life of ^{99m}Tc, because the agent is permanently deposited in the liver. ^{99m}Tc-albumin colloid is obtained by adding $^{99m}TcO_4^-$ to a mixture of human serum albumin colloid and $SnCl_2$. This agent was observed to clear from the blood into the liver faster than ^{99m}Tc-sulphur colloid [120].

6.6 Renal imaging agents

^{99m}Tc radiopharmaceuticals for renal imaging are, in general, hydrophilic complexes of relatively low molecular weight. The clinically approved, commercially available, and frequently used functional imaging agents are $[^{99m}Tc^{V}O(MAG_3)]^-$ and $[^{99m}Tc(DTPA)]^{2-}$. Approved and marketed agents for evaluation of kidney morphology are [^{99m}Tc-DMSA] and $[^{99m}Tc(glucoheptonate)_2]^-$.

6.6.1 $[^{99m}Tc^{V}O(MAG_3)]^-$

^{99m}TcO-mercaptoacetyltriglycine (Fig. 12.28A) was developed more than ten years ago and evaluated as a renal tubular function agent [121]. To prepare the compound, $^{99m}TcO_4^-$ in generator saline and benzoyl-mercaptoacetyltriglycine are reduced by $SnCl_2$ upon heating at 95 °C with the concomitant elimination of the benzoyl protecting group. The radiochemical purity is 96.6 %. The placement of a substituent containing a carboxylate group was deemed useful in providing efficient renal secretion. Since $[^{99m}TcO(MAG_3)]^-$ has no chiral centers, no isomer problems are associated with its preparation and purification. Upon coordination to Tc(V), the thiolate sulphur and each of the three amide nitrogens of MAG_3 lose their protons to yield a monoanionic complex. Tc(V) resides above the basal plane in a distorted square pyramidal environment. It is surrounded by three nitrogen atoms and one sulphur atom in the basal plane and one oxygen atom at the apex. The structure agrees with that found for the analogous complex anion of Re(V) [122,123]. A more convenient preparation of $[^{99m}TcO(MAG_3)]^-$ without heating the reaction mixture has been described. The procedure involves the reduction of $^{99m}TcO_4^-$ in saline with Sn(II) in alkaline solution in the presence of S-unprotected mercaptoacetyltriglycine and the co-ligand tartrate, followed by neutralization with a phophate buffer. A radiochemical purity of the agent of more than 98 % was achieved [124,125].

Studies of $[^{99m}Tc^{V}O(MAG_3)]^-$ in normal subjects and in patients indicate that the complex is an excellent renal tubular agent, but its plasma clearance rate was found to be only 50–60 % that of orthoiodohippurate (OIH). Approximately 3 % of the injected radioactivity was taken up by liver, gall bladder and gastrointestinal tract [126]. In all subjects the quality of the images obtained with $[^{99m}TcO(MAG_3)]^-$ was clearly superior to the images achieved with OIH [127–130]. $[^{99m}Tc^{V}O(MAG_3)]^-$ is protein-bound to almost 90 %, is transported by the proximal renal tubules, and is not retained in the parenchyma of normal kidneys [131].

6.6.2 $[^{99m}Tc(DTPA)]^{2-}$

This complex was already described as a brain imaging agent in Sect. 6.1.6. It is approved for assessing the glomerular filtration rate and provides a clearance measurement with only 3–5 % below the true glomerular filtration rate obtained with inulin, a fructose polymer [132]. $[^{99m}Tc(DTPA)]^{2-}$ shows a rapid plasma clearance with a half-life of about 70 min. Urinary excretion amounts to about 90 % in 24 h and its plasma protein binding is 5–10 % in 60 min. The dynamic renal flow study provides

information about blood perfusion in the kidneys [14]. The agent is approved for kidney imaging.

6.6.3 [^{99m}Tc-DMSA] and [$^{99m}Tc^{V}O$(glucoheptonate)$_2$]$^-$

The chelate of ^{99m}Tc with 2,3-dimercaptosuccinic acid, [^{99m}Tc-DMSA], and the [$^{99m}Tc^{V}O$(glucoheptonate)$_2$]$^-$ agent provide information (Fig. 6.15.B) on the morphology of the kidneys. [^{99m}Tc-DMSA] is prepared by reduction of $^{99m}TcO_4$ with excess $SnCl_2$ and coordination of ^{99m}Tc at pH 2.5–3.5, with DMSA. Composition and structure of this agent are not unambiguously defined. The oxidation state of ^{99g}Tc in the purple complex is suggested to be +3 [133–135]. Approximately 50 % of the injected dose of [^{99m}Tc-DMSA] accumulates in the cortical tubules within 1 h and remains in the renal cortex up to 24 h post-injection. 4–8 % of the injected radioactivity is excreted in the urine within 1 h via glomerular filtration and tubular secretion and up to 30 % after 14 h [131]. The complex is excreted unaltered into the urine. Plasma clearance with normal renal function was 34 ml/min and urinary clearance 12 ml/min [136].

Preparation, composition, and structural formula of [$^{99m}Tc^{V}O$(glucoheptonate)$_2$]$^-$ are reported in Sect. 6.1.6 under the aspect of brain perfusion imaging agents. The renal imaging agent is cleared by glomerular filtration with a small component of tubular extraction. Its plasma clearance half-time is only a few minutes [113]. 30–45 % of the injected dose is excreted into the urine within 1 h, and this fact is used to delineate the pelvocalyceal system. Since 5–15 % of the dose remains bound to the renal tubular cells, excellent cortical images can be obtained 1–2 h post-injection [131]. Urinary excretion is about 70 % in 24 h after administration [113].

[^{99m}Tc-DMSA] and [$^{99m}Tc^{V}O$(glucoheptonate)$_2$]$^-$ are not frequently used in clinics for imaging kidney morphology, since ultrasound, magnetic resonance, and X-ray computer tomography provide higher resolution and more precise information.

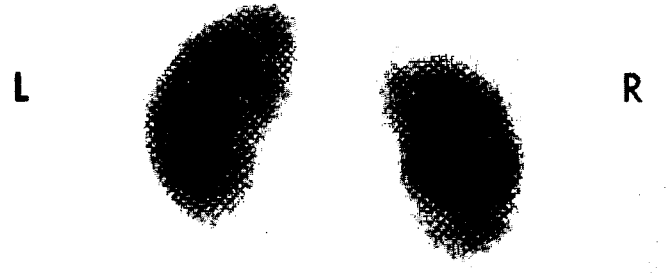

Fig. 6.15.B Scintiphotograph of normal kidneys (posterior view) obtained with [^{99m}Tc-DMSA] [84]

6.6.4 $[^{99m}Tc^{V}O\text{-}L,L\text{-}EC]^{2-}$

This new renal imaging agent was prepared by reaction of $^{99m}TcO_4^-$ saline with $SnCl_2$ in the presence of the ligand L,L-ethylenedicysteine at room temperature. The anionic complex is the diacid derivative of the brain perfusion imaging agent $[^{99m}Tc^{V}O\text{-}L,L\text{-}ECD]^0$ described in Sect. 6.1.2. $[^{99m}Tc^{V}O\text{-}L,L\text{-}EC]^{2-}$ is obtained in high radiochemical purity [137]. Its proposed molecular structure is shown in Fig. 6.16.B. The mean 1 h plasma clearance of the agent in normal volunteers was 460 ml/min per 1.73 m^2. The urinary excretion 30 min post-injection was 67 % of the injected dose and at 60 min post-injection it was 80 %. The agent has a very low plasma protein binding of 31 %. $[^{99m}Tc^{V}O\text{-}L,L\text{-}EC]^{2-}$ merits further clinical evaluation for renal function studies in humans [138–140a].

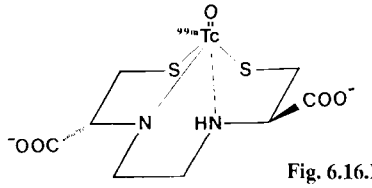

Fig. 6.16.B Proposed structural formula of $[Tc^{V}O\text{-}L,L\text{-}EC]^{2-}$ [138]

6.7 Bone imaging agents

Complexes of ^{99m}Tc with the diphosphonate ligands (Fig. 6.17.B) are clinically approved and widely used bone imaging radiopharmaceuticals. They are prepared by reduction of $^{99m}TcO_4^-$ saline with Sn^{2+} or $[BH_4]^-$ in the presence of a diphosphonate ligand added in excess. Neither the composition of the ^{99m}Tc-diphosphonate complexes nor their structures have not been established to date. Obviously, the preparation performed with one pure ligand results in a mixture of many different complexes. Anion-exchange HPLC separation of [^{99m}Tc-HEDP] revealed as many as 13 components. The separated species exhibited average charges ranging from –1.5 to –8.0. Approximate chromatographic partial molar volumes between 500–1600 ml/mole indicate the possibility of dimeric or polymeric complexes. Size-exclusion chromatography and mass spectrometry support a polynuclear structure [141,142]. The distribution of the components in such mixtures depends strongly on the mode of preparation and the reaction time [143]. The most important variables affecting the relative abundance of the various components are the pH and the ligand concentration [144,145]. In spite of the failure to isolate any ^{99}Tc-diphosphonate complex in a reproducible stoichiometric composition, much effort has been devoted to determine the oxidation state of Tc in reaction products with different diphosphonate ligands. In [^{99g}Tc-HEDP] the oxidation state +4 was suggested by evaluating spectrophotometric and potentiometric measurements [146], while polarographic studies revealed the reduction of $^{99g}TcO_4^-$ in complexing MDP or HEDP to Tc(III), Tc(IV), and Tc(V), depending on the pH [147]. More recently, potentiometric titrations yielded similar results for [^{99g}Tc-HEDP] [148]. At about neutral pH, Tc(IV) was found for [^{99g}Tc-MDP] and Tc(III) for [^{99g}Tc-DPD] [149].

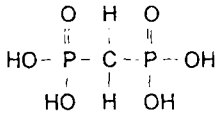

Methylene diphosphonate
(MDP)

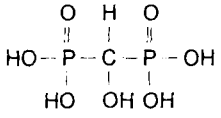

Hydroxymethylene diphosphonate
(HMDP)

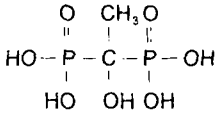

1-Hydroxyethylidene diphosphonate
(HEDP)

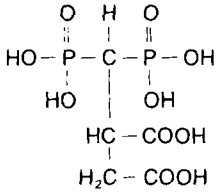

2,3- Dicarboxypropane- 1,1- diphosphonate
(DPD)

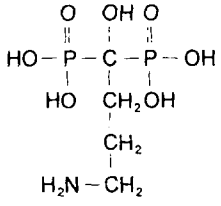

1- Hydroxy- 4- amino- butylidene-
1,1- diphosphonate (alendronate)
(ABP)

Fig. 6.17.B *Diphosphonate ligands for* ^{99m}Tc bone imaging agents

Some time ago, a [^{99g}Tc-MPD] complex, prepared by reaction of $[TcBr_6]^{2-}$ with excess MDP and isolated as brown crystals, was structurally characterized by X-ray diffraction analysis. The solid state structure of the compound was reported to consist of infinite polymeric chains. Each MDP ligand bridges two symmetry related Tc atoms and each Tc atom is bound to two symmetry related MDP ligands (Fig. 6.18.B). The MDP:Tc ratio within the polymer is 1:1. The polymeric repeat unit is completed by an oxygen atom, presumably in the form of a hydroxyl ion, which bridges two symmetry related Tc atoms. The assumed Tc(IV) oxidation state cannot be established definitely. Each Tc center has approximately octahedral coordination geometry. The bridging oxygen to technetium bond distance is 1.94(2) Å on average [150]. EXAFS analysis of an HPLC-purified [^{99g}Tc-MDP] complex in aqueous solution provided evidence that the separated fraction was a mixture of several oligomers. The oligomeric-polymeric nature of the dissolved compound was based on the suggested Tc–Tc interaction [152]. Raman spectra of mixtures of [^{99g}Tc-HEDP] complexes in aqueous solu-

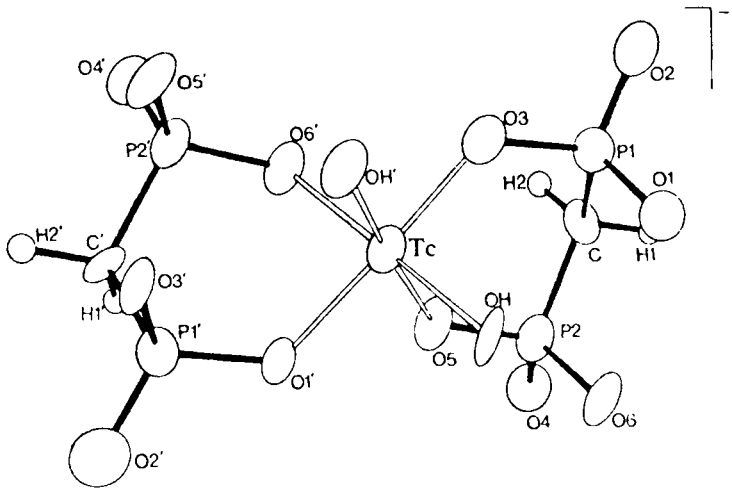

Fig. 6.18.B Portion of the structure of $\{[Tc^{IV}(OH)\ (MDP)]\}_n$ showing one Tc center bridging two MDP ligands [150].

tion indicated the presence of Tc–oxo cores by frequencies observed at 970 and 878 cm^{-1} that were assigned to Tc=0 and 0=Tc=0 vibrations, respectively [151].

A comparative evaluation of bone imaging agents in a whole-body retention of normal volunteers revealed the skeletal uptake in the order [^{99m}Tc-HMDP] > [^{99m}Tc-MDP] > [^{99m}Tc-HEDP]. The superior [^{99m}Tc-HMDP] bone specifity clearly demonstrates that slight alterations of the complex compositions yield a significant effect [153]. These results are in agreement with studies on the uptake of the agents in osteogenic animal models and form a working rationale for the clinically observed high contrasts obtained with [^{99m}Tc-HMDP] between normal bone and soft tissue and between normal and abnormal bone [154]. The binding of ^{99m}Tc-diphosphonate complexes to calcium at the surface of bone appears to be an important step in the *in vivo* action of skeletal imaging agents [155]. The bone imaging agents are bone seekers because the coordinated phosphonate ligands still have considerable affinity for calcium [150], in particular for sites of actively growing bone, i.e. areas of osteoblastic activity [5]. The diphosphonate ligands may be considered as doubly bidentate or bidentate-tridentate [6] ligands, with the ability to complex not only technetium, but also calcium. OH substituents in [^{99m}Tc-HMDP] and [^{99m}Tc-HEDP] or carboxyl groups in [^{99m}Tc-DPD] provide additional binding sites.

The [^{99m}Tc-diphosphonate] agents are administered to diagnose fracture, bone tumor, metastatic lesion, sarcoma, arthritis, osteomyelitis, and other bone diseases that result in the occurrence of growing bone with readily accessible coordination of calcium in the hydroxyapatite bone structure [132]. The bone scanning is performed 2–3 h post-injection to reduce the background radioactivity in the body. In 24 h 75 to 85 % of the activity is excreted in the urine [84].

Very recently another bone imaging agent [^{99m}Tc-ABP], prepared by reduction of $^{99m}TcO_4$ with SnF_2 in the presence of 1-hydroxy-4-amino-butylidene-1,1-diphospho-

nate (alendronate) has been reported to be a better bone scanning radiopharmaceutical than [^{99m}Tc-MDP], because of its shorter mean residence time, lower protein binding, and more rapid renal clearance. The agent exhibits a radiochemical purity of > 98 % up to 5 h after preparation. Composition and structure of [^{99m}Tc-ABP] are still unknown [156].

6.8 ^{99m}Tc-labeled red blood cells (^{99m}Tc-RBCs) and white blood cells (^{99m}Tc-WBCs)

The efficacy of ^{99m}Tc-RBCs is based on its ability to distribute within the intravascular pool of the body and to leave this compartment slowly. ^{99m}Tc-RBCs is a major diagnostic agent in cardiovascular nuclear medicine and is also used for blood pool imaging of other organs. It is administered for the investigation of the ventricular functioning of the heart, for measuring the cardiac output or for the detection of gastrointestinal hemorrhages [6,157]. Recent applications include diagnosis of deep vein thrombosis and hepatic hemangiomas [159]. For spleen imaging the labeled red blood cells are denatured by heating at 50 °C for 20 min prior to injection.

The ^{99m}Tc labeling of the red blood cells is based on the reduction of $^{99m}TcO_4^-$ by Sn^{2+} inside the cells and binding of the reduced ^{99m}Tc species predominantly to the β-chain of the globin moiety of hemoglobin [158]. Both $^{99m}TcO_4^-$ and Sn^{2+} are able to diffuse into the red blood cells.

Three different procedures are currently used for the labeling of RBCs with ^{99m}Tc, the *in vitro* method, the *in vivo* method, and the modified *in vivo* method. For *in vitro* labeling, blood drawn from the subject is heparinized and incubated with stannous citrate. Excess extracellular Sn(II) is oxidized with dilute NaOCl to Sn(IV) in order to prevent reduction of the subsequently added $^{99m}TcO_4^-$, before it has diffused into the RBCs. ^{99m}Tc-RBCs are then obtained by incubating $^{99m}TcO_4^-$ for 15 min. The labeling yield is better than 97 %. The labeled RBCs are reinjected into the patient for diagnostic imaging. The blood radioactivity levels remained essentially unchanged over 3 h post-injection [6,113,159].

In the *in vivo* method a solution of stannous pyrophosphate containing 10 to 20 μg Sn(II) per kg is injected intravenously. After waiting about 30 min for biological clearance of extracellular stannous pyrophosphate, 20–30 mCi (0.74–1.11 GBq) $^{99m}TcO_4^-$ is injected, tagging the RBCs immediately with an efficiency of 80–90 %. After equilibration of ^{99m}Tc-RBCs with the blood pool, imaging can be executed [113]. In the modified method for the *in vivo* labeling of RBCs the patients receive approximately 500 μg Sn(II) as stannous pyrophosphate intravenously. 20 min later, 3 ml of blood with *in vivo* tinned red blood cells are withdrawn into a syringe containing 20 mCi (0.74 GBq) of $^{99m}TcO_4^-$. After 10 min of incubation, the labeled RBCs are reinjected into the patient. $^{99m}TcO_4^-$ is thus prevented from distributing to extravascular compartments. 90 % of the injected ^{99m}Tc is bound to the RBCs [161].

White blood cells (WBCs), in particular polymorphonuclear leucocytes and monocytes, accumulate in high concentrations at sites of infection. Radiolabeled leucocytes or granulocytes now are widely established as a means of localizing various forms of

inflammatory disease and infections. Diseases in which radiolabeled leucocytes made a significant contribution to clinical management include inflammatory bowel disease, postoperative sepsis, intra-abdominal and soft tissue sepsis, and acute and chronic osteomyelitis [162].

^{99m}Tc phagocytic labeling of leucocytes proceeded for instance with a commercial ^{99m}Tc-albumin colloid kit. The leucocytes were separated from 40 ml heparinized blood. The preparation appeared to be stable for 2–3 h after labeling. Imaging time was 30 min to 4 h post-administration. About 20 % of the labeled colloid remained unbound to the WBCs. The preparation contained approximately equal activities of granulocytes and monocytes [163].

Recently, efforts for imaging infections are more devoted to the application of ^{99m}Tc-hexamethyl propylene amine oxime, [^{99m}Tc^{V}O-*d,l*-HM-PAO]^{o}, labeled leucocytes. The labeling is performed by mixing leucocytes, obtained from 50–100 ml blood and suspended in plasma/ACD (acid-citrate-dextrose) with [^{99m}TcO-*d,l*-HM-PAO]^{o}, freshly prepared from a commercial kit. After incubating the mixture 10 min at room temperature, the preparation is washed with and resuspended in plasma and injected. The lipophilic ^{99m}Tc-complex can penetrate the blood cell membranes. The labeling efficiency is 50–60 %, while 80 % of the cell-bound activity is found on granulocytes. The white blood cell labeling efficiency is reported to be increased to 85 % when only one-fifth of the lyophilized HM-PAO kit was used [160]. The label stability *in vitro* is 90 % for 1 h in plasma [159,164]. The clinical value of [^{99m}TcO-*d,l*-HM-PAO]^{o} labeled leucocytes is now clearly established, although some areas of application, such as chronic osteomyelitis and occult fever, require further evaluation [162].

6.9 Tumor imaging agents

Benign or malignant tumors exhibit characteristics, such as enhanced metabolic activity and blood flow, high vascular permeability and the formation of tumor-associated antigens. Tumor imaging can be accomplished by evaluating any of these characteristics [113].

6.9.1 [^{99m}Tc^{V}O(DMSA)$_2$]$^{-}$

While the composition and structure of the renal agent [^{99m}Tc-DMSA] are not defined (only the oxidation state of technetium was suggested to be +3), the tumor imaging agent [^{99m}Tc^{V}O(DMSA)$_2$]$^{-}$ was recently identified by the chemical characterization of the analogous compound of long-lived ^{99g}Tc. [Bu$_4$N][^{99g}TcO(DMSA)$_2$] was obtained in orange-red crystals when TcO_4^- was reduced with $S_2O_4^{2-}$ in the presence of DMSA in alkaline solution and the reaction solution was treated with excess [Bu$_4$N]Br. Elemental analysis confirmed the composition of the complex salt. In the IR an absorption at 958 cm^{-1} was assigned to a terminal Tc=O bond. The ^{1}H NMR was consistent with the presence of three stereoisomers (Fig. 6.19.B) the *syn-endo*, *syn-exo*, and *anti*-configuration. The electronic spectrum showed a peak in the visible at 418 nm. The preparation of the corresponding complex of ^{99m}Tc under alkaline

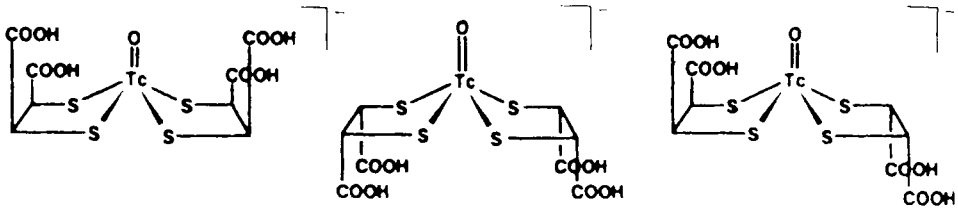

Fig. 6.19.B Stereoisomers of $[Tc^{V}O(DMSA)_2]$ [165]

conditions [166] yielded a compound that was distinct from the $[^{99m}Tc^{III}$-DMSA] renal agent. In addition, HPLC confirmed the occurrence of three isomers in $[^{99g}Tc^{V}O(DMSA)_2]^-$ as well as in $[^{99m}Tc^{V}O(DMSA)_2]^-$ [165]. The X-ray structure analysis of $[^{99}Tc^{V}O\ (DMSA)_2]$ is still not available, but the *syn-endo* isomer of the analogous rhenium complex $[Re^{V}O(DMSA)_2]^-$ has been structurally characterized. Also this rhenium compound was shown to localize in certain human tumors. The complex anion adopts an approximately square pyramidal configuration [167] with the terminal oxygen in the apical position. The geometry of the coordination is shown in Fig. 6.20.B.

The tumor imaging agent was designed in Japan in the early eighties [168,169] and used for the detection of medullary thyroid carcinomas and head and neck tumors in patients [170,171]. Planar and SPECT imaging were applied to rapidly assess head

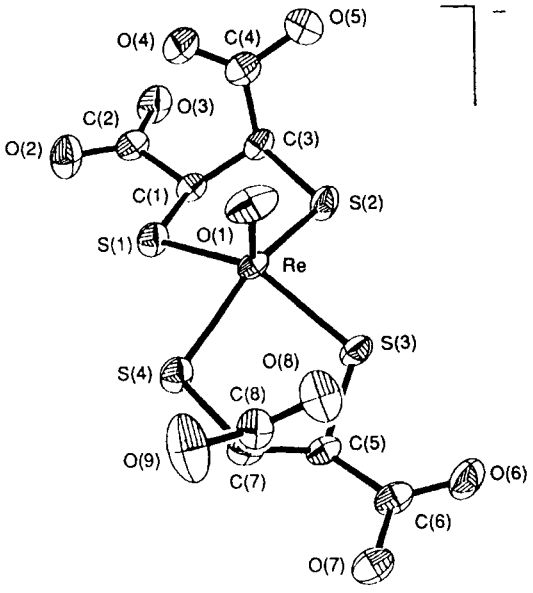

Fig. 6.20.B Structure of the *syn-endo*-isomer of $[Re^{V}O(DMSA)_2]^-$ [167].

and neck squamous carcinomas in patients with high sensitivity and specificity [172]. The usefulness of this agent for detecting medullary thyroid carcinoma and its soft tissue metastases was again demonstrated recently. The scintigraphic studies were carried out two hours after intravenous injection. The sensitivity for the detection of bone and soft tissue metastases was 92 and 100 %, respectively [173].

6.9.2 $[^{99m}Tc^{I}(MIBI)_6]^+$, $[^{99m}Tc^{V}O_2(tetrofosmin)_2]^+$, and $[^{99m}Tc^{V}O$-*d,l*-HM-PAO$]^\circ$

The myocardial perfusion imaging agents $[^{99m}Tc^{I}(MIBI)_6]^+$ and $[^{99m}Tc^{V}O_2(tetrofosmin)_2]^+$ recently found increasing application in tumor detection. Malignant breast tumors and axillary node metastases were detected with high sensitivity and specificity. 20 mCi (740 MBq) of the tetrofosmin agent was administered intravenously. Imaging began 10 min post-injection. Both agents exhibited high diagnostic accuracy and are promising breast tumor radiopharmaceuticals. However, the sensitivity in detection appeared to be low for lesions smaller than 10 mm [174–178]. $[^{99m}Tc^{I}(MIBI)_6]^+$ was also used for the localization of parathyroid enlargement. The agent showed higher parathyroid to thyroid uptake and accumulation in a thyroid adenoma [179]. The sensitivity for the detection of hyperparathyroidism was 95 % and images of superior quality were obtained. The MIBI agent seems to be the radiopharmaceutical of choice for parathyroid scintigraphy [180,181]. It was more sensitive in detecting adenomas than hyperplasia [182]. The uptake of $[^{99m}Tc^{V}O_2(tetrofosmin)_2]^+$ in malignant lung tumors was demonstrated recently [183]. After intravenous injection of 20 mCi (740 MBq) of this agent, 89 % of the primary lung cancers in patients were visualized by SPECT, showing the tetrofosmin agent to be highly effective in the delineation of lung cancer [184]. The neutral brain perfusion imaging agent $[^{99m}Tc^{V}O$-*d,l*-HM-PAO$]^\circ$ appeared to be a useful radiopharmaceutical for the localization of both the primary focus and metastatic lesions of malignant melanoma in patients by SPECT [185].

6.9.3 ^{99m}Tc-labeled monoclonal antibodies

The immunoscintigraphy of tumors, using ^{99m}Tc-labeled monoclonal antibodies, has been developed since the beginning of the eighties. Antibodies can accumulate specifically in tumor tissue by binding to tumor markers, such as proteins, glycoproteins, glycolipids, or polysaccharides that are formed by tumor cells. However, unspecific binding to normal tissue cannot be excluded. With ^{99m}Tc-labeled monoclonal antibodies it was possible to gain high contrast images. Several techniques for labeling monoclonal antibodies with ^{99m}Tc are used at present.

The labeling can be performed directly [186] by incubation of the antibody protein with $^{99m}TcO_4^-$ and $SnCl_2$. ^{99m}Tc is probably reduced to the oxidation state +5 and is bound to thiol (HS) groups formed by reductive partial cleavage of the disulphide bridges in the antibody. Unfortunately, the capacity of binding sites of strong bonding was only 16–24 % [189]. Incubation of the antibody overnight with 12 mM $SnCl_2$ (pretinning method) [191] and subsequent labeling with ^{99m}Tc appears to increase the sites

of strong bonding. On the other hand the disulphide bonds are essential for maintaining the structural integrity of the immunoglobulin molecule which, however, seems to be preserved if less than 4 % of the disulphide bonds are reduced. 100 μg of an antibody could be labeled with 20 mCi (740 MBq) of ^{99m}Tc, if less than 1 % of its disulphide bridges are cleaved by reduction [187].

Another direct method for the labeling of monoclonal antibodies is the reduction of the antibody by a thiol reagent such as 2-mercaptoethanol or 2-aminoethanethiol-hydrochloride, the subsequent purification of the reduced antibody by column chromatography and the labeling of the HS-groups, generated in the antibody, with ^{99m}Tc by transcomplexation of the ^{99m}Tc from a weaker complexing ligand such as pyrophosphate, phosphonates or iminodiacetic acid derivatives (Fig. 6.21.B). The labeling yield was better than 95 %. This is one of the most frequently used techniques [188–191]. Monoclonal antibodies have also been effectively reduced with dithiothreitol, dithioerythritol, and ascorbic acid [187]. Labeling efficiencies of > 97 % were achieved when after prereduction of the antibody with 2-mercaptoethanol, the $^{99m}TcO_4^-$ reduction was performed with an aliquot of a stannous kit containing glucoheptonate [192]. Recently, direct ^{99m}Tc-labeling of prereduced human immunoglobulin succeeded in using an insoluble macromolecular Sn(II) complex containing aminophosphonic acid groups [193]. Water-soluble phosphines are alternative reducing agents to generate high affinity binding sites, i.e. thiol groups, in monoclonal antibodies for binding reduced ^{99m}Tc [194].

The indirect labeling of antibodies is based on bifunctional ligands that complex ^{99m}Tc and also bind to the antibody. In the preconjugation labeling procedure, a strong ^{99m}Tc chelate is preformed and subsequently bound to the immunoglobulin through reactive functional groups of the chelate. For instance, the diaminodithiol ligand system is well known to form strong tetradentate complexes with $Tc^{V}O^{3+}$. Antibodies and their fragments were labeled by conjugating the tetrafluorophenyl active ester of ^{99m}Tc-4,5-bis(thioacetamido)pentanoate to the protein amine groups (Fig. 6.22.B). High stability and retention of immunoreactivity were demonstrated for ^{99m}Tc-labeled antibodies and their fragments. Together with rapid clearance of antibody fragments and lack of normal tissue accumulation, optimal imaging was reported to be achieved. However, the overall labeling efficiency was only 35 to 50 % and the total time for the procedure about 3 h [195]. Nevertheless, some advantages are the stable labeling of the antibody and the defined chemical structure of the ^{99m}Tc chelate.

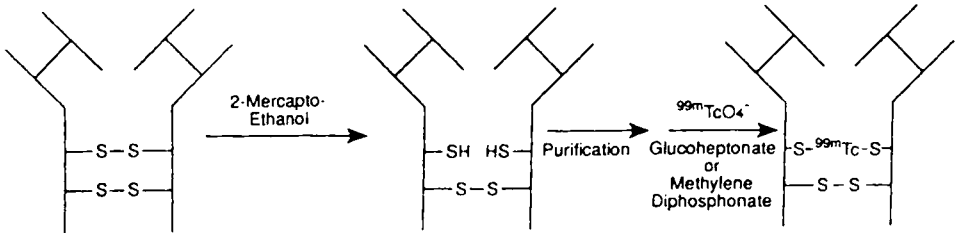

Fig. 6.21.B Direct labeling of monoclonal antibodies [188,189]

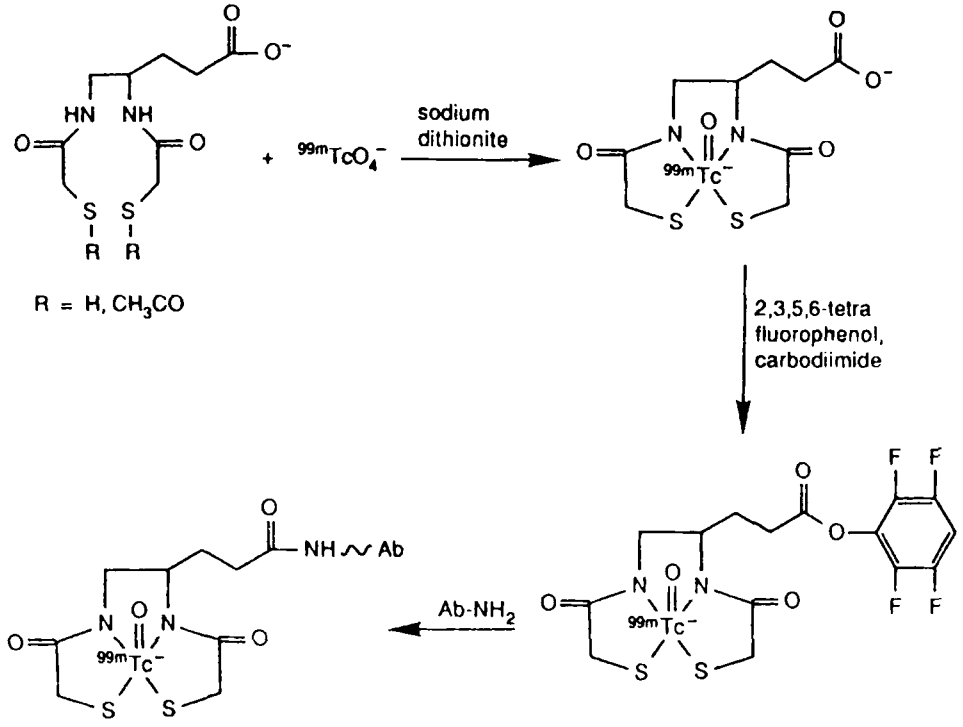

Fig. 6.22.B Synthesis of ^{99m}Tc-N_2S_2-antibody by formation of ^{99m}Tc-4,5-bis(thioacetamido)pentanoate, which is converted to an active ester by water-soluble carbodiimide and finally conjugated to antibody (Ab) via acylation of amino groups [195]

Another recently proposed indirect labeling procedure, a so-called pretargeting method, uses the high affinity of biotin (M=244 g·mole^{-1}) to the glycoprotein avidin (M = 68000 g·mole^{-1}). Avidin has four binding sites that are highly specific for biotin. Biotin is labeled with ^{99m}Tc by binding the ^{99m}Tc chelating ligand of propylene-amine-oxime (pnao) to biotin (Fig. 6.23.B). The tumor-specific monoclonal antibody is bonded to avidin, and this non-radioactive conjugate is injected into the patient for accumulation in the tumor, allowing a period of some days. Subsequently the ^{99m}Tc labeled biotin derivative is injected and binds rapidly and irreversibly to tumor-localized avidin [196]. The affinity of avidin and biotin for each other is 5–7 orders of magnitude higher than those of antibodies for tumors [197]. Long incubations of labeled monoclonal antibodies in the blood can be avoided by this pretargeting method.

Since the preconjugation labeling methods are relatively time consuming, procedures were developed for binding the bifunctional ligand at first to the antibody and thereafter labeling the purified conjugate with ^{99m}Tc (postconjugation labeling). For instance, a bis(aminoethanethiol) ligand with an activated N-hydroxysuccinimide ester (Fig. 6.24.B) for protein conjugation was conjugated to monoclonal antibodies at pH 8.5 with about 40 % yield. Subsequently, $^{99m}TcO_4^-$ was reduced with Sn(II) and complexed with the bis(aminoethanethiol) ligand at ambient temperature. The stabil-

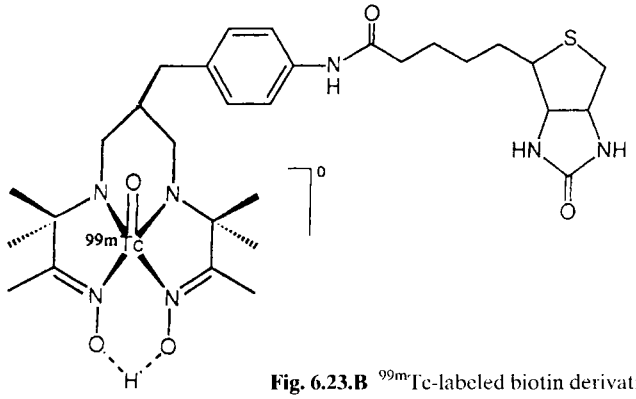

Fig. 6.23.B ^{99m}Tc-labeled biotin derivative [132]

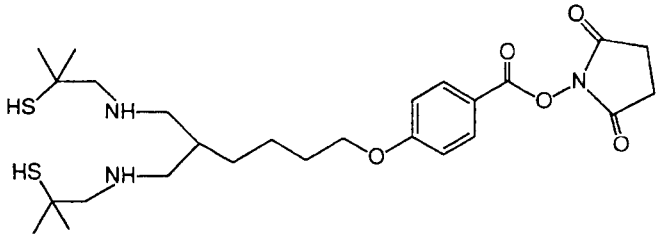

Fig. 6.24.B N-hydroxysuccinimide ester of 6-(4′-(4″-carboxyphenoxy)butyl)-2,10-dimercapto-2,10-dimethyl-4,8-diazaundecane for conjugation to monoclonal antibodies and subsequent bis(aminoethanethiol) complexation of ^{99m}Tc [198]

ity of the ^{99m}Tc labeled antibody was reported to be excellent and the labeling efficiency > 90 % [198].

Numerous clinical tumor studies using ^{99m}Tc labeled monoclonal antibodies have been recently performed. Melanoma, colon, breast, lung, head and neck, ovary, and lymphoma tumors were successfully detected with varying sensitivity depending both on the size of the lesion and its location [189]. The novel pretargeting immunodetection method succeeded in localizing cerebral gliomas in patients. The tumors were detected in 15/18 glioma patients with a mean tumor to non-tumor ratio of 6.2. 0.2 mg pnao-biotin was labeled with 15–20 mCi (555–740 MBq) ^{99m}Tc. ^{99m}Tc-pnao-biotin was rapidly cleared from the blood and was primarily excreted through the biliary system. Brain tomographic images were obtained 1–2 h post-injection of ^{99m}Tc-pnao-biotin [199].

6.10 Some future prospects

6.10.1 Brain

^{99m}Tc is not a physiological nuclide as, for instance, ^{11}C, which is accepted by the body and metabolized in biomolecules [200]. However, specially designed ^{99m}Tc labeled biomolecules can be taken up by the body as analogue tracers. ^{99m}Tc brain imaging agents devel-

oped up to now cross the blood-brain-barrier by diffusion, depending on the concentration difference between the two sides of the capillary wall. But carrier systems in the endothelial cells of the BBB are capable of transporting selected substances, such as glucose or large neutral amino acids, through the barrier without the normal passive diffusion (Sect. 6.1). On this basis, novel brain imaging agents could be designed for potentially accelerating the passage of ^{99m}Tc into the brain [39]. In a first recent approach, L-phenylalanine, which is known to penetrate the BBB by the endothelial carrier for large, neutral amino acids, was bound to a tripodal ligand forming a small, neutral diaminodithiolate complex with $Tc^{V}O^{3+}$ (Fig. 6.25.B). The Tc complex was shown to be sterically less demanding than the bis(2-chloroethyl)amino substituent in melphalan, an antitumor drug which is also transported through the BBB by the carrier for large, neutral amino acids. The accumulation of the ^{99m}Tc-labeled compound in brains of mice was established, but till now the biodistribution measurements were not fully conclusive [201]. Recently, the complexing of ^{99}Tc/^{99m}Tc by a functionalized D-glucose, i.e. 2-amino-2-deoxy-D-glucose-oxime, was successful. Significant accumulations in the brain or in the myocardium were, however, not observed [202].

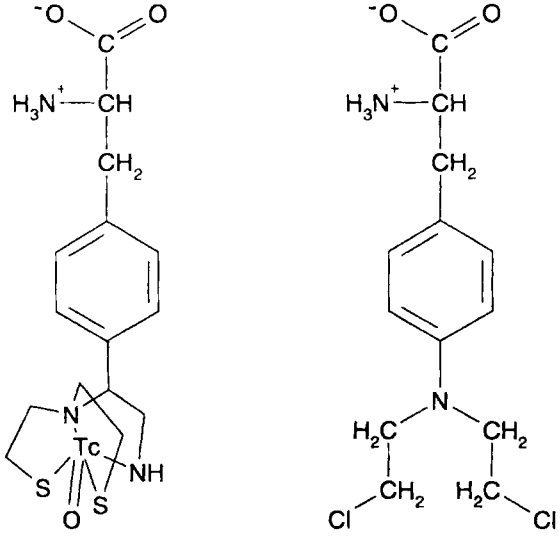

Fig. 6.25.B a) Tripodand Tc-complex bound to L-phenylalanine [201]
b) Melphalan

6.10.2 Myocardium

Some promising myocardial perfusion imaging agents were developed in the last decade. Reactions of $^{99m}TcO_4^-$ with both 2-phenylene-bis(dimethylarsine) (diars) and various thiols (RSH) yielded a series of monocationic $[^{99m}Tc^{III}(diars)_2(SR)_2]^+$ complexes. The analogous complex cations of long-lived ^{99g}Tc were identified by FAB mass spectroscopy. All the $[^{99m}Tc^{III}(diars)_2(SR)_2]^+$ cations, which are *in vivo* non-reducible,

were shown to accumulate rapidly in the myocardium of rats with an uptake of 1.5–2.0 % of the injected dose/g at 30 min, without the rapid myocardial washout observed for the *in vivo* reducible dihalo analogues $[Tc^{III}(dmpe)_2X_2]^+$. The blood clearance of the diarsinedithiol complexes was very rapid with 0.3 % of the injected dose/g at 30 min post-injection. A fast liver clearance of $[^{99m}Tc^{III}(diars)_2(SR)_2]^+$ was observed for the RS ligands 2-methoxyethanethiolate and 1-methoxy-2-(methoxymethylene)pentane-5-thiolate, which can be attributed to the ether functionalities of these thiolato ligands. The judicious choice of R groups in this series of complexes may finally lead to clinically interesting myocardial imaging agents [203,204].

Bis(dithiocarbamato)nitrido^{99m}Tc(V) complexes of the general formula $[^{99m}Tc^{V}N(R^1R^2NCS_2)_2]^0$, with R^1 and R^2 indicating variable lateral groups, were reported to be a new class of neutral myocardial imaging agents. The preparation involves the initial reaction of $^{99m}TcO_4^-$ with S-methyl.N-methyl-dithiocarbazate ($H_2NN(CH_3)CSSCH_3$) in the presence of tertiary phosphines or Sn^{2+} as reductants, followed by the addition of the sodium salt of the monoanionic ligand $R^1R^2NCS_2^-$. $H_2NN(CH_3)CSSCH_3$ behaves as an efficient donor of nitride (N^{3-}) to produce the $[^{99m}Tc^{V}{\equiv}N]^{2+}$ core. The complex $[^{99g}TcN\{Et(EtO)NCS_2\}_2]^0$ was obtained in pale yellow crystals. The coordination geometry is distorted square pyramidal with four sulphur atoms in the basal plane and the Tc≡N group in the apical position. The analogous ^{99m}Tc compound revealed, in comparison to other derivatives, the most favorable biodistribution and best quality of myocardial images in dogs and monkeys. No decomposition of the compound occurred over 6 h. About 4 % of the injected activity was observed in the myocardium of monkeys, however, along with significant activity uptake in the liver. Slow washout from the heart was reported, in spite of the neutral character of the complex. Trials in human subjects may be promising [205–208]. Also, the neutral complex $[^{99m}TcN\{Me(CH_2COOMe)NCS_2\}_2]^0$ has been recently reported to show high brain uptake in primates [209].

Substantial myocardial uptake of a series of cationic bis(arene)^{99m}Tc(I) complexes in rats has been described. The compound may be prepared in a sealed vial by reaction of $NaTcO_4$ with zinc dust in a cyclohexane-arene mixture that is purged with HCl. Complex ions containing benzene rings substituted with about four to six carbon atoms revealed significant uptake in the myocardium of up to 3.8 % dose/g 5 min post-injection. In addition, excellent heart/blood ratios were observed, heart/liver ratios exceeded in certain cases a value of 5.0, and heart/lung ratios approached 3.0 as an upper limit. For the complex cations [bis(1,3,5-trimethylbenzene)^{99m}Tc]$^+$ and [bis(1,2,3,5-tetramethylbenzene)^{99m}Tc]$^-$ the activity in the heart reached its maximum within 45 min and cleared slowly to about 50 % after 24 h. Preliminary results in human volunteers also indicate the low plasma binding, but some lower target/non-target ratios. However, the preparation of the complexes needs to be simplified in order for them to be adopted in clinical use [210,211].

6.10.3 Hypoxic tissue

Since the beginning of the 1990s, much effort has been devoted to develop ^{99m}Tc radiopharmaceuticals for the detection of hypoxic tissue in the myocardium, brain,

and tumors. Tissue hypoxia are important in evaluating several disease states. Appropriate imaging agents could be clinically useful, for instance, in the identification of tissue at risk in myocardial ischemia, in the designing of strategies for revival of jeopardized tissue after stroke or in early assessment of tumors that may be resistant to radiotherapy and/or chemotherapy because of their hypoxic status [212]. Nitroimidazole can be selectively trapped with reactive metabolites in hypoxic cells by enzymatic reduction of the nitro group in the absence of adequate supplies of oxygen. The redox potential of the nitroimidazole derivative appears to be a measure of the intensity of the reduction and the trapping.

The $^{99g}Tc^{V}O$-propylene-amine-oxime ($Tc^{V}O$-pnao) complex was bound through a methylene group to 2-nitroimidazole (Fig. 6.26.B). $[^{99g}Tc^{V}O\{pnao\text{-}1\text{-}(2\text{-nitroimidazole})\}]^{\circ}$ was prepared in red crystals by reacting the ligand pnao-1-(2-nitroimidazole) with $^{99}TcO_4^-$ and Sn^{2+} in saline. The compound was characterized spectroscopically and by single crystal X-ray analysis. The Tc=0 stretch at 918 cm^{-1} falls within the range observed for Tc=0 amine oxime compounds. The complex has square pyramidal geometry with the oxygen in the apical position. The plane of the nitroimidazole ring is approximately perpendicular to the plane given by the four coordinated nitrogen atoms of the complex; the nitro group has a *trans* position with respect to the Tc=0 group. The two amines and one oxime of the complex are deprotonated. There is no evidence of interaction between the nitroimidazole and the technetium core. The redox potential of $[^{99g}Tc^{V}O\{pnao\text{-}1\text{-}(2\text{-nitroimidazole})\}]^{\circ}$ in CH_3CN at E= –1.45 V *vs* $Ag/AgNO_3$ can be assigned to the reversible reduction of the nitro group [212,213].

The imaging agent $[^{99m}Tc^{V}O\{pnao\text{-}1\text{-}(2\text{-nitroimidazole})\}]^{\circ}$ of analogous composition was prepared by a similar route using the generator eluant containing up to 100 mCi ($3.7 \cdot 10^3$ MBq) of $^{99m}TcO_4$. The radiochemical purity of the labeled compound was better than 90 % [214]. Animal studies demonstrated that the agent is selectively retained in hypoxic myocardium and marks the ischemic border zone [215]. It is cleared quickly from the normoxic heart [216]. The ischemic/non-ischemic radioactivity ratio was about 3/1 at 30 min post-injection [215]. $[^{99m}Tc^{V}O\{pnao\text{-}1\text{-}(2\text{-nitroimidazole})\}]^{\circ}$ (BMS-181321) appears to be a sensitive marker of hypoxic myocardium [217], where its binding is essentially irreversible [218]. The clinical applicability of the agent in the imaging of myocardial hypoperfusion has been suggested [219], however, an unfavorable heart-to-liver ratio was observed with *in vivo* planar imaging of a canine model, which may limit its use in clinical myocardial imaging [220]. Further animal studies showed the agent to be also selectively retained in acutely ischemic brain, but not in the ischemic infarct. It is therefore a marker of ischemic tissue at risk of infarction and may contribute to the clinical management of acute stroke [221]. In addition, BMS-181321 was recently reported to be taken up in solid mice tumors with a tumor-to-muscle activity ratio of 3.5–4.0 at 4–8 h after injec-

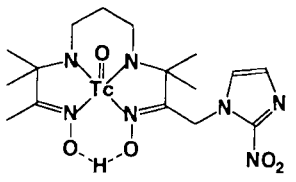

Fig. 6.26.B The hypoxic cell imaging agent $[Tc^{V}O\{pnao\text{-}1\text{-}(2\text{-nitroimidazole})\}]^{\circ}$ [212]

tion. The agent could potentially be useful in clinics to investigate the status of hypoxia in solid tumors [222]. Nitroimidazoles and the imaging of hypoxia was excellently reviewed some years ago [223].

When $^{99m}TcO_4^-$ is reduced with Sn(II) and complexed with the ligand 4,9-diaza-3,3,10,10-tetramethyldodecane-2,11-dione-dioxime (Fig. 6.27.B) a ^{99m}Tc compound was obtained which possesses intrinsic bioreductive properties and is reduced in hypoxic tissue to trapped species without having bound before nitroimidazole to the ligand. The complex is reported to show high retention in carcinomas with hypoxic fraction in mice and significant tumor-to-background ratios at 4 h post-injection [225]. Also, increased myocardial accumulation and retention in normal-flow-hypoxic and low-flow-ischemic viable myocardial models (isolated perfused rat hearts) were observed. After 60 min of clearance a low-flow-ischemic/control heart activity ratio of 13.6:1 was achieved [224]. The complex is superior to carbon-142-deoxyglucose in detecting damaged but viable myocardium [224a].

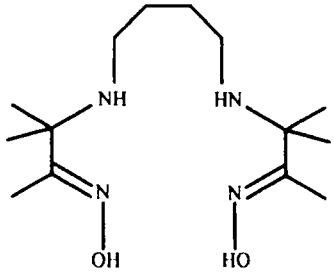

Fig. 6.27.B 4,9-Diaza-3,3,10,10-tetramethyldodecane-2,11-dione-dioxime [224]

6.10.4 Receptor binding

The physiological function of organs, the testing of which is the predominant aim of the application of radiopharmaceuticals, is often controlled by receptors. They are found as glycoproteins on the cell surface or as soluble proteins inside a cell and bind the associated ligands through complementary structures. Receptors exhibit high ligand affinity, specificity, stereoselectivity, and saturability. Radiopharmaceuticals bound to receptors permit insight into special physiological processes; in particular, changes in receptor concentration are thought to be related to certain disease states of an organ [226,227]. Many receptor-specific radiopharmaceuticals with nuclides such as ^{11}C, ^{18}F, ^{75}Br, ^{77}Br or ^{123}I are known, but only a few receptor-binding ^{99m}Tc imaging agents.

^{99m}Tc-galactosyl-neoglycoalbumin (^{99m}Tc–NGA) is a labeled ligand analogous to the hepatocyte-specific receptor, i.e. the hepatic binding protein (HBP) [228,229]. The ligand (NGA) was synthesized by coupling 2-imino-2-ethyloxymethyl-1-thiogalactose (IME-thiogalactose) to human serum albumin (HSA) [232]:

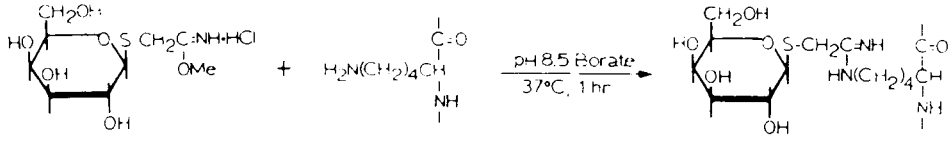

IME-thiogalactose HSA NGA

The ^{99m}Tc labeling of the ligand was performed by controlled potential electrolytic reduction of $^{99m}TcO_4^-$ [230,231] with yields ranging from 92 to 99 %. ^{99m}Tc-NGA remained stable for at least 4 h [232]. This receptor-binding radiopharmaceutical provides the assessment of liver function and is a quantitative probe for the HBP receptor. Clinical tests after injection of 5 mCi (185 MBq) ^{99m}Tc-NGA indicated that with liver diseases, such as hepatoma, liver metastases, and cirrhosis, the hepatic binding protein (HBP) concentration appears to be a measure of functional hepatocyte mass [233–238]. In patients with advanced breast cancer, ^{99m}Tc-NGA was exclusively trapped by the liver. The images revealed cold spots in areas of liver metastases formation. This receptor radiopharmaceutical is promising to be clinically useful for both quantification of liver function and assessment of liver morphology [239].

To develop a ^{99m}Tc radiopharmaceutical useful for the diagnostic imaging of steroid receptor-positive breast tumors, an analogue of mefipristone was modified to incorporate an N_2S_2 chelate system in the 11β-position and labeled with ^{99m}Tc after reduction of $^{99m}TcO_4$ in saline with $SnCl_2$ in the presence of glucoheptonate (Fig. 6.28.B). The insertion of the Tc=O core into the N_2S_2 ligand can result in the formation of four diastereomeric products, which are denoted as the *syn* and *anti* diastereomeric pairs, *syn* and *anti* being defined by the orientation of the steroid substituent and the Tc-oxo group relative to the N_2S_2 plane. The *syn* diastereomeric pair was obtained in higher yield (43 %) than the *anti* pair. The specific-to-non-specific binding ratio of the ^{99m}Tc linked *syn* system *in vitro* was 75/25. *In vivo*, the progestin conjugate showed progesterone receptor-mediated uptake in rat uterus, but also high uptake in non-target tissues. Modified systems of ^{99m}Tc progestin conjugates with improved target uptake efficiency and selectivity may be candidates for future studies aimed at the goal of obtaining images of progesterone receptor-positive breast tumors [240–244].

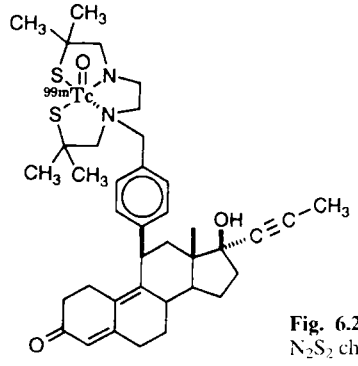

Fig. 6.28.B An analogue of mefipristone, modified to incorporate an N_2S_2 chelate system in the 11β-position and labeled with ^{99m}Tc [240,242]

Venous or arterial thrombus formations are potentially life-threatening events. The diagnosis, treatment, and prevention of thromboembolic diseases has gained considerable attention recently. A thrombus is an intravascular deposit mainly comprising fibrin, aggregates of platelets, and red blood cells. Platelet aggregation is mediated by fibrinogen, which binds via the Arg-Gly-Asp (RGD) tripeptide sequence to the platelet glycoprotein GPIIb/IIIa receptor expressed on activated platelets. Small molecule antagonists of the fibrinogen receptor GPIIb/IIIa represent a class of potential antithrombotics. ^{99m}Tc labeled fibrinogen receptor antagonists, which bind to the GPIIb/IIIa receptor on activated platelets, are potential radiopharmaceuticals for the detection of thrombi. The cyclic Arg-Gly-Asp GPIIb/IIIa receptor antagonists, conjugated to 4,5-bis(S-1-ethoxyethyl-mercaptoacetamido)pentanoic acid, were labeled with ^{99m}Tc using the exchange labeling with $[^{99m}Tc^{V}O(glucoheptonate)_2]^-$. A promising compound for diagnosing the presence of thrombi by imaging, demonstrated in a canine deep vein thrombosis model, is given in Fig. 6.29.B. By 50 min post-injection the thrombus/blood and thrombus/muscle ratios were 6–8:1 [245,246]. In addition, a hydrazinonicotinamide functionalized GPIIb/IIIa receptor antagonist was labeled with ^{99m}Tc using tricine and a water soluble phosphine as coligands [245a].

Not long ago, an α-melanotropin peptide analogue, cyclized through ^{99m}Tc coordination, was synthesized while retaining high affinity for receptors present on melanoma cells. *In vivo* the complex revealed selective accumulation in a murine melanoma tumor [246a].

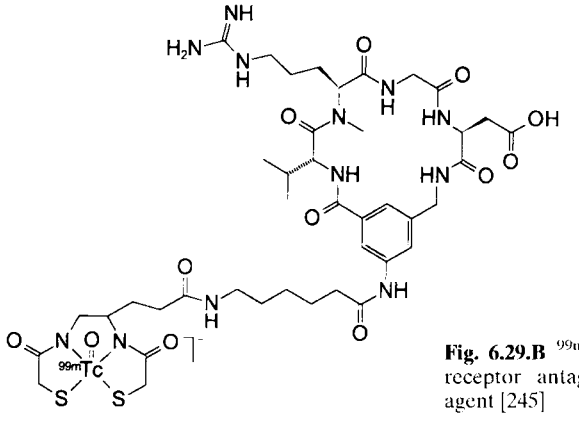

Fig. 6.29.B ^{99m}Tc labeled analogue of the GPIIb/IIIa receptor antagonist as potential thrombus imaging agent [245]

6.10.5 Dopamine transporter

Recently, the development of ^{99m}Tc-labeled tropane derivatives used as dopamine transporter imaging agents has been reported. The dopamine transporter is a protein complex located presynaptically at dopaminergic nerve terminals [247]. It is depleted in Parkinson's disease, and the extent of depletion correlates with the loss of dopamine [248]. Among a series of tropane derivatives [249,250] labeled with ^{99m}Tc, two compounds deserve more attention.

The tropane derivative TRODAT-1 was labeled with ^{99m}Tc and yielded ^{99m}Tc-TRODAT-1 (Fig. 6.30a.B). The agent was obtained in a good yield of 80 % and high radiochemical purity of more than 95 %. The bis(amino-ethanethiol) ligand is attached at the 2β position of the tropane core structure. ^{99m}Tc-TRODAT-1 displayed an initial uptake in rat brain of 0.4 % at 2 min post-injection, the striatal/cerebellar ratio reached 2.8 at 60 min and a maximum of 4.07 at 4 h after injection. It is selectively localized in the striatum region consistent with a profile of specific binding to dopamine transporters [247,251]. In non-human primates a maximal target/non-target ratio of 3.5 between striatum and cerebellum was obtained [251a]. A dose of 11.2 mCi (414 MBq) of ^{99m}Tc-TRODAT-1 was injected intravenously into a normal human volunteer. The agent quickly penetrated the blood-brain-barrier. At 120–140 min post-injection, SPECT images gave the best contrast between the basal ganglia where dopamine transporters are located and the occipital area devoid of dopamine transporters [252]. ^{99m}Tc-TRODAT-1 forms diastereomers that display different binding affinities and distinct localization in the striatum region [252a].

Another ^{99m}Tc labeled imaging agent that targets the dopamine transporter is the so-called Technepine. The compound is also based on the tropane skeleton and the square pyramidal diamide-dithiolate complex of the $^{99m}TcO^{3+}$ core (Fig. 6.30b.B). SPECT images in rhesus monkeys were obtained over 3 h. The striatum was localized by co-registration of the SPECT images with magetic resonance imaging. The selectivity of Technepine was confirmed by comparing the striatum versus cerebellum radioactive labeling, which was found to be 2:1 in a female monkey and 3:1 in a male monkey [248,253].

The development of ^{99m}Tc labeled dopamine transporters has been excellently reviewed very recently [254].

a

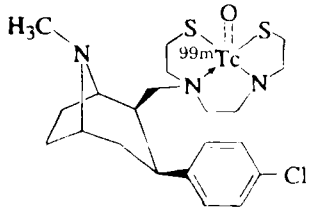

b

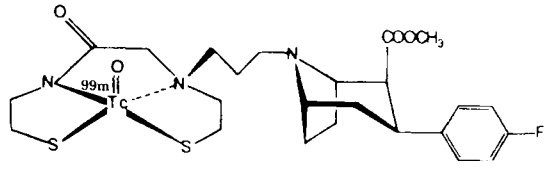

Fig. 6.30.B The dopamine transporter imaging agents ^{99m}Tc-TRODAT-1 (a) [251] and Technepine (b) [248,253]

7 Summary of ^{99m}Tc radiopharmaceuticals

A summary of ^{99m}Tc radiopharmaceuticals is given in Table 7.1.B.

Table 7.1.B ^{99m}Tc Radiopharmaceuticals for imaging and functional studies of organs.

Organ	Radio-pharmaceutical	Tradename	Producer (incomplete list)	Dosage [mCi (MBq)]	Application
Brain	[^{99m}Tc^{V}O-*d,l*-HM-PAO]	Ceretec	Amersham International	10–20 (370–740)	Regional blood perfusion, cerebral stroke, ischemia, dementia, tumors, trauma, hematoma
	[^{99m}Tc^{V}O-L,L-ECD]	Neurolite	DuPont	10–20 (370–740)	Regional blood perfusion, cerebral stroke, focal epilepsy
	[^{99m}Tc^{III}Cl(DMG)2MP]	Neurovue	Bristol-Myers Squibb	25 (925)	Regional perfusion
	[^{99m}Tc^{V}O(MRP-20)]	-	Medgenix, Belgium	–	
	[^{99m}Tc^{V}O(NEP-DADT)]	–			
	[^{99m}Tc(DTPA)]$^{2-}$	Teceren	Hoechst	10–15 (370–555)	Blood perfusion, tumor localization
	[^{99m}Tc^{V}O(gluco-heptonate)$_3$]	Glucosan	DuPont	20 (740)	Blood perfusion, brain lesions
	Na^{99m}TcO$_4$	–	–	10–20 (370–740)	Blood perfusion, lesions
Myocardium	[^{99m}Tc^{I}(MIBI)$_6$]$^{+}$	Cardiolite	DuPont	10–30 (370–1110)	Blood perfusion, ischemia, infarction
	[^{99m}Tc^{III}(teboroxime)]	Cardiotec	Bristol-Myers Squibb	15 (555)	Blood perfusion, coronary diseases
	[^{99m}Tc^{V}O$_2$(tetrofos-min)$_2$]$^{+}$	Myoview	Amersham International	5–24 (185–888)	Blood perfusion, ischemia, infarction
	[^{99m}Tc^{III}(furifosmin)]$^{+}$	Technescan	Mallinckrodt	14 (518)	Blood perfusion
	[^{99m}Tc-Pyrophosphate]	Tecephos	Hoechst	15–20 (555–740)	Acute myocardial infarcts
Thyroid	Na^{99m}TcO$_4$	–	-	0.5–2 (18.5–74)	Morphology, vascularity, function
Lungs	^{99m}Tc-MAA	Tecepart	Behring	1 – 16 (37–600)	Blood perfusion, shunt diagnosis, angio- and phleboscintigraphy
	[^{99m}Tc(DTPA)] aerosol	Teceren	Behring	5.4 (200)	Ventilation
Liver, gall bladder	[^{99m}Tc^{III}(disofenin)]	Hepatolite	DuPont	3 (111)	Liver and gall bladder function
	^{99m}Tc-PMT]	–	Nihon Medi-Physics	–	
	^{99m}Tc-sulphur colloid	Tesuloid	Bristol-Myers Squibb	1–3 (37–111)	Liver and spleen morphology, tumors and abscesses
	^{99m}Tc-albumin colloid	Microlite	DuPont	5 (185)	
Kidneys	[^{99m}Tc^{V}O(MAG$_3$)]	MAG3	Mallinckrodt	5–20 (185–740)	Tubuli function, flow studies
	[^{99m}Tc(DTPA)]$^{2-}$	DTPA	Amersham Buchler	5–12 (185–444)	Glomerular filtration rate, renal perfusion
	[^{99m}Tc-DMSA]	DMSA	Amersham Buchler	1–2 (37–74)	Morphology, function diagnosis

Table 7.1.B Continued.

Organ	Radio-pharmaceutical	Tradename	Producer (incomplete list)	Dosage [mCi (MBq)]	Application
	[^{99m}Tc^{V}O(gluco-heptonate)$_2$]$^{-}$	Gluceptate	Mallinckrodt	10–15 (370–555)	Morphology, renal perfusion
	[^{99m}Tc^{V}O-L,L-EC]$^{?}$		–	–	Renal function
Skeleton	[^{99m}Tc-HMDP]	Osteoscan HDP	Mallinckrodt	10–20 (370–740)	Bone fracture, tumor, metastatic lesion, sarcoma, arthritis, osteomyelitis and other bone diseases
	[^{99m}Tc-MDP]	Tecebon	Hoechst	10–15 (370–555)	
	[^{99m}Tc-DPD]	Teceos	Behring	10–15 (370–555)	
	[^{99m}Tc-HEDP]	–			
	[^{99m}Tc-ABP]		–	20 (740)	
Red blood cells	[^{99m}Tc-RBCs]	Ultra Tag	Mallinckrodt	15–20 (555–740)	Ventricular functioning, cardiac output, gastrointestinal hemorrhages, vein thrombosis, internal bleeding, hepatic hemangiomas
White blood cells	[^{99m}Tc-WBCs]		–	–	Inflammatory bowel disease, tissue sepsis, osteomyelitis
Tumors	[^{99m}Tc^{V}O(DMSA)$_2$]$^{-}$		Amersham International	10 (370)	Medullary thyroid carcinoma, head and neck tumors
	[^{99m}Tc^{I}(MIBI)$_6$]$^{+}$	Cardiolite	DuPont	3–15 (111–555)	Hyperparathyroidism, breast tumors, axillary node metastases
	[^{99m}Tc^{V}O$_2$(tetrofosmin)$_2$]$^{+}$	Myoview	Amersham International	20 (740)	Breast and lung tumors
	[^{99m}Tc^{V}O-*d,l*-HM-PAO]°	Ceretec	Amersham International	20 (740)	Malignant melanoma, primary focus and metastatic lesions
	^{99m}Tc-Mab BW 431/26	Scintimum CEA	Behring	18.9–29.7 (700–1100)	Colorectal cancer, gastric cancer
	^{99m}Tc-Mab BW 250/183	Scintimum Granulozyt	Behring	27 (1000)	Mammary and prostatic carcinoma, lymphoma, small cell lung cancer

8 References

[1] K. Schwochau, Angew. Chem, Int. Ed. Engl. *33*, 2258–2267 (1994)
[2] E. Browne and R.B. Firestone, Table of Radioactive Isotopes (V.S. Shirley, ed.), Wiley, New York (1986)
[3] E. Deutsch and K. Libson, Comments Inorg. Chem. *3*, 83–103 (1984)
[4] M.J. Clarke and L. Podbielski, Coord. Chem. Rev. *78*, 253–331 (1987)
[5] W.A. Volkert and S. Jurisson, Topics in Current Chemistry *176*, 123–148 (1996). In: Technetium and Rhenium. Their Chemistry and its Application. Ed. K. Yoshihara and T. Omori
[6] S. Jurisson, D. Berning, Wei Jia, and Dangshe Ma, Chem. Rev. *93*, 1137–1156 (1993)
[7] J. Steigman and W.C. Eckelman, The Chemistry of Technetium in Medicine, Nuclear Science Series, NAS-NS-3204 (1992)

[8] T.R. Carroll, Technetium Heart and Brain Perfusion Imaging Agents, Advances in Metals in Medicine *1*, 1–27 (1993)
[9] A.D. Nunn, Semin. Nucl. Med. *20*, 111–118 (1990)
[10] W.C. Eckelman, Eur. J. Nucl. Med. *22*, 249–263 (1995)
[11] J.R. Dilworth and S.J. Parrott, Dev. Nucl. Med. *30*, 1–20 (1996)
[12] S. Liu, D.S. Edwards, and J.A. Barrett, Bioconjugate Chem. *8*, 621–636 (1997)
[13] A.D. Nunn (ed.), Radiopharmaceuticals, Chemistry and Pharmacology, Marcel Dekker, Inc. New York (1992)
[14] G.B. Saha, Fundamentals of Nuclear Pharmacy, 4th ed., Springer, New York (1998)
[15] Nuclear Data Center, Brookhaven, BNL 325 (1973)
[16] Gmelin Handbook of Inorganic Chemistry, Technetium, Suppl. Vol. 1, 8th ed., (H. K. Kugler and C. Keller, eds.), Springer, Berlin (1982) p. 145
[17] W.D. Tucker, M.W. Greene, A.J. Weiss, and A.P. Murrenhoff (BNL 3746) Trans. Am. Nucl. Soc. *1*, 160 (1958)
[18] P. Richards, W.D. Tucker, and S.C. Srivastava, Int. J. Appl. Radiat. Isot. *33*, 793–799 (1982)
[19] Monograph of the European Pharmacopoeia Commission PA, PH, Exp. 14. T(76)1, Com. 9.1.1977
[20] K. Jordan, Meßtechnik in der Emissions-Computertomographie in: Handbuch der Medizinischen Radiologie Bd XV, Teil 1B (L. Diethelm, F. Heuck, O. Olsson, F. Strnad, H. Vieten, A. Zuppinger, eds.), Springer, Berlin, 1983
[21] D. Lange, Nuklearmedizinische bildgebende Verfahren in: Physik der bildgebenden Verfahren in der Medizin (H.-J. Maurer, E. Zieler, eds.), Springer, Berlin, 1984
[22] H.J. Hermann, Nuklearmedizin, 2nd ed., Urban und Schwarzenberg, München, 1989
[23] R.C. Walovitch, S.J. Williams, and N.D. Lafrance, Nucl. Med. Biol. *17*, 77–83 (1990)
[24] K. Schwochau, Radiochim. Acta *32*, 139–152 (1983)
[25] H.F. Kung, Brain Radiopharmaceuticals in: Radiopharmaceuticals: Progress and clinical Perspectives, Vol. 1 (A.R. Fritzberg, ed.), CRC, Boca Raton, FL, 1986, pp. 21–39
[26] E. Deutsch, R.C. Elder, B.A. Lange, M.J. Vaal, and D.H. Lay, Proc. Natl. Acad. Sci. *73*, 4287–4289 (1976)
[27] K.E. Linder, M.F. Malley, J.Z. Gougoutas, S.E. Unger, and A.D. Nunn, Inorg. Chem. *29*, 2428–2434 (1990)
[28] M. Nakayama, T. Terahara, M. Wada, K. Harada, A. Sugii, M. Hara, O. Shimomura, A. Kojima, S. Tomiguchi, H. Izunaga, Y. Hirota, and M. Takahashi, Nucl. Med. Commun. *12*, 147–152 (1991)
[29] M.C. Day, Jr. and J. Selbin, Theoretical Inorganic Chemistry, 2nd ed., Reinhold Book, New York, 1969
[30] C.D. Russel and J. Majerik, Int. J. Appl. Radiat. Isot. *29*, 109–114 (1978)
[31] D.P. Nowotnik in: Textbook of Radiopharmacy (C.B. Sampson, ed.). Gordon and Breach Science Publishers, New York (1994), pp. 53–72
[32] W.M. Pardridge, Ann. Rev. Pharmacol. Toxicol. *28*, 25–39 (1988)
[33] G.W. Goldstein and A.L. Betz, Spektrum der Wissenschaft, November 1986, pp. 82–91
[34] D.D. Dischino, M.J. Welch, M.R. Kilbourn, and M.E. Raichle, J. Nucl. Med. *24*, 1030–1038 (1983)
[35] K. Leesmeister and K. Schwochau, Nucl. Med. Biol. *19*, 73–78 (1992)
[36] A.D. Nunn, T. Feld, and R.K. Narra in: Technetium and rhenium in chemistry and nuclear medicine 3 (M. Nicholini, G. Bandoli, and U. Mazzi eds.), Publ. Cortina International (1990), pp. 399–403
[37] V.A. Levin, J. Med. Chem. *23*, 682–684 (1980)
[38] D.P. Nowotnik, Technetium based Brain Perfusion Agents in: Radiopharmaceuticals, Chemistry and Pharmacology (A.D. Nunn, ed.), Dekker, New York (1992), pp. 37–95
[39] U. Pleger and K. Schwochau (Forschungszentrum Jülich), Patent DE 4128183 C1 (1993)
[40] S. Jurisson, E.D. Schlemper, D.E. Troutner, L.R. Canning, D.P. Nowotnik, and R.D. Neirinckx, Inorg. Chem. *25*, 543–549 (1986)
[41] W.A. Volkert, T.J. Hoffman, C. Roth, M. Corlija, and R.A. Holmes, Radiochim. Acta *63*, 205–208 (1993)
[42] P.F. Sharp, F.W. Smith, H.G. Gemmell, D. Lyall, N.T.S. Evans, D. Gvozdanovic, J. Davidson, D.A. Tyrrell, R.D. Pickett, and R.D. Neirinckx, J. Nucl. Med. *27*, 171–177 (1986)
[43] H.F. Kung, Semin. Nucl. Med. *20*, 150–158 (1990)
[44] A.R. Andersen, Cerebrovasc. Brain Metab. Rev. *1*, 288–318 (1989)
[45] R.D. Neirinckx, J.F. Burke, R.C. Harrison, A.M. Forster, A.R. Andersen, and N.A. Lassen, J. Cereb. Blood Flow Metab. *8*, Suppl. 1, S4–S12, (1988)

[46] C.A. Roth, T.J. Hoffman, M. Corlija, W.A. Volkert, and R.A. Holmes, Nucl. Med. Biol. *19*, 783-790 (1992)
[47] M.R. Jacquier-Sarlin, B.S. Polla, and D.O. Slosman, J. Nucl. Med. *37*, 1413-1416 (1996)
[48] J.C. Hung, M. Corlija, W.A. Volkert, and R.A. Holmes, J. Nucl. Med. *29*, 1568-1576 (1988)
[49] J.C. Hung, W.A. Volkert, and R.A. Holmes, Nucl. Med. Biol. *16*, 675-680 (1989)
[50] H.Y. Ding, S.J. Yeh, C.C. Yang, J.T. Hsu, and C.C. Tzeng, Appl. Radioat. Isot. *48*, 311-317 (1997)
[51] M.W. Billinghurst, D.N. Abrams, and M.S. Lawson, Appl. Radiat. Isot. *42*, 607-612 (1991)
[52] K. Tubergen, M. Corlija, W.A. Volkert, and R.A. Holmes, J. Nucl. Med. *32*, 111-115 (1991)
[53] R.D. Neirinckx, L.R. Canning, J.M. Piper, D.P. Nowotnik, R.D. Pickett, R.A. Holmes, W.A. Volkert, A.M. Forster, P.S. Weisner, J.A. Marriott, and S.B. Chaplin, J. Nucl. Med. *28*, 191-202 (1987)
[54] J.-P. Leonard, D.P. Nowotnik, and R.D. Neirinckx, J. Nucl. Med. *27*, 1819-1823 (1986)
[55] H.G. Gemmell, P.F. Sharp, J.A.O. Besson, J.R. Crawford, K.P. Ebmeier, J. Davidson, and F.W. Smith, J. Comput. Assist. Tomogr. *11*, 398-403 (1987)
[56] D. Neary, J.S. Snowden, R.A. Shields, A.W.I. Burjan, B. Northen, N. Macdermott, M.C. Prescott, and H.J. Testa, J. Neurol. Neurosurg. Psychiatry *50*, 1101-1109 (1987)
[57] B.L. Holman, K.A. Johnson, B. Gerada, P.A. Carvalho, and A. Satlin, J. Nucl. Med. *33*, 181-185 (1992)
[58] H.J. Biersack, D. Linke, F. Brassel, R. Reichmann, M. Kurthen, H.F. Durwen, B.M. Reuter, J. Wappenschmidt, and H. Stefan, J. Nucl. Med. *28*, 1763-1767 (1987)
[59] B.G. Gray, M. Ichise, D.-G. Chung, J.C. Kirsh, and W. Franks, J. Nucl. Med. *33*, 52-58 (1992)
[60] Y. Isaka, M. Imaizumi, Y. Itoi, K. Ashida, and K. Horibe, J. Nucl. Med, *33*, 246-248 (1992)
[61] J.W. Babich, M.A. Flower, F. Keeling, S. Fielding, S. Chittenden, L. Repetto, A. Whitton, and V.R. McCready, J. Nucl. Med. *27*, 1030 (1986)
[62] N.R. Laurin, A.A. Driedger, G.A. Hurwitz, A.G. Mattar, J.E. Powe, M.J. Chamberlain, P.L. Zabel, and W.F. Pavlosky, J. Nucl. Med. *30*, 1627-1635 (1989)
[63] R.H. Reid, K.Y. Gulenchyn, and J.R. Ballinger, J. Nucl. Med. *30*, 1621-1626 (1989)
[64] J. Léveillé, G. Demonceau, M. DeRoo, P. Rigo, R. Taillefer, R.A. Morgan, D. Kupranick, and R.C. Walovitch, J. Nucl. Med. *30*, 1902-1910 (1989)
[65] D.S. Edwards, E.H. Cheesman, M.W. Watson, L.J. Maheu, S.A. Nguyen, L. Dimitre, T. Nason, A.D. Watson, and R. Walovitch in: Technetium and Rhenium in Chemistry and Nuclear Medicine 3 (M. Nicolini, G. Bandoli, U. Mazzi, eds.), Cortina International/ Verona and Raven/New York, 1990, pp. 433-444
[66] R.C. Walovitch, E.H. Cheesman, L.H. Maheu, and K.M. Hall, J. Cereb. Blood Flow Metab. *14*, S4-S11 (1994)
[67] M.R. Jacquier-Sarlin, B.S. Polla, and D.O. Slosman, J. Nucl. Med. *37*, 1694-1697 (1996)
[68] R.C. Walovitch, T.C. Hill, S.T. Garrity, E.H. Cheesman, B.A. Burgess, D.H. O'Leary, A.D. Watson, M.V. Ganey, R.A. Morgan, and S.J. Williams, J. Nucl. Med. *30*, 1892-1901 (1989)
[69] S. Vallabhajosula, R.E. Zimmerman, M. Picard, P. Stritzke, I. Mena, R.S. Hellman, R.S. Tikofsky, M.G. Stabin, R.A. Morgan, and S.J. Goldsmith, J. Nucl. Med. *30*, 599-604 (1989)
[70] B.L. Holman, R.S. Hellman, S.J. Goldsmith, I.G. Mena, J. Leveille, P.G. Gherardi, J.-L. Moretti, A. Bischof-Delaloye, T.C. Hill, P.M. Rigo, R.L. Van Heertum, P.J. Ell, U. Buell, M.C. DeRoo, and R.A. Morgan, J. Nucl. Med. *30*, 1018-1024 (1989)
[71] K.E. Linder, M.F. Malley, J.Z. Gougoutas, S.E. Unger, and A.D. Nunn, Inorg. Chem. *29*, 2428-2434 (1990)
[72] R.K. Narra, A.D. Nunn, B.L. Kuczynski, R.J. Di Rocco, T. Feld, D.A. Silva, and W.C. Eckelman, J. Nucl. Med. *31*, 1370-1377 (1990)
[73] D.P. Nowotnik and A.D. Nunn, Drugs News and Perspectives *5*, 174-183 (1992)
[74] G.F. Morgan, M. Deblaton, P. Clemens, P. Van den Broeck, A. Bossuyt, and J.R. Thornback, J. Nucl. Med. *32*, 500-505 (1991)
[75] A. Bossuyt, G.F. Morgan, M. Deblaton, R. Pirrotte, A. Chirico, P. Clemens, P. Vandenbroeck, and J.R. Thornback, J. Nucl. Med. *32*, 399-403 (1991)
[76] G.F. Morgan, M. Deblaton, P. Clemens, P. Van den Broeck, W. Hussain, A. Bossuyt, and J.R. Thornback in: Technetium and Rhenium in Chemistry and Nuclear Medicine 3 (M. Nicolini, G. Bandilo, U. Mazzi, eds.) Cortina International/ Verona and Raven/New York (1990) pp. 419-423
[77] S.Z. Levey, D.H. Burns, T.M. Kervitsky, H.W. Goldfarb, D.V. Woo, D.F. Wong, L.A. Epps, A.V. Kramer, and H.N. Wagner, Jr., J. Nucl. Med. *26*, 1287-1294 (1985)
[78] L.A. Epps, H.D. Burns, S.Z. Lever, H.W. Goldfarb, and H.N. Wagner, Jr., Appl. Radiat. Isot. *38*, 661-664 (1987)

[79] U. Scheffel, H.W. Goldfarb, S.Z. Lever, R.L. Gungon, H.D. Burns, and H.N. Wagner, Jr., J. Nucl. Med. *29*, 73–82 (1988)
[80] C.D. Russel, R.C. Crittenden, and A.G. Cash, J. Nucl. Med. *21*, 354–369 (1980)
[81] P. Bläuenstein, K. Girgenrath, H. Hügli, G. Anderegg, P. Jordan, and K. May, J. Labelled Compd. Radiopharm *18*, 194–195 (1981)
[82] S. Seifert, B. Noll, and R. Münze, Int. J. Appl. Radiat. Isot. *33*, 1393–1398 (1982)
[83] E. Ianovici, M. Kosinski, P. Lerch, and A.G. Maddock, Dev. Nucl. Med. *10*, 161–172 (1986)
[84] G.B. Saha, Fundamentals of Nuclear Pharmacy, 2nd ed., Springer, New York (1984)
[85] W. de Kieviet, J. Nucl. Med. *22*, 703–709 (1981)
[86] E. Deutsch, W. Bushong, K.A. Glavan, R.C. Elder, V.J. Sodd, K.L. Scholz, D.L. Fortman, and S.J. Lukes, Science *214*, 85–86 (1981)
[87] D.M. Wieland and E.A. Deutsch, Cationic Radiotracers as myocardial Radiopharmaceuticals in: Radiopharmaceuticals: Progress and Clinical Perspectives, Vol. 1 (A.R. Fritzberg, ed.), CRC, Boca Raton, Florida (1986), pp. 1–20
[88] A.D. Nunn, Single Photon Radiopharmaceuticals for Imaging Myocardial Perfusion in: Radiopharmaceuticals, Chemistry and Pharmacology (A.D. Nunn, ed.), Dekker, New York (1992), pp. 97–140
[89] D. Piwnica-Worms, J.F. Kronauge, B.L. Holman, A. Davison, and A.G. Jones, Invest. Radiol. *24*, 25–29 (1989)
[90] Du Pont Radiopharmaceutical Division, Billerica, Massachusetts, USA 01862, J. Nucl. Med. *34*, Nr. 6 (1993)
[91] T.H. Tulip, J. Calabrese, J.F. Kronauge, A., Davison, and A.G. Jones in: Technetium in Chemistry and Nuclear Medicine 2 (M. Nicolini, G. Bandoli, U. Mazzi, eds.), Cortina International, Verona/ Raven, New York, 1986, pp. 119–121
[92] F.J.T. Wackers, D.S. Berman, J. Maddahi, D.D. Watson, G.A. Beller, H.W. Strauss, C.A. Boucher, M. Picard, B.L. Holman, R. Fridrich, E. Inglese, B. Delaloye, A. Bischof-Delaloye, L. Camin, and K. McKusick, J. Nucl. Med. *30*, 301–311 (1989)
[93] D. Piwnica-Worms, J.F. Kronauge, B.L. Holman, J. Lister-James, A. Davison, and A.G. Jones, J. Nucl. Med. *29*, 55–61 (1988)
[94] H. Sands, M.L. Delano, and M. Gallagher, J. Nucl. Med. *27*, 404–408 (1986)
[95] R. Taillefer, L. Laflamme, G. Dupras, M. Picard, D.-C. Phaneuf, and J. Léveillé, Eur. J. Nucl. Med. *13*, 515–522 (1988)
[96] S. Jurisson, Drugs of the Future *15*, 1085–1086 (1990)
[97] E.N. Treher, L.C. Francesconi, J.Z. Gougoutas, M.F. Malley, and A.D. Nunn, Inorg. Chem. *28*, 3411–3416 (1989)
[98] S.S. Jurisson, W. Hirth, K.E. Linder, R.J. Di Rocco, R.K. Narra, D.P. Nowotnik, and A.D. Nunn, Nucl. Med. Biol. *18*, 735–744 (1991)
[99] A.D. Nunn, Dev. Nucl. Med. 22, 55–65 (1992)
[100] D.W. Seldin, L.L. Johnson, D.K. Blood, M.J. Muschel, K.F. Smith, R.M. Wall, and P.J. Cannon, J. Nucl. Med. *30*, 312–319 (1989)
[101] J.D. Kelly, A.M. Forster, B. Higley, C.M. Archer, F.S. Booker, L.R. Canning, K.W. Chiu, B. Edwards, H.K. Gill, M. McPartlin, K.R. Nagle, I.A. Latham, R.D. Pickett, A.E. Storey, and P.M. Webbon, J. Nucl. Med. *34*, 222–227 (1993)
[102] S. Jones and R.C. Hendel, J. Nucl. Med. Technol. *21*, 191–195 (1993)
[103] B. Higley, F.W. Smith, T. Smith, H.G. Gemmell, P.D. Gupta, D.V. Gvozdanovic, D. Graham, D. Hinge, J. Davidson, and A. Lahiri, J. Nucl. Med. *34*, 30–38 (1993)
[104] P.J. Thorley, J. Ball, K.L. Sheard, and U.M. Sivananthan, Nucl. Med. Commun. *16*, 733–740 (1995)
[105] S.S. Jurisson, K. Dancey, M. MacPartlin, P.A. Tasker, and E. Deutsch, Inorg. Chem. *23*, 4743–4749 (1984)
[106] E. Deutsch, J.-L. Vanderheyden, P. Gerundini, K. Libson, W. Hirth, F. Colombo, A. Savi, and F. Fazio, J. Nucl. Med. *28*, 1870–1880 (1987)
[107] J.E. Bugaj, M.A. De Rosch, M.F. Marmion, R.H. Quint, K.F. Deutsch, and E. Deutsch, J. Nucl. Med. *35*, 139P (1994)
[108] C. Rossetti, G. Vanoli, G. Paganelli, M. Kwiatkowski, F. Zito, F. Colombo, E. Deutsch, and F. Fazio, J. Nucl. Med. *32*, 1007 (1991)
[109] M.T. Hays and B. Wesselossky, J. Nucl. Med. *14*, 785–792 (1973)

[110] A.R. Fritzberg in: Radiopharmaceuticals. Progress and Clinical Perspectives Vol. 1, (A.R. Fritzberg, ed.), CRC Press, Inc., Boca Raton, Florida (1986), Chapter 5, pp. 89–116
[111] M.D. Loberg and A.T. Fields, Int. J. Appl. Radiat. Isot. *29*, 167–173 (1978)
[112] C.E. Costello, J.W. Brodack, A.G. Jones, A. Davison, D.L. Johnson, S. Kasina, and A.R. Fritzberg, J. Nucl. Med. *24*, 353–355 (1983)
[113] G.B. Saha, Fundamentals of Nuclear Pharmacy, 3rd ed., Springer, New York (1992)
[114] A.D. Nunn, M.D. Loberg, and R.A. Conley, J. Nucl. Med. *24*, 423–430 (1983)
[115] M. Kato-Azuma, J. Nucl. Med. *23*, 517–524 (1992)
[116] M. Kato-Azuma, Int. J. Appl. Radiat. Isot. *32*, 187–189 (1981)
[117] A.R. Fritzberg, D.C. Bloedow, D. Eshima, D.L. Johnson, and W.C. Klingensmith, J. Nucl. Med. *24*, 10 (1983)
[118] Y. Hasegawa, S. Nakano, K. Ibuka, T. Hashizume, Y. Sasaki, S. Imaoka, S. Ishiguro, H. Kasugai, Y. Okano, S. Tanaka, M. Ehara, T. Morii, J. Kojima, and S. Ishigami, J. Nucl. Med. *25*, 1122–1126 (1984)
[119] J. Steigman, N.A. Solomon, and L.L.-Y. Hwang, Appl. Radiat. Isot. *37*, 223–229 (1986)
[120] M.W. Billinghurst in: Radiopharmaceuticals. Progress and Clinical Perspectives Vol. 2, (A.R. Fritzberg, ed.), CRC Press, Inc., Boca Raton, Florida (1986), Chapter 4, pp. 61–87
[121] A.R. Fritzberg, S. Kasina, D. Eshima, and D.L. Johnson, J. Nucl. Med. *27*, 111–116 (1986)
[122] D.L. Nosco, R.G. Manning, and A. Fritzberg, J. Nucl. Med. *27*, 939 (1986)
[123] T.N. Rao, D. Adhikesavalu, A. Camerman, and A.R. Fritzberg, Inorg. Chim. Acta *180*, 63–67 (1991)
[124] B. Noll, B. Johannsen, K. May, and H. Spies, Appl. Radiat. Isot. *43*, 899–901 (1992)
[125] G. Bormans, B. Cleynhens, P. Adriaens, H. Vanbilloen, M. DeRoo, and A. Verbruggen, Nucl. Med. Biol. *22*, 339–349 (1995)
[126] D. Eshima, A.R. Fritzberg, and A. Taylor, Jr., Semin. Nucl. Med. *20*, 28–40 (1990)
[127] A. Taylor, Jr., D. Eshima, A.R. Fritzberg, P.E. Christian, and S. Kasina, J. Nucl. Med. *27*, 795–803 (1986)
[128] A. Taylor, Jr., D. Eshima, and N. Alazraki, Eur. J. Nucl. Med. *12*, 510–514 (1987)
[129] A. Taylor, Jr., D. Eshima, P.E. Christian, W.W. Wooten, L. Hansen, and K. McElvany, J. Nucl. Med. *29*, 616–622 (1988)
[130] A.A. Al-Nahhas, R.A. Jafri, K.E. Britton, K. Solanki, J. Bomanji, S. Mather, M.A. Carroll, M. Al-Janabi, V. Frusciante, B. Ajdinowic, F. Fiore, S. Demena, and C.C. Nimmon, Eur. J. Med. *14*, 453–462 (1988)
[131] A. Taylor, Jr., Crit. Rev. Diag. Imag. *32*, 1–36 (1991)
[132] H.R. Maecke and M. Eisenhut in: Handbook of Metal-Ligand Interactions in Biological Fluid: Bioinorganic Chemistry, Vol. 2, (G. Berthon, ed.), New York, Dekker (1995) pp. 1079–1092
[133] I. Ikeda, O. Inoue, and K. Kurata, Int. J. Appl. Radiat. Isot. *27*, 681–688 (1976)
[134] J.L. Moretti, J.R. Rapin, J.C. Saccavini, A. Lageron, M.L. Poncin, and A. Bardy, Int. J. Nucl. Med. Biol. *11*, 270–274 (1984)
[135] R. Garcia, J. Galvez, and J.L. Moreno, Int. J. Appl. Radiat. Isot. *33*, 521–524 (1982)
[136] M. J. de Lange, D.A. Piers, J.G.W. Kosterink, W.H.J. van Luijk, S. Meijer, D. de Zeeuw, and G.K. van der Hem, J. Nucl. Med. *30*, 1219–1223 (1989)
[137] A.M. Verbruggen, D.L. Nosco, C.G. Van Nerom, G.M. Bormans, P.J. Adriaens, and M.J. DeRoo, J. Nucl. Med. *33*, 551–557 (1992)
[138] C.G. Van Nerom, G.M. Bormans, M.J. De Roo, and A.M. Verbruggen, Eur. J. Nucl. Med. *20*, 738–746 (1993)
[139] M. Misra, H.S. Sarkar, M. Chakravarty, S. Sanyal, S. Ganguly, B.R. Sarkar, J. Chatterjee, P. Dobe, S. Ghosh, and S. Banerjee, Nucl. Med. Commun. *15*, 878–885 (1994)
[140] Y.-Z. Liu, L. Zhu, Z. Zhang, F. Guo, and X.-J. Liu, J. Radioanal. Nucl. Chem., Articles, *206*, 127–132 (1996)
[140a] A.-Y. Wang, J. Radioanal. Nucl. Chem. *230*, 79–82 (1998)
[141] G.M. Wilson and T.C. Pinkerton, Anal. Chem. *57*, 246–253 (1985)
[142] T.C. Pinkerton, C.P. Desilets, D.J. Hoch, M.V. Mikelsons, and G.M. Wilson, J. Chem. Educ. *62*, 965–973 (1985)
[143] T.C. Pinkerton, W.R. Heineman, and E. Deutsch, Anal. Chem. *52*, 1106–1110 (1980)
[144] C.L. De Ligny, W.J. Gelsema, T.G. Tji, Y.M. Huigen, and H.A. Vink, Nucl. Med. Biol. *17*, 161–179 (1990)
[145] C.L. De Ligny, W.J. Gelsema, and W.E. Meijs, Nucl. Med. Biol. *18*, 173–178 (1991)

[146] R. Münze, J. Labelled Compd. Radiopharm. *15*, 215–224 (1978)
[147] C.D. Russel and A.G. Cash, J. Nucl. Med. 20, 532–537 (1979)
[148] T.G. Tji, H.A. Vink, W.J. Gelsema, and C.L. De Ligny, Appl. Radiat. Isot. *41*, 17–28 (1990)
[149] N. Vanlic-Razumenic, D. Jankovic, and D. Veselinovic, J. Radioanal. Nucl. Chem., Articles, *190*, 149–154 (1995)
[150] K. Libson, E. Deutsch, and B.L. Barnett, J. Am. Chem. Soc. *102*, 2476–2478 (1980)
[151] M.V. Mikelsons and T.C. Pinkerton, Appl. Radiat. Isot. *38*, 569–570 (1987)
[152] J.L. Martin, Jr., J. Yuan, C.E. Lunte, R.C. Elder, W.R. Heineman, and E. Deutsch, Inorg. Chem. *28*, 2899–2901 (1989)
[153] I. Fogelman, A.J. Tofe, and M.D. Francis, J. Nucl. Med. *22*, 78 (1981)
[154] M.D. Francis, D.L. Ferguson, A.J. Tofe, J.A. Bevan, and S.E. Michaels, J. Nucl. Med. *21*, 1185–1189 (1980)
[155] S.S. Jurisson, J.J. Benedict, R.C. Elder, R. Whittle, and E. Deutsch, Inorg. Chem. *22*, 1332–1338 (1983)
[156] C.A. de Murphy, L. Meléndez-Alafort, C.E. Montoya-Molina, and J. Sepúlveda-Méndez, Nucl. Med. Biol. *24*, 27–39 (1997)
[157] R.J. Callahan in: Radiopharmaceuticals, Progress and Clinical Perspectives Vol. 2, (A.R. Fritzberg, ed.) CRC Press, Inc., Boca Raton, Florida (1986), Chapter 3, pp. 41–60
[158] M.K. Dewanjee, Semin. Nucl. Med. *20*, 5–27 (1990)
[159] S.C. Srivastava and R.F. Straub, Semin. Nucl. Med. *20*, 41–51 (1990)
[160] K. Ozker, B.D. Collier, R.S. Hellman, A.T. Isitman, A.Z. Krasnow, F. Uzum, and F.S. Steffel, Nucl. Med. Commun. *17*, 342–345 (1996)
[161] R.J. Callahan, J.W. Froelich, K.A. McKusick, J. Leppo, and H.W. Strauss, J. Nucl. Med. *23*, 315–318 (1982)
[162] A.M. Peters, Semin. Nucl. Med. *24*, 110–127 (1994)
[163] C.S. Marcus, J.H. Kuperus, J.A. Butler, P.L. Henneman, R.D. Salk, B.-Y. Chen, M.R.P. Vivian, and L.M. Yamanaka, Nucl. Med. Biol. *15*, 673–682 (1988)
[164] M. Papós, J. Láng, M. Rajtár, and L. Csernay, Nucl. Med. Biol. *21*, 893–895 (1994)
[165] P.J. Blower, J. Singh, and S.E.M. Clarke, J. Nucl. Med. *32*, 845–849 (1991)
[166] C.B. Sampson, Nucl. Med. Comm. *8*, 184–185 (1987)
[167] J. Singh, A.K. Powell, S.E.M. Clarke, and P.J. Blower, J. Chem. Soc., Chem. Commun. 115–117 (1991)
[168] H. Ohta, K. Yamamoto, K. Endo, T. Mori, D. Hamanaka, A. Shimazu, K. Ikekubo, K. Makimoto, Y. Iida, J. Konishi, R. Morita, N. Hata, K. Horiuchi, A. Yokoyama, K. Torizuka, and K. Kuma, J. Nucl. Med. *25*, 323–325 (1984)
[169] A. Yokoyama, N. Hata, K. Horiuchi, H. Masuda, H. Saji, H. Ohta, K. Yamamoto, K. Endo, and K. Torizuka, Int. J. Nucl. Med. Biol. *12*, 273–279 (1985)
[170] H. Ohta, K. Endo, T. Fujita, T. Nakashima, H. Sakahara, K. Torizuka, Y. Shimizu, Y. Ishii, K. Makomoto, N. Hata, K. Horiuchi, A. Yokoyama, and M. Ishii, Clin. Nucl. Med. *10*, 855–860 (1985)
[171] H. Ohta, K. Endo, T. Fujita, J. Konishi, K. Torizuka, K. Horiuchi, and A. Yokoyama, Nucl. Med. Comm. *9*, 105–116 (1988)
[172] J.C. Watkinson, C.R. Lazarus, R. Mistry, O.H. Shaheen, M.N. Maisey, and S.E. Clarke, J. Nucl. Med. *30*, 174–180 (1989)
[173] Ö. Ugur, L. Kostakoglu, N. Güler, B. Caner, U. Uysal, N. Elahi, M. Haliloglu, D. Yüksel, T. Aras, H. Bayhan, and C. Bekdik, Eur. J. Nucl. Med. *23*, 1367–1371 (1996)
[174] M.R. Vieira and J.H.B. Weinholtz, Eur. J. Surgical Oncology, *22*, 331–334 (1996)
[175] N. Fukumitsu, M. Tozaki, M. Uchiyama, Y. Mori, K. Kawakami, and K. Uchida, Nippon Igaku Hoshasen Gakkai Zasshi, *56*, 974–979 (1996)
[176] J. Maublant, Eur. J. Radiology *24*, 2–10 (1997)
[177] O. Schillaci, F. Scopinaro, R. Danieli, V. Picardi, R. Tavolaro, P. Cannas, and A.C. Colella, Anticancer Research, *17*, 1623–1626 (1997)
[178] O. Schillaci, F. Scopinaro, R. Danieli, R. Tavolaro, P. Cannas, V. Picardi, and A.C. Colella, Anticancer Research, *17*, 1607–1610 (1997)
[179] A.J. Coakley, A.G. Kettle, C.P. Wells, M.J. O'Doherty, and R.E.C. Collins, Nucl. Med. Commun. *10*, 791–794 (1989)
[180] O. Geatti, B. Shapiro, P.G. Orsolon, G. Proto, U.P. Guerra, F. Antonucci, and D. Gasparini, Eur. J. Nucl. Med. *21*, 17–22 (1994)

[181] G.S. Waters, G.J. Burke, J.H. Corley, and J.P. Wei, Am. Surg. *63*, 195–198 (1997)
[182] A.H. Cheung, M.S. Weeler, L.D. Madanay, E. Hew, M.N. Coel, and L.M. Wong, Hawaii Med. J. *56*, 114–117 (1997)
[183] T. Basoglu, M. Sahin, C. Coskun, A. Koparan, I. Bernay, and L. Erkan, Eur. J. Nucl. Med. *22*, 687–698 (1995)
[184] H. Takekawa, K. Takaoka, F. Tsukamoto, K. Kanegae, Y. Kozeki, A. Yamaya, F. Miller, and Y. Kawakami, Nucl. Med. Commun. *18*, 341–345 (1997)
[185] Y.H. Ryu, T.S. Chung, J.D. Lee, J.H. Suh, T.J. Lee, and C.Y. Park, Clin. Nucl. Med. *20*, 528–530 (1995)
[186] W.C. Eckelman and J. Steigman, Nucl. Med. Biol. *18*, 3–7 (1991)
[187] M.L. Thakur, J. DeFulvio, M.D. Richard, and C.H. Park, Nucl. Med. Biol. *18*, 227–233 (1991)
[188] A. Schwarz and A. Steinsträßer, J. Nucl. Med. *28*, 721 (1987)
[189] R.M. Reilly, Nucl. Med. Commun. *14*, 347–359 (1993)
[190] S.J. Mather and D. Ellison, J. Nucl. Med. *31*, 692–697 (1990)
[191] B.A. Rhodes, Nucl. Med. Biol. *18*, 667–676 (1991)
[192] Z.M. Zhang, J.R. Ballinger, K. Sheldon, and I. Boxen, Nucl. Med. Biol. *19*, 607–609 (1992)
[193] M. Nakayama, M. Wada, N. Araki, Y. Ginoza, T. Terahara, K. Harada, A. Sugii, S. Tomiguchi, A. Kojima, M. Hara, and M. Takahashi, Nucl. Med. Biol. *22*, 795–802 (1995)
[194] H. Koprivova, A. Pèlegrin, J.P. Mach, and H.R. Mäcke, Eur. J. Nucl. Med. *20*, 999 (1993)
[195] A.R. Fritzberg, P.G. Abrams, P.L. Beaumier, S. Kasina, A.C. Morgan, T.N. Rao, J.M. Reno, J.A. Sanderson, A. Srinivasan, D.S. Wilbur, and J.-L. Vanderheyden, Proc. Natl. Acad. Sci. USA, *85*, 4025–4029 (1988)
[196] P. Koch and H.R. Mäcke, Angew. Chem. Int. Ed. Engl. *31*, 1507–1509 (1992)
[197] M. Magerstädt, J.H. Hachmann, L. Kuhlmann, and L. Seidel, Chemiker-Ztg. *114*, 123–128 (1990)
[198] M. Eisenhut, M. Mißfeldt, W.D. Lehmann, and M. Karas, J. Labelled Compd. Radiopharm. *29*, 1283–1291 (1991)
[199] G. Paganelli, P. Magnani, F. Zito, G. Lucignani, F. Sudati, G. Truci, E. Motti, M. Terreni, B. Pollo, M. Giovanelli, N. Canal, G. Scotti, G. Comi, P. Koch, H.R. Maecke, and F. Fazio, Eur. J. Nucl. Med. *21*, 314–321 (1994)
[200] G. Stöcklin, Eur. J. Nucl. Med. *19*, 527–551 (1992)
[201] U.-M. Pleger, Dissertation, Technische Hochschule Aachen (1997)
[202] H.J. Steinmetz, Dissertation, Technische Hochschule Aachen (1993)
[203] F. Tisato, T. Maina, L.-R. Shao, M.J. Heeg, and E. Deutsch, J. Med. Chem. *39*, 1253–1261 (1996)
[204] E. Deutsch and W. Hirth, J. Nucl. Med. *28*, 1491–1500 (1987)
[205] R. Pasqualini and A. Duatti, J. Chem. Soc., Chem. Commun. 1354–1355 (1992)
[206] R. Pasqualini, V. Comazzi, E. Bellande, A. Duatti, and A. Marchi, Appl. Radiat. Isot. *43*, 1329–1333 (1992)
[207] R. Pasqualini, A. Duatti, E. Bellande, V. Comazzi, V. Brucato, D. Hoffschir, D. Fagret, and M. Comet, J. Nucl. Med. *35*, 334–341 (1994)
[208] C. Ghezzi, D. Fagret, C.C. Arvieux, J.-P. Mathieu, R. Bontron, R. Pasqualini, J. de Leiris, and M. Comet, J. Nucl. Med. *36*, 1069–1077 (1995)
[209] A. Duatti, C. Bolzati, L. Uccelli, and G.L. Zucchini, Transition Met. Chem. *22*, 313–124 (1997)
[210] D.W. Wester, J.R. Coveney, D.L. Nosco, M.S. Robbins, and R.T. Dean, J. Med. Chem. *34*, 3284–3290 (1991)
[211] D.L. Nosco, D.W. Wester, F. Fazio, A. Verbruggen, and M. De Roo, J. Nucl. Med. *31*, 907 (1990)
[212] K.E. Linder, Y.-W. Chan, J.F. Cyr, M.F. Malley, D.P. Nowotnik, and A.D. Nunn, J. Med. Chem. *37*, 9–17 (1994)
[213] K.E. Linder, J. Cyr, Y.W. Chan, N. Raju, K. Ramalingam, D.P. Nowotnik, and A.D. Nunn, J. Nucl. Med. *33*, 919 (1992)
[214] W.L. Rumsey, B. Patel, and K.E. Linder, J. Nucl. Med. *36*, 632–636 (1995)
[215] R.J. Di Rocco, A. Bauer, B.L. Kuczynski, J.P. Pirro, K.E. Linder, R.K. Narra, and A.D. Nunn, J. Nucl. Med. *33*, 865 (1992)
[216] H. Kusuoka, K. Hashimoto, K. Fukuchi, and T. Nishimura, J. Nucl. Med. *35*, 1371–1376 (1994)
[217] W.L. Rumsey, J.E. Cyr, N. Raju, and R.K. Narra, Biochem. Biophys. Res. Commun. *193*, 1239–1246 (1993)
[218] C.K. Ng, A.J. Sinusas, B.L. Zaret, and R. Soufer, Circulation *92*, 1261–1268 (1995)
[219] C.K. Stone, T. Mulnix, R.J. Nickles, B. Renstrom, S.H. Nellis, A.J. Liedtke, A.D. Nunn, B.L. Kuczynski, and W.L. Rumsey, Circulation *92*, 1246–1253 (1995)

[220] C.Q.-X. Shi, A.J. Sinusas, D.P. Dione, M.J. Singer, L.H. Young, E.N. Heller, B.D. Rinker, F.J.T. Wackers, and B.L. Zaret, J. Nucl. Med. *36*, 1078–1086 (1995)
[221] R.J. DiRocco, B.L. Kuczynski, J.P. Pirro, A. Bauer, K.E. Linder, K. Ramalingam, J.E. Cyr, Y.W. Chan, N. Raju, R.K. Narra, D.P. Nowotnik, and A.D. Nunn, J. Cereb. Blood Flow Metab. *13*, 755–762 (1993)
[222] J.R. Ballinger, J.W.M. Kee, and A.M. Rauth, J. Nucl. Med. *37*, 1023–1031 (1996)
[223] A. Nunn, K. Linder, and H.W. Strauss, Eur. J. Nucl. Med. *22*, 265–280 (1995)
[224] R.D. Okada, G. Johnson III, K.N. Nguyen, B. Edwards, C.M. Archer, and J.D. Kelly, Circulation *95*, 1892–1899 (1997)
[224a] K. Fukuchi, H. Kusuoka, K. Yutani, S. Hasegawa, and T. Nishimura, Eur. J. Nucl. Med. *25*, 361–366 (1998)
[225] C.M. Archer, B. Edwards, J.D. Kelly, A.C. King, J.F. Burke, and A.L.M. Riley, in: Technetium and Rhenium in Chemistry and Nuclear Medicine 4, (M. Nicolini, G. Bandoli, U. Mazzi, eds.), SGE ditoriali, Padova, Italy (1995) pp. 535–539
[226] W.C. Eckelman, Clinical potential of receptor based radiopharmaceuticals, in Radiopharmaceuticals: Progress and clinical Perspectives, Vol. II, Ed. A.R. Fritzberg, CRC, Boca Raton, Florida, pp. 89–113 (1986)
[227] W.C. Eckelman, The development of single-photon emitting receptor-binding radiotracers, in Radiopharmaceuticals: Chemistry and Pharmacology, (A.D. Nunn, ed.), Marcel Dekker, Inc., New York, pp. 167–219 (1992)
[228] D.R. Vera, K.A. Krohn, R.C. Stadalnik, and P.O. Scheibe, Radiology *151*, 191–196 (1984)
[229] D.R. Vera, K.A. Krohn, R.C. Stadalnik, and P.O. Scheibe, J. Nucl. Med. *25*, 779–787 (1984)
[230] P.P. Benjamin, Int. J. Appl. Radiat. Isot. *20*, 187–194 (1969)
[231] H.J. Dworkin and R.F. Gutkowski, J. Nucl. Med. *12*, 562–565 (1971)
[232] D.R. Vera, R.C. Stadalnik, and K.A. Krohn, J. Nucl. Med. *26*, 1157–1167 (1985)
[233] R.C. Stadalnik, D.R. Vera, E.S. Woodle, W.L. Trudeau, B.A. Porter, R.F. Ward, K.A. Krohn, and L.F. O'Grady, J. Nucl. Med. *26*, 1233–1242 (1985)
[234] J. Virgolini, C. Müller, W. Klepetko, P. Angelberger, H. Bergmann, J. O'Grady, and H. Sinzinger, Br. J. Cancer *61*, 937–941 (1990)
[235] M. Kudo, D.R. Vera, W.L. Trudeau, and R.C. Stadalnik, Nucl. Med. Biol. *18*, 663–666 (1991)
[236] D.R. Vera, R.C. Stadalnik, W.L. Trudeau, P.O. Scheibe, and K.A. Krohn, J. Nucl. Med. *32*, 1169–1176 (1991)
[237] M. Kudo, D.R. Vera, W.L. Trudeau, and R.C. Stadalnik, J. Nucl. Med. *32*, 1177–1182 (1991)
[238] J.C. Xu, D.R. Vera, and R.C. Stadalnik, J. Nucl. Med. *37*, 1896–1902 (1996)
[239] I. Virgolini, G. Kornek, J. Höbart, S.R. Li, M. Raolerer, H. Bergmann, W. Scheithauer, T. Pantev, P. Angelberger, H. Sinziger, and R. Höfer, Br. J. Cancer *68*, 549–554 (1993)
[240] J.P. DiZio, C.J. Anderson, A. Davison, G.J. Ehrhardt, K.E. Carlson, M.J. Welch, and J.A. Katzenellenbogen, J. Nucl. Med. *33*, 558–569 (1992)
[241] J.P. DiZio, R. Fiaschi, A. Davison, A.G. Jones, and J.A. Katzenellenbogen, Bioconjugate Chem. *2*, 353–366 (1991)
[242] J.P. O'Neil, K.E. Carlson, C.J. Anderson, M.J. Welch, and J.A. Katzenellenbogen, Bioconjugate Chem. *5*, 182–193 (1994)
[243] R.K. Hom, D.Y. Chi, and J.A. Katzenellenbogen, J. Org. Chem. *61*, 2624–2631 (1996)
[244] R.K. Hom and J.A. Katzenellenbogen, J. Org. Chem. *62*, 6290–6297 (1997)
[245] M. Rajopadhye, D.S. Edwards, J.P. Bourque, and T.R. Carroll, Bioorg. Med. Chem. Letters *6*, 1737–1740 (1996)
[245a] J.A. Barrett, A.C. Crocker, D.J. Damphousse, S.J. Heminway, S. Liu, D.S. Edwards, J.L. Lazewatsky, M. Kagan, T.J. Mazaika, and T.R. Carroll, Bioconjugate Chem. *8*, 155–160 (1997)
[246] T.D. Harris, M. Rajopadhye, P.R. Damphousse, D. Glowacka, K. Yu, J.P. Bourque, J.A. Barrett, D.J. Damphousse, S.T. Heminway, J. Lazewatsky, T. Mazaika, and T.R. Carroll, Bioorg. Med. Chem. Letters *6*, 1741–1746 (1996)
[246a] M.F. Giblin, N. Wang, T. Hoffmann, S.S. Jurisson, and T.P. Quinn, Proc. Natl. Acad. Sci. USA *95*, 12814–12818 (1998)
[247] M.-P. King, D.A. Stevenson, K. Plössl, S.K. Meegalla, A. Beckwith, W.D. Essman, M. Mu, I. Lucky, and H.F. Kung, Eur. J. Nucl. Med. *24*, 372–380 (1997)
[248] P.C. Meltzer, P. Blundell, A.G. Jones, A. Mahmood, B. Garada, R.E. Zimmerman, A. Davison, B.L. Holman, and B.K. Madras, J. Med. Chem. *40*, 1835–1844 (1997)

[249] S.K. Meegalla, K. Plössl, M.-P. Kung, D.A. Stevenson, L.M. Liable-Sands, A.L. Rheingold, and H.F. Kung, J. Am. Chem. Soc. *117*, 11037–11038 (1995)
[250] S. Meegalla, K. Plössl, M.-P. Kung, S. Chumpradit, D.A. Stevenson, D. Frederick, and H.F. Kung, Bioconjugate Chem. 7, 421–429 (1996)
[251] S. Meegalla, K. Plössl, M.-P. Kung, S. Chumpradit, D.A. Stevenson, S.A. Kushner, W.T. McElgin, P.D. Mozley, and H.F. Kung, J. Med. Chem. *40*, 9 17 (1997)
[251a] S.A. Kushner, W.T. McElgin, M.-P. Kung, P.D. Mozley, K. Plössl, S.K. Meegalla, M. Mu, S. Dresel, J.M. Vessotskie, N. Lexow, and H.F. Kung, J. Nucl. Med. *40*, 150–158 (1999)
[252] H.F. Kung, H.-J. Kim, M.-P. Kung, S.K. Meegalla, K. Plössl, and H.-K. Lee, Eur. J. Nucl. Med. *23*, 1527–1530 (1996)
[252a] S.K. Meegalla, K. Plössl, M.-P. Kung, D.A. Stevenson, M. Mu, S. Kushner, L.M. Liable-Sands, A.L. Rheingold, and H.K. Kung, J. Med. Chem. *41*, 428–436 (1998)
[253] B.K. Madras, A.G. Jones, A. Mahmood, R.E. Zimmerman, B. Garada, B.L. Holman, A. Davison, P. Blundell, and P.C. Meltzer, Synapse, *22*, 239–246 (1996)
[254] H.F. Kung, S. Meegalla, M.-P. Kung, and K. Pössl, Transition Met. Chem. *23*, 531 536 (1998)

C. Acronyms and abbreviations

This Page Intentionally Left Blank

ABP: : 1-hydroxy-4-amino-butylidene-1,1-diphosphonate

$abtH(H_2)$: 2-aminobenzenethiol

acacH : acetylacetone

$(acac)_2enH_2$: N,N′-ethylene-bis(acetylacetoneimine)

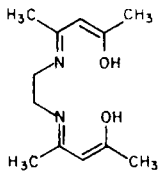

acdH : 2-amino-1-cyclopentene-1-dithiocarboxylic acid

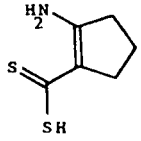

Acm : (acetylamino)methyl

ADP : adenosine diphosphate

aec : N-(2-aminoethyl)carbamic acid

amt_1H : 2-(methylamino)thiazole

amt_2H : 2-(4-methoxyphenylamino)thiazole

$14ane\text{-}N_2S_2$: 1,4-dithia-8,11-diazacyclotetradecane

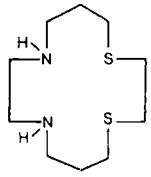

apH : 2-aminophenol

$apaH_3$: N,N′–3-azapentane-1,5-diyl-bis{3-(1-iminoethyl)-6-methyl-2H-pyran-2,4-dione}

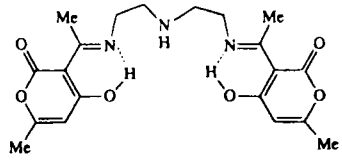

appH : 2-aminophenyldiphenylphosphine

$apsH_3$: N,N′–3-azapentane-1,5-diyl-bis(salicylideneimine)

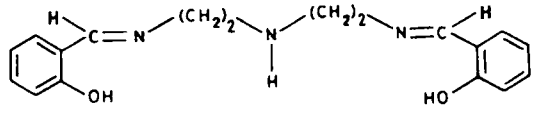

apy : 4-aminopyridine
Ar : 2,6-diisopropylphenyl
Ar′ : 2,6-dimethylphenyl
atpH : 2-aminothiophenol
$(BAT\text{-}TE)H_3$: ethane-1,2-bis(N-1-amino-3-ethyl-butyl-3-thiol)

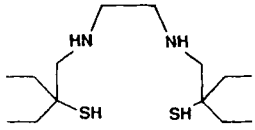

BBB : blood-brain barrier
bdi : butane-2,3-dione-imine-oxime
$bdtH_2$: 1,2-benzenedithiol
bemH : benzylidine-2-thioaniline

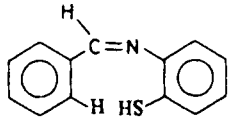

bgoH : 2-benzimidazol-2′-yl-methanol

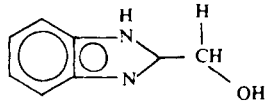

bloH : 2-benzimidazol-2′-yl-ethanol
blsH : 2-benzimidazol-2′-yl-ethanethiol
B.M. : Bohr magneton
BPA : N′-benzylpiperazinyl
$(BP\text{-}BAT\text{-}TM)H_3$: biphenyl-2,2′-bis(N-1-amino-2-methyl-propane-2-thiol)

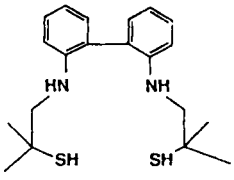

BPHA : N-benzoyl-N-phenyl hydroxylamine
bpm : 2,2′-bipyrimidine
bptz : 3,6-bis(2′-pyridyl)-1,2,4,5-tetrazine

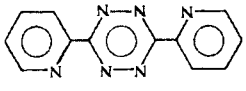

bpy : 2,2′-bipyridine
$(brac)_2enH_2$: N,N′-ethylene-bis(3-bromoacetylacetone imine)

btH : benzenethiol
Bu : *n*-butyl
Bu^i : *iso*-butyl
$(buac)_2enH_2$: N,N′-ethylene-bis(*tert*-butylacetyl-acetone imine)
$butriH_3$: 1,2,4-butanetriol
bztH : benzylthiol
$catH_2$: 1,2-dihydroxybenzene
CBF : cerebral blood flow
$(CDO\text{-}MeB)H_3$: tris(cyclohexanedionedioxime)methylboron
cep : tris(2-cyanoethyl)phosphine

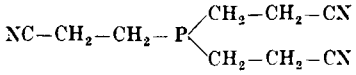

C.F.A.E. : crystal field activation energy
C.F.S.E. : crystal field stabilization energy
CNmxyl : 2,6-dimethylphenylisocyanide
Cp : cyclopentadienyl
Cp* : pentamethylcyclopentadienyl
15-Crown-5 : 1,4,7,10,13-pentaoxacyclopentadecane
csaH : cysteamine
Cy : cyclohexyl
cysH : L-cysteine
(cys-OEt)H : L-cysteineethylester
$dataH_4$: cyclohexanediaminetetraacetic acid
$dbcatH_2$: 3,5-di-*tert*-butylcatechol
$DBDSH_4$: N,N′-bis(mercaptoacetyl)butane-1,4-diamine

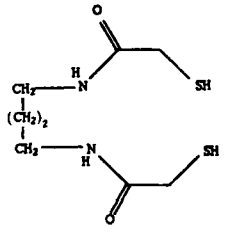

dbmH : dibenzoylmethane
dctH : N,N′-bis(4-chlorophenyl)triazenide
$dddH_2$: 3,6-dimethyl-3,6-diazaoctane-1,8-dithiol
$dedtH_2$: 2,2′-dimethyl-1,1-{(N,N′-H_2)ethylene-diamino}dipropane-2-thiol
depe : bis(1,2-diethylphosphino)ethane
diars : 1,2-phenylene-bis-(dimethylarsine)
diglyme : diethyleneglycoldimethylether

dioxocyclamH_2 : 1,4,8,11-tetraazacyclotetradecane-5,7-dione

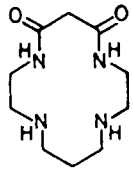

dithiadod : 5,8-dithiadodecane
dithiaoct : 3,6-dithiaoctane
dmapy : 4-(dimethylamino)pyridine
dmbtH : 2,6-dimethylbenzenethiol
dme : 1,2-dimethoxyethane
(DMG)2MPH_2 : dimethylglyoxime-(2-methyl-1-propyl)boron
dmitH_2 : isotrithionedithiol

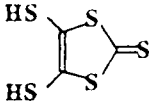

dmpe : bis(1,2-dimethylphosphino)ethane
DMSAH_2 : 2,3-dimercaptosuccinic acid
DMSEH_2 : 2,3-dimercaptosuccinic acid dimethylester
dpaH : N,N′-diphenylacetamidine
DPD : 2,3-dicarboxypropane-1,1-diphosphonate
dpfH : diphenylformamidine
dpk : bis(2-pyridyl)ketone
dpmH : dipivaloylmethane
dpp : 2,3-bis(2-pyridyl)pyrazine

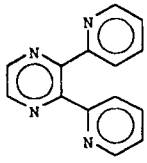

dppH : 1,2-dimethyl-3-hydroxy-4-pyridinone
dppb : 1,2-bis(diphenylphosphino)benzene
dppbtH : 2-(diphenylphosphino)benzenethiol
dppdH_2 : N,N′-bis{2-(diphenylphosphino)phenyl}-propane-1,3-diamine

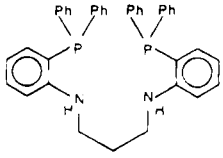

dppe : 1,2-bis(diphenylphosphino)ethane

dppv : *cis*-bis(1,2-diphenylphosphino)ethylene
dpq : 2,3-bis(2-pyridyl)quinoxaline

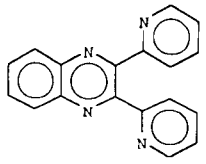

dta-morphH_3 : N,N-bis(2,2-dimethyl-2-mercapto-ethyl)(2-morpholine-4-yl-ethyl)amine
dtcbH(H_2) : S-methyl-3-(2′-hydroxybenzylidene) dithiocarbazate

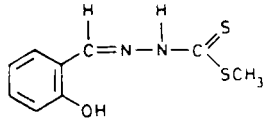

dtfH : N,N′-di-4-tolylformamidine
dttH : N,N′-di-4-tolyltriazenide
E_a : activation energy
ecbapH_2 : N-{2-ethoxycarbonyl-3-oxo-but-(1)-ene(1)yl}-2-aminophenol

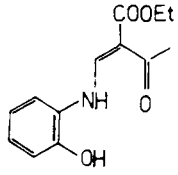

eddaH_2 : ethylenediaminediacetic acid
edtH_2 : ethane-1,2-dithiol
e=dtH_2 : ethene-1,2-dithiol
edtaH_4 : ethylenediaminetetraacetic acid
Eh : redox potential *vs* normal hydrogen electrode
egH_2 : 1,2-ethanediol
emaH_4 : N,N′-ethylene-bis(2-mercaptoacetamide)
epaH_4 : N,N′-ethylene-bis(2-phenoxyacetamide)
Et_4dadtH_2 : 3,10-diethyl-5,8-diazadodecane-3,10-dithiol
Et_2dtcH : diethyldithiocarbamic acid
Et_2tcbH : N-(N,N-diethylthiocarbamoyl)benzamidine

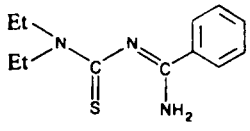

Et_2tu : N,N′-diethylthiourea
EXAFS : extended X-ray absorption fine structure

FAB-MS : fast atom bombardment mass spectrometry

furifosmin : 1,2-bis{dihydro-2,2,5,5-tetramethyl-3(2H)-furanato-4-methyl-encamino} ethane, bis{tris(3-methoxy-1-propyl)phosphine}

$glucaH_2$: N-salicylidene-D-glucosamine

$hafH_2$: S-methyl-β-N-(2-hydroxyphenylethylidene)dithiocarbazate

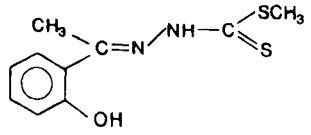

hbaH : 2′-hydroxybenzylidine-aniline

$hbdnpH_2$: N,N′-bis(2-hydroxybenzyl)-1,3-diamino-2-(4-nitrobenzyl) propane

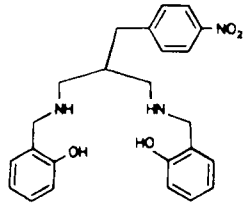

$hbdpH_2$: N,N′-bis(2-hydroxybenzyl)-1,3-diaminopropane

$hbhH_2$: 2′-hydroxybenzylidine-2-hydroxyaniline

$HB(pz)_3^-$: hydro-tris(1-pyrazolyl)borate

hbtH : 2-(2-hydroxyphenyl)benzothiazol

$hbtaH_2$: 2′-hydroxybenzylidine-2-thioaniline

HEDP : 1-hydroxyethylidene diphosphonate

$hedtaH_3$: N-(2-hydroxymethyl)-ethylenediamine-N,N′,N′-triacetic acid

Hep : *n*-heptyl

Hex : *n*-hexyl

hfaH : hexafluoroacetylacetone

HMDP : hydroxymethylene diphosphonate

HM-PAO : hexamethyl-propyleneamineoxime

hmpoH : 3-hydroxy-2-methyl-4H-pyran-4-one

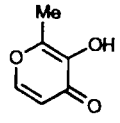

$hpaH_2$: 4′-hydroxypentyl-2′-idine-2-hydroxyaniline

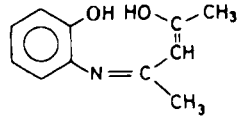

$hptH_2$	:	4′-hydroxypentyl-2′-idine-2-thioaniline
HR-ICP-MS	:	high resolution inductively coupled plasma mass spectrometry
im	:	imidazole
IT	:	isomeric transition
$L,L\text{-}ECDH_3$	:	N,N′–1,2-ethanediyl-bis(L-cysteinediethylester)
LPAS	:	laser induced photoacoustic spectroscopy
lut	:	3,5-dimethylpyridine
$mactH_2$	:	N,N′-ethylene-bis(methyl-2-amino-cyclopentane-1-dithiocarboxylate)

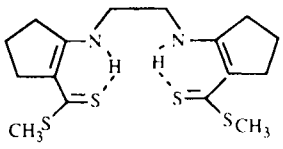

$(MAG)_3H_4$	:	mercaptoacetylglycylglycylglycine
$(MAG)_2H_4$	:	2-mercaptoacetyl diglycine

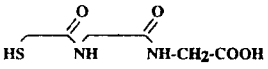

$mapH_4$	:	2,3-bis(mercaptoacetamido)propanoic acid
MDP	:	methylene diphosphonate
mdtcH	:	morpholine-4-dithiocarbamic acid

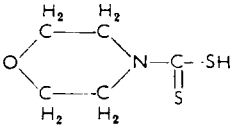

$mephH_2$	:	2-mercaptophenol
MequinH	:	2-methyl-8-hydroxyquinoline
MesalH	:	N-methylsalicylidenemine
Me_2tu	:	N,N′-dimethylthiourea
MIBI	:	hexakis(2-methoxy-2-methylpropyl-1-isonitrile)
$mnsH_2$	:	1,2-dicyanoethenediselenol
$mntH_2$	:	1,2-dicyanoethenedithiol

MPH_2 : *meso*-porphyrin IX dimethylester

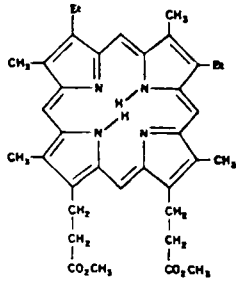

morphtcbH : N-(N′-morpholinylthiocarbonyl)benzamidine

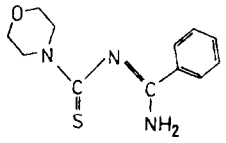

$mpdH_3$: N(mercaptoacetyl)-N′-{4-(pentenc-3-one-2)}ethane-1,2-diamine

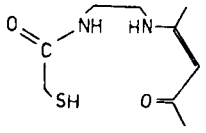

$(MRP\text{-}2O)H_3$: N-{2(1H-pyrolylmethyl)}N′-(4-pentenc-3-one-2)ethane-1,2-diamine

9N3 : 1,4,7-triazacyclononane

$NADP^+$: nicotinamide adenine dinucleotide phosphate

$(NEP\text{-}DADT)H_3$: N-ethyl-piperidinyl-hexamethyl-diaminodithiol

$Net\text{-}tmdadtH_3$: 4-N-ethyl-2,9-dimethyl-4,7-diaza- 2,9-decanedithiol

NHE : normal hydrogen electrode

$NMe\text{-}tmdadtH_3$: 4-N-methyl-2,9-dimethyl-4,7-diaza- 2,9-decanedithiol

NP_3 : 2-diphenylphosphino-N,N′-bis(2-diphenylphosphino-ethyl)ethanamine

nPe : neopentyl

$ntaH_3$: nitrolotriacetic acid

$oepH_2$: octaethylporphyrin

$ophsalH_2$: N-(2-hydroxyphenyl)salicylidenimine

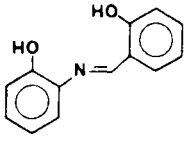

oxH_2 : oxalic acid

pacH : S-methyl-β-N-(isopropylidene)dithiocarbazate

pbtH : 2-(diphenylphosphino)benzenethiol

$pedH_3$: N-{2(1H-pyrolylmethyl)}-N′-(4-pentene-3-one-2)-ethane-1,2-diamine

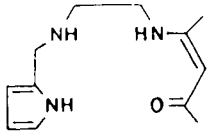

Pen : *n*-pentyl

$penamineH_3$: D-penicillamine-N,S,O-D-penicillamine-N,S

$pent(ao)_2H$: 3,3,11,11-tetramethyl-4,10-diazatridecane-2,12-dionedioxime

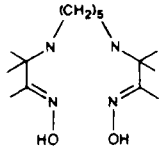

Ph : phenyl

phen : 1,10-phenanthroline

phsalH : N-phenylsalicylideneimine

$PICH_3$: N-[2-{(2-mercaptoacetyl)amino}-ethyl]-2-pyridine-carboxamide

pico : 4-methylpyridine

PMT : N-pyridoxyl-5-methyltryptophan

pn : 1,3-propanediamine

$pnaoH_3$: 3,3,9,9-tetramethyl-4,8-diazaundecane-2,10-dionedioxime

PP_3 : tris-2-diphenylphosphinoethylphosphine

ppme : 1,1,1-tris(diphenylphosphinomethyl)-ethane

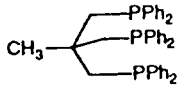

ppoo : 1,8-bis(diphenylphosphino)-3,6-dioxaoctane

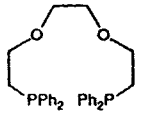

PPP : 4-phenylpiperidinyl

pppa : bis(diphenylphosphinoethyl)propylamine

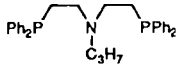

pppz : 4-phenyl-3,6-bis(2′-pyridyl)pyridazine

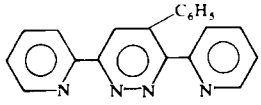

Pr^i : isopropyl
psi : pounds per square inch, 14.22 psi ≈ 1 bar
psig : pounds per square inch gauge (pressure measured with respect to that of the atmosphere)
ptfaH : pivaloyltrifluoroacetone
py : pyridine
pybta : bis(2-pyridylmethyl)-2-benzylthio-2,2-dimethylethylamine

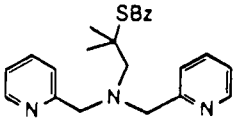

Pyr* : 2,3,4,5-tetramethylpyrrolyl
quinH : 8-hydroxyquinoline
quinim-naphH : 1-(8′-quinolyliminomethyl)-2-naphthol

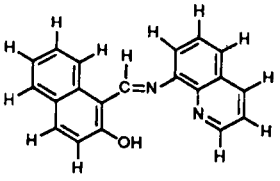

RIMS : laser resonance ionization mass spectroscopy
RH^+Cl : rhodamine-B hydrochloride
9S3 : 1,4,7-trithiacyclononane
14S4 : 1,4,8,11-tetrathiacyclotetradecane
16S4 : 1,5,9,13-tetrathiacyclohexadecane
16S4-$(OH)_2$: 1,5,9,13-tetrathiacyclohexadecane-3,11-diol
18S6 : 1,4,7,10,13,16-hexathiacyclooctadecane
$(sacac)_2enH_2$: N,N′-ethylene-bis(acetylacetonethioimine)
salH : salicylaldehyde
$salabtH_2$: N-salicylidene-2-aminothiophenol

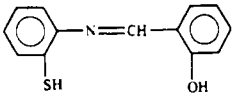

$salbdH_2$: N,N′-butane-1,4-diyl-bis(salicylidenimine)
$salcysH_3$: N-salicylidenecystein

: N,N′-ethylene-bis(salicylideneimine)

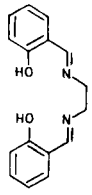

: N,N′–2-hydroxypropane-1,3-bis(salicylideneimine)
: N,N′-propane-1,3-bis(salicylideneimine)
: single photon emission computed tomography
: N-(2-mercaptophenyl)salicylideneimine
: 2-mercaptopyridine
: 1,5,8,12-tetraazadodecane
: monothiodibenzoylmethane
: tri-*n*-butyl phosphate
: 4-*tert*-butylpyridine
: S-methyl-3-(2′-hydroxy-1′-naphthylmethylene)dithiocarbazate

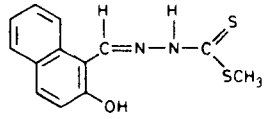

: 1,4,7-triazacyclononane-N,N′,N″-triacetic acid
: 3,4-toluenedithiol
: 2,2:6′,2″-terpyridine
: 1,4,8,11-tetraazaundecane
: 1,2-bis{bis(2-ethoxyethyl)phosphino}ethane trifluoroacetylacetone
: trifluoroacetylacetone
: tris(hydroxymethyl)(trimethylammonium)methane cation
: 2-(2′-hydroxyphenyl)-2-thiazoline

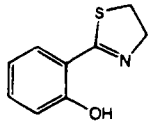

: 2,4,6-tri-*iso*-propylbenzenethiol
: triisooctylamine
: 2,3,5,6-tetramethylbenzenethiol
: trimethylphosphite
: N,N,N′,N′-tetramethylthiourea
: tri-*n*-octylamine
: *meso*-tetraphenylporphine

tppz : 2,3,5,6-tetrakis(2-pyridyl)pyrazine

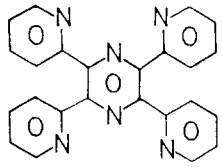

tren-py$_3$: tris{4-(2-pyridyl)-3-aza-3-butenyl} amine

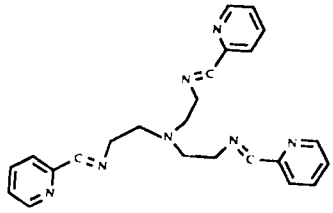

ttod : 1,5,11,14-tetrathiaoctadecane

tu : thiourea

Index

J

K

L

M

N

O

P

Q

R

S

T

X

This Page Intentionally Left Blank